agronomy

Special Issue Reprint

Sustainable Agricultural Systems

Enhancing Efficiency and Reducing Environmental Impact

Edited by
Thiago Libório Romanelli

mdpi.com/journal/agronomy

MDPI

Sustainable Agricultural Systems: Enhancing Efficiency and Reducing Environmental Impact

Sustainable Agricultural Systems: Enhancing Efficiency and Reducing Environmental Impact

Guest Editor

Thiago Libório Romanelli

MDPI

Basel • Beijing • Wuhan • Barcelona • Belgrade • Novi Sad • Cluj • Manchester

Guest Editor
Thiago Libório Romanelli
Department of Biosystems
Engineering
University of Sao Paulo
Piracicaba, SP
Brazil

Editorial Office
MDPI AG
Grosspeteranlage 5
4052 Basel, Switzerland

This is a reprint of the Special Issue, published open access by the journal *Agronomy* (ISSN 2073-4395), freely accessible at: https://www.mdpi.com/journal/agronomy/special_issues/GPW2XMK9YR.

For citation purposes, cite each article independently as indicated on the article page online and as indicated below:

Lastname, A.A.; Lastname, B.B. Article Title. *Journal Name* **Year**, *Volume Number*, Page Range.

ISBN 978-3-7258-9295-2 (Hbk)
ISBN 978-3-7258-9296-9 (PDF)
https://doi.org/10.3390/books978-3-7258-9296-9

© 2026 by the authors. Articles in this reprint are Open Access and distributed under the Creative Commons Attribution (CC BY) license. The reprint as a whole is distributed by MDPI under the terms and conditions of the Creative Commons Attribution-NonCommercial-NoDerivs (CC BY-NC-ND) license (https://creativecommons.org/licenses/by-nc-nd/4.0/).

Contents

About the Editor . . . . . **vii**

Thiago Libório Romanelli
Overview of Sustainable Agricultural Systems: Enhancing Efficiency and Reducing Environmental Impact
Reprinted from: *Agronomy* **2026**, *16*, 1164, https://doi.org/10.3390/agronomy16121164 . . . . . **1**

Anita Boros, Eszter Szólik, Goshu Desalegn and Dávid Tőzsér
A Systematic Review of Opportunities and Limitations of Innovative Practices in Sustainable Agriculture
Reprinted from: *Agronomy* **2025**, *15*, 76, https://doi.org/10.3390/agronomy15010076 . . . . . **5**

Sung Yung Yoo, Jun-Ki Son, Kyoung-Sik Jun and Hyun-Hwoi Ku
Effects of GroMore® Program on Rice Yield and GHG Emissions in a Korean Paddy Rice
Reprinted from: *Agronomy* **2024**, *14*, 2448, https://doi.org/10.3390/agronomy14102448 . . . . . **45**

Ana Paula Pereira Carvalho, Ana Claudia Pereira Carvalho, Mirian Yasmine Krauspenhar Niz, Fabrício Rossi, Giovana Tommaso and Tamara Maria Gomes
Multi-Criteria Analysis for Geospatialization of Potential Areas for Water Reuse in Irrigated Agriculture in Hydrographic Regions
Reprinted from: *Agronomy* **2024**, *14*, 2689, https://doi.org/10.3390/agronomy14112689 . . . . . **59**

Ana Carolina Murad Lima, Lisiane Brichi, Lucas Renato Trevisan, André Leão de Souza Dominguez, Gustavo Nocera Santiago, Tamara Maria Gomes and Fabrício Rossi
Effects of Irrigation with Treated Slaughterhouse Effluent and *Bradyrhizobium* spp. Inoculation on Soybean Development and Productivity: Strategies for Sustainable Management
Reprinted from: *Agronomy* **2025**, *15*, 167, https://doi.org/10.3390/agronomy15010167 . . . . . **89**

Camila Fabiani, María V. Valero, Jessica Basualdo, Marco Allegrini, Gastón A. Iocoli, María B. Villamil and María C. Zabaloy
Exploratory Field Case Study of Microbial and Resistance Genes Dynamics in the Maize Phyllosphere Following Fertigation with Anaerobic Digestate
Reprinted from: *Agronomy* **2025**, *15*, 2398, https://doi.org/10.3390/agronomy15102398 . . . . . **110**

Guilherme Rosa da Silva, Adam J. Liska and Cimélio Bayer
Cover Crops Can Reduce Greenhouse Gas Emissions from No-Till Maize in Southern Brazil: Insights from a Long-Term Field Experiment
Reprinted from: *Agronomy* **2025**, *15*, 267, https://doi.org/10.3390/agronomy15020267 . . . . . **126**

Xingyuan Xiao, Xuanming Hu, Yaqun Liu and Changhe Lu
Long-Term Annual Changes in Agricultural Carbon Footprints and Associated Driving Factors in China from 2000 to 2020
Reprinted from: *Agronomy* **2025**, *15*, 453, https://doi.org/10.3390/agronomy15020453 . . . . . **140**

Adéla Kalkušová, Jaroslav Neumann, Nina Veselovská, Eliška Kůrková, Petr Konvalina, Reinhard W. Neugschwandtner and Jaroslav Bernas
Rethinking Efficiency: How Increased Electricity Use Can Reduce Environmental Impacts in Controlled Hemp Cultivation—A Life Cycle Assessment (LCA) Study
Reprinted from: *Agronomy* **2025**, *15*, 2400, https://doi.org/10.3390/agronomy15102400 . . . . . **160**

Ibrahim M. Al-Helal, Abdullah A. Alsadon, Abdullah A. Ibrahim and Mohamed R. Shady
Optimizing Vents Opening Configurations and Orientations for Effective Natural Ventilation in Sustainable Greenhouses: A Case Study
Reprinted from: *Agronomy* **2025**, *15*, 2454, https://doi.org/10.3390/agronomy15112454 . . . . . **182**

Marianna Cardi Peccinelli, Marcos Milan and Thiago Libório Romanelli
Integrating Management and Digital Tools to Reduce Waste in Plant Protection Process
Reprinted from: *Agronomy* **2025**, *15*, 2276, https://doi.org/10.3390/agronomy15102276 . . . . . **196**

Asi Lazar, Inbar Meir, Ran Nisim Lati and Avital Bechar
Weed Detection: Innovative Hyperspectral Image Analysis for Classification and Band Selection of Site-Specific and Selective Weeding Robot
Reprinted from: *Agronomy* **2025**, *15*, 2576, https://doi.org/10.3390/agronomy15112576 . . . . . **211**

About the Editor

Thiago Libório Romanelli

Thiago Libório Romanelli is full Professor in the Department of Biosystems Engineering (LEB), Luiz de Queiroz College of Agriculture, University of Sao Paulo. His research interests include material flows, energy and environmental footprints in production systems, sustainability, lifecycle assessments, and the economic feasibility of technology adoption. He holds a degree in Agronomy, a Master's degree in Agricultural Machinery and a PhD in Forest Resources. He was a Research Associate at the Center for Environmental Policy at the University of Florida, and a Fulbright Scholar at the Chair of Agricultural Sciences at the University of Nebraska/Lincoln.

agronomy

MDPI

Editorial

Overview of Sustainable Agricultural Systems: Enhancing Efficiency and Reducing Environmental Impact

Thiago Libório Romanelli

Department of Biosystems Engineering, Luiz de Queiroz College of Agriculture, University of Sao Paulo, Sao Paulo 13418-900, SP, Brazil; romanelli@usp.br

In recent decades, globally, consumers, society, and policymakers have increased their awareness of environmental issues. The need to feed the increasing population has also highlighted the inefficiencies in agricultural and livestock management and their consequences [1]. The environmental context is frequently used as a barrier to international trade and as a promoter of new market niches [2,3]. Biosystems have been identified as sources of environmental impact, which has led to the constant aim for improvement, including the adoption of rational input use in decision-making, technology, and waste reduction [4,5].

Based on this context, this Special Issue titled "Sustainable Agricultural Systems: Enhancing Efficiency and Reducing Environmental Impact" was launched in 2024, successfully gathering studies that contribute to environmental awareness through systemic approaches focused on viable production chains or their components. The eleven articles cover topics from agricultural practices and the rationalization of input use to the circular economy through wastewater reuse, greenhouse gas (GHG) mitigation, carbon footprint consideration, energy efficiency, and precision agriculture.

1. Agricultural Practices and the Rationalization of Input Use

Boros et al. (2025) presented a systematic literature review of 291 studies on the progress and future opportunities of "sustainable agricultural practices". The research classified the most promising practices into three groups:

1. Agroecological Practices: Integrating ecological principles such as crop diversification and organic fertilizers.
2. Sustainable Agricultural Intensification: Focusing on increasing the productivity per unit area through genetic improvement and resource efficiency.
3. Technological Innovations: Using cutting-edge technologies including AI, biotechnology, drones, and big data to optimize resources.

This framework was corroborated in [6], where researchers evaluated integrated crop–livestock systems (ICLS) effects on crop yields and soil fertility. They concluded that an intermittent pasture system for legume crops in sequence is an alternative that can maintain or improve soil chemical composition and highlighted that conventional tillage systems should be avoided for tropical sandy soils.

In another study, Yoo et al. (2025) analyzed the effects of combining pesticides and amino acids in South Korean rice fields, finding that this practice sustains productivity while mitigating the environmental impact by reducing GHG emission intensity and the amount of pesticide applied. Their findings complement studies that approached amino acids as tools for toxicity mitigation [7].

2. Circular Economy: Water and Waste Reuse

Several studies evaluated the application of wastewater for irrigation, due to its economic and environmental impacts, in addition to its technological requirements [8,9]. To address freshwater scarcity—with agriculture consuming about 70% of the world's supply—Carvalho et al. (2025) proposed a method to identify ideal areas for treated wastewater reuse in Brazil. The study concluded that using wastewater from industries such as dairies and sugar mills provides a stable supply of nutrients, reducing the dependence on synthetic fertilizers.

Additionally, Murad Lima et al. (2025) researched the use of treated slaughterhouse effluent (TSE) in soybean cultivation. The authors indicated that TSE is a viable and sustainable strategy for soybean production, but it requires the longer-term monitoring of soil sodium levels to avoid salinization. Regarding environmental safety, Fabiani et al. (2025) found that using anaerobic digestate in corn fertigation is safe, as long as there is an adequate interval (21 days) between application and harvest to allow the plant's natural microbiota to recover.

3. Greenhouse Gas (GHG) Mitigation and Carbon Footprint (CF)

Studies considering GHG emissions and the CF of crops determined the equivalence of carbon dioxide or the amounts of carbon, respectively [10], and considered the energy provided by the mitigation routes [11]. Both ways help to map the production systems' components, to both enable effective decision-making and consider the energy nexus, since energy is the main reason mitigation is necessary.

In their research in Southern Brazil, Silva et al. (2025) demonstrated that replacing winter fallow with cover crops (legumes or grasses) in no-till corn systems is highly effective. These practices increase carbon sequestration in the soil and drastically reduce the crop's climate footprint.

More broadly, Xiao et al. (2025) analyzed China's agricultural carbon footprint from 2000 to 2020. While the total emissions increased by 21.32% due to chemical fertilizers and energy consumption, the carbon intensity (emissions per value generated) decreased, indicating more economically efficient production over time.

4. Technological Intensification and Energy Efficiency

Technology adoption either for assets or for their management through data science can provide more benefits than traditional methods for controlled cultivation [12]. Kalkušová et al. (2025) challenged the idea that high electricity consumption is always environmentally harmful by using Life Cycle Assessment (LCA) on indoor hemp cultivation. They determined that high-intensity systems are more environmentally efficient, because the drastic increase in productivity offsets the additional energy expenditure.

In their study on arid regions, Al-Helal et al. (2025) investigated how the orientation of ventilation openings in greenhouses can improve natural cooling. This "intelligent design" serves as a powerful tool to reduce the reliance on costly mechanical cooling systems and lower the carbon footprint.

5. Precision Agriculture and Digitalization (Waste Reduction)

The digitalization of crop production has high potential for monitoring environmental impacts. Since the input utilization determines both the production cost and environmental footprints, two-thirds of sustainability issues are addressed when the material flows of production systems are determined [13].

Peccinelli et al. (2025) integrated Lean Thinking with digital technologies to reduce waste in sugarcane crop protection. By using digital maps and variable rate applications, they reduced pesticide overlap and improved operational efficiency. Tools from total

https://doi.org/10.3390/agronomy16121164

quality management (TQM), similar to those used in technological adoption, supported efficiency improvements and, consequently, reduced the environmental impacts [14].

Finally, Lazar et al. (2025) used hyperspectral cameras and machine learning (with over 94% accuracy) to differentiate tomato plants from weeds. The study identified that using only 10 to 20 specific spectral bands is sufficient, allowing faster data processing, which is essential for real-time robotic field decisions. This study highlights how data science can support decision-making through remote sensing to promote sustainability [15].

Over the next 20 years, biobased production systems, including agriculture, forestry, and livestock, will likely face a paradox. Global food production will need to increase to supply a population of around 10 billion, and it will need to reduce its carbon footprint, water usage, and chemical dependency. There will be room for technology adoption, such as precision agriculture, autonomous and robotic farming, and real-time IoT sensing. Niche markets, either locally or internationally, may rely on natural ecosystem restoration, regenerative agriculture, and carbon-based farming. Further, the search for biological options to replace the chemical control of pests and diseases may pose changes in input management. Water may also benefit from data science to support decision-making in irrigation systems.

Funding: This research received no external funding.

Data Availability Statement: No new data were created or analyzed in this study. Data sharing is not applicable to this article.

Conflicts of Interest: The author declares no conflicts of interest.

List of Contributions:

1. Boros, A.; Szólik, E.; Desalegn, G.; Tőzsér, D. A Systematic Review of Opportunities and Limitations of Innovative Practices in Sustainable Agriculture. *Agronomy* **2025**, *15*, 76. https://doi.org/10.3390/agronomy15010076.
2. Yoo, S.Y.; Son, J.-K.; Jun, K.-S.; Ku, H.-H. Effects of GroMore® Program on Rice Yield and GHG Emissions in a Korean Paddy Rice. *Agronomy* **2024**, *14*, 2448. https://doi.org/10.3390/agronomy14102448.
3. Carvalho, A.P.P.; Carvalho, A.C.P.; Niz, M.Y.K.; Rossi, F.; Tommaso, G.; Gomes, T.M. Multi-Criteria Analysis for Geospatialization of Potential Areas for Water Reuse in Irrigated Agriculture in Hydrographic Regions. *Agronomy* **2024**, *14*, 2689. https://doi.org/10.3390/agronomy14112689.
4. Murad Lima, A.C.; Brichi, L.; Trevisan, L.R.; Leão de Souza Dominguez, A.; Nocera Santiago, G.; Gomes, T.M.; Rossi, F. Effects of Irrigation with Treated Slaughterhouse Effluent and *Bradyrhizobium* spp. Inoculation on Soybean Development and Productivity: Strategies for Sustainable Management. *Agronomy* **2025**, *15*, 167. https://doi.org/10.3390/agronomy15010167.
5. Fabiani, C.; Valero, M.V.; Basualdo, J.; Allegrini, M.; Iocoli, G.A.; Villamil, M.B.; Zabaloy, M.C. Exploratory Field Case Study of Microbial and Resistance Genes Dynamics in the Maize Phyllosphere Following Fertigation with Anaerobic Digestate. *Agronomy* **2025**, *15*, 2398. https://doi.org/10.3390/agronomy15102398.
6. Silva, G.R.d.; Liska, A.J.; Bayer, C. Cover Crops Can Reduce Greenhouse Gas Emissions from No-Till Maize in Southern Brazil: Insights from a Long-Term Field Experiment. *Agronomy* **2025**, *15*, 267. https://doi.org/10.3390/agronomy15020267.
7. Xiao, X.; Hu, X.; Liu, Y.; Lu, C. Long-Term Annual Changes in Agricultural Carbon Footprints and Associated Driving Factors in China from 2000 to 2020. *Agronomy* **2025**, *15*, 453. https://doi.org/10.3390/agronomy15020453.
8. Kalkušová, A.; Neumann, J.; Veselovská, N.; Kůrková, E.; Konvalina, P.; Neugschwandtner, R.W.; Bernas, J. Rethinking Efficiency: How Increased Electricity Use Can Reduce Environmental Impacts in Controlled Hemp Cultivation—A Life Cycle Assessment (LCA) Study. *Agronomy* **2025**, *15*, 2400. https://doi.org/10.3390/agronomy15102400.

9. Al-Helal, I.M.; Alsadon, A.A.; Ibrahim, A.A.; Shady, M.R. Optimizing Vents Opening Configurations and Orientations for Effective Natural Ventilation in Sustainable Greenhouses: A Case Study. *Agronomy* **2025**, *15*, 2454. https://doi.org/10.3390/agronomy15112454.
10. Peccinelli, M.C.; Milan, M.; Romanelli, T.L. Integrating Management and Digital Tools to Reduce Waste in Plant Protection Process. *Agronomy* **2025**, *15*, 2276. https://doi.org/10.3390/agronomy15102276.
11. Lazar, A.; Meir, I.; Lati, R.N.; Bechar, A. Weed Detection: Innovative Hyperspectral Image Analysis for Classification and Band Selection of Site-Specific and Selective Weeding Robot. *Agronomy* **2025**, *15*, 2576. https://doi.org/10.3390/agronomy15112576.

References

1. Silveira, J.G.D.; d'Almeida, F.S.; Silva, D.A.; de Oliveira, S.R.M.; de Faria, L.C. Land Use, Land Cover Change and Sustainable Intensification of Agriculture and Livestock in the Amazon and the Atlantic Forest in Brazil. *Sustainability* **2022**, *14*, 2563. [CrossRef]
2. Liu, Z.; Zhang, M.; Li, Q.; Zhao, X. The impact of green trade barriers on agricultural green total factor productivity: Evidence from China and OECD countries. *Econ. Anal. Policy* **2023**, *78*, 697–710. [CrossRef]
3. Zhao, X.; Gao, Y. Green Trade Barriers, Financial Support and Agricultural Exports. *Int. Rev. Econ. Financ.* **2024**, *97*, 103758. [CrossRef]
4. Sangaletti-Gerhard, N.; Romanelli, T.L.; Vieira, T.M.F.S. Energy flow in the soybean biodiesel production chain using ethanol as solvent extraction of oil from soybeans. *Biomass Bioenergy* **2014**, *65*, 24–31. [CrossRef]
5. Da Silva Lopes, J.; Kiperstok, A.; De Figueirêdo, M.C.B.; De Almeida Neto, J.A.; Rodrigues, L.B. Assessing the Eco-nomic and Environmental Performance of Cleaner Production Practices in Eucalyptus Planted Forests Using Life Cycle Assessment. *J. Clean. Prod.* **2022**, *380*, 134757. [CrossRef]
6. Soares, D.A.; Modesto, V.C.; Crusciol, C.A.C.; Pavinato, P.S.; Andreotti, M. Accumulated Carbon Fractions in Tropical Sandy Soils and Their Effects on Fertility and Grain Yield in an Integrated Crop–Livestock System. *Agronomy* **2024**, *14*, 2071. [CrossRef]
7. Zhao, G.p.; Cheng, W.l.; Zhang, Z.h.; Li, Y.x.; Li, Y.q.; Yang, F.w.; Wang, Y.b. The use of amino acids and their derivates to mitigate against pesticide-induced toxicity. *Ecotoxicol. Environ. Saf.* **2024**, *276*, 116340. [CrossRef] [PubMed]
8. Ukoha-Onuoha, E.; Taiwo Horsfall, I. The evolution of wastewater reuse for irrigation: Lessons learned and future directions. *Next Sustain.* **2026**, *4*, 100253. [CrossRef]
9. Awad, H.; Alalm, M.G. Toward a circular economy and sustainability: Evaluating resource recovery and reuse strategies in source-separated wastewater treatment systems in rural Egypt. *J. Water Process Eng.* **2026**, *89*, 110228. [CrossRef]
10. Cerri, C.E.P.; You, X.; Cherubin, M.R.; Moreira, C.S.; Raucci, G.S.; Almeida Castigioni, B.; Alves, P.A.; Cerri, D.G.P.; Castro Mello, F.F.; Cerri, C.C. Assessing the Greenhouse Gas Emissions of Brazilian Soybean Biodiesel Production. *PLoS ONE* **2017**, *12*, e0176948. [CrossRef] [PubMed]
11. Rosen, M.A.; Dincer, I. On exergy and environmental impact. *Int. J. Energy Res.* **1998**, *21*, 643–654. [CrossRef]
12. Gerampinis, E.; Kalafati, F.; Matsatsinis, N.; Arampatzis, G. Towards Digital Twin-Enabled Greenhouse Management: Enhancing Climate Resilience and Sustainability through Machine Learning-Driven Controlled Environmental Agriculture. *Sustain. Comput. Inform. Syst.* **2026**, *50*, 101343. [CrossRef]
13. Colaço, A.F.; Pagliuca, L.G.; Romanelli, T.L.; Molin, J.P. Economic viability, energy and nutrient balances of site-specific fertilisation for citrus. *Biosyst. Eng.* **2020**, *200*, 138–156. [CrossRef]
14. Lajnef, M.; Zaidi, A.; Lakhal, L.; Pasin, F. The effect of TQM on firms' performance: The mediating role of environmental management practices and green innovation. *J. Manuf. Technol. Manag.* **2025**, *36*, 1555–1575. [CrossRef]
15. Abdul-Gafaar, S.; Boamah, P.E.; Awad, M.; Al-Ansari, N.; Elbeltagi, A.; Hazazi, N.A.; El-Metwally, S.M.; El-Sawy, S.M.; Moustafa, M.; Al-Olayan, E.M.; et al. Integrating machine learning and drone technology for precision agriculture: A smart solution for automated irrigation and crop management. *Environ. Chall.* **2026**, *22*, 101393. [CrossRef]

Disclaimer/Publisher's Note: The statements, opinions and data contained in all publications are solely those of the individual author(s) and contributor(s) and not of MDPI and/or the editor(s). MDPI and/or the editor(s) disclaim responsibility for any injury to people or property resulting from any ideas, methods, instructions or products referred to in the content.

agronomy

MDPI

Review

A Systematic Review of Opportunities and Limitations of Innovative Practices in Sustainable Agriculture

Anita Boros [1,2,3], Eszter Szólik [1], Goshu Desalegn [4] and Dávid Tőzsér [5,*]

[1] Greenology Green Innovation Sustainability Knowledge Center, H-1031 Budapest, Hungary; boros.anita@uni-nke.hu (A.B.); szolik.eszter@uni-mate.hu (E.S.)
[2] Lajos Lőrincz Department of Administrative Law, Ludovika University of Public Service (NKE), Ludovika sq. 2, H-1083 Budapest, Hungary
[3] Institute of Agricultural and Food Economics, Hungarian University of Agriculture and Life Sciences (MATE), Páter Károly str. 1, H-2100 Gödöllő, Hungary
[4] Doctoral School of Economics and Regional Sciences, Hungarian University of Agriculture and Life Sciences (MATE), Páter Károly str. 1, H-2100 Gödöllő, Hungary; goshudasalegn@gmail.com
[5] Department of Ecology, Faculty of Science and Technology, University of Debrecen, Egyetem sq. 1, H-4032 Debrecen, Hungary
* Correspondence: tozser.david@science.unideb.hu

Abstract: A transformation is needed in agricultural production to satisfy the growing population-based increased food demands and overcome food safety challenges while supporting human health and the preservation of natural resources. Improving sustainable agricultural practices is essential for developing a long-term and resilient economy. This systematic review with meta-analyses aims to overview sustainable agriculture's progress, trends, and future opportunities, focusing primarily on integrating novel technologies into recently prevailing agricultural operations. As a basis, an extensive literature search was conducted, identifying nearly 45,000 records related closely to various dimensions of sustainable agriculture. Out of these, based on a thorough selection process, 291 were included in further evaluations. The temporal distribution and content analyses indicated an improvement in the number of papers and the spectrum of addressed agricultural aspects. The analysis of the publications revealed that most traditional farming practices focus on mass food production and cannot deal with further interrelated sustainability challenges. On the other hand, sustainable agricultural practices consider sustainability's environmental, economic, and social aspects, thereby preserving environmental health and supporting economic viability and social well-being. The integrative assessment in this study suggests that adopting novel, innovative practices can achieve the most significant progress toward agricultural sustainability. At the same time, a broad range of limitations and challenges are listed, which widely hinder the penetration of sustainability initiatives. To eliminate these barriers, consistent policy regulations are required, targeting specific agricultural problems, alongside a complex, education-based support system, further boosting initiatives related to the green transition in agriculture.

Keywords: green transition; agricultural sustainability; agricultural innovation; agro-economy; food production

1. Introduction

Agricultural activities have a significant impact on the condition of the environment and natural resources through various mechanisms. The most environmentally adverse agricultural practices include excessive use of chemical fertilizers and pesticides and mono-cultural mass production, leading to soil degradation, water pollution, and deterioration of

organisms [1–5]. Intensive animal husbandry and synthetic fertilizers contribute significantly to the emission of greenhouse gases such as methane, dinitrogen oxide, and carbon dioxide [6,7]. In some areas, the inappropriate disposal of plant residues or the burning of the remains instead of recycling results in extensive greenhouse gas emissions [8]. Using fertilizers and pesticides leads to the eutrophication of lakes, fostering damage to aquatic ecosystems [9]. In addition, soil's physical and agrochemical degradation, including the loss of humus and essential nutrients, is a major environmental burden, especially in regions where acidification of soil or radionuclide (e.g., ^{210}Pb, ^{226}Ra, ^{90}Sr) pollution are causes for concern [10,11]. These suggest that land use faces several challenges in terms of agricultural utilization.

The United Nations (UN) estimates that the global population could increase to 8.6 billion by 2030 [12]. This also means that the agricultural food industry needs to intensify its production. All this is executed with a focus on the fact that existing agricultural areas should not be further increased based on the recent intensity of their management [13–15]. In addition, a reduction in global biological diversity significantly hinders the involvement of new food sources (e.g., seaweed or plant-based alternatives to animal-derived products) and adversely affects food quality and nutrient content [16,17], putting pressure on agricultural systems. With eco-efficient agricultural operations, however, some adverse trends can be counteracted. Binding greenhouse gases in soil and plants, reducing biodiversity loss through new species with elevated resilience, changing nutritional habits through the diversification of diet, and using modern soil cultivation practices to reduce soil depletion and flood risk are all among potential solutions [18,19].

Based on the above, this paper seeks to introduce the development of sustainable agriculture and its practices in the last ten years by conducting meta-analyses of the available literature. Here, the most decisive farming technologies are assessed, focusing on innovations and their adoption in actual practice. Therefore, the implementation conditions of these innovations and their influence on production and the environment are also evaluated. Additionally, the major factors that hinder the spread of these sustainable practices are underlined, thereby determining the areas where there is space for further improvement.

1.1. The Concept of Sustainable Agriculture and Sustainable Agricultural Practices

The Food Agricultural Organization (FAO) defines the concept of sustainable agriculture as follows: "the management and conservation of the natural resource base, and the orientation of technological and institutional change in such a manner as to ensure the attainment and continued satisfaction of human needs for present and future generations" [20]. As a prelude, the formation of sustainable agriculture frameworks resulted from a long-term evolution lasting several decades. In the early 1980s, many American and European farmers recognized that their operations could hardly be maintained due to financial and environmental constraints; therefore, an alternative approach was required [21]. In this initial period, the proposal widely divided the scientific community, and its progress did not get the boost it deserved. By the late 1980s, however, the deterioration of soil and water bodies, the accumulation of toxic substances, and related health issues became highly evident and perceptible for society, researchers, and also legal bodies, which facilitated the wider acceptance and actual manifestation of sustainable agricultural interventions [22–24]. Since then, the concept has been continuously evolving with consistent debate, with multiple perspectives reflecting the preferences of stakeholders or authors. The approach of a sustainable farming system suggests that agriculture contributes to general well-being by providing sufficient food and other goods and services in an economically efficient, socially responsible, and profitable manner while also improving the quality of the environment [25]. Some authors emphasize that sustainable agriculture should be assessed from a

holistic farming aspect that aims to meet the needs of current and future generations by ensuring profitability, environmental health, and social and economic equity [26].

As a closely related subject, sustainable agricultural practices are tools and measures that support the reform of the whole agrarian sector along complex environmental-social-economic demands. These rely on previously developed methods with recent technological advances (e.g., low/no-emission machinery) and novel solutions (e.g., artificial intelligence) that aim to increase agricultural standards and productivity and subordinate total agricultural production to sustainability purposes [27]. From an ecological perspective, sustainable practices aim to maintain and improve the quality of the environment, even under the pressure of extensive farming operations. From an economic point of view, sustainable agricultural practices must ensure the long-term maintenance of farming activities, maintain economic resistance to market fluctuations, and meet the changing needs of consumers. These practices include the social aspect of sustainability by promoting the life quality of farmers, agricultural workers, and wider society, and improving food safety and healthy nutritional opportunities [28]. Additionally, sustainable agriculture based on innovative practices can contribute to achieving the Sustainable Development Goals (SDGs) of the United Nations, especially no poverty (SDG 1), zero hunger (SDG 2), decent work and economic growth (SDG 8), reduced inequalities (SDG 10), responsible consumption and production (SDG 12), climate action (SDG 13), life below water (SDG 14), and life on land (SDG 15) [29]. Thus, according to unanimous opinion, sustainable agriculture and its supporting practices are critical elements of future development.

1.2. New Research Directions Related to Sustainable Agricultural Practices

Considering the core focus areas, ecological intensification is a key strategy in sustainable agriculture, advocating for replacing anthropogenic inputs with environmentally friendly and sustainable alternatives. As suggested by scientific representatives, this approach underscores the need for the sustainable use of natural resources such as soil, water, nutrients, and other biotic and abiotic factors to achieve high performance and efficiency of agricultural yields. With similar goals, sustainable intensification has a broader definition range, including a wide variety of models and novel technologies that serve eco-efficient operations [30–32]. In addition to ecological intensification, genetic and socio-economic intensification are also evaluated in the literature. Genetic intensification, for instance, focuses on enhancing the genetic structure of plants to improve yield, resist pests and illnesses, tolerate harsh weather conditions, and enhance nutritional quality [33–36]. Socio-economic intensification, on the other hand, evaluates economic and social factors that can help improve farming, including the establishment of better markets for farmers. Further, it promotes the creation of training and education platforms related to modern technologies, the appropriate governmental regulatory and support policy systems, and the building of communities [37–40].

Another direction is climate-smart agriculture, which is considered the manifestation of intelligent agriculture [41]. The FAO defined climate-smart agriculture as "*an approach for transforming and reorienting agricultural production systems and food value chains so that they support sustainable development and can ensure food security under climate change*." [42]. Researchers are looking for practices that use the latest technological achievements and aim to reduce greenhouse gas emissions and water use while helping farmers adapt to and relieve the effects of climate change. Thus, these methods (e.g., cover cropping and nutrient recycling) promote the resistance of the sector to changing environmental conditions [43–48]. General resistance of the sector is a highly important issue, while current agronomic practices reportedly face three interrelated challenges: the spread of

pathogens in soil-human microbial loops, antibiotic-resistant genes in agroecosystems, and the impact of chemical pesticides on human and environmental health [49].

Among the trends in sustainable agriculture, research in agroecology stands out for its holistic approach. Agroecology, which integrates ecological principles with agricultural practices, aims to create sustainable and resilient food systems. This trend emphasizes the interconnectedness of plants, animals, humans, and the environment to balance food security and promote biodiversity and environmental health [50,51]. According to the most common views, agroecology deals with the exploration of the underlying causes of unsustainable agricultural systems but also links environmental security, production, consumption, and social innovation by promoting strong social movements, participatory frameworks, and alternative markets [52].

2. Materials and Methods

A systematic approach was used to review the relevant recent literature (published since 2015) for a thorough and accurate overview. As a first step, the database of Web of Science was scanned to find relevant publications using the topic search term "sustainable agriculture". Further, the databases of Google Scholar, PubMed, Scopus, and ResearchGate were also inspected using the aforementioned keyword. The resulted publications have been cumulated and listed with their bibliometric data, keywords, and abstract. According to the titles of listed publications, a pre-filtering of duplications was performed in Microsoft Excel. A summary of the literature selection process can be seen in Figure 1.

The first phase of this identification procedure resulted in more than 42,600 hits. Additionally, the reference list of 1000 randomly selected papers (from the 42,646 hits) was also revised to reveal additional publications outside of the studied databases but within the scope of this analysis. This complementary search yielded 1983 publications. After that, duplications were filtered out using the Bramer methodology [53]. Following the identification process, the key search terms "sustainable agricultural practice", "agricultural technology", and "sustainable management" were designated by the authors of this paper. These keywords were selected and used with the aim of including general aspects (with the keyword "sustainable agricultural practice") and more specific ones ("technology" and "management") simultaneously, thereby representing some of the most studied directions in sustainable agriculture in the literature. To combine or exclude keywords, "AND" and "OR" Boole operators were used, according to Booth and his co-author [54]. The refinement targeted papers in English, published between 1 January 2015 and 30 June 2023. However, to obtain a more comprehensive overview, discussions were also crafted based on publications from the year 2024. Studies were subject to specific criteria: we only assessed documents that were research papers, review articles, and book chapters focusing on sustainable agricultural practices. With these prerequisites, we selected 5800 sources for the subsequent analysis phase. In the following selection process, a two-step filtration approach was applied. First, relevant studies (research papers, review articles, book chapters) were identified by reviewing titles and abstracts, and it was then determined based on a complete text overview whether to involve the given source of literature in further research phases [55]. In more than 4100 cases, abstracts of papers referred to sustainable agriculture; however, the text scanning revealed no actual inclusion. The topic remained at the level of mention without in-depth assessment or critical scientific approach to any extent. In this stage, the number of selected studies was reduced to 1227. We made a template for the selected studies according to Clarke and Braun's guidelines that allowed systematic data recovery from studies. Due to this, we recorded details such as the scientific field of study. Here, we excluded scientific fields outside of the agricultural economy, food economy, and sustainability sciences based on the year of publication, abstract, methods,

main findings, and the exclusion of sustainable farming practices [56]. After excluding papers with the features above, 291 studies remained compliant. For these publications, we also considered the yearly progress of research and, where possible, highlighted the literature-based development of each concept. From the last ten years, such studies and their main research focuses were highlighted, which, based on the number of papers with similar topics from specific years and according to a content analysis, covered and introduced the presented agricultural issues the most extensively (see Table 1).

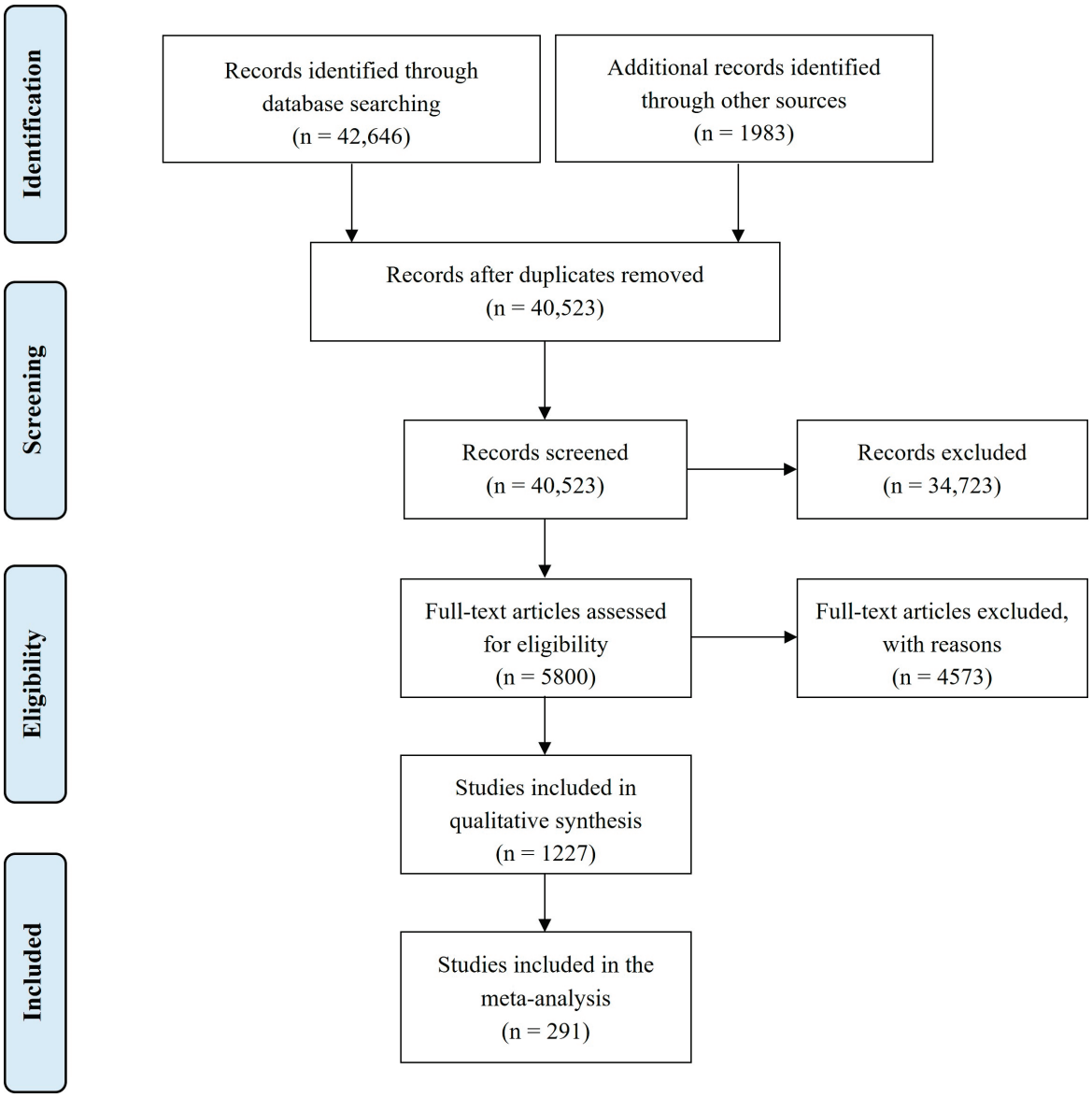


Figure 1. PRISMA flow diagram demonstrating the selection process within the analysis (i.e., the number of studies identified, excluded, and included).

Table 1. Some of the most significant practices in sustainable agriculture according to the time series of the literature.

Sustainable Agricultural Practices	Geographical Scope Discussed in the Paper	Source
Seed treatment methods for sustainable agriculture: (a) physical seed treatment, (b) hot water treatment, (c) dry heat treatment, (d) aerated heat treatment, (e) radiation treatment, (f) chemical and biological treatment, (g) seed soak in aqueous fungicides, (h) use of antibiotics, (i) seed soak in inorganic chemicals, (j) seed dressing, (k) seed coating, (l) seed pelleting, (m) permeability, (n) fluid drilling, (o) seed priming, (p) microorganisms, (q) future bioprotectants.	Global (general)	[57]
Strategies for the sustainable agricultural framework: (a) adaptive management, (b) cooperation, (c) ecology-based strategy, (d) economics-based strategy, (e) holistic and complex systems thinking, (f) knowledge and science, (g) subsidiarity.	Global (general)	[58]
Cultivation patterns: (a) crop diversification, (b) intercropping of maize with food crops.	South Africa (Kwazulu-Natal)	[59]
Conservation agriculture: (a) direct sowing, (b) rip line seeding, (c) planting basins.	Zimbabwe	[60]
Practices to increase maize yield: (a) establishment of furrows against soil erosion and for increased water retention, (b) cultivation of species with specific root structure against soil erosion, (c) rainwater retention, (d) application of inorganic fertilizers, (e) seasonal crop rotation, (f) application of green fertilizers, (g) mulching for better soil health, (h) application of lime for soil pH optimization.	Southern Africa (Chinyanja Triangle)	[61]
Soil protection: (a) organic manuring, (b) precision manuring, (c) integrated manuring, (d) green manuring.	Finland	[62]

Table 1. *Cont.*

Sustainable Agricultural Practices	Geographical Scope Discussed in the Paper	Source
Automation of conservation agriculture: (a) seeders and planters, (b) power sources, (c) weed control and cover crop management.	Africa, Asia	[63]
(a) agroforestry, (b) intercropping, (c) overcrops.	Zambia	[64]
Role of nanotechnology: (a) nanoencapsulation, (b) nanopesticides, nanoherbicides, (c) nanobiofertilizers, (d) nanoclay, (e) nano-assisted release of genetic material for quality upgrading.	India	[65]
Stakeholders' evaluation on climate-smart agriculture: (a) dugwell excavation, (b) livestock insurance, (c) tubewell, (d) climate-smart housing for livestock, (e) crop insurance, (f) drip irrigation, (g) sprinkler irrigation, (h) check dams, (i) vermicompost, (j) farmyard manure.	India (Maharashtra)	[66]
Resource management: (a) integrated plant protection, (b) integrated nutrient management, (c) soil protection, (d) water management.	Global (general)	[18]
(a) conservation agriculture (CA), (b) climate-resilient agriculture (CRA), (c) climate-smart agriculture (CSA), (d) sustainable agriculture (SA), (e) sustainable agricultural intensification (SAI), (f) sustainable agricultural extensification (SAE).	Global (general)	[67]
(a) agroecology, (b) nature-inclusive agriculture, (c) permaculture, (d) conservation agriculture, (e) regenerative agriculture, (f) carbon farming, (g) low external input agriculture, (h) organic farming, (i) high nature value farming, (j) climate-smart agriculture, (k) ecological intensification, (l) circular agriculture, (m) biodynamic agriculture, (n) sustainable intensification.	Global (general)	[68]
(a) automation of various practices (e.g., irrigation, tillage, harvesting, yield maximization), (b) use of resistant seeds, (c) modern irrigation techniques (e.g., sprinklers, drip irrigation), (d) use of renewable resources, (e) maintaining healthy soil conditions by supplementing essential nutrients, water, and oxygen.	Global (general)	[69]

Table 1. *Cont.*

Sustainable Agricultural Practices	Geographical Scope Discussed in the Paper	Source
(a) farm management plan, (b) farming cooperation, (c) sustainable crop rotation plan, (d) soil management, (e) crop nutrient management and organic-based fertilizers, (f) crop protection management, (g) management plan for efficient energy use, (h) farm waste management, (i) use of renewable energy, (j) energy production from biomass and liquid manure, (k) water conservation and management, (l) irrigation evaluation and monitoring, (m) reduction in CO_2 emissions from machinery and fuel use, (n) reduction in methane emissions from livestock, (o) maintenance and calibration of spraying equipment, (p) use of catch crops, (q) integrated pest management, (r) reuse of agricultural residues, (s) precision agriculture.	Europe, Asia	[70]
(a) conservation agriculture, (b) crop diversification, (c) organic farming, (d) agroforestry.	Europe, North Africa	[71]
(a) conservation agriculture, (b) good agricultural practices (GAP), (c) organic farming, (d) sustainable intensification, (e) permaculture.	Global (general)	[72]
(a) organic farming, (b) conservation agriculture, (c) precision agriculture, (d) agroecology.	Global (general)	[73]
(a) genetic intensification, improvement of crop yields, resistance to pests and illnesses, tolerance to abiotic stress, improving the nutritional quality of food, (b) use of precision breeding with genetic and genomic devices, (c) ecological intensification and increased diversification, farming, cultivation systems, resource efficiency, integrated water and nutrient management, (d) socio-economic benefits.	West Africa	[74]
(a) artificial intelligence, (b) machine learning.	Global (general)	[75]
RNAi-based biopesticides and strategies, including genomics, transcriptomics, metabolomics, and bioinformatics.	Global (general)	[76]
(a) climate-intelligent agriculture, (b) organic farming, (c) biodynamic agriculture, (d) conservation intensification, (e) regenerative agriculture.	Global (general)	[47]
artificial intelligence-based nanotechnology.	Global (general)	[8]

Table 1. *Cont.*

Sustainable Agricultural Practices	Geographical Scope Discussed in the Paper	Source
(a) precision agriculture, (b) organic farming, (c) agroforestry, (d) aquaponics and hydroponics, (e) biotechnology, (f) AI and BigData, (g) drones and satellite imagery, (h) conservation agriculture.	Global (general)	[77]
(a) crop rotation, (b) cover cropping, (c) conservation tillage, (d) organic farming, (e) integrated pest management, (f) agroforestry, (g) precision agriculture.	Global (general)	[78]
Main focuses of agriculture in the next few years: (a) organic farming, (b) climate-smart agriculture, (c) integrated farming, (d) best practices in management.	Southeast Asia	[79]
The role of artificial intelligence in: (a) production efficiency, (b) yield quantity and quality, (c) food production.	Global (general)	[80]

The selected 291 publications were involved in a meta-analysis; we determined the general topic trends by combining data from the studies. The use of meta-analysis provides an overview of the research topic of sustainable agricultural practices, allowing researchers, farmers, decision-makers, and other stakeholders to draw more clear conclusions about the effectiveness of each agrarian practice. In addition, this method increases the reliability of the findings of our study, as it is based on a higher amount of data, which reduces the possible variability, shortcomings, and methodological differences in investigations in certain studies [81].

However, it is worth noting that due to the very high number of involved studies, the publication list consists of papers of highly varied quality, which is a factor to consider when determining the explanatory power of the related statements. For instance, information disclosed in titles and abstracts sometimes does not entirely cover the main text's subject. Further potential limitations can emerge from the publication bias caused by not incorporating smaller studies (e.g., by assessing a reference list of only 1000 publications from the initial search). Additionally, the high heterogeneity arising from the experimental setup (e.g., location and statistical methods) may also influence the outcome of this analysis [82]. At the same time, in this study, these potential shortcomings are considerably counterweighted by the in-depth keyword search and the complementary scan for further research items in the reference list of papers. Along with this, a solid basis was established for the core conclusions in this paper by highlighting the issues represented most frequently and underlining similar methodology proposals across studies.

3. Results and Discussion

3.1. Scientometric Information on the Relevant Literature

In the preliminary analysis of the 291 publications, the temporal change in the relevant studies was evaluated. The result of the 8-year-long overview is presented in Figure 2.

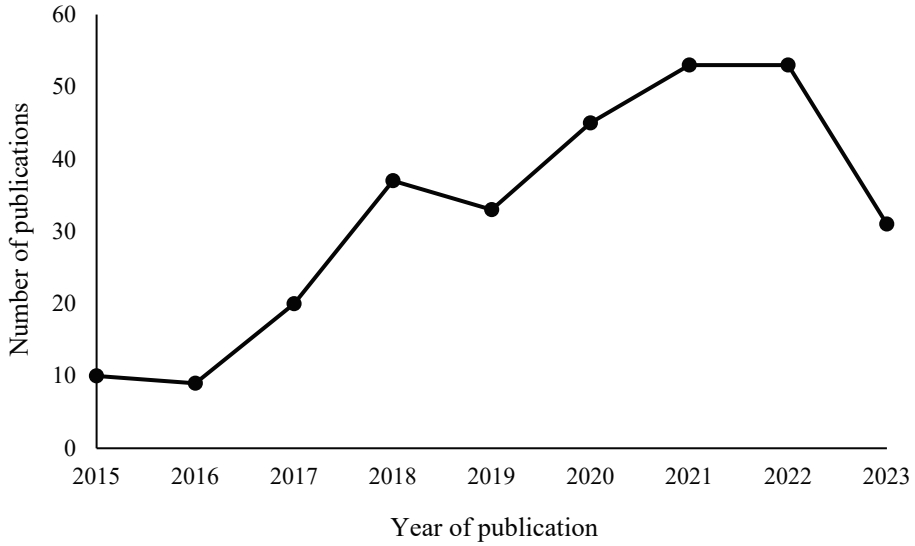


Figure 2. Change in the number of publications related to sustainable agricultural practices between 2015 and 2023.

After the initial low number of papers published in 2015 and 2016, a dynamic increase started in 2017. The publication intensity on the topic reached the highest numbers in 2021 and 2022, with 53 papers in both years. The result for 2023 should be interpreted considering the specific methodology of this paper: the latest studies involved were published in June 2023. During the first six months of the year, 31 papers were published, projecting a continuation of the previous years' ascending trend.

It was also assessed as to which leading journals featured the most publications. The related report for the 2015–2023 period is presented in Figure 3.

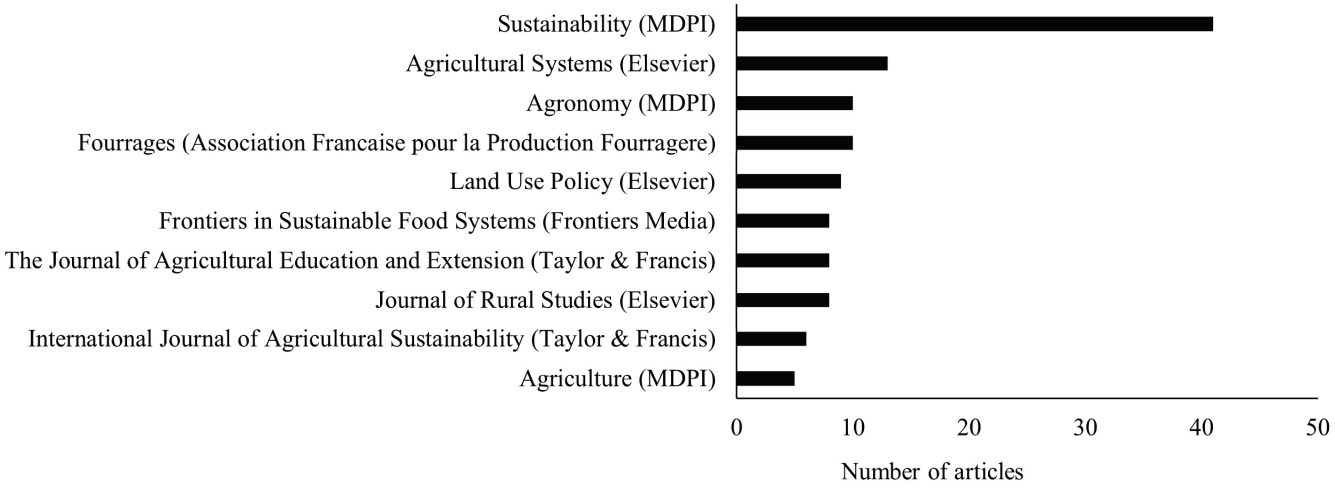


Figure 3. The top 10 journals with the most articles published related to sustainable agricultural practices between 2015 and 2023. (In parentheses: publisher).

It can be seen that 41 of the 118 research articles can be linked to one journal (*Sustainability*), indicating its primary importance in the field. Further journals in the list also

represent the high added value in assessing relevant agricultural issues. Apart from the journal in first place, the distribution of papers among journals (and their publishers) is considered even, which suggests the general relevance of the topic according to the scientific community.

3.2. Practices in Sustainable Agriculture

After the short scientometric introduction, it is worth highlighting the significant characteristics discussed in the literature on sustainable agricultural practices and related fields. It became evident from our review that most authors focus on specific segments rather than overgeneralizing farming issues. According to the literature of the last ten years, authors have determined which agricultural practices and technologies are classified as sustainable. Table 1 highlights some of the most intensely studied aspects of the literature for each year.

The findings in Table 1 suggest that the most studied sustainable agriculture-related aspects in the literature are strongly associated with technological improvements (e.g., the permeation of AI solutions and climate-smart farming technologies). This introduction and distribution of innovations by the scientific community establishes a solid basis for practical implementation, which often lacks theoretical fundamentals, even in some regions with high agricultural potential (e.g., favorable climate and soil characteristics) [83]. It can also be seen that issues are primarily studied as global phenomena; however, geographical involvement in many papers covers regions with much space for agricultural development and efficiency enhancement (e.g., African and Asian territories).

3.3. Types of Sustainable Agricultural Practices

As seen above, evaluating sustainable agricultural practices is a hot topic in the literature. Below, such operations are presented that are considered the most forward-looking and practical based on a meta-analysis of literature findings from the past ten years.

3.3.1. Agroecological Practices

Agroecological practices are methods that integrate ecological principles to create sustainable farming systems. The practices classified in this group emphasize respecting wildlife and the need to maintain an environmental balance [27,50]. In other words, such agricultural practices aim to consistently use natural resources by supporting appropriate and profitable food systems, food safety, and flexibly developing agricultural systems.

The most widely studied techniques include crop diversification, poly-cropping, agro-forestry, and the use of local varieties [84], organic fertilizers, intercropping, crop rotation, and cover crops to enhance soil fertility, pest control, and pollination [85,86], and promote organic farming [28]. According to some authors, agroecology-based farms generally provide more ecosystem services than traditional farms, thus improving productivity and promoting environmental health [85]. For instance, in Latin America, agroecological practices have been integrated into broader rural and regional development strategies, supporting socioeconomic development and ecological sustainability [87]. In addition, agroecology also motivates farmers to transform their practices radically, change their thinking, and facilitate participation in local knowledge distribution [88].

For the evaluation of agroecological systems, the Tool for Agroecology Performance Evaluation (TAPE) was developed under FAO coordination to measure the performance of methods concerning governance, culture, health, and nutrition [89]. Preliminary results of TAPE applications show that agroecological practices improve ecosystem services such as soil fertility, pest control, and pollination compared to conventional farming methods. A positive effect on farmers' well-being and food safety, especially in regions with scarce resources and high biodiversity, such as Tanzania and Malawi, was also reported [87,90,91].

3.3.2. Sustainable Agricultural Intensification

Sustainable agricultural intensification refers to a process that enhances the productivity of agricultural land by increasing the yield per unit by adopting various measures, such as automation, innovative plant varieties, and advanced farming techniques [92]. It includes three main components: (i) genetic intensification, which focuses on the improvement of yield, pest resistance, and nutritional quality through precision breeding and genomics; (ii) eco-intensification, which increases general efficiency while respecting environmental conditions and needs; and (iii) socio-economic intensification, which includes market development, political support and social capital construction [93]. The main characteristics of sustainable agricultural intensification are overviewed in Table 2, while some significant barriers to implementation and their policy-assisted potential solution proposals are found below.

Table 2. The main characteristics of sustainable agricultural intensification.

Nr.	Type of Sustainable Agricultural Practice	Components	Aims of Implementation	The Effect on the Production	The Effects on the Environment	Factors Hindering Practical Implication	Source
I.	Sustainable intensification of crop production	(a) Optimization of tillage	It aims to support yield stability by optimizing the water-holding capacity of soils and making farming methods more cost- and eco-efficient.	Increased yield and improved plant fertility.	Contributes to maintaining soil health by minimizing soil characteristics-based disturbance, maintaining soil structure, and providing better soil quality.	Local conditions, soil characteristics, and the economic viability of various soil cultivation methods influence the optimization of tillage methods.	[74,94–101]
		(b) Optimization of water management	It attempts to map multiple supply and demand scenarios using computational techniques and algorithms to set the most optimal water use.	Improved water management efficiency and increased productivity.	Contributes to the protection of water resources, to prevent water waste, and to enhance the quality of water.	The complexity and uncertainty of water systems, the lack of adequate water management policies, the variability of water resources, the economic interests.	[98,101–109]
		(c) Mixed farming integrating crop production and animal husbandry	It focuses on utilizing synergies between plants and livestock, such as nutrient recycling and diversified production, thereby increasing ecological and economic resistance.	Increased productivity and optimized resources by providing healthier flora and livestock and implementing more flexible agricultural systems.	Creates a more balanced ecosystem and supports biological diversity.	Lack of knowledge, skilled workforce, handling of synergies characteristic of mixed systems, uncontrolled material flow.	[98,103,110–115]

Table 2. *Cont.*

Nr.	Type of Sustainable Agricultural Practice	Components	Aims of Implementation	The Effect on the Production	The Effects on the Environment	Factors Hindering Practical Implication	Source
		(d) Precision crop management	It aims to manage agricultural areas' geographical and temporal diversity, including using advanced technologies to optimize resources and improve yields.	Uses advanced technologies and data analysis, provides more efficient plant treatment, optimized nutrient distribution, and maximized yield, cost savings by the reduced use of chemicals such as fertilizers and pesticides, increased overall profitability.	Contributes to preserving and restoring sensitive and vulnerable habitats. It helps to reduce the environmental impact of farming by minimizing the use of chemicals, conserving water resources, and reducing waste.	High initial cost and energy requirements, lack of knowledge and technical expertise, falsely addressed space-specific features.	[99,116–123]
		(e) Bioremediation	It uses living organisms such as bacteria, fungi, and plants to break down, remove, or transform environmental contaminants into less harmful substances.	More cost-effective compared to traditional clean-up methods as it often requires less equipment and workforce and can be used on a large scale.	Natural metabolic processes of organisms involved in bioremediation organize harmful substances into less toxic or non-toxic substances, promoting the restoration of the natural balance of the environment and improving soil health.	The complexity of microbial processes adversely influences the efficiency of integration, the lack of related knowledge, the type and metabolic activity of the microorganisms used, the high cost, the high variability of environmental factors, slow procedure flow, selectivity for contaminant type.	[98,103,124–134]

Table 2. *Cont.*

Nr.	Type of Sustainable Agricultural Practice	Components	Aims of Implementation	The Effect on the Production	The Effects on the Environment	Factors Hindering Practical Implication	Source
II.	Integrated Pest Management (IPM)		It seeks to combine cultural, physical, mechanical, biological, and chemical methods to keep pest populations below economic thresholds, thereby minimizing risks to human health and the environment.	Increased yields, reduced pesticide use, and enhanced overall environmental sustainability.	The purpose of these methods is to reduce the dependence on pesticides and to minimize the adverse effects on the environment.	The lack of appropriate knowledge. of crop production methods or pests.	[99,135–140]
III.	Integrated Nutrient Management (INM)		It aims to combine organic and inorganic fertilizers to improve soil health and crop productivity sustainably.	Increased yields by improved soil quality, increased nutrient use, and productivity.	Due to its application, soil health can be maintained or improved.	Higher levels of expertise and monitoring compared to traditional methods, the low availability and quality of organic materials, the lack of proper policy support.	[141–148]
IV.	Climate-smart agriculture	(a) Minimum tillage and no tillage (MT and NT)	It supports the decrease in farming intensification by mitigating as much physical impact on the soil system as possible.	Improved agricultural productivity and soil health, alleviated exposure to climate change.	These practices minimize soil disturbances, reduce erosion, enhance soil organic matter content, and improve water infiltration and retention.	Lack of practical knowledge, cost factors, need for special machines, and technological challenges.	[144,149–156]
		(b) Cover cropping	It supports the growing of certain crops primarily for the benefit of the soil rather than for direct harvest.	Improved soil biological activity and health and increased productivity.	It contributes to the quality of the soil by improving its physical, chemical, and biological properties, increasing organic matter and nutrient content, suppressing weeds, and eradicating pests.	High related costs (maintenance), the lack of expertise, and practical knowledge needed to select the appropriate species.	[144,157–164]

Table 2. *Cont.*

Nr.	Type of Sustainable Agricultural Practice	Components	Aims of Implementation	The Effect on the Production	The Effects on the Environment	Factors Hindering Practical Implication	Source
		(c) Nutrient recycling from livestock	It aims to minimize waste and optimize material use by recirculating reusable materials into different farming phases.	Increased productivity, improved cost-efficiency by recovering secondary, mineral-rich and organic products.	Animal fertilizers are rich in organic matter and nutrients that support the fertility of the soil, and these measures also reduce animal waste, while the involvement of external agents is minimized.	Cultural, educational, and institutional hiatus, technical, and economic constraints.	[144,165–170]

(I) Sustainable intensification of crop production

Sustainable crop intensification practices positively affect yields and farmers' income; however, obstacles to their widespread adoption still exist. One significant barrier is the perception of risk among small producers, who often see new technologies as a risky investment [171,172]. In addition, the lack of participation of agricultural producers in developing such technologies and the absence of a supportive policy environment hinder widespread integration [98]. Ecological concerns, such as land degradation and the adverse effects of previous agricultural intensification practices, are also significant challenges [173]. Insufficient experience with sustainable production concepts and the need for stakeholder-driven approaches to agricultural intensification are realized as additional limitations [174,175]. Like each method listed, the solution should be provided primarily by adequate and tailored policies. Establishing market opportunities and fostering/inhibiting the use of agriculture-related products (e.g., fertilizers and genetically modified seeds) are significant aspects of the process [176].

(Ia) Optimization of tillage methods

Although the literature contains several promising practices, many factors hinder the optimization of tillage methods, including soil compression, the decrease in soil organic matter content, the loss of nutrients required for optimal soil cultivation, and the low economic viability of non-destructive cultivation techniques [177–179]. These diverse challenges require a comprehensive and location-specific approach for optimization, including, among others, nutrient supplementation, soil amendment use, and the timing of field operation, all executed with data collection and calculations based on reliable logging and methods.

(Ib) Optimization of water resources management

The optimization of water resources management faces some significant obstacles, including the complexity and uncertainty of water systems, the lack of adequate water management policies, inadequate decision-making frameworks [180], spatial and temporal changes in water resources, and conflicts between stakeholders [102]. In addition, the consolidation of modeling results and the time-consuming justification process of their efficiency are also significant challenges for adopting best practices with regard to water resources [107]. Therefore, handling these shortcomings requires coordinated efforts

involving advanced optimization techniques, stakeholder agreements, and integrating adaptive management strategies. As actual evidence, resource policies make a significant contribution by recognizing local characteristics (e.g., water stress in the Middle East) and supporting joint technological (e.g., water recycling and reuse, rainwater harvesting, desalination) solutions [181].

(Ic) Mixed farming integrating crop production and animal husbandry

The spread of mixed farming, combining crop production and animal husbandry, is significantly hindered by the high labor intensity and time consumption associated with integrating plant and animal breeding systems [114]. Additionally, the heterogeneity of mixed management systems, high general costs, and initial capital investments into crop production systems are limiting factors [110]. Further, the need to reduce functional interactions between plants and livestock [115] and the availability of a skilled workforce [182] are also weaknesses. In addition, nutrient recycling and the complexity of resource distribution between food, feed, and animal products are challenging, especially in maximizing the efficiency of food production [183]. These should be resolved by supporting policy and complementary training opportunities and subsidies to enable farmers to acquire modern tools and machinery.

(Id) Precision crop management

Despite several technical and economic obstacles, precision crop management techniques hold immense potential for widespread application [184]. Significant barriers include high initial costs and energy requirements, a lack of knowledge and technical expertise, the complexity of managing site-specific inputs, and the challenges of climate and topography. However, with efficient cooperation between science, policymakers, and actors in the agricultural system, these obstacles can be overcome, paving the way for more efficient and sustainable crop management [118,185,186].

(Ie) Bioremediation

Being a promising and environmentally friendly approach to treating environmental pollutants, bioremediation faces several difficulties that hinder its widespread application [125]. These include the complexity of microbial processes, the type and metabolic activity of microorganisms used, the dynamic nature of the environment, and the variability of environmental factors (e.g., availability of nutrients, temperature, pH, toxicity, and concentration of compounds that can adversely affect the bioremediation process) [187]. In addition, bioremediation's nature and efficiency are highly varied by the contaminant type (e.g., inorganic vs. organic), which requires specific knowledge in the field [188]. Many innovative engineering tools, such as remote sensing and GIS-based mapping, support bioremediation practices in determining the degree of contamination. Still, a more intensive interaction of scientific fields and a multidisciplinary approach is also necessary [189]. As polluters lack accountability in many regions of the world due to insufficient legislation, policies should target this shortcoming by creating legal incentives, which would provide a boost to clean-up technologies such as bioremediation [190].

(II) Integrated pest management (IPM)

The extensive manifestation of IPM principles is primarily hindered by their cost and a lack of knowledge. In addition, the increased workload associated with IPM, and the uncertainty of the actual effectiveness of the methods against pests, do not support the spread of these techniques [140]. Overcoming these barriers requires a complex approach that includes better training, economic incentives, and improved communication strategies. The spread of these practices and a reduction in the use of pesticides can, however, best be facilitated by appropriate regulation. For instance, Directive 2009/128/EC of the European Parliament and of the Council aims to reduce the risks and impacts of pesticide use on human health and the environment and to promote integrated pest management and the

use of alternative approaches or techniques to reduce dependency on pesticide use. In 2017, the Commission undertook the development of a consensus in cooperation with the Member States on the development of harmonized risk indicators to monitor trends in the risks arising from the use of pesticides at the EU level [191]. Additionally, in February 2023, within the framework of the "Farmer's Toolbox for Integrated Pest Management" program, the European Commission developed a toolbox of proven IPM practices. This toolbox encourages national authorities and agricultural actors to use best practice techniques and technologies, such as crop rotation and balanced fertilization, monitoring harmful organisms, targeted and reduced application, and non-chemical pest control methods. The database also contains 273 plant-specific guidelines. In this regard, the European Commission highlighted that reducing the use of pesticides often works best when combined with other goals, such as soil conservation practices, reducing the use of fertilizers, and providing ecosystem services [192].

(III) Integrated nutrient management (INM)

Integrated nutrient management faces many obstacles, despite its proven benefits for sustainable agriculture. One of the significant drawbacks is the dependence on chemical fertilizers [193] and farmers' lack of awareness and knowledge of the long-term benefits of INM (e.g., improved soil health, increased crop yields, and reduced pollution) [194,195]. In addition, the inconsistent availability and quality of organic materials such as farmyard manure, compost, and bio-fertilizers may also hinder the consistent application of INM practices [196]. A decent solution could be a balanced and site-specific combination of organic and inorganic nutrients, but this would require more expertise and monitoring than conventional methods [197]. Overall, barriers can be removed through education, financial support, improving the supply chain of ecological inputs, and setting stricter policy frameworks. As for the latter, legal documents created at the community and state levels to limit inorganic fertilizer use and foster the application of organic compounds have proven to be efficient [198]. Therefore, adapting best practice policies is key to the efficient sector-level coordination of nutrient use.

(IV) Climate-smart agriculture (CSA) practices

This group of techniques includes conservation agriculture, integrated soil fertility management, plant diversification, and agroforestry, which improve yields and farm income while reducing greenhouse gas emissions [41,199]. CSA practices also include advanced irrigation techniques, such as subsurface drip irrigation, which improve soil properties and increase crop yields [200]. In addition, for example, early planting and using organic fertilizers have been beneficial in drought-prone areas, significantly increasing maize and bean yields [201].

(IVa) Minimum tillage (MT) and no-tillage (NT) management

As realized barriers ahead of this group of methods, the lack of practical knowledge, the initial costs of such practices, and the need for special machines capable of handling different soil hardness and operating speeds have been identified. Further, technological barriers to related solutions can also inhibit these sustainable practices in many regions [154,156]. Recently, policymakers have focused on MT and NT management, which, in a small group of high-income countries, has resulted in incentives toward the continuous implementation of afore management techniques [202].

(IVb) Cover cropping

Although these practices are becoming more and more popular, it is necessary to consider the variability in the costs (e.g., increases in the price of seeds, the high cost of labor and equipment) and the lack of expertise related to the selection of the appropriate cover crop type [161]. Besides these factors, in some cases, the inconsistent effect of cover crops on soil water retention and excessive competition for water between cover plants

and cultivated plants (e.g., in Mediterranean regions) should be assessed appropriately, as these are potential limits to the spread of this practice [203]. Research shows that targeted education programs and cost-sharing initiatives can help alleviate financial problems and promote wider adoption. In addition, selecting less competitive cover plant species and optimizing management practices can reduce interspecific competition [204].

(IVc) Nutrient recycling from livestock

Nutrient recycling from livestock faces many cultural, educational, and institutional challenges, as well as technical and economic limitations. Cultural and educational barriers often stem from a lack of awareness and knowledge about the benefits and methods of manure recycling [205]. Institutional barriers include inadequate policies and regulations that do not encourage nutrient recycling in many regions of the world [206]. Technical challenges cover the complexity of livestock waste processing and specialized technologies supporting efficient nutrient recovery, which is not readily available or affordable for all farmers [168]. Economic factors also play a significant role: costs associated with the transport and distribution of manure, the market demand for recycled manure products, and the lack of quality standards limit the economic viability of nutrient recycling [170]. Addressing these barriers requires a multifaceted approach that includes policy reforms, educational initiatives, and the adaptation of state-of-the-art technologies to promote sustainable recycling of livestock nutrients.

It can be concluded that many factors, including farm size, access to financial resources, and genetic, ecological, and socio-economic intensification components, influence the adoption of solutions. The successful integration of such practices requires an interdisciplinary approach, the involvement of the public and private sectors [207], and more intensive regional cooperation. Further, future progress in sustainable agricultural practices cannot be accomplished without the support of legal frameworks and policies built on local demands.

3.3.3. Sustainable Innovative Agricultural Practices

The practices mentioned above cannot be separated from the technological development routes, as they are also vital to increasing resource efficiency, reducing environmental degradation, and improving agriculture's resilience to climate change. To provide a more detailed but concise thought-provoking overview, Table 3 presents the most decisive and promising practices with the potential for innovation to make agricultural operations more sustainable.

Table 3. The most frequently studied sustainable innovative agricultural practices in the literature.

Nr.	Type of Sustainable Innovative Agricultural Practice	Components	Aims of Implementation	Effects on Production	Effects on the Environment	Factors Hindering Practical Implication	Source
I.	Biotechnology	(a) General biotechnology	Aims to use biological organisms and systems to develop quantitative and qualitative agricultural production for specific farming purposes.	Improved productivity, resilience, effective management of natural resources, and satisfied human nutritional needs.	Biotechnology can create plants resistant to pests and diseases, thereby reducing the need for chemicals to protect the quality of the environment and reducing the use of pesticides through stress tolerance genes.	High related costs, regulatory deficiencies, the lack of social acceptance, and inadequate/outdated infrastructural conditions.	[208–210]

Table 3. *Cont.*

Nr.	Type of Sustainable Innovative Agricultural Practice	Components	Aims of Implementation	Effects on Production	Effects on the Environment	Factors Hindering Practical Implication	Source
		(b) Genetic engineering	Modifies the genes of organisms to establish characteristics enabling more resilience and productivity under specific conditions.	Improved quality and quantity of crop production, reduced costs, and improved nutrient utilization.	Improve plant properties and strengthen resistance to pests, diseases, and adverse environmental conditions.	Environmental and health consequences include possible allergenic effects, unintended ecological risks, genetic pollution, and a deficit in social acceptance.	[211–219]
		(c) Marker-assisted selection	Operates to enhance crop yield by selecting the most favorable gene alleles using DNA markers, thus improving the targeted trait in the population.	Increased efficiency, reduced costs, accelerated development of improved varieties, improved crop yield, and increased genetic gain of better populations by increasing selection accuracy and reducing generation intervals.	It supports the selection of traits that increase resistance to environmental stress factors, reduce the need for chemicals, and improve resource efficiency.	High costs, lack of expertise, time-scale of development, unsupportive regulations.	[211,220–224]
		(d) Tissue culture and micropropaga-tion	These aim to multiply and regenerate plant materials under laboratory conditions; many individuals with the same characteristics can be cultivated in the field.	More balanced production of seeds, setting priorities for propagation conditions, and better rooting performance.	Optimization of growth conditions by selecting the most appropriate environment for the species.	High costs from testing to application, lack of trained experts.	[225–228]
		(e) Omics	Analyses data on the structure and function of biological systems at specific levels within the fields of genomics, proteomics, transcriptomics, metabolomics, and phenomics.	Improved plant traits (with focus areas such as gene characterization, protein regulation patterns, and metabolite composition) to achieve global food security.	Increases drought tolerance, improves the efficiency of nutrient use and pest resistance.	Regulatory/legal barriers, lack of expertise to carry out extensive research.	[229–233]
		(f) Bioinformatics	Collects, organizes, and processes information on genes and molecules with software to interpret genetic processes to be highlighted during cultivation.	Better seed quality, improved plant resistance, enhanced soil quality, and support of plant-based human disease diagnosis based on large datasets.	Helps the better understanding of the environmental systems as a whole.	Educational difficulties in training scientists, accep-tance/adoption of tools, high software and hardware costs.	[234–238]

Table 3. *Cont.*

Nr.	Type of Sustainable Innovative Agricultural Practice	Components	Aims of Implementation	Effects on Production	Effects on the Environment	Factors Hindering Practical Implication	Source
II.	Tools of eco-efficiency		Considers adopting practices and technologies that operate with low energy consumption and undesired emissions.	Increased crop quality/quantity with reduced resources invested, optimized supply chain, support of technological progress.	Supports reduced resource use resulting in lower emission levels, establishes programs promoting environmental sustainability.	Lack of expertise and holistic/systematic approach, inconsistent legal frameworks, climate change.	[239–244]
III.	Artificial intelligence (AI)		Its integration will provide better calculations, forecasting, and more reliable decisions throughout the agricultural value chain.	Precise and controlled management, including (among others) plant selection, procedure timing, irrigation, weeding, anti-pest measures, and nutrition supply, increased overall production efficiency.	Helps the removal of pests, weather prediction-based software for a more conscious use of renewables, emission tracking to locate pollution sources.	Low social acceptance rate, lack of technological knowledge, lack of strategies.	[194,245–250]
IV.	Drones	(a) Remote inspection and data gathering	Provides more accurate and time-saving solutions for field evaluation.	The identification of diseases, yield loss, and other discrepancies, monitoring of real-time livestock movement, and support of rapid soil and water sampling for plot assessment.	Fosters quick intervention in plant/plantation impairments and directed intervention instead of extensive intervention with environmental deterioration.	High initial and maintenance costs of equipment, need for potential authorization.	[251–256]
		(b) Fertilizer and pesticide application	Enables a precise and timely output of agents to save human workload, time, and overall energy investment.	Directed and reduced use of chemicals for balanced plant development, time-saving compared to conventional methods.	Eliminates the physical burden (e.g., soil deterioration) of heavy machinery.	High equipment initial and maintenance costs, need for potential authorization and social concerns around inappropriate airborne spraying.	[253,255–260]
V.	Satellites		Establishes continuous surveillance of crops for better yield and pest management.	Crop health monitoring, yield assessment, soil mapping, irrigation management, pest and disease control, and overall food security with the potential to increase efficiency by attaching AI and machine learning.	Enables early-stage intervention to avoid environmental deterioration and contributes to the establishment of databases by data collection.	High setup, maintenance, and reparation costs, high energy consumption, lack of expertise, and lack of farmer willingness to implement due to its inaccessible nature.	[261–265]

Table 3. *Cont.*

Nr.	Type of Sustainable Innovative Agricultural Practice	Components	Aims of Implementation	Effects on Production	Effects on the Environment	Factors Hindering Practical Implication	Source
VI.	Sensors	(a) Optical sensors	Their application is aimed at favoring general crop protection.	Surface reflection- and material-based data collection with installation on different vehicles and tools (e.g., diseases and irrigation requirements).	Indication of unfavorable changes in soil and plant characteristics.	High costs, lack of trained professionals.	[266–268]
		(b) Electro-chemical sensors	Supports the accurate determination of beneficial and undesired ions in soil layers to favor biological processes.	Quantification and qualification of soil parameters (e.g., pH, ion composition, and concentration) and monitoring pollution spread and hot spots.	Real-time overview of soil health to maintain an adequate habitat for species.	Laboratory infrastructure required for further soil analyses.	[269–271]
		(c) Mechanical sensors	Determines the physical properties of soils to maintain adequate structure.	Assessment of mechanical soil parameters by evaluating physical resistance.	Determines the location of areas affected by undesired soil compaction to prevent irreversible damage to soil organisms.	High cost of tools, lack of technical personnel.	[272,273]
		(d) Dielectric sensors	Aims to determine soil water conditions and supports the setting of proper moisture values.	Determination and adjustment of soil and tissue moisture levels for appropriate plant development.	Helps determine sites sensitive to drought and monitor seasonal changes in the soil water phase.	High cost of tools, lack of technical personnel.	[274–277]
		(e) Location sensors	These are applied to prevent the effects of unfavorable weather conditions on crops.	Information on environmental (primarily weather) conditions based on GPS data.	The sensors log data in different intervals to create a time series of information (e.g., being practical for climate change studies).	High tools, data storage, processing costs, and a lack of proper interpretation of results due to insufficient training.	[272,278,279]
		(f) Air-flow sensors	Determines the physical properties of soils to maintain adequate structure.	Data collection regarding various soil parameters by penetrating air into the depths.	A comprehensive evaluation of soil characteristics aids farming efficiency and provides data for science-related research.	High costs of tools and lack of farmers' information on specific devices and functions.	[273,280,281]
VII.	Forecasting systems	(a) Weather forecasting systems	Helps avoid the detrimental consequences of weather/ environmental extremes by enabling premature preparation.	Preparation for indices risking crop health and food safety, decreased im-port/transportation dependency due to the realization of projected yield.	Managers of adjacent sites can also be involved in the data access to broaden the range of areas with protective measures against forecasted weather phenomena (e.g., hail).	High cost of the establishment of a network of units and the high cost of tools needed for the prevention.	[282,283]

Table 3. *Cont.*

Nr.	Type of Sustainable Innovative Agricultural Practice	Components	Aims of Implementation	Effects on Production	Effects on the Environment	Factors Hindering Practical Implication	Source
		(b) Market forecasting systems/models	Aims to inform stakeholders on future processes by past and recent data processed with statistical analyses, aids the potential restructuring of the cultivation portfolio.	Indication of the short- and mid-term changes in product prices, whereby the individual agricultural portfolios can be restructured.	Monocultural cultivation depletes soil nutrients, while intermittent crop rotation can positively influence physicochemical soil properties.	Lack of relevant economic/scientific knowledge, insufficient/nonreliable raw data results in biased outcomes, nonresilient farming structures.	[284–286]
VIII.	Simulations		Aims to present possible future scenarios based on past data for farmers.	Scenarios for crop yield and quality, water and fertilizer use, and weather conditions to support efficient adaptation and mitigation measures in farming.	Simulations predict changes in climate parameters, whereby local and regional scenarios can be formed regarding the potential environmental consequences.	Insufficient input data (quantity and quality), high software costs, and the lack of trained experts.	[287–289]
IX.	Big Data		Supports modern, data-based farming operations with reliable information.	Reliable forecasting and decision-making, assessment of water use, and optimization of energy and costs, enhanced product safety.	Access to extensive data and its appropriate interpretation also support minimizing environmental burden by proposing farming practices with the least stress exerted.	Data security concerns among farmers, lack of human and financial resources, and low technological maturity level.	[290–292]
X.	Special vehicles		Aims to provide machinery in any cultivated area to broaden the range of arable lands and enhance the quality of farming operations.	Increased accuracy and decreased loss by planting and fertilizing, increased harvesting efficiency with time-saving operation.	Lower emission than conventional vehicles, a more efficient operation requiring less resource use.	Fear of environmental threat, low adaptation to novel solutions, local regulations, high costs.	[293–296]
XI.	Nanotechnology		Enables the improvement of desired traits of tools by implementing state-of-the-art technologies.	Improved crop quantity, quality, and security, support of the controlled application of soil/plant fertilizers and amendments, and more efficient agricultural operation through the value chain.	Enables decreased resource use (e.g., raw materials), energy generation from renewables (e.g., solar panels), and contamination remediation using nanomaterials.	Lack of expertise, health risks upon misuse of persistent nanomaterials, and high related costs.	[297–301]

Table 3. *Cont.*

Nr.	Type of Sustainable Innovative Agricultural Practice	Components	Aims of Implementation	Effects on Production	Effects on the Environment	Factors Hindering Practical Implication	Source
XII.	Innovative seeds		Aims to develop seeds with better characteristics in terms of resilience and yield.	Increased stress tolerance, higher yield, shorter cultivation periods, and better product transportability and keepability.	Due to the seeds' benefits, lower amounts of water and fertilizers are required, and transportation routes are shorted by cultivation in areas formerly considered infertile.	Regulation of (genetically) modified crops, low innovation willingness/uncertainty of farmers, lack of knowledge.	[302–305]
XIII.	Innovative food production systems		Helps provide food in remote areas with resource deficiencies, replace foods in the diet with less ecological footprint.	Market establishment by novel foods and foods with novel methods, increasing demand triggers higher production quality and quantity standards.	Contribution to decreased water consumption (e.g., plant-based meats), direct and indirect enhancement of consumers' environmental consciousness.	Aversion of consumers, sluggish licensing and regulation of products, high developmental costs, and lengthy experimental procedures.	[306–308]

It is worth noting that the classifications above are not considered a universal and exhaustive listing; however, these highlighted segments appear in the literature the most frequently and, according to several authors, have a core role in forming recent and future advances in agriculture. Thus, the transition to more sustainable agriculture is determined by integrating novel technologies (e.g., AI, drones), which, upon successful implementation, will significantly contribute to the eco-efficient operation of the sector. However, the actual adoption of these solutions is burdened by several common challenges. Based on the classifications in Table 3, a short overview of the most frequently highlighted issues can be found below.

(Ia) General biotechnology

The spread of biotechnology faces several financial, regulatory, social, and infrastructural obstacles. High investment and production costs represent significant economic and regulatory challenges, as different national and international regulatory frameworks form trade barriers. Among the difficulties, various levels of social acceptance of technologies can be underlined, hindering innovations' market integration [309–311].

(Ib) Genetic engineering

As Table 3 indicates, several environmental and health concerns may arise from the use of genetically modified organisms [216]. Partly due to these potential risks, the social acceptance of the genetic modification of organisms is also low. As a first phase, a solid regulatory framework is essential for initial support in integrating this technology. At the same time, well-founded information has to be published to a wider breadth of society to help people be more informed and thereby provide sufficient background for individuals to distinguish between actual and presumed concerns.

(Ic) Marker-assisted selection

Obstacles to the practical spread of marker-assisted selection include, among others, the high costs associated with genotyping a large number of plants, the low economic return on investment in the breeding of plant species, and the limited knowledge of the technical features [219,220,222]. In addition, this technology is considered adequate in the case of testing properties that can be measured only to a limited extent [312]. Therefore,

specific subsidies and governmental programs should support the spread of such scientific initiatives, with significant expenditures in the research and development procedures.

(Id) Tissue culture and micropropagation

Like marker-assisted selection, tissue culture and micropropagation adoption face multiple challenges. Knowledge and expertise in this domain are still moderate among farmers, which does not form sufficient demand and hinders the execution of extensive laboratory experiments. Thus, the crop yield and overall market competitiveness remain lower than for those areas with massive scientific backgrounds (e.g., biotechnology) [313]. According to some authors, the education of scientists, professionals, and farmers, along with complementary regulatory support, would be giant steps toward resolving these barriers, and rectifying the significant lagging of this area [228].

(Ie) Omics technologies

Despite the advances in genomics, proteomics, transcriptomics, metabolomics, and phenomics demonstrated in Table 3, challenges such as public perception, an immature regulatory environment, and a lack of robust training and capacity building remain. Further, compliance with data sharing and privacy standards often hinders the adequate exploitation of technological potential [314]. Additionally, the lack of standardization and efficient analytical methods due to insufficient resources are significant factors to eliminate [315]. These require transparent communication and substantial investment in research and development to realize the full potential of agricultural biotechnology [224]. Therefore, the penetration of omics technologies would greatly benefit from loosening regulatory frameworks based on scientifically supported decisions and presenting this information on multiple societal scales.

(If) Bioinformatics

As shown in Table 3 above, a wide range of modern approaches has been considered in the scientific literature. Bioinformatics enables the interconnectivity of specific farming practices, thereby providing all-pervasive technological solutions surrounding food safety, both in quality and quantity. However, many bioinformatics implementations face difficulties arising from insufficient educational systems and the lack of individual competencies (e.g., simultaneous biological and informatics knowledge), which are additional barriers besides the high emerging costs [238]. These obstacles can be widely overcome by fostering digital progress on each level of the educational system, whereby a higher number of professionals can be trained with dual (biology-informatics) interests.

(II) Tools of eco-efficiency

The problems raised regarding agricultural eco-efficiency are multifold, specifically since the measures of eco-efficient operation (modern technologies to reduce environmental burden) can cover nearly all segments of agricultural sustainability. This approach can seem overgeneralized; however, barriers are often related to the limitations of individual tools (see below). To highlight some of the most common issues, the low number of trained personnel, the challenging and sometimes contradictory regulatory frameworks, and climate change are the primary aspects to address. As these concerns emerge, a systematic approach is required across societal and economic perspectives. Approaches should focus on adopting the best available techniques implemented by appropriately qualified professionals, keeping, at the same time, societal, economic, and ecological demands in mind [239].

(III) Artificial intelligence (AI)

While it possesses immense potential in agriculture, artificial intelligence is considered to have many barriers to its implementation in the field. AI's relatively novel methods are still scarcely known and bear social uncertainty. Users' skills are usually insufficient, aggravated by the lack of joint strategies. Further, data quality issues and ethical concerns are

also barriers to AI integration. These shortcomings could be efficiently handled by uniform legislation and related attitude formation of affected parties, providing a framework and knowledge enabling conscious decisions in its application, even in farming practices [316].

(IV) Drones

The use of drones provides a wide range of benefits in farming. However, factors like high costs and regulation hinder their extensive use among farmers. The concerns linked to drones are enhanced in cases when they are used for chemical agent application; spraying into the atmosphere is considered a health risk by many people. Therefore, general governmental and regulatory confirmation would be needed to emphasize advances and resolve the doubt regarding the presumed hazards, highlighting the benefits, drawing the scope of application, and triggering the sparing use of drones and chemicals [260].

(V) Satellites

The barriers to the application of satellites comprise the need for high financial, energetic, and expert investment into the technology, whereby these technologies are attainable only for major institutions possessing these resources. Some mapping services are also available for public use, but the skills required for proper interpretation of the information are often lacking. Training should be directed at farmers to aid this concern, during which basic information on the appropriate use of satellite images in their agricultural practices should be forwarded. Further, primary sources for such data should also be reflected on, which help farmers gather as much relevant data as possible [264].

(VI) Sensors

Using sensors gives a thorough overview of the relevant processes in soil and vegetation. However, the application level of these instruments remains below a certain standard. Unfortunately, farmers' economic opportunities and know-how in several geographical areas enable them to use only a few or none of these during general fieldwork. This means that the first challenge is to get the farmers familiar with the instruments available for data collection, fostering the exchange of information. These measures should be followed by establishing funds for a dedicated governmental budget to help procure essential tools [285,289].

(VIIa) Weather forecasting systems

The formation of weather forecasting systems is burdened primarily by high costs related to the weather/environmental forecasting apparatus. Along with this, regional differences can be perceived in this field regarding the actual infrastructure and background expertise, raising the need for governmental intervention. However, in many countries, efficient bound forecasting and averting systems are already in operation (e.g., hail forecasting), providing up-to-date information to farmers. Analogous to this, more weather phenomenon-related cross-boundary forecasting systems should be installed and maintained with easily attainable online information for all stakeholders [317].

(VIIb) Market forecasting systems

The use intensity of this type of forecasting has barely been examined; however, the reliability of sources for relevant information, the ability of farmers to evaluate the credibility of data, and even the continuously changing economic environment make it extremely difficult to assess the actual role of market forecasting systems. While the data quality and critical attitudes in this area can be enhanced, the uncertainty of the economy cannot be eliminated, and this remains a major weak spot [284].

(VIII) Simulations

Using simulations can be beneficial for planning farming management schemes; however, some factors prevent the efficient use of technology in this domain. Data given as input lack adequate quality and quantity in many cases, which should be eliminated by standardized measurements, resulting in validated outcomes that are easily accessible

for further use. Fluent data processing of simulations has high software and hardware costs. Therefore, the license and technical guidance for their use should be integrated into services tailored to farmers (e.g., bank products) to encourage their use and thus favor food safety [318].

(IX) Big Data

Integrating Big Data (e.g., huge and progressively increasing amounts of data on environmental/cultural parameters) has already penetrated agricultural practices. Still, its comprehensive application is limited by data quality and security and human and financial resource-based and technological issues. Long-term data storage should be fostered by establishing dedicated, cloud-based data platforms with continuous data input, basic tutorials, and calculation proposals to aid the utilization of information gathered during farmers' operations. With such systems available, human resource dependencies could be sharply decreased, and with targeted agricultural subsidies for each farmer, technological barriers should also be eliminated [319].

(X) Special vehicles

The agricultural use of special vehicles has proved to provide high farming efficiency. However, conservative approaches from farmers, the fear of environmental deterioration caused, regulative hindrances, and high purchase and maintenance costs all counteract the widespread application of such machinery. To move forward, a thorough conversation should be conducted among developers, legal representatives, and farmers to map the needs and opportunities in each potential case. After outlining the aforementioned conditions, future measures could include the publication of relevant agricultural tenders and policy revisions [294].

(XI) Nanotechnology

Practices in nanotechnology have the potential to revolutionize agricultural production. Along with this feature, some significant concerns around its use are highly related to those presented for biotechnology. The lack of expertise, the health risks associated with the materials used, and the high emerging costs hinder its general integration. Considering these obstacles, actions should focus on training groups of researchers for nanotechnological applications and promoting the development of materials and products to eliminate their health-threatening characteristics. Then, after familiarizing farmers with fundamental information, forming demands should be followed by governmental legal and financial support [320].

(XII) Innovative seeds

The development of innovative seeds has had immense relevance during the recent decades of barely predictable climate change patterns. While a great proportion of farmers still insist on conventional solutions, the societal and legal doubt around genetically modified organisms and a significant knowledge gap leave huge unexploited potential in this technological direction. These obstacles are not often set aside. However, reliable and convincing scientific information on the actual ecological and health risks bound to genetically modified organisms (GMOs), and thereby reconsidered legislation, would shift the recent state toward a more open reception of innovative seeds from both farmers and consumers [305,321].

(XIII) Innovative food production systems

The appearance of foods in the market produced using innovative/alternative methods (e.g., underground horizontal or rooftop farming, vertical farming, urban agriculture) has occurred in direct response to unsustainable food supply schemes (e.g., long-distance shipping with economic and ecological concerns) that have predominated previously. These unconventionally produced foods can feed populations remote from conventional food production with novel methods that have decreased ecological footprints. However, there

is much debate regarding the actual sustainability benefits of some of these (e.g., vertical farming and its high related energy intensity). Additionally, with the features above being highly advantageous, consumers still strongly resist food innovation due to production technology-based deviations in taste, consistency, and individual conviction. Moreover, developing and licensing products takes a long time, slowing down their distribution. Science and nutrition-based popularization of these foods would influence the social acceptance of these novelties. At the same time, additional support for the development and shortening of the licensing procedure of foods should also be beneficial to distribution and guaranteeing food safety in the long run [307,322].

According to the literature, each of the technologies above has a particular potential to elevate agricultural production's efficiency and climate resilience. At the same time, farmers have individual opportunities and preferences regarding their operation. The most efficient exploitation of resources requires the education of farmers and smallholders regarding the technological and methodological options via professional assistance, through which specific demands are shaped. Once the future progress directions are formulated, legislation complemented with tailored financial subsidies should be made available for farmers. This would aid more sustainable and efficient operations that serve high-scale agricultural objectives.

4. Conclusions

This study aimed to evaluate significant trends and progress directions in sustainable agriculture, focusing on integrating novel technologies into the sector's operation. This meta-analysis-based literature review relied on a list of 44,629 items published between 2015 and 2023, which was, through screening and eligibility assessment, narrowed down to 291 papers. Further analyses of these publications indicated a yearly improvement in the number of manuscripts, while the quantitative distribution of publications was uneven among the journals. It was found that many techniques are available to foster agricultural sustainability. However, adopting these innovative solutions faces multiple challenges, which hinder their deeper penetration and, thus, the better utilization of technological opportunities. Limitations of this nature also have economic, social, and governmental aspects. Among the most common barriers, high related investment costs, unwillingness to innovate, social awareness, acceptance, and impenetrable legal frameworks were mentioned in several cases. The complexity of the limitations above justifies the need for joint, intersectoral measures to aid agriculture prospects. This study provides insight into the prevailing agricultural processes and localizes focus areas to advance future investigations. These aspects should be addressed even more to help farmers with practical implementation in order to keep up with the expectations of the changing natural, social, governmental, and economic environment. Future environmental legislation and associated financial subsidies must also be directed to favor the evolution of agriculture-related sustainability progress.

Author Contributions: A.B.: conceptualization, methodology, validation, formal analysis, investigation, data curation, writing—original draft, writing—review and editing, visualization, supervision; E.S.: methodology, investigation, writing—original draft, writing—review and editing; G.D.: visualization, writing—original draft, writing—review and editing; D.T.: methodology, formal analysis, investigation, writing—original draft, writing—review and editing, visualization, project administration, funding. All authors have read and agreed to the published version of the manuscript.

Funding: This work was financed by the NRDI (National Research, Development and Innovation Office) Fund [grant number 138806].

Data Availability Statement: Data will be made available upon request.

Conflicts of Interest: The authors declare that they have no known competing financial interests or personal relationships that could have appeared to influence the work reported in this paper.

Abbreviations

AI	Artificial intelligence
CA	Conservation agriculture
CRA	Climate-resilient agriculture
CSA	Climate-smart agriculture
FAO	Food Agricultural Organization
GAP	Good agricultural practices
GHGs	Greenhouse gases
INM	Integrated Nutrient Management
IPM	Integrated Pest Management
MT	Minimum tillage
NT	No tillage
SA	Sustainable agriculture
SAE	Sustainable agricultural extensification
SAI	Sustainable agricultural intensification
SDGs	Sustainable Development Goals
TAPE	Tool for Agroecology Performance Evaluation

References

1. Saxena, L.K.; Jain, P.K.; Sharma, A.K. Tactical supply chain planning for tyre remanufacturing considering carbon tax policy. *Int. J. Adv. Manuf. Tech.* **2018**, *97*, 1505–1528. [CrossRef]
2. Uddin, M.E.; Kebreab, E. Impact of food and climate change on pastoral industries. *Front. Sustain. Food Syst.* **2020**, *4*, 543403. [CrossRef]
3. Farooq, M.S.; Uzair, M.; Raza, A.; Habib, M.; Xu, Y.; Yousuf, M.; Yang, S.H.; Ramzan Khan, M. Uncovering the research gaps to alleviate the negative impacts of climate change on food security: A review. *Front. Plant Sci.* **2022**, *13*, 927535. [CrossRef] [PubMed]
4. Ratnadass, A.; Sarter, S. How agricultural practices affect the risk of human contamination by infectious pathogens: The need for a 'One Health' perspective. *CABI Rev.* **2023**. [CrossRef]
5. Ullah, M.K.; Shabir, S. The Significant Effects of Agricultural Systems on The Environment. *J. World Sci.* **2023**, *2*, 798–805. [CrossRef]
6. Bulut, S.; Gökalp, Z. Agriculture and environment interaction. *Curr. Trends Nat. Sci.* **2022**, *11*, 372–380. [CrossRef]
7. Palapa, N.; Honchar, S.Y. Environmental risks associated with human agricultural activity. *Agroèkologičeskij Žurnal* **2022**, *1*, 68–80. [CrossRef]
8. Singh, A.D.; Bakshi, P.; Kumar, P.; Kour, J.; Dhiman, S.; Ibrahim, M.; Madaan, I.; Kapoor, D.; Mir, B.A.; Bhardwaj, R. Effects of Agricultural Wastes on Environment and Its Control Measures. In *Agricultural and Kitchen Waste*; Pal, D.B., Tiwari, A.K., Eds.; CRC Press: Boca Raton, USA, 2022; pp. 219–239. [CrossRef]
9. Kaur, G.; Singh, G. Environmental impacts of agriculture. *J. Pharmacogn. Phytochem.* **2019**, *8*, 23–25.
10. Mathur, R.; Srivastava, V.K. Crop Residue Burning: Effects on Environment. In *Greenhouse Gas Emissions. Energy, Environment, and Sustainability*; Shurpali, N., Agarwal, A., Srivastava, V., Eds.; Springer: Singapore, 2019. [CrossRef]
11. Tan, K.; Cai, X.; Kwan, K.T. A review of natural and anthropogenic radionuclide pollution in marine bivalves. *Sci. Total Environ.* **2023**, *896*, 165030. [CrossRef] [PubMed]
12. UN. *World Population Prospects: The 2024 Revision*; United Nations: New York, NY, USA, 2024. Available online: https://population.un.org/wpp/ (accessed on 3 December 2024).
13. Padulosi, S.; Heywood, V.; Hunter, D.; Jarvis, A. Underutilized species and climate change: Current status and outlook. In *Crop Adaptation to Climate Change*; Yadav, S.S., Redden, R.J., Hatfield, J.L., Lotze-Campen, H., Hall, A.E., Eds.; Wiley: Hoboken, NJ, USA, 2011; pp. 507–521. [CrossRef]
14. Herrero, M.; Havlík, P.; Valin, H.; Notenbaert, A.; Rufino, M.C.; Thornton, P.K.; Blümmel, M.; Weiss, F.; Grace, D.; Obersteiner, M. Biomass use, production, feed efficiencies, and greenhouse gas emissions from global livestock systems. *PNAS* **2013**, *110*, 20888–20893. [CrossRef] [PubMed]

15. NCD-RisC. Worldwide trends in body-mass index, underweight, overweight, and obesity from 1975 to 2016: A pooled analysis of 2416 population-based measurement studies in 128.9 million children, adolescents, and adults. *Lancet* **2017**, *390*, 2627–2642. [CrossRef]
16. Díaz, S.; Settele, J.; Brondízio, E.S.; Ngo, H.T.; Agard, J.; Arneth, A.; Balvanera, P.; Brauman, K.A.; Butchart, S.H.M.; Chan, K.M.A.; et al. Pervasive human-driven decline of life on Earth points to the need for transformative change. *Science* **2019**, *366*, eaax3100. [CrossRef]
17. Dembedza, V.P.; Chopera, P.; Mapara, J.; Macheka, L. Impact of climate change-induced natural disasters on intangible cultural heritage related to food: A review. *J. Ethn. Foods* **2022**, *9*, 32. [CrossRef]
18. Peshin, R.; Bano, F.; Kumar, R. Diffusion and Adoption: Factors Impacting Adoption of Sustainable Agricultural Practices. In *Natural Resource Management: Ecological Perspectives. Sustainability in Plant and Crop Protection*; Peshin, R., Dhawan, A., Eds.; Springer: Cham, Switzerland, 2019. [CrossRef]
19. Owino, V.; Kumwenda, C.; Ekesa, B.; Parker, M.E.; Ewoldt, L.; Roos, N.; Lee, W.T.; Tome, D. The impact of climate change on food systems, diet quality, nutrition, and health outcomes: A narrative review. *Front. Clim.* **2022**, *4*, 941842. [CrossRef]
20. FAO. Conservation Agriculture | Food and Agriculture Organization of the United Nations. 2006. Available online: http://www.fao.org/conservation-agriculture/en/ (accessed on 2 June 2024).
21. Sampson, R.N. Saving agricultural land: Environmental issue of the 1980's. *Environmentalist* **1982**, *2*, 321–332. [CrossRef]
22. Keeney, D. Sustainable Agriculture: Definition and Concepts. *J. Prod. Agric.* **1990**, *3*, 281–285. [CrossRef]
23. Altieri, M.A. *Agroecology: The Science of Sustainable Agriculture*, 2nd ed.; CRC Press: Boca Raton, FL, USA, 1996; 448p. [CrossRef]
24. Alshaal, T.; El-Ramady, H. Sustainable Agriculture: Towards Holistic Overview. *J. Sustain. Agric. Sci.* **2017**, *43*, 65–67. [CrossRef]
25. Sirmour, A.; Pandey, M.K.; Verma, A. Adoption of new resource conservation technology for sustainable production. *J. Pharmacogn. Phytochem.* **2017**, *6*, 655–661.
26. Liu, S. Towards a sustainable agriculture: Achievements and challenges of Sustainable Development Goal Indicator 2.4.1. *Glob. Food Secur.* **2023**, *37*, 100694. [CrossRef]
27. Akanmu, A.O.; Akol, A.M.; Ndolo, D.O.; Kutu, F.R.; Babalola, O.O. Agroecological techniques: Adoption of safe and sustainable agricultural practices among the smallholder farmers in Africa. *Front. Sustain. Food Syst.* **2023**, *7*, 1143061. [CrossRef]
28. Saikanth, D.R.K.; Gupta, K.; Srivastava, P.; Saryam, M.; Rani, K.S.; Jena, P.; Rout, S. Environmental Sustainability and Food Security of Traditional Agricultural Practices in India: A Review. *Int. J. Environ. Clim.* **2023**, *13*, 1847–1856. [CrossRef]
29. UN. *The 17 Goals*; United Nations: New York, NY, USA, 2024. Available online: https://sdgs.un.org/goals (accessed on 5 December 2024).
30. Tittonell, P. Ecological intensification of agriculture—Sustainable by nature. *Curr. Opin. Environ. Sustain.* **2014**, *8*, 53–61. [CrossRef]
31. Jhariya, M.K.; Meena, R.S.; Banerjee, A. (Eds.) *Ecological Intensification of Natural Resources for Sustainable Agriculture*; Singapore: Springer, 2021. [CrossRef]
32. Pupos, T.; Nábrádi, A. A fenntarthatóság értelmezése, annak komplex elméleti háttere. *Gazdalkodas* **2022**, *66*, 493–531. [CrossRef]
33. Arzu, Ü.N.A.L. The Importance of Microbial Genetic Resources for Food and Agriculture in the Bioeconomy. *J. Agric.* **2020**, *3*, 33–42. [CrossRef]
34. Suroso, A.I.; Pahan, I.; Maesaroh, S.S. New Plantation Moratorium Policy and Smallholders Palm Oil Rejuvenation for Increasing Productivity of Indonesian Palm Oil. *J. Manaj. Agribisnis* **2020**, *17*, 138–152. [CrossRef]
35. Saputra, G.E. Keragaman Genetik Sepuluh Galur F3 Hasil Persilangan Double Cross Tanaman Tomat (*Solanum lycopersicum* L.) Menggunakan Marka SRAP. Ph.D. Thesis, Universitas Gadjah Mada, Yogyakarta, Indonesia, 2023.
36. Putri, L.E.; Anhar, A.; Violita, V.; Vauzia, V. The Effect of Giving Trichoderma asperellum on Rice Plant Height in Organic and Inorganic Cultivation. *J. Biol. Trop.* **2024**, *24*, 100–105. [CrossRef]
37. Boeckx, P.; Bauters, M.; Dewettinck, K. Poverty and climate change challenges for sustainable intensification of cocoa systems. *Curr. Opin. Environ. Sustain.* **2020**, *47*, 106–111. [CrossRef]
38. Haggar, J.; Nelson, V.; Lamboll, R.; Rodenburg, J. Understanding and informing decisions on sustainable agricultural intensification in Sub-Saharan Africa. *Int. J. Agric. Sustain.* **2021**, *19*, 349–358. [CrossRef]
39. Mucheru-Muna, M.W.; Ada, M.A.; Mugwe, J.N.; Mairura, F.S.; Mugi-Ngenga, E.; Zingore, S.; Mutegi, J.K. Socio-economic predictors, soil fertility knowledge domains and strategies for sustainable maize intensification in Embu County, Kenya. *Heliyon* **2021**, *7*, e06345. [CrossRef] [PubMed]
40. Silva, J.V.; Reidsma, P.; Baudron, F.; Laborte, A.G.; Giller, K.E.; van Ittersum, M.K. How sustainable is sustainable intensification? Assessing yield gaps at field and farm level across the globe. *Glob. Food Secur.* **2021**, *30*, 100552. [CrossRef]
41. Mizik, T. Climate-smart agriculture on small-scale farms: A systematic literature review. *Agronomy* **2021**, *11*, 1096. [CrossRef]
42. FAO. Climate-Smart Agriculture Sourcebook, Module A1-2: Introducing Climate-Smart Agriculture. 2021. Available online: https://www.fao.org/climate-smart-agriculture-sourcebook/en/ (accessed on 3 December 2024).
43. Abegunde, V.O.; Sibanda, M.; Obi, A. Mainstreaming climate-smart agriculture in small-scale farming systems: A holistic nonparametric applicability assessment in South Africa. *Agriculture* **2020**, *10*, 52. [CrossRef]

44. Mazzetto, F.; Gallo, R.; Sacco, P. Reflections and methodological proposals to treat the concept of "information precision" in smart agriculture practices. *Sensors* **2020**, *20*, 2847. [CrossRef] [PubMed]
45. Navarro, E.; Costa, N.; Pereira, A. A systematic review of IoT solutions for smart farming. *Sensors* **2020**, *20*, 4231. [CrossRef]
46. Branca, G.; Arslan, A.; Paolantonio, A.; Grewer, U.; Cattaneo, A.; Cavatassi, R.; Lipper, L.; Hillier, J.; Vetter, S. Assessing the economic and mitigation benefits of climate-smart agriculture and its implications for political economy: A case study in Southern Africa. *J. Clean. Prod.* **2021**, *285*, 125161. [CrossRef]
47. Muhie, S.H. Novel approaches and practices to sustainable agriculture. *J. Agric. Food Res.* **2022**, *10*, 100446. [CrossRef]
48. Taimour, H.; Farhadian, H.; Saadvandi, M. Adoption of climate-smart agriculture practices in the Gorganrood basin in Golestan province. *Ecohydrol. Hydrobiol.* **2023**, *23*, 678–687. [CrossRef]
49. Yan, Z.; Xiong, C.; Liu, H.; Singh, B.K. Sustainable agricultural practices contribute significantly to One Health. *J. Sustain. Agric. Environ.* **2022**, *1*, 165–176. [CrossRef]
50. Al-Yahyai, R.; Al-Hashmi, K.; Janke, R. Agroecological Practices on Traditional Date Farms. In *Date Palm*; CABI International: Wallingford, UK, 2023; pp. 367–398. [CrossRef]
51. Knapp, J.L.; Sciarretta, A. Agroecology: Protecting, restoring, and promoting biodiversity. *BMC Ecol. Evol.* **2023**, *23*, 29. [CrossRef]
52. Bisht, I.S.; Rana, J.C.; Jones, S.; Estrada-Carmona, N.; Yadav, R. Agroecological approach to farming for sustainable development: The Indian scenario. In *Biodiversity of Ecosystems*; Hufnagel, L., Ed.; IntechOpen Ltd.: London, UK, 2022. [CrossRef]
53. Bramer, W.M.; Giustini, D.; de Jonge, G.B.; Holland, L.; Bekhuis, T. De-duplication of database search results for systematic reviews in EndNote. *J. Med. Libr. Assoc.* **2016**, *104*, 240. [CrossRef]
54. Booth, A.; Papaioannou, D.; Sutton, A. *Systematic Approaches to a Successful Literature Review*, 2nd ed.; SAGE Publications Ltd.: London, UK, 2016; 336p.
55. Arksey, H.; O'Malley, L. Scoping studies: Towards a methodological framework. *Int. J. Soc. Res. Methodol.* **2005**, *8*, 19–32. [CrossRef]
56. Clarke, V.; Braun, V. Thematic analysis. *J. Posit. Psychol.* **2017**, *12*, 297–298. [CrossRef]
57. Sharma, K.K.; Singh, U.S.; Sharma, P.; Kumar, A.; Sharma, L. Seed treatments for sustainable agriculture—A review. *J. Appl. Nat. Sci.* **2015**, *7*, 521–539. [CrossRef]
58. Velten, S.; Leventon, J.; Jager, N.; Newig, J. What Is Sustainable Agriculture? A Systematic Review. *Sustainability* **2015**, *7*, 7833–7865. [CrossRef]
59. Hitayezu, P.; Zegeye, E.W.; Ortmann, G.F. Farm-level crop diversification in the Midlands region of Kwazulu-Natal, South Africa: Patterns, microeconomic drivers, and policy implications. *Agroecol. Sustain. Food Syst.* **2016**, *40*, 553–582. [CrossRef]
60. Mafongoya, P.; Rusinamhodzi, L.; Siziba, S.; Thierfelder, C.; Mvumi, B.M.; Nhau, B.; Hove, L.; Chivenge, P. Maize productivity and profitability in conservation agriculture systems across agro-ecological regions in Zimbabwe: A review of knowledge and practice. *Agric. Ecosyst. Environ.* **2016**, *220*, 211–225. [CrossRef]
61. Makate, C.; Makate, M.; Mango, N. Sustainable agriculture practices and livelihoods in pro-poor smallholder farming systems in southern Africa. *Afr. J. Sci. Technol. Innov. Dev.* **2017**, *9*, 269–279. [CrossRef]
62. Huttunen, S.; Oosterveer, P. Transition to sustainable fertilisation in agriculture, a practices approach. *Sociol. Rural.* **2017**, *57*, 191–210. [CrossRef]
63. Sims, B.; Kienzle, J. Sustainable Agricultural Mechanization for Smallholders: What Is It and How Can We Implement It? *Agriculture* **2017**, *7*, 50. [CrossRef]
64. Nkomoki, W.; Bavorová, M.; Banout, J. Adoption of sustainable agricultural practices and food security threats: Effects of land tenure in Zambia. *Land Use Policy* **2018**, *78*, 532–538. [CrossRef]
65. Pandey, G. Challenges and future prospects of agri-nanotechnology for sustainable agriculture in India. *Environ. Technol. Innov.* **2018**, *11*, 299–307. [CrossRef]
66. Khatri-Chhetri, A.; Pant, A.; Aggarwal, P.K.; Vasireddy, V.V.; Yadav, A. Stakeholders prioritization of climate-smart agriculture interventions: Evaluation of a framework. *Agric. Syst.* **2019**, *174*, 23–31. [CrossRef]
67. Kumar, N.; Chhokar, R.S.; Tripathi, S.C.; Sharma, R.K.; Gill, S.C.; Kumar, M. Role of Conservation Agriculture in Sustainable Food Production and Challenges. *Find. Agric. Res. Manag. (FARM) J.* **2020**, *4*, 5–11.
68. Oberč, B.P.; Schnell, A.A. *Approaches to Sustainable Agriculture: Exploring the Pathways Towards the Future of Farming*; International Union for Conservation of Nature (IUCN): Brussels, Belgium, 2020; pp. 1–92.
69. Srivastava, R.K. Influence of Sustainable Agricultural Practices on Healthy Food Cultivation. In *Environmental Biotechnology Vol. 2. Environmental Chemistry for a Sustainable World*; Gothandam, K., Ranjan, S., Dasgupta, N., Lichtfouse, E., Eds.; Springer: Cham, Switzerland, 2020. [CrossRef]
70. Baptista, F.; Lourenço, P.; da Cruz, V.F.; Silva, L.L.; Silva, J.R.; Correia, M.; Picuno, P.; Dimitriou, E.; Papadakis, G. Which are the best practices for MSc programmes in sustainable agriculture? *J. Clean. Prod.* **2021**, *303*, 126914. [CrossRef]
71. Choden, T.; Ghaley, B.B. A Portfolio of Effective Water and Soil Conservation Practices for Arable Production Systems in Europe and North Africa. *Sustainability* **2021**, *13*, 2726. [CrossRef]

72. Coulibaly, T.P.; Du, J.; Diakité, D. Sustainable agricultural practices adoption. *Agriculture* **2021**, *67*, 166–176. [CrossRef]
73. Landers, J.N.; de Freitas, P.L.; de Oliveira, M.C.; da Silva Neto, S.P.; Ralisch, R.; Kueneman, E.A. Next steps for conservation agriculture. *Agronomy* **2021**, *11*, 2496. [CrossRef]
74. Owusu Danquah, E.; Danquah, F.O.; Frimpong, F.; Dankwa, K.O.; Weebadde, C.K.; Ennin, S.A.; Asanta, M.O.O.; Brempong, M.B.; Dwamena, H.A.; Addo-Danso, A.; et al. Sustainable intensification and climate-smart yam production for improved food security in West Africa: A review. *Front. Agron.* **2022**, *4*, 858114. [CrossRef]
75. Chauhan, U.; Sharma, D.; Saleem, S.; Kumar, M.; Singh, S.P. Artificial intelligence-based sustainable agricultural practices. In *Artificial Intelligence Applications in Agriculture and Food Quality Improvement*; Khan, M.A., Khan, R., Praveen, P., Eds.; IGI Global: Hershey, PA, USA, 2022. [CrossRef]
76. Kumari, I.; Hussain, R.; Sharma, S.; Geetika; Ahmed, M. Microbial biopesticides for sustainable agricultural practices. *Biopesticides* **2022**, *2*, 301–317. [CrossRef]
77. Saikanth, D.R.K.; Supriya; Singh, B.V.; Rai, A.K.; Bana, S.R.; Singh, B. Advancing Sustainable Agriculture: A Comprehensive Review for Optimizing Food Production and Environmental Conservation. *Int. J. Plant Soil Sci.* **2023**, *35*, 417–425. [CrossRef]
78. Saliu, F.; Luqman, M.; AlKhaza'leh, H. A Review on the Impact of Sustainable Agriculture Practices on Crop Yields and Soil Health. *Int. J. Res. Adv. Agric. Sci.* **2023**, *2*, 1–13.
79. Chang, S.H.E.; Benjamin, E.O.; Sauer, J. Factors influencing the adoption of sustainable agricultural practices for rice cultivation in Southeast Asia: A review. *Agron. Sustain. Dev.* **2024**, *44*, 27. [CrossRef]
80. El Jarroudi, M.; Kouadio, L.; Delfosse, P.; Bock, C.H.; Mahlein, A.K.; Fettweis, X.; Mercatoris, B.; Adams, F.; Lenné, J.M.; Hamdioui, S. Leveraging edge artificial intelligence for sustainable agriculture. *Nat. Sustain.* **2024**, *7*, 846–854. [CrossRef]
81. Konstantinos, C.; Charoula, D.; Grigorios, E.; Michail, T.; Vangelis, T. Factors shaping innovative behavior: A meta-analysis of technology adoption studies in agriculture. *Can. J. Agric. Econ.* **2024**. [CrossRef]
82. Fernández-Castilla, B.; Said-Metwaly, S.; Kreitchmann, R.S.; Van Den Noortgate, W. Guidelines and the SEMI checklist for facilitating cumulative knowledge. *Behav. Res.* **2024**, *56*, 3315–3329. [CrossRef] [PubMed]
83. Siebrecht, N. Sustainable Agriculture and Its Implementation Gap—Overcoming Obstacles to Implementation. *Sustainability* **2020**, *12*, 3853. [CrossRef]
84. Lianu, C.; Simion, V.-E.; Urdes, L.; Bucea-Manea-Ţoniş, R.; Radulescu, I.G.; Lianu, C. Agroecological Approaches in the Context of Innovation Hubs. *Sustainability* **2023**, *15*, 4335. [CrossRef]
85. Shankland, A. Practising agroecology for sustainable diets and healthy communities. In *Routledge Handbook of Sustainable Diets*; Kevany, K., Prosperi, P., Eds.; Routledge: London, UK, 2022; pp. 69–79. [CrossRef]
86. Niggli, U.; Sonnevelt, M.; Kummer, S. Pathways to Advance Agroecology for a Successful Transformation to Sustainable Food Systems. In *Science and Innovations for Food Systems Transformation*; von Braun, J., Afsana, K., Fresco, L.O., Hassan, M.H.A., Eds.; Springer: Cham, Switzerland, 2023. [CrossRef]
87. Palomo-Campesino, S.; García-Llorente, M.; Hevia, V.; Boeraeve, F.; Dendoncker, N.; González, J.A. Do agroecological practices enhance the supply of ecosystem services? A comparison between agroecological and conventional horticultural farms. *Ecosyst. Serv.* **2022**, *57*, 101474. [CrossRef]
88. Lacombe, C.; Couix, N.; Hazard, L. Designing agroecological farming systems with farmers: A review. *Agric. Syst.* **2018**, *165*, 208–220. [CrossRef]
89. Namirembe, S.; Wezi, M.; Njoroge, R.; Tchuwa, F.; Wellard, K.; Coe, R. Grounding a global tool—Principles and practice for agroecological assessments inspired by TAPE. *Elementa* **2022**, *10*, 00022. [CrossRef]
90. Mottet, A.; Bicksler, A.; Lucantoni, D.; de Rosa, F.; Scherf, B.; Scopel, E.; Lopez-Ridaura, S.; Gemmil-Herren, B.; Kerr, R.B.; Sourisseau, J.-M.; et al. Assessing Transitions to Sustainable Agricultural and Food Systems: A Tool for Agroecology Performance Evaluation (TAPE). *Front. Sustain. Food Syst.* **2020**, *4*, 579154. [CrossRef]
91. Milheiras, S.G.; Sallu, S.M.; Loveridge, R.; Nnyiti, P.; Mwanga, L.; Baraka, E.; Lala, M.; Moore, E.; Shirima, D.D.; Kioko, E.N.; et al. Agroecological practices increase farmers' well-being in an agricultural growth corridor in Tanzania. *Agron. Sustain. Dev.* **2022**, *42*, 56. [CrossRef] [PubMed]
92. Pereira, P.; Bogunović, I.; Inácio, M.; Zhao, W.; Barcelo, D. Agriculture intensification impacts on soil and water ecosystem services. In Proceedings of the EGU General Assembly 2023, EGU23-1423, Vienna, Austria, 24–28 April 2023. [CrossRef]
93. Haldar, N.; Pearlin, R. Sustainable and Climate Smart Agriculture for Food Security: A Review. *J. Exp. Agric. Int.* **2023**, *45*, 229–239. [CrossRef]
94. Niu, K.; Yuan, Y.; Zhang, J.; Wang, F.; Liu, Y.; Fang, X.; Cheng, H. Design Optimization and Performance Evaluation of a Tillage Depth Precision Measurement System. In Proceedings of the Computer and Computing Technologies in Agriculture X: 10th IFIP WG 5.14 International Conference, CCTA 2016, Dongying, China, 19–21 October 2016; Li, D., Ed.; Springer: Cham, Switzerland, 2016. [CrossRef]
95. Paruelo, J.M. The Challenge of Making the Idea of Sustainable Intensification Operational. *Agrociencia* **2019**, *23*, e140. [CrossRef]

96. Minikayev, R.V.; Gulia, S.; Saifiyeva; Irina, G.; Manukova. Optimization of the main tillage in the grey forest rotation of the Predkamye region of the Republic of Tatarstan. *BIO Web Conf.* **2020**, *17*, 00066. [CrossRef]
97. Schiefer, J.; Lair, G.J.; Mueller, L.; Blum, W.E.H. Evaluation of Framework Conditions and Soil Potentials for Sustainable Intensification of Agriculture. In *Exploring and Optimizing Agricultural Landscapes. Innovations in Landscape Research*; Mueller, L., Sychev, V.G., Dronin, N.M., Eulenstein, F., Eds.; Springer: Cham, Switzerland, 2021. [CrossRef]
98. Fayose, C.A. Efficient Management of Environmental Resources through Sustainable Crop Production Intensification. In *Sustainable Management of Natural Resources*; Suratman, M.N., Ariff, E.A.R.E., Gandaseca, S., Eds.; IntechOpen: London, UK, 2022. [CrossRef]
99. Samuel, A.; Dines, L.; Finch, S.; Lane, G.P. (Eds.) *Lockhart and Wiseman's Crop Husbandry Including Grassland*, 10th ed.; Woodhead Publishing: Cambridge, UK, 2022.
100. Sowmya, K.; Bindhu, J.S.; Shalini Pillai, P. Agro-ecological Sustainability with Pulses under System of Crop Intensification: A Review. *Agric. Rev.* **2022**, *44*, 385–388. [CrossRef]
101. Joseph, J.; Tramberend, S.; Gonzalez, D.L.; Fischer, G.; Kahil, T. Modeling Sustainable Intensification of Agriculture under Resource Constraints. In Proceedings of the EGU General Assembly 2023, EGU23-6817, Vienna, Austria, 24–28 April 2023. [CrossRef]
102. Yeomans, J.S. Water resource management using stochastic multicriteria population-based algorithms for producing alternatives. *J. Earth Environ. Sci.* **2019**, *3*, 1–10.
103. Shrestha, J.; Subedi, S.; Prasad Timsina, K.; Subedi, S.; Pandey, M.; Shrestha, A.; Shrestha, S.; Anwar Hossain, M. Sustainable Intensification in Agriculture: An Approach for Making Agriculture Greener and Productive. *J. Nepal Agric. Res. Counc.* **2021**, *17*, 133–150. [CrossRef]
104. Zeinalie, M.; Bozorg-Haddad, O.; Azamathulla, H.M. Optimization in Water Resources Management. In *Essential Tools for Water Resources Analysis, Planning, and Management. Springer Water*; Bozorg-Haddad, O., Ed.; Springer: Singapore, 2021. [CrossRef]
105. Bajpai, M.; Mishra, S.; Gaur, S.; Ohri, A.; Piégay, H.; Graillot, D. Optimization of Groundwater Pumping and River-Aquifer Exchanges for Management of Water Resources. *Water Resour. Manag.* **2022**, *36*, 1863–1878. [CrossRef]
106. Bhardwaj, R.; Garg, S. Multi-Objective Optimization in Water Resource Management. In *Modeling and Simulation of Environmental Systems*; Maurya, S.P., Yadav, A.K., Singh, R., Eds.; CRC Press: Boca Raton, FL, USA, 2022; pp. 65–82. [CrossRef]
107. Bhavya, R.L.; Elango, L. Ant-Inspired Metaheuristic Algorithms for Combinatorial Optimization Problems in Water Resources Management. *Water* **2023**, *15*, 1712. [CrossRef]
108. Patil, D.; Kar, S.; Gupta, R. An efficient urban water management practice based on optimum LPCD estimated using the MLR-GA optimization approach—A case study for Jaipur, Rajasthan (India). In Proceedings of the 2023 IEEE Conference on Technologies for Sustainability (SusTech), Portland, OR, USA, 19–22 April 2023; pp. 275–279. [CrossRef]
109. Wang, H.; Wanakule, N.; Asefa, T.; Erkyihun, S.; Basdekas, L.; Hayslett, R. Application of Multiobjective Optimization to Provide Operational Guidance for Allocating Supply among Multiple Sources. *J. Water Resour. Plan. Manag.* **2023**, *149*, 04023004. [CrossRef]
110. Zull, A.F.; Owens, J.; Bourgault, M.; Johnson, B.; Peck, G.N.; Christodoulou, N. Mixed farming diversification may be costly: Southern Queensland case study. *Crop Pasture Sci.* **2017**, *68*, 378–389. [CrossRef]
111. Ismail, H.M.; Al-Sadek, A.F.; Ashmawy, A.A.; Khalil, M.A.I.; Elsayed, M. Computational model to improve dairy animal feeding under mixed farming system (crops/livestock) as study case. *Arab. Univ. J. Agric. Sci.* **2018**, *26*, 1053–1064. [CrossRef]
112. Moraine, M.; Fuselier, M.; Moerman, M. Pathways of sustainability in organic mixed livestock farms are based on local embeddedness: Case studies in France and Belgium. In *Organic Animal Husbandry Systems–Challenges, Performance and Potentials: Proceedings of the IAHA Video-Conference on Organic Animal Husbandry 111, Bonn, Germany, 21–22 September 2020*; Schmid, O., Johnson, M., Vaarst, M., Früh, B., Eds.; Animal Husbandry Alliance of International Federation of Organic Agriculture Movements: Frick, Switzerland, 2020.
113. Mugnier, S.; Husson, C.; Cournut, S. Why and how farmers manage mixed cattle–sheep farming systems and cope with economic, climatic and workforce-related hazards. *Renew. Agric. Food Syst.* **2021**, *36*, 344–352. [CrossRef]
114. Fanchone, A.; Alexandre, G.; Hostiou, N. Work organization as a barrier to crop–livestock integration practices: A case study in Guadeloupe. *Agron. Sustain. Dev.* **2022**, *42*, 54. [CrossRef]
115. Pédèches, R.; Aubron, C.; Philippon, O.; Bainville, S. An Ecological Reading of Crop–Livestock Interactions—Gers, Southwestern France, 1950 to the Present. *Sustainability* **2023**, *15*, 10234. [CrossRef]
116. Hedley, C. The role of precision agriculture for improved nutrient management on farms. *J. Sci. Food Agric.* **2015**, *95*, 12–19. [CrossRef]
117. Whattoff, D.; Mouazen, A.; Waine, T. A multi sensor data fusion approach for creating variable depth tillage zones. *Adv. Anim. Biosci.* **2017**, *8*, 461–465. [CrossRef]
118. Ahmad, L.; Mahdi, S.S. Feasibility and Evaluation of Precision Farming. In *Satellite Farming*; Ahmad, L., Mahdi, S.S., Eds.; Springer: Cham, Switzerland, 2018. [CrossRef]

119. Monteiro, A.; Santos, S.; Gonçalves, P. Precision agriculture for crop and livestock farming—Brief review. *Animals* **2021**, *11*, 2345. [CrossRef]
120. Dwivedi, N.; Kumar, D.; Suryavanshi, P. Precision farming techniques for sustainable weed management. *Emergent Life Sci. Res.* **2022**, *8*, 142–149. [CrossRef]
121. Mohanty, S.; Singh, D. Optimal Resource Utilization In precision agriculture. In Proceedings of the 2022 2nd International Conference on Advance Computing and Innovative Technologies in Engineering (ICACITE), Greater Noida, India, 28–29 April 2022; pp. 1608–1612. [CrossRef]
122. Punithavathi, R.; Rani, A.D.C.; Sughashini, K.R.; Kurangi, C.; Nirmala, M.; Ahmed, H.F.T.; Balamurugan, S.P. Computer Vision and Deep Learning-enabled Weed Detection Model for Precision Agriculture. *Comput. Syst. Sci. Eng.* **2023**, *44*, 2759–2774. [CrossRef]
123. Weddell, B.J. Precision Agriculture. *Int. J. Comput. Algorithm* **2023**, *12*, 4. [CrossRef]
124. Sales da Silva, I.G.; Gomes de Almeida, F.C.; Padilha da Rocha e Silva, N.M.; Casazza, A.A.; Converti, A.; Asfora Sarubbo, L. Soil bioremediation: Overview of technologies and trends. *Energies* **2020**, *13*, 4664. [CrossRef]
125. Sharma, I. Bioremediation techniques for polluted environment: Concept, advantages, limitations, and prospects. In *Trace Metals in the Environment-New Approaches and Recent Advances*; Murillo-Tovar, M.A., Saldarriaga-Noreña, H., Saeid, A., Eds.; IntechOpen Ltd.: London, UK, 2020. [CrossRef]
126. Gu, J.D. On environmental biotechnology of bioremediation. *Appl. Environ. Biotechnol.* **2021**, *5*, 3–8. [CrossRef]
127. Kour, D.; Kaur, T.; Devi, R.; Yadav, A.; Singh, M.; Joshi, D.; Singh, J.; Suyal, D.C.; Kumar, A.; Rajput, V.D.; et al. Beneficial microbiomes for bioremediation of diverse contaminated environments for environmental sustainability: Present status and future challenges. *Environ. Sci. Pollut. Res.* **2021**, *28*, 24917–24939. [CrossRef] [PubMed]
128. Ahmed, F.J. Microbial Biotechnology and Bioremediation. *Futur. Biotechnol.* **2022**, *2*, 1. [CrossRef]
129. Bala, S.; Garg, D.; Thirumalesh, B.V.; Sharma, M.; Sridhar, K.; Inbaraj, B.S.; Tripathi, M. Recent strategies for bioremediation of emerging pollutants: A review for a green and sustainable environment. *Toxics* **2022**, *10*, 484. [CrossRef]
130. Patel, A.K.; Singhania, R.R.; Albarico, F.P.J.B.; Pandey, A.; Chen, C.W.; Dong, C.D. Organic wastes bioremediation and its changing prospects. *Sci. Total Environ.* **2022**, *824*, 153889. [CrossRef]
131. Ayilara, M.S.; Babalola, O.O. Bioremediation of environmental wastes: The role of microorganisms. *Front. Agron.* **2023**, *5*, 1183691. [CrossRef]
132. Singal, N.; Kaur, S. Bioremediation: Sustainable Approach for Pollution Control. *Asian J. Environ. Ecol.* **2023**, *20*, 1–18. [CrossRef]
133. Wróbel, M.; Śliwakowski, W.; Kowalczyk, P.; Kramkowski, K.; Dobrzyński, J. Bioremediation of Heavy Metals by the Genus Bacillus. *Int. J. Environ. Res. Public Health* **2023**, *20*, 4964. [CrossRef]
134. Tóth, C.; Simon, L.; Tóth, B. Microanatomical Properties of Energy Willow (*Salix* spp.) Leaves after Exposure to Potentially Toxic Elements from Wastewater Solids and Wood Ash. *Agronomy* **2024**, *14*, 1625. [CrossRef]
135. Riyaz, S.U.M.; Kathiravan, K. Integrated Pest Management Approaches. In *Geminiviruses*; Kumar, R., Ed.; Springer: Cham, Switzerland, 2019. [CrossRef]
136. Karlsson Green, K.; Stenberg, J.A.; Lankinen, Å. Making sense of Integrated Pest Management (IPM) in the light of evolution. *Evol. Appl.* **2020**, *13*, 1791–1805. [CrossRef] [PubMed]
137. Jack, C.J.; Ellis, J.D. Integrated Pest Management Control of Varroa destructor (Acari: Varroidae), the Most Damaging Pest of (*Apis mellifera* L. (Hymenoptera: Apidae)) Colonies. *J. Insect Sci.* **2021**, *21*, 6. [CrossRef]
138. Binks, R.H. Practical applications of integrated pest management in horticultural cultivation: The cases of protected tomato and outdoor Brassica production. In *Improving Integrated Pest Management in Horticulture*; Collier, R., Ed.; Burleigh Dodds Science Publishing: Cambridge, UK, 2022; pp. 387–420. [CrossRef]
139. Matthews, G. The Need for Integrated Pest Management (IPM). *Outlooks Pest Manag.* **2022**, *33*, 174–176. [CrossRef]
140. Ghabeish, I.H.; Al-Zyoud, F.A.; Mamkagh, A.M.; Al-Nawaiseh, R.A. Sustainable Control Measures Towards Integrated Pest Management of the Cereal Leafminer *Syringopais temperatella* Led. (Lep.; Scythrididae): Tillage System as Cultural Control Method. *Rev. Colomb. Entomol.* **2023**, *49*, e11487. [CrossRef]
141. Borase, D.N.; Nath, C.P.; Hazra, K.K.; Senthilkumar, M.; Singh, S.S.; Praharaj, C.S.; Singh, U.; Kumar, N. Long-term impact of diversified crop rotations and nutrient management practices on soil microbial functions and soil enzymes activity. *Ecol. Indic.* **2020**, *114*, 106322. [CrossRef]
142. Selim, M.M. Introduction to the integrated nutrient management strategies and their contribution to yield and soil properties. *Int. J. Agron.* **2020**, *2020*, 2821678. [CrossRef]
143. Zhang, X.; Davidson, E.A.; Zou, T.; Lassaletta, L.; Quan, Z.; Li, T.; Zhang, W. Quantifying nutrient budgets for sustainable nutrient management. *Glob. Biogeochem. Cycles* **2020**, *34*, e2018GB006060. [CrossRef]
144. Caporali, F. Sustainable Agriculture Through Ecological Intensification. In *Ethics and Sustainable Agriculture*; Springer: Cham, Switzerland, 2021. [CrossRef]

145. Paramesh, V.; Mohan Kumar, R.; Rajanna, G.A.; Gowda, S.; Nath, A.J.; Madival, Y.; Jinger, D.; Bhat, S.; Toraskar, S. Integrated nutrient management for improving crop yields, soil properties, and reducing greenhouse gas emissions. *Front. Sustain. Food Syst.* **2023**, *7*, 1173258. [CrossRef]
146. Puneeth Raj, M.S.; Narender; Pavitra, B.V. Review on Effect of Integrated Nutrient Management on Seed Yield and Quality of Pulses. *Int. J. Plant Soil Sci.* **2023**, *35*, 404–409. [CrossRef]
147. Sarkar, P.; David, A.; Thomas, T.; Reddy, I.S. Integrated Nutrient Management in Green Gram (*Vigna radiata* L.) for Enhancing Soil Health. *Int. J. Environ. Clim.* **2023**, *13*, 815–819. [CrossRef]
148. Shafi, U.; Mumtaz, R.; Mahmood, Z.; Muhammad, M.D.M.; Khanp, R.U.; Tanveer, S.I.H.K. Assessment of Wheat Productivity Enhancement by Integrated Nutrient Management (INM) using Remote Sensing. In Proceedings of the 2023 International Conference on Machine Intelligence for GeoAnalytics and Remote Sensing (MIGARS), Hyderabad, India, 27–29 January 2023; pp. 1–4. [CrossRef]
149. Awe, G.O.; Reichert, J.M.; Fontanela, E. Sugarcane production in the subtropics: Seasonal changes in soil properties and crop yield in no-tillage, inverting and minimum tillage. *Soil Tillage Res.* **2020**, *196*, 104447. [CrossRef]
150. Castellini, M.; Vonella, A.V.; Ventrella, D.; Rinaldi, M.; Baiamonte, G. Determining soil hydraulic properties using infiltrometer techniques: An assessment of temporal variability in a long-term experiment under minimum-and no-tillage soil management. *Sustainability* **2020**, *12*, 5019. [CrossRef]
151. Peixoto, D.S.; da Silva, L.D.C.M.; de Melo, L.B.B.; Azevedo, R.P.; Araújo, B.C.L.; de Carvalho, T.S.; Moreira, S.G.; Silva, B.M. Occasional tillage in no-tillage systems: A global meta-analysis. *Sci. Total Environ.* **2020**, *745*, 140887. [CrossRef] [PubMed]
152. Jiang, S.; Wang, Q.; Zhong, G.; Tong, Z.; Wang, X.; Xu, J. Brief Review of Minimum or No-Till Seeders in China. *AgriEngineering* **2021**, *3*, 605–621. [CrossRef]
153. Smith, C.; Chalk, P.M. Carbon ($\delta^{13}C$) dynamics in agroecosystems under traditional and minimum tillage systems: A review. *Soil Res.* **2021**, *59*, 661–672. [CrossRef]
154. Williams, J.D.; Wuest, S.B. Minimum tillage and no-tillage winter wheat–summer fallow for low precipitation regions. *J. Soil Water Conserv.* **2021**, *76*, 246–255. [CrossRef]
155. Xu, H. Effect of No-Tillage Management on Soil Organic Matter and Net Greenhouse Gas Fluxes in a Rice-Oilseed Rape Cropping System. *Agriculture* **2022**, *12*, 918. [CrossRef]
156. Yemadje, P.L.; Takpa, O.; Amonmidé, I.; Balarabe, O.; Sêkloka, E.; Guibert, H.; Tittonell, P. Limited yield penalties in an early transition to conservation agriculture in cotton-based cropping systems of Benin. *Front. Sustain. Food Syst.* **2022**, *6*, 1041399. [CrossRef]
157. Blanco-Canqui, H.; Shaver, T.M.; Lindquist, J.L.; Shapiro, C.A.; Elmore, R.W.; Francis, C.A.; Hergert, G.W. Cover crops and ecosystem services: Insights from studies in temperate soils. *Agron. J.* **2015**, *107*, 2449–2474. [CrossRef]
158. Wittwer, R.; Dorn, B.; Jossi, W.; van der Heijden, M.G.A. Cover crops support ecological intensification of arable cropping systems. *Sci. Rep.* **2017**, *7*, 41911. [CrossRef] [PubMed]
159. Adetunji, A.T.; Ncube, B.; Mulidzi, R.; Lewu, F.B. Management impact and benefit of cover crops on soil quality: A review. *Soil Tillage Res.* **2020**, *204*, 104717. [CrossRef]
160. Quintarelli, V.; Radicetti, E.; Allevato, E.; Stazi, S.R.; Haider, G.; Abideen, Z.; Bibi, S.; Jamal, A.; Mancinelli, R. Cover Crops for Sustainable Cropping Systems: A Review. *Agriculture* **2022**, *12*, 2076. [CrossRef]
161. Ingram, M. Building cover crop expertise with citizen science in the upper Midwest: Supporting farmer innovation in a time of change. *Front. Sustain. Food Syst.* **2023**, *7*, 1045769. [CrossRef]
162. Trueman, C.L.; Awrey, J.C.; Delaporte, A.; Kerr, J.; Weersink, A.; Van Eerd, L.L. Long-term cover cropping suppresses foliar and fruit disease in processing tomatoes. *Plant Dis.* **2023**, *107*, 2160–2168. [CrossRef] [PubMed]
163. Zhang, H.; Ghahramani, A.; Aram, A.; Erbacher, A. Cover cropping impacts on soil water and carbon in dryland cropping system. *PLoS ONE* **2023**, *18*, e0286748. [CrossRef]
164. Dasgupta, D.; Ries, M.; Walter, K.; Zitnick-Anderson, K.; Camuy-Vélez, L.A.; Gasch, C.; Banerjee, S. Cover cropping reduces the negative effect of salinity on soil microbiomes. *J. Sustain. Agric. Environ.* **2023**, *2*, 140–152. [CrossRef]
165. Szogi, A.A.; Vanotti, M.B.; Ro, K.S. Methods for treatment of animal manures to reduce nutrient pollution prior to soil application. *Curr. Pollut. Rep.* **2015**, *1*, 47–56. [CrossRef]
166. Bergfeldt, B.; Tomasi Morgano, M.; Leibold, H.; Richter, F.; Stapf, D. Recovery of Phosphorus and other Nutrients during Pyrolysis of Chicken Manure. *Agriculture* **2018**, *8*, 187. [CrossRef]
167. Tullo, E.; Finzi, A.; Guarino, M. Environmental impact of livestock farming and Precision Livestock Farming as a mitigation strategy. *Sci. Total Environ.* **2019**, *650*, 2751–2760. [CrossRef]
168. Spiegal, S.; Kleinman, P.J.; Endale, D.M.; Bryant, R.B.; Dell, C.; Goslee, S.; Meinen, R.J.; Colton Flynn, K.; Baker, J.M.; Browning, D.M.; et al. Manuresheds: Advancing nutrient recycling in US agriculture. *Agric. Syst.* **2020**, *182*, 102813. [CrossRef]
169. Hidalgo, D.; Corona, F.; Martín-Marroquín, J.M. Nutrient recycling: From waste to crop. *Biomass Convers. Biorefinery* **2021**, *11*, 207–217. [CrossRef]

170. González-García, I.; Oliveira, V.; Molinuevo-Salces, B.; García-González, M.C.; Dias-Ferreira, C.; Riaño, B. Two-phase nutrient recovery from livestock wastewaters combining novel membrane technologies. *Biomass Convers. Biorefinery* **2022**, *12*, 4563–4574. [CrossRef]
171. Ajibade, S.; Simon, B.; Gulyás, M.; Balint, C. Sustainable intensification of agriculture as a tool to promote food security: A bibliometric analysis. *Front. Sustain. Food Syst.* **2023**, *7*, 1101528. [CrossRef]
172. Jain, M.; Barrett, C.B.; Solomon, D.; Ghezzi-Kopel, K. Surveying the Evidence on Sustainable Intensification Strategies for Smallholder Agricultural Systems. *Annu. Rev. Environ. Resour.* **2023**, *48*, 347–369. [CrossRef]
173. Buerkert, A.; Schlecht, E. Toward sustainable intensification of agriculture in sub-Saharan Africa. *Front. Agric. Sci. Eng.* **2020**, *7*, 401–405. [CrossRef]
174. Van Campenhout, B.; Bizimungu, E. Risk and returns of sustainable crop intensification: The case of smallholder rice and potato farmers in Uganda. *Dev. Policy Rev.* **2018**, *36*, 605–633. [CrossRef]
175. Ratnadass, A. Crop Protection for Agricultural Intensification Systems in Sub-Saharan Africa. In *Sustainable Agriculture Reviews*; Lichtfouse, E., Ed.; Springer: Cham, Switzerland, 2020; Volume 39. [CrossRef]
176. Kassie, M.; Teklewold, H.; Jaleta, M.; Marenya, P.; Erenstein, O. Understanding the adoption of a portfolio of sustainable intensification practices in eastern and southern Africa. *Land Use Policy* **2015**, *42*, 400–411. [CrossRef]
177. Alfyorov, O.; Grynchenko, O.; Ponomarenko, V.; Shchur, T.; Tomporowski, A.; Kruszelnicka, W.; Walichnowska, P. Agricultural Equipment Design Optimization Based on the Inversion Method. *Agriculture* **2022**, *12*, 1410. [CrossRef]
178. Okoko, P.; Nwabueze, O.D. Performance optimization of draft and power requirement for some tillage implements in a loamy soil: A response surface approach. *Poljopr. Teh.* **2023**, *48*, 79–86. [CrossRef]
179. Veselovska, N.; Burlaka, S.A. Methods and techniques combination working bodies of complex soil processing machines. *Vìsnik Hmel′nic′kogo Nacìonal′nogo Unìversitetu* **2023**, *217*, 42–47. [CrossRef]
180. Nie, S.; Huang, C.Z.; Huang, W.W.; Liu, J. A Non-Deterministic Integrated Optimization Model with Risk Measure for Identifying Water Resources Management Strategy. *J. Environ. Inf.* **2021**, *38*, 41–55. [CrossRef]
181. Wang, G.; Kumar, S.; Huang, Z.; Liu, R. Water resource management and policy evaluation in Middle Eastern countries: Achieving sustainable development goal 6. *Desalination Water Treat.* **2024**, *320*, 100829. [CrossRef]
182. Ryschawy, J.; Moraine, M.; Péquignot, M.; Martin, G. Trade-offs among individual and collective performances related to crop–livestock integration among farms: A case study in southwestern France. *Org. Agric.* **2019**, *9*, 399–416. [CrossRef]
183. Puech, T.; Stark, F. Diversification of an integrated crop-livestock system: Agroecological and food production assessment at farm scale. *Agric. Ecosyst. Environ.* **2023**, *344*, 108300. [CrossRef]
184. Trivelli, L.; Apicella, A.; Chiarello, F.; Rana, R.; Fantoni, G.; Tarabella, A. From precision agriculture to Industry 4.0: Unveiling technological connections in the agrifood sector. *Br. Food J.* **2019**, *121*, 1730–1743. [CrossRef]
185. Javaid, M.; Haleem, A.; Singh, R.P.; Suman, R. Enhancing smart farming through the applications of Agriculture 4.0 technologies. *Int. J. Intell. Netw.* **2022**, *3*, 150–164. [CrossRef]
186. Hundal, G.S.; Laux, C.M.; Buckmaster, D.; Sutton, M.J.; Langemeier, M. Exploring barriers to the adoption of internet of things-based precision agriculture practices. *Agriculture* **2023**, *13*, 163. [CrossRef]
187. Nandy, S.; Andraskar, J.; Lanjewar, K.; Kapley, A. Challenges in bioremediation: From lab to land. In *Bioremediation for Environmental Sustainability. Toxicity, Mechanisms of Contaminants Degradation, Detoxification, and Challenges*; Saxena, G., Kumar, V., Shah, M.P., Eds.; Elsevier: Amsterdam, The Netherlands, 2021; pp. 561–583. [CrossRef]
188. Vishwakarma, G.S.; Bhattacharjee, G.; Gohil, N.; Singh, V. Current status, challenges and future of bioremediation. In *Bioremediation of Pollutants. From Genetic Engineering to Genome Engineering*; Pandey, V.C., Singh, V., Eds.; Elsevier: Amsterdam, The Netherlands, 2020; pp. 403–415. [CrossRef]
189. Rehan, M.; Alsohim, A.S. Bioremediation of Heavy Metals. In *Environmental Chemistry and Recent Pollution Control Approaches*; Saldarriaga-Noreña, H., Murillo-Tovar, M.A., Farooq, R., Dongre, R., Riaz, S., Eds.; IntechOpen Ltd.: London, UK, 2019. [CrossRef]
190. Rodovalho Gonçalves, C.; da Silva Delabona, P. Strategies for bioremediation of pesticides: Challenges and perspectives of the Brazilian scenario for global application—A review. *Environ. Adv.* **2024**, *8*, 100220. [CrossRef]
191. EU. Commission Communication in the Framework of the Implementation of Directive 2009/128/EC of the European Parliament and of the Council of 21 October 2009 Establishing a Framework for Community Action to Achieve the Sustainable Use of Pesticides. 2009. Available online: https://eur-lex.europa.eu/legal-content/EN/TXT/?uri=CELEX:52015XC0612(03) (accessed on 16 June 2024).
192. EC. Using Less Chemical Pesticides: European Commission Publishes Toolbox of Good Practices. 2023. Available online: https://agriculture.ec.europa.eu/news/using-less-chemical-pesticides-european-commission-publishes-toolbox-good-practices-2023-02-28_en (accessed on 16 June 2024).
193. Tufa, T. Role of Integrated Nutrient Management on Nutrient Uptake, Soil Physicochemical Properties and Maize Yield Improvement: Review. *J. Biol. Agric. Healthc.* **2019**, *9*, 14–21. [CrossRef]

194. Sharma, S.; Verma, K.; Hardaha, P. Implementation of Artificial Intelligence in Agriculture. *J. Comput. Cogn. Eng.* **2022**, *2*, 155–162. [CrossRef]
195. Paramesh, V.; Kumar, P.; Bhagat, T.; Nath, A.J.; Manohara, K.K.; Das, B.; Desai, B.F.; Jha, P.K.; Prasad, P.V.V. Integrated Nutrient Management Enhances Yield, Improves Soil Quality, and Conserves Energy under the Lowland Rice–Rice Cropping System. *Agronomy* **2023**, *13*, 1557. [CrossRef]
196. Randhawa, M.K.; Dhaliwal, S.S.; Sharma, V.; Toor, A.S.; Sharma, S.; Kaur, M. Impact of Integrated Nutrient Management on Transformations of Micronutrients and Uptake by Wheat Crop in North-western India. *J. Soil Sci. Plant Nutr.* **2021**, *21*, 2932–2945. [CrossRef]
197. Kumar, S.; Sagwal, D.P.; Garhwal, R.S.; Kumar, A.; Gill, A.; Sharma, J.C. Efficacy of integrated nutrient management on soil properties and wheat yield. *Int. J. Agric. Sci.* **2022**, *18*, 888–892. [CrossRef]
198. Ali, A.; Niu, G.; Masabni, J.; Ferrante, A.; Cocetta, G. Integrated Nutrient Management of Fruits, Vegetables, and Crops through the Use of Biostimulants, Soilless Cultivation, and Traditional and Modern Approaches—A Mini Review. *Agriculture* **2024**, *14*, 1330. [CrossRef]
199. Azadi, H.; Moghaddam, S.M.; Burkart, S.; Mahmoudi, H.; Van Passel, S.; Kurban, A.; Lopez-Carr, D. Rethinking resilient agriculture: From climate-smart agriculture to vulnerable-smart agriculture. *J. Clean. Prod.* **2021**, *319*, 128602. [CrossRef]
200. Johnson, D.; Almaraz, M.; Rudnick, J.; Parker, L.E.; Ostoja, S.M.; Khalsa, S.D.S. Farmer Adoption of Climate-Smart Practices Is Driven by Farm Characteristics, Information Sources, and Practice Benefits and Challenges. *Sustainability* **2023**, *15*, 8083. [CrossRef]
201. Adesipo, A.; Fadeyi, O.; Kuca, K.; Krejcar, O.; Maresova, P.; Selamat, A.; Adenola, M. Smart and climate-smart agricultural trends as core aspects of smart village functions. *Sensors* **2020**, *20*, 5977. [CrossRef]
202. Adam, B.; Abdulai, A. Minimum tillage as climate-smart agriculture practice and its impact on food and nutrition security. *PLoS ONE* **2023**, *18*, e0287441. [CrossRef] [PubMed]
203. Moore, E.B. Challenges and Opportunities for Cover Crop Mediated Soil Water Use Efficiency Enhancements in Temperate Rain-Fed Cropping Systems: A Review. *Land* **2023**, *12*, 988. [CrossRef]
204. Rodrigues, M.A.; Raimundo, S.; Arrobas, M. Cover Cropping in Rainfed Fruticulture. *World J. Agric. Soil Sci.* **2019**, *1*, 1–3. [CrossRef]
205. Tadesse, S.T.; Oenema, O.; van Beek, C.; Ocho, F.L. Manure recycling from urban livestock farms for closing the urban–rural nutrient loops. *Nutr. Cycl. Agroecosyst.* **2021**, *119*, 51–67. [CrossRef]
206. Lam, K.L.; Zlatanović, L.; van der Hoek, J.P. Life cycle assessment of nutrient recycling from wastewater: A critical review. *Water Res.* **2020**, *173*, 115519. [CrossRef]
207. Semalulu, O.; Kibaya, P.; Kyebogola, S.; Mworozi, E.; Sewankambo, N.; Gebru, B. Enhancing Farmer Resilience through Profitable and Farmer-Acceptable Climate Smart Technologies and Practices. In *Research Highlights in Agricultural Sciences*; Elkhalifa, A.E.O., Ed.; B P International: Kolkata, India, 2023; Volume 9, pp. 1–32. [CrossRef]
208. Das, S.; Ray, M.K.; Panday, D.; Mishra, P. Role of biotechnology in creating sustainable agriculture. *PLoS Sustain. Transform.* **2023**, *2*, e0000069. [CrossRef]
209. Krishna Kumar, R.; Senthamizhkumaran, V.R.; Alagendran, S.; Chitra, M.; Ramesh Kumar, K.; Tyagi, T.; Tyagi, A. Advances in Agricultural Biotechnology: Enhancing Productivity and Sustainability in India: A Review. *J. Sci. Res. Rep.* **2024**, *30*, 366–383. [CrossRef]
210. Ma, Q.P. Biotechnology: Recent Developments, Emerging Trends, and Implications for Business. In *Research Anthology on Bioinformatics, Genomics, and Computational Biology*; IGI Global Scientific Publishing: Hershey, PA, USA, 2024; pp. 335–355. [CrossRef]
211. Gupta, V.; Sengupta, M.; Prakash, J.; Tripathy, B.C. Plant Biotechnology and Agriculture. In *Basic and Applied Aspects of Biotechnology*; Springer: Singapore, 2017; pp. 415–452. [CrossRef]
212. Khan, F.F.; Ahmad, K.; Ahmed, A.; Haider, S. Applications of biotechnology in agriculture—Review article. *World J. Biol. Biotechnol.* **2017**, *2*, 139–142. [CrossRef]
213. Van Eenennaam, A.L.; De Figueiredo Silva, F.; Trott, J.F.; Zilberman, D. Genetic engineering of livestock: The opportunity cost of regulatory delay. *Annu. Rev. Anim. Biosci.* **2021**, *9*, 453–478. [CrossRef] [PubMed]
214. Begna, T. Genetic engineering for enhancement of crop productivity. *Int. J. Res. Agron.* **2022**, *5*, 29–34. [CrossRef]
215. Ghorbani-Asl, M. Impact of Genetic Engineering on Agriculture Applications. *Recent Res. Rev. J.* **2022**, *1*, 38–49. [CrossRef]
216. Magray, J.A.; Zargar, S.A.; Islam, T. Use of Metabolic Engineering/Biotechnology in Crops Breeding and Development of New Crops. In *Metabolic Engineering in Plants*; Aftab, T., Hakeem, K.R., Eds.; Springer: Singapore, 2022; pp. 301–319. [CrossRef]
217. Petersen, B. Editorial: Genetic engineering in farm animals. *Front. Genet.* **2023**, *14*, 1155201. [CrossRef]
218. Kwon, D.H.; Gim, G.M.; Yum, S.Y.; Jang, G.O. Current Status and Future of Gene Engineering in Livestock. *J. Biochem. Mol. Toxicol.* **2024**, *57*, 50–59. [CrossRef] [PubMed]

219. Yogi, L.N.; Kathayat, A.; Bhandari, S.R.; Paudel, P.; Mishra, P.K. An overview on the impact of genetically engineered organisms on crop yield and safety. *Arch. Agric. Environ. Sci.* **2024**, *9*, 175–179. [CrossRef]
220. Yang, H.; Jian, J.; Li, X.; Renshaw, D.; Clements, J.; Sweetingham, M.; Tan, C.; Li, C. Application of whole genome re-sequencing data in the development of diagnostic DNA markers tightly linked to a disease-resistance locus for marker-assisted selection in lupin (*Lupinus angustifolius*). *BMC Genom.* **2015**, *16*, 660. [CrossRef] [PubMed]
221. Bonnecarrere, V.; Rosas, J.; Ferraro, B. Economic impact of marker-assisted selection and rapid generation advance on breeding programs. *Euphytica* **2019**, *215*, 197. [CrossRef]
222. Shimizu, T.; Kaçar, Y.A.; Cristofani-Yaly, M.; Curtolo, M.; Machado, M.A. Markers, Maps, and Marker-Assisted Selection. In *The Citrus Genome. Compendium of Plant Genomes*; Gentile, A., La Malfa, S., Deng, Z., Eds.; Springer: Cham, Switzerland, 2020. [CrossRef]
223. Hasan, N.; Choudhary, S.; Naaz, N.; Sharma, N.; Laskar, R.A. Recent advancements in molecular marker-assisted selection and applications in plant breeding programmes. *J. Genet. Eng. Biotechnol.* **2021**, *19*, 128. [CrossRef]
224. Kumari, M.; Dubey, A.; Kumar, R.; Kumar, A. Marker-assisted selection in plant breeding for stress tolerance. In *Improving Stress Resilience in Plants*; Abass Ahanger, M., Ahmad, P., Bhat, J.A., John, R., Eds.; Academic Press: Cambridge, MA, USA, 2024; pp. 371–387. [CrossRef]
225. Ng, T.J. Use of Tissue Culture for Micropropagation of Vegetable Crops. In *Tissue Culture as a Plant Production System for Horticultural Crops, Proceedings of the Conference on Tissue Culture as a Plant Production System for Horticultural Crops, Beltsville, MD, USA, 20–23 October 1985*; Zimmerman, R.H., Griesbach, R.J., Hammerschlag, F.A., Lawson, R.H., Eds.; Springer: Dordrecht, The Netherlands, 1986; Volume 2, p. 2. [CrossRef]
226. Pant, M.; Husen, A. In vitro micrografting to induce juvenility and improvement of rooting. In *Environmental, Physiological and Chemical Controls of Adventitious Rooting in Cuttings*; Husen, A., Ed.; Academic Press, Elsevier Inc.: Cambridge, MA, USA, 2022; pp. 439–453. [CrossRef]
227. Chaudhari, V.M. Tissue Culture: Aeon of Micro Propagation in Vegetable Crops. *Int. J. Environ. Clim.* **2023**, *13*, 1989–1999. [CrossRef]
228. Guerra, F.; Cautín, R.; Castro, M. In Vitro Micropropagation of the Vulnerable Chilean Endemic *Alstroemeria pelegrina* L. *Horticulturae* **2024**, *10*, 674. [CrossRef]
229. Van Emon, J.M. The Omics Revolution in Agricultural Research. *J. Agric. Food Chem.* **2016**, *64*, 36–44. [CrossRef]
230. Dai, X.; Shen, L. Advances and Trends in Omics Technology Development. *Front. Med.* **2022**, *9*, 911861. [CrossRef]
231. Debener, T. State of the art of omics technologies in horticultural crops. In *Omics in Horticultural Crops*; Rout, G.R., Peter, K.V., Eds.; Academic Press, Elsevier Inc.: Cambridge, MA, USA, 2022; pp. 1–14. [CrossRef]
232. Kumar, P.; Singh, J.; Kaur, G.; Adunola, P.M.; Biswas, A.; Bazzer, S.; Kaur, H.; Kaur, I.; Kaur, H.; Sandhu, K.S.; et al. OMICS in Fodder Crops: Applications, Challenges, and Prospects. *Curr. Issues Mol. Biol.* **2022**, *44*, 5440–5473. [CrossRef]
233. Bai, L.; Zhang, Z.; Peng, X.; Gao, Z.; Zhao, Y.; Liang, K. Application of omics technology in the storage and transportation of agricultural products. *Front. Sustain. Food Syst.* **2023**, *7*, 1249199. [CrossRef]
234. Shachak, A.; Shuval, K.; Fine, S. Barriers and enablers to the acceptance of bioinformatics tools: A qualitative study. *J. Med. Libr. Assoc.* **2007**, *95*, 454–458. [CrossRef]
235. Xue, J.; Zhao, S.; Liang, Y.; Hou, C.; Wang, J. Bioinformatics and its Applications in Agriculture. In *Computer and Computing Technologies in Agriculture, Volume II: First IFIP TC 12 International Conference on Computer and Computing Technologies in Agriculture (CCTA 2007), Wuyishan, China, 18–20 August 2007*; Li, D., Ed.; Springer: Boston, MA, USA, 2008; Volume 259. [CrossRef]
236. Singh, V.K.; Singh, A.K.; Chand, R.; Kushwaha, C. Role of bioinformatics in agriculture and sustainable development. *Int. J. Bioinform. Res. Appl.* **2011**, *3*, 221–226.
237. Tan, Y.C.; Kumar, A.U.; Wong, Y.P.; Ling, A.P.K. Bioinformatics approaches and applications in plant biotechnology. *J. Genet. Eng. Biotechnol.* **2022**, *20*, 106. [CrossRef]
238. Drew, J.; Morgan, W.; Galindo, S.; Kleinschmit, A.J.; McWilliams, M.; Pauley, M.; Triplett, E.W.; Williams, J.; Murdoch, B.; Rosenwald, A. Revisiting barriers to implementation of bioinformatics into life sciences education. *Front. Educ.* **2023**, *8*, 1317191. [CrossRef]
239. Keating, B.A.; Carberry, P.S.; Bindraban, P.S.; Asseng, S.; Meinke, H.; Dixon, J. Eco-efficient Agriculture: Concepts, Challenges, and Opportunities. *Crop Sci.* **2010**, *50*, 109–119. [CrossRef]
240. Zhao, R.; Liu, Y.; Zhang, Z.; Guo, S.; Tseng, M.L.; Wu, K.J. Enhancing Eco-Efficiency of Agro-Products' Closed-Loop Supply Chain under the Belt and Road Initiatives: A System Dynamics Approach. *Sustainability* **2018**, *10*, 668. [CrossRef]
241. Giles, J.; Grosjean, G.; Le Coq, J.F.; Huber, B.; Bui, V.L.; Läderach, P. Barriers to Implementing Climate Policies in Agriculture: A Case Study from Viet Nam. *Front. Sustain. Food Syst.* **2021**, *5*, 439881. [CrossRef]
242. Zeng, J.; Han, J.; Qu, J.; Maraseni, T.N.; Xu, L.; Li, H.; Liu, L. Ecoefficiency of China's agricultural sector: What are the spatiotemporal characteristics and how are they determined? *J. Clean. Prod.* **2021**, *325*, 129346. [CrossRef]
243. Wang, G.; Shi, R.; Mi, L.; Hu, J. Agricultural Eco-Efficiency: Challenges and Progress. *Sustainability* **2022**, *14*, 1051. [CrossRef]

244. Yang, B.; Zhang, Z.; Wu, H. Detection and attribution of changes in agricultural eco-efficiency within rapid urbanized areas: A case study in the Urban agglomeration in the middle Reaches of Yangtze River, China. *Ecol. Indic.* **2022**, *144*, 109533. [CrossRef]
245. Talaviya, T.; Shah, D.; Patel, N.; Yagnik, H.; Shah, M. Implementation of artificial intelligence in agriculture for optimisation of irrigation and application of pesticides and herbicides. *Artif. Intell. Agric.* **2020**, *4*, 58–73. [CrossRef]
246. Zha, J. Artificial Intelligence in Agriculture. *J. Phys. Conf. Ser.* **2020**, *1693*, 012058. [CrossRef]
247. Indira, P.; Arafat, I.S.; Karthikeyan, R.; Selvarajan, S.; Balachandran, P.K. Fabrication and investigation of agricultural monitoring system with IoT & AI. *SN Appl. Sci.* **2023**, *5*, 322. [CrossRef]
248. Mendoza, Q.A.; Pordesimo, L.; Neilsen, M.; Armstrong, P.; Campbell, J.; Mendoza, P.T. Application of Machine Learning for Insect Monitoring in Grain Facilities. *AI* **2023**, *4*, 348–360. [CrossRef]
249. Oliveira, R.C.d.; Silva, R.D.d.S.e. Artificial Intelligence in Agriculture: Benefits, Challenges, and Trends. *Appl. Sci.* **2023**, *13*, 7405. [CrossRef]
250. Restrepo-Arias, J.F.; Branch-Bedoya, J.W.; Awad, G. Image classification on smart agriculture platforms: Systematic literature review. *Artif. Intell. Agric.* **2024**, *13*, 1–17. [CrossRef]
251. van der Merwe, D.; Burchfield, D.R.; Witt, T.D.; Price, K.P.; Sharda, A. Drones in agriculture. *Adv. Agron.* **2020**, *162*, 1–30. [CrossRef]
252. Ahmad, A.; Ordoñez, J.; Cartujo, P.; Martos, V. Remotely Piloted Aircraft (RPA) in Agriculture: A Pursuit of Sustainability. *Agronomy* **2021**, *11*, 7. [CrossRef]
253. Rejeb, A.; Abdollahi, A.; Rejeb, K.; Treiblmaier, H. Drones in agriculture: A review and bibliometric analysis. *Comput. Electron. Agric.* **2022**, *198*, 107017. [CrossRef]
254. Chin, R.; Catal, C.; Kassahun, A. Plant disease detection using drones in precision agriculture. *Precis. Agric.* **2023**, *24*, 1663–1682. [CrossRef]
255. Hafeez, A.; Husain, M.A.; Singh, S.P.; Chauhan, A.; Khan, M.T.; Kumar, N.; Chauhan, A.; Soni, S.K. Implementation of drone technology for farm monitoring & pesticide spraying: A review. *Inf. Process. Agric.* **2023**, *10*, 192–203. [CrossRef]
256. Lawrence, I.D.; Agnishwar, J.; Vijayakumar, R. Drone technology in agriculture for surveillance and inspection. *Eur. Chem. Bull.* **2023**, *12*, 1253–1263. [CrossRef]
257. Subramanian, K.S.; Pazhanivelan, S.; Srinivasan, G.; Santhi, R.; Sathiah, N. Drones in Insect Pest Management. *Front. Agron.* **2021**, *3*, 640885. [CrossRef]
258. Borikar, G.P.; Gharat, C.; Deshmukh, S.R. Application of Drone Systems for Spraying Pesticides in Advanced Agriculture: A Review. *IOP Conf. Ser. Mater. Sci. Eng.* **2022**, *1259*, 012015. [CrossRef]
259. Lopes, L.d.L.; Cunha, J.P.A.R.d.; Nomelini, Q.S.S. Use of Unmanned Aerial Vehicle for Pesticide Application in Soybean Crop. *AgriEngineering* **2023**, *5*, 2049–2063. [CrossRef]
260. Das, A.; Kadawla, K.; Nath, H.; Chakraborty, S.; Ali, H.; Singh, S.; Dubey, V.K. Drone-Based Intelligent Spraying of Pesticides: Current Challenges and Its Future Prospects. In *Applications of Computer Vision and Drone Technology in Agriculture 4.0*; Chouhan, S.S., Singh, U.P., Jain, S., Eds.; Springer: Singapore, 2024. [CrossRef]
261. Brown, M.E. Satellite Remote Sensing in Agriculture and Food Security Assessment. *Procedia Environ. Sci.* **2015**, *29*, 307. [CrossRef]
262. Weiss, M.; Jacob, F.; Duveiller, G. Remote sensing for agricultural applications: A meta-review. *Remote Sens. Environ.* **2020**, *236*, 111402. [CrossRef]
263. Johri, P.; Singh, J.N.; Khatri, S.K.; Bagchi, A.; Rajesh, E. Role of Satellites in Agriculture. In *Smart IoT for Research and Industry. EAI/Springer Innovations in Communication and Computing*; Moh, M., Sharma, K.P., Agrawal, R., Garcia Diaz, V., Eds.; Springer: Cham, Switzerland, 2022. [CrossRef]
264. Fakhar, M.; Khalid, M.N. Satellites to agricultural fields: The role of remote sensing in precision agriculture. *Biol. Agric. Sci. Res. J.* **2023**, *2*, 14. [CrossRef]
265. Dainelli, R.; Saracco, F. Bibliometric and Social Network Analysis on the Use of Satellite Imagery in Agriculture: An Entropy-Based Approach. *Agronomy* **2023**, *13*, 576. [CrossRef]
266. Yule, I.; Pullanagari, R. Optical Sensors to Assist Agricultural Crop and Pasture Management. In *Smart Sensing Technology for Agriculture and Environmental Monitoring*; Lecture Notes in Electrical Engineering; Mukhopadhyay, S., Ed.; Springer: Berlin/Heidelberg, Germany, 2012; Volume 146. [CrossRef]
267. Nogueira-Martins, R.; de Carvalho Pinto, F.A.D.; de Moura, A.D.; da Cunha Siqueira, W.; de Melo Villar, F.M. Economic feasibility of optical sensors for variable rate nitrogen fertilization in corn. *Idesia* **2022**, *40*, 2022. [CrossRef]
268. Umapathi, R.; Park, B.; Sonwal, S.; Rani, G.M.; Cho, Y.; Huh, Y.S. Advances in optical-sensing strategies for the on-site detection of pesticides in agricultural foods. *Trends Food Sci. Technol.* **2022**, *119*, 69–89. [CrossRef]
269. Lin, J.; Wang, M.; Zhang, M.; Zhang, Y.; Chen, L. Electrochemical Sensors for Soil Nutrient Detection: Opportunity and Challenge. In *Computer and Computing Technologies in Agriculture, Volume II: First IFIP TC 12 International Conference on Computer and Computing Technologies in Agriculture (CCTA 2007), Wuyishan, China, 18–20 August 2007*; Springer: Boston, MA, USA, 2008; Volume 259. [CrossRef]

270. Chugh, B.; Thakur, S.; Singh, A.K.; Joany, R.M.; Rajendran, S.; Nguyen, T.A. Electrochemical sensors for agricultural application. In *Nanosensors for Smart Agriculture*; Denizli, A., Nguyen, T.A., Rajendran, S., Yasin, G., Nadda, A.K., Eds.; Elsevier Inc.: Amsterdam, The Netherlands, 2022. [CrossRef]
271. Kim, M.Y.; Lee, K.H. Electrochemical Sensors for Sustainable Precision Agriculture—A Review. *Front. Chem.* **2022**, *10*, 848320. [CrossRef] [PubMed]
272. Rajak, P.; Ganguly, A.; Adhikary, S.; Bhattacharya, S. Internet of Things and smart sensors in agriculture: Scopes and challenges. *J. Agric. Food Res.* **2023**, *14*, 100776. [CrossRef]
273. Soussi, A.; Zero, E.; Sacile, R.; Trinchero, D.; Fossa, M. Smart Sensors and Smart Data for Precision Agriculture: A Review. *Sensors* **2024**, *24*, 2647. [CrossRef] [PubMed]
274. Nelson, S.O. Dielectric spectroscopy in agriculture. *J. Non-Cryst. Solids* **2005**, *351*, 2940–2944. [CrossRef]
275. Jones, S.B.; Sheng, W.; Or, D. Dielectric Measurement of Agricultural Grain Moisture—Theory and Applications. *Sensors* **2022**, *22*, 2083. [CrossRef]
276. Abdulraheem, M.I.; Chen, H.; Li, L.; Moshood, A.Y.; Zhang, W.; Xiong, Y.; Zhang, Y.; Taiwo, L.B.; Farooque, A.A.; Hu, J. Recent Advances in Dielectric Properties-Based Soil Water Content Measurements. *Remote Sens.* **2024**, *16*, 1328. [CrossRef]
277. Mane, S.; Das, N.; Singh, G.; Cosh, M.; Dong, Y. Advancements in dielectric soil moisture sensor Calibration: A comprehensive review of methods and techniques. *Comput. Electron. Agric.* **2024**, *218*, 108686. [CrossRef]
278. Botero-Valencia, J.S.; Mejia-Herrera, M.; Pearce, J.M. Low cost climate station for smart agriculture applications with photovoltaic energy and wireless communication. *HardwareX* **2022**, *11*, e00296. [CrossRef] [PubMed]
279. Xu, J.; Gu, B.; Tian, G. Review of agricultural IoT technology. *Artif. Intell. Agric.* **2022**, *6*, 10–22. [CrossRef]
280. García-Ramos, F.J.; Vidal, M.; Boné, A.; Malón, H.; Aguirre, J. Analysis of the Air Flow Generated by an Air-Assisted Sprayer Equipped with Two Axial Fans Using a 3D Sonic Anemometer. *Sensors* **2012**, *12*, 7598–7613. [CrossRef]
281. Ma, Z.; Shen, D. Flexible flow sensors-enabled intelligent life. *J. Micromech. Microeng.* **2024**, *34*, 073001. [CrossRef]
282. Agyekum, T.P.; Antwi-Agyei, P.; Dougill, A.J. The contribution of weather forecast information to agriculture, water, and energy sectors in East and West Africa: A systematic review. *Front. Environ. Sci.* **2022**, *10*, 935696. [CrossRef]
283. Pujahari, R.M.; Yadav, S.P.; Khan, R. Intelligent farming system through weather forecast support and crop production. In *Application of Machine Learning in Agriculture*; Khan, M.A., Khan, R., Ansari, A., Eds.; Academic Press, Elsevier Inc.: Cambridge, MA, USA, 2022. [CrossRef]
284. Purohit, S.K.; Panigrahi, S.; Sethy, P.K.; Behera, S.K. Time Series Forecasting of Price of Agricultural Products Using Hybrid Methods. *Appl. Artif. Intell.* **2021**, *35*, 1388–1406. [CrossRef]
285. Sun, F.; Meng, X.; Zhang, Y.; Wang, Y.; Jiang, H.; Liu, P. Agricultural Product Price Forecasting Methods: A Review. *Agriculture* **2023**, *13*, 1671. [CrossRef]
286. Mohamed-Amine, N.; Abdellatif, M.; Belaid, B. Artificial intelligence for forecasting sales of agricultural products: A case study of a moroccan agricultural company. *J. Open Innov. Technol. Mark. Complex.* **2024**, *10*, 100189. [CrossRef]
287. Kephe, P.N.; Ayisi, K.K.; Petja, B.M. Challenges and opportunities in crop simulation modelling under seasonal and projected climate change scenarios for crop production in South Africa. *Agric. Food Secur.* **2021**, *10*, 10. [CrossRef]
288. da Silveira, F.; da Silva, S.L.C.; Machado, F.M.; Barnedo, J.G.A.; Amaral, F.G. Farmers' perception of the barriers that hinder the implementation of agriculture 4.0. *Agric. Syst.* **2023**, *208*, 103656. [CrossRef]
289. Timlin, D.; Paff, K.; Han, E. The role of crop simulation modeling in assessing potential climate change impacts. *Agrosystems Geosci. Environ.* **2024**, *7*, e20453. [CrossRef]
290. Osinga, S.A.; Paudel, D.; Mouzakitis, S.A.; Athanasiadis, I.N. Big data in agriculture: Between opportunity and solution. *Agric. Syst.* **2022**, *195*, 103298. [CrossRef]
291. Perçin, S. Identifying barriers to big data analytics adoption in circular agri-food supply chains: A case study in Turkey. *Environ. Sci. Pollut. Res.* **2023**, *30*, 52304–52320. [CrossRef]
292. Sullivan, C.S.; Gamtou, M.; Anastasiou, E.; Fountas, S. Building trust: A systematic review of the drivers and barriers of agricultural data sharing. *Smart Agric. Technol.* **2024**, *8*, 100477. [CrossRef]
293. Yao, L.; Li, L.; Zhang, M.; Minzan, L. Automatic Guidance of Agricultural Vehicles Based on Global Positioning System. In *Artificial Intelligence Applications and Innovations: IFIP TC12 WG12. 5-Second IFIP Conference on Artificial Intelligence Applications and Innovations (AIAI2005), Beijing, China, 7–9 September 2005*; Li, D., Wang, B., Eds.; Springer: Boston, MA, USA, 2005; Volume 187. [CrossRef]
294. Roshanianfard, A.; Noguchi, N.; Okamoto, H.; Ishii, K. A review of autonomous agricultural vehicles (The experience of Hokkaido University). *J. Terramechanics* **2020**, *91*, 155–183. [CrossRef]
295. Kamon, S.; di Maria, E.; Giannoccaro, N.I.; Ishii, K. A New Reconfigurable Agricultural Vehicle Controlled by a User Graphical Interface: Mechanical and Electronic Aspects. *Machines* **2023**, *11*, 795. [CrossRef]
296. Puppala, H.; Peddinti, P.R.T.; Tamvada, J.P.; Ahuja, J.; Kim, B. Barriers to the adoption of new technologies in rural areas: The case of unmanned aerial vehicles for precision agriculture in India. *Technol. Soc.* **2023**, *74*, 102335. [CrossRef]

297. Fraceto, L.F.; Grillo, R.; de Medeiros, G.A.; Scognamiglio, V.; Rea, G.; Bartolucci, C. Nanotechnology in Agriculture: Which Innovation Potential Does It Have? *Front. Environ. Sci.* **2016**, *4*, 20. [CrossRef]
298. Usman, M.; Farooq, M.; Wakeel, A.; Nawaz, A.; Cheema, S.A.; ur Rehman, H.; Ashraf, I.; Sanaullah, M. Nanotechnology in agriculture: Current status, challenges and future opportunities. *Sci. Total Environ.* **2020**, *721*, 137778. [CrossRef] [PubMed]
299. Taran, M.; Safaei, M.; Karimi, N.; Almasi, A. Benefits and Application of Nanotechnology in Environmental Science: An Overview. *Biointerface Res. Appl. Chem.* **2021**, *11*, 7860–7870. [CrossRef]
300. Saritha, G.N.G.; Anju, T.; Kumar, A. Nanotechnology—Big impact: How nanotechnology is changing the future of agriculture? *J. Agric. Food Res.* **2022**, *10*, 100457. [CrossRef]
301. Shukla, K.; Mishra, V.; Singh, J.; Varshney, V.; Verma, R.; Srivastava, S. Nanotechnology in sustainable agriculture: A double-edged sword. *J. Sci. Food Agric.* **2024**, *104*, 5675–5688. [CrossRef]
302. Zolkin, A.L.; Matvienko, E.V.; Shavanov, M.V. Innovative technologies in agricultural crops breeding and seed farming. *IOP Conf. Ser. Earth Environ. Sci.* **2021**, *677*, 022092. [CrossRef]
303. Buckseth, T.; Tiwari, J.K.; Singh, R.K.; Kumar, V.; Sharma, A.K.; Dalamu, D.; Bhardwaj, V.; Sood, S.; Kumar, M.; Sadawarti, M.; et al. Advances in innovative seed potato production systems in India. *Front. Agron.* **2022**, *4*, 956667. [CrossRef]
304. Moumni, M.; Brodal, G.; Romanazzi, G. Recent innovative seed treatment methods in the management of seedborne pathogens. *Food Secur.* **2023**, *15*, 1365–1382. [CrossRef]
305. Wu, H.; Song, Y.; Yu, L.; Ge, Y. Uncertainty aversion and farmers' innovative seed adoption: Evidence from a field experiment in rural China. *J. Integr. Agric.* **2023**, *22*, 1928–1944. [CrossRef]
306. Ukhurebor, K.E.; Aidonojie, P.A. The influence of climate change on food innovation technology: Review on topical developments and legal framework. *Agric. Food Secur.* **2021**, *10*, 50. [CrossRef]
307. Hussain, M.A.; Bekhit, A.E.A. Innovative Foods: The Future Food Supply, Nutrition and Health. *Foods* **2023**, *12*, 1359. [CrossRef] [PubMed]
308. Wang, N.; Shah, K.A.M. The impact of ecological innovation on the food production quality: Mediating role of environmental awareness. *Ekon. Istraz.* **2023**, *36*, 2163682. [CrossRef]
309. Smyth, S.Y.; Kerr, W.A.; Gray, R. Regulatory barriers to international scientific innovation: Approving new biotechnology in North America. *Can. Foreign Policy J.* **2017**, *23*, 134–145. [CrossRef]
310. Dahabieh, M.S.; Bröring, S.; Maine, E. Overcoming barriers to innovation in food and agricultural biotechnology. *Trends Food Sci. Technol.* **2018**, *79*, 204–213. [CrossRef]
311. Valieva, O.V. Pharmaceuticals and biotechnology: Institutional barriers in the context of the world pandemic. *Interexpo GEO-Sib.* **2020**, *3*, 44–52. [CrossRef]
312. Eze, F. Marker-assisted Selection in Fish: A Review. *Asian J. Fish. Aquat. Res.* **2019**, *3*, 1–11. [CrossRef]
313. Malakar, M.; Beruto, M.; Barba-Gonzalez, R. Biotechnological approaches to overcome hybridization barriers and use of micropropagation tool for further improvement in *Heliconia*: A review. *Plant Cell Tissue Organ Cult.* **2022**, *149*, 503–522. [CrossRef]
314. Ying, W. Phenomic Studies on Diseases: Potential and Challenges. *Phenomics* **2023**, *3*, 285–299. [CrossRef] [PubMed]
315. Desaire, H.; Go, E.P.; Hua, D. Advances, obstacles, and opportunities for machine learning in proteomics. *Cell Rep. Phys. Sci.* **2022**, *3*, 101069. [CrossRef] [PubMed]
316. Gardezi, M.; Joshi, B.; Rizzo, D.M.; Ryan, M.; Prutzer, E.; Brugler, S.; Dadkhah, A. Artificial intelligence in farming: Challenges and opportunities for building trust. *Agron. J.* **2024**, *116*, 1217–1228. [CrossRef]
317. Guido, Z.; Lopus, S.; Waldman, K.; Hannah, C.; Zimmer, A.; Krell, N.; Knudson, C.; Estes, L.; Caylor, K.; Evans, T. Perceived links between climate change and weather forecast accuracy: New barriers to tools for agricultural decision-making. *Clim. Change* **2021**, *168*, 9. [CrossRef]
318. Matthews, R.B.; Rivington, M.; Muhammed, S.; Newton, A.C.; Hallett, P.D. Adapting crops and cropping systems to future climates to ensure food security: The role of crop modelling. *Glob. Food Secur.* **2013**, *2*, 24–28. [CrossRef]
319. Weersink, A.; Fraser, E.; Pannell, D.; Duncan, E.; Rotz, S. Opportunities and challenges for big data in agricultural and environmental analysis. *Annu. Rev. Resour. Econ.* **2018**, *10*, 19–37. [CrossRef]
320. Garg, S.; Rumjit, N.P.; Roy, S. Smart agriculture and nanotechnology: Technology, challenges, and new perspective. *Adv. Agrochem.* **2024**, *3*, 115–125. [CrossRef]
321. Kolur, S.M.; Burud, A.; Ramasamy, M.; Sampath, V.; Chellem, S.R.; Satapathy, S.N.; Rout, A. A review on biotech innovations in seed technology for robust crop production. *J. Adv. Biol. Biotechnol.* **2024**, *27*, 535–550. [CrossRef]
322. Kilimova, L.; Nishnianidze, O.; Cherkashin, M.; Pykhtin, A. Problems of regional management of innovative food industry development. *BIO Web Conf.* **2021**, *32*, 03018. [CrossRef]

Disclaimer/Publisher's Note: The statements, opinions and data contained in all publications are solely those of the individual author(s) and contributor(s) and not of MDPI and/or the editor(s). MDPI and/or the editor(s) disclaim responsibility for any injury to people or property resulting from any ideas, methods, instructions or products referred to in the content.

agronomy

MDPI

Article

Effects of GroMore® Program on Rice Yield and GHG Emissions in a Korean Paddy Rice

Sung Yung Yoo [1], Jun-Ki Son [2], Kyoung-Sik Jun [3] and Hyun-Hwoi Ku [4,5,*]

[1] Institute of Ecological Phytochemistry, Hankyong National University, 327 Chungang-ro, Anseong City 17579, Gyeonggi, Republic of Korea; lsn136@hknu.ac.kr
[2] Syngenta Korea Jincheon Station, CP Development Korea, 330-11 Chogeum-ro, Deoksan-eup, Jincheon-gun 27855, Chungcheongbuk-do, Republic of Korea; junki.son@syngenta.com
[3] Syngenta Korea Seoul Office, CP Marketing Korea, 47 Jong-ro, Jongno-gu, Seoul 03160, Republic of Korea; kyoungsik.jun@syngenta.com
[4] Department of Plant Resources and Landscape Architecture, Hankyong National University, 327 Chungang-ro, Anseong City 17579, Gyeonggi, Republic of Korea
[5] Soil Environment Research Institute, Hankyong National University, 327 Chungang-ro, Anseong City 17579, Gyeonggi, Republic of Korea
* Correspondence: seanku@hknu.ac.kr

Abstract: The agronomic benefits of pesticides combined with amino acid application to increase rice production have been recognized, but they are still not well-known for greenhouse gas (GHG) emissions and mitigation in irrigated paddy fields. Thus, this study was conducted to investigate the combined effects of pesticide and amino acid application on rice yield and methane (CH_4) emissions in a Korean rice paddy. A field experiment was conducted with five levels: none (no pesticide application, T1), different conventional practices (combined application of insecticides and fungicide, T2 and T3), and GroMore® programs (combined application of insecticides, fungicides, and amino acids, T4 and T5). Rice grain yield and yield components were obtained using agronomic measurements. To determine the greenhouse gas intensity (GHGI) of each treatment, CH_4 emissions were measured throughout the rice growing period. Results showed that the chemical applications in combination with amino acids in T4 obtained a higher grain yield and number of panicles per plant compared to T1, T2, and T3, while T4 and T5 showed no difference on filled spikelets except for T2. T3 and T5 showed lower respective cumulative CH_4 emissions by 30% and 32% during the entire rice growing season, compared to no chemical application (T1). Meanwhile, N_2O emissions were negligible in all treatments because the paddy field was flooded most of the growing season. The results of the impact of GroMore® programs on relatively higher grain yield and lower GHG emissions are presented. In conclusion, the application of pesticides combined with amino acids obtained lower GHGI values.

Keywords: insecticides; fungicides; amino acids; rice productivity; methane emission

1. Introduction

In agricultural fields, rice cultivation practices, such as the application of chemical fertilizers, pesticides, tillage, amendment of organic material, flooding paddy fields, etc., contribute approximately 10% of global man-made methane (CH_4) and nitrous oxide (N_2O), a potent GHG [1–4]. Meanwhile, sustaining rice productivity is most important in meeting the increasing demand for food security since increasing greenhouse gas (GHG) emissions worldwide have been attributed to global warming and climate change, which has affected drought, flood, and extreme temperatures that devastate crops. Recent agricultural practices face different challenges, such as sustaining crop productivity and increasing pathogen and pest attacks in relation to fluctuating climatic factors [5,6]. Crop pests especially influence super threats to global agricultural production [7].

Large amounts of agrochemicals such as herbicides, insecticides, fungicides, and plant growth regulators in terms of pesticides are used to control weeds, pests, and pathogens in agricultural fields. In Korea, the total use of agricultural pesticides amounted to 19,882 tons in 2022 [8]. Frequently, the application of pesticides leads to chemical residue accumulation in intensive agriculture, causing contamination of water and soil and killing off useful or harmful organisms, and throwing off the ecological balance of the agroecosystem [9–13]. There are benefits of pesticide usage on agricultural productivity and possible negative effects on health and the environment. Tremendous benefits such as improving crop productivity, protection of crop losses (yield reduction), and disease control have been derived from the use of pesticides in agriculture [14–16]. There are potential benefits of pesticides: controlling diseases and weeds and vectors of crop disease and organisms (human and livestock) disease and preventing harmful organisms that influence human activities [17]. Particularly, pests reduce agricultural income in most developing countries since farm and postharvest losses contribute to hunger and malnutrition. According to the United Nations Children's Fund (UNICEF), malnutrition is "largely a silent and invisible emergency, exacting a terrible toll on children and their families" [18]. Although, the credits of pesticides include enhanced economic benefits such as increased production of food and fiber, and amelioration of vector-borne diseases, their negative effects have resulted in critical health implications to man and his environment such as pesticide contamination and degradation of soil, water, and other vegetation in addition to possible negative effects on organisms (birds, fish, beneficial insects, non-target plants, etc.) [19].

The use of agrochemicals can effectively suppress the growth of weeds and the threat of insects, and thus improve crop growth, yet influence GHG emissions directly or indirectly [1,20,21]. Much research on the influence of agrochemicals used in croplands is focused on the mode of action, efficacy, resistance of plants, nitrogen-use efficiency, and therefore higher crop production [10,19,22–26]. Research attempted on foliar spray plant growth regulators to increase rice yield reported that amino acids absorbed from the leaves increase the mineral nutrients content of the grain and improve its quality [27]. Foliar spray of amino acids (with the recommended dose of fertilizers for plant growth) on rice leaves rapidly absorbs and assimilates them, increasing the number of leaves, leaf area index (LAI), crop growth rate (CGR), total chlorophyll content, and yield [28,29]. When the nitrogen content of rice leaves increases, a great deal of N is invested in Rubisco protein, the primary CO_2 fixation enzyme [30], and the CO_2 conductivity of mesophyll cells is improved [31], which increases photosynthesis.

Currently, only a few studies on the impact of agrochemical application on GHG emissions in agriculture have been reported. Gianessi (2013) [32] reported that herbicide application to manage weeds reduced GHG emissions by saving the fuel consumption of traditional farming machinery. Jiang et al., (2015) [33] reported that the application of herbicides reduced N_2O emissions in winter wheat fields and CH_4 and N_2O fluxes in irrigated rice paddy fields. While another study reported that the combination of two herbicides (Bensulfuron-methyl and Pretilachlor) increased the emissions of N_2O and CH_4 [34]. The use of pesticides plays an important role in increasing crop production, but its impact on GHG emissions and mitigation in irrigated paddy fields is not well-known. Additionally, there have been no research reports on the effect of synthetic agrochemical and amino acid applications on rice production and GHG emissions.

Agriculture is directly impacted by climate change and extreme weather, which alters the dynamics of pest occurrence, the length of the rainy season, the amount of rainfall, the timing and course of typhoons, and the amount of sunlight. These changes have an impact on agricultural production both directly and indirectly. In terms of pest management and prevention, granular insecticides have a 30- to 60-day pest control efficacy, whereas Syngenta Korea's GroMore® program, which combines insecticides, fungicides, and amino acids, has a 100-day pest control efficacy. The fungicides, insecticides, and amino acids in the drenching speed up the early growth of rice, prolonging the tillering period, increasing the number of panicles, and further increasing rice yield. This enables the number of foliar

sprays to be reduced from two times to one during the heading stage. Since its introduction in the Korean market in 2016, the GroMore® program has been implemented all over the country, covering an area of almost 20,000 hectares as of 2024. It has been acknowledged for its effectiveness and is recommended as a local government subsidy program. Therefore, the purpose of this study was to look into how the use of GroMore® programs affected rice yield and greenhouse gas emissions.

2. Materials and Methods

2.1. Field Experiment

A field experiment was conducted at a local rice paddy field in Pyeongtaek-si, Gyeonggi province, Korea (26°58′ N, 127°10′ E) from May to October 2023. The climatic condition is characterized by an annual average air temperature of 13.2 °C, radiation of 13.1 MJ m^{-2}, and cumulative precipitation of 1356.5 mm (Figure 1), where the average air temperature in the area ranges from around 10 to 16 °C of the average annual temperature in Korea. The experiment field belongs to a relatively humid region, having a significantly similar amount of precipitation to the average in Korea. Precipitation is mostly concentrated in the summer season. During the rice growing season, the average air temperature, radiation, and cumulative precipitation were 22.4 °C, 16.2 MJ m^{-2}, and 1094 mm, respectively.

Soil type for the experiment is classified as Alisols [35]. Soils are used mainly for paddy rice. The soil physico-chemical properties are shown in Table 1. It is loam, 0 to 1% slopes, drained, and permeable. Based on the local field and climate conditions in the region, the experiment was set up in a completely randomized block design, consisting of five plots with three replications. The treatments for each plot (300 m^2, 6 × 50 m) is shown in Table 2. To prevent mixing chemicals from water between the treatment areas, polyvinyl chloride (PVC) with 200 mm in height was installed in between plots.

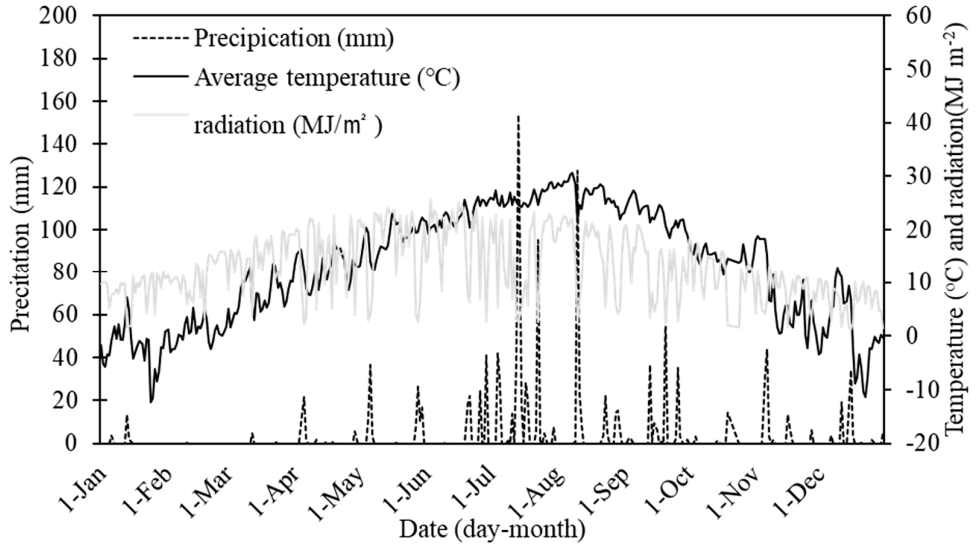


Figure 1. The mean of the average air temperature and radiation and amount of rainfall observed at the regional climate station of Pyeongtaek-si (climate datasets available from National Institute of Agricultural Sciences for agricultural climatic information [36].

Table 1. Soil chemical properties of the rice paddy field.

Soil Texture	pH	O.M [1]	Av. P_2O_5	Av. SiO_2	K^+	Ca^{2+}	Mg^{2+}
	(1:5)	(g kg^{-1})	(mg kg^{-1})	(mg kg^{-1})	($cmol_c$ kg^{-1})		
Loam	6.5	13.3	23	173.7	0.5	4.4	1.5

[1] organic matter.

Table 2. Specific chemical sources, purpose, and the recommended rate in the treatments.

Treatment	Chemicals	Purpose	Recommended Rate (g, mL ha^{-1})
T1	-	-	-
T2	Fipronil	Insecticide	10,000
	Orysastrobin	Fungicide	10,000
T3	Clothianidin	Insecticide	10,000
	Thifluzamide	Fungicide	10,000
	Tiadinil		10,000
T4	Cyantraniliprole	Insecticide	800
	Pymetrozine		800
	Clothianidin		2000
	Orysastrobin	Fungicide	2000
	Amino acid (water soluble)	Nutrition	1500
T5	Cyantraniliprole	Insecticide	400
	Thiamethoxam		400
	Clothianidin		2000
	Orysastrobin	Fungicide	2000
	Amino acid (water soluble)	Nutrition	1500

T1: none, T2 and T3: conventional practices, but different chemicals of insecticide and fungicide, T4 and T5: GroMore® programs (T4 = GroMore_Star, T5 = GroMore_Duo).

2.2. Management of the Chemicals and Fertilizer Application, Water Irrigation, and Rice Cultivation

For chemical application, recommended treatment amounts of T4–T5 in Table 2 were diluted based on 80 L ha^{-1} of water to make a diluted solution. The granular type of pesticide for T2 and T3 was sprayed to the plots directly on transplanting day, while 400 mL of stock solution per seedling box for T4 and T5 was applied to the seeding box using a 10 L PVC water drench can (Jinsan Inc., Jeonnam, Republic of Korea) at 1 day before transplanting. This cultivar (Kosihikari, *Oryza sativa* L.) is a broad rice variety in Gyeonggi-do, Korea, and it has a medium–late maturity (150 d). Three to four seedlings per hill were established with a density of 30 cm × 15 cm.

For each treatment, urea, superphosphate, and potassium chloride were used as sources of N-P_2O_5-K_2O for rice cultivation. The amounts of N-P_2O_5-K_2O were 90-45-57 kg ha^{-1} following the recommended amount of fertilizer for paddy rice in Korea [37]. Urea was applied three times on −1 (30%), 40 (40%), and 70 (30%) days after transplanting (DAT). The entire amount of superphosphate (45 kg P ha^{-1}) was basally applied. Potassium chloride was split into two applications and applied on −1 (60%) and 70 (40%) DAT.

Water management practice was continuously flooded from −20 DAT to 30 DAT at the beginning of the rice growing season. When the rice plant reached the tillering stage on 30 DAT, mid-season drainage was applied for three weeks (late June to mid-July) to suppress the non-productive tiller, and then irrigation was applied until the physiological maturity stage. During the flooded period, the water level was continuously maintained at a depth of approximately 5 cm from the soil surface. The rice was harvested at 145 DAT.

2.3. Agronomic Measurements

The rice was harvested at 145 DAT. Grain yield (GY) and other yield components (thousand-grain weight, number of panicles per plant, total spikelets per panicle, and % filled spikelets) of rice were obtained after harvest. GY was measured after oven drying at 70 °C for 3 days.

2.4. Measurement of CH_4 and N_2O

The closed chamber method was used to examine the plot's gas flux [38]. For collecting gas samples, a 60 × 60 × 120 cm acrylic chamber with a fan and thermometer within the lid was employed in each plot.

CH_4 and N_2O were sampled in the morning (10:00 to 12:00) one to two times per week using a 50 mL plastic syringe at 0, 30, and 60 min after closing the chamber. The collected gas samples were analyzed with a gas chromatography (Agilent, California, USA) equipped with FID and ECD detectors to determine the concentrations of CH_4 and N_2O, respectively. Except for the period of gas sampling, the chambers were kept open during the rice growing season to prevent the greenhouse effect on rice growth. The CH_4 and N_2O emissions were calculated using the following equation [39]:

$$F = \rho \times \frac{V}{A} \times \frac{\Delta c}{\Delta t} \times \frac{273}{(273 + T)} \times \frac{P_a}{760} \times 60 \times 24$$

where F is the flux (mg CH_4 m^{-2} d^{-1} or mg N_2O m^{-2} d^{-1}), ρ is the gas density (ρ = 0.714 g m^{-3} for CH_4 and ρ = 1.964 kg m^{-3} for N_2O at 273 K and 101.325 kPa (760 mmHg)), V is the volume of the chamber (m^3), A is the cross-sectional area of the chamber (m^2), $\Delta c/\Delta t$ is the change in gas concentration inside the chamber as a function of time t (10^{-6} m^3 m^{-3} min^{-1}), T is the air temperature inside the chamber (°C), 273 is a correction factor between °C and K, and Pa is the air pressure (kPa). The value of Pa was assumed to be 760 mmHg (101.325 kPa) in our calculation.

To estimate the daily data of gas emissions, linear interpolation between the observed values of gas concentrations was used [2], and summed up to estimate its GWP in CO_2 terms through multiplying by 25 or 300 for CH_4 or N_2O, respectively [40]. The standard curve was calibrated at 0.00, 0.10, 0.50, and 1.00 mg L^{-1} of N_2O and 0, 3, 5, and 10 mg L^{-1} of CH_4 every week before gas analysis [41].

2.5. Greenhouse Gas Intensity (GHGI) Estimated with Aggregate Emission of CH_4 and N_2O

The cumulative amounts of CH_4 and N_2O emissions in the CO_2 equivalent for the 100-year horizon of each treatment were calculated, projecting the global warming potential (GWP) of CH_4 and N_2O as 25 and 300, respectively [40]. The GHGI (kg CO_2-eq. t^{-1} per grain yield) was interpreted as yield-scaled aggregate emission of CH_4 and N_2O in the CO_2 equivalent at the 100-year horizon and calculated using the below equation:

GHGI = aggregate emission in the 100-year CO_2 equivalent per grain yield.

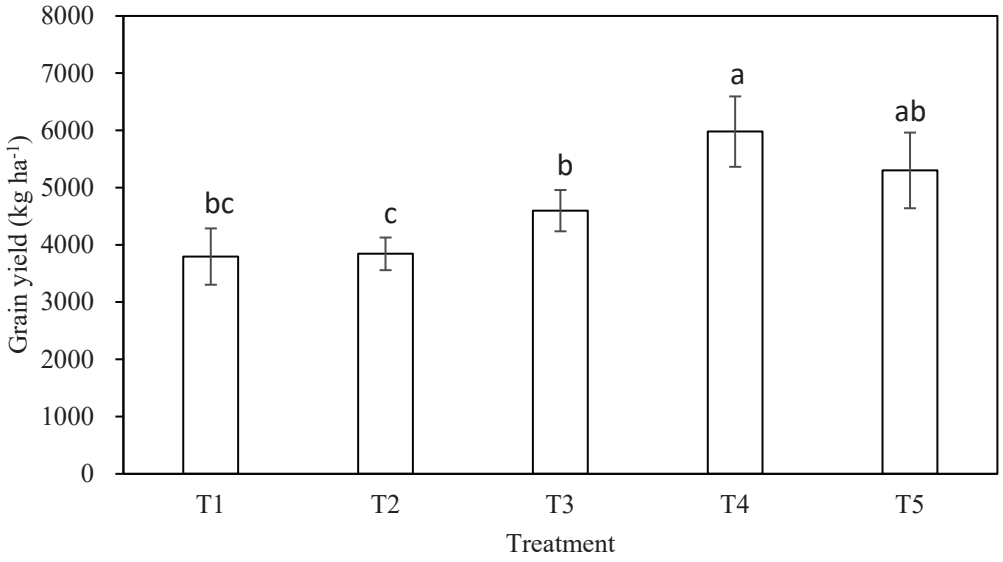
2.6. Statistical Analysis

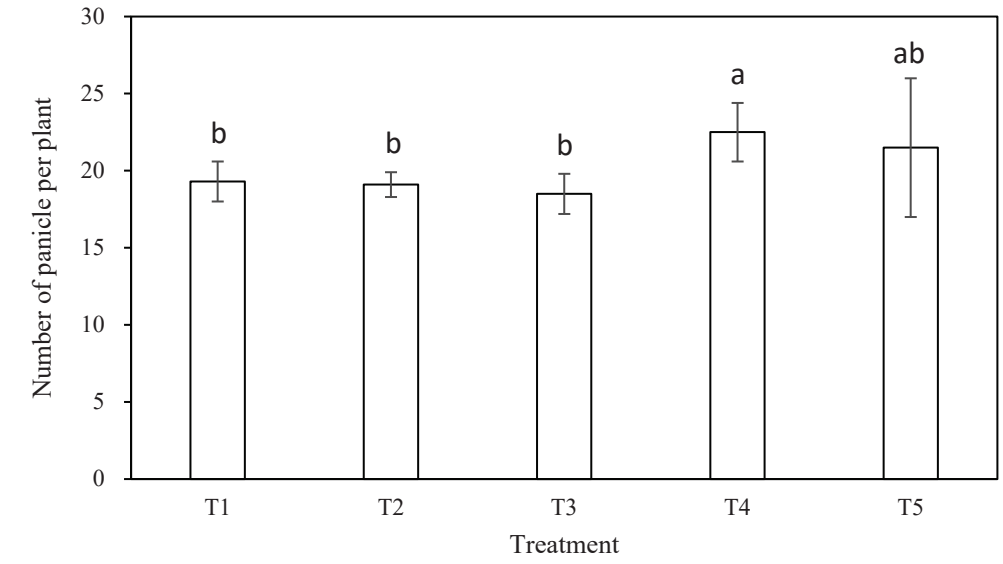
ANOVA (analysis of variance) was conducted using the XLSTAT V.2023 software while the differences between the treatments were analyzed using Duncan's multiple range test (DMRT) at $p < 0.05$ of probability. Principal component analysis (PCA) was applied using the XLSTAT software to clarify the effect of each treatment on rice productivity and GWP.

3. Results and Discussions

3.1. Rice Yield Characteristics

The chemical applications in combination with amino acids in T4 obtained higher grain yield and number of panicles per plant compared to T1, T2, and T3, although there were no different total spikelets per panicle, filled spikelet (%), and thousand-grain weight (g) among them (Figure 2). In the results, the effect of pesticides combined with amino acids as biostimulants was remarkable. Although T5 was not statistically significant with T1, T2, and T3, the higher grain yields due to amino acids including phenylalanine, tryptophan, and tyrosine improved the number of panicles per plant and seed-setting rate [42–44].





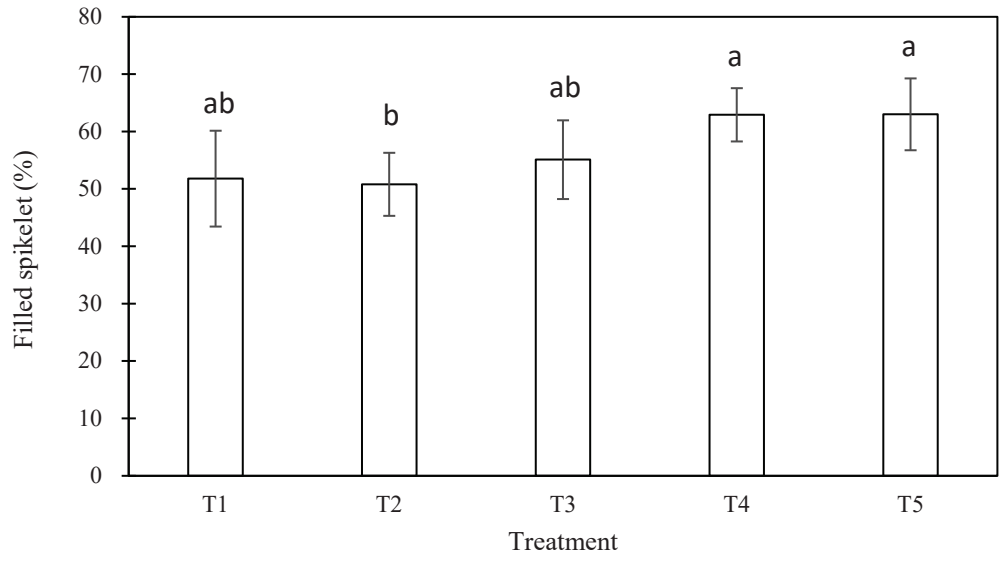


Figure 2. *Cont*.

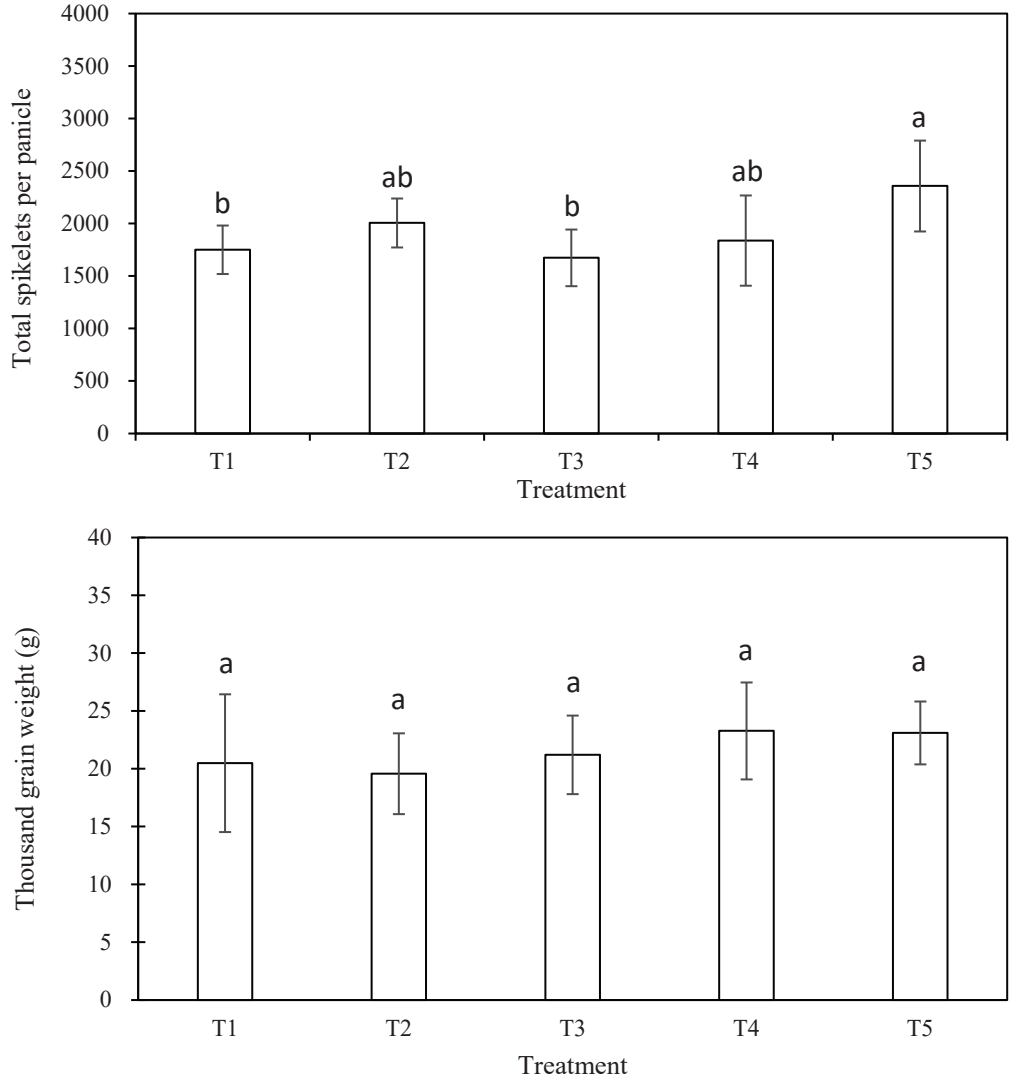


Figure 2. Effect of the different chemical applications with/without amino acids on rice yield characteristics (T1: none, T2 and T3: conventional practices, but different chemicals of insecticide and fungicide, T4 and T5: GroMore® programs (T4 = GroMore_Star, T5 = GroMore_Duo) (Different letter indicates a significantly different at $p < 0.05$ of probability).

Foliar application of amino acids supports rice growth by improving photosynthesis and biosynthesis within the plant. Also, water-soluble amino acids improve the accumulation of the amino acid content in plants. Garcia et al., (2011) [45] reported that the application of single or complex forms of different amino acids supplied essential nutrients for plant growth. Amino acids accelerate the absorption of micronutrients such as metal ions that are chelated with different amino acids in the plant [46]. As a source of nitrogen (N), amino acids can enhance nutrient N availability in the soil by promoting the activity of beneficial soil microorganisms involved in nutrient cycling. When applied to paddy soil, amino acids serve as organic substrates for soil microorganisms. Soil microorganisms, such as bacteria, fungi, and archaea, play crucial roles in the decomposition of organic matter. Upon deposition in the soil, amino acids are metabolized by microbial communities as a source of carbon (C), nitrogen (N), and energy. During microbial metabolism, amino acids undergo a process called mineralization, where the organic nitrogen (N) within the amino acids is converted into inorganic forms, such as ammonium (NH_4^+). This process releases mineralized N into the soil solution, making it available for rice uptake in flooded paddy soils [47].

On the other hand, there are various types and dosages of fungicides and insecticides used in the experiment. Most of the pesticides such as fipronil, clothianidin, and

cyantraniliprole for insecticides and orysastrobin, thifluzamide, and tiadinil for fungicides in T2 and T3 are commonly used domestically in Korean paddy fields, and the recommended amount was 10 kg ha^{-1} for T2 and T3 (Table 2). T4 and T5 consist of these pesticides (cyantraniliprole, clothianidin, and orysastrobin) and thiamethoxam (THMX) and pymetrozine (PYME), the recommended amount is 3.6 L ha^{-1}. THMX is a small molecule (molecular weight 291) with a balanced lipophilicity/hydrophilicity (log Pow is −0.13) and an optimal water solubility (4100 mg L^{-1} at 20 °C). It has a high availability in soils, rapid uptake by roots, and good distribution in plants. THMX uptake was compared with imidacloprid and clothianidin under normal humid soil conditions. Due to its optimal physicochemical properties, THMX is taken up and distributed more evenly in the plant as demonstrated by the greater amount. In addition, THMX's optimal water solubility provides good uptake and translocation properties even under dry conditions. In seed care, THMX benefits from its lipophilicity (as measured by the log P or log Kow value), where it binds to organic matter in the soil. If the log P is greater than zero, the compound is attracted to organic matter. If the log P is less than zero, the compound is more soluble in water and is less attracted to organic matter. Mobility of the active compound is required in order to maintain a sufficient concentration in the root hair zone. Seed coatings with restricted mobility will form only a small zone around the seed, and uptake of the compound from this reservoir will cease over time as the roots and root hairs grow away from the concentrated zone. In contrast to those compounds, THMX is soluble enough to be translocated with and within the growing root [48]. PYME is a modulator in the TRPV channels of the chordotonal organs, which is systemically active through xylem transportation, allowing movement of PYME from the point of application to the outer edges or growing points of the plant leaf. Leaf uptake is moderate in comparison with other insecticides. There is no or little phloem movement, so downward movement in the plant or translocation to new leaves is not possible. However, redistribution of PYME can occur after a rain event, as demonstrated in the control of brown planthoppers in rice after PYME applications made to the upper parts of the plant are redistributed by rainfall. PYME is a small molecule (molecular weight 217.23) with hydrophilicity (log Pow is −0.19) and is slightly soluble in water (270 mg L^{-1} at 20 °C) [48]. Although pesticides have various purposes and modes of action (Table S1), grain yield and number of particles per $hill^{-1}$, and filled spikelet were higher in T4 and T5. Meanwhile, a few studies suggest that the combined application of amino acids and pesticides can have synergistic effects on rice growth. Amino acids can act as biostimulants, promoting root development, nutrient uptake, and stress tolerance in plants. When applied in conjunction with pesticides, amino acids may enhance the efficacy of the pesticides by improving their absorption and translocation within the plant, thereby increasing pest control while supporting plant growth [49–51].

3.2. Effect of the Chemical Applications With/Without Amino Acids on CH_4 Emissions and GHGI

The CH_4 emissions over the rice growing periods are presented in Figure 3. The flux and its trend of CH_4 emissions were related to rice growing development and the water regime associated with air temperature. From transplanting to tillering stages (7 June to 7 August), CH_4 emissions had increased in all treatments and showed the highest peaks on 7 August. Increasing rice growth and air temperature can lead to increased CH_4 emissions during the rice growing stages. This is because more vigorous rice plants produce more root exudates and organic matter, which provide substrates for methanogenic archaea in the soil [52,53]. These microorganisms use the exudates and decaying plant material to produce CH_4 under anaerobic conditions typical of flooded rice paddies. Additionally, larger and more developed root systems enhance the transport of CH_4 from the soil to the atmosphere via the aerenchyma (air spaces) in the plant tissues. This accounts for about 90% of CH_4 emissions under submerged soil conditions. Although mid-season drainage on July 19 was implemented, the CH_4 emission still increased due to rainfall events and temperature. Additionally, Conant et al., (2008) [54] reported that concern in increasing air temperature accelerates the decomposition of organic substances in soils,

thus stimulating methanogenic activities. The trend of CH_4 flux was attributed to soil water and temperature affected by the amount of rainfall and air temperature (Figure 3). On the other hand, the tendencies of T3 and T5 showed lower CH_4 emissions than the others. The application of the chemicals (T3 and T5) reduced cumulative CH_4 emissions during the entire rice-growing season, as compared to no chemical application (T1). Among the chemical treatments, T2 and T4 showed a similar amount of CH_4 emissions to T1 (Figure 4). Meanwhile, N_2O emissions were negligible in all treatments because the paddy field was flooded most of the growing season and it has high water solubility.

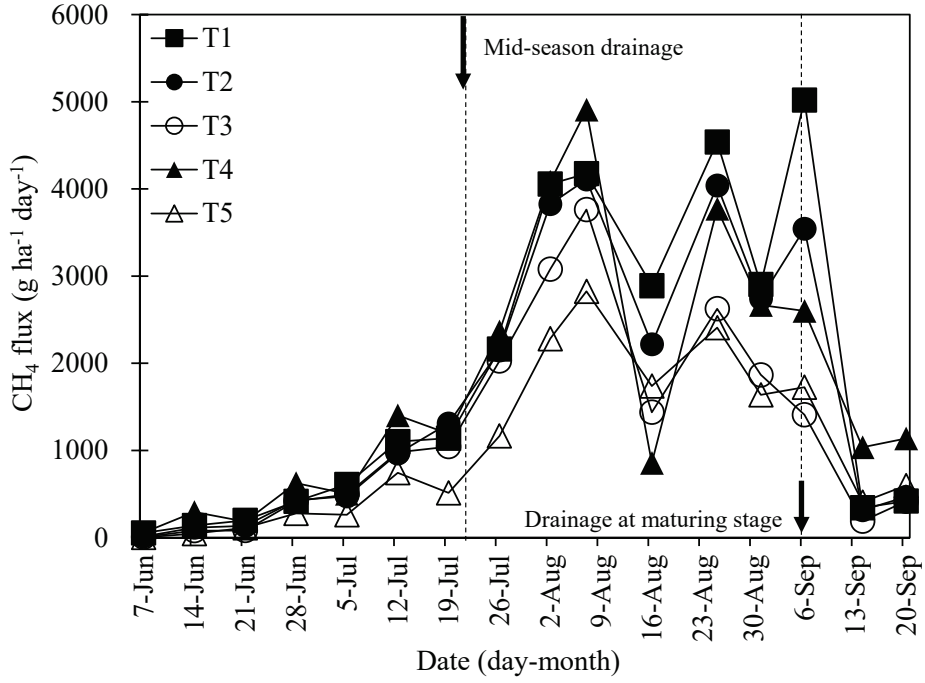


Figure 3. Daily methane fluxes during the rice growing season (T1: none, T2 and T3: conventional practices, but different chemicals of insecticide and fungicide, T4 and T5: GroMore® programs (T4 = GroMore_Star, T5 = GroMore_Duo).

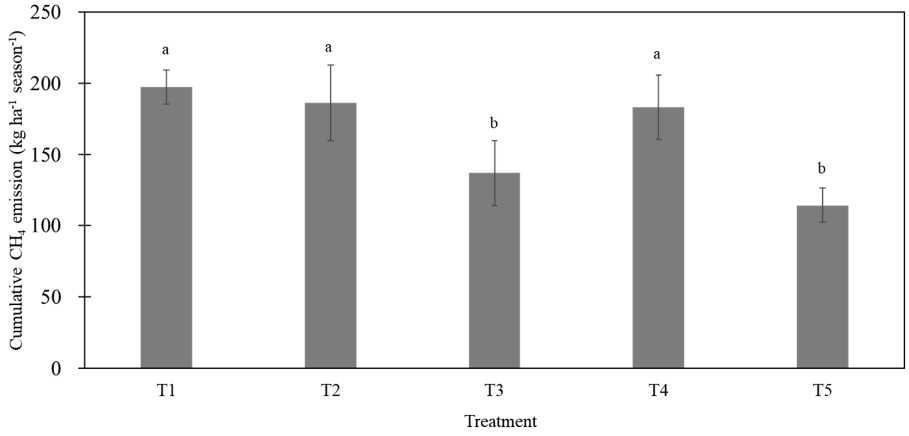


Figure 4. Cumulative methane emission during the rice growing season (T1: none, T2 and T3: conventional practices, but different chemicals of insecticide and fungicide, T4 and T5: GroMore® programs (T4 = GroMore_Star, T5 = GroMore_Duo) (Different letter indicates a significantly different at $p < 0.05$ of probability).

Among the chemicals used in our experiment, fipronil, clothianidin, cyantraniliprole, pymetrozine, and thiamethoxam seem to have no specific evidence for the reduction in methanogenesis in paddy soils since these control insects. Thifluzamide and tiadinil: T3,

and ozysastrobin: T5, showed a reduction in CH_4 emissions in paddy rice since these are fungicides affecting the microbial communities in soils. We assumed that the reduction in CH_4 emissions from T3 and T5 was derived from the different application methods of the chemicals with/without amino acids. In the treatments, T4 and T5 as the GroMore® program provide a rice seedling box drench application of a mixture of pesticides (insecticide, fungicide, and biostimulant) in water-soluble form 1 day before transplanting, while T2 and T3 are the conventional methods of farmers who evenly broadcast pesticides in granular form (mixture of fungicide and insecticide) on the seedling box 1 day before transplanting to prevent diseases and pests that occur from immediately after transplanting to before the heading stage of rice. The granule form of the chemicals (thifluzamide and tiadinil) in T3 may influence the reduction in CH_4 emissions because the chemicals may remain and affect methanogens in the soil. While T2, T4, and T5 treated with the same fungicide (ozysastrobin) showed different results in CH_4 emissions, the results seemed to be attributed to the amino acid. Amino acids including biostimulant components accelerate the early growth of rice, extending the tillering period, and increasing the number of panicles per plant [55]. When applied to paddy soil, amino acids serve as the organic substrates for soil microorganisms. We assumed that the release of organic compounds (root exudates) from the rice roots into the surrounding soil influences CH_4 emissions. These exudates provide substrates such as sugars, amino acids, and organic acids that are utilized by soil microbes, including methanogenic archaea. The presence of these substrates stimulates microbial activity, leading to increased production of intermediates like acetate and hydrogen, which are then converted to methane by methanogens under anaerobic conditions. The process significantly contributes to CH_4 emissions from paddy fields [56]. Meanwhile, T4 included with amino acids appeared to have an effect on increasing CH_4 emissions with the higher grain yield and number of panicles per plant because root exudates appeared to have decreased relatively as the carbon assimilation rate within the plant improved. However, T5 showed a reduction in CH_4 emissions in the experiment, although the same amount of chemicals was used with T4. Probably, further study is needed to clarify this difference.

To evaluate GHGI, this study considered the yield-scaled aggregate emission of CH_4 in the CO_2 equivalent. Our result showed that significantly lower GHGI values in T4 and T5 were observed because of higher grain yields and comparatively lower CH_4 emissions (Figure 5). Hughes et al., (2010) [57] reported that disease control reduced 15 to 20% of GHG emissions associated with higher crop yields.

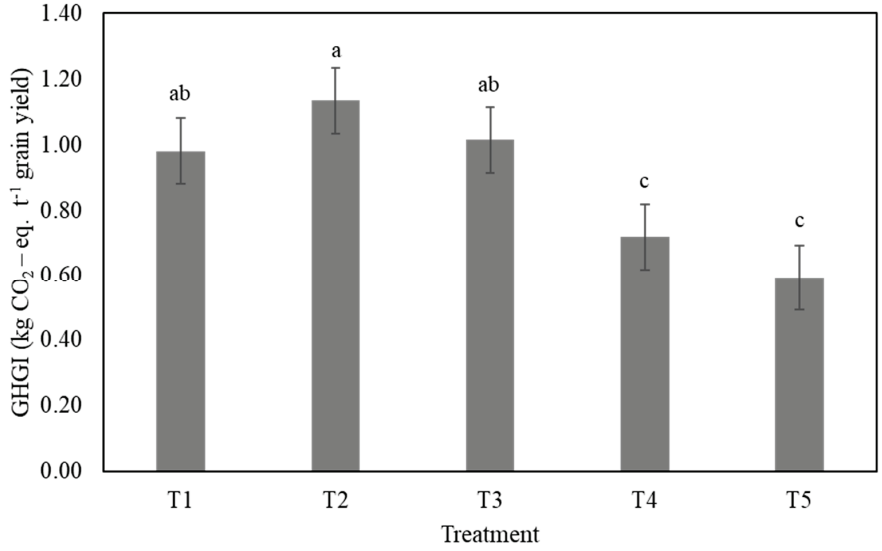


Figure 5. Effect of the pesticides combined with/without amino acid application on GHGI over the rice growing season (T1: none, T2 and T3: conventional practices, but different chemicals of insecticide and fungicide, T4 and T5: GroMore® programs (T4 = GroMore_Star, T5 = GroMore_Duo) (Different letter indicates a significantly different at $p < 0.05$ of probability).

3.3. PCA Analysis

PCA analysis was conducted to assess the effect of each treatment. Table 3 indicates eigenvalue, cumulative proportion, and 1st and 2nd PC for factor loading. For this analysis, grain yield, number of panicles per plant, percentage filled spikelet, thousand-grain weight, and CH_4 emissions were engaged, and the analysis result was significant because the eigenvalue was more than 1.0 for the 2nd PC, and 97.5% of information was explained with the 1st and 2nd PC. The 1st PC was interpreted as P since grain yield, number of panicles per plant, percentage filled spikelet, and thousand-grain weight were highly contributing factors. On the other hand, the 2nd PC was explained as GWP since CH_4 showed a high eigenvector. Figure 3 presents the scattered diagram of the PC scores, with P on the *x*-axis and GWP on the *y*-axis. The T5 is in the 4th quadrant, indicating a high contribution of both P and GWP, in contrast with T1 and T2. The T4 is in the 1st quadrant, indicating relatively high P and low GWP, which is in contrast with T3 showing high GWP, but relatively low P (Figure 6).

Table 3. Factor loading, eigenvalue, and cumulative proportion of PCA in each treatment.

Factor Loading	1st PC	2nd PC
Grain yield (kg ha^{-1})	0.937	0.011
Number of panicles per plant	0.797	0.159
Percentage filled spikelet (%)	0.999	0.001
Thousand-grain weight (g)	0.978	0.000
CH_4 (kg ha^{-1})	0.251	0.743
Eigenvalue	3.96	1.0
Cumulative proportion	79.2	97.5

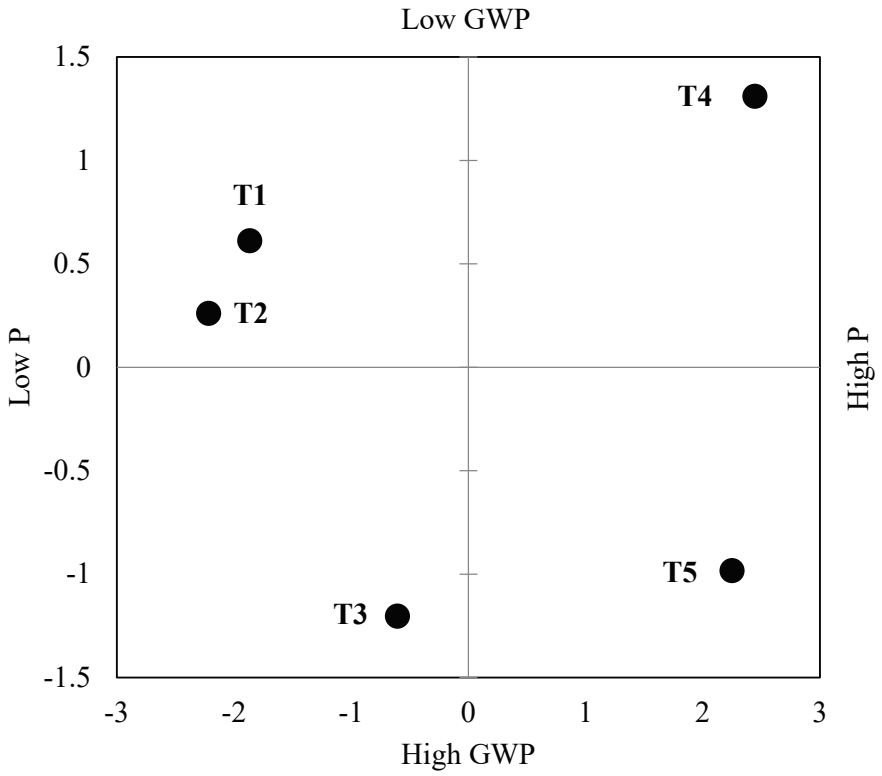


Figure 6. Assessment of rice productivity (P) and global warming potential (GWP) on the treatments (● = mean values of PCA scores in all treatments, (T1: none, T2 and T3: conventional practices, but different chemicals of insecticide and fungicide, T4 and T5: GroMore® programs (T4 = GroMore_Star, T5 = GroMore_Duo).

4. Conclusions

The intensively irrigated rice field increases GHG emissions, and contributes to elevated global average temperature. Additionally, the use of fertilizers and pesticides to increase crop yield and control disease in crop fields may cause global environmental effects. Thus, an appropriate practice of chemical application for sustaining rice productivity and reducing GHG emissions should be implemented in rice cultivation. In the experiment, GroMore® programs (T4 and T5), which is a combined application method of pesticides and amino acids, avoid yield loss compared to T2 and T3, although it shortens the spraying time by 95% and uses 64% less pesticide amount than conventional practices (T2 and T3). In addition, the cumulative amount of GHG emissions in T4 and T5 showed similar and lower GHG emissions compared to T2 and T3 during the rice growing season. These results of the impact of GroMore® programs on relatively lower GHGI values have herein been presented. However, in order to have sustainable and productive rice production, pesticide application needs to be performed at an appropriate rate through either synthetic or organic N fertilizers. Also, it is imperative to test an optimal practice for pesticides in future research to compromise the negative impact of agrochemical application in rice production.

Supplementary Materials: The following supporting information can be downloaded at: https://www.mdpi.com/article/10.3390/agronomy14102448/s1, Table S1: Specific chemical sources, purpose, and mode of action (MoA) in the treatments.

Author Contributions: S.Y.Y.: Conceptualization, methodology, data curation, writing—original draft preparation; J.-K.S. and K.-S.J.: Conceptualization, methodology, investigation, and resources; H.-H.K.: writing—review and editing, visualization, supervision, project administration, funding acquisition. All authors have read and agreed to the published version of the manuscript.

Funding: This research was funded by Syngenta Korea.

Data Availability Statement: Data will be made available on request.

Acknowledgments: The authors respectfully recognize the staff at the Soil Environment Research Institute, Hankyong National University, and Syngenta Korea.

Conflicts of Interest: Author Jun-Ki Son was employed by the company CP Development Korea. Author Kyoung-Sik Jun was employed by the company CP Marketing Korea. The remaining authors declare that the research was conducted in the absence of any commercial or financial relationships that could be construed as a potential conflict of interest.

References

1. Audsley, E.; Stacey, K.; Parsons, D.J.; Williams, A.G. *Estimation of the Greenhouse Gas Emissions from Agricultural Pesticide Manufacture and Use*; Crop Protection Association: Bedford, UK, 2009; pp. 1–20.
2. Ku, H.H.; Hayashi, K.; Agbisit, R.; Villegas-Pangga, G. Evaluation of fertilizer and water management effect on rice performance and greenhouse gas intensity in different seasonal weather of tropical climate. *Sci. Total Environ.* **2017**, *601*, 1254–1262. [CrossRef] [PubMed]
3. Jeong, S.T.; Kim, G.W.; Hwang, H.Y.; Kim, P.J.; Kim, S.Y. Beneficial effect of compost utilization on reducing greenhouse gas emissions in a rice cultivation system through the overall management chain. *Sci. Total Environ.* **2018**, *613*, 115–122. [CrossRef] [PubMed]
4. Kim, G.W.; Gutierrez-Suson, J.; Kim, P.J. Optimum N rate for grain yield coincides with minimum greenhouse gas intensity in flooded rice fields. *Field Crops Res.* **2019**, *237*, 23–31. [CrossRef]
5. Burke, M.; Lobell, D. Food security and adaptation to climate change: What do we know? In *Climate Change and Food Security: Adapting Agriculture to a Warmer World*; Springer: New York, NY, USA, 2010; pp. 133–153.
6. Barth, H.G.; Sun, S.T. Particle size analysis. *Anal. Chem.* **1989**, *61*, 143–152. [CrossRef] [PubMed]
7. Bradshaw, C.J.; Leroy, B.; Bellard, C.; Roiz, D.; Albert, C.; Fournier, A.; Barbet-Massin, M.; Salles, J.-M.; Simard, F.; Courchamp, F. Massive yet grossly underestimated global costs of invasive insects. *Nat. Commun.* **2016**, *7*, 12986. [CrossRef]
8. FAO. Pesticides Use. Available online: https://www.fao.org/faostat/en/#data/RP (accessed on 2 October 2024).
9. Tosun, N.; Karabay, N.Ü.; Sayım, F. Pesticide usage and their potential adverse impacts on living organisms. *Anadolu J. AARI* **2001**, *11*, 113–125.
10. Kalia, A.; Gosal, S. Effect of pesticide application on soil microorganisms. *Arch. Agron. Soil Sci.* **2011**, *57*, 569–596. [CrossRef]

11. Zacharia, J.T. Ecological effects of pesticides. In *Pesticides in the Modern World-Risks and Benefits*; IntechPublisher: Rijeka, Croatia, 2011; pp. 129–142.
12. Liu, X.; Xu, X.; Li, C.; Zhang, H.; Fu, Q.; Shao, X.; Ye, Q.; Li, Z. Degradation of chiral neonicotinoid insecticide cycloxaprid in flooded and anoxic soil. *Chemosphere* **2015**, *119*, 334–341. [CrossRef]
13. Prudnikova, S.; Streltsova, N.; Volova, T. The effect of the pesticide delivery method on the microbial community of field soil. *Environ. Sci. Pollut. Res.* **2021**, *28*, 8681–8697. [CrossRef]
14. Behera, B.; Singh, G.S. Studies on weed management in monsoon season crop of tomato. *Indian J. Weed Sci.* **1999**, *31*, 67–70.
15. Webster, J.; Bowles, R.; Williams, N. Estimating the economic benefits of alternative pesticide usage scenarios: Wheat production in the United Kingdom. *Crop Prot.* **1999**, *18*, 83–89. [CrossRef]
16. Ross, G. Risks and benefits of DDT. *Lancet* **2005**, *366*, 1771–1772. [CrossRef]
17. Cooper, J.; Dobson, H. The benefits of pesticides to mankind and the environment. *Crop Prot.* **2007**, *26*, 1337–1348. [CrossRef]
18. Bellamy, C. *The State of the World's Children 1998*; Oxford University Press for UNICEF: New York, NY, USA, 1998.
19. Aktar, W.; Sengupta, D.; Chowdhury, A. Impact of pesticides use in agriculture: Their benefits and hazards. *Interdiscip. Toxicol.* **2009**, *2*, 1–12. [CrossRef] [PubMed]
20. Ahmed, S.; Chauhan, B.S.; Humphreys, E. Effect of application timings of soil applied herbicides on weed growth and crop yield in dry-seeded rice in Bangladesh. In Proceedings of the Weed Science Society Conference, Bandung, Indonesia, 22–25 October 2013.
21. Cederberg, C.; Persson, U.M.; Schmidt, S.; Hedenus, F.; Wood, R. Beyond the borders–burdens of Swedish food consumption due to agrochemicals, greenhouse gases and land-use change. *J. Clean. Prod.* **2019**, *214*, 644–652. [CrossRef]
22. Mithila, J.; Hall, J.C.; Johnson, W.G.; Kelley, K.B.; Riechers, D.E. Evolution of resistance to auxinic herbicides: Historical perspectives, mechanisms of resistance, and implications for broadleaf weed management in agronomic crops. *Weed Sci.* **2011**, *59*, 445–457. [CrossRef]
23. Karimmojeni, H.; Pirbaloti, A.G.; Kudsk, P.; Kanani, V.; Ghafori, A. Influence of Postemergence Herbicides on Weed Management in Spring-Sown Linseed. *Agron. J.* **2013**, *105*, 821–826. [CrossRef]
24. Owen, M.J.; Martinez, N.J.; Powles, S.B. Multiple herbicide-resistant *Lolium rigidum* (annual ryegrass) now dominates across the W estern A ustralian grain belt. *Weed Res.* **2014**, *54*, 314–324. [CrossRef]
25. Oyeogbe, A.I.; Das, T.; Bhatia, A.; Singh, S.B. Adaptive nitrogen and integrated weed management in conservation agriculture: Impacts on agronomic productivity, greenhouse gas emissions, and herbicide residues. *Environ. Monit. Assess.* **2017**, *189*, 198. [CrossRef]
26. Grichar, W.J.; Rose, J.J.; Dotray, P.A.; Baughman, T.A.; Langham, D.R.; Werner, K.; Bagavathiannan, M. Response of sesame to selected herbicides applied early in the growing season. *Int. J. Agron.* **2018**, *2018*, 9373721. [CrossRef]
27. Mirtaleb, S.H.; Niknejad, Y.; Fallah, H. Foliar spray of amino acids and potassic fertilizer improves the nutritional quality of rice. *J. Plant Nutr.* **2021**, *44*, 2029–2041. [CrossRef]
28. Abbasi, P.A.; Cuppels, D.A.; Lazarovits, G. Effect of foliar applications of neem oil and fish emulsion on bacterial spot and yield of tomatoes and peppers. *Can. J. Plant Pathol.* **2003**, *25*, 41–48. [CrossRef]
29. Priyanka, B.; Ramesh, T.; Rathika, S.; Balasubramaniam, P. Foliar application of fish amino acid and egg amino acid to improve the physiological parameters of rice. *Int. J. Curr. Microbiol. Appl. Sci.* **2019**, *8*, 3005. [CrossRef]
30. Makino, A. Photosynthesis, grain yield, and nitrogen utilization in rice and wheat. *Plant Physiol.* **2011**, *155*, 125–129. [CrossRef] [PubMed]
31. Caemmerer, S.; Evans, J.R. Determination of the average partial pressure of CO_2 in chloroplasts from leaves of several C3 plants. *Funct. Plant Biol.* **1991**, *18*, 287–305. [CrossRef]
32. Gianessi, L.P. The increasing importance of herbicides in worldwide crop production. *Pest Manag. Sci.* **2013**, *69*, 1099–1105. [CrossRef]
33. Jiang, J.; Chen, L.; Sun, Q.; Sang, M.; Huang, Y. Application of herbicides is likely to reduce greenhouse gas (N_2O and CH_4) emissions from rice–wheat cropping systems. *Atmos. Environ.* **2015**, *107*, 62–69. [CrossRef]
34. Das, S.; Ghosh, A.; Adhya, T. Nitrous oxide and methane emission from a flooded rice field as influenced by separate and combined application of herbicides bensulfuron methyl and pretilachlor. *Chemosphere* **2011**, *84*, 54–62. [CrossRef]
35. Korean Soil Information System. Soil Classification. Available online: http://soil.rda.go.kr/geoweb/soilmain.do (accessed on 4 March 2023).
36. Agricultural Weather 365. Agricultural Climatic Information. Available online: https://weather.rda.go.kr (accessed on 4 March 2024).
37. Lee, K.S.; Park, W.K.; Jeong, B.K.; Song, Y.S.; Jeon, H.J.; Jeong, K.S.; Lee, C.S. *Fertilizer Recommendation Standards for Various Crops*; Rural Development Administration: Suwon, Republic of Korea, 2006; pp. 19–25.
38. Hutchinson, G.; Mosier, A. Improved soil cover method for field measurement of nitrous oxide fluxes. *Soil Sci. Soc. Am. J.* **1981**, *45*, 311–316. [CrossRef]
39. Rolston, D. *Methods of Soil Analysis. Part 1. Physical and Mineralogical Methods*; Klute, A., Ed.; American Society of Agronomy, Inc.: Madison, WI, USA, 1986; pp. 1103–1119.
40. Solomon, S.; Qin, D.; Manning, M.; Alley, R.B.; Berntsen, T.; Bindoff, N.L.; Chen, Z.; Chidthaisong, A.; Gregory, J.M.; Hegerl, G.C. *Technical summary. Climate Change 2007: The Physical Science Basis. Contribution of Working Group I to the Fourth Assessment Report of the Intergovernmental Panel on Climate Change*; Solomon, S., Qin, D., Manning, M., Chen, Z., Marquis, M., Averyt, K.B., Tignor, M., Miller, H.L., Eds.; Cambridge University Press: New York, NY, USA, 2007.

41. Ku, H.H.; Hayashi, K.; Agbisit, R.; Villegas-Pangga, G. Effect of calcium silicate on nutrient use of lowland rice and greenhouse gas emission from a paddy soil under alternating wetting and drying. *Pedosphere* **2020**, *30*, 535–543. [CrossRef]
42. Luo, H.; Zhang, Y.; Yi, W.; Zhang, S.; Zhang, Q.; Xing, P.; Tang, X. Foliar application of phenylalanine, tryptophan, and tyrosine in fragrant rice production: Aroma, yield, grain quality, and economic return. *Eur. J. Agron.* **2024**, *155*, 127117. [CrossRef]
43. Decouard, B.; Bailly, M.; Rigault, M.; Marmagne, A.; Arkoun, M.; Soulay, F.; Caïus, J.; Paysant-Le Roux, C.; Louahlia, S.; Jacquard, C. Corrigendum: Genotypic Variation of Nitrogen Use Efficiency and Amino Acid Metabolism in Barley. *Front. Plant Sci.* **2022**, *13*, 893540. [CrossRef] [PubMed]
44. Wang, G.; Xu, M.; Wang, W.; Galili, G. Fortifying horticultural crops with essential amino acids: A review. *Int. J. Mol. Sci.* **2017**, *18*, 1306. [CrossRef] [PubMed]
45. Garcia, A.; Madrid, R.; Gimeno, V.; Rodriguez-Ortega, W.; Nicolas, N.; Garcia-Sanchez, F. The effects of amino acids fertilization incorporated to the nutrient solution on mineral composition and growth in tomato seedlings. *Span. J. Agric. Res.* **2011**, *9*, 852–861. [CrossRef]
46. Popko, M.; Michalak, I.; Wilk, R.; Gramza, M.; Chojnacka, K.; Górecki, H. Effect of the new plant growth biostimulants based on amino acids on yield and grain quality of winter wheat. *Molecules* **2018**, *23*, 470. [CrossRef]
47. Havlin, J.L. Soil: Fertility and nutrient management. In *Landscape and Land Capacity*; CRC Press: Boca Raton, FL, USA, 2020; pp. 251–265.
48. IRAC.org. Available online: https://irac-online.org (accessed on 1 March 2023).
49. Chotsaeng, N.; Laosinwattana, C.; Charoenying, P. Enantioselective and synergistic herbicidal activities of common amino acids against Amaranthus tricolor and Echinochloa crus-galli. *Molecules* **2021**, *26*, 2071. [CrossRef]
50. Zhao, P.; Wang, C.; Zhang, S.; Zheng, L.; Li, F.; Cao, C.; Cao, L.; Huang, Q. Fungicide-loaded mesoporous silica nanoparticles promote rice seedling growth by regulating amino acid metabolic pathways. *J. Hazard. Mater.* **2022**, *425*, 127892. [CrossRef]
51. Zhao, G.-P.; Cheng, W.-L.; Zhang, Z.-H.; Li, Y.-X.; Li, Y.-Q.; Yang, F.-W.; Wang, Y.-B. The use of amino acids and their derivates to mitigate against pesticide-induced toxicity. *Ecotoxicol. Environ. Saf.* **2024**, *276*, 116340. [CrossRef]
52. Chen, Y.; Guo, W.; Ngo, H.H.; Wei, W.; Ding, A.; Ni, B.; Hoang, N.B.; Zhang, H. Ways to mitigate greenhouse gas production from rice cultivation. *J. Environ. Manag.* **2024**, *368*, 122139. [CrossRef]
53. Ding, H.; Liu, T.; Hu, Q.; Liu, M.; Cai, M.; Jiang, Y.; Cao, C. Effect of microbial community structures and metabolite profile on greenhouse gas emissions in rice varieties. *Environ. Pollut.* **2022**, *306*, 119365. [CrossRef]
54. Conant, R.T.; Steinweg, J.M.; Haddix, M.L.; Paul, E.A.; Plante, A.F.; Six, J. Experimental warming shows that decomposition temperature sensitivity increases with soil organic matter recalcitrance. *Ecology* **2008**, *89*, 2384–2391. [CrossRef] [PubMed]
55. Sowmya, R.; Warke, V.G.; Mahajan, G.B.; Annapure, U.S. Effect of amino acids on growth, elemental content, functional groups, and essential oils composition on hydroponically cultivated coriander under different conditions. *Ind. Crops Prod.* **2023**, *197*, 116577.
56. Cai, Z.; Shan, Y.; Xu, H. Effects of nitrogen fertilization on CH4 emissions from rice fields. *Soil Sci. Plant Nutr.* **2007**, *53*, 353–361. [CrossRef]
57. Hughes, D.J.; West, J.S.; Atkins, S.D.; Gladders, P.; Jeger, M.J.; Fitt, B.D. Effects of disease control by fungicides on greenhouse gas emissions by UK arable crop production. *Pest Manag. Sci.* **2011**, *67*, 1082–1092. [CrossRef]

Disclaimer/Publisher's Note: The statements, opinions and data contained in all publications are solely those of the individual author(s) and contributor(s) and not of MDPI and/or the editor(s). MDPI and/or the editor(s) disclaim responsibility for any injury to people or property resulting from any ideas, methods, instructions or products referred to in the content.

agronomy

MDPI

Article

Multi-Criteria Analysis for Geospatialization of Potential Areas for Water Reuse in Irrigated Agriculture in Hydrographic Regions

Ana Paula Pereira Carvalho [1], Ana Claudia Pereira Carvalho [1], Mirian Yasmine Krauspenhar Niz [2], Fabrício Rossi [1], Giovana Tommaso [3] and Tamara Maria Gomes [1,*]

[1] Department of Biosystems Engineering, Faculty of Animal Science and Food Engineering, University of São Paulo, Pirassununga 13635-900, SP, Brazil; ana.carvalho02@alumni.usp.br (A.P.P.C.); ana.carvalho01@alumni.usp.br (A.C.P.C.); fabricio.rossi@usp.br (F.R.)
[2] Institute of Science and Technology, Federal University of Alfenas, Alfenas 37130-001, MG, Brazil; mirian.niz@gmail.com
[3] Department of Foods Engineering, Faculty of Animal Science and Food Engineering, University of São Paulo, Pirassununga 13635-900, SP, Brazil; tommaso@usp.br
* Correspondence: tamaragomes@usp.br

Abstract: As the climate crisis progresses, droughts and the seasonal availability of fresh water are becoming increasingly common in different regions of the world. One solution to tackle this problem is the reuse of treated wastewater in agriculture. This study was carried out in two significant hydrographic regions located in the southeast of Brazil (Mogi Guaçu River Water Management Unit—UGRHI-09 and Piracicaba River Basin—PRB) that have notable differences in terms of land use and land cover. The aim of this study was to carry out a multi-criteria analysis of a set of environmental attributes in order to classify the areas under study according to their levels of soil suitability and runoff potential. The integrated analysis made it possible to geospatialize prospective regions for reuse, under two specified conditions. In the UGRHI-09, condition 1 corresponds to 3373.24 km^2, while condition 2 comprises 286.07 km^2, located mainly in the north-western and central-eastern portions of the unit. In the PRB, condition 1 was also more expressive in occupational terms, corresponding to 1447.83 km^2; and condition 2 was perceptible in 53.11 km^2, predominantly in the central region of the basin. The physical characteristics of the areas studied were decisive in delimiting the areas suitable for the reuse of treated wastewater.

Keywords: geoprocessing; GIS; land suitability; water reuse; spatial analysis; surface runoff

1. Introduction

Water has great relevance in the global economic scenario. However, it is a finite element and currently scarce in some regions of the planet [1]. With climate change and the increase in population and goods and food production, it is clear that water resources are being seriously impacted. Against this background, the introduction of sustainable practices in the most diverse activities that depend on this resource is increasingly necessary for conservation and protection purposes, especially in the agricultural sector [2].

In this regard, wastewater reuse in irrigated agriculture has been used and improved over the years, becoming an alternative source of water and nutrients for agricultural production [3,4], as well as a sustainable alternative for water resource management [5,6], stimulated by the sixth Sustainable Development Goal (SDG)–Drinking Water and Sanitation [7]. This practice, beyond improving wastewater management, reduces water course pollution, contributing to a circular economy [8].

However, before reuse, it is essential to treat wastewater, in order to avoid the accumulation of contaminants in the soil, causing damage to agricultural crops [9], human health,

and the environment. Therefore, for reuse, it is necessary to select the most appropriate effluent treatment system for the local context. This step is essential to obtain reliable information about the benefits and challenges of the various water and nutrient recovery system options [10].

The practice of wastewater reuse consists of using water produced from wastewater, which after treatment, acquires characteristics with potential for reuse in different categories, such as recycling and reuse in industrial areas [11], in recreational areas [12], in aquifer recharge [13], and in agricultural irrigation [14–16].

Besides contributing to the reduction in water resource exploitation, treated wastewaters, mainly from agro-industrial sources (dairies, slaughterhouses, beverage manufacturing, sugar and ethanol plants, among others), provide essential macro- and micronutrients for the development of plants, reducing the need for synthetic fertilizers [17], and are a supplementary source of biodegradable water, free of toxic chemicals [18].

Irrigated agriculture is the largest water resource consumer, using around 70% of the volume of freshwater withdrawn on a global scale [19]. The challenge for the agricultural sector is to achieve sustainable practices while maintaining productivity. Even though it has made progress, it suffers from increased pressure on freshwater resources, given that more than 60% of irrigated crops globally are located in regions with a high exploitation of water resources [20].

Although wastewater reuse is considered a strategy to reduce the use of better-quality water, in current times, this practice in irrigation is far from its potential use. This is due to society's lack of trust, in addition to the absence of standards on wastewater reuse [21]. It is important for managers, planners, and society to understand that treated wastewater currently is no longer a waste, but rather a resource [22].

Thereby, it is mandatory to acknowledge the physical characteristics of a given area, to delineate the appropriate and inappropriate locations for adopting wastewater reuse practice. Just like water, soil is also one of the most significant natural resources in the world and is fundamental for all aspects of life [23,24]; therefore, responsible care for this resource is also crucial for adequate agricultural management, with a view to protecting soil and increasing ecosystem services [25].

Land suitability maps are an extremely important tool, as they show the levels of suitability for agricultural production. The assessment of land suitability helps in sustainable agricultural development [26,27], as in this process different environmental attributes of a given region are integrated and analyzed, considering its specificities [28–31].

Land suitability is an instrument that indicates potential areas for agricultural production, with a view to the sustainable use of natural resources without affecting ecosystems, in line with SDG2 (Zero Hunger and Sustainable Agriculture) and SDG 15 (Life on Land) [32–34].

For the reuse of wastewater in irrigation, in addition to agricultural sustainability, it is also essential to map the areas regarding the potential for surface runoff, a process that occurs when the volume of precipitation is greater than the water storage capacity of the land [35]. This information enables recognizing which areas are most in need of water resources, that is, those that have a shorter water concentration time in a microbasin and/or those that have physical characteristics that provide a higher rate of infiltration into groundwater and aquifers, and consequently, greater need for a supplementary water source in dry periods.

To create these maps, it is necessary to use geospatial techniques, which have been improved with the advancement in technology. Geospatial studies are gaining greater scope at different scales and environmental issues as they provide, quickly and efficiently, the integration and analysis of a set of attributes.

The analysis of land suitability, as well as the classification of a hydrographic region in terms of the surface runoff process, can be carried out using the Analytic Hierarchy Process (AHP) technique associated with the use of specific tools from a Geographic Information System (GIS) [36,37].

In the Nile River, the capacity of agricultural areas was assessed based on the Cervatana module of the MicroLEIS DSS agricultural model, integrating NDVI data, pedological maps, and land assessment. The methods used involved the assistance of GIS tools, geoprocessing techniques, and agricultural and ecosystem service models. The procedures adopted helped guide more sustainable recommendations for the conservation of areas that present limitations to agricultural production, with the intention of increasing productivity and reducing the negative environmental impacts, such as the use of high quantities of water [38].

Ref. [39] also carried out land aptness mapping; the work involved all of Europe, and the geospatial data used included seventeen eco-pedological indicators. The authors also evaluated land use, using an integrated analysis of aptness maps with the crop map. In the work of [29], the AHP technique was used to analyze a series of data: the slope, altitude, land use and cover, soil texture, moisture and pH, precipitation, temperature, and distances to rivers and roads. These variables showed a greater relationship in the land aptness analysis (Republic of Tatarstan's, Russia), after pairwise comparison.

The AHP technique was proposed by Saaty in the 1970s and is still widely used today to establish priority between various attributes, through pairwise comparisons [16,40]. This technique is based on the opinion and knowledge of experts to weigh sustainability criteria and create a score made up of the weighted sum of all attributes [4,41].

In this context, this study aimed to analyze the land suitability associated with the levels of surface runoff potential using a multivariate hierarchical analysis integrated with geoprocessing techniques in a GIS, to verify the feasibility of irrigation with an alternative water source. The identification of areas with high agricultural suitability in conjunction with areas of low surface runoff has been demonstrated to represent priority areas for the reuse of water. This study was conducted in the Mogi Guaçu Water Resources Management Unit (UGRHI-09) and the Piracicaba River Basin (PRB), which corresponds to one of the basins of the Fifth Water Resources Management Unit (UGRHI-05), located in the state of São Paulo, Brazil. The objective was to contribute to the development of sustainable practices for the conservation and utilization of water and soil resources, with the aim of ensuring water and food security.

2. Materials and Methods

2.1. Study Area

The first study area comprises the UGRHI-09, while the second corresponds to the PRB, which represents the largest river basin in the UGRHI-05; both areas are located in the state of São Paulo, Brazil. The first unit has a territorial extension of 15,068.54 km^2, and is considered a predominantly agricultural region, with temporary and permanent crops, as well as pastures for cattle. The second area covers 12,655.01 km^2, and has a large population and an intense industrial complex (Figure 1A,B).

Cultivation activities and livestock breeding in UGRHI-09 and agricultural and industrial activities in PRB contribute to the regional economy. In addition to these activities, the various agro-industries also contribute to the economic development of the units, being responsible for the production of sugar and ethanol, beverages (distilled and concentrated orange juice), oils, meat, dairy products, and vegetable processing, among other activities.

According to the Köppen classification, the UGRHI-09 has the Cwa climate type, considered to be mesothermal, with hot, rainy summers and an average temperature of over 22 °C for the hottest month; and the Aw climate type, which has hot, rainy summers and dry winters, with an average temperature of over 18 °C for the coldest month [42]. According to the same classification, the PRB has four types of climate: Cfa (subtropical with no dry season and hot summer); Cfb (subtropical with no dry season and mild summer); Cwa (subtropical with dry winter and hot summer); and Cwb (subtropical with dry winter and mild summer) [43].

In terms of physical aspects, the UGRHI-09 predominantly has altitudes between 600 and 800 m above sea level. According to the Brazilian Soil Classification System, the most common soils in these regions are Oxisols (1085.61 km^2 of the total area of the unit),

which have a clayey texture (clay content between 350 g·kg^{-1} and 600 g·kg^{-1}) and an effective depth of more than 2 m. Argisols, on the other hand, are the second largest soil class, occurring on hilly to very hilly terrain (8% to 45%) and found in the eastern part of UGRHI-09, where the areas with the greatest tourist potential in the region are concentrated [44]. The PRB has more areas at altitudes up to 677 m, with the presence of red Oxisols, red-yellow Oxisols, and red-yellow Argisols. The eastern region of the PRB also has steeper terrain and altitudes up to 2037 m.

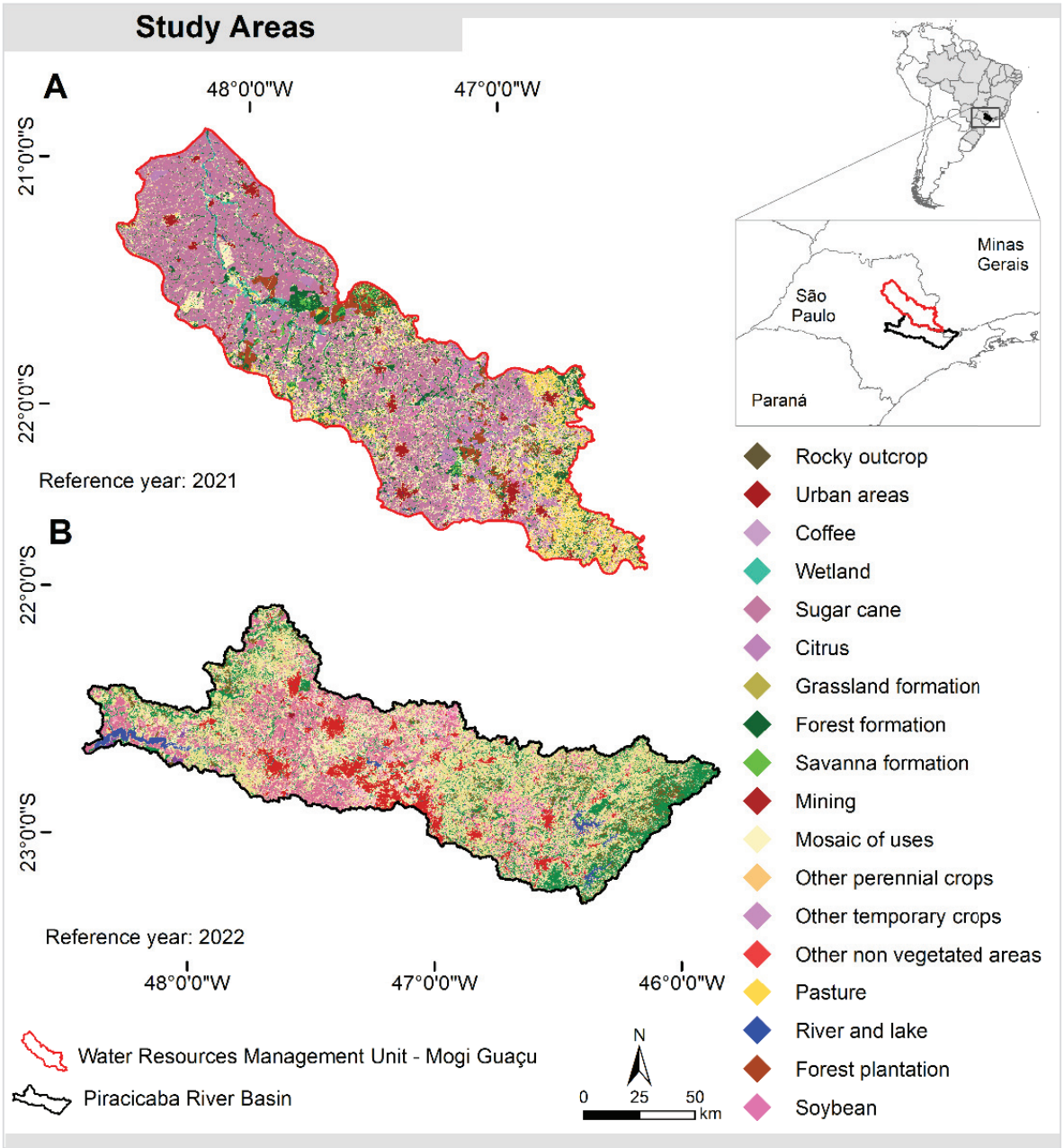


Figure 1. Location of study areas. Land use and land cover maps of UGRHI-09 (**A**) and PRB (**B**). Source: Adapted from [45,46].

2.2. Methods

The methods used involved geoprocessing techniques for weighting and overlaying the environmental attributes that were considered for the UGRHI-09 and PRB classification regarding land suitability and potential levels for surface runoff, to assist in the practice

of reusing treated wastewater from agro-industrial sources in the hydrographic region (Figure 2). It is worth noting that the PRB runoff levels were mapped by [47].

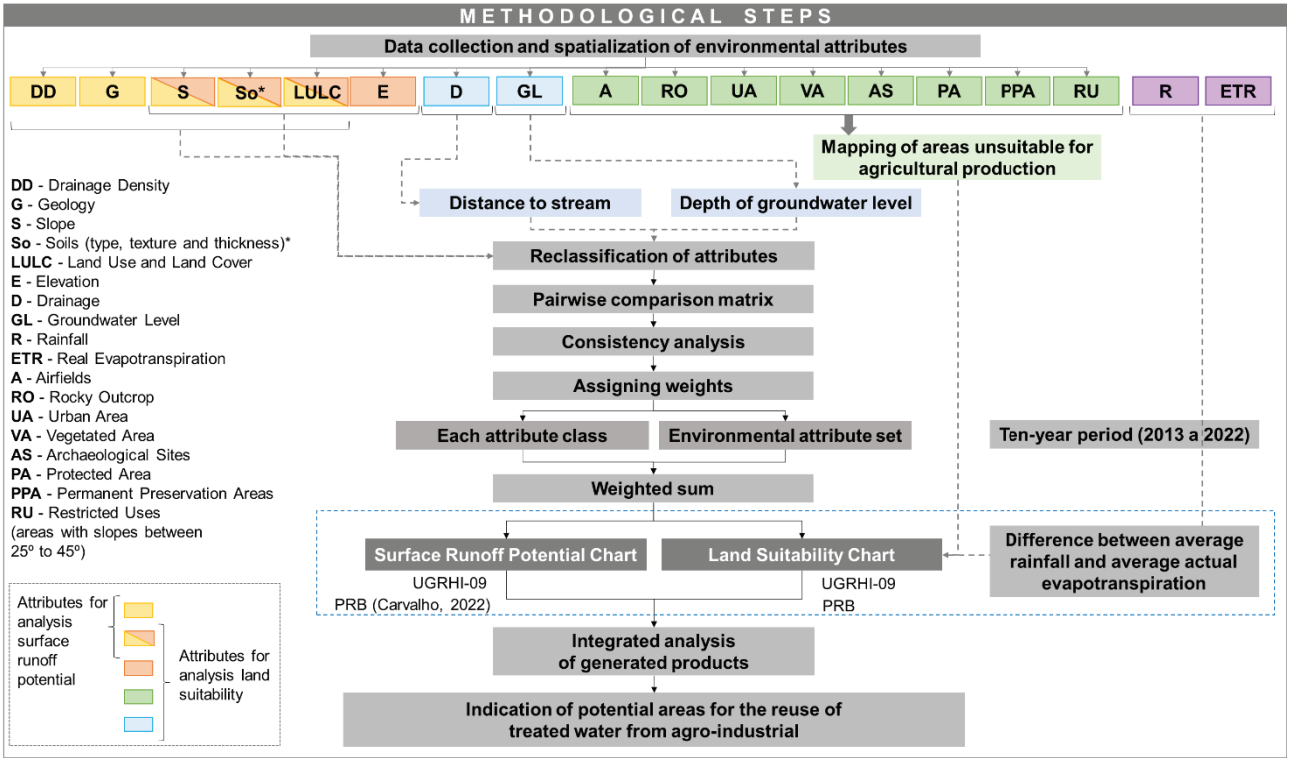


Figure 2. Methodological steps developed in the study. * So: soils (type, texture and thickness). It is worth noting that the PRB runoff levels were mapped by [47].

2.2.1. Data Collection

The data were collected from different official platforms; Table 1 presents the information on each attribute considered for the elaboration of the interpretative cartographic products.

Table 1. Information on the environmental attributes considered in this work.

Attributes	Information	Scale	Source/Year—Unit
Airfield	-	-	[48]—UGRHI-09 and PRB https://metadados.snirh.gov.br/geonetwork/srv/api/records/ce6bb0fe-ccfc-4cbf-9ff6-929ba80b47db (accessed on 31 January 2023)
Rocky Outcrop	Images from Landsat satellite, with spatial resolution of 30 m	1:50,000	[45]—UGRHI-09 https://mapbiomas.org/ (accessed on 30 January 2023) [46]—PRB https://mapbiomas.org/ (accessed on 21 February 2024)
Urban Area			
Vegetated Area			
Land Use and Land Cover			
Permanent Preservation Areas (PPAs)	Law no. 12651/2012		[49]—UGRHI-09 https://www.car.gov.br/#/ (accessed on 25 January 2023) [50]—PRB
Restricted Uses (areas with slopes between 25° and 45°)			[49]—UGRHI-09 https://www.car.gov.br/#/ (accessed on 25 January 2023) [51]—PRB https://www.car.gov.br/#/ (accessed on 21 February 2024)

Table 1. *Cont.*

Attributes	Information	Scale	Source/Year—Unit
Archaeological Sites	Representation in points Decree Law no. 25/1937 Technical note no. 7/2020/CGN/DEPAM [52]	-	[53]—UGRHI-09 and PRB http://portal.iphan.gov.br/pagina/detalhes/1701/ (accessed on 24 January 2023)
Protected Area Conservation Unit—Integral Protection	Law no. 9985/2000 [54]	-	[55]—UGRHI-09 and PRB https://www.gov.br/icmbio/pt-br/assuntos/dados_geoespaciais/mapa-tematico-e-dados-geoestatisticos-das-unidades-de-conservacao-federais (accessed on 24 January 2023)
Geology	Limits of geological units	1:250,000	[56]—UGRHI-09 https://www.ibge.gov.br/geociencias/ininformaco-ambientais/geologia/15822-geologia-1-250-000.html?=&t=downloads (accessed on 7 February 2023) [57]—PRB
Soils	Type, texture, and thickness	1:750,000	[44]—UGRHI-09 [47]—PRB
Elevation	Digital Elevation Model (DEM), using orbital images from Alos Palsar remote sensor, with spatial resolution of 12.5 m	1:50,000	[58] UGRHI-9 and PRB https://search.asf.alaska.edu/# (accessed on 27 September 2022)
Slope	Slope classes generated through MDE, using orbital images from Alos Palsar remote sensor, with spatial resolution of 12.5 m		
Drainage Density	Made from drainage		[59]—UGRHI-09 [60]—PRB
Depth of Groundwater Level	Static level of registered wells	-	[61]—UGRHI-09 https://siagasweb.sgb.gov.br/layout/pesquisa_complexa.php (accessed on 14 March 2023) [62]—PRB https://siagasweb.sgb.gov.br/layout/pesquisa_complexa.php (accessed on 19 February 2024)
Surface Runoff	Surface runoff levels	1:50,000	[47]—PRB
Rainfall	Ten-year period (2013 to 2022)	-	[63] UGRHI-9 and PRB https://data.chc.ucsb.edu/products/CHIRPS-2.0/ (accessed on 20 September 2024)
Real Evapotranspiration	Ten-year period (2013 to 2022)	-	[64] UGRHI-9 and PRB https://earlywarning.usgs.gov/fews (accessed on 20 September 2024)

2.2.2. Inapt Area Mapping

At this stage, areas considered inapt for agricultural production were those whose function is to ensure the conservation and preservation of natural resources based on environmental legislation at the regional and national level, as well as areas already consolidated.

The areas of rocky outcrops, urbanized areas, and areas with native vegetation cover were extracted from the land use and cover map prepared by MapBiomas®, through a download on the Google Earth Engine® platform.

The Conservation Unit (CU) delimitations were acquired from the Chico Mendes Institute for Biodiversity Conservation (ICMBIO). The study areas were considered sustainable

use CUs, which according to Law no. 9.985/2000 are areas that make it possible to reconcile nature conservation with the sustainable use of part of their natural resources [54].

For permanent preservation areas (PPAs), the limits surrounding springs and watercourses were considered. The limits of the PPAs were obtained individually for the municipal limits that fully or partially cover the UGRHI-09 and PRB areas. At this stage of mapping, the limits of existing aerodromes in the studied areas were also considered. For areas that do not have the delimitation of aerodromes, it was necessary to identify these locations and then vectorize them on the Google Earth Pro® platform.

In relation to archeological sites, it was necessary to apply a buffer of 3 km to delimit the area surrounding each point that represents the archeological site, according to the criteria defined by technical note no. 7/2020/CGN/DEPAM [52].

After the acquisition and reprojection of the mentioned environmental attributes, the shapefiles were joined using ArcGIS® 10.8 software resources. This procedure allowed the environmental attributes to be connected, avoiding overlapping information.

2.2.3. The Selection of Environmental Attributes for the Land Suitability Chart (LSC) and the Surface Runoff Potential Chart (SRPC)

This stage involved the selection of environmental attributes for the construction of the Land Suitability Chart (LSC) and the Surface Runoff Potential Chart (SRPC) for the two areas under study. The choice of attributes was based on the influence of physical and anthropogenic characteristics on the suitability of the land, as well as the interference of these characteristics in surface runoff. The set of environmental attributes used is presented below:

Slope: The slope of the land was employed in the delineation of the LSC and SRPC. In consideration of agricultural suitability, this attribute represents a fundamental factor in the evaluation of irrigation potential. Areas exhibiting steeper slopes are less conducive to irrigation and can exert an influence on runoff and the manifestation or exacerbation of erosion processes. Conversely, flatter areas, exhibiting a slope of less than 2%, are more conducive to surface irrigation [65]. Slope also influences various soil properties such as soil moisture, clay composition, and nutrient availability (e.g., nitrogen, calcium, and magnesium) [66].

In terms of surface runoff, slope was the most important attribute as it is a determining factor in surface runoff. The steeper the slope, the greater the potential for runoff, while flatter areas favor the process of water infiltration into the soil. In the UGRHI-09, the areas with steep slopes are mainly located in the extreme east, whereas in the PRB, the steepest slopes are found in the extreme west and in the eastern part of the basin (Figure 3).

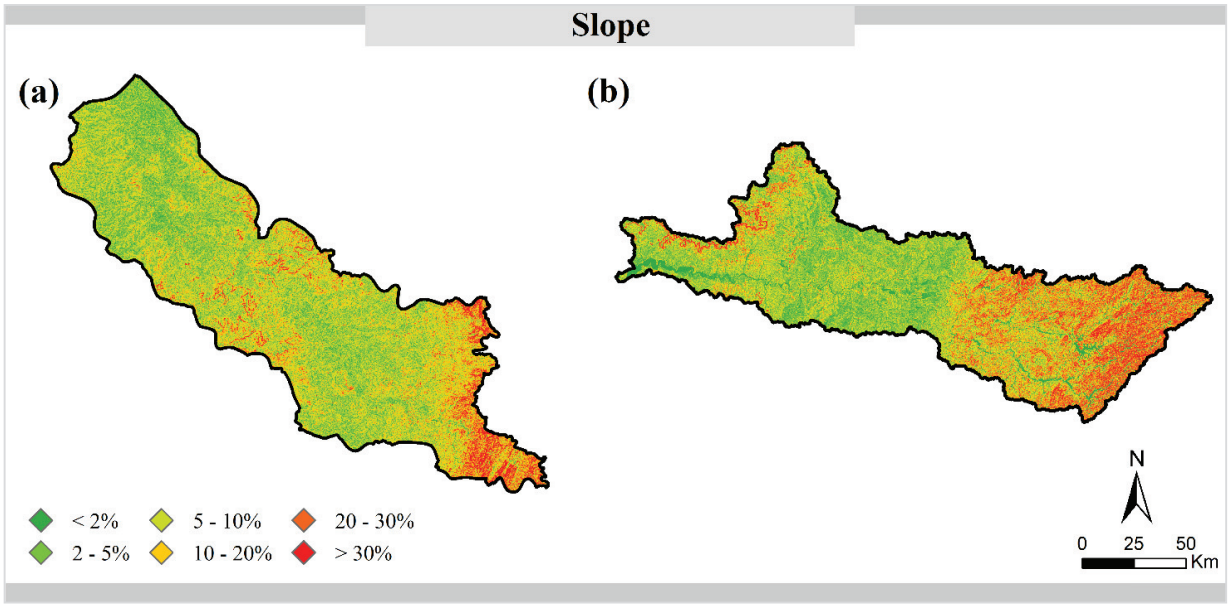


Figure 3. Slope chart of UGRHI-09 (**a**) and PRB (**b**).

Elevation: This attribute (Figure 4) was one of the information plans used to prepare the LSC, given that elevation has a significant impact on the distribution and activity of microorganisms, soil organic matter, and the development of crops [67].

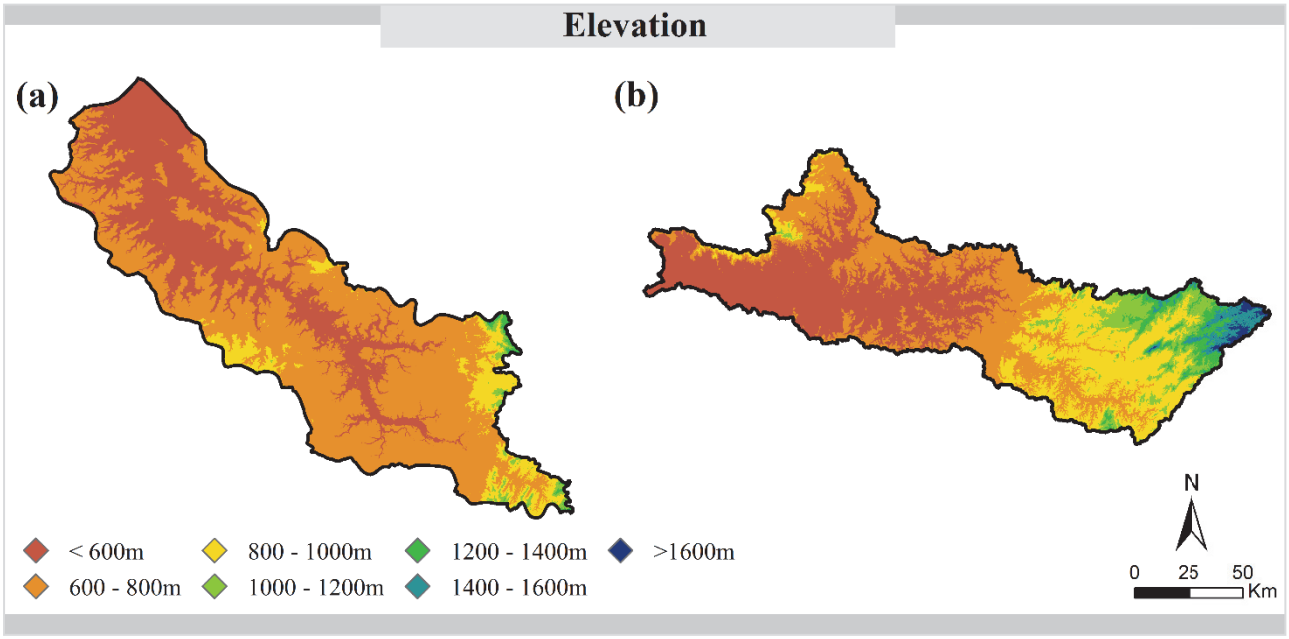


Figure 4. Elevation map of UGRHI-09 (**a**) and PRB (**b**).

Soils: This is a crucial factor in determining agricultural suitability (Figure 5), as soil properties can significantly influence productivity and irrigation operations [36]. Soil depth is a significant factor that influences the root system of crops and can affect their growth and yield [68].

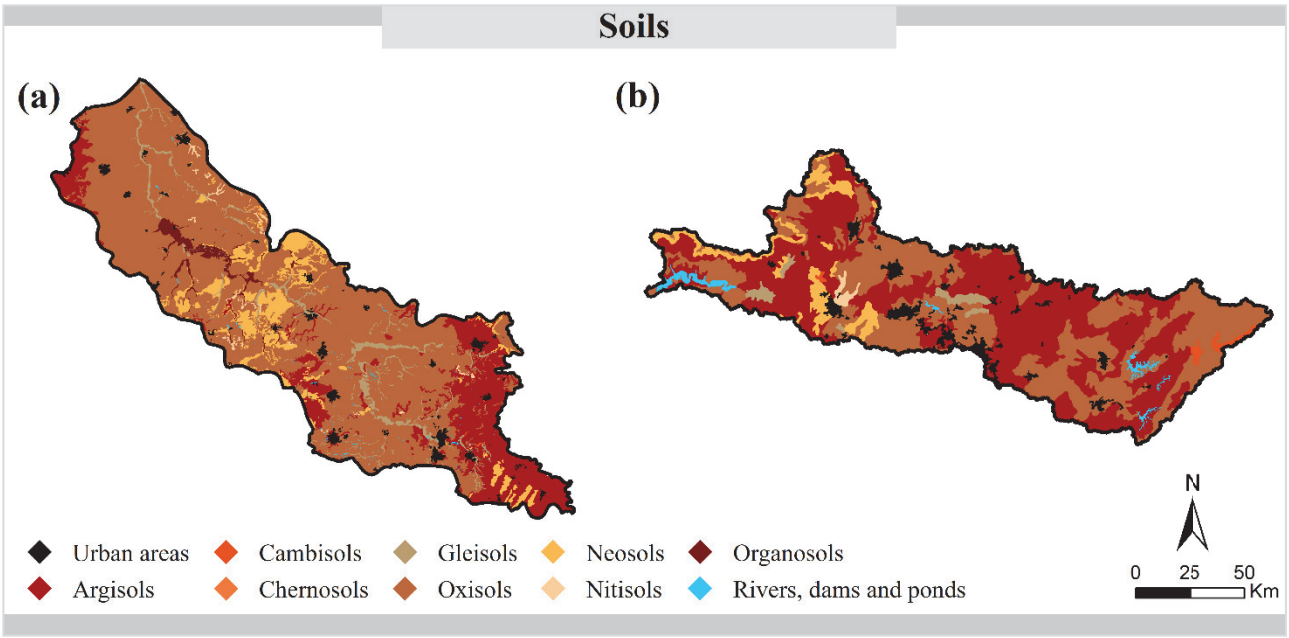


Figure 5. Soil maps of UGRHI-09 (**a**) and PRB (**b**).

Soil texture is typically indicative of its capacity to retain water and nutrients. For instance, soils with a sandy texture are generally unsuitable for agricultural use due to their

limited capacity to retain water and nutrients [69]. In terms of surface runoff, soil characteristics are also of great importance; the prevalence of sandy soils with thick profiles facilitates greater water infiltration, thus reducing the likelihood of surface runoff [37]. On the other hand, clay soils have lower permeability, which predisposes them to surface runoff.

Drainage density: As drainage density is inversely proportional to permeability, this attribute was included in the preparation of the SRPC (Figure 6). It is evident that an area with a low drainage density can exhibit a higher infiltration rate, which in turn affects groundwater recharge [70]. Consequently, low-density areas are assigned a lower weighting, whereas high-density drainage areas are given a higher weighting, as they contribute more significantly to surface runoff.

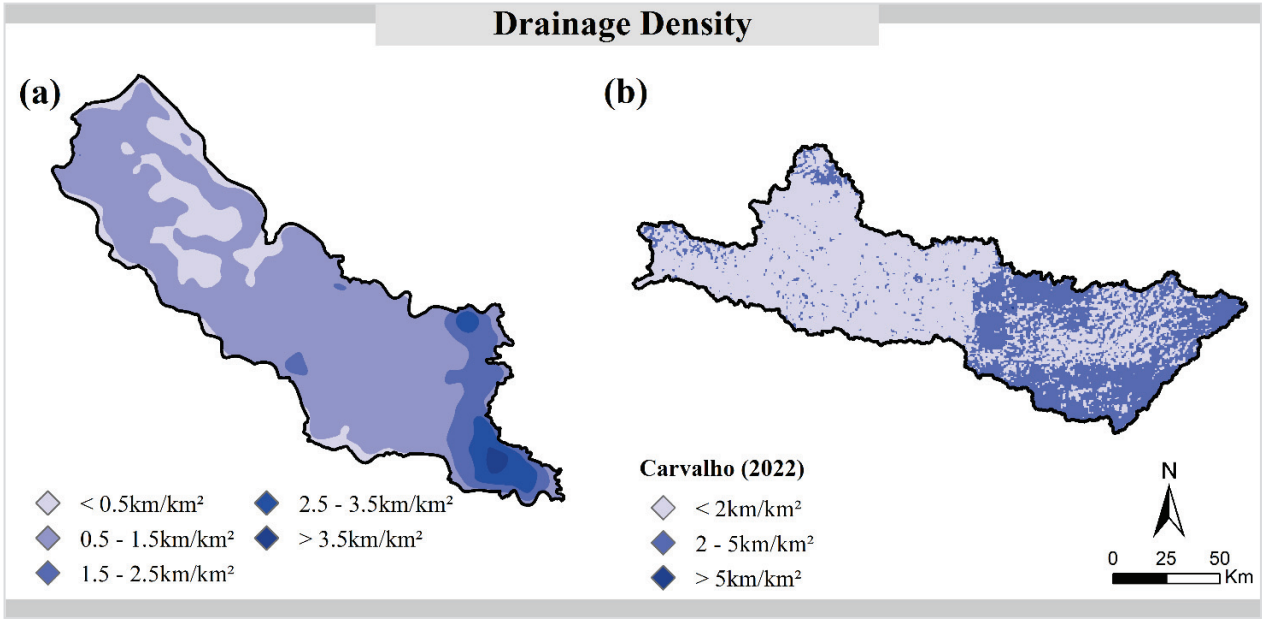


Figure 6. Drainage density map of UGRHI-09 (**a**) and PRB (**b**) [47].

Drainage density was calculated using the drainage network of the areas under study and the Kernel Density tool in ArcGIS® software. The radius established was 1128; this value was more representative of the density of the channels [71]. The relationship between drainage density and potential runoff levels means that the greater the length of drainage per square kilometer, the greater the surface flow in the area [47].

Geology: This attribute was also taken into account when drawing up the SRPC. Geological units can be associated with the type and properties of soils in an area, as well as portraying their permeability (Figure 7) [72].

Land use and land cover: It is an indispensable criterion for discerning the distinctive attributes of each area within a hydrographical region. It was essential for the preparation of both the LSC and the SRPC, as agricultural suitability is also defined based on the respective land uses of a given area [4]. Furthermore, surface runoff is influenced by the composition of surface uses [73]. For instance, areas with dense vegetation are less prone to runoff with greater flow, while areas with less dense vegetation contribute to greater runoff action.

The land use and land cover maps for the areas under investigation were obtained from the MapBiomas platform, which mapped land use and land cover classes for the entirety of Brazil using images from the Landsat sensor. Figures 1A and 1B illustrate the land use and land cover maps for UGRHI-09 and PRB, respectively.

Depth of groundwater levels: This variable is of great significance, as it is associated with the types of aquifers and their porosities, the proximity of drainage channels, and the production of wells under diverse hydrogeological conditions [74].

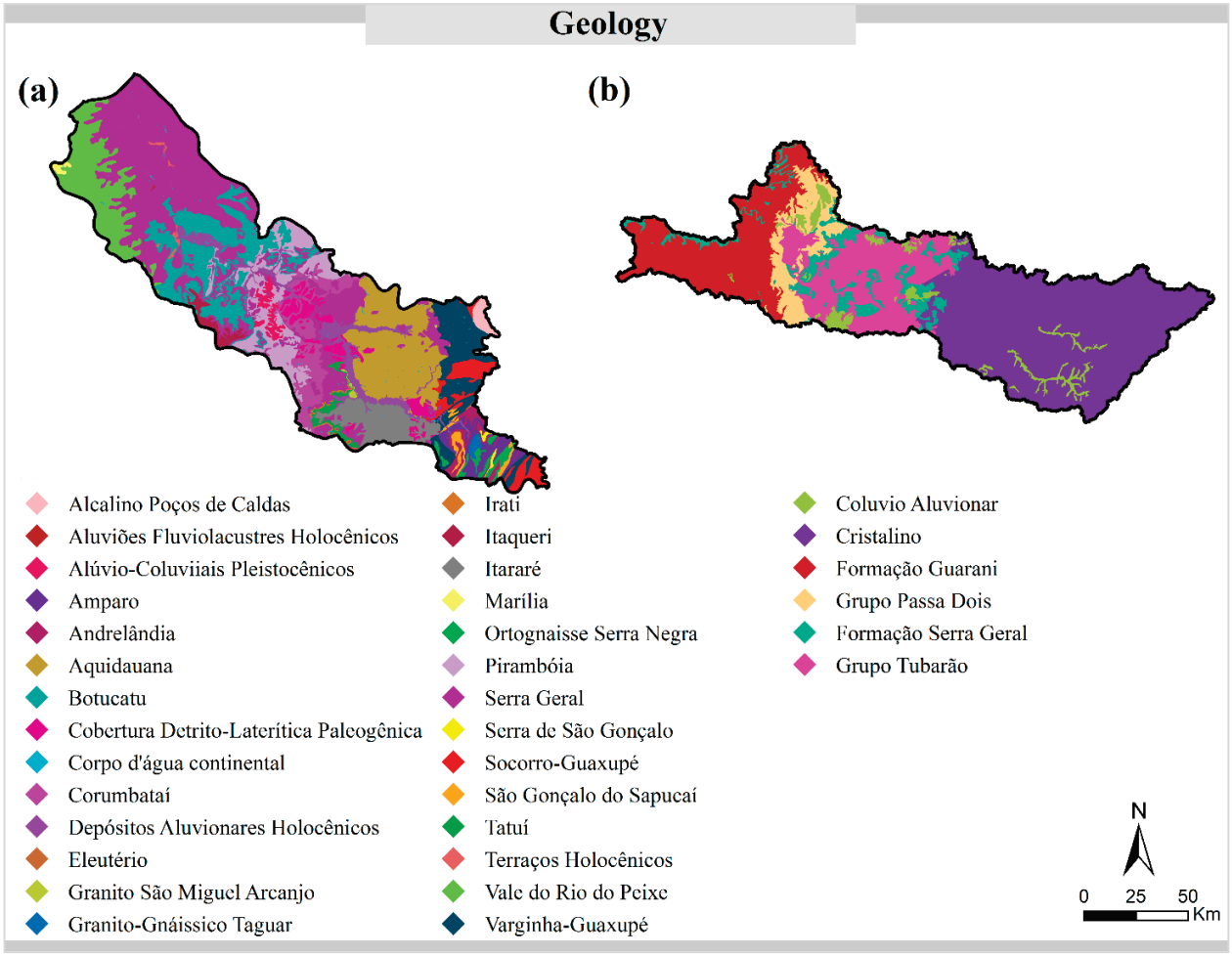


Figure 7. Geology map of UGRHI-09 (**a**) and PRB (**b**).

The depth of the groundwater level involved the interpolation of 1374 points and 2669 points that represent the wells that have the static level value in UGRHI-09 and PRB (Figure 8). For interpolation, the Inverse Distance Weighted (IDW) method was used, which is adopted for the spatial distribution of both the groundwater level, as well as precipitation and temperature. This method is considered a convex interpolation mapping technique that fits continuous models of spatial variations [75].

Distance from nearest drainage: This attribute was employed in the formulation of the LSC and constitutes a pivotal element in the evaluation of agricultural suitability. Areas in closer proximity to watercourses are accorded greater significance, as they indicate a higher probability of irrigation, thereby reducing water distribution costs and ensuring an adequate supply [65].

To delimit the distance to the nearest drainage channel, the ottocoded hydrographic database was used, available at the National Water and Basic Sanitation Agency [59] (Figure 9a), and in PRB the hydrographic base was also obtained in vector format from the Geonetwork platform of the National Water and Sanitation Agency [60] (Figure 9b). These hydrographic bases were reprojected to the Datum SIRGAS 2000 and cropped for the study areas. They were then entered into ArcGIS® software to create the Euclidean distance. The generated products represent the closest straight-line distance to a water channel drainage [36,65,76,77] (Figure 9c,d).

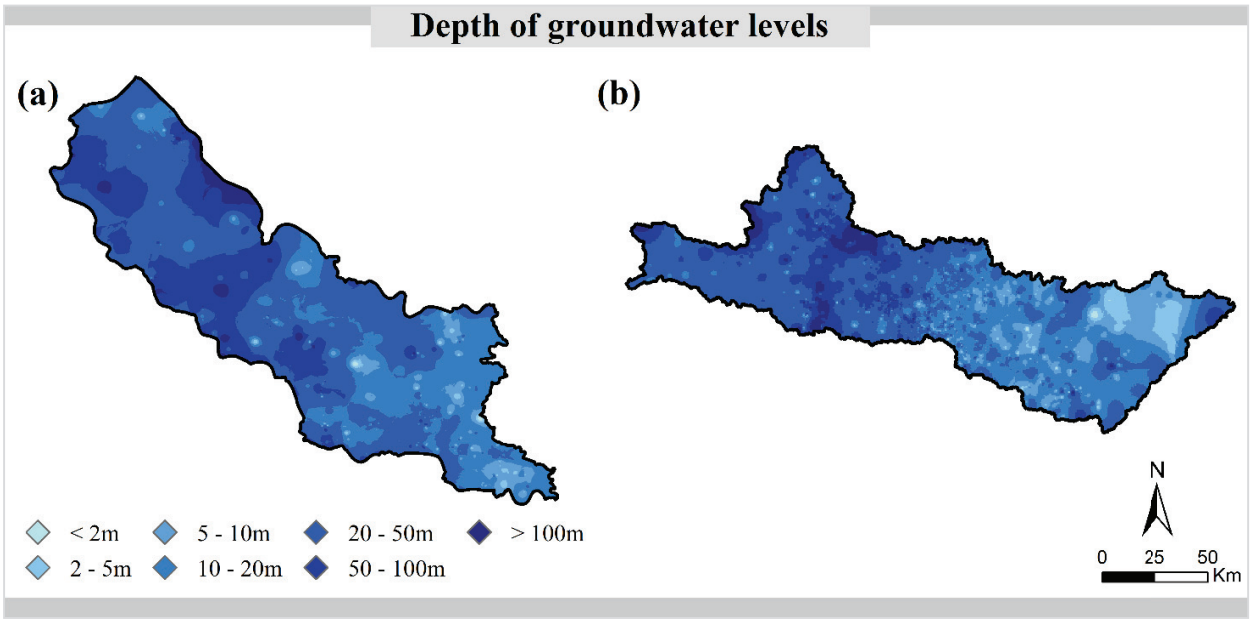


Figure 8. Depth of groundwater level map of UGRHI-09 (**a**) and PRB (**b**).

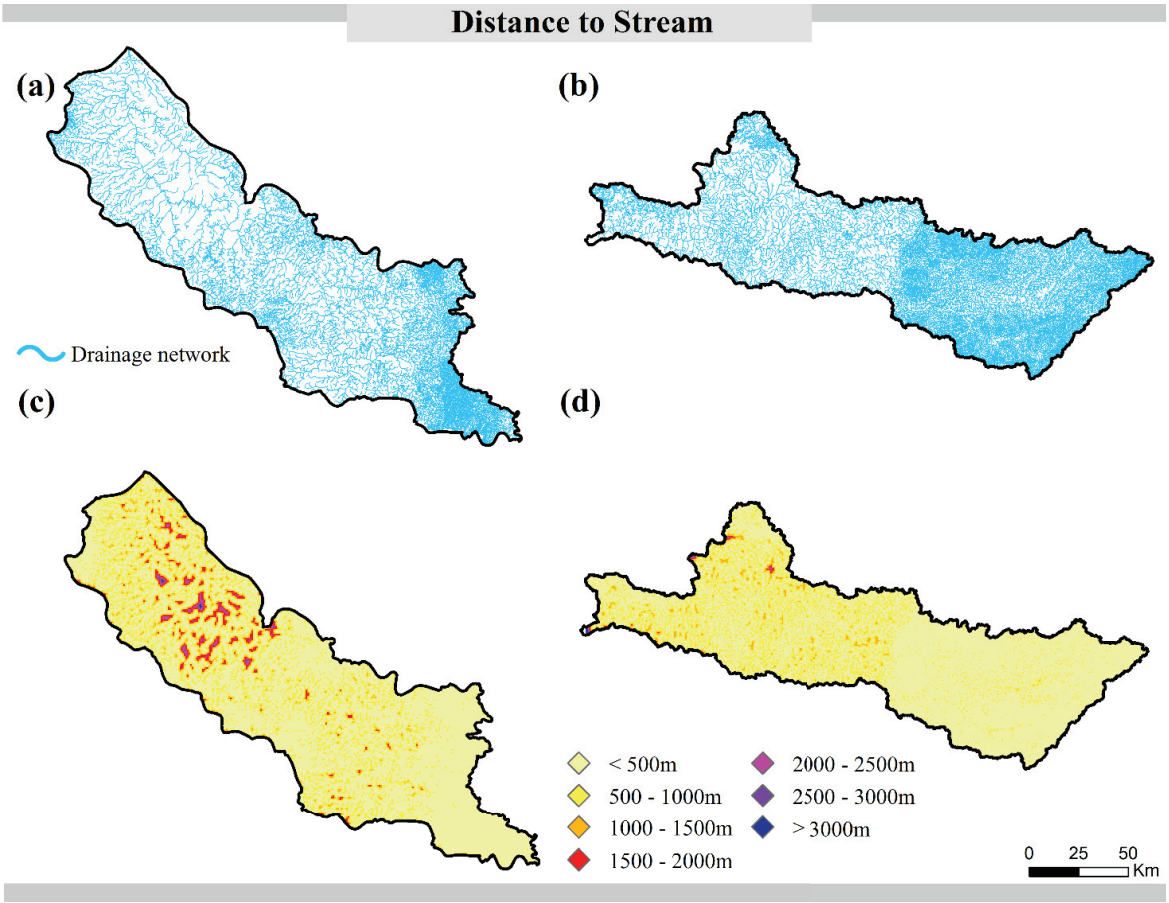


Figure 9. Drainage network map of UGRHI-09 (**a**) and PRB (**b**); distance to stream map of UGRHI-09 (**c**) and PRB (**d**).

2.2.4. Analytics Hierarchy Process (AHP)

At this stage, the AHP method was applied to consider environmental attributes regarding their influence on land suitability and surface runoff in the hydrographic region.

This method is widely used in environmental studies that require joint analyses of several factors, facilitating the interpretation and identification of their specificities.

Once the environmental attributes had been reprojected in accordance with the SIRGAS 2000 Datum, the weights for each class of attribute were defined. The weights were assigned by comparing the importance between the classes of each environmental attribute, as well as comparing the importance of the respective attributes considered in the preparation of agricultural suitability and surface runoff maps, respectively. At this stage, pairwise comparison matrices were created, as indicated below.

$$A = \begin{bmatrix} a_{11} & a_{12} & \cdots & a_{1n} \\ a_{21} & a_{22} & \cdots & a_{2n} \\ \vdots & \vdots & \vdots & \vdots \\ a_{n1} & a_{n2} & \cdots & a_{nn} \end{bmatrix}$$

Weights were assigned to each class of environmental attributes analyzed, as well as to each attribute, considering the hierarchical value scale established by [78] (Table 2).

Table 2. Hierarchical value scale for assigning weights.

Scale of Values			
Value	**Importance**	**Value**	**Importance**
1/9	Extremely less important	3	Moderate significance
1/7	Much less strongly important	5	Essential significance
1/5	Strongly less important	7	Very strong significance
1/3	Moderately less important	9	Extreme significance
1	Equal significance	2, 4, 6 and 8	Intermediate values

Scheme 78.

The weight was obtained by dividing each element by the sum of the elements in the same column to which it belongs and then calculating the arithmetic mean of all the columns to establish the final weight of each class and attribute. It is noteworthy that the aforementioned procedures were conducted for both the classes of each attribute and the set of attributes utilized in the construction of the LSC and SRPC. For instance, the influence of each slope class on land suitability and surface runoff was quantified and assigned a weight.

As an example, Tables 3 and 4 present, respectively, the pairwise comparison matrix between the slope attribute classes and the normalized matrix slope attribute, with the respective weights for each slope attribute class employed in the preparation of the two charts.

Table 3. Comparison matrix of slope classes.

Slope	**<2%**	**2–5%**	**5–10%**	**10–20%**	**20–30%**	**>30%**
<2%	1	2	3	5	7	9
2–5%	1/2	1	2	4	5	7
5–10%	1/3	1/2	1	3	4	6
10–20%	1/5	1/4	1/3	1	3	4
20–30%	1/7	1/5	1/4	1/3	1	3
>30%	1/9	1/7	1/6	1/4	1/3	1
Sum	2.29	4.09	6.75	13.58	20.33	30.00

The 2–5% slope class, which has similar characteristics to the less-than-2% class, received an intermediate value of 2 in the comparison matrix according to the Saaty scale. These classes contribute to low potential surface runoff and are at the same time favorable for agricultural management, in contrast to areas with steep slopes (e.g., >30%).

Table 4. Normalized matrix of slope attribute.

Slope	Normalized Matrix						Weight (W)
	<2%	2–5%	5–10%	10–20%	20–30%	>30%	
<2%	0.44	0.49	0.44	0.37	0.34	0.30	0.40
2–5%	0.22	0.24	0.30	0.29	0.25	0.23	0.26
5–10%	0.15	0.12	0.15	0.22	0.20	0.20	0.17
10–20%	0.09	0.06	0.05	0.07	0.15	0.13	0.09
20–30%	0.06	0.05	0.04	0.02	0.05	0.10	0.05
>30%	0.05	0.03	0.02	0.02	0.02	0.03	0.03
$W(<2\%) = 0.44 + 0.49 + 0.44 + 0.37 + 0.34 + 0.30/6$							

Subsequently, the assigned weights to the attribute classes and attributes were subjected to a consistency analysis, employing the Consistency Ratio (CR) (Equation (1)) and the Consistency Index (CI) (Equation (2)), as outlined by Saaty [78]. In order for the weights to be deemed appropriate, the CR must be less than 10%.

$$CR = \frac{CI}{RI} \tag{1}$$

where

CR = Consistency Ratio;
CI = Consistency Index;
RI = Random Consistency Index (Figure 10).

$$CI = \frac{(\lambda mx - n)}{(n - 1)} \tag{2}$$

where

n = number representing the order of the matrix;
$\lambda máx$ = maximum eigenvalue, defined using Equation (3).

$$\lambda mx = T \times W \tag{3}$$

where

T = normalized eigenvector;
W = sum of the columns of the comparison matrix for each attribute.

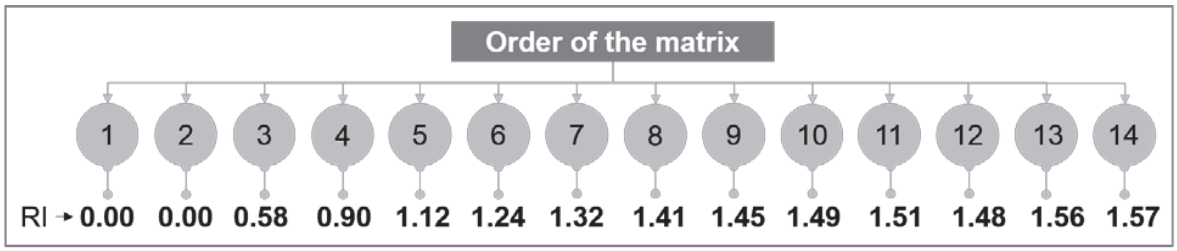


Figure 10. Random Consistency Index values considering the order of the matrix.

The criterion for establishing the weights is related to the physical characteristics of the classes that directly influence land suitability and surface runoff potential; i.e., regions with classes favorable to land suitability and surface runoff have higher weights, while the lower weights are represented by attribute classes that hinder agricultural practice (steep slopes, greater distance from a drainage channel, sandy-textured and shallow soils, etc.) and the runoff process (low slope, low drainage density, very deep soils, etc.). Tables 5 and 6 show the weights of the environmental attribute classes considered in the preparation of the LSC and SRPC, respectively.

Table 5. Weights of the classes of environmental attributes used to prepare the LSC.

Weights of the Classes of Environmental Attributes Used to Prepare the Land Suitability Chart							
Slope	<2%	2–5%	5–10%	10–20%		20–30%	>30%
Weights	0.40	0.26	0.17	0.09		0.05	0.03
Elevation	<600 m	600–800 m	800–1000 m	1000–1200 m	1200–1400 m	1400–1600 m	>1600 m
Weights	0.37	0.24	0.17	0.09	0.06	0.04	0.03
Distance to stream	<0.5 km	0.5–1.0 km	1.0–1.5 km	1.5–2.0 km	2.0–2.5 km	2.5–3.0 km	>3.0 km
Weights	0.37	0.24	0.17	0.09	0.06	0.04	0.03
Depth of groundwater level	<2 m	2–5 m	5–10 m	10–20 m	20–50 m	50–100 m	>100 m
Weights	0.03	0.04	0.06	0.09	0.17	0.24	0.37
Soils (Type)	Chernosols	Oxisols	Argisols	Gleisols	Nitisols	Organosols	Cambisols	Neosols
Weights	0.33	0.23	0.17	0.10	0.07	0.05	0.03	0.02
Soils (Thickness)	≥2 m		1–2 m		0.5–1 m		≤0.5 m	
Weights	0.47		0.28		0.17		0.08	
Soils (Texture)	Very clayey		Clayey	Average	Sandy		Indiscriminate	
Weights	0.43		0.27	0.17	0.09		0.04	
Land use and land cover	Coffee, sugar cane, citrus, other perennial crops, other temporary crops, soybean, and mosaic of uses				Pasture	Grassland formation, forest formation, savanna formation		
Weights	0.71				0.22	0.07		

Table 6. Weights of the classes of environmental attributes used to prepare the SRPC.

Weights of the Classes of Environmental Attributes Used to Prepare the Surface Runoff Potential Chart								
Slope	<2%		2–5%	5–10%	10–20%	20–30%		>30%
Weights	0.03		0.05	0.09	0.17	0.26		0.40
Drainage density	>3.5 km/km^2		2.5–3.5 km/km^2	1.5–2.5 km/km^2		0.5–1.5 km/km^2		<0.5 km/km^2
Weights	0.43		0.27	0.17		0.09		0.04
Geology	Aluviões, Aluvios-Coluviais, Aquidauana, Corpo D'Água Continental, Depósitos Aluvionares Holocênicos, Eleutério, Irati, Itararé, Marília, Tatuí, Terraços Holocênicos, Vale do Rio do Peixe			Andrelândia, Botucatu, Cobertura Detrito-Lateritica, Itaqueri, Pirambóia, Serra de São Gonçalo, Varginha-Guaxupé		Alacalino Poços de Caldas, Amparo, Corumbataí, Granito São Miguel Arcanjo, Granito-Gnaissico Taguar, Ortognaisse Serra Negra, Serra Geral		
Weights	0.49			0.31		0.20		
Soils (Type)	Chernosols	Oxisols	Argisols	Gleisols	Nitisols	Organosols	Cambisols	Neosols
Weights	0.33	0.23	0.17	0.10	0.07	0.05	0.03	0.02
Soils (Thickness)	≥2 m		1–2 m	0.5–1 m		≤0.5 m		
Weights	0.08		0.17	0.28		0.47		
Soils (Texture)	Very clayey		Clayey	Average		Sandy		Indiscriminate
Weights	0.43		0.27	0.17		0.09		0.04
Land use and land cover	Mining and other non-vegetated areas		Sugar cane	Coffee, citrus, soybean, mosaic of uses, other perennial crops, other temporary crops, and pasture		Urban areas and forest plantation		Rocky outcrop, wetland, grassland formation, forest formation, savanna formation, rivers, and lake
Weights	0.43		0.27	0.17		0.09		0.04

The same procedures were carried out for the other attributes separately, as exemplified for the slope attribute. The same method was employed to assign the final weights to the set of attributes used in the LSC and the SRPC. Figure 11 shows the normalized matrices made up of all the environmental attributes used to draw up the LSC and SRPC.

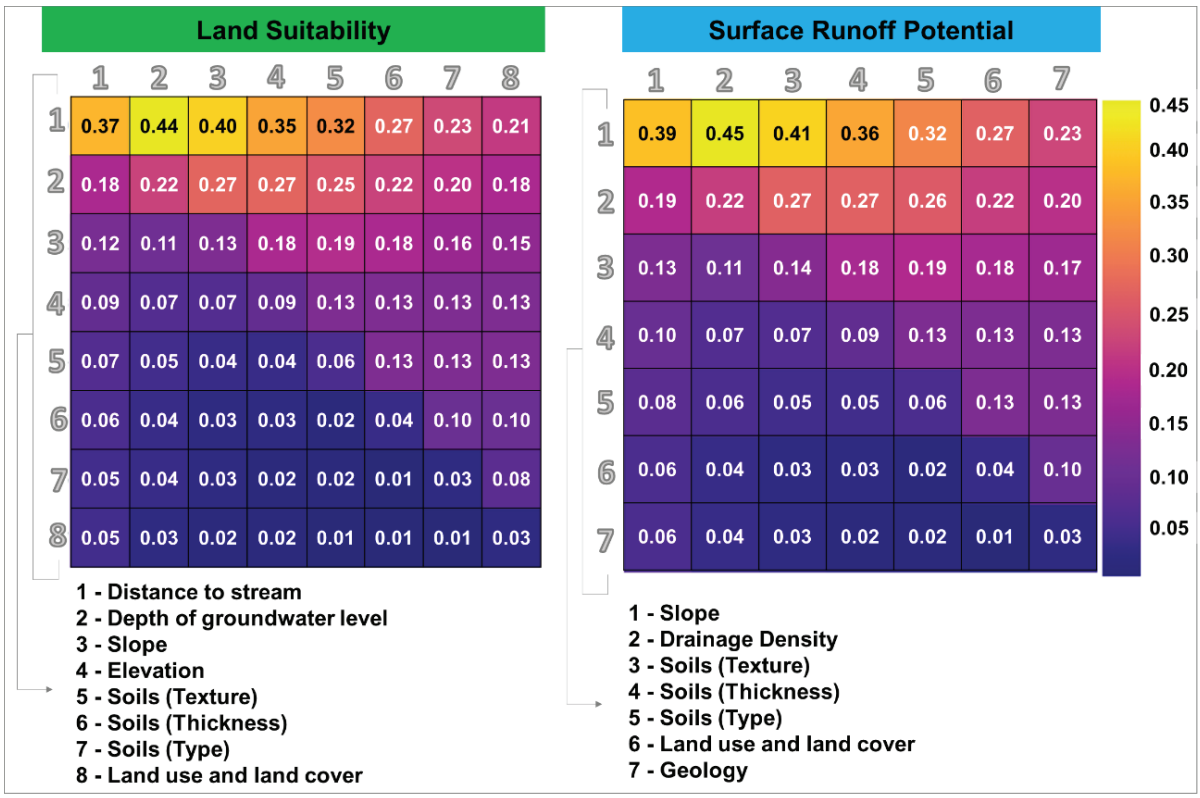


Figure 11. Normalized matrices considering the environmental attributes of the LSC and the SRPC.

Figure 12 illustrates the final weights assigned to the environmental attributes utilized in the production of the interpretive cartographic products. It was necessary to utilize disparate sets of environmental attributes to generate the LSC and SRPC, as each cartographic document is designed to represent the areas under study in a specific manner. Consequently, the final weights assigned to each environmental attribute reflect the importance of each attribute in terms of land suitability and potential surface runoff. However, it is noteworthy that the assignment of final weights for the two maps was conducted in accordance with the procedures outlined in this section.

2.2.5. Analysis of Climate Variables

The LSC and SRPC were constructed using physical attributes that are relatively stable in the short and medium term. Consequently, in this study, the analysis of these two cartographic products was compared with the difference between actual evapotranspiration (ETa) and rainfall in order to identify relationships with the levels of agricultural suitability and surface runoff in the two areas under investigation.

The ETa data are produced using the Simplified Surface Energy Balance (SSEBop) operational model [79], which are obtained annually from the Famine Early Warning Systems Network (FEWS NET) platform. The estimation of ETa by the SSEBop model uses the evapotranspiration fraction—ETf (which varies from 0 to ~1)—based on air temperature and surface temperature data obtained from remote sensing images. The ETf is then multiplied by the reference evapotranspiration (ETr), usually estimated by the Penman–Monteith method for a grass surface in the region of interest. Precipitation was obtained from the Climate Hazards Group InfraRed Precipitation with Station data (CHIRPS) dataset, which

uses data from rain gauges and observations captured by orbital sensors. Precipitation data were also obtained on an annual basis.

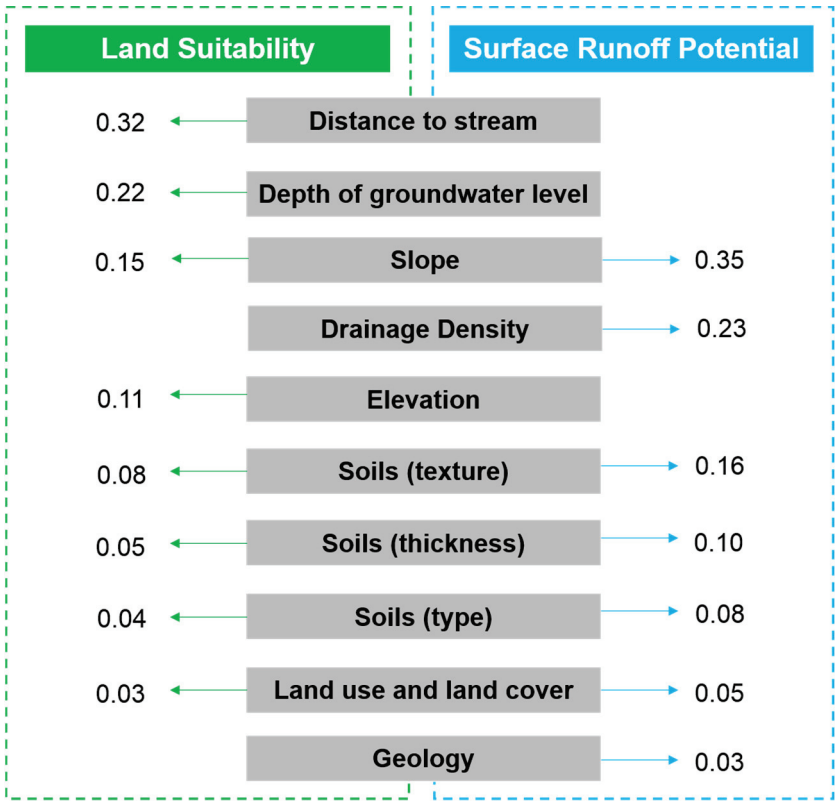


Figure 12. Final weights of environmental attributes used to prepare interpretative cartographic products.

The data on the two climatic variables were obtained for the areas under study between 2013 and 2022. Once the data had been acquired, the Raster Calculator tool was used to calculate the sum and then the arithmetic mean of the ETa and rainfall, with consideration given to the established periods.

Subsequently, the mean decadal ETa was subtracted from the mean decadal rainfall, thus enabling the identification of the relationship between climatic variables, land suitability, and potential runoff levels. This approach facilitated the validation of the regions most conducive to irrigation.

2.2.6. Joint Analysis of Interpretative Cartographic Products

This stage comprised an integrated analysis of the cartographic products, specifically the LSC and PSRC. The agricultural suitability classes were correlated with the surface runoff classes in the ArcGIS® software, revealing that the classes on the first chart correlated with all the classes on the second chart, with the exception of the very-low-suitability class of the PRB, which correlated with the first four surface runoff classes of this unit.

In this way, the areas that present very high and high agricultural aptness and very low and low surface runoff were separated, in order to indicate the potential areas that can adopt the practice of reusing treated wastewater from agro-industrial sources in irrigation, considering the specificities of each location in the UGRHI-09 and the PRB.

These classes were selected because their locations have potential for cultivation; however, they have low levels of surface runoff, and this last factor generally means that these areas have a higher infiltration rate for aquifer recharge. In this case, potential arable areas may have a greater need for irrigation from a supplementary source of water, especially during the dry season. Figure 13 illustrates the descriptions of potential areas for adopting the practice of reusing treated wastewater from agro-industrial sources.

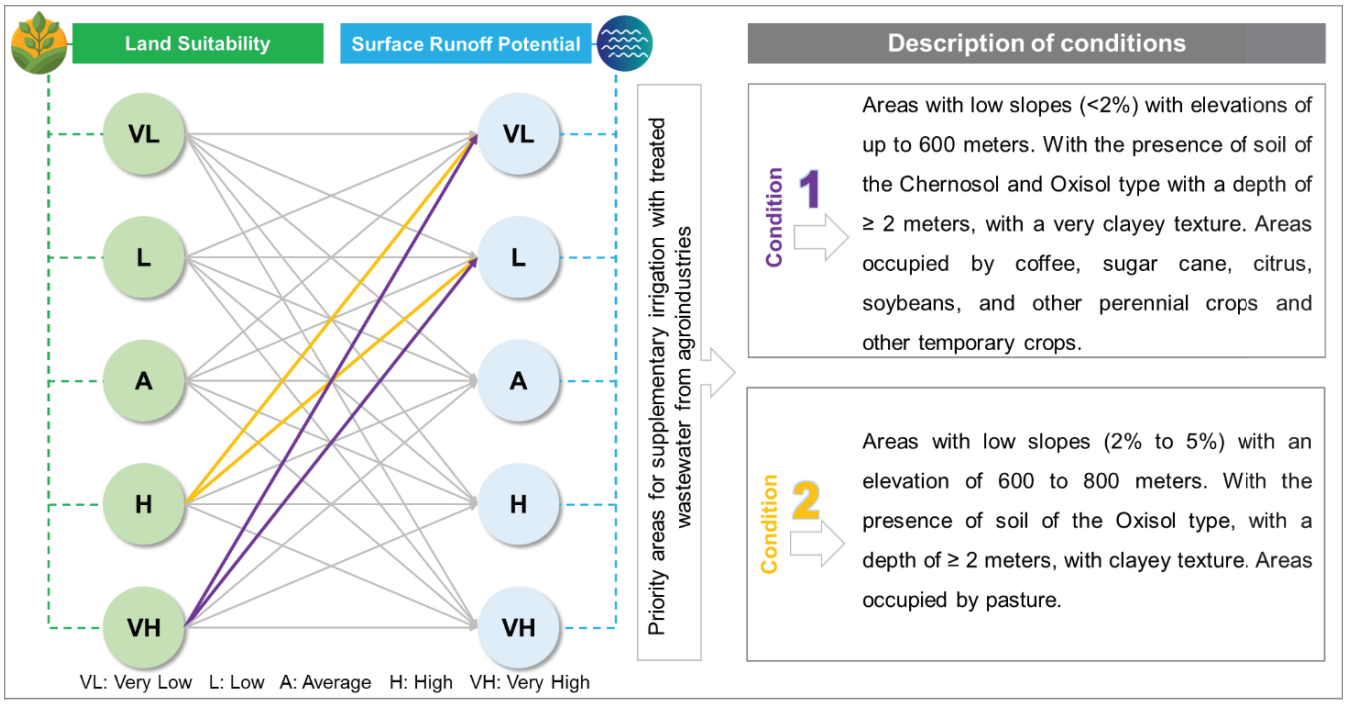


Figure 13. Descriptions of potential areas for the reuse of treated wastewater from agro-industrial sources in irrigation.

3. Results

3.1. Analysis of Inapt Areas for Agricultural Production

The UGRHI-09 area has an agricultural character and is therefore considered an important supply region in the state of São Paulo. The PRB is also an important region, as it has a well-developed industrial complex and is home to a large population. In addition, the PRB transfers part of its water supply to supply part of the metropolitan region of the city of São Paulo (Brazil's most populous city). Thus, with the intention of assisting development linked to environmental issues, in order to avoid inappropriate occupation in areas that require protection, the map of inapt areas for agricultural production in the areas studied was created (Figure 14a,b).

Inapt areas account for 22% and 39% of the total extension of the UGRHI-09 and PRB, respectively. These areas do not have potential for agricultural occupation; those areas are protected by environmental legislation, for natural resource preservation in vegetated areas along water courses (PPAs), for biodiversity maintenance in CUs, and for the preservation of cultural assets found in archeological sites. Consolidated areas, such as urbanized areas, were also considered inapt areas.

Consolidated areas, especially aerodromes, rocky outcrop areas, and areas with use restrictions due to high slopes (slope between 25° and 45°), have small extents within UGRHI-09 and PRB. Regarding urbanized areas, those with the largest population centers are located in the eastern region of the UGRHI-09. However, the PRB has more than twice as many urban areas as the UGRHI-09, corresponding to 949.26 km^2. These areas are distributed throughout the PRB, but the most prominent urban conglomerations are in the central part of the PRB, where the metropolitan region of the city of Campinas is located.

The CUs considered in the mapping of inapt areas in the UGRHI-09 and PRB were those of integral protection. According to Brazilian legislation (Law no. 9985/2000), these areas aim to preserve nature, with indirect use of natural resources permitted. UGRHI-09 has six CUs, including one biological reserve, two ecological stations, and three state parks, covering around 131 km^2. The PRB has five CUs, two of which are ecological stations, two are state parks, and one is a natural monument, totaling an area of 86.27 km^2.

Table 7 shows the specific characteristics of each category of CUs according to the country's environmental legislation.

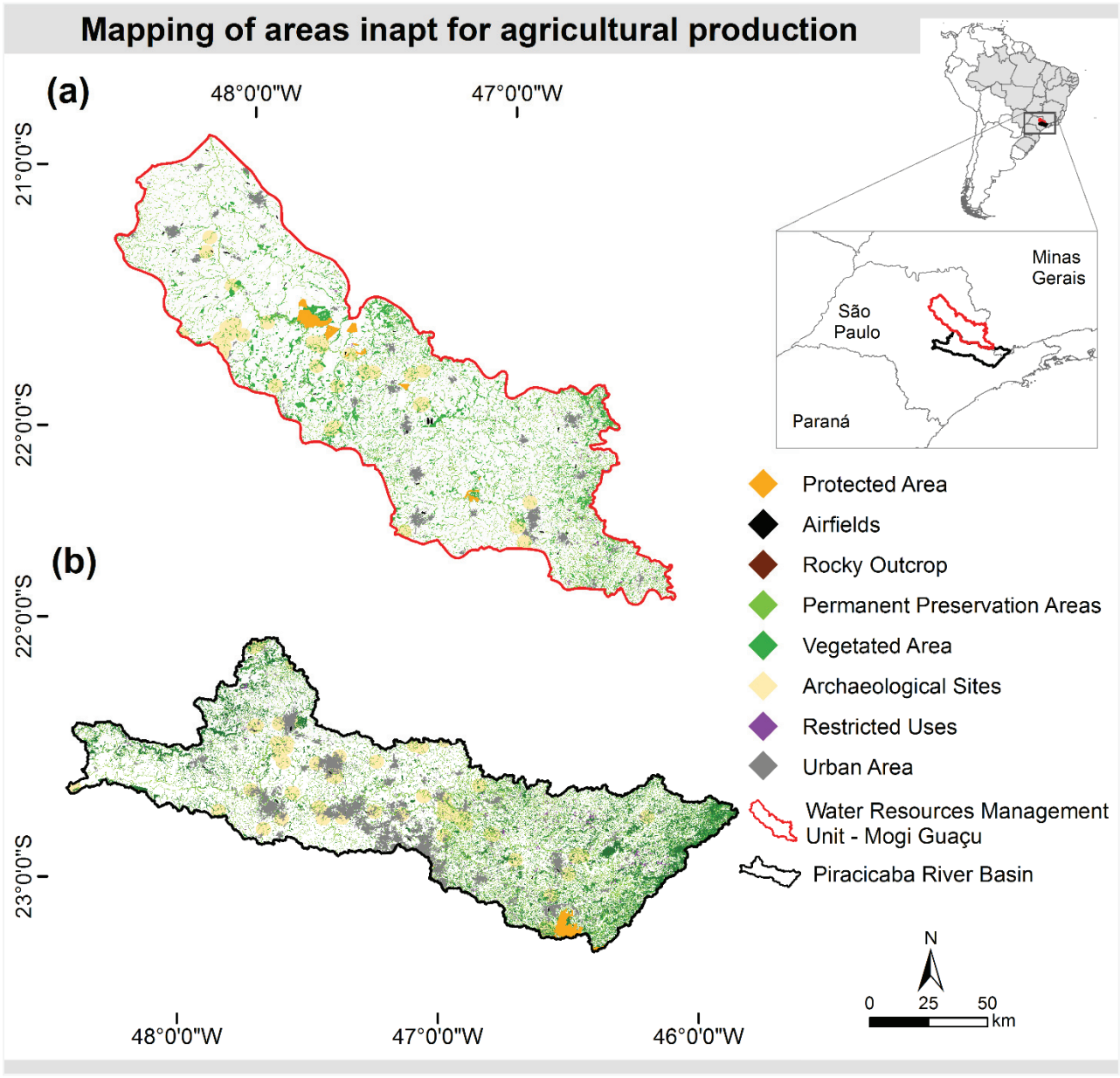


Figure 14. Map of inapt areas at UGRHI-09 (**a**) and PRB (**b**).

The vegetated areas are composed of forest, savanna, and Campestre formations, distributed by UGRHI-09 and PRB. The two study areas are characterized by a predominance of forest formation, corresponding to 2235.11 km^2 (UGRHI-09) and 1698.74 km^2 (PRB). According to [80], the suppression of native vegetation by agricultural cultivation and pastures interferes with the functional diversity of plants and ecosystem functions, such as pollination and seed dispersal; thus, the preservation of native forests is essential for the environmental balance of a certain region. Permanent preservation areas consist of protected areas with or without the presence of native vegetation cover, which border watercourses and springs; among their objectives are to avoid silting of water bodies, preserve the landscape, facilitate fauna and flora gene flow, preserve biodiversity, and protect the soil [81].

Table 7. Specific characteristics of the categories of CUs in the areas studied.

Categories of CUs (Integral Protection)	Specific Characteristics *
Biological Reserve	The objective of the reserve is the integrated conservation of the biota and other natural attributes within its boundaries, without direct anthropogenic intervention or environmental modification. Public access is prohibited within the reserve, except for educational visits.
Ecological Stations	The area in question is in the public domain and its objective is to preserve nature and carry out scientific research. Public visitation is also forbidden, being permitted only for educational purposes. In this category of CUs, modifications to ecosystems are permitted in the case of measures that promote the restoration of modified ecosystems; species management with the aim of preserving biological diversity; the collection of ecosystem components for scientific purposes; and scientific research in an area of a maximum of three percent of the total extension of the CU, and up to a limit of one thousand and five hundred hectares.
State Parks	The objective of the park is to conserve natural ecosystems of great ecological importance and scenic beauty, to allow scientific research and the development of educational activities and environmental interpretation, as well as recreation and ecotourism.
Natural Monument	The objective of this category of CU is the preservation of rare and unique natural sites or sites of significant scenic beauty. It is possible for this category of CU to be located in private areas, provided that the objectives of the unit can be made compatible with the use of the land and natural resources of the site by the owners.

* Chapter III—The categories of Conservation Units of Law no. 9985/2000 [51].

Clearly, there is a strong relationship between the native vegetation around the springs and the freshwater ecosystems. This relationship interferes both in the functioning and structure of the streams, and helps to maintain ecological functions. The authors of [82] found that streams close to sugarcane crops had less shade and protection, and streams close to forested areas had riparian forests along the channel. In these regions, no occurrences of erosion or silting were found. The authors of [83] concluded that the conservation of riparian forests reduces the impacts of agricultural crops, increases litter, and also regulates water temperature. Therefore, these factors together provide an increase in richness and taxonomic diversity.

Regarding archeological sites, protection zones were delimited considering a 3 km radius. These areas are concentrated in the central portion of the UGRHI-09, further away from the large urban perimeters. Meanwhile, in the PRB, the areas that represent the protection zone for this attribute are close to and within the boundaries of some cities; this situation is due to the characteristics of each area studied.

3.2. Environmental Attribute Analysis Regarding Land Suitability and Surface Runoff Potential

UGRHI-09 predominantly presents areas with gentle slopes (<2% to 10%), corresponding to 69.7% of the total area, well distributed throughout the unit's area. The steepest slopes and highest altitudes are found at the east end of the unit. Meanwhile, the PRB has a predominance of areas with slopes between 5 and 20%, comprising 52% of the basin's total area. The areas with the steepest slopes (>30%) are also more prevalent in the far east of the PRB, where altitudes of over 1000 m are more frequent, occupied by forestry, where agricultural activity is less significant. According to [84], higher altitudes tend to present greater precipitation volumes and increased temperatures, directly affecting the development and agricultural production of some crops. According to [85,86], relief is responsible for redistributing climate resources, as well as affecting the activity and phenology of vegetation.

The eastern region of the unit has greater potential for tourism, due to the existence of the São Paulo water circuit (hot springs, waterfalls, dams, lakes), which stands out for its thermal waters and mineral properties. The circuit is made up of nine municipalities; among them, Águas de Lindóia, Lindóia, Serra Negra, and Socorro are located in UGRHI-09. In this region, the drainage is dendritic and has characteristics typical of reliefs derived from folded structures, with parallel quartzite and gneissic ridges and subsequent valleys (orthoclinal) [87].

Furthermore, the slope has a direct influence on soil thickness and high potential for nutrient leaching [88]. The extreme east of the studied areas, despite being favored in water availability, presents a quite rugged relief, meaning that agricultural practice did not develop, due to the difficulty in using machinery and soil management. Land with a slope up to 5° is suitable for agricultural production, as opposed to land with a slope greater than 25°, considered unsuitable for cultivation [84].

In addition, the depth of the groundwater level in the eastern region of the two areas studied varies between 10 and 20 m, which would also make it impossible to have high agricultural suitability. Particularly in the eastern region of UGRHI-09, in the Lindóia region, wells located in areas with gneiss show the highest yields, followed by areas composed of migmatite and mylonite. The wells with the lowest yields are located in areas of granite and granitoid, regions with a low degree or absence of fracturing [89].

In relation to the western region of the UGRHI-09, it presents high agricultural aptness (Figure 15a), with the presence of Oxisols with depths greater than 2 m, with clay as the predominant fraction in its composition, which demonstrates the existence of less permeable surfaces, favoring surface runoff [25]. However, these areas have gentler slopes, which makes it easier for water to infiltrate the soil, potentially resulting in a scenario dependent on irrigation, especially during the dry season. In addition to natural characteristics, soil management such as the liming process to correct the pH of acidic soils can also interfere with surface runoff. This practice can reduce the diameters of larger pores, and consequently increase the specific surface area, favoring flow on the ground surface [90].

The western portion of the PRB is characterized by a predominantly medium level of land suitability. This is associated with the existing soil texture, which varies from medium to sandy. In addition, other locational characteristics also interfere with the suitability of the reuse practice, such as distance from the nearest drainage channel, altitude, and land use and cover (Figure 15b). The central region of the PRB is characterized by areas inapt for agricultural production, including urban areas, protection zones for archeological sites, and permanent preservation areas on the banks of watercourses.

The central-eastern portion of the UGRHI-09 presents low aptness for irrigated agriculture. Even though the soil presents suitable properties for cultivation, Oxisol with deep thickness, and altitudes of less than 600 m, the main factor that influences the aptness of this area is the distance to the watercourse, greater than 3.0 km.

The distance to a water course is considered one of the most important parameters in the aptness of the land when applying surface irrigation, as it indicates the extent of the surface close to rivers with permanent flow [36]. According to [29], when there is a significant distance from streams and rivers from agricultural areas, these are more likely to have lower soil moisture content; therefore, the distance from the river connection is a fundamental factor in increasing agricultural productivity. Furthermore, soil quality may be influenced by proximity to rivers [91].

Therefore, the reuse of treated wastewater should be considered in irrigation, as it is a low-cost resource, in addition to being more accessible, compared to water transfers over greater distances, which are normally more expensive [92], due to the need for specific infrastructure. Furthermore, it may compromise the supplying region at some point, due to the high resource exploitation. Treated wastewaters can be a source of a stable supply of nutrients (nitrogen, phosphorus, and potassium) and organic matter that are fundamental for soil fertility [93].

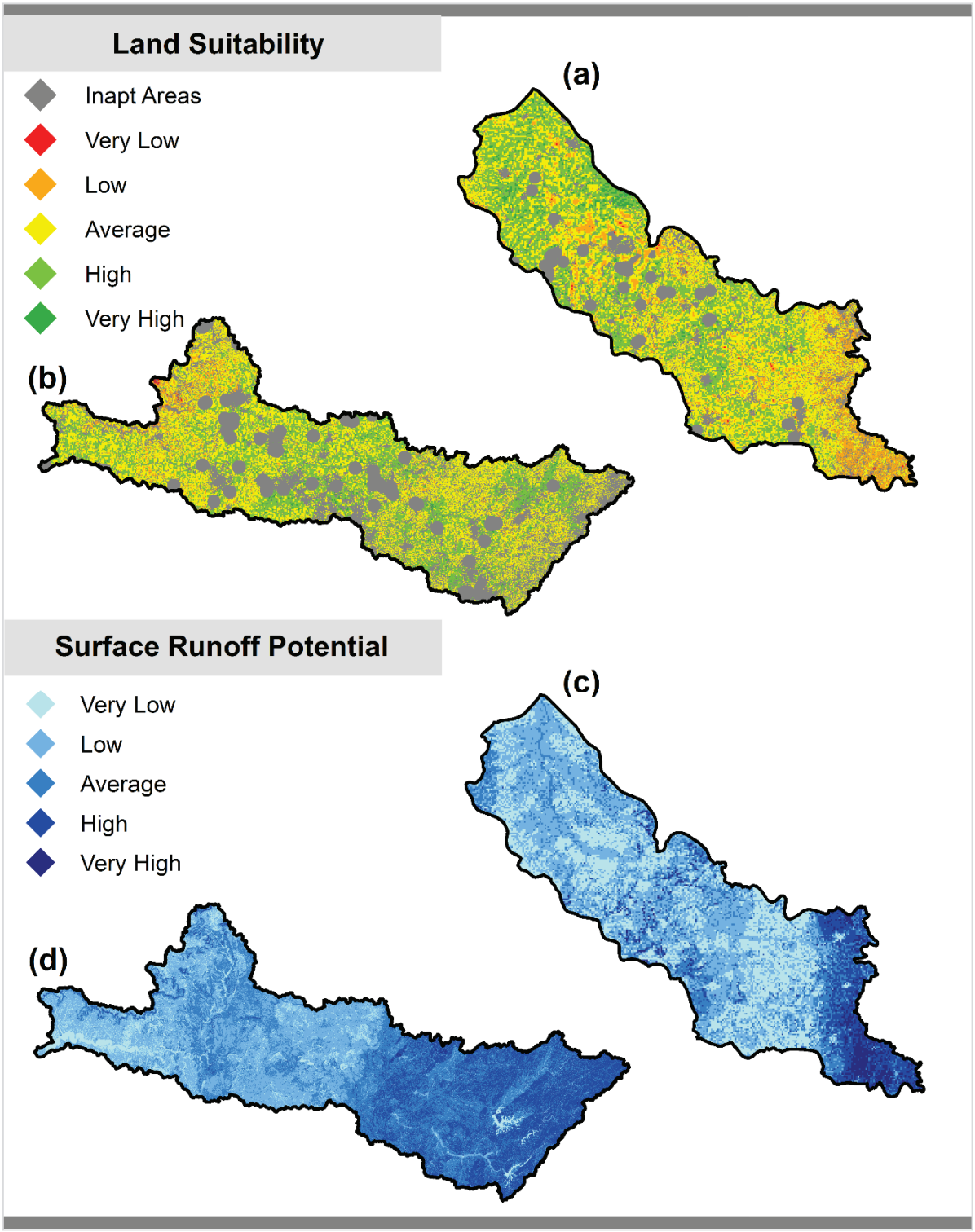


Figure 15. UGRHI-09 Land Suitability Chart (**a**), PRB Land Suitability Chart (**b**), UGRHI-09 Surface Runoff Potential Chart (**c**), and PRB Surface Runoff Potential Chart (**d**).

Very-high-agricultural-aptness areas are distributed across the UGRHI-09 to minor extents, corresponding to 231.9 km^2 of the total area. They are mainly located in areas with altitudes below 600 m, with soils with a predominantly clayey texture in gently undulating relief. The depth of the groundwater level varies from 10 to 50 m in these regions. The nearest distance to a surface drainage channel is generally less than 0.5 km. This region has low potential for surface runoff (Figure 15c), due to the influence of low drainage density, ranging from less than 0.5 $km \cdot km^{-2}$ to 1.5 $km \cdot km^{-2}$. Drainage density has an opposite functionality to permeability, and is related to the distance between channels. An area with lower drainage density results in less runoff, presenting a greater infiltration of water into the subsoil [94]; it is also noticeable in the western region of the PRB.

As in this work, the study by [95], conducted in the Tabuk basin (Saudi Arabia), also found low drainage density in the area (<1.5 km/km^2); this characteristic reflects high surface permeability, and consequently, low surface runoff, facilitated by the sedimentary cover, the articulated and fractured igneous rocks, and the Quaternary sediments existing in the basin.

Taking into account the areas in the eastern portion of the PRB, these are regions with a higher drainage density when compared to its western region, which has a more sparse drainage network. It should be noted that this region has a high drainage density due to its physical characteristics; due to the existence of a crystalline rocky substrate and the high slope of the terrain, this environmental configuration allows for greater surface runoff (Figure 15d) [47,96]. However, agricultural use in areas with a more pronounced slope is prone to the loss of nutrients through surface runoff, which could have adverse effects on downstream water bodies [97]. Consequently, the highest levels of surface runoff in the PRB, which account for 22% of the total area, are observed in regions with medium agricultural suitability.

Drainage density values can vary greatly, as they will depend on the intrinsic physical characteristics of each region, such as climatic variables, soil properties, and geological units, as well as slope and soil use and coverage.

A comparative analysis of the climatic variables (average accumulated rainfall and average real evapotranspiration over a 10-year period) reveals that the two areas under study exhibit a comparable rainfall regime. In the easternmost regions of the study area, average rainfall volumes exceed 1400 mm per year (Figure 16a), accompanied by elevated levels of potential surface runoff. This phenomenon is linked to the physical characteristics and land use and cover patterns observed in these areas.

With regard to ETa for the period analyzed, the two areas studied stand out with a predominance of the 700 to 900 mm range (Figure 16b), in regions with temporary and permanent crops. The regions with an ETa of less than 500 mm include urbanized areas.

The relationship between rainfall and evapotranspiration is well known in agricultural and environmental studies [47,98,99]. In this study, the difference between the two variables showed that the areas studied for the periods analyzed did not present a water deficit. Figure 16c shows the difference between average accumulated rainfall and average ETa (2013 to 2022).

The UGRHI-09 region exhibits a greater prevalence of water surplus in the 300 to 500 mm range. These regions are predominantly characterized by medium to very high agricultural suitability, and have the potential to adopt the practice of reusing treated wastewater from agro-industries.

The western part of the PRB exhibits a greater prevalence of agricultural activities, which contributes to a lower water surplus compared to other regions within the basin. This region is predominantly occupied by pastures, sugar cane, and citrus, and is characterized by a medium level of agricultural suitability. In the majority of the PRB, the water surplus falls within the 500 to 700 mm range.

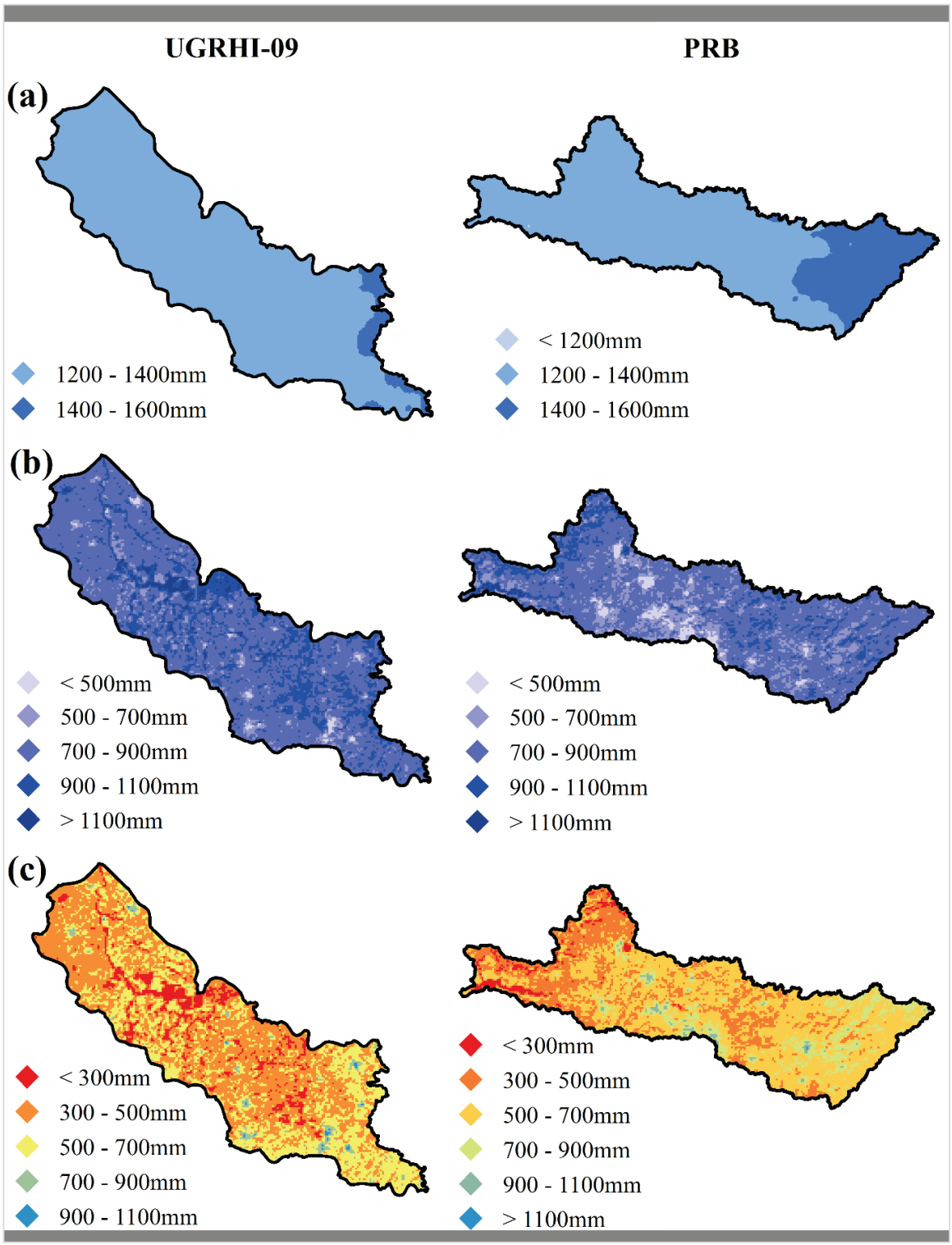


Figure 16. Decadal average rainfall (2013 to 2022) (**a**), decadal average actual evapotranspiration (2013 to 2022) (**b**), and the difference between the decadal average rainfall and the decadal average actual evapotranspiration (**c**).

3.3. Integrated Analysis of Cartographic Products to Determine Areas with Potential for Treated Wastewater Reuse

Changes in climate can make access to water for irrigation difficult, negatively affecting the agricultural sector [100]. In this sense, aiming to meet target 2.3 of the second SDG (Zero Hunger and Sustainable Agriculture) and target 6.3 of the sixth SDG (Drinking Water

and Sanitation), an integrated analysis was carried out between agricultural suitability and the potential for surface runoff to identify which regions can adopt the practice of reusing treated wastewater in the irrigation process, with the intention of helping small producers. Small-scale irrigation has been seen as sustainable agriculture, to increase production and reduce the effects of the climate crisis [101].

Many studies have used the reuse of treated wastewaters for irrigation [1,15,102–105]; however, no comprehensive analyses, considering the various aspects of the physical environment, were presented. The present work presents this analysis.

It is important to know and define which areas of a hydrographic region are potentially capable of developing and producing crops, based on the knowledge of soil thickness and texture, geological groups, and formations, slope, hypsometry, water level depth, distance from the channel nearest to the drainage system, and surface runoff.

After the elaboration and analysis of the interpretative products of aptness for rural production and potential for surface runoff, two conditions were considered. The first consists of areas with gentle terrain slopes (<2%), with altitudes of up to 600 m. This is with the presence of soil of the Chernosol type, with a very clayey texture and depth $\geq$2 m. Regarding the second condition, areas with low slopes (2% to 5%) stand out, with altitudes between 600 and 800 m. This is with the presence of soil of the Oxisol type, with a depth of $\geq$2 m, with a clayey texture. Thereby, the total area of the UGRHI-09 suitable for receiving treated wastewater considering the aptness of the land and surface runoff in condition 1 corresponds to 3373.24 km^2, while in condition 2, it consists of 286.07 km^2. The total area of the two conditions represents 24.28% of the territorial extension of UGRHI-09. The areas are most prominently located in the northwest and central-east portion of the unit (Figure 17a).

With regard to the PRB, the potential areas for the reuse of treated wastewater from agro-industries in the PRB total 1500.94 km^2, comprising 11.86% of the basin's total area. The first condition is taken into account, and it is found that the area in question covers 1447.83 km^2, where there is a predominance of red Oxisol, red-yellow Oxisol, red Argisol, and red-yellow Argisol soils. These are characterized as deep and very deep, with a texture ranging from medium to clayey. These regions are predominantly occupied by sugar cane, which is mainly used to produce ethanol. As in UGRHI-09, the second condition is less common, covering no more than 53.11 km^2 (Figure 17b), and is found in regions where the soil has a higher clay fraction and thicknesses of more than 2 m.

It is important to note that while the potential areas of the UGRHI-09 and PRB have characteristics that make it feasible to reuse wastewater from agro-industrial sources after treatment, these waters must not contain any heavy metals or other chemical elements that affect irrigation water or soil [6].

According to [106], to implement wastewater reuse, a comprehensive approach is needed, taking into account several factors, including environmental aspects. In this way, the result achieved in this research can be used as a subsidy for managers and planners in the creation of public policies on the reuse of treated wastewater in agriculture, with the aim of reducing the demand on surface and underground water, in addition to avoiding the dumping of wastewaters in receiving water bodies, indicating an alternative combined with the circular economy. As a result, new policies based on the circular economy can achieve a "paradigm shift", proposing a more sustainable model in wastewater management with better resource use [106].

To develop public policies aimed at establishing specific guidelines for these areas, it is necessary to have prior knowledge of the phenological stages of the crops to be planted, and the physical, chemical, and biological properties of the soils and treated wastewater, as well as an understanding of the rainfall regime in the areas, due to climate change.

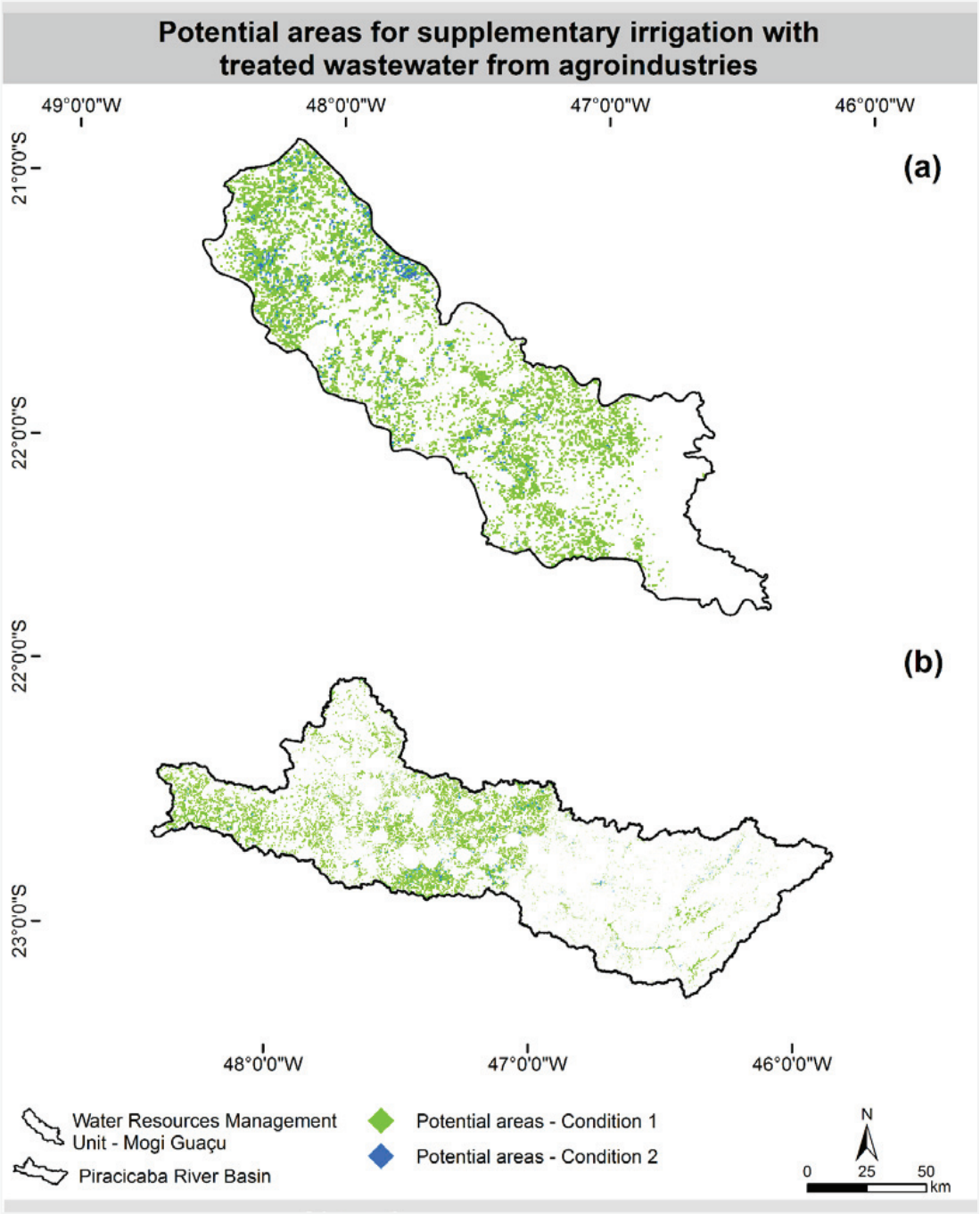


Figure 17. Potential areas in UGRHI-09 (**a**) and PRB (**b**) for adopting the practice of reusing treated wastewater from agro-industries.

4. Conclusions

Changes in the environment as a result of human actions encourage the adoption of sustainable practices throughout the production chain, especially in agriculture. In this study, the mapping of land suitability and the classification into levels of potential surface runoff in two hydrographic regions with consolidated agriculture were presented, which can be used as indicators for the adoption of the practice of reusing treated wastewater from an agro-industrial source for irrigation.

The multivariate analysis facilitated a more effective interaction between the attributes under study, enabling the identification of locations exhibiting favorable conditions (comprising 24.28% of the UGRHI-09 area and 11.86% of the PRB area) for the implementation

of wastewater reuse. It is noteworthy that the integrated analysis of physical characteristics contributed positively to the specialization of agricultural areas. However, a limiting factor was the lack of availability of data at the same mapping scale. This situation is acceptable for studies of this type, but the creation of a thematic geospatial database with higher resolutions and a consistent scale would improve the cartographic quality of the products to be produced. When applying AHP, future work should take into account the experience and knowledge of farmers, technicians, and extension workers, as the social dimension is very important in management and decision making.

The western region of the two areas under study displays a greater propensity for the adoption of this sustainable practice, where the terrain properties are conducive to soil management and more intensive agricultural activities. However, in the easternmost regions of the UGRHI-09 and PRB, despite greater water availability, the physical characteristics directly influence agricultural practices. For instance, surface slope plays a role in this region of the UGRHI-09, where there is greater tourist exploitation, and in the PRB, where larger forest fragments are important for the regional microclimate.

The methodology adopted in this work can be reapplied to other hydrographic regions of the world, to promote better use of water, especially in regions that suffer from water scarcity. It is worth mentioning, however, that beyond mapping, physical and chemical analyses of the treated wastewater, as well as the soil, are essential for the effective adoption of the reuse practice.

The cartographic products created in this work are easy to read and aim to assist managers and planners in the formulation of public policies aimed at areas' suitable reuse of treated wastewater from agro-industrial sources in irrigated agriculture, eliminating obstacles to the implementation of this practice, and promoting a broad conservation and maintenance of water resources.

Author Contributions: Conceptualization, A.P.P.C., A.C.P.C., M.Y.K.N., F.R., G.T. and T.M.G.; methodology, A.P.P.C., A.C.P.C., F.R. and T.M.G.; software, A.P.P.C. and A.C.P.C.; validation, A.P.P.C., A.C.P.C., M.Y.K.N., F.R., G.T. and T.M.G.; formal analysis, A.P.P.C., A.C.P.C., M.Y.K.N., F.R., G.T. and T.M.G.; investigation, A.P.P.C., A.C.P.C., F.R. and T.M.G.; data curation, A.P.P.C. and A.C.P.C.; writing—original draft preparation, A.P.P.C., A.C.P.C., M.Y.K.N., F.R., G.T. and T.M.G.; writing—revision and editing, A.P.P.C., A.C.P.C., M.Y.K.N., F.R., G.T. and T.M.G.; visualization, A.P.P.C. and A.C.P.C.; supervision, T.M.G. All authors have read and agreed to the published version of the manuscript.

Funding: This research received no external funding. The APC was funded by Luiz de Queiroz Agricultural Studies Foundation (Fealq).

Data Availability Statement: The original contributions presented in the study are included in the article, further inquiries can be directed to the corresponding author.

Acknowledgments: The authors thank the Rectory of the University of São Paulo for the postdoctoral fellowships in the USP Sustainability Program, for the authors Ana Claudia, Ana Paula, and Mirian. The authors would also like to thank the Luiz de Queiroz Agricultural Studies Foundation (Fealq) for its financial support for the publication of this article.

Conflicts of Interest: The authors declare that they have no known competing financial interests or personal relationships that could have appeared to influence the work reported in this paper.

References

1. Gonçales Filho, M.; Nunhes, T.V.; Barbosa, L.C.F.M.; de Campos, F.C.; de Oliveira, O.J. Opportunities and Challenges for the Use of Cleaner Production to Reduce Water Consumption in Brazilian Sugar-Energy Plants. *J. Clean. Prod.* **2018**, *186*, 353–363. [CrossRef]
2. Carvalho, A.P.P.; Lorandi, R.; Collares, E.G.; Di Lollo, J.A.; Moschini, L.E. Potential Water Demand from the Agricultural Sector in Hydrographic Sub-Basins in the Southeast of the State of São Paulo-Brazil. *Agric. Ecosyst. Environ.* **2021**, *319*, 107508. [CrossRef]
3. Hsien, C.; Low, J.S.C.; Chung, S.Y.; Tan, D.Z.L. Quality-Based Water and Wastewater Classification for Waste-to-Resource Matching. *Resour. Conserv. Recycl.* **2019**, *151*, 104477. [CrossRef]
4. Paul, M.; Negahban-Azar, M.; Shirmohammadi, A.; Montas, H. Assessment of Agricultural Land Suitability for Irrigation with Reclaimed Water Using Geospatial Multi-Criteria Decision Analysis. *Agric. Water Manag.* **2020**, *231*, 105987. [CrossRef]

5. Chen, Z.; Wu, Q.; Wu, G.; Hu, H.Y. Centralized Water Reuse System with Multiple Applications in Urban Areas: Lessons from China's Experience. *Resour. Conserv. Recycl.* **2017**, *117*, 125–136. [CrossRef]
6. Burak, S.; Samanlioglu, F.; Ulker, D.; Kup, E.T. Ranking Willingness to Reuse Water in Cotton Irrigation with Hybrid MCDM Methods: Soke Plain Case Study. *Agric. Water Manag.* **2024**, *301*, 108920. [CrossRef]
7. Singh, A. A Review of Wastewater Irrigation: Environmental Implications. *Resour. Conserv. Recycl.* **2021**, *168*, 105454. [CrossRef]
8. Jones, E.R.; Van Vliet, M.T.H.; Qadir, M.; Bierkens, M.F.P. Country-Level and Gridded Estimates of Wastewater Production, Collection, Treatment and Reuse. *Earth Syst. Sci. Data* **2021**, *13*, 237–254. [CrossRef]
9. Ahmadi-Jouibari, T.; Ahmadi Jouybari, H.; Sharafi, K.; Heydari, M.; Fattahi, N. Assessment of Potentially Toxic Elements in Vegetables and Soil Samples Irrigated with Treated Sewage and Human Health Risk Assessment. *Int. J. Environ. Anal. Chem.* **2021**, *103*, 2351–2367. [CrossRef]
10. Woltersdorf, L.; Zimmermann, M.; Deffner, J.; Gerlach, M.; Liehr, S. Benefits of an Integrated Water and Nutrient Reuse System for Urban Areas in Semi-Arid Developing Countries. *Resour. Conserv. Recycl.* **2018**, *128*, 382–393. [CrossRef]
11. Partal, R.; Basturk, I.; Murat Hocaoglu, S.; Baban, A.; Yilmaz, E. Recovery of Water and Reusable Salt Solution from Reverse Osmosis Brine in Textile Industry: A Case Study. *Water Resour. Ind.* **2022**, *27*, 100174. [CrossRef]
12. Winker, M.; Gehrmann, S.; Schramm, E.; Zimmermann, M.; Rudolph-Cleff, A. Greening and Cooling the City Using Novel Urban Water Systems. In *Approaches to Water Sensitive Urban Design*; Sharma, A.K., Gardner, T., Begbie, D., Eds.; Elsevier: Amsterdam, The Netherlands, 2019; pp. 431–454, ISBN 978-0-12-812843-5.
13. Gdoura, K.; Anane, M.; Jellali, S. Geospatial and AHP-Multicriteria Analyses to Locate and Rank Suitable Sites for Groundwater Recharge with Reclaimed Water. *Resour. Conserv. Recycl.* **2015**, *104*, 19–30. [CrossRef]
14. Wanner, J.; Srb, M.; Beneš, O. Water Reuse in the Frame of Circular Economy. In *Current Developments in Biotechnology and Bioengineering*; Mannina, G., Pandey, A., Sirohi, R., Eds.; Elsevier: Amsterdam, The Netherlands, 2022; pp. 221–266, ISBN 978-0-32-399920-5.
15. Partyka, M.L.; Bond, R.F. Wastewater Reuse for Irrigation of Produce: A Review of Research, Regulations, and Risks. *Sci. Total Environ.* **2022**, *828*, 154385. [CrossRef] [PubMed]
16. Anane, M.; Bouziri, L.; Limam, A.; Jellali, S. Ranking Suitable Sites for Irrigation with Reclaimed Water in the Nabeul-Hammamet Region (Tunisia) Using GIS and AHP-Multicriteria Decision Analysis. *Resour. Conserv. Recycl.* **2012**, *65*, 36–46. [CrossRef]
17. Menegassi, L.C.; Rossi, F.; Dominical, L.D.; Tommaso, G.; Montes, C.R.; Gomide, C.A.; Gomes, T.M. Reuse in the Agro-Industrial: Irrigation with Treated Slaughterhouse Effluent in Grass. *J. Clean. Prod.* **2020**, *251*, 119698. [CrossRef]
18. Emara, M.M.; Abd, A.M.A.; Amir, E.-R.; Sayedahmed, A.M. Industrial Food Processing Wastewater Treatment by Modified Moving Bed Biofilm Reactor (MBBR). *Int. J. Sci. Eng. Res.* **2017**, *8*, 929–934.
19. UN-Water. *The United Nations World Water Development Report 2023: Partnerships and Cooperation for Water*; UNESCO: Paris, France, 2023.
20. Fernandes, L.S.; Galvão, A.; Santos, R.; Monteiro, S. Impact of Water Reuse on Agricultural Practices and Human Health. *Environ. Res.* **2023**, *216*, 114762. [CrossRef] [PubMed]
21. Radini, S.; González-Camejo, J.; Andreola, C.; Eusebi, A.L.; Fatone, F. Risk Management and Digitalisation to Overcome Barriers for Safe Reuse of Urban Wastewater for Irrigation—A Review Based on European Practice. *J. Water Process Eng.* **2023**, *53*, 103690. [CrossRef]
22. Yadav, G.; Mishra, A.; Ghosh, P.; Sindhu, R.; Vinayak, V.; Pugazhendhi, A. Technical, Economic and Environmental Feasibility of Resource Recovery Technologies from Wastewater. *Sci. Total Environ.* **2021**, *796*, 149022. [CrossRef]
23. Anusha, B.N.; Babu, K.R.; Kumar, B.P.; Sree, P.P.; Veeraswamy, G.; Swarnapriya, C.; Rajasekhar, M. Integrated Studies for Land Suitability Analysis towards Sustainable Agricultural Development in Semi-Arid Regions of AP, India. *Geosyst. Geoenviron.* **2023**, *2*, 100131. [CrossRef]
24. Keson, J.; Silalertruksa, T.; Gheewala, S.H. Land Suitability Class and Implications to Land-Water-Food Nexus: A Case of Rice Cultivation in Thailand. *Energy Nexus* **2023**, *10*, 100205. [CrossRef]
25. Samanta, S.; Ale, S.; Bagnall, D.K.; Morgan, C.L. Assessing the Watershed-Scale Effects of Tillage Management on Surface Runoff and Sediment Loss Using a Curve Number-Precipitation Relationship Based Approach. *J. Hydrol.* **2023**, *625*, 130130. [CrossRef]
26. Sadiq, F.K.; Ya'u, S.L.; Aliyu, J.; Maniyunda, L.M. Evaluation of Land Suitability for Soybean Production Using GIS-Based Multi-Criteria Approach in Kudan Local Government Area of Kaduna State Nigeria. *Environ. Sustain. Indic.* **2023**, *20*, 100297. [CrossRef]
27. Akpoti, K.; Kabo-bah, A.T.; Zwart, S.J. Agricultural Land Suitability Analysis: State-of-the-Art and Outlooks for Integration of Climate Change Analysis. *Agric. Syst.* **2019**, *173*, 172–208. [CrossRef]
28. Agrawal, N.; Govil, H.; Kumar, T. Agricultural land suitability classification and crop suggestion using machine learning and spatial multicriteria decision analysis in semi-arid ecosystem. *Environ. Dev. Sustain.* **2024**, 1–38. [CrossRef]
29. Choudhary, K.; Boori, M.S.; Shi, W.; Valiev, A.; Kupriyanov, A. Agricultural Land Suitability Assessment for Sustainable Development Using Remote Sensing Techniques with Analytic Hierarchy Process. *Remote Sens. Appl. Soc. Environ.* **2023**, *32*, 101051. [CrossRef]
30. Akpoti, K.; Higginbottom, T.P.; Foster, T.; Adhikari, R.; Zwart, S.J. Mapping Land Suitability for Informal, Small-Scale Irrigation Development Using Spatial Modelling and Machine Learning in the Upper East Region, Ghana. *Sci. Total Environ.* **2022**, *803*, 149959. [CrossRef]

31. El Behairy, R.A.; El Arwash, H.M.; El Baroudy, A.A.; Ibrahim, M.M.; Mohamed, E.S.; Rebouh, N.Y.; Shokr, M.S. Artificial Intelligence Integrated GIS for Land Suitability Assessment of Wheat Crop Growth in Arid Zones to Sustain Food Security. *Agronomy* **2023**, *13*, 1281. [CrossRef]
32. Franco, L.; Magalhães, M.R. Assessing the Ecological Suitability of Land-Use Change. Lessons Learned from a Rural Marginal Area in Southeast Portugal. *Land Use Policy* **2022**, *122*, 106381. [CrossRef]
33. Zhang, C.; Di, L.; Lin, L.; Li, H.; Guo, L.; Yang, Z.; Yu, E.G.; Di, Y.; Yang, A. Towards Automation of In-Season Crop Type Mapping Using Spatiotemporal Crop Information and Remote Sensing Data. *Agric. Syst.* **2022**, *201*, 103462. [CrossRef]
34. Di Minin, E.; Soutullo, A.; Bartesaghi, L.; Rios, M.; Szephegyi, M.N.; Moilanen, A. Integrating Biodiversity, Ecosystem Services and Socio-Economic Data to Identify Priority Areas and Landowners for Conservation Actions at the National Scale. *Biol. Conserv.* **2017**, *206*, 56–64. [CrossRef]
35. Liu, L.; Ouyang, W.; Liu, H.; Zhu, J.; Ma, Y.; Wu, Q.; Chen, J.; Zhang, D. Potential of Paddy Drainage Optimization to Water and Food Security in China. *Resour. Conserv. Recycl.* **2021**, *171*, 105624. [CrossRef]
36. Wubalem, A. Modeling of Land Suitability for Surface Irrigation Using Analytical Hierarchy Process Method in Belessa Districts, Northwestern Ethiopia. *Heliyon* **2023**, *9*, e13937. [CrossRef]
37. Arantes, L.T.; Carvalho, A.C.P.; Carvalho, A.P.P.; Lorandi, R.; Moschini, L.E.; Di Lollo, J.A. Surface Runoff Associated with Climate Change and Land Use and Land Cover in Southeast Region of Brazil. *Environ. Chall.* **2021**, *3*, 100054. [CrossRef]
38. Abd-Elmabod, S.K.; Fitch, A.C.; Zhang, Z.; Ali, R.R.; Jones, L. Rapid Urbanisation Threatens Fertile Agricultural Land and Soil Carbon in the Nile Delta. *J. Environ. Manag.* **2019**, *252*, 109668. [CrossRef]
39. Dornik, A.; Chet, M.A.; Cris, T.E. International Soil and Water Conservation Research Geospatial Evaluation of the Agricultural Suitability and Land Use Compatibility in Europe's Temperate Continental Climate Region. *Int. Soil Water Conserv. Res.* **2024**, *12*, 908–919. [CrossRef]
40. Burayu, D.G.; Karuppannan, S.; Shuniye, G. Identifying Flood Vulnerable and Risk Areas Using the Integration of Analytical Hierarchy Process (AHP), GIS, and Remote Sensing: A Case Study of Southern Oromia Region. *Urban Clim.* **2023**, *51*, 101640. [CrossRef]
41. Muhammad Anwar, S.N.B.; Alvarado, V.; Hsu, S.C. A Socio-Eco-Efficiency Analysis of Water and Wastewater Treatment Processes for Refugee Communities in Jordan. *Resour. Conserv. Recycl.* **2021**, *164*, 105196. [CrossRef]
42. Secretaria de Estado de Saneamento e Recursos Hídricos e Consórcio Enecorps/Maubertec (SSRH/CSAN). *Plano de Plano Regional Integrado de Saneamento Básico—Relatório Síntese*; SSRH/CSAN: São Paulo, Brazil, 2015.
43. Alvares, C.A.; Stape, J.L.; Sentelhas, P.C.; De Moraes Gonçalves, J.L.; Sparovek, G. Köppen's climate classification map for Brazil. *Meteorol. Z.* **2013**, *22*, 711–728. [CrossRef]
44. Rossi, M. *Mapa Pedológico do Estado de São Paulo: Revisado e Ampliado*; Instituto Florestal: São Paulo, Brazil, 2017; 118p.
45. MapBiomas. Coleção 7 da Série Anual de Mapas de Cobertura e Uso de Solo do Brasil. 2021. Available online: https://brasil.mapbiomas.org/map/colecao-7/ (accessed on 30 January 2023).
46. MapBiomas. Coleção 8 da Série Anual de Mapas de Cobertura e Uso de Solo do Brasil. 2022. Available online: https://brasil.mapbiomas.org/map/colecao-8/ (accessed on 21 February 2024).
47. Carvalho, A.C.P. Proposição de uma Sistemática para Avaliação Qualitativa da Oferta Hídrica Superficial Aplicada em Sub-bacias Hidrográficas da Bacia Hidrográfica do Rio Piracicaba—Região Sudeste do Estado de São Paulo. Ph.D. Thesis, Federal University of São Carlos, São Carlos, Brazil, 2022.
48. Agência Nacional de Águas (ANA). Airfields. 2010. Available online: https://metadados.snirh.gov.br/geonetwork/srv/api/records/ce6bb0fe-ccfc-4cbf-9ff6-929ba80b47db (accessed on 31 January 2023).
49. Sistema Nacional de Cadastro Ambiental Rural (SICAR). Permanent Preservation Areas and Restricted Uses. 2021. Available online: https://www.car.gov.br/publico/imoveis/index (accessed on 25 January 2023).
50. Agência das Bacias PCJ. Meu Mapa. 2018. Available online: https://mapas.agenciapcj.org.br/portal/home/webmap/viewer.html?useExisting=1 (accessed on 14 August 2018).
51. Sistema Nacional de Cadastro Ambiental Rural (SICAR). Restricted Uses. 2024. Available online: https://www.car.gov.br/publico/imoveis/index (accessed on 21 February 2024).
52. Contribuição do Patrimônio Material para o Protocolo do SAIP. Nota Técnica nº7/CGN/DEPAM. 2020. Available online: https://sei.iphan.gov.br/sei/modulos/pesquisa/md_pesq_documento_consulta_externa.php?9LibXMqGnN7gSpLFOOgUQFziRouBJ5VnVL5b7-UrE5TIlA4YrIW0lcDMPGm5IUPfBQxJPChXxXYetl3gOytduuIJGAed0ZuPs26LTAYHvimGO9lB5GsDzSqFwYJt4Pzs (accessed on 30 January 2023).
53. Instituto do Património Histórico e Artístico Nacional (IPHAN). Archaeological Sites. 2022. Available online: http://portal.iphan.gov.br/pagina/detalhes/1701/ (accessed on 24 January 2023).
54. Lei Federal nº 9.985, de 18 de Janeiro de 2000. Sistema Nacional de Unidades de Conservação da Natureza. 2000. Available online: https://www.planalto.gov.br/ccivil_03/leis/l9985.htm (accessed on 2 January 2024).
55. Instituto Chico Mendes de Conservação da Biodiversidade (ICMBIO). Protected Area. 2022. Available online: https://www.gov.br/icmbio/pt-br/assuntos/dados_geoespaciais/mapa-tematico-e-dados-geoestatisticos-das-unidades-de-conservacao-federais (accessed on 24 January 2023).
56. Instituto Brasileiro de Geografia e Estatística (IBGE). Limits of Geological Units. 2021. Available online: https://www.ibge.gov.br/geociencias/informacoes-ambientais/geologia/15822-geologia-1-250-000.html?=&t=downloads (accessed on 7 February 2023).

57. Instituto de Pesquisas Tecnológicas (IPT). *Mapa Geológico do Estado de São Paulo*; IPT: São Paulo, Brazil, 1981.
58. ASF Data Search Vertex. Digital Elevation Model. 2010/2011. Available online: https://search.asf.alaska.edu/#/ (accessed on 27 September 2022).
59. Agência Nacional de Águas (ANA). Ottocoded Hydrographic Base of the Rio Grande Basin. 2014. Available online: https://metadados.snirh.gov.br/geonetwork/srv/api/records/b13fa102-148d-4c4a-b7cd-02f23027e5c1 (accessed on 10 March 2023).
60. Agência Nacional de Águas (ANA). Catálogo de Metadados da ANA: Base Hidrográfica Ottocodificada das Bacias. Base Hidrográfica Ottocodificada das Bacias. 2013. Available online: https://metadados.snirh.gov.br/geonetwork/srv/por/catalog.search#/metadata/9a761447-7aa2-470e-a5f0-9ad63468fa3c (accessed on 9 January 2019).
61. Sistema de Informações de Águas Subterrâneas (SIAGAS). Static Level of Registered Wells. 2023. Available online: https://siagasweb.sgb.gov.br/layout/pesquisa_complexa.php (accessed on 14 March 2023).
62. Sistema de Informações de Águas Subterrâneas (SIAGAS). Static Level of Registered Wells. 2024. Available online: https://siagasweb.sgb.gov.br/layout/pesquisa_complexa.php (accessed on 19 February 2024).
63. CHIRPS. Available online: https://data.chc.ucsb.edu/products/CHIRPS-2.0/ (accessed on 20 September 2024).
64. USGS FEWS NET Data Portal. Available online: https://earlywarning.usgs.gov/fews (accessed on 20 September 2024).
65. Wanyama, J.; Nakawuka, P.; Bwambale, E.; Kiraga, S.; Kiggundu, N.; Barasa, B.; Katimbo, A. Evaluation of Land Suitability for Surface Irrigation under Changing Climate in a Tropical Setting of Uganda, East Africa. *Agric. Syst.* **2024**, *217*, 103937. [CrossRef]
66. Sadiq, F.K.; Maniyunda, L.M.; Anumah, A.O.; Adegoke, K.A. Variation of Soil Properties under Different Landscape Positions and Land Use in Hunkuyi, Northern Guinea Savanna of Nigeria. *Environ. Monit. Assess.* **2021**, *193*, 178. [CrossRef] [PubMed]
67. Gizawu Garbaba, F.; Negasa Wolteji, B. Application of Geospatial Technology on Land Suitability Analysis for Wheat and Maize Farming: In a Case of Guder Sub-Watershed North West Oromia, Ethiopia. *Heliyon* **2024**, *10*, e33557. [CrossRef] [PubMed]
68. Ramamurthy, V.; Reddy, G.P.O.; Kumar, N. Assessment of Land Suitability for Maize (*Zea mays* L.) in Semi-Arid Ecosystem of Southern India Using Integrated AHP and GIS Approach. *Comput. Electron. Agric.* **2020**, *179*, 105806. [CrossRef]
69. Xue, L.; Cao, P.; Xu, D.; Guo, Y.; Wang, Q.; Zheng, X.; Han, R.; You, A. Agricultural Land Suitability Analysis for an Integrated Rice—Crayfish Culture Using a Fuzzy AHP and GIS in Central China. *Ecol. Indic.* **2023**, *148*, 109837. [CrossRef]
70. Arunbose, S.; Srinivas, Y.; Rajkumar, S.; Nair, N.C.; Kaliraj, S. Groundwater for Sustainable Development Remote Sensing, GIS and AHP Techniques Based Investigation of Groundwater Potential Zones in the Karumeniyar River Basin, Tamil Nadu, Southern India. *Groundw. Sustain. Dev.* **2021**, *14*, 100586. [CrossRef]
71. Dias, C.C. Avaliação Geoambiental da Região do Médio Rio Grande. Master's Dissertation, Escola de Engenharia de São Carlos, Universidade de São Paulo (EESC/USP), São Carlos, Brazil, 2013.
72. Reis, P.E.; Parizzi, M.G.; de Magalhães, D.M.; Moura, A.C.M. O Escoamento Superficial Como Condicionante de Inundações Em Belo Horizonte, MG: Estudo de Caso Da Sub-Bacia Córrego Do Leitão, Bacia Do Ribeirão Arrudas. *Geociencias* **2012**, *31*, 31–46.
73. Risal, A.; Parajuli, P.B.; Dash, P.; Ouyang, Y.; Linhoss, A. Sensitivity of Hydrology and Water Quality to Variation in Land Use and Land Cover Data. *Agric. Water Manag.* **2020**, *241*, 106366. [CrossRef]
74. MacDonald, A.M.; Bonsor, H.C.; Dochartaigh, B.É.Ó.; Taylor, R.G. Quantitative Maps of Groundwater Resources in Africa. *Environ. Res. Lett.* **2012**, *7*, 024009. [CrossRef]
75. Patra, S.; Sahoo, S.; Mishra, P.; Mahapatra, S.C. Impacts of Urbanization on Land Use /Cover Changes and Its Probable Implications on Local Climate and Groundwater Level. *J. Urban Manag.* **2018**, *7*, 70–84. [CrossRef]
76. Penny, J.; Ordens, C.M.; Barnett, S.; Djordjević, S.; Chen, A.S. Small-Scale Land Use Change Modelling Using Transient Groundwater Levels and Salinities as Driving Factors—An Example from a Sub-Catchment of Australia's Murray-Darling Basin. *Agric. Water Manag.* **2023**, *278*, 108174. [CrossRef]
77. Akpoti, K.; Dossou-Yovo, E.R.; Zwart, S.J.; Kiepe, P. The Potential for Expansion of Irrigated Rice under Alternate Wetting and Drying in Burkina Faso. *Agric. Water Manag.* **2021**, *247*, 106758. [CrossRef]
78. Saaty, T.L. *The Analytic Hierarchy Process*; McGraw-Hil: New York, NY, USA, 1980.
79. Senay, G.B.; Bohms, S.; Singh, R.K.; Gowda, P.H.; Velpuri, N.M.; Alemu, H.; Verdin, J.P. Operational Evapotranspiration Mapping Using Remote Sensing and Weather Datasets: A New Parameterization for the SSEB Approach. *J. Am. Water Resour. Assoc.* **2013**, *49*, 577–591. [CrossRef]
80. Martello, F.; dos Santos, J.S.; Silva-Neto, C.M.; Cássia-Silva, C.; Siqueira, K.N.; de Ataíde, M.V.R.; Ribeiro, M.C.; Collevatti, R.G. Landscape Structure Shapes the Diversity of Plant Reproductive Traits in Agricultural Landscapes in the Brazilian Cerrado. *Agric. Ecosyst. Environ.* **2023**, *341*, 108216. [CrossRef]
81. Lei Federal nº 12.651, de 25 de Janeiro de 2012. Novo Código Florestal. 2012. Available online: https://www.planalto.gov.br/ccivil_03/_ato2011-2014/2012/lei/l12651.htm (accessed on 2 January 2024).
82. França, M.V.; Shimabukuro, E.M.; Fushita, Â.T.; Smith, W.S.; Benassi, R.F.; Cunha, D.G.F.; Taniwaki, R.H. Structural Characteristics of Tropical Headwater Streams Draining Native Vegetation and Sugarcane Cultivation. *Limnologica* **2023**, *101*, 126099. [CrossRef]
83. Rojas-Castillo, O.A.; Kepfer-Rojas, S.; Vargas, N.; Jacobsen, D. Forest Buffer-Strips Mitigate the Negative Impact of Oil Palm Plantations on Stream Communities. *Sci. Total Environ.* **2023**, *873*, 162259. [CrossRef]
84. Zhu, X.; Xiao, G.; Wang, S. Suitability Evaluation of Potential Arable Land in the Mediterranean Region. *J. Environ. Manag.* **2022**, *313*, 115011. [CrossRef]
85. Chen, S.; Ma, M.; Wu, S.; Tang, Q.; Wen, Z. Topography Intensifies Variations in the Effect of Human Activities on Forest NPP across Altitude and Slope Gradients. *Environ. Dev.* **2023**, *45*, 100826. [CrossRef]

86. Lisso, L.; Lindsay, J.B.; Berg, A. Evaluating the Topographic Factors for Land Suitability Mapping of Specialty Crops in Southern Ontario. *Agronomy* **2024**, *14*, 319. [CrossRef]
87. Madrucci, V. Prospecção de Água Subterrânea em Terreno Cristalino Utilizando-Se Análise Integrada de Dados de Sensoriamento Remoto, Geofísicos e Técnicas de Geoprocessamento, Região de Lindóia, SP. Ph.D. Thesis, Universidade de São Paulo, São Paulo, Brazil, 2004.
88. Osei-gyabaah, A.P.; Antwi, M.; Addo, S.; Osei, P. Smart Agricultural Technology Land Suitability Analysis for Cocoa (Theobroma Cacao) Production in the Sunyani Municipality, Bono Region, Ghana. *Smart Agric. Technol.* **2023**, *5*, 100262. [CrossRef]
89. Madrucci, V.; Taioli, F.; de Araújo, C.C. Groundwater Favorability Map Using GIS Multicriteria Data Analysis on Crystalline Terrain, São Paulo State, Brazil. *J. Hydrol.* **2008**, *357*, 153–173. [CrossRef]
90. Bölscher, T.; Koestel, J.; Etana, A.; Ulén, B.; Berglund, K.; Larsbo, M. Changes in Pore Networks and Readily Dispersible Soil Following Structure Liming of Clay Soils. *Geoderma* **2021**, *390*, 114948. [CrossRef]
91. Sarkar, D.; Saha, S.; Mondal, P. Green Technologies and Sustainability Modelling Agricultural Land Suitability for Vegetable Crops Farming Using RS and GIS in Conjunction with Bivariate Techniques in the Uttar Dinajpur District of Eastern India. *Green Technol. Sustain.* **2023**, *1*, 100022. [CrossRef]
92. Chen, S.; Chen, Z.; Zhang, Y.; Huang, J. A Coupled Modeling Framework to Screen Reclaimed Water Supplement Schemes in an Urban Watershed. *J. Hydrol. Reg. Stud.* **2023**, *50*, 101602. [CrossRef]
93. Ricart, S.; Rico, A.M. Assessing Technical and Social Driving Factors of Water Reuse in Agriculture: A Review on Risks, Regulation and the Yuck Factor. *Agric. Water Manag.* **2019**, *217*, 426–439. [CrossRef]
94. Bera, A.; Mukhopadhyay, B.P.; Barua, S. Delineation of Groundwater Potential Zones in Karha River Basin, Maharashtra, India, Using AHP and Geospatial Techniques. *Arab. J. Geosci.* **2020**, *13*, 693. [CrossRef]
95. Yawar, M.; Khan, A.; Elkashouty, M. Watershed Prioritization and Hydro-Morphometric Analysis for the Potential Development of Tabuk Basin, Saudi Arabia Using Multivariate Statistical Analysis and Coupled RS-GIS Approach. *Ecol. Indic.* **2023**, *154*, 110766. [CrossRef]
96. Carvalho, A.C.P.; Lorandi, R.; Di Lollo, J.A.; Collares, E.G.; Moschini, L.E. Hydrological Response of Hydrographic Sub-Basins in the Piracicaba River Basin—Southeast Region of Brazil. *Soc. Nat.* **2022**, *34*, 1–17. [CrossRef]
97. Wang, W.; Wu, X.; Yin, C.; Xie, X. Nutrition Loss through Surface Runoff from Slope Lands and Its Implications for Agricultural Management. *Agric. Water Manag.* **2019**, *212*, 226–231. [CrossRef]
98. Chen, Y.; Li, H.; Xu, Y.; Fu, Q.; Wang, Y.; He, B.; Li, M. Sustainable Management in Irrigation Water Distribution System under Climate Change: Process-Driven Optimization Modelling Considering Water-Food-Energy-Environment Synergies. *Agric. Water Manag.* **2024**, *302*, 108990. [CrossRef]
99. Adeyeri, O.E.; Ishola, K.A. Variability and Trends of Actual Evapotranspiration over West Africa: The Role of Environmental Drivers. *Agric. For. Meteorol.* **2021**, *308–309*, 108574. [CrossRef]
100. Mannina, G.; Gulhan, H.; Ni, B.J. Water Reuse from Wastewater Treatment: The Transition towards Circular Economy in the Water Sector. *Bioresour. Technol.* **2022**, *363*, 127951. [CrossRef] [PubMed]
101. Bojago, E.; Abrham, Y. Small-Scale Irrigation (SSI) Farming as a Climate-Smart Agriculture (CSA) Practice and Its Influence on Livelihood Improvement in Offa District, Southern Ethiopia. *J. Agric. Food Res.* **2023**, *12*, 100534. [CrossRef]
102. Crovella, T.; Paiano, A.; Falciglia, P.P.; Lagioia, G.; Ingrao, C. Wastewater Recovery for Sustainable Agricultural Systems in the Circular Economy—A Systematic Literature Review of Life Cycle Assessments. *Sci. Total Environ.* **2024**, *912*, 169310. [CrossRef] [PubMed]
103. Giacobbo, A.; Oliveira, M.; Bernardes, A.M.; de Pinho, M.N. Winery Wastewater Treatment for Biomolecules Recovery and Water Reuse Purposes. In *Advanced Technologies in Wastewater Treatment*; Basile, A., Cassano, A., Conidi, C., Eds.; Elsevier: Amsterdam, The Netherlands, 2023; pp. 311–354, ISBN 978-0-323-88510-2.
104. Radcliffe, J.C. Current Status of Recycled Water for Agricultural Irrigation in Australia, Potential Opportunities and Areas of Emerging Concern. *Sci. Total Environ.* **2022**, *807*, 151676. [CrossRef]
105. Wang, H.-J.; Wang, J.; Yu, X. Wastewater Irrigation and Crop Yield: A Meta-Analysis. *J. Integr. Agric.* **2022**, *21*, 1215–1224. [CrossRef]
106. Sgroi, M.; Vagliasindi, F.G.A.; Roccaro, P. Feasibility, Sustainability and Circular Economy Concepts in Water Reuse. *Curr. Opin. Environ. Sci. Health* **2018**, *2*, 20–25. [CrossRef]

Disclaimer/Publisher's Note: The statements, opinions and data contained in all publications are solely those of the individual author(s) and contributor(s) and not of MDPI and/or the editor(s). MDPI and/or the editor(s) disclaim responsibility for any injury to people or property resulting from any ideas, methods, instructions or products referred to in the content.

agronomy

MDPI

Article

Effects of Irrigation with Treated Slaughterhouse Effluent and *Bradyrhizobium* spp. Inoculation on Soybean Development and Productivity: Strategies for Sustainable Management

Ana Carolina Murad Lima [1], Lisiane Brichi [1], Lucas Renato Trevisan [1], André Leão de Souza Dominguez [1], Gustavo Nocera Santiago [2], Tamara Maria Gomes [1,3] and Fabrício Rossi [1,3,*]

[1] College of Agriculture "Luiz de Queiroz", University of São Paulo, Piracicaba 13418-900, SP, Brazil; ana.murad.lima@usp.br (A.C.M.L.); lisiane.brichi@alumni.usp.br (L.B.); lucas.renato.trevisan@alumni.usp.br (L.R.T.); andre.dominguez@usp.br (A.L.d.S.D.); tamaragomes@usp.br (T.M.G.)

[2] Agronomy Department, Kansas State University, 1712 Claflin Rd, Manhattan, KS 66502, USA; gsantiago@ksu.edu

[3] Department of Biosystems Engineering, School of Animal Science and Food Engineering, University of São Paulo, Pirassununga 13635-900, SP, Brazil

* Correspondence: fabricio.rossi@usp.br

Abstract: Water scarcity challenges in agriculture are prompting the exploration of alternative irrigation sources, including treated effluents. This study investigates the effects of irrigation with treated slaughterhouse effluent on soybean productivity and development, with and without inoculation, over two cropping cycles. Plant performance was significantly influenced by environmental factors and the interaction between effluent and inoculation. Plant height and leaf area were greater in the second cycle, with effluent enhancing growth and foliar development. Fresh and dry shoot biomass showed significant interactions among cycle, inoculation, and effluent, with higher effluent concentrations combined with inoculation being most effective in the first cycle. Foliar nitrogen concentrations were higher in the first cycle, particularly at elevated effluent doses, while foliar sodium showed a positive correlation with nitrogen and a negative correlation with magnesium. Chlorophyll indices varied across developmental stages, with maximum chlorophyll *b* estimated at 85.35% effluent irrigation. Soybean yield did not vary significantly with effluent dilutions, suggesting environmental factors had a greater influence. In conclusion, treated effluent irrigation represents a sustainable strategy for soybean production, optimizing water and nutrient use while reducing reliance on chemical fertilizers.

Keywords: *Glycine max*; legumes; agricultural reuse; wastewater; nodulation; symbiotic bacteria

1. Introduction

Water scarcity is an increasing global challenge exacerbated by population growth and climate change. Currently, about 40% of the world's population faces some degree of water stress, and this situation is expected to worsen by 2050 [1,2]. In Brazil, agriculture accounts for over 50% of total water consumption, while industrial sectors such as meat processing and slaughterhouses also make substantial withdrawals, further intensifying pressure on water resources [3]. In this context, water reuse has become a vital strategy for promoting sustainability and water security. It aligns with the principles of a circular economy by reducing the consumption of higher-quality water, minimizing effluent discharge, and decreasing the reliance on mineral fertilizers [4]. However, the application of treated

effluents in agriculture requires careful management to prevent soil salinization and adverse environmental impacts [5,6].

Soybean (*Glycine max*), one of the most important crops for Brazilian agribusiness, is especially relevant in this scenario. Brazil is the largest global producer of soybeans, contributing approximately 33% of the world's production [7,8]. In addition to its economic value, soybeans possess advantageous agronomic characteristics, such as the ability to fix atmospheric nitrogen biologically through symbiosis with bacteria of the genus *Bradyrhizobium* spp., which reduces the need for nitrogen fertilization and enhances the sustainability of production systems [9,10]. However, the interaction between effluent irrigation and biological nitrogen fixation (BNF) can be complex, as high concentrations of nutrients and salts in the effluent may negatively influence nodulation and the nitrogen fixation process [11].

Recent studies suggest that while irrigation with treated effluents can increase agricultural productivity, excessive nitrogen doses and soil salinity can reduce BNF efficacy and limit legume growth [12,13]. Conversely, moderate nitrogen doses may complement BNF and improve soybean development [14,15]. These findings highlight the need to explore management practices that maximize the benefits of effluent reuse while preserving soil health and symbiotic performance.

This study, therefore, investigates the effects of irrigation with treated slaughterhouse effluent on soybean productivity, with and without *Bradyrhizobium* spp. inoculation. The hypothesis is that treated effluent when applied at appropriate doses and combined with *Bradyrhizobium* spp. inoculation can meet the plant's nitrogen demand independently of BNF, promoting a viable and sustainable alternative for soybean crop irrigation. This study aims to contribute to the advancement of sustainable agricultural management practices, particularly in water-scarce regions, by providing an in-depth analysis of the interaction between effluent irrigation and biological nitrogen fixation.

2. Materials and Methods

2.1. Experimental Conditions

The experiment was conducted in the experimental area of the School of Animal Science and Food Engineering, University of São Paulo (FZEA/USP), located in Pirassununga, São Paulo, Brazil (latitude: 21°59′ S, longitude: 47°23′ W). The regional climate is classified as Cwa, a humid subtropical climate with dry winters. During the two experimental cycles (2020/2021 and 2021/2022), the average recorded temperatures from October to February over the past 10 years were 30 °C maximum and 19 °C minimum, with an accumulated rainfall of 772 mm. Figure 1 shows the 10-year temperature and rainfall patterns compared to the climate conditions for the 2020–2021 and 2021–2022 seasons.

The experiment followed a split-plot design arranged in randomized complete blocks. The main plots consisted of five dilutions of treated slaughterhouse effluent (0%, 25%, 50%, 75%, and 100%), while the subplots comprised two *Bradyrhizobium* spp. inoculation treatments, with inoculation (WI) and without inoculation (NI). Each treatment combination was replicated across four blocks in a randomized way, totaling 40 experimental units. Each experimental subplot comprised a useful area of 21 m^2, with border rows to minimize edge effects.

The effluent used was sourced from the Scholar Slaughterhouse of the University of São Paulo, School of Animal Science and Food Engineering, "Fernando Costa" (Pirassununga, SP), and was treated through a system consisting of a solid separation tank, an Upflow Anaerobic Sludge Blanket (UASB) reactor, and a polishing pond. The UASB reactor had a total volume of 13 m^3 and a working volume of 8.7 m^3, with an application rate varying from 2 to 4 kg of COD/m^3 and a detention time ranging from 24 to 48 h. Effluent

samples were collected and analyzed biweekly following the methodology proposed by APHA/AWWA/WEF [16].

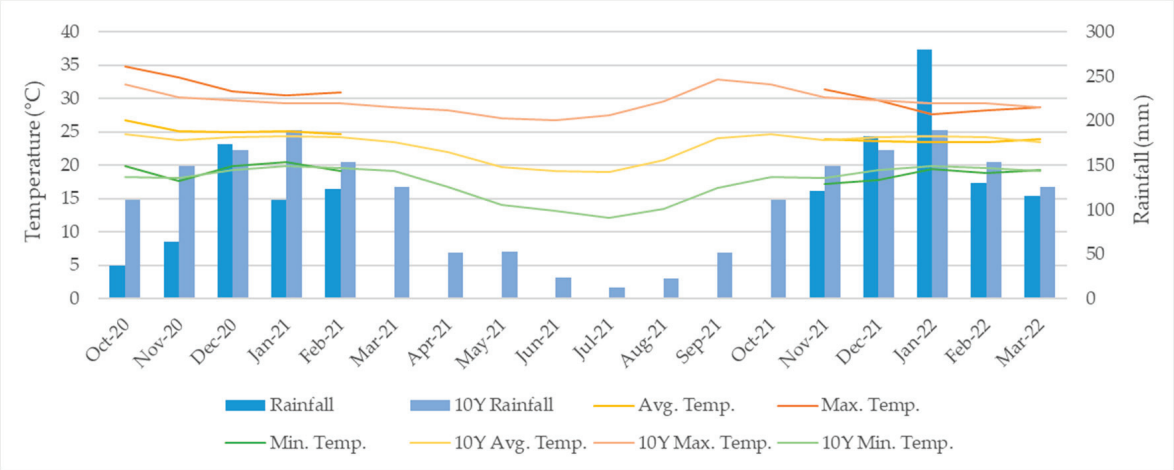


Figure 1. Average monthly temperatures (Avg. Temp.), maximum (Max. Temp.) and minimum temperatures (Min. Temp.), and precipitation during the experimental period (cycle 1, 20 October to 21 February; and cycle 2, 21 November to 22 March) compared to the historical averages (10Y) over the past ten years for the experimental area location. Source: Author's work, created with data from the Power Project (NASA, 2023).

2.2. Soybean Cultivation

In both cycles, soybean cultivation was preceded by black oat cultivation during winter. In the first cycle, the soybean seeds used were of the Agroeste® AS 3590 (Bayer S.A., Santo Antônio da Platina, Brazil) variety, sown at a density of 30 seeds per linear meter. The inoculated treatment (WI) received inoculation with *Bradyrhizobium japonicum* from Biosphera (Nitrosphera High Soja TS liquid and Nitrosphera Ultra peat—Agrocete Ind. De Fertilizantes LDTA, Ponta Grossa, Brazil). In both cycles, the inoculant was applied directly to the seeds right before sowing, following the manufacturer's recommended concentration per kilogram of seed to ensure uniform coverage. Soybeans were sown on 14 October 2020 and harvested 127 days later.

In the second cycle, the soybean seeds used were of the Intacta RR2 PRO® (KWS Sementes LDTA, Patos de Minas, Brazil) variety, sown at a density of 35 seeds per linear meter. Inoculation was performed with *Bradyrhizobium elkanii* from Biomax® Premium (liquid plus peat—Vittia Fertilizantes e Biológicos S.A., São Joaquim da Barra, Brazil). Soybeans were sown on 29 October 2021 and harvested 133 days later. Both soybean seeds used were varieties widely accepted and used by local rural producers in respective years.

In both cycles, weed control was performed using glyphosate. In the 2020–2021 cycle, glyphosate was applied at a rate of 1 kg ha^{-1} five days after sowing, while in the 2021–2022 cycle, the application was increased to 2 kg ha^{-1} in the second week after sowing. No additional herbicide applications were necessary during the cultivation cycles. *Brachiaria* grass around the plots was managed with a backpack mower.

Phosphorus and potassium fertilization were performed consistently across both cycles, following the recommendations of the Soybean Crop Fertilization Guide [17]. Simple superphosphate and potassium chloride were used as fertilizers. A total of 40 kg ha^{-1} of P_2O_5 was applied immediately after sowing, while 80 kg ha^{-1} of K_2O was applied in five split doses throughout the cultivation cycle, both delivered via fertigation.

Micronutrient applications were also performed via fertigation using the Agrucon Green Italia foliar micronutrient blend. This provided, per hectare, 350 g manganese, 1050 g zinc, 23 g iron, 58 g boron, 992 g sulfur, 175 g magnesium, and 1867 g nitrogen.

Micronutrients were applied twice in the 2020–2021 cycle (at 23 and 37 DAS) and once in the 2021–2022 cycle (at 42 DAS).

The soybean growth stages referenced in this study were defined according to the widely recognized and accepted scale developed by Embrapa (Brazilian Agricultural Research Corporation, Brasília, Brazil), which operates under the Ministry of Agriculture, Livestock, and Food Supply [18].

2.3. Irrigation Management

Irrigation was managed based on the soil water retention curve, established from soil samples collected at depths of 0–20 cm and 20–40 cm and determined using a Richards chamber, with adjustments made according to the Van Genuchten model (1980). Soil moisture was monitored every 48 h by frequency domain reflectometry (FDR) using the Sentek Diviner 2000 probe, with readings taken in the experimental plots of three of the four blocks. The average moisture content was used to calculate the irrigation depth needed to bring soil moisture to field capacity. The irrigation system consisted of separate tanks for water and effluent, connected to centrifugal pumps for precise control of effluent dilutions (0, 25, 50, 75, and 100%) through solenoid valves programmed for each treatment. Application was carried out via adjustable sector sprinklers set to operate at 90°, with two sprinklers per plot installed at opposite ends to ensure uniform distribution.

2.4. Biometric Analyses

The biometric parameters evaluated included plant height, plant stand, fresh and dry shoot biomass, fresh root biomass, and leaf area. Plant height was measured at three points (V7 seventh node, R1 beginning bloom, and R5 beginning seed) throughout the cycle, while the other variables were analyzed at stages R5 beginning seed (2020–2021) and R2 full bloom (2021–2022). Destructive sampling was conducted in three areas of 0.0625 m^2 per subplot to minimize impact on plant stand. Plants were washed, separated into shoots and roots, and weighed to obtain fresh biomass. Leaf area was measured with an area integrator (LI-3100, LI-COR®, Inc., Lincoln, NE, USA) and extrapolated per square meter. Leaves were then dried at 65 °C to obtain dry mass. Roots were photographed and analyzed using Safira© software, version 1.1, to calculate volume and surface area per square meter.

2.4.1. Foliar Diagnosis

Foliar diagnosis sampling took place about 50 days after sowing (DAS) at the R2 full bloom stage. Fifteen newly mature leaves with petioles were collected per subplot. After drying in a forced-air oven at 65 °C to a constant weight, samples were ground and sent to the Laboratory of Agricultural Sciences (FZEA/USP) for macronutrient and sodium analysis.

2.4.2. Instrumentation: Chlorophyll Index and Normalized Difference Vegetation Index

Chlorophyll content was determined indirectly using a chlorophyll meter (Clorofilog®, Falker, Porto Alegre, Brazil) to measure relative chlorophyll index (RCI) for chlorophyll *a*, *b*, and total. Readings were taken from 15 plants per subplot, always on the first fully expanded leaf of each plant, at phenological stages V3 third node, R1 beginning bloom, R2 full bloom, and R4 full pod in both cycles. Normalized Difference Vegetation Index (NDVI) was collected using the GreenSeeker® (Trimble Agriculture, Sunnyvale, CA, USA) device. NDVI measurements were taken along the five central rows of the subplot, positioning the device about 1 m above the canopy at stages V7 seventh node, R1 beginning bloom, R2 full bloom, and R4 full pod in the 2020–2021 cycle and at R2 full bloom, R4 full pod, and R5 beginning seed in the 2021–2022 cycle. Differences in collection dates were due to technical issues and challenges during rainy periods.

2.4.3. Yield and Bromatological Analysis of Grains

Sample collection to determine yield was conducted manually when the soybeans reached physiological maturity (R8 full maturity stage), occurring at 127 DAS (days after sowing) in the 2020–2021 cycle and at 133 DAS in the 2021–2022 cycle in a 3 m^2 area at the center of the subplot. The plants were bagged whole and processed in a plot thresher (TP SB01, SB Máquinas Agrícolas, Cambé, Brazil). The grains were dried in an oven at 45 °C, with moisture adjusted to 13% using a moisture meter (G600, Gehaka Agri, Sao Paulo, Brazil) before weighing to calculate yield per subplot. Due to the low physiological quality of the grains in the 2020–2021 cycle, only samples from the 2021–2022 cycle were analyzed at the Nutrition Laboratory (FZEA/USP) to determine bromatological parameters: dry matter, mineral matter, crude protein, crude fiber, ether extract, nitrogen-free extract, acid detergent fiber, and ash-free neutral detergent fiber.

2.5. Statistical Analysis

The variance analyses were conducted using the Sisvar statistical software, version 5.8, [19] following a split-plot block design and considering the repetition across two growing seasons and, where applicable, in time (phenological stages). For factors with significant differences ($p < 0.05$), the comparisons for the effluent factor were performed using Tukey's test and regression analysis, while comparisons for inoculation and cycle factors were carried out using the t-test. Comparisons over time or depth, with statistical significance, were also conducted using Tukey's test and regression analysis.

2.6. Generative AI Assistance

During the preparation of this manuscript, a generative artificial intelligence tool, ChatGPT, GPT-4-turbo (from OpenAI), was utilized to assist with the refinement of academic language, the structuring of the manuscript, and ensuring adherence to the submission guidelines of the journal. The tool provided suggestions for text revisions, scientific phrasing, and formatting in line with high-impact publication standards in agronomy. The authors reviewed and edited all AI-generated content to ensure its accuracy and relevance to this study.

3. Results

3.1. Irrigation Management and Nitrogen Incoming

Soil moisture varied similarly between the experimental plots in both cropping cycles, with greater uniformity from the onset of the reproductive phase when soybean water demand reached its peak. In cycle 1, both rainfall and effluent were more evenly distributed throughout the cycle, with higher effluent volumes applied at the beginning to meet initial water demand. In cycle 2, most of the effluent was applied up to 48 DAS (days after sowing) before the increase in rainfall, which had more intense and heterogeneous volumes. Effluent characterization showed a higher nutrient concentration in cycle 2, including nitrogen, phosphorus, and calcium, possibly due to variations in the abattoir processing and climatic conditions (Table 1).

The average nitrogen concentration in the effluent was similar to values reported in the literature, and electrical conductivity remained below the limit of 3.30 dS m^{-1}, posing no risk to soybean productivity. Due to the higher nitrogen concentration in cycle 2, nutrient input was higher, although the irrigated volume was similar in both cycles (Table 2). The total applied volume exceeded the crop's maximum demand (800 mm), especially in cycle 2, where rainfall exceeded the crop's requirement by 240 mm.

Table 1. Characterization of the effluent from Scholar Slaughterhouse of the University of São Paulo, "Fernando Costa" *campus*, collected after the polishing pond stage, during the first and second experimental cycles in comparison with previous studies.

Parameter	This Study			Oliveira et al. [20]	Araújo et al. [21]	Emerick et al. [22]	Kanafin et al. [23]	Madeira et al. [24]
	2020–2021	2021–2022	Average					
Slaughterhouse Type		**General**		**NP**	**Poultry**	**Swine**	**Poultry**	**General**
Treatment Type		**Anaerobic**		**Physical**	**Aerobic**	**Physical Chemist**	**Photochemical**	**Physical Chemist**
pH	8.12 ± 0.75	7.45 ± 0.12	7.79 ± 0.63	7.70 ± 0.30	7.00 ± 0.10	8.20 ± 0.71	7.53 ± 0.22	7.50 ± 0.10
EC (dS m^{-1})	0.4 ± 0.07	0.77 ± 0.09	0.58 ± 0.20	1.20 ± 0.10	0.01 ± 0.00	2.82 ± 0.53	-	3.00 ± 0.10
COD (mg L^{-1})	96.04 ± 42.25	178.46 ± 80.67	279.62 ± 243.00	5.81 ± 3007.00	80.90 ± 14.70	405.00 ± 8.20	155.00 ± 15.00	226.00 ± 41.00
TKN (mg L^{-1})	34.03 ± 9.27	77.49 ± 7.74	53.34 ± 23.25	157.50 ± 27.00	48.70 ± 11.50	9.20 ± 2.52	-	58.00 ± 0.00
N-NH_4^+ (mg L^{-1})	22.19 ± 8.88	59.71 ± 9	40.95 ± 20.79	-	-	-	0.84	52.00 ± 0.00
Nitrate (mg L^{-1})	0.32 ± 0.18	ND	0.32 ± 0.18	-	-	-	2.98	-
Nitrite (mg L^{-1})	ND	ND	ND	-	-	-	-	-
Soluble Phosphoru (mg L^{-1})	3.57 ± 0.4	5.46 ± 0.99	4.62 ± 1.22	-	-	-	-	-
Total Phosphorus (mg L^{-1})	7.16 ± 2.9	7.98 ± 0.87	7.61 ± 2.08	11.90 ± 9.60	20.20 ± 5.50	0.26 ± 0.06	-	-
Potassium (mg L^{-1})	14.88 ± 3.31	NA	14.88 ± 3.31	12.60 ± 5.00	-	-	14.86	-
Calcium (mg L^{-1})	17.97 ± 0.95	23.25 ± 1.45	17.97 ± 0.95	65.00 ± 38.10	-	-	132.43	190.50 ± 0.00
Magnesium (mg L^{-1})	1.58 ± 0.29	2.44 ± 0.19	1.58 ± 0.29	89.00 ± 52.20	-	-	67.27	60.20 ± 4.20
Sulfur (mg L^{-1})	2.12 ± 2.35	NA	2.12 ± 2.35	-	-	-	-	-
Iron (mg L^{-1})	2.61 ± 2.94	NA	2.61 ± 2.94	-	-	-	-	-
Manganese (mg L^{-1})	0.06 ± 0.02	0.12 ± 0.02	0.06 ± 0.02	-	-	-	-	-
Sodium (mg L^{-1})	35.7 ± 9.59	NA	35.70 ± 9.59	21.50 ± 3.60	-	-	141.87	-
SAR (mmol $L^{-1})^{-0.5}$	3.34 ± 0.89	-	-	-	-	-	-	-

EC: electrical conductivity; COD: chemical oxygen demand; TKN: total Kjeldahl nitrogen; SAR: Sodium adsorption ratio; ND: not detectable; NA: not analyzed; NP: not provided.

Table 2. Water input (via precipitation and irrigation) and nitrogen input during the two soybean growing cycles.

Treatment	Precipitation	Tap Water Irrigation	Effluent Irrigation	Total Irrigation	Total Depth	Nitrogen Input
2020–2021			(mm)			(kg ha^{-1})
0%	468.54	395.79	0.00	395.79	864.33	0.00
25%	468.54	338.91	76.37	415.28	883.82	25.96
50%	468.54	277.82	161.82	439.64	908.18	55.02
75%	468.54	181.89	223.65	405.54	874.08	76.04
100%	468.54	107.34	298.20	405.54	874.08	101.39
2021–2022			(mm)			(kg ha^{-1})
0%	756.85	287.93	0.00	287.93	1044.78	0.00
25%	756.85	248.43	54.40	302.84	1059.69	41.89
50%	756.85	205.94	115.54	321.47	1078.32	88.96
75%	756.85	136.21	159.18	295.38	1052.23	122.56
100%	756.85	83.15	212.23	295.38	1052.23	163.42

3.2. Biometric Analyses

3.2.1. Plant Height and Stand

The average plant height varied according to the interaction between the growing cycle and the effluent concentrations (Figure 2). In the first cycle, the plants showed a linear response to the increase in effluent doses, suggesting that the nutrient input, especially nitrogen, was crucial for initial growth. In the second cycle, the highest plant heights were observed in plots with 50%, 75%, and 100% effluent, indicating that intermediate and high effluent doses promote an optimal height for soybean development. The difference between cycles can be attributed to better water and nutrient availability in the second cycle, as well as a higher nitrogen concentration in the applied effluent or even to higher plant stand, which was bigger for the second cycle (Figure 3b) and also presented difference for the effluent factor, fitting a second-degree polynomial equation (Figure 3a).

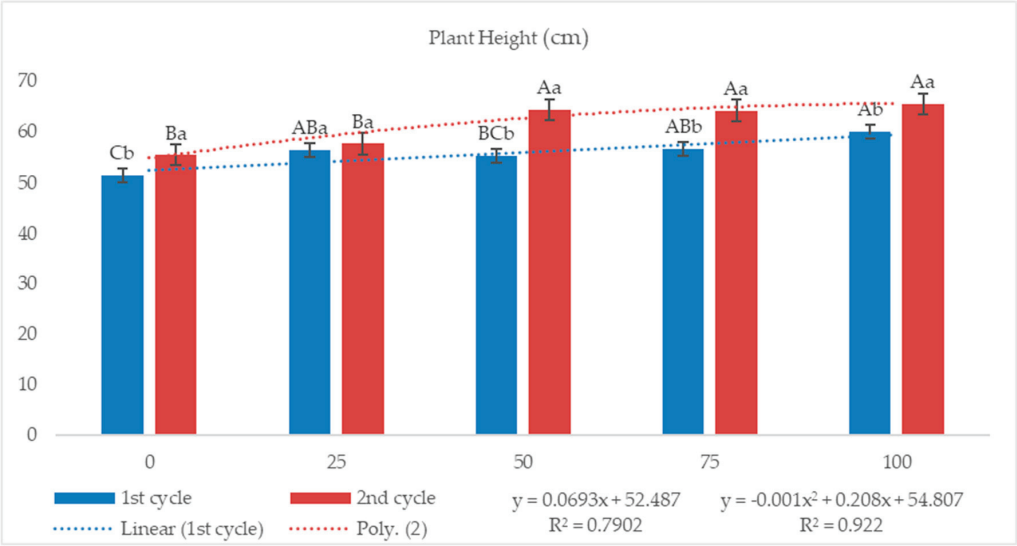


Figure 2. Result of the statistical analysis for plant height in the effluent-cycle interaction. Uppercase letters indicate differences for the effluent factor, and lowercase letters indicate differences for the cycle factor ($p < 0.05$).

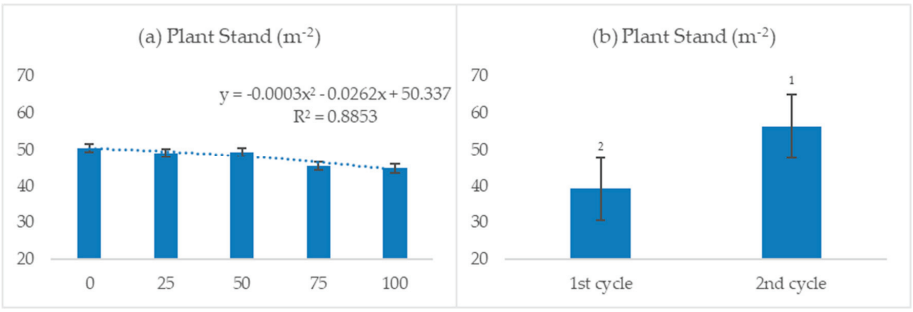


Figure 3. Result of the statistical analysis for plant stand in response to (**a**) effluent and (**b**) growing cycle. Different numbers indicate differences in the cycle factor ($p < 0.05$).

3.2.2. Fresh and Dry Shoot Mass

The results for fresh shoot biomass showed a significant interaction among effluent concentration, inoculation, and cultivation cycle (Figure 4a). A significant effect of inoculation was observed only at the 100% effluent dose. In cycle 1, the rhizobium-inoculated subplots had greater fresh biomass, whereas in cycle 2, the non-inoculated subplots performed better. No differences were observed in either cycle for the effluent levels in inoculated subplots. During cycle 1, the non-inoculated subplots did not show differences across effluent doses but fit a second-degree polynomial equation, indicating that the highest fresh biomass accumulation would occur at 64% effluent in the absence of inoculation. In cycle 2, the 50% and 100% effluent doses yielded the best results. At these same concentrations and with inoculation, plants accumulated more fresh biomass in cycle 1 than in cycle 2, suggesting that the impact of effluent on fresh biomass in inoculated soybeans depends on environmental conditions during cultivation.

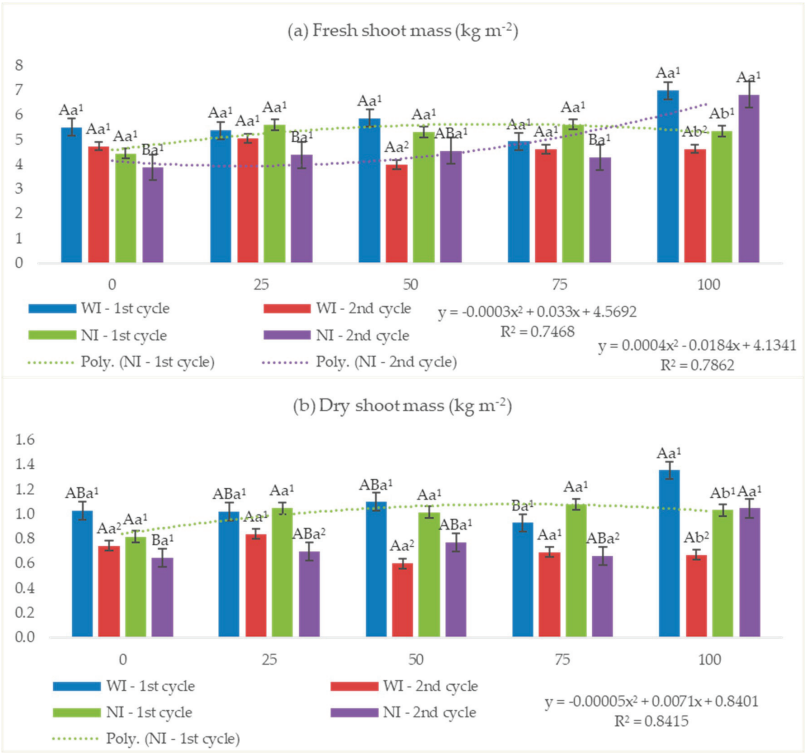


Figure 4. Result of the statistical analysis for fresh shoot biomass (**a**) and dry shoot biomass (**b**) in the interaction between effluent, inoculum, and cycle. Uppercase letters differ for the effluent factor, lowercase letters differ for the inoculum factor, and numbers differ for the cycle factor ($p < 0.05$). WI: with inoculation; NI: without inoculation.

Dry shoot biomass results mirrored the fresh biomass findings, as expected (Figure 4b). However, in the 25% and 75% effluent treatments, the absence of inoculant resulted in lower dry biomass accumulation in cycle 2 compared to cycle 1. This may indicate that, without inoculation, these effluent doses were less effective in optimizing conversion to structural biomass. Effluent doses did not show differences in dry biomass accumulation in non-inoculated subplots in cycle 1 or in inoculated subplots in cycle 2.

3.2.3. Leaf Area and Normalized Difference Vegetation Index

Leaf area measurements using the integrator showed differences only between cultivation cycles, with higher values observed in cycle 2 (Figure 5a). Considering that sampling for this analysis was conducted at stage R5 in cycle 1 and at stage R2 in cycle 2, the increased leaf area observed in the second cycle indicates favorable plant development during that year (2021–2022). Normalized Difference Vegetation Index (NDVI) values obtained showed statistical differences in response to interactions between cycle and inoculation (Figure 5b), cycle and phenological stage (Figure 5c), and effluent and phenological stage (Figure 5d). In the latter case, the data fit a second-degree polynomial equation, allowing us to estimate that the effluent dose maximizing NDVI at stage R2 is 86%.

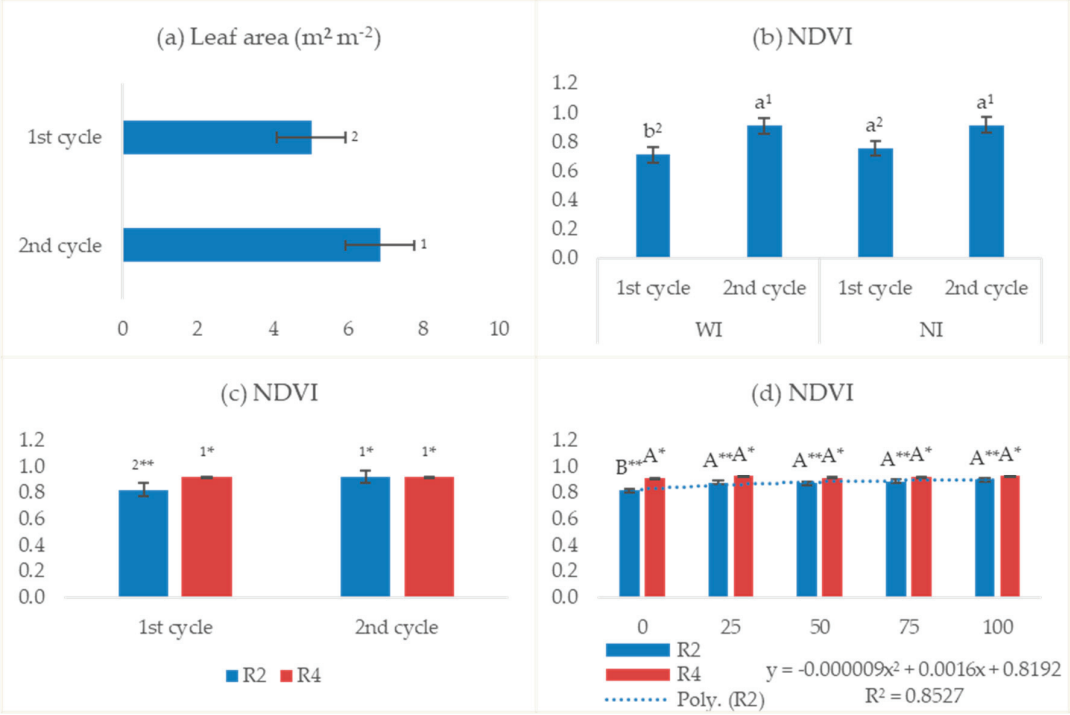


Figure 5. Result of the statistical analysis for (**a**) leaf area in response to the cycle factor and Normalized Difference Vegetation Index (NDVI) in response to (**b**) interaction between inoculum and cycle, as well as (**c**) phenological stage and cycle and (**d**) effluent and phenological stage. Uppercase letters differ for effluent, lowercase letters differ for inoculum, numbers differ for cycle, and asterisks differ for phenological stage ($p < 0.05$). WI: with inoculation; NI: without inoculation.

3.2.4. Root Parameters

The difference between cultivation cycles was significant for both root fresh biomass and root surface area (Figure 6a,d). However, the greater root biomass observed in cycle 1 did not correspond to an increase in root surface area or volume (Figure 6d,f). This result suggests a higher accumulation of structural biomass in cycle 1, whereas in cycle 2, the root architecture likely shifted toward a denser, more branched structure. Root surface area was highest with the 100% effluent dose, comparable with 25% and 50% dosages, while the 0%

effluent treatment showed a lower response (Figure 6b). Root volume varied significantly with both effluent and inoculation treatments (Figure 6e,f); the optimal effluent doses for volume were 25% and 100%, and the absence of inoculation further increased both root volume and surface area (Figure 6c).

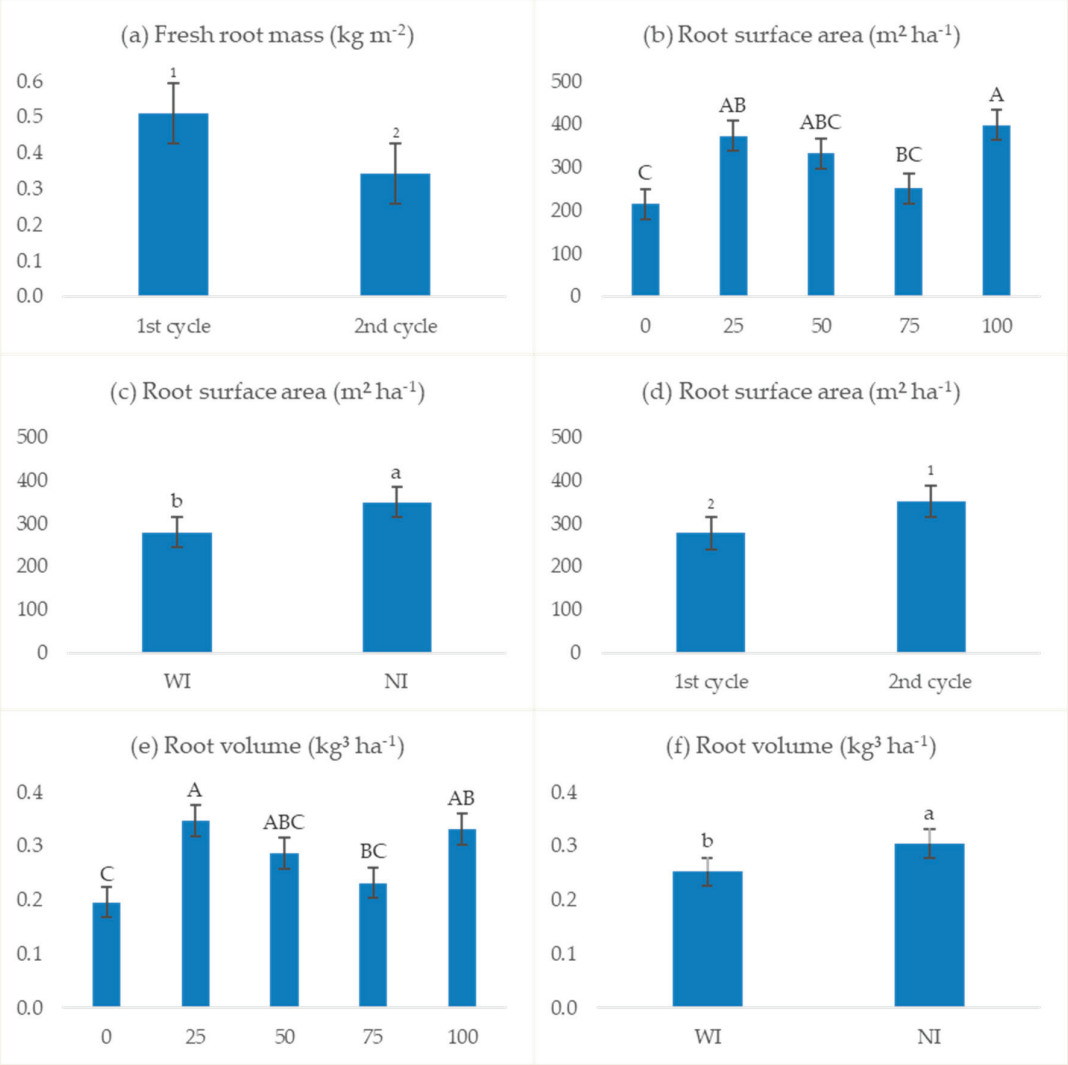


Figure 6. Result of the statistical analysis for (**a**) fresh root mass in response to the cycle factor; root surface area in response to (**b**) effluent, (**c**) inoculation, and (**d**) cycle; and root volume in response to (**e**) effluent and (**f**) inoculation. Uppercase letters differ for effluent, lowercase letters differ for inoculum, and numbers differ for cycle ($p < 0.05$). WI: with inoculation; NI: without inoculation.

3.2.5. Foliar Diagnosis

The statistical analysis results for foliar concentrations of nitrogen, potassium, phosphorus, sodium, calcium, magnesium, and sulfur are presented in Table 3. All analyzed nutrients showed significant differences for the effluent factor, either alone or within interactions. The mean values obtained from the statistical analysis are shown in the table alongside reference values for legumes [25], except for sodium. The averages for magnesium and calcium fell within the recommended range, while phosphorus and potassium were slightly below, and nitrogen and sulfur varied according to the treatments.

Table 3. Leaf diagnosis analysis result for macronutrients and sodium.

	N	P	Ca	Mg	S	Na		P	K	Ca	Mg	Na
						(g kg^{-1})						
Min.	40.00	2.50	4.00	3.00	2.10	-		2.50	17.00	4.00	3.00	-
Max.	54.00	5.00	20.00	10.00	4.00	-		5.00	25.00	20.00	10.00	-
2020–2021	49.04	2.17 [1]	8.95 [2]	6.32	1.26	0.68						
0	46.37 B[1]	2.10	8.40	6.52 A[2]	1.03	0.19						
WI	46.16	2.09	7.93	6.38	1.04 Aa[2]	0.00	0	2.03	16.15 A	12.69 B	6.91	0.29
NI	46.57	2.11	8.87	6.66	1.03 Aa[2]	0.38						
25	46.64 B[1]	2.19	8.49	6.84 A[2]	1.32	0.45	WI	2.09 Aa	15.83	12.37	6.83	0.17 Ba
WI	47.26	2.08	8.67	6.88	1.33 Aa[2]	0.47						
NI	46.01	2.30	8.31	6.80	1.30 Aa[2]	0.42	NI	1.97 Ba	16.46	13.02	6.99	0.40 BCa
50	46.90 B[1]	2.17	8.66	6.63 A[2]	1.21	0.58						
WI	45.48	2.15	8.77	6.68	1.13 Aa[2]	0.35	25	2.06	14.82 AB	13.67 AB	7.51	0.40
NI	48.32	2.20	8.55	6.58	1.28 Aa[2]	0.80						
75	51.11 AB[1]	2.10	8.77	6.00 AB[2]	1.34	0.53	WI	1.96 Ab	14.39	13.81	7.46	0.41 Ba
WI	52.69	2.04	9.00	5.87	1.31 Aa[2]	0.48						
NI	49.53	2.17	8.54	6.14	1.37 Aa[2]	0.57	NI	2.17 ABa	15.24	13.53	7.57	0.39 Ca
100	54.19 A[1]	2.26	10.45	5.61 B[2]	1.39	1.65						
WI	54.10	2.17	10.31	5.44	1.37 Aa[2]	1.72	50	2.11	15.59 AB	13.61 AB	7.39	0.51
NI	54.28	2.35	10.59	5.78	1.41 Aa[2]	1.58						
2021–2022	39.10	2.01 [2]	19.81 [2]	8.18	3.68	0.31	WI	2.11 Aa	15.73	13.65	7.43	0.20 Bb
0	38.71 A[2]	1.94	18.42	7.43 B[1]	3.29	0.42						
WI	37.54	2.09	18.29	7.43	4.38 Aa[1]	0.40	NI	2.10 ABa	15.44	13.58	7.36	0.81 ABa
NI	39.88	1.80	18.55	7.44	2.19 Bb[1]	0.43						
25	38.01 A[2]	1.89	20.57	8.40 A[1]	4.29	0.33	75	2.10	14.33 B	13.69 AB	7.10	0.37
WI	38.86	1.80	20.66	8.22	4.55 Aa[1]	0.33						
NI	37.16	1.99	20.48	8.58	4.03 Aa[1]	0.33	WI	2.00 Ab	14.29	13.75	6.89	0.31 Ba
50	39.95 A[2]	2.02	20.21	8.41 A[1]	3.31	0.42						
WI	41.45	2.06	20.14	8.43	4.10 ABa[1]	0.00	NI	2.19 Aa	14.37	13.63	7.31	0.43 BCa
NI	38.44	1.98	20.28	8.39	2.52 Bb[1]	0.83						
75	38.30 A[2]	2.08	20.24	8.55 A[1]	4.04	0.17	100	2.20	14.70 AB	14.36 A	6.68	1.04
WI	36.86	1.94	20.07	8.24	3.56 ABb[1]	0.10						
NI	39.74	2.23	20.41	8.86	4.53 Aa[1]	0.23	WI	2.13 Aa	14.76	13.86	6.38	1.07 Aa
100	40.52 A[2]	2.11	19.58	8.09 AB[1]	3.49	0.23	NI	2.27 Aa	14.64	14.86	6.97	1.01 Aa
WI	39.83	2.08	18.61	7.63	3.19 Ba[1]	0.20	WI	2.06	15.00	13.49	7.00 a	0.43
NI	41.22	2.15	20.56	8.56	3.79 Aa[1]	0.27	NI	2.14	15.23	13.72	7.24 b	0.61

Uppercase letters differ for effluent, lowercase letters differ for inoculum, and numbers differ for cycle ($p < 0.05$). WI: with inoculation; NI: without inoculation.

No interaction was observed between the higher nitrogen and phosphorus concentrations in the effluent during cycle 2 and foliar levels of these nutrients in the same cycle, as their leaf concentrations were lower in cycle 2. This suggests that the cycle-related differences are associated with other factors, such as nitrogen translocation within the plant and phosphorus's low soil mobility. In contrast, calcium, magnesium, and sulfur levels were higher in cycle 2, likely due to the increased application of these nutrients via effluent. Sodium concentrations showed significant differences between cycles under 75% and 100% effluent irrigation, with higher levels in cycle 1. Sodium content also differed for the inoculation factor at the 50% concentration, with significantly higher means in non-inoculated treatments.

Foliar nitrogen concentrations were higher in cycle 1 and at the 75% and 100% effluent doses. Despite the higher nitrogen application rate in cycle 2, increased precipitation in the second cycle and nitrogen's high soil mobility led to lower leaf concentrations in the second year of cultivation. Nitrogen averages in cycle 1 were within reference values, except for the 100% dose, which was slightly above (54.19 g kg^{-1}). In cycle 2, only the 100% dose fell within the recommended range, while the other doses ranged from 38.01 to 39.95 g kg^{-1}. Despite significant differences, foliar nitrogen levels in the effluent-cycle interaction were close to recommended values.

Foliar potassium content responded significantly to the effluent doses applied. The highest potassium average was observed in the 0% dose, while the lowest was observed at the 75% dose. This response may be linked to the competitive relationship between potassium and sodium, with effluent application and subsequent sodium accumulation possibly influencing K uptake. The potassium means ranged from 14.29 to 16.15 g kg^{-1}. Phosphorus content averaged between 1.94 and 2.25 g kg^{-1} and increased with effluent dose in the absence of inoculation.

Foliar calcium levels were higher in the second cycle and varied according to the effluent concentration, with averages between 8.95 and 19.81 g kg^{-1}, remaining within recommended values. Magnesium levels also fell within the recommended range, ranging from 5.61 to 8.55 g kg^{-1}, with the highest means at intermediate effluent doses in the second cycle. Sulfur levels in the first cycle were all below the recommended range (average of 1.26 g kg^{-1}), while in cycle 2, some treatments met the recommended range, and others exceeded it. In cycle 2, the sulfur content in inoculated plants decreased with increasing effluent doses, while in non-inoculated plants, sulfur concentrations were lowest at 25% and 50% effluent doses.

3.2.6. Chlorophyll Index

The relative chlorophyll index is directly related to chlorophyll content in the leaf and, consequently, to its photosynthetic capacity, serving as an indicator of plant health. The results obtained in this study show that the chlorophyll *a* index responded significantly to the interaction among inoculation, cycle, and vegetative stage (Figure 7a), while the chlorophyll *b* index responded to the effluent dose applied (Figure 7b) to the interaction between inoculation and phenological stage (Figure 7c), and to the interaction between cycle and phenological stage (Figure 7d).

For chlorophyll *a*, the highest means were observed at stage V3 in cycle 1 and at stages R1 and R2 in cycle 2 in both inoculated and non-inoculated plants. For chlorophyll *b*, the effluent dose that maximizes the response is approximately 85.35%, with the highest values observed in reproductive stages when inoculation was present and in R4 without inoculation. When comparing cycles, the best chlorophyll *b* results were obtained at V3 in cycle 1 and at R2 and R4 in cycle 2.



Figure 7. Result of the statistical analysis for (**a**) chlorophyll *a* in response to the inoculation and cycle factor; chlorophyll *b* in response to (**b**) effluent, (**c**) inoculation and phenological stage, and (**d**) cycle and phenological state; and total chlorophyll in response to (**e**) cycle and phenological state. Lowercase letters differ for inoculum, numbers differ for cycle, and asterisks differ for phenological stage ($p < 0.05$). WI: with inoculation; NI: without inoculation.

3.2.7. Yield and Grain Quality

The physiological quality of grains in the first cultivation cycle was lower than in the second, resulting in a reduced yield that fell below the national average of 3202 kg ha^{-1} (CONAB, 2024) [8]. Higher temperatures during the first cycle likely contributed to this outcome, as did the increased rainfall during the late developmental stages in the first cycle, beginning around 110 days after sowing (DAS), corresponding to stages R7 and R8 (beginning of maturity and full maturity). In response to the rainfall, plants started producing new shoots at the nodes, which likely redirected photoassimilates and compromised both plant maturation and grain quality.

Soybean yield did not respond significantly to different doses of treated slaughterhouse effluent used for irrigation. The primary factors influencing yield in this study were inoculation and cultivation cycle, with their interaction showing significant effects (Figure 8a). Non-inoculated soybeans in cycle 1 were the only group with a significantly lower mean yield compared to the others.

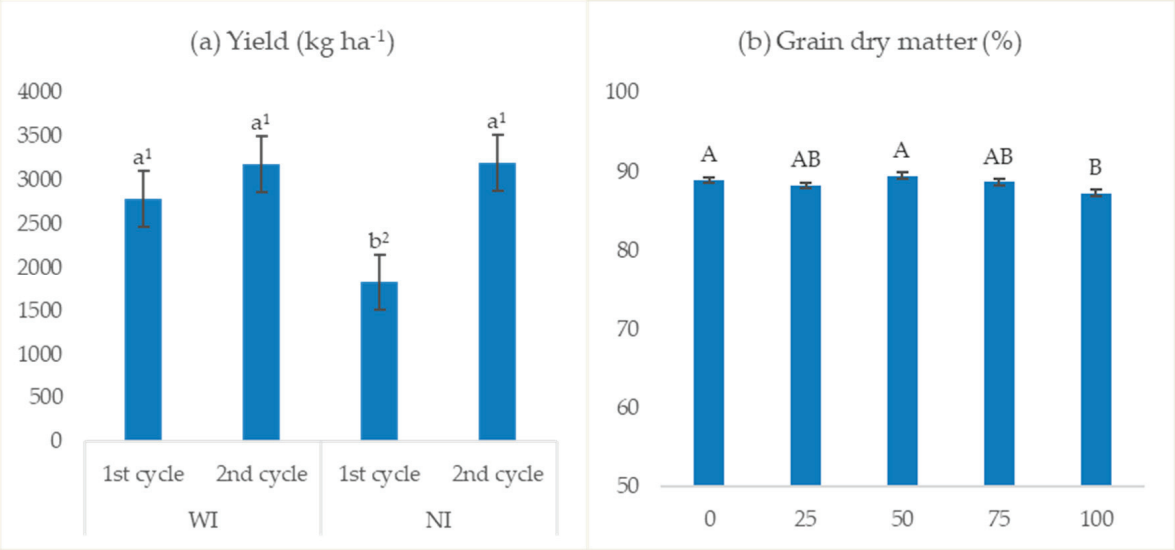


Figure 8. Result of the statistical analysis for (**a**) yield in the interaction for the factors inoculum and cycle and (**b**) grain dry matter in response to the effluent factor. Uppercase letters differ for effluent, lowercase letters differ for inoculum, and numbers differ for cycle ($p < 0.05$). WI: with inoculation; NI: without inoculation.

The bromatological analysis results for soybeans harvested in the second cycle are presented in Table 4 in comparison with other studies and reference values from the Organization for Economic Co-operation and Development (OECD). Most parameters evaluated did not show significant differences for the factors studied, except for the dry matter percentage, which showed a significant response to the effluent factor (Figure 8b), with the lowest value observed in the 100% effluent treatment. However, all treatments remained within the recommended range. This variation is likely associated with the sodium applied to the soil, affecting the dynamics of photoassimilate accumulation in the plants.

Table 4. Average result of the bromatological analysis of soybean grains in the present study compared with other studies and references.

	This Study	Etiosa et al. [26]	Qin et al. [27]	Alghamdi et al. [28]	OECD [29]		
	Average	Average	cv Poongsan	Average	Average	Min.	Max.
Dry Matter	88.52	91.93	-	95.1	89.9	65.6	95.3
Mineral Matter	4.62	4.29	5.01	5.44	5.3	3.9	7
Crude Protein	45.03	37.69	35.05	39.02	39.5	33.2	45.5
Crude Fiber	11.8	5.44	4.75	-	7.8	-	-
Ether Extract	22.55	28.2	17.27	21.16	16.7	8.1	23.6
Nitrogen-Free Extract	15.97	-	-	-	-	-	-
Acid Detergent Fiber	10.5	-	-	-	12	7.8	18.6
Neutral Detergent Fiber	17.19	-	-	-	12.3	8.5	21.3

4. Discussion

4.1. Plant Height and Stand

The results align with findings from other studies, indicating that plant height varied significantly by soybean genotype but not by the presence or absence of rhizobium inoculation [30]. Kakabouki et al. [31] observed an increase in soybean plant height with higher nitrogen doses, with 120 kg ha^{-1} providing the best results compared to lower doses and unfertilized soybeans. The higher plant stand in cycle 2 is consistent with the increased plant height observed, as denser plantings tend to promote etiolation due to light competition, though this response is also influenced by each cultivar's intrinsic characteristics [32]. Serafin-Andrzejewska et al. (2024) [14] reported that nitrogen application combined with inoculation optimized germination and survival rates, resulting in higher plant density, especially with moderate nitrogen dosages (30 kg ha^{-1}). However, the results of this study differed from these findings, as the nitrogen dose–response curve peaked near 0%. Tukey's test showed no significant differences in plant stand across effluent doses, indicating minimal variation, which was also reflected in the low absolute values of coefficients in the dose–response equation. The limited effect of effluent on plant stand was expected, as stand establishment occurs within the first weeks after sowing when salt and nutrient accumulation from effluent is still low.

4.2. Fresh and Dry Shoot Mass

As previously mentioned, higher temperatures and lower precipitation in cycle 1 (see Materials and Methods) created conditions that negatively affected soybean and rhizobium fitness [33]. Under these conditions, high nitrogen doses combined with inoculation allowed the plants to accumulate more fresh shoot biomass. In more favorable environmental conditions, high effluent doses may have impaired symbiosis. Kakabouki et al. [31] reported that applying 120 kg ha^{-1} of nitrogen increased dry shoot biomass. However, environmental factors are known to have a significant impact on soybean yield, accounting for 68% of variability, with nitrogen management practices contributing less than 1% [34]. Therefore, the more stressful environmental conditions in cycle 1 likely influenced soybean response more than nitrogen supplied via effluent. In cycle 2, under more favorable conditions for soybean development, the 100% effluent dose effectively increased dry shoot biomass in the absence of inoculation.

4.3. Leaf Area and Normalized Difference Vegetation Index

Similar to the plant height response, leaf area may have been positively influenced by denser planting in the second cycle, consistent with findings by Jańczak-Pieniążek [35]. These results also align with those of Szpunar-Krok et al. [10], who reported higher leaf area index (LAI) in inoculated treatments; however, they found maximum LAI at stage R3, whereas Montoya et al. [36] observed a peak between stages R4 and R5. Other studies report positive leaf area index responses to nitrogen application. Gai et al. [12] found that

LAI was higher in soybeans fertilized with 50 kg ha^{-1} nitrogen compared to 0, 25, and 75 kg ha^{-1} doses. Basal and Szabó [37] also reported LAI increases with nitrogen application, especially under water-stress conditions.

4.4. Root Parameters

Conversely, Da Silva [38] observed higher soybean yields associated with lower root dry mass, suggesting that conditions that discourage root growth, such as higher soil moisture and water availability, may positively influence grain yield. In line with our findings, Gai et al. [12] reported negative root parameter responses to high nitrogen concentrations. While the 50 kg ha^{-1} dose had positive effects on root parameters, a 75 kg ha^{-1} nitrogen dose inhibited root activity and reduced root dry mass. McCoy et al. [39] corroborated this, reporting a 19% reduction in belowground biomass, with shorter root length and smaller root area in plants receiving 135 kg ha^{-1} nitrogen. Samudin and Kuswantoro [30] observed that inoculants increased root dry matter while reducing root length in soybeans. In the presence of *Bradyrhizobium* spp. inoculation, no difference was found in foliar phosphorus levels, possibly due to phosphorus retention in the roots to support nitrogen fixation [33].

4.5. Foliar Diagnosis

The foliar nutrient diagnosis revealed significant variations in macronutrient and sodium concentrations in response to treated effluent application, inoculation, and cultivation cycle. The observed nitrogen concentrations were higher in the first cycle compared to the second, aligning with nitrogen translocation within plants and the high mobility of this nutrient in soil. Although nitrogen application rates were increased in the second cycle, precipitation may have diluted its soil availability, resulting in lower leaf concentrations. Despite these variations, nitrogen levels in most treatments fell within or near the reference range for legumes, demonstrating the feasibility of effluent irrigation as an alternative nitrogen source.

Potassium concentrations were highest in the absence of effluent application and decreased with increased sodium accumulation from effluent treatments, supporting evidence of competitive absorption between these cations. This interaction has been widely documented as a limiting factor in potassium uptake under saline conditions. Similarly, phosphorus concentrations showed treatment-specific variations, with the absence of *Bradyrhizobium* spp. inoculation enhancing phosphorus uptake at higher effluent doses. This pattern is likely due to reduced phosphorus retention in roots under non-symbiotic conditions, as previously reported in soybean studies [33].

Conversely, calcium, magnesium, and sulfur concentrations were elevated in the second cycle, potentially due to the increased application of these nutrients via effluent. Calcium and magnesium levels consistently met the recommended ranges, highlighting the effluent's role in supplementing essential secondary macronutrients. In contrast, sulfur concentrations varied by treatment, with inoculated plants demonstrating lower sulfur content under higher effluent doses, potentially due to the metabolic demands of nitrogen fixation on sulfur assimilation pathways.

Sodium accumulation showed a notable interaction with the effluent and inoculation factors. Higher sodium levels were detected in non-inoculated treatments, suggesting that *Bradyrhizobium* spp. may mitigate sodium uptake, potentially by enhancing plant resilience to osmotic stress through improved nitrogen assimilation. Additionally, sodium concentrations were higher in the first cycle under 75% and 100% effluent treatments, correlating with lower rainfall and reduced leaching.

4.6. Chlorophyll Index

The highest total chlorophyll levels were observed at V3 in cycle 1 and at R2 in cycle 2, followed by treatments at R1 in cycle 2, R4 in both cycles, and, lastly, the lowest values were seen in R1 and R2 in cycle 1 and V3 in cycle 2. The chlorophyll index is positively influenced by nitrogen and sulfur application, rhizobium inoculation, and higher plant water content [12,37,38,40]. Accordingly, chlorophyll index results from this study indicate that, generally, plants were healthier at V3 than at reproductive stages during cycle 1, while in cycle 2, plant health peaked near stage R2. In interaction with the inoculation factor, inoculation improved chlorophyll b levels during reproductive stages but did not positively affect chlorophyll a when interacting with the cycle, instead showing a reduction at R4 in the second cycle.

4.7. Yield and Grain Quality

Higher maximum temperatures in the first cycle likely contributed to the difference in grain quality, as reported by other authors; elevated temperatures negatively affect soybean fitness and yield [33,41]. This result suggests that under more limiting environmental conditions, rhizobium inoculation supports soybean response, whereas inoculation has no significant effect in favorable conditions. The positive effect of inoculation on soybean yield has been documented in several studies [10,14], as well as its beneficial effects on physiological responses [30]. This positive effect can occur due to various factors reported in the literature, including improved nutrient availability and uptake, enhanced plant growth, increased pathogen resistance, greater biomass accumulation [42], and increased salt stress tolerance [43]. The latter effect is particularly relevant to this study, as sodium concentrations in leaves correlated positively with effluent application in cycle 1.

The average yields in this study are compared with those from other scientific studies in Table 5. Other authors also found no significant yield difference in response to nitrogen application [10,11,44]. Kakabouki et al. [31], however, noted a significant yield increase with higher nitrogen doses. La Menza et al. [45] compared soybean production under limited versus abundant nitrogen supply across 13 environments, concluding that nitrogen limitation affects yield in high-productivity environments, with the extent of this limitation modulated by pre-existing soil nitrogen.

Table 5. Comparison of soybean yield values in the present study with average soybean yields found in the literature. Uppercase letters differ for effluent, lowercase letters differ for inoculum ($p < 0.05$) in this study, while different letters within each study denote specific treatment differences. WI: with inoculation; NI: without inoculation.

This Study SP-Brasil		Santachiara et al. [11] Argentina		Flajšman et al. [44] Slovenia		Kakabouki et al. [31] Greece		Szpunar-Krok et al. [10] Poland	
Treatment	**kg ha^{-1}**	**Treatment**	**kg ha^{-1}**	**Treatment**	**kg ha^{-1}**	**Treatment**	**kg ha^{-1}**	**Treatment**	**kg ha^{-1}**
WI Cycle 1	2782 Aa	0 kg N ha^{-1}	4968	WI	3093	0 kg N ha^{-1}	4066–4095 c	0 kg N ha^{-1}	3740
NI Cycle 1	1823 Bb	600 kg N ha^{-1}	5081	NI	3162	80 kg N ha^{-1}	4208–4225 bc	30 kg N ha^{-1}	3860
WI Cycle 2	3180 Aa			Control	3044	100 kg N ha^{-1}	4327–4343 ab	60 kg N ha^{-1}	3950
NI Cycle 2	3190 Aa			Zeolite 600 kg ha^{-1} + 30 kg N ha^{-1} + 72–90 kg N ha^{-1}	3161	120 kg N ha^{-1}	4441–4462 a	NI	3610 b
					3174			WI HiStick®	4010 a
				Zeolite 600 kg ha^{-1} + 30 kg N ha^{-1} + 72–90 kg N ha^{-1}	3132			WI Nitragina	3940 a

Mourtzinis et al. [34] assessed nitrogen application in soybeans under different management practices, noting that split applications, surface applications, and applications distributed across vegetative and reproductive stages (rather than solely reproductive) yielded better results. However, only 1% of environmental variation was attributed to

nitrogen fertilization. Hoffaman et al. [46] supported this, showing that soybeans are more sensitive to water deficiency than nitrogen deficiency, a finding mirrored by Montoya et al. [36] in their yield responses to irrigation. Recent studies in Brazil found significant soybean yield differences when grown after sorghum fertilized with increasing nitrogen doses (0, 50, and 100 kg ha^{-1}), with higher yields when nitrogen application was combined with no-till soybean planting after sorghum [15]. Yield averages in this study also varied by production year, with estimated yields ranging from 2250 to 3250 kg ha^{-1} in the 2019–2020 season and 2500 to 3500 kg ha^{-1} in the 2021–2022 season.

While numerous studies report that biological nitrogen fixation (BNF) is inhibited by nitrogen fertilization [11,47,48], this process is also strongly modulated by other factors. According to Santachiara, Salvagiotti, and Rotundo [33], phosphorus and potassium are major BNF promoters, while sulfur and other micronutrients also have positive impacts. It is also important to note that reduced BNF due to nitrogen application is not directly related to decreased yield, as soils with adequate mineral nitrogen supply can balance nitrogen sources [49].

The lack of significant yield response to effluent suggests that nitrogen sources compensated sufficiently to meet soybean needs, even if some biometric parameters were affected, as seen earlier. However, the importance of *Bradyrhizobium* spp. inoculation in mitigating adverse effects on soybean performance is evident.

The quality of grains from the second cycle was satisfactory, not only meeting established nutrient levels but also exhibiting high crude protein content compared to other studies. Since nitrogen application can increase seed protein content [37,50], the high crude protein values and lack of significant differences in this variable support the earlier discussion that nitrogen deficiency was not a concern in the second cycle due to the balance between nitrogen sources.

5. Conclusions

This study evaluated the impact of irrigation with treated slaughterhouse effluent on soybean growth, development, and yield under different effluent concentrations, with and without *Bradyrhizobium* spp. inoculation. Effluent application enhanced plant height, leaf area, and biomass, with the most significant effects observed at higher effluent concentrations combined with inoculation in the first cycle. Foliar nitrogen increased with elevated effluent doses in the first cycle, while chlorophyll *b* index peaked at 85.35% effluent irrigation. Yield was not significantly affected by effluent dilutions, highlighting the dominant influence of environmental factors.

Cycle-dependent variations in environmental factors, particularly rainfall and nitrogen concentrations in the effluent, influenced crop responses, underlining the importance of adjusting effluent application to the specific climatic conditions of each growing season. Inoculation with *Bradyrhizobium* spp. proved beneficial in promoting plant health and yield, particularly under suboptimal conditions, reinforcing the importance of microbial symbiosis for sustainable crop management.

Overall, this study supports the viability of using treated effluent as an alternative irrigation source in soybean production, with potential benefits for reducing reliance on chemical fertilizers and conserving freshwater resources. Careful management of effluent dosage is essential to maximize yield and ensure the compatibility of effluent irrigation with sustainable agricultural practices. Further research is recommended to explore the long-term agronomic impacts and the economic feasibility of large-scale effluent reuse in soybean and other legume crops, contributing to more sustainable agriculture in water-scarce regions.

Author Contributions: A.C.M.L.: conceptualization, methodology, formal analysis, investigation, data curation, and writing—original draft preparation; L.B. and L.R.T.: conceptualization, methodology, formal analysis, investigation, and data curation; A.L.d.S.D. and G.N.S.: investigation and data curation; T.M.G.: writing—review and editing, supervision, and funding acquisition; F.R.: writing—review and editing, supervision, project administration, and funding acquisition. All authors have read and agreed to the published version of the manuscript.

Funding: This research received no external funding.

Data Availability Statement: Data will be made available on request.

Acknowledgments: The authors would like to thank CAPES (Brazil) for the scholarship (Financing Code 001, process 88887.484379/2020-00), the University of Sao Paulo—*Campus* "Fernando Costa" for supplying the space, and all of the Grupo de Estudos em Engenharia de Biossistemas (GEBio) team for their hard work collecting data. During the preparation of this manuscript, the authors used ChatGPT and GPT-4-turbo (from OpenAI) for the purposes of academic language refinement, manuscript structuring, and adherence to journal formatting standards. The authors have reviewed and edited the output and take full responsibility for the content of this publication.

Conflicts of Interest: The authors declare no conflicts of interest.

References

1. Ribeiro, W.C.; Conferência da Água da ONU: A Contribuição da USP. Jornal da USP, São Paulo, 12 April 2023. Available online: https://jornal.usp.br/?p=626794 (accessed on 20 October 2024).
2. Bruyninckx, H.; Hatfield-Dodds, S.; Hellweg, S.; Schandl, H.; Vidal, B.; Razian, H.; Nohl, R.; Marcos-Martinez, R.; West, J.; Lu, Y.; et al. *Global Resources Outlook 2024: Bend the Trend—Pathways to a Liveable Planet as Resource Use Spikes*; International Resource Panel: Nairobi, Kenya, 2024; Available online: https://wedocs.unep.org/20.500.11822/44901 (accessed on 20 October 2024).
3. Agência Nacional de Águas e Saneamento Básico (ANA). *Conjuntura dos Recursos Hídricos no Brasil 2023: Informe Anual*; ANA: Brasília, Brazil, 2024; 118p.
4. Chojnacka, K.; Moustakas, K.; Witek-Krowiak, A.; Skrzypczak, D.; Mikula, K.; Loizidou, M. A transition from conventional irrigation to fertigation with reclaimed wastewater: Prospects and challenges. *Renew. Sustain. Energy Rev.* **2020**, *130*, 109959. [CrossRef]
5. Almeida, I.C.C.; Fernandes, R.B.A.; Neves, J.C.L.; Ruiz, H.A.; De Lima, T.L.B.; Hoogmoed, W. Soil quality after six years of paper mill industrial wastewater application. *Rev. Bras. Ciênc. Solo* **2017**, *41*, e0160400. [CrossRef]
6. Wang, H.; Wang, J.; Yu, X. Wastewater irrigation and crop yield: A meta-analysis. *J. Integr. Agric.* **2022**, *21*, 1215–1224. [CrossRef]
7. Food and Agriculture Organization of the United Nations (FAO). FAOSTAT: Crops. Available online: https://www.fao.org/faostat/en/#data/QCL (accessed on 29 September 2024).
8. Companhia Nacional de Abastecimento (CONAB). Boletim da Safra de Grãos. 12° Levantamento—Safra 2023/24. Available online: https://www.conab.gov.br/info-agro/safras/graos/boletim-da-safra-de-graos (accessed on 14 October 2024).
9. Ramlal, A.; Nautiyal, A.; Lal, S.K.; Chigeza, G. A wonder legume, soybean: Prospects for improvement. *Front. Plant Sci.* **2023**, *14*, 1294185. [CrossRef]
10. Szpunar-Krok, E.; Bobrecka-Jamro, D.; Pikuła, W.; Jańczak-Pieniążek, M. Effect of nitrogen fertilization and inoculation with *Bradyrhizobium japonicum* on nodulation and yielding of soybean. *Agronomy* **2023**, *13*, 1341. [CrossRef]
11. Santachiara, G.; Salvagiotti, F.; Rotundo, J.L. Does biological nitrogen fixation modify soybean nitrogen dilution curves? *Field Crops Res.* **2018**, *223*, 171–178. [CrossRef]
12. Gai, Z.; Zhang, J.; Li, C. Effects of starter nitrogen fertilizer on soybean root activity, leaf photosynthesis and grain yield. *PLoS ONE* **2017**, *12*, e0174841. [CrossRef]
13. Liu, Y.; Yin, X.; Xiao, J.; Tang, L.; Zheng, Y. Interactive influences of intercropping by nitrogen on flavonoid exudation and nodulation in faba bean. *Sci. Rep.* **2019**, *9*, 4818. [CrossRef]
14. Serafin-Andrzejewska, M.; Jama-Rodzeńska, A.; Helios, W.; Kozak, M.; Lewandowska, S.; Zalewski, D.; Kotecki, A. Influence of nitrogen fertilization, seed inoculation and the synergistic effect of these treatments on soybean yields under conditions in south-western Poland. *Sci. Rep.* **2024**, *14*, 6672. [CrossRef]
15. Da Silva, G.F.; Calonego, J.C.; Luperini, B.C.O.; Chamma, L.; Zanetti, W.A.L.; Borghi, E.; Parrella, R.A.C.; Putti, F.F. Nitrogen fertilization in biomass sorghum improves the yield and quality of soybeans grains grown in succession in long-term management systems. *Eur. J. Agron.* **2024**, *158*, 127206. [CrossRef]

16. American Public Health Association (APHA); American Water Works Association (AWWA); Water Environment Federation (WEF). *Standard Methods for the Examination of Water and Wastewater*, 22nd ed.; APHA: Washington, DC, USA, 2012; 1496p.
17. Farias, J.R.B.; Nepomuceno, A.L.; Neumaier, N. *Ecofisiologia da Soja*; Circular Técnica No. 48; Embrapa Soja: Londrina, Brazil, 2007. Available online: http://www.infoteca.cnptia.embrapa.br/infoteca/handle/doc/470308 (accessed on 20 August 2024).
18. Braga, N.R.; Reco, P.C.; Galo, P.B.; de Miranda, M.A.C.; Mascarenhas, H.A.A. Soybean: *Glycine max* (L.) Merrill. In *Boletim 200: Instruções agrícolas para as principais culturas econômicas*, 7th ed.; da Eira Aguiar, A.T., Gonçalves, C., Zagatto Paterniani, M.E.A.G., Tucci, M.L.S.A., de Castro, C.E.F., Eds.; Instituto Agronômico: Campinas, Brazil, 2014; p. 452.
19. Ferreira, D.F. Sisvar: A computer statistical analysis system. *Ciênc. Agrotec.* **2011**, *35*, 1039–1042. [CrossRef]
20. Oliveira, J.F.D.; Rodrigues, F.N.; Fia, R.; Vilela, H.S.; Landim, D.V. Chemical properties of soil fertirrigated with dairy and slaughterhouse wastewater. *Eng. Agríc.* **2017**, *37*, 1244–1253. [CrossRef]
21. Araujo, I.R.; Sampaio, S.C.; Paz-Gonzalez, A.; Vilas-Boas, M.A.; Gonçalves, A.C.; Szekut, F.D. Reforested soil under drip irrigation with treated wastewater from poultry slaughterhouse. *Rev. Bras. Eng. Agríc. Ambient.* **2019**, *23*, 439–445. [CrossRef]
22. Emerick, T.; Vieira, J.L.; Silveira, M.H.L.; João, J.J. Ultrasound-assisted electrocoagulation process applied to the treatment and reuse of swine slaughterhouse wastewater. *J. Environ. Chem. Eng.* **2020**, *8*, 104308. [CrossRef]
23. Kanafin, Y.N.; Makhatova, A.; Meiramkulova, K.; Poulopoulos, S.G. Treatment of a poultry slaughterhouse wastewater using advanced oxidation processes. *J. Water Process Eng.* **2022**, *47*, 102694. [CrossRef]
24. Madeira, L.; Carvalho, F.; Almeida, A.; Teixeira, M.R. Optimization of atmospheric carbonation in the integrated treatment immediate one-step lime precipitation and atmospheric carbonation: The case study of slaughterhouse effluents. *Results Eng.* **2023**, *17*, 100807. [CrossRef]
25. Van Raij, B.; Cantarella, H.; Quaggio, J.A.; Furlani, A.M.C. *Recomendações de Adubação e Calagem para o Estado de São Paulo*, 2nd ed.; Boletim Técnico 100; Instituto Agronômico de Campinas: Campinas, Brasil, 1997; 285p.
26. Etiosa, O.R.; Chika, N.B.; Benedicta, A. Mineral and proximate composition of soya bean. *Asian J. Phys. Chem. Sci.* **2017**, *4*, 1–6. [CrossRef]
27. Qin, Y.; Park, S.Y.; Oh, S.W.; Lim, M.H.; Shin, K.S.; Cho, H.S.; Lee, S.K.; Woo, H.J. Nutritional composition analysis for beta-carotene-enhanced transgenic soybeans (*Glycine max* L.). *Appl. Biol. Chem.* **2017**, *60*, 299–309. [CrossRef]
28. Alghamdi, S.S.; Khan, M.A.; El-Harty, E.H.; Ammar, M.H.; Farooq, M.; Migdadi, H.M. Comparative phytochemical profiling of different soybean (*Glycine max* (L.) Merr) genotypes using GC–MS. *Saudi J. Biol. Sci.* **2018**, *25*, 15–21. [CrossRef]
29. Organisation for Economic Co-operation and Development (OECD). *Revised Consensus Document on Compositional Considerations for New Varieties of Soybean [Glycine max (L.) Merr.]: Key Food and Feed Nutrients, Anti-Nutrients, Toxicants and Allergens*; Series on the Safety of Novel Foods and Feeds; No. 25; OECD: Paris, France, 2012; Available online: https://www.oecd.org (accessed on 26 October 2024).
30. Samudin, S.; Kuswantoro, H. Effect of rhizobium inoculation to nodulation and growth of soybean [*Glycine max* (L.) Merrill] germplasm. *Legume Res.* **2018**, *41*, 303–310. [CrossRef]
31. Kakabouki, I.; Zisi, C.; Mavroeidis, A.; Kouneli, V.; Karydogianni, S.; Folina, A.; Triantafyllidis, V.; Efthimiadou, A.; Roussis, I.; Zotos, A.; et al. Effects of nitrogen fertilization on weed flora and productivity of soybean [*Glycine max* (L.) Merr.] crop. *Nitrogen* **2022**, *3*, 284–297. [CrossRef]
32. Do Carmo, E.L.; Rocha, A.G.C.; Simon, G.A.; Da Silva, A.G.; Braz, G.B.P. Adensamento de plantas e épocas de cultivo de soja no cerrado. *Colloq. Agrar.* **2018**, *14*, 1–12. [CrossRef]
33. Santachiara, G.; Salvagiotti, F.; Rotundo, J.L. Nutritional and environmental effects on biological nitrogen fixation in soybean: A meta-analysis. *Field Crops Res.* **2019**, *240*, 106–115. [CrossRef]
34. Mourtzinis, S.; Gurpreet Kaur, G.; Orlowski, J.M.; Shapiro, C.A.; Lee, C.D.; Wortmann, C.; Holshouser, D.; Nafziger, E.D.; Kandel, H.; Niekamp, J.; et al. Soybean response to nitrogen application across the United States: A synthesis-analysis. *Field Crops Res.* **2018**, *215*, 74–82. [CrossRef]
35. Jańczak-Pieniążek, M.; Buczek, J.; Bobrecka-Jamro, D.; Szpunar-Krok, E.; Tobiasz-Salach, R.; Jarecki, W. Morphophysiology, productivity and quality of soybean (*Glycine max* (L.) Merr.) cv. Merlin in response to row spacing and seeding systems. *Agronomy* **2021**, *11*, 403. [CrossRef]
36. Montoya, F.; García, C.; Pintos, F.; Otero, A. Effects of irrigation regime on the growth and yield of irrigated soybean in temperate humid climatic conditions. *Agric. Water Manag.* **2017**, *193*, 30–45. [CrossRef]
37. Basal, O.; Szabó, A. The combined effect of drought stress and nitrogen fertilization on soybean. *Agronomy* **2020**, *10*, 384. [CrossRef]
38. Da Silva, G.F.; Calonego, J.C.; Luperini, B.C.O.; Chamma, L.; Alves, E.R.; Rodrigues, S.A.; Putti, F.F.; Silva, V.M.; Silva, M.A. Soil–Plant relationships in soybean cultivated under conventional tillage and long-term no-tillage. *Agronomy* **2022**, *12*, 697. [CrossRef]
39. McCoy, J.M.; Kaur, G.; Golden, B.R.; Orlowski, J.M.; Cook, D.R.; Bond, J.A.; Cox, M.S. Nitrogen fertilization of soybean affects root growth and nodulation on two soil types in Mississippi. *Commun. Soil Sci. Plant Anal.* **2018**, *49*, 181–187. [CrossRef]

40. Bi, Y.; Fan, C.; Liang, W.; Liao, Y.; Han, D.; Li, W.; Chen, X.; Liu, M.; Liu, J.; Di, S.; et al. Combination effects of sulfur fertilizer and rhizobium inoculant on photosynthesis dynamics and yield components of soybean. *Agronomy* **2024**, *14*, 794. [CrossRef]
41. Allen Jr, L.H.; Zhang, L.; Boote, K.J.; Hauser, B.A. Elevated temperature intensity, timing, and duration of exposure affect soybean internode elongation, mainstem node number, and pod number per plant. *Crop J.* **2018**, *6*, 148–161. [CrossRef]
42. Kebede, E. Competency of rhizobial inoculation in sustainable agricultural production and biocontrol of plant diseases. *Front. Sustain. Food Syst.* **2021**, *5*, 728014. [CrossRef]
43. Fu, X.; Bian, D.; Gu, X.; Cao, J.; Liu, J. Combination of graphene oxide and rhizobium improved soybean tolerance in saline-alkali stress. *Agronomy* **2023**, *13*, 1637. [CrossRef]
44. Flajšman, M.; Mihelič, R.; Kolmanič, A.; Ačko, D.K. Influence of soil amended with zeolite and/or mineral N on agronomic performance and soil mineral N dynamics in a soybean–winter triticale crop rotation field experiment. *Cereal Res. Commun.* **2020**, *48*, 239–246. [CrossRef]
45. La Menza, N.C.; Monzon, J.P.; Specht, J.E.; Lindquist, J.L.; Arkebauer, T.J.; Graef, G.; Grassini, P. Nitrogen limitation in high-yield soybean: Seed yield, N accumulation, and N-use efficiency. *Field Crops Res.* **2019**, *237*, 74–81. [CrossRef]
46. Hoffmann, B.; Varga, B.; Nagy, E.; Hoffmann, S.; Darkó, É.; Tajti, J.; Janda, T. Effects of nitrogen and water deficiency on agronomic properties, root characteristics and expression of related genes in soybean. *Agronomy* **2021**, *11*, 1329. [CrossRef]
47. Shin, C.; Sharif, M.O.; Lee, H. Evaluating the effect of bacterial inoculation and fertilization on the soil nutrient status of coal mine soil by growing soybean (*Glycine max*) and shrub lespedeza (*Lespedeza bicolor*). *Sustainability* **2018**, *10*, 4793. [CrossRef]
48. Ciampitti, I.A.; de Borja Reis, A.F.; Córdova, S.C.; Castellano, M.J.; Archontoulis, S.V.; Correndo, A.A.; De Almeida, L.F.A.; Rosso, L.H.M. Revisiting biological nitrogen fixation dynamics in soybeans. *Front. Plant Sci.* **2021**, *12*, 727021. [CrossRef]
49. Santachiara, G.; Borrás, L.; Salvagiotti, F.; Gerde, J.A.; Rotundo, J.L. Relative importance of biological nitrogen fixation and mineral uptake in high yielding soybean cultivars. *Plant Soil.* **2017**, *418*, 191–203. [CrossRef]
50. La Menza, N.C.; Monzon, J.P.; Specht, J.E.; Grassini, P. Is soybean yield limited by nitrogen supply? *Field Crops Res.* **2017**, *213*, 204–212. [CrossRef]

Disclaimer/Publisher's Note: The statements, opinions and data contained in all publications are solely those of the individual author(s) and contributor(s) and not of MDPI and/or the editor(s). MDPI and/or the editor(s) disclaim responsibility for any injury to people or property resulting from any ideas, methods, instructions or products referred to in the content.

agronomy

MDPI

Communication

Exploratory Field Case Study of Microbial and Resistance Genes Dynamics in the Maize Phyllosphere Following Fertigation with Anaerobic Digestate

Camila Fabiani [1,2], María V. Valero [1], Jessica Basualdo [2], Marco Allegrini [3], Gastón A. Iocoli [1,2], María B. Villamil [4,†] and María C. Zabaloy [1,2,*,†]

[1] Centro de Recursos Naturales Renovables de la Zona Semiárida (CERZOS), Universidad Nacional del Sur (UNS), CONICET, Bahía Blanca 8000, Argentina; camila.fabiani@uns.edu.ar (C.F.); mvvalero@cerzos-conicet.gob.ar (M.V.V.); gastoniocoli@yahoo.com.ar (G.A.I.)
[2] Departamento de Agronomía, Universidad Nacional del Sur (UNS), San Andrés 800, Bahía Blanca 8000, Argentina; jessica.basualdo@uns.edu.ar
[3] Instituto de Investigaciones en Ciencias Agrarias de Rosario (IICAR), Facultad de Ciencias Agrarias, Universidad Nacional de Rosario, CONICET, Zavalla 2170, Argentina; allegrini@iicar-conicet.gob.ar
[4] Department of Crop Sciences, University of Illinois, Urbana, IL 61801, USA; villamil@illinois.edu
* Correspondence: mzabaloy@uns.edu.ar
† These authors contributed equally to this work.

Abstract

Anaerobic digestate from manure, a byproduct of biogas production, is increasingly used as an organic fertilizer in circular agriculture systems. This study assessed the microbiological impact of maize fertigation with anaerobic digestate, focusing on fecal indicators (*Escherichia coli*, *Salmonella*), antibiotic resistance genes (ARGs), and integrons. The trial was conducted in a commercial maize field, where on-site manure-based anaerobic digestate was applied via center-pivot irrigation. Leaf samples were collected two days (2 dai) and four weeks (4 wai) after the last fertigation. *E. coli* and *Salmonella* were assessed by culturable methods, while ARGs and integrons were analyzed by qPCR. Results showed that *E. coli* (3 MPN/g) and *Salmonella* were detected at 2 dai but were undetectable at 4 wai and in the control condition, suggesting transient contamination. The abundance of *tetW* was approximately tenfold higher in digestate-treated plants than in the control, while no consistent changes were observed for the other genes. Overall, fertigation with anaerobic digestate appears to pose minimal microbiological impact within the specific conditions of this study, although it may act as a source of specific resistance determinants. Although limited by the use of single treated and control plots, this study offers preliminary insight into microbial and resistance gene dynamics in the phyllosphere, providing a basis for future replicated hypothesis-driven studies.

Keywords: feedlot manure; anaerobic digestion; fecal indicators; antibiotic resistance genes; *tetW*; *ermB*; $bla_{CTX\text{-}M}$; *intI1*; *a-int1*

1. Introduction

The "One Health" concept emphasizes the link between human, animal, and environmental health, proposing a unified approach to global health challenges [1]. Antimicrobial resistance (AMR) is a priority concern under this framework, as the misuse and overuse of antibiotics in recent decades in both human medicine and livestock production is accelerating its emergence and dissemination [2,3]. Globally, antimicrobials used in food animals

represent approximately 73% of total antibiotic consumption, with a projected increase of 11.5% by 2030 relative to 2017 [3]. In livestock farming, a significant portion of these antibiotics is used for non-therapeutic purposes, including growth promotion and disease prophylaxis, contributing to the spread of AMR [3].

Unmetabolized antibiotics in manure promote an increase in antimicrobial resistance genes (ARGs) levels, recognized by the WHO as contaminants of emerging concern, by applying selective pressure on microbial communities [2,4]. These genes can be transferred between bacteria in animal populations and from animals to humans, increasing the risk of treatment failures in both veterinary and human healthcare [5]. There is strong scientific evidence indicating that antimicrobial use on farms imposes a public health impact due to infections with resistant pathogens [6]. As many of the microbes that are pathogenic in livestock animals are also pathogenic in humans, there is a potential for resistant strains to develop in animals and subsequently infect humans [1].

The dissemination of ARGs represents one of the main challenges to global public health [2,3,7]. On the other hand, mobile genetic elements (MGEs), such as integrons, play a crucial role in the spread and assembly of ARGs by facilitating horizontal gene transfer both within and between bacterial populations. This makes them a significant reservoir of resistance determinants, which should be regarded as a threat from the "One Health" perspective [3].

Without effective measures to stop the spread of AMR, it is projected to result in 10 million deaths per year by 2050. To address this urgent issue, a "One Health" approach would be necessary, involving multidisciplinary strategies and the collaboration of various national and international agencies to combat this problem [1].

A Circular Economy is a systemic framework intended to address global challenges such as waste, climate change, pollution, and biodiversity loss. As a sustainable alternative to the traditional linear economic model, it represents a new paradigm focused on minimizing waste and pollution, optimizing resource efficiency by keeping products and materials in use, and restoring natural systems [8]. Within this framework, waste is redefined as a resource that can be reintegrated into the production process [9]. Agricultural operations generate substantial volumes of agro-waste, generally accompanied by limited disposal options. As a result, it contributes to exacerbating various key problems like greenhouse gas emissions, soil degradation, and biodiversity loss [10]. Taking this into account, it is urgent to consider innovative solutions to transform agro-waste into valuable resources. One critical aspect of this challenge is the improper disposal of animal manure, which, despite its potential to cause ecological damage, can be a valuable resource if integrated into a circular concept [11]. In this regard, anaerobic digestion of manure emerges as an attractive and cost-effective treatment. This process consists of the microbial decomposition of organic material in a bioreactor under anaerobic conditions, generating biogas. The biogas is then converted into electrical and thermal energy or, more recently, upgraded to biomethane, while anaerobic digestate, a byproduct, holds significant potential as a sustainable fertilizer in agricultural systems [12]. Animal manure anaerobic digestate contributes to nutrient recycling, reduces reliance on chemical fertilizers, and ultimately supports environmental sustainability [13]. However, its use presents certain risks that need to be carefully considered.

The influence of the anaerobic digestion process on the survival of pathogenic or multidrug-resistant bacteria is a topic that has received considerable attention. In many cases, the persistence of antibiotics, ARGs to commonly used antibiotics in the livestock sector, as well as MGEs involved in the spread of resistance in agroecosystems, has been reported [14,15]. These compounds can be exchanged between bacteria in the microbiota of animals, plants, soils, and humans through horizontal gene transfer, thus contributing to

the global problem of AMR and multidrug resistance [7]. This horizontal gene transfer also extends to plant-associated environments. Specifically, microorganisms establish a diverse range of intimate associations with plants, inhabiting the phyllosphere (the above-ground plant surface), the plant interior as endophytes, and the rhizosphere (the surrounding soil and roots) [16]. In fact, the presence of ARGs has been detected in the phyllosphere of many plants, among them maize (*Zea mays* L.), even though little is known about the composition of the antibiotic resistome and the factors influencing the diversity and abundance of ARGs [17]. Maize is a versatile cereal crop that plays a central role in global agriculture. Approximately 60% of its production is dedicated to livestock feed. It is a primary energy source in diets for poultry, swine, and cattle due to its high energy value, palatability, and digestibility. In beef and dairy cattle, maize forages, including silage, are extensively utilized due to its unique nutritional and functional properties, including their starch content and presence of essential fatty acids, with feedlot diets often comprising around 75–80% of maize [18].

The use of anaerobic digestate as a fertilizer may introduce complex interactions that could influence the composition and dynamics of microbial communities, potentially allowing the persistence of pathogens and ARGs within the phyllosphere and, consequently, threatening the health of cattle fed with maize silage. In agricultural practice, fertigation—the application of liquid fertilizers through irrigation systems—is a common approach to efficiently deliver nutrients to crops. Therefore, it is crucial to investigate how the application of anaerobic digestates by fertigation could affect the spread of ARGs, providing a deeper understanding of the potential risks and benefits associated with using anaerobic digestate as a fertilizer in sustainable agricultural practices. This study aimed to evaluate microbiological impacts of fertigation with anaerobic digestate within a privately managed, commercial maize operation practicing circular agriculture. Anaerobic digestate generated on-site from feedlot manure was applied through the system's only available center pivot. While replication was limited by the realities of large-scale farming infrastructure, this case study offers valuable, context-specific data on pathogen and ARG dynamics, providing insight for both scientific advancement and sustainable practice.

2. Materials and Methods

2.1. Study Site and Climate Context

This study was carried out in collaboration with a privately owned commercial maize operation located in Coronel Suárez, Buenos Aires Province, Argentina. The farm is actively implementing a circular agriculture model, whereby anaerobic digestate produced on-site from cattle manure is reused as fertigation input for maize. The climate in Coronel Suárez is temperate, with a mean annual temperature of approximately 15 °C and annual rainfall averaging 800 to 1000 mm, relatively evenly distributed. In 2023, the site received approximately 870.7 mm of precipitation, with a typical dry period in late winter and occasional semi-dry conditions in mid-summer (January–February). The soils in both fields are classified as clay loam Petrocalcic Hapludols [19].

2.2. Field Design and Agronomic Practices

The study was conducted in two maize fields. The treated field (37°39′30″ S, 61°52′19″ W) is equipped with the operation's only center-pivot irrigation system, delivering overhead sprinkler application that fully wets the canopy. This field received liquid anaerobic digestate through fertigation. The control field (37°32′48.39″ S, 61°56′25.92″ W) was located 14 km northwest of the treated site to avoid cross-contamination, while maintaining similar environmental and soil conditions. Neither field had a history of animal grazing, and both are exclusively dedicated to crop production. Maize was sown in De-

cember 2023 using DUO 30 (Corteva Agriscience, Buenos Aires, Argentina) at a density of 65,000 plants/ha in the anaerobic digestate-treated field (60 ha), and NK 897 (Syngenta, Buenos Aires, Argentina) at 40,000 plants/ha in the control field (26 ha). Diammonium phosphate was applied prior to sowing at 60 kg/ha (treated) and 80 kg/ha (control), and light harrowing was conducted only in the treated field to prepare the seedbed. Due to logistical and operational constraints on this commercial farm, only one digestate-treated field and one control field were available for study. Therefore, differences in hybrid, plant density, and base fertilizer rates may act as potential confounding factors in the interpretation of results.

2.3. Anaerobic Digestate Source and Application

The liquid anaerobic digestate used in this study was produced on-site at the BiodeS plant operated by Agro De Souza S.A. (Coronel Suárez, Argentina), using two complete mix anaerobic reactors fueled entirely by feedlot cattle manure. The system features a European-style design and includes key components from Vogelsang® GmbH & Co. KG, (Essen, Oldenburg, Germany). Anaerobic digestion is carried out under mesophilic conditions (39 °C), with a hydraulic retention time of 40 days. Starting December 12th, a total of 100,842 L per hectare of anaerobic digestate was applied to 50 ha of maize via the pivot system. Anaerobic digestate was pumped directly from the plant's settling lagoon to the center pivot for fertigation. Due to the operational realities of working within a commercial circular system with a single pivot, only one field per treatment was available. Although this limits field-level replication, the study design reflects applied sustainability practices already in use, offering a unique opportunity to assess microbial and antimicrobial resistance dynamics under real-world conditions. Photographic documentation is provided in the Supplementary Material (Figure S1).

2.4. Use of Antibiotics in Cattle

Throughout the duration of the trial, the animals in the feedlot were administered the following antibiotics: Maxibiotic™ (a tetracycline-based antibiotic, Biogenesis Bagó, Garín, Argentina), and Maxytil Platinum™ (Biogenesis Bagó, Garín, Argentina), and Biomacrotil™ (Calier, Buenos Aires, Argentina) (all of which are macrolides containing tylosin). Macrolides and tetracyclines are two classes of antibiotics commonly used in veterinary medicine. Macrolides, such as erythromycin and tylosin, are often used to control respiratory diseases and gastrointestinal infections in animals, while tetracyclines, like oxytetracycline and chlortetracycline, are frequently employed for a broad range of bacterial infections, including those affecting the respiratory tract, digestive system, and reproductive health of animals [20,21].

2.5. Characterization of Anaerobic Digestate

The following parameters were determined: NH_4^+-N, NO_3^--N and total Kjeldahl nitrogen (TKN) by the semi-micro-Kjeldahl method. Total carbon (C) was determined by dry combustion (Elemental Analyser Exeter CE 440, Exeter Analytical UK Ltd., Coventry, England). Total solid (TS) was determined by drying samples at 105 °C to constant weight. The ash content was determined by burning samples at 550 °C for 2 h. The volatile solid (VS) was calculated by subtracting the ash mass from the TS mass. The determinations for total and available phosphorus (TP and AP, respectively) and heavy metals were carried out with an Inductively Coupled Plasma Optical Emission Spectrometer (ICP-OES), Shimadzu Simultaneous 9000 (Shimadzu, Canby, OR, USA) (Table 1). In Argentina, digestate application is regulated by Resolution 19/2019 [22]. In compliance with this normative, stability measurements were performed using Residual Biogas Potential (RB) and Volatile Fatty Acids (VFA). The obtained values (RB = 0.107 L/g organic matter and

VFA = 0.042 chemical oxygen demand/g organic matter) were within the regulatory limits (<0.25 and <0.43, respectively), confirming that the digestate was stable. Total coliforms, *E. coli*, and *Salmonella* were determined prior to the field sampling, following the standard methodology specified by Resolution 19/2019 [22]. In the initial anaerobic digestate sample, the total coliform count was 43 MPN/g fresh weight, with fecal coliforms and *E. coli* present at levels below detection (<3 MPN/g). However, the *Salmonella* count was 113 MPN/4 g fresh weight, which exceeded the limit set by the regulation for this pathogen (<3 MPN/4 g).

Table 1. Chemical and spectroscopy characterization of digestate.

Parameters									
% (Mean ± S.E.)									
TS		VS		C		NTK	$N\text{-}NH_4^+$	$N\text{-}NO_3^-$	
6.150 ± 0.007		61.060 ± 0.16		30.470 ± 0.22		6.729 ± 0.288	4.947 ± 0.174	0.067 ± 0.003	
mg/kg									
TP	AP	As	Cd	Cr	Cu	Hg	Ni	Pb	Zn
9790	903	0.78	<0.1	9.1	59.6	<0.1	8.5	1.5	334

2.6. Plant Sampling

The first sampling was conducted 2 days after the final fertigation event with anaerobic digestate (2 dai, 16 March 2024), allowing time for plant surfaces to dry. The second sampling occurred 4 weeks later (4 wai, 12 April 2024), just before the scheduled maize harvest for silage. In the control field (Figure 1a), three 100 m transects (T1, T2, T3) were established in a North–South direction, spaced 20 m apart. At each transect, leaf samples were collected from the top to bottom of three maize plants at three different points (0, 50, and 100 m), using nitrile gloves to prevent contamination. These nine leaflets were composited into one sample per transect (N = 3). In the digestate-treated field (Figure 1b), a similar approach was used. Three transects (T1, T2, T3), spaced 20 m apart and aligned North–South, were sampled at 0 m (upslope), 50 m (mid-slope), and 250 m (downslope). Again, leaf samples were collected from three plants at each point and combined into a composite sample per transect (N = 3). Each transect thus represented a composite sampling unit within its respective field. These transects serve as subsamples rather than independent replicates, consistent with field-based ecological studies where logistical or landscape constraints precluded full replication. While the experimental design lacks field-level replication, the sampling structure allows meaningful comparison between treatment conditions and provides valuable insight into microbial and ARG dynamics under real-world conditions.

2.7. Screening for Indicators of Fecal Contamination and Pathogens

Total coliforms, *E. coli*, and *Salmonella* were determined in the phyllosphere of maize plants. Since there is no specific regulation, the standard established in the Argentine Food Code for the analysis of fresh leafy vegetables [23] was used as a reference. To estimate the concentration of coliforms in each sample, the Most Probable Number (MPN) method was used. Briefly, 20 g of leaf were added to a flask with 180 mL of peptone water (PW, Britania Laboratories, Buenos Aires, Argentina) and shaken for 2 min to obtain the first dilution 1:10 (10^{-1}). Decimal dilutions were prepared by adding 1 mL of the 1:10 dilution to a tube containing 9 mL of peptone water until reaching the 10^{-3} dilution. Then, 1 mL of each prepared dilution was inoculated in triplicate into tubes with 9 mL of Lauryl sulfate medium (Britania Laboratories, Buenos Aires, Argentina) with a Durham tube inside. Tubes were incubated at 37 °C ± 2 °C for 24 h. After incubation, the tubes were examined for gas

production and turbidity. For positive tubes, the procedure continued with inoculation in MacConkey broth and agar plates (Britania Laboratories, Buenos Aires, Argentina). The detection limit was 3 MPN/g. For screening of *Salmonella* spp., 20 g of leaf was added to a flask with 180 mL of PW, shaken for 2 min and incubated at 35 °C for 24 ± 2 h. Following, 0.1 mL of the culture was transferred into a tube with 10 mL of Rappaport Vassiliadis broth (RV, Britania Laboratories, Buenos Aires, Argentina) and 1 mL into a tube with 10 mL of Tetrathionate Broth (TT, Britania Laboratories, Buenos Aires, Argentina). The RV tubes were incubated for 24 ± 2 h at 42 ± 0.2 °C, and the TT tubes for 24 ± 2 h at 35 ± 2 °C. Then, 10 µL of each tube was streaked onto three different media plates: brilliant green agar (Britania Laboratories, Buenos Aires, Argentina), Xylose Lysine Deoxycholate agar (Britania Laboratories, Buenos Aires, Argentina) and Hektoen Enteric agar (Britania Laboratories, Buenos Aires, Argentina) and incubated at 35 °C for 24 ± 2 h.

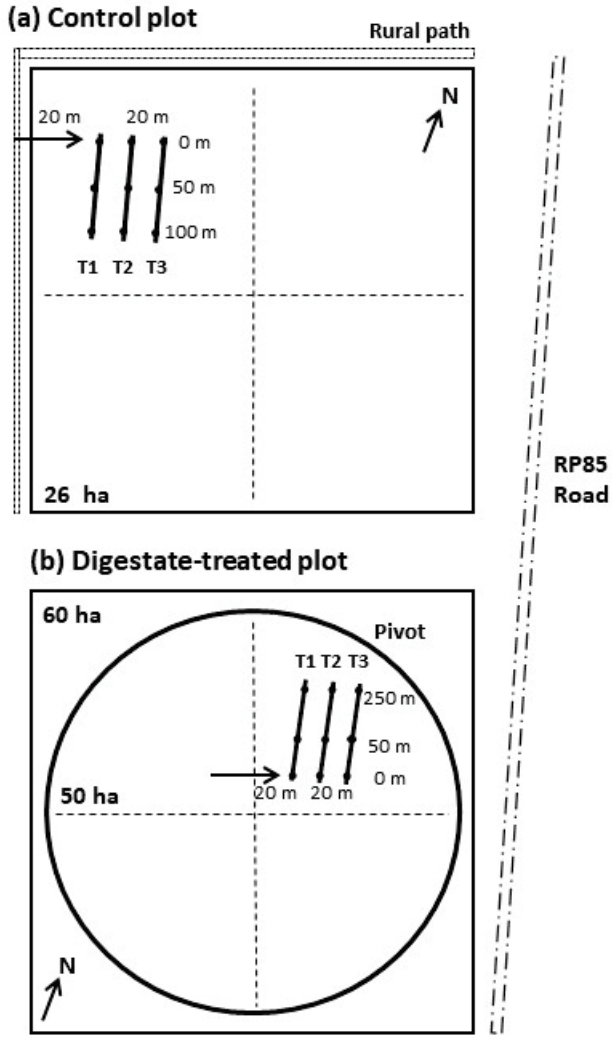


Figure 1. Spatial representation of the control and digestate-irrigated fields. The control field is located 14 km north of the digestate–irrigated plot, along Provincial Road N°85. Three transects (T1–T3) were established in each plot, proportional to the area of each one. Plots and their elements are not drawn to scale. (**a**) In the control plot, the transects were 100 m long, separated by approximately 20 m. Samples were taken at 0 m, 50 m, and 100 m. (**b**) In the digestate-treated plot, the transects were 250 m long, separated by approximately 20 m. Samples were taken at the Upslope (0 m), Mid-slope (50 m), and Downslope (250 m) locations. The 50-ha circle represents the area irrigated by the pivot.

2.8. Extraction of Total DNA from the Microbial Community

The extraction and purification of metagenomic DNA were performed using the DNeasy PowerSoil Pro Kits® (Qiagen, Hilden, Germany). For the anaerobic digestate, extraction was performed using 2 mL of homogenized fresh sample, which was centrifuged at 10,000× *g* for 10 min to obtain a pellet. The supernatant was discarded, and the pellet was stored at −20 °C until extraction. For DNA extraction from the phyllosphere, the procedure described by Zhu et al. (2017) was followed with minor modifications [24]. Briefly, 10 g of leaf (cut into 2 cm pieces) were soaked in 40 mL of Phosphate Buffer (60 mM pH 7.6) with 10% Tween, left for 1 h under reciprocal shaking, filtered and then centrifuged for 15 min at 10,000 rpm (Heraeus Biofuge pico centrifuge, Kendro, Germany). The pellets were recovered, and the DNeasy PowerSoil Pro Kits® (Qiagen, Hilden, Germany) was followed. The obtained DNA was subsequently quantified using the QuantiFluor® dsDNA System (Promega Corporation, Madison, WI, USA) in a Quantus fluorometer (Promega Corporation, Madison, WI, USA). The quality and integrity of the DNA were assessed from 1% agarose gel and absorbance ratios (260:230 and 260:280 nm ratio) in a DS-11 FX spectrophotometer (DeNovix Inc., Wilmington, DE, USA).

2.9. Analysis of Total Bacteria, Resistance Genes and Integrons

To study the treatment effect on the total number of bacteria, a quantitative real-time PCR (qPCR) of the *16S rRNA* gene was conducted. Antibiotic resistance in the samples was determined using previously optimized qPCR protocols evaluated in different environmental samples [3]. Specifically, the genes *ermB*, *tetW*, $bla_{CTX\text{-}M}$ group 1, associated with resistance to different antibiotics (Tables 2 and 3), and the integrons *intI1* and *a-int1* (Table 2), associated with horizontal gene transfer, were assessed. All amplifications, baseline corrections, melting curve analysis, and standard curve assessments were conducted in ABI 7500 Real—Time System and its associated software (7500 Software v2.0.3, Applied Biosystems, Foster City, CA, USA). In all cases, the SYBR Green system was used. SYBR Green reactions were conducted using SsoAdvanced™ Universal SYBR® Green Supermix (BioRad, Hercules, CA, USA), employing two different thermocycler programs. For *16S rRNA*, the protocol was as follows: 5 min of initial denaturation at 95 °C, and 35 cycles of 15 s denaturation at 95 °C, 30 s annealing (see temperature in Table 2) and 45 s extension at 72 °C. For resistance genes and integrons, 10 min of initial denaturation at 95 °C, and 40 cycles of 15 s denaturation at 95 °C, 20 s annealing (see temperatures in Table 2) and 30 s extension at 72 °C. In all cases, the melt curve analysis was at 65–95 °C and the detection limit was approximately 2×10^1 gene copies per reaction.

Table 2. Primers used in this study to quantify total bacteria (*16s rRNA*), resistance genes (*tetW*, *ermB*, bla_{CTX-M}), integrons (*intI1*) and anthropogenic class 1 integrons (*a-int1*).

Target	Primer	Sequence (5′–3′)	Amplicon Size (bp)	Annealing (°C)	Reference
16S rRNA	338_F 518_R	ACTCCTACGGGAGGCAGCAG ATTACCGCGGCTGCTGG	~180	53	Pollock et al., 2020 [25]
tetW	tetW_F tetW_R	GAGAGCCTGCTATATGCCAGC GGGCGTATCCACAATGTTAAC	168	65	Aminov et al., 2004 [26]
ermB	ermB_F ermB_R	AGCCATGCGTCTGACATCTA CTGTGGTATGGCGGGTAAGT	193	56	Szczepanowski et al., 2009 [27]
bla_{CTX-M}	RTCTX-M-F RTCTX-M-R	CTATGGCACCACCAACGATA ACGGCTTTCTGCCTTAGGTT	101	61	Marti et al., 2013 [28]
intI1	intI1_LC1 F intI1_LC5 R	GCCTTGATGTTACCCGAGAG GATCGGTCGAATGCGTGT	196	60	Barraud et al., 2010 [29]
a-int1	aint1_F aint1_R	GCACTAAGCACATAATTG CCAACTATTGCGATAACA	140	50	Quintela-Baluja et al., 2021 [30]

Table 3. Antibiotic resistance mechanisms of the ARGs *tetW*, *ermB* and bla_{CTX-M}.

ARG	Mechanisms of Resistance	Class of Antibiotic
tetW	Protection of the target site (ribosomal protection protein)	Tetracyclines
ermB	Modification of the target by methylation (23S rRNA)	Macrolides, lincosamides and group B streptogramins
bla_{CTX-M}	Antibiotic deactivation by hydrolysis of beta-lactam ring	Expanded-spectrum cephalosporins and monobactams (not cephamycins or carbapenems)

2.10. Statistical Analysis

MPN of bacteria was reported as the median and 95% confidence interval of three replicates. Statistical analyses of the resistance genes data were performed as repeated measures analysis of variance (RM-ANOVA) using R studio version 4.4.2 [31]. Data were analyzed using a linear mixed-effects model (lme procedure fit with REML) in the nlme package (version 3.1-90) in R. The analysis tested the effects of fertilization treatment and time elapsed since fertilization on the abundance of resistance genes. Statistical analyses were conducted using linear mixed-effects models, accounting for repeated measures. Due to the logistical limitations of conducting research within a production-scale circular agriculture system, our statistical approach permits exploratory conclusions, appropriate for this real-world case study context [32]. Transect was included as a random effect, and fertilization treatment, time, and their interaction as fixed effects. The Compound Symmetry (CS) model was selected, using Aikake's Information criterion (AIC), Bayesian information criterion (BIC) and log of restricted maximum likelihood (logLik) criterion. Comparisons were calculated using the emmeans function from the emmeans package version 1.10.5. This function provides adjusted means for each factor level and was used to conduct pairwise comparisons to assess the differences between group means. Given the absence of true replication at the field level, statistical comparisons should be interpreted as indicative of trends rather than definitive inferences.

3. Results

3.1. Detection of Indicators of Fecal Contamination and Pathogens

As shown in Table 4, in the 2 dai sampling, the control situation showed low levels of total coliforms and fecal coliforms, with no detection of *E. coli* or *Salmonella*, consistent with the fact that maize was not irrigated with anaerobic digestate. In contrast, the phyllosphere of maize that was fertigated with anaerobic digestate (AD) exhibited higher levels of total coliforms, with both *E. coli* and *Salmonella* present. In the 4 wai sampling, the control had no detectable total coliforms or fecal coliforms and neither *E. coli* nor *Salmonella* were detected, as observed in 2 dai sampling. The AD phyllosphere sampled 4 wai showed a lower concentration of total coliforms than in the first sampling date, and no detectable fecal coliforms, *E. coli*, or *Salmonella* (Table 4).

3.2. Analysis of Antibiotic Resistance Genes

Due to the absence of field-level replication, statistical tests cannot be interpreted as confirmatory. For transparency, descriptive *p*-values are provided in the Supplementary Material (Tables S1 and S2) but are not shown in the main text. Differences in *16S rRNA* gene abundance were examined across treatments (control and AD) and sampling times (2 dai and 4 wai) (Tables 5 and S1). At 2 dai, levels were generally lower in the control than in AD, with a similar pattern observed in the control across the sampling times. The abundances of the ARGs *tetW*, *ermB*, $bla_{CTX\text{-}M}$, and integrons *intI1* and *a-int1* were also analyzed. Most genes showed no apparent differences among treatments or sampling times, except for two cases (Tables 5 and S1). Levels of *tetW* were generally higher in AD than in the control (Table 5, Figure S2), with values in AD around tenfold greater. Patterns for *a-int1*, varied across treatments and sampling times. At the second sampling, levels tended to be lower in AD than in the control, and in AD they were lower at 4 wai compared with 2 dai. No notable differences between treatments were observed at 2 dai (Tables 5 and S1). No clear differences were observed in the other ARGs tested *(ermB,* $bla_{CTX\text{-}M}$, and *intI1*). Similar patterns were observed for relative abundances (i.e., resistance gene abundance normalized to *16S rRNA* gene abundance). Specifically, *tetW* relative abundance tended to be higher in digestate-treated plants, whereas *a-int1* relative abundance tended to be lower in the AD treatment at 4 wai compared with the earlier sampling (2 dai) and with the control at both time points (Tables S2 and S3).

Table 4. Detection of total coliforms, fecal coliforms, *E. coli*, and *Salmonella* in maize leaves in both sampling dates (2 days after last irrigation with digestate, 2 dai, and 4 weeks after last irrigation with digestate, 4 wai) for treated (AD) and control samples. Results are presented as the median of MPN/g (Most Probable Number per gram) along with the corresponding 95% confidence intervals (CI). The presence or absence of *Salmonella*/20 g of leaves is noted for each sample.

Sampling	Treatment	Coliforms						*Salmonella*/20 g
		Total Coliforms		Fecal Coliforms		*E. coli*		
		MPN/g	CI	MPN/g	CI	MPN/g	CI	
2 dai	Control	3	0.15–9.6	<3	0–9.5	<3	0–9.5	absence
	AD	1100	180–4100	3	0.15–9.6	3	0.15–9.6	presence
4 wai	Control	<3	0–9.5	<3	0–9.5	<3	0–9.5	absence
	AD	43	9–180	<3	0–9.5	<3	0–9.5	absence

Table 5. Mean values of absolute abundance [$\log_{10}$ (gene copies μg^{-1} DNA)]. The mean values, standard errors of the mean (S.E.) and number of observations (n) are indicated. T represents the effect of fertilization treatment (Control vs. AD), S refers to the sampling time (2 dai vs. 4 wai), and T × S indicates the interaction between fertilization treatment and sampling time. Boldface denotes the lowest mean values among treatments, indicating comparative trends.

Gene or Integron	*16S*			*tetW*			*ermB*			bla_{CTX-M}			*intI1*			*a-int1*		
	n	Mean	S.E.	n	Mean	S.E.	n	Mean	S.E.	n	Mean	S.E.	n	Mean	S.E.	n	Mean	S.E.
Treatment (T) *																		
Control	6	8.87	0.02	6	**4.35**	0.16	6	5.54	0.47	5	4.82	0.38	6	4.04	0.12	6	5.78	0.09
AD	6	8.98	0.02	6	5.22	0.16	6	5.57	0.47	5	4.76	0.38	6	4.23	0.12	6	5.33	0.09
Sampling (S)																		
2 dai	6	8.87	0.02	6	4.79	0.16	6	6.05	0.47	4	4.40	0.42	6	3.98	0.12	6	5.81	0.09
4 wai	6	8.98	0.02	6	4.78	0.16	6	5.06	0.47	6	5.18	0.34	6	4.29	0.12	6	5.30	0.09
T × S																		
Control, 2 dai	3	**8.73**	0.03	3	4.18	0.26	3	5.99	0.63	2	4.57	0.57	3	4.54	0.15	3	5.78	0.14
AD, 2 dai	3	9.00	0.03	3	5.40	0.26	3	6.10	0.63	2	4.23	0.57	3	4.75	0.15	3	5.83	0.14
Control, 4 wai	3	9.00	0.03	3	4.52	0.26	3	5.09	0.63	3	5.08	0.47	3	4.22	0.15	3	5.78	0.14
AD, 4 wai	3	8.95	0.03	3	5.04	0.26	3	6.04	0.63	3	5.28	0.47	3	4.37	0.15	3	**4.83**	0.14

* Note: Statistical details (*p*-values) are provided in Supplementary Table S1. Given the absence of field-level replication, these values are for descriptive purposes only and should not be interpreted as confirmatory evidence of treatment effects.

4. Discussion

This study offers valuable preliminary data from a commercial circular agriculture system, where on-site anaerobic digestate was applied to maize through the farm's existing irrigation infrastructure. While the field-level design was constrained by the realities of production-scale farming, the findings represent a rare insight into pathogen and ARG behavior under real-world, sustainability-oriented conditions. Our approach is consistent with other field studies conducted under similar constraints [32], where data were still recognized as valuable contributions to the broader understanding of environmental change. Although field-level replication was not feasible, our findings highlight potential short-term microbial impacts and set the stage for future research involving replicated experimental designs. In this research, we focused on exploring the microbial impacts associated with the use of anaerobic digestate from manure for the fertigation of maize using a center-pivot system that results in full wetting of the foliage. Emphasis was placed on the potential presence of pathogenic microorganisms and the persistence and spread of ARGs. One of the key findings was the detection of *E. coli* and *Salmonella* in maize plants that were irrigated with anaerobic digestate. In addition, we identified the presence of ARGs in these plants, suggesting that anaerobic digestate could serve as a vector for the transmission of ARGs into the agricultural environment.

In anaerobic digestates, the survival of bacteria is influenced by various factors, such as oxygen concentration, temperature, pH, and moisture content. Moreover, the risk of pathogen presence is higher when manure is used as a feedstock, as it commonly contains coliforms and pathogens such as *Salmonella*, *Campylobacter*, and some protozoa, which can persist in anaerobic digestates [33,34]. Their inactivation during the anaerobic process is highly variable and depends on many factors [35]. For example, while anaerobic digestion is generally effective at reducing microbial load, the process tends to be more efficient in laboratory-scale digesters than in full-scale systems [35]. Temperature also plays a crucial role in pathogen inactivation, with digesters operating at thermophilic temperatures typically achieving more effective microbial reduction than mesophilic ones [36]. In our research, the initial anaerobic digestate sample had undetectable levels of *E. coli*, but a count of *Salmonella* which exceeded the limit set by the regulation for this pathogen (Table 4). This could be influenced by the conditions during anaerobic digestion, as observed in other

studies, as well as by the storage conditions [35,37]. The presence of pathogens in the anaerobic digestate emphasizes the importance of conducting thorough microbiological evaluations to assess potential health risks for humans and animals [35]. Regarding the effects of anaerobic digestate applied to soil or plants, it is known that microbial populations associated with manure vary significantly depending on the animal source, its feeding regime, and waste management practices, among others [38,39]. The application of manure and anaerobic digestate can enrich the soil with pathogens, which poses a potential risk to crops, livestock, and humans, especially in areas with intensive agricultural practices [40]. In our study, *E. coli* and *Salmonella* were detected in the phyllosphere of maize 2 days after the last irrigation with anaerobic digestate (2 dai), but not in the second sampling (4 wai) nor in the non-irrigated crops (Table 4). The results of our research may suggest that the presence of these pathogens is transient and potentially linked to the immediate effects of fertigation with anaerobic digestate, with their prevalence decreasing over time. Nevertheless, even though the prevalence of *E. coli* and *Salmonella* appears to decline over time, their short-term detection may still pose a temporary risk that requires careful consideration in terms of management and food safety. Notably, the absence of these pathogens at four weeks should not be interpreted as a lack of risk, since harvest in commercial systems may occur earlier, during the period when pathogens were still detectable.

The antibiotics administered to livestock are often excreted in their feces, and traces of these antibiotics can be detected in the fecal anaerobic fermentation byproducts and in the soil, promoting the increment of ARGs [4,14]. The *tetW* gene has frequently been reported as persistent in anaerobic digestates derived from different feedstocks, showing undesirable removal efficiencies or even increments in its abundance compared to raw manure [41,42]. Our observations suggested an enrichment of *tetW* in AD maize samples. This may be linked to the fact that, during the trial, the animals in the feedlot were administered a tetracycline-based antibiotic. Since the increase in the abundance of this gene in maize phyllosphere was only observed at the first sampling (2 dai, Tables 5 and S1, Figure S2), this transient rise may be attributed to short-term enrichment from the anaerobic digestate. While *tetW* has been detected in soils treated with organic amendments [43–45], the risk of its transfer to the phyllosphere has received little attention. To our knowledge, no previous studies have reported the presence of *tetW* in the phyllosphere.

The gene *ermB*, together with the $bla_{CTX\text{-}M}$ gene, is among the recommended targets for monitoring resistance [46]. In addition, they have been classified as posing the highest risk for human health based on several factors, including their presence in human-associated environments, their ability to spread through MGEs, and their prevalence in many pathogens [3,47]. Regarding *ermB*, our observations did not indicate notable differences between treated and untreated crops or across sampling dates (Table 5). Although previous studies have reported the environmental persistence of *ermB* in soils [48,49], the phyllosphere may not sustain comparable microbial dynamics. Consequently, the addition of anaerobic digestate might have little influence on the occurrence of this gene in plant tissues. Even though macrolides were administered to the animals in the feedlot, potentially introducing *ermB*-carrying bacteria through manure, no evident changes were detected in our study. This could be related to low concentrations of antibiotic residues in the manure or digestate, insufficient to affect *ermB* in the phyllosphere, or to a rapid degradation of the gene in this environment [45]. Similarly, no notable differences in $bla_{CTX\text{-}M}$ were observed between treatments or across sampling dates (Table 5). Previous studies have reported contrasting results regarding $bla_{CTX\text{-}M}$ responses to the application of animal-derived fertilizers. While some studies observed increases in its relative abundance in treated soils [15,50], others found no clear effects. For instance, Allegrini et al. (2024) reported stable $bla_{CTX\text{-}M}$ levels in the rhizosphere of ryegrass following anaerobic digestate

application even after 190 days of cultivation [45]. Additionally, it is important to note that $bla_{CTX\text{-}M}$ represents a family of resistance genes, with *M* being just one of its many subtypes. Other bla_{CTX} variants were not assessed; therefore, our observations do not exclude the presence or persistence of other bla_{CTX} subtypes, and, given the lack of field replication, should be interpreted as preliminary trends rather than generalizable patterns.

Among the three documented classes of integrons, class 1 (*intI1*) has been found mostly among clinical and environmental isolates. Class 1 integrons have been detected in soils treated with both raw and digested manures, as well as in the rhizosphere of plants fertilized with these materials [14,45,49]. We evaluated the presence and persistence of *intI1* and *a-int1*, a specific type of class 1 integron that is primarily associated with antibiotic resistance in environments impacted by human activities [30]. While no differences were apparent between irrigated and non-irrigated crops, nor across sampling dates for *intI1*, *a-int1* displayed a different pattern (Tables 5 and S1). In particular, a trend toward lower abundance of this integron was observed in the AD phyllosphere at 4 wai (Tables 5 and S1). Although somewhat unexpected, this result could be explained by considering the changes in the environmental conditions within the phyllosphere of the treated plants, which may differ from those of the control crop. In plants treated with anaerobic digestate, which involves the addition of organic matter and microbial load, there is potential for increased microbial competition [51]. The introduction of a complex mixture of microorganisms could alter the composition of the microbial community, potentially influencing the behavior of specific microorganisms associated with the integron. Furthermore, the effects of anaerobic digestate on the phyllosphere are likely to vary over time [45], as natural processes, including microbial degradation and plant physiological responses, may progressively reduce the abundance of the *a-int1* integron.

The benefits of using anaerobic digestates as organic fertilizers have been widely recognized [12,13,37]. However, while they could improve soil health and crop productivity, their use also presents potential risks related to the persistence and spread of pathogens and ARGs, which should not be overlooked. Our study highlights the importance of evaluating the microbiological quality of anaerobic digestate both before and after its application to soil or crops to minimize the risks of pathogen and ARGs transmission. As agricultural systems increasingly rely on organic amendments like anaerobic digestates, it is crucial to consider better practices for managing and reducing the risks associated with their use. Further research is needed to find a balance between the benefits of the obtention and use of anaerobic digestates and the potential environmental and public health concerns, ensuring their responsible and sustainable use.

Limitations and Scope of the Study

This study was conducted under real-world conditions on a working commercial farm, which provides practical relevance but also entails design constraints. Only one digestate-treated field and one control field were available, with inherent differences in maize variety, planting density, and soil preparation. Maize leaves from three composite transects were sampled per field, but these represent subsamples rather than true replicates. Consequently, the study design does not permit statistical inference or broad generalization beyond the specific site and timeframe examined. Observed patterns in microbial markers may also reflect site-specific variables not captured in the design, and therefore, *p*-values should be viewed as exploratory.

Our intent was not to present a replicated field trial, but to document trends under commercial conditions and generate hypotheses for future research. Given that the work was restricted to a single farm, crop, climate, and type of digestate, the findings should be regarded as context-dependent and hypothesis-generating rather than conclusive.

5. Conclusions

Despite the aforementioned constraints, the study provides preliminary insights into short-term microbial dynamics of maize phyllosphere following digestate fertigation and highlights key parameters that warrant further investigation in future trials. The main observations include the transient detection of *E. coli* and *Salmonella* shortly after digestate application (2 dai) and a temporary increase in the *tetW* resistance gene in the maize phyllosphere, while other ARGs and integrons showed no notable changes. Overall, under the conditions of this study, fertigation with anaerobic digestate appears to pose minimal short-term impact on the phyllosphere, though these conclusions are based on limited data and should be interpreted with caution.

From an environmental and economic perspective, the use of on-site manure-based digestate contributes to circular agriculture and nutrient recycling, with potential benefits for soil health and crop productivity. Nevertheless, careful management is recommended to reduce potential microbial risks. Suggested best practices include microbiological assessment of the anaerobic digestate before application, monitoring of indicators of fecal contamination, pathogens, and ARGs, and careful consideration of the timing and method of fertigation to minimize transient contamination. In this regard, guidelines developed under the Nitrates Directive (91/676/EEC) recommend composting of solids and pasteurization of the liquid fraction to ensure regulatory compliance while preserving agronomic benefits [52].

Future research should therefore focus on replicated field trials to confirm the observations reported here, assess the fate of a wider spectrum of ARGs and mobile genetic elements, and evaluate their persistence through subsequent steps of the agricultural cycle, including various time points throughout the crop cycle and in silage fed to livestock. Integrating agronomic, microbiological, and regulatory perspectives will support the development of improved management strategies and promote the safe, sustainable use of digestates. This will align with One Health principles, balancing agricultural productivity with environmental and public health considerations.

Supplementary Materials: The following supporting information can be downloaded at: https://www.mdpi.com/article/10.3390/agronomy15102398/s1, Figure S1. Photographic overview of the experimental site: (a) General view of the plant and the feedlot area, with the digestate lagoon visible in the lower left, (b) Irrigation area showing the circular pattern traced by the pivot (seen from a distance), and (c) Pivot in operation. Table S1. Differences in gene absolute abundance. *p*-values and degrees of freedom associated with the main effects (T, S and T × S). Due to the absence of true replication at the field level, statistical comparisons should be interpreted as indicative trends rather than confirmed differences. Table S2. Differences in gene absolute abundance. *p*-values and degrees of freedom associated with the main effects (T, S and T × S). Due to the absence of true replication at the field level, statistical comparisons should be interpreted as indicative trends rather than confirmed differences. Table S3. Mean values of relative abundance [$\log_{10}$ (gene copies μg^{-1} DNA)]. The mean values, standard errors of the mean (S.E.) and number of observations (n) are indicated. T represents the effect of fertilization treatment (Control vs. AD), S refers to the sampling time (2 dai vs. 4 wai), and T × S indicates the interaction between fertilization treatment and sampling. Boldface denotes the lowest mean values among treatments, indicating comparative trends. Figure S2. Changes in the abundance of the *tetW* gene between control and AD samples. Values are expressed as the mean of absolute abundances [$\log_{10}$ (gene copies μg^{-1} DNA)], with error bars representing the S.E. Because true field replication was not performed, statistical comparisons should be interpreted as indicative of trends rather than confirmed differences.

Author Contributions: Conceptualization, M.C.Z.; methodology, C.F., M.V.V., J.B. and G.A.I.; resources, M.C.Z. and G.A.I.; formal analysis and data curation, C.F., M.C.Z. and M.B.V.; writing—original draft preparation, C.F.; writing—review and editing, M.B.V., G.A.I., M.C.Z. and

M.A.; supervision, project administration, and funding acquisition, M.C.Z. and M.B.V. All authors have read and agreed to the published version of the manuscript.

Funding: This research was funded by the Agencia Nacional de Promoción Científica (ANPCyT, PICT 2020-02289), the Secretaría de Ciencia y Tecnología—UNS (PGI 24/A276), and the United States Department of Agriculture, USDA-NIFA (HATCH Grant, Nº. ILLU-802-978).

Data Availability Statement: Dataset is available on request from the authors.

Acknowledgments: C.F and M.V.V acknowledge CONICET for the fellowships granted. Artificial intelligence tools (ChatGPT, OpenAI, GPT-5) were used solely to improve the English language and readability of the manuscript. No AI tools were used for the generation of scientific content, data analysis, or interpretation.

Conflicts of Interest: The authors declare no conflicts of interest.

Abbreviations

The following abbreviations are used in this manuscript:

ARG	Antibiotic Resistance Genes
AMR	Antimicrobial Resistance
WHO	World Health Organization
MGEs	Mobile genetic elements
MPN	Most Probable Number
AD	Sample fertigated with Digestate
dai	Days After Fertigation
wai	Weeks After Fertigation

References

1. Pitt, S.J.; Gunn, A. The One Health Concept. *Br. J. Biomed. Sci.* **2024**, *81*, 12366. [CrossRef]
2. World Health Organization. Antimicrobial Resistance; Fact Sheet. WHO. 2021. Available online: https://www.who.int/news-room/fact-sheets/detail/antimicrobial-resistance (accessed on 22 January 2025).
3. Allegrini, M.; Zabaloy, M.C. Anaerobic digestates in agricultural soils: A systematic review of their effects on antibiotic resistance genes. *Rev. Argent. Microbiol.* **2024**, *56*, 394–401. [CrossRef]
4. Huang, Z.; Hu, L.X.; Yang, J.B.; Liu, Y.S.; He, L.Y.; Zhao, J.L.; Ying, G.G. Comprehensive discovery and migration evaluation of antimicrobial drugs and their transformation products in a swine farm by target, suspect, and nontarget screening. *Environ. Int.* **2023**, *181*, 108304. [CrossRef]
5. Samreen, A.I.; Malak, H.A.; Abulreesh, H.H. Environmental antimicrobial resistance and its drivers: A potential threat to public health. *J. Glob. Antimicrob. Resist.* **2021**, *27*, 101–111. [CrossRef] [PubMed]
6. Hoelzer, K.; Wong, N.; Thomas, J.; Talkington, K.; Jungman, E.; Coukell, A. Antimicrobial drug use in food-producing animals and associated human health risks: What, and how strong, is the evidence? *BMC Vet. Res.* **2017**, *13*, 211. [CrossRef] [PubMed]
7. Forsberg, K.J.; Reyes, A.; Wang, B.; Selleck, E.M.; Sommer, M.O.; Dantas, G. The shared antibiotic resistome of soil bacteria and human pathogens. *Science* **2012**, *337*, 1107–1111. [CrossRef] [PubMed]
8. Ellen MacArthur Foundation. It's Time for a Circular Economy. 2021. Available online: https://www.ellenmacarthurfoundation.org/topics/circular-economy-introduction/overview (accessed on 3 December 2024).
9. Abad-Segura, E.; González-Zamar, M.D.; Belmonte-Ureña, L.J. Effects of circular economy policies on the environment and sustainable growth: Worldwide research. *Sustainability* **2020**, *12*, 5792. [CrossRef]
10. Sathish Kumar, R.K.; Sasikumar, R.; Dhilipkumar, T. Exploiting agro-waste for cleaner production: A review focusing on biofuel generation, bio-composite production, and environmental considerations. *J. Clean. Prod.* **2024**, *435*, 140536. [CrossRef]
11. Hollas, C.E.; Guedes Cubas do Amaral, K.; Valles Lange, M.; Mayumi Higarashi, M.; Radis Steinmetz, R.L.; Barros, E.C.; Ferronato Mariani, L.; Nakano, V.; Kunz, A.; Sanches-Pereira, A.; et al. Life cycle assessment of waste management from the Brazilian pig chain residues in two perspectives: Electricity and biomethane production. *J. Clean. Prod.* **2022**, *354*, 131654. [CrossRef]
12. Iocoli, G.A.; Zabaloy, M.C.; Pasdevicelli, G.; Gómez, M.A. Use of biogas digestates obtained by anaerobic digestion and codigestion as fertilizers: Characterization, soil biological activity and growth dynamic of *Lactuca sativa* L. *Sci. Total Environ.* **2019**, *647*, 11–19. [CrossRef]

13. Zoui, O.; Baroudi, M.; Drissi, S.; Abouabdillah, A.; Abd-Elkader, O.H.; Plavan, G.; Bourioug, M. Utilization of digestate as an organic manure in corn silage culture: An in-depth investigation of its profound influence on soil's physicochemical properties, crop growth parameters, and agronomic performance. *Agronomy* **2023**, *13*, 1715. [CrossRef]
14. Cao, H.; Jiao, Q.; Cheng, L.; Song, L.; Xun, M.; Yang, H. Occurrence and prevalence of antibiotic resistance genes in apple orchard after continual application of anaerobic fermentation residues of pig manure. *Environ. Sci. Pollut. Res. Int.* **2023**, *30*, 29229–29242. [CrossRef] [PubMed]
15. Nõlvak, H.; Truu, M.; Kanger, K.; Tampere, M.; Espenberg, M.; Loit, E.; Raave, H.; Truu, J. Inorganic and organic fertilizers impact the abundance and proportion of antibiotic resistance and integron integrase genes in agricultural grassland soil. *Sci. Total Environ.* **2016**, *562*, 678–689. [CrossRef]
16. Methe, B.A.; Hiltbrand, D.; Roach, J.; Xu, W.; Gordon, S.G.; Goodner, B.W.; Stapleton, A.E. Functional gene categories differentiate maize leaf drought-related microbial epiphytic communities. *PLoS ONE* **2020**, *15*, e0237493. [CrossRef]
17. Chen, Q.L.; An, X.L.; Zheng, B.X.; Ma, Y.B.; Su, J.Q. Long-term organic fertilization increased antibiotic resistome in phyllosphere of maize. *Sci. Total Environ.* **2018**, *645*, 1230–1237. [CrossRef]
18. Kaul, J.; Jain, K.; Olakh, O. An overview on role of yellow maize in food, feed and nutrition security. *Int. J. Curr. Microbiol. Appl. Sci.* **2019**, *8*, 3037–3048. [CrossRef]
19. USDA Natural Resources Conservation Service. Soil Survey Staff. In *Keys to Soil Taxonomy*, 13th ed.; USDA Natural Resources Conservation Service: Washington, DC, USA, 2022.
20. Cameron, A.; McAllister, T.A. Antimicrobial usage and resistance in beef production. *J. Anim. Sci. Biotechnol.* **2016**, *7*, 68. [CrossRef]
21. Dinos, G.P. The macrolide antibiotic renaissance. *Br. J. Pharmacol.* **2017**, *174*, 2967–2983. [CrossRef] [PubMed]
22. Norma Técnica Para la Aplicación Agrícola de Digerido Proveniente de Plantas de Digestión Anaeróbica. Available online: https://servicios.infoleg.gob.ar/infolegInternet/anexos/315000-319999/319167/res19.pdf (accessed on 27 September 2025).
23. Código Alimentario Argentino, Capítulo XI. Alimentos Vegetales. Available online: https://www.argentina.gob.ar/sites/default/files/capitulo_xi_vegetales_actualiz_2025-071.pdf (accessed on 27 September 2025).
24. Zhu, B.; Chen, Q.; Chen, S.; Zhu, Y.G. Does organically produced lettuce harbor higher abundance of antibiotic resistance genes than conventionally produced? *Environ. Int.* **2017**, *98*, 152–159. [CrossRef]
25. Pollock, J.; Muwonge, A.; Hutchings, M.R.; Mainda, G.; Bronsvoort, B.M.; Gally, D.; Corbishley, A. Resistance to change: AMR gene dynamics on a commercial pig farm with high antimicrobial usage. *Sci. Rep.* **2020**, *10*, 1708. [CrossRef]
26. Aminov, R.I.; Chee-Sanford, J.C.; Garrigues, N.; Mehboob, A.; Mackie, R.I. Detection of tetracycline resistance genes by PCR methods. *Methods Mol. Biol.* **2004**, *268*, 3–13. [CrossRef]
27. Szczepanowski, R.; Linke, B.; Krahn, I.; Gartemann, K.H.; Gützkow, T.; Eichler, W.; Pühler, A.; Schlüter, A. Detection of 140 clinically relevant antibiotic-resistance genes in the plasmid metagenome of wastewater treatment plant bacteria showing reduced susceptibility to selected antibiotics. *Microbiology* **2009**, *155*, 2306–2319. [CrossRef] [PubMed]
28. Marti, E.; Jofre, J.; Balcazar, J.L. Prevalence of antibiotic resistance genes and bacterial community composition in a river influenced by a wastewater treatment plant. *PLoS ONE* **2013**, *8*, e78906. [CrossRef]
29. Barraud, O.; Baclet, M.C.; Denis, F.; Ploy, M.C. Quantitative multiplex real-time PCR for detecting class 1, 2 and 3 integrons. *J. Antimicrob. Chemother.* **2010**, *65*, 1642–1645. [CrossRef] [PubMed]
30. Quintela-Baluja, M.; Frigon, D.; Abouelnaga, M.; Jobling, K.; Romalde, J.L.; Gomez Lopez, M.; Graham, D.W. Dynamics of integron structures across a wastewater network—Implications to resistance gene transfer. *Water Res.* **2021**, *206*, 117720. [CrossRef]
31. *R—"Pile of Leaves"*, version 4.4.2; The R Foundation for Statistical Computing: Vienna, Austria, 2024.
32. Reemts, C.M.; Hansen, L.L. Short-term effects of repeated wildfires in oak-juniper woodlands. *Fire Ecol.* **2013**, *9*, 64–79. [CrossRef]
33. Bicudo, J.R.; Goyal, S.M. Pathogens and manure management systems: A review. *Environ. Technol.* **2003**, *24*, 115–130. [CrossRef]
34. Spencer, J.L.; Guan, J. Public health implications related to spread of pathogens in manure from livestock and poultry operations. *Methods Mol. Biol.* **2004**, *268*, 503–515. [CrossRef]
35. Burch, T.R.; Spencer, S.K.; Borchardt, S.S.; Larson, R.A.; Borchardt, M.A. Fate of manure-borne pathogens during anaerobic digestion and solids separation. *J. Environ. Qual.* **2018**, *47*, 336–344. [CrossRef]
36. Gantzer, C.; Gaspard, P.; Galvez, L.; Huyard, A.; Dumouthier, N.; Schwartzbrod, J. Monitoring of bacterial and parasitological contamination during various treatments of sludge. *Water Res.* **2001**, *35*, 3763–3770. [CrossRef]
37. Ndubuisi-Nnaji, U.; Ofon, U.; Asira, A.E.; Dickson, N. Anaerobic digestion of untreated manure: Environmental risk assessment of resultant digestates. *World J. Appl. Sci. Technol.* **2023**, *14*, 73–79. [CrossRef]
38. Albihn, A.; Vinnerås, B. Biosecurity and arable use of manure and biowaste—Treatment alternatives. *Livest. Sci.* **2007**, *112*, 232–239. [CrossRef]
39. Lopatto, E.; Choi, J.; Colina, A.; Ma, L.; Howe, A.; Hinsa-Leasure, S. Characterizing the soil microbiome and quantifying antibiotic resistance gene dynamics in agricultural soil following swine CAFO manure application. *PLoS ONE* **2019**, *14*, e0220770. [CrossRef] [PubMed]

40. Luo, H.; Lv, T.; Shi, M.; Wu, S.; Carvalho, P.N.; Dong, R. Stabilization of preliminary anaerobically digested slurry in post-storage: Dynamics of chemical characteristics and hygienic quality. *Water Air Soil Pollut.* **2017**, *306*, 3493. [CrossRef]
41. Ben, W.; Wang, J.; Cao, R.; Yang, M.; Zhang, Y.; Qiang, Z. Distribution of antibiotic resistance in the effluents of ten municipal wastewater treatment plants in China and the effect of treatment processes. *Chemosphere* **2017**, *172*, 392–398. [CrossRef]
42. Chen, X.; Tang, R.; Wang, Y.; Yuan, S.; Wang, W.; Ali, I.M.; Hu, Z.H. Effect of ultrasonic and ozone pretreatment on the fate of enteric indicator bacteria and antibiotic resistance genes, and anaerobic digestion of dairy wastewater. *Bioresour. Technol.* **2021**, *320*, 124356. [CrossRef] [PubMed]
43. Pu, C.; Liu, H.; Ding, G.; Sun, Y.; Yu, X.; Chen, J.; Ren, J.; Gong, X. Impact of direct application of biogas slurry and residue in fields: In situ analysis of antibiotic resistance genes from pig manure to fields. *J. Hazard. Mater.* **2018**, *344*, 441–449. [CrossRef]
44. Tran, T.T.; Scott, A.; Tien, Y.C.; Murray, R.; Boerlin, P.; Pearl, D.L.; Liu, K.; Robertson, J.; Nash, J.H.E.; Topp, E. On-farm anaerobic digestion of dairy manure reduces the abundance of antibiotic resistance associated gene targets and the potential for plasmid transfer. *Appl. Environ. Microbiol.* **2021**, *87*, e0298020. [CrossRef]
45. Allegrini, M.; Iocoli, G.A.; Zabaloy, M.C. Combined use of digestate and inorganic fertilizer alleviates the burden of class 1 integrons in perennial ryegrass rhizosphere without compromising aerial biomass production. *Environ. Sci. Pollut. Res. Int.* **2024**, *31*, 47132–47143. [CrossRef]
46. Luby, E.; Ibekwe, A.M.; Zilles, J.; Pruden, A. Molecular methods for assessment of antibiotic resistance in agricultural ecosystems: Prospects and challenges. *J. Environ. Qual.* **2016**, *45*, 441–453. [CrossRef]
47. Zhang, A.N.; Gaston, J.M.; Dai, C.L.; Zhao, S.; Poyet, M.; Groussin, M.; Yin, X.; Li, L.G.; van Loosdrecht, M.C.M.; Topp, E.; et al. An omics-based framework for assessing the health risk of antimicrobial resistance genes. *Nat. Commun.* **2021**, *12*, 4765. [CrossRef] [PubMed]
48. Scott, A.; Tien, Y.C.; Drury, C.F.; Reynolds, W.D.; Topp, E. Enrichment of antibiotic resistance genes in soil receiving composts derived from swine manure, yard wastes, or food wastes, and evidence for multiyear persistence of swine *Clostridium* spp. *Can. J. Microbiol.* **2018**, *64*, 201–208. [CrossRef] [PubMed]
49. Zeng, J.Y.; Meng, M.; Qi, L.; Li, Y.; Yao, H. Environmental risks in swine biogas slurry-irrigated soils: A comprehensive analysis of antibiotic residues, resistome, and bacterial pathogens. *Environ. Int.* **2024**, *191*, 108954. [CrossRef]
50. Nüesch-Inderbinen, M.; Stephan, R. Epidemiology of extended-spectrum β-lactamase producing *Escherichia coli* in the human-livestock environment. *Curr. Clin. Microbiol. Rep.* **2016**, *3*, 1–9. [CrossRef]
51. De Mandal, S.; Jeon, J. Phyllosphere Microbiome in Plant Health and Disease. *Plants* **2023**, *12*, 3481. [CrossRef] [PubMed]
52. Huygens, D.; Orveillon, G.; Lugato, E.; Tavazzi, S.; Comero, S.; Jones, A.; Gawlik, B.; Saveyn, H.G.M. *Technical Proposals for the Safe Use of Processed Manure Above the Threshold Established for Nitrate Vulnerable Zones by the Nitrates Directive (91/676/EEC)*; Publications Office of the European Union: Luxembourg, 2020. [CrossRef]

Disclaimer/Publisher's Note: The statements, opinions and data contained in all publications are solely those of the individual author(s) and contributor(s) and not of MDPI and/or the editor(s). MDPI and/or the editor(s) disclaim responsibility for any injury to people or property resulting from any ideas, methods, instructions or products referred to in the content.

agronomy

MDPI

Article

Cover Crops Can Reduce Greenhouse Gas Emissions from No-Till Maize in Southern Brazil: Insights from a Long-Term Field Experiment

Guilherme Rosa da Silva [1], Adam J. Liska [2,*] and Cimélio Bayer [1]

[1] Department of Soil Science, Federal University of Rio Grande do Sul, 7712 Bento Gonçalves Ave., Porto Alegre 91540-000, RS, Brazil; mutadagui@gmail.com (G.R.d.S.); cimelio.bayer@ufrgs.br (C.B.)
[2] Department of Biological Systems Engineering, University of Nebraska-Lincoln, Lincoln, NE 68583, USA
* Correspondence: aliska2@unl.edu

Abstract: Brazil is one of the countries that has the most agricultural area under no-till (NT) management. This research study aims to evaluate life-cycle greenhouse gas (GHG) emissions from maize (M) grain production in agroecosystems that used different cover crops under NT management in southern Brazil. The data for this study were from a long-term 41-year field experiment in southern Brazil. The long-term experiment evaluated the effects of fallow (F) and cover crops (oat (O), vetch (V), cowpea (B), pigeon pea (P), and lablab (L)) on nitrous oxide and methane emissions and soil carbon (C) sequestration in maize agroecosystems. Five cropping systems, FM, OV/M, OV/MB, PM, and LM, were evaluated. Our results show that cover crops can reduce life-cycle GHG emissions by ~40 to >100% through increased soil C sequestration. The agroecosystems with winter cover crops (OV/M and OV/MB) had higher life-cycle GHG emissions (0.5 kg CO_2e kg^{-1} of M or 2.6 Mg CO_2e ha^{-1}) than the agroecosystem with winter F (0.06 kg CO_2e kg^{-1} of M or 0.2 Mg CO_2e ha^{-1}). Summer cover crops (P and L) resulted in negative life-cycle GHG emissions (an average of −0.2 kg CO_2e kg M^{-1} or −1.2 Mg CO_2e ha^{-1}) and increased the M grain yield. This study shows that cover crops can reduce greenhouse gas emissions from NT M in southern Brazil.

Keywords: soil organic carbon; Brazilian agriculture; subtropical climate; methane; nitrous oxide; life-cycle assessment

1. Introduction

In the last decade (2010–2019), global greenhouse gas (GHG) emissions were the highest on record, with an average annual emission value of 56 Gt CO_2e [1]. The primary contributing sources of GHG emissions to the atmosphere are the following: CO_2 from fossil fuel combustion and industrial processes; CO_2 from land use, land use change, and forestry; methane (CH_4); nitrous oxide (N_2O); and fluorinated gases (F-gases: HFCs, PFCs, SF_6, and NF_3) [1]. These sources contribute to annual GHG emissions by 36, 5.7, 10, 2.6, and 1.2 Gt CO_2e, respectively [1]. The sector of agriculture, forestry, and other land use (AFOLU) accounts for 22% (13 Gt CO_2e) of the total global GHG emissions, being the second largest emitting sector that is also significantly affected by climate change [1]. The main regions in the world responsible for GHG emissions from the AFOLU sector are Africa, Latin America, and Southeast Asia, with Latin America having the highest absolute and per capita AFOLU GHG emissions of any world region [1]. Brazil, one of the seventh largest emitters of GHGs globally, is responsible for 3% of global emissions. In 2021, 2.4 Gt CO_2e were emitted, with the

AFOLU sector being the largest source of Brazilian emissions, 74% of its total GHG emissions. These emissions are divided between agriculture, which is responsible for 25%, and land use change and forest use, which account for 49% of Brazilian GHG emissions [2]. On the other hand, the agricultural sector, which is responsible for GHG emissions, can also promote their mitigation [2]. The Greenhouse Gas Emissions and Removals Estimation System (SEEG) at the Brazilian Climate Observatory [2] estimated a carbon balance for Brazil in 2021 and found the agricultural sector has a net removal of 229 Mt of CO_2e. No-till (NT) systems were responsible for the removal of −67.5 Mt CO_2e [2].

NT management is known as the most practiced conservation agricultural technique in the world and is used on approximately 125 million hectares of cultivated land globally [3]. As opposed to traditional tillage practices, NT management only clears a line of above-ground crop residue for direct planting at a specified depth, with minimal disturbance to soil below a few centimeters. However, NT land represented only ~10% of cultivated land, and its adoption rate depends on the context or country-specific factors [3]. The countries with the largest NT area are the USA, Brazil, Argentina, Canada, and Australia, in descending order. Latin America is the region with the highest percentage of NT land by area globally, with Brazil, Argentina, and Paraguay representing >70% of the total croplands under NT management in the world [3]. According to Kassam et al. [4], 68.7% of the cropland area in Latin America is under conservation agriculture. In Brazil, 19% of the farmers used NT management, with an average of 33 million hectares under NT management [5].

The use of NT management brings some benefits to farming systems, mainly related to soil quality and reductions in labor and energy use, resulting in reduced environmental impacts [6]. The use of NT management can reduce GHG emissions from agriculture, especially CO_2 and N_2O emissions from fields, and can sequester carbon in the soil [7,8]. According to Zaher et al. [9], NT management decreased nitrification and denitrification rates and reduced N_2O emissions from soil. However, during the first years of NT management, there can be higher N_2O emissions that are followed by a decrease because of increased soil aggregation [10]. Converting to NT management from conventional tillage (CT) practices could reduce GHG emissions associated with field emissions of maize by 53% because of more carbon (C) sequestered and less N_2O emission from the soil; in addition, NT management can reduce diesel fuel use by 12% to 44% [11]. NT management's reduced use of resources, like labor, machinery, and energy, have allowed farmers to increase their land area for farming systems [12]. According to Kim and Dale [13], negative GHG emissions in maize production are associated with increases in soil organic carbon levels under NT conditions, which could sequester between 1.0 and 1.4 kg CO_2e per kilogram of maize, while N_2O emissions from fields ranged from 10 to 13 g CO_2e per kilogram of maize. Silva et al. [7] also found in NT systems with cover crops that soil C sequestration can mitigate all the GHG emissions from maize production farming systems in Brazil. In fact, obtaining the ability to fully mitigate GHG emissions is not dependent on tillage only, but on numerous practices, one of which is the use of cover crops.

Farming's CO_2 emissions have been found to mainly be dependent on the characteristics of individual agroecosystems [9]. The use of NT management with large amounts of crop residues in fields can contribute significantly to the reduction in GHG emissions in maize production [7]. Thus, according to Abdalla et al. [14], the use of cover crops in agroecosystems can supply a larger amount of crop residues than cropping systems that use only maize or cash crops with fallow. These agroecosystems could be annual, biennial, or perennial herbaceous plants grown in a pure or mixed stand [14]. When using legume cover crops, they can reduce N fertilizer requirements for the subsequent crops through biological N fixation, while non-legume crops can increase the plant biomass input to the soil. In

conditions of the USA, Camargo et al. [15] found that NT maize cultivation using a legume cover crop can reduce GHG emissions by 42% compared to CT using N mineral fertilization. Silva et al. [7] found in their study on southern Brazil that the use of non-legume winter cover crops had lower GHG emissions by area than using legume winter cover crops under NT management, because of reductions in N_2O emissions, although the agroecosystem with the legume cover crop had a higher yield because of N supplied by the legume. Malhi et al. [16] found in a long-term study that maintaining crop residues in soil with the use of NT management improved soil properties more than CT, whereas N fertilization in CT resulted in higher N_2O emissions than those in NT management. Poeplau and Don [17] in a meta-analysis found that cover crops could reduce GHG emissions from agriculture by 8% at a soil organic carbon (SOC) sequestration rate of 0.12 Pg C yr^{-1}. Bayer et al. [18] found in their study that summer cover crops in succession or in consortium with maize can mitigate GHG emissions by soil C sequestration, although they can have higher N_2O and CH_4 emissions than simpler agroecosystems because of a high amount and the quality of biomass input to the soil. Therefore, the potential of cover crops to mitigate GHG emissions depends on the species used and the arrangement present in the agroecosystem.

In this study, our focus was to evaluate how the use of cover crops influences GHG emissions from NT agroecosystems that produce maize grain in southern Brazil. Quantification of GHG emissions in distributed complex systems uses the life-cycle assessment (LCA) method to quantify resource use and emissions that occur in supply chains in the production of specific products. The LCA can be used to estimate the environmental impacts from a farming system, but the results depend on the context and system boundaries of the study, being either "cradle to grave" or "cradle to farm gate" [19]. The LCA includes an evaluation of the processes of resource acquisition, production of primary materials and infrastructure, transport, processing, and recycling associated with the supply chain [20]. All the resources used and related emissions are summarized into impact categories, such as the GHG emission intensity [19]. The central aim of this study was to use the LCA to evaluate and compare the life-cycle GHG emissions from NT agroecosystems in a long-term experiment that incorporates different cover crops. Net life-cycle GHG emissions were estimated primarily based on measurements of changes in soil organic C (SOC) and chamber measurements of N_2O and CH_4. Through this study, we aimed to identify the primary sources and magnitudes of individual GHG emissions and, thus, the leverage points for the optimization of NT agroecosystems that produce maize grain.

2. Materials and Methods

2.1. Description of Field Experimental Design

This research was carried out in a long-term field experiment that evaluates NT management and cover crops installed at the Agricultural Experimental Station of the Federal University of Rio Grande do Sul—EEA/UFRGS. EEA/UFRGS is located at geographic coordinates 30° 50′ 52″ S and 51° 38′ 08″ W in Eldorado do Sul, RS. The area's relief is undulating, with an average altitude of 46 m, and the predominant native vegetation is grassland, mainly composed of low grasses, such as *Paspalum* and *Andropogon*, with *Desmodium*.

The experimental soil is classified as a sandy clay loam granite-derived Acrisol [21] or Typic Paleudult, according to soil taxonomy [22], with 220 g kg^{-1} of clay. The main minerals in the clay fraction are kaolinite (720 g kg^{-1}) and iron oxides (109 g kg^{-1}). The experimental NT maize agroecosystems began in 1983 in an area that had been previously cultivated for 14 years with rapeseed and sunflower under CT. The experimental design is composed of three randomized blocks containing five treatments with plots of a size of 80 m^2 (16 × 5 m). Five agroecosystem treatments were cultivated: uncovered soil, fallow/maize (*Zea mays* L.) (F/M), oat (*Avena strigosa* Schreb.) + vetch (*Vicia sativa* L.)/maize

(OV/M), oat + vetch/maize + cowpea (*Vigna unguiculata* L.) (OV/MB), pigeon pea (*Cajanus cajan* L.) + maize (PM), and lablab (*Lablab purpureus* L.) + maize (LM). Annual fertilization was 50 kg ha^{-1} of P_2O_5 and 50 kg ha^{-1} of K_2O incorporated into the sowing line; all the treatments had no nitrogen applied. Winter cover crops were sown in May, while summer cover crops were sown in December. Maize was always planted with an NT planter in September–October, with minimal disruption below the soil surface, at an approximate population of 50 to 60 thousand plants per hectare.

2.2. Goal and Scope

The goal of this study was to evaluate the life-cycle GHG emissions from the production of maize grain in southern Brazil by employing different configurations of agroecosystems. The methodology employed used the Feedstock Carbon Intensity Calculator (FD-CIC), a field-to-farm-gate LCA model derived from the GREET model (https://greet.anl.gov/tool_fd_cic; accessed on 1 December 2023) [23]. The treatments used F/M, OV/M, OV/MB, PM, LM. We chose these farming systems because we have GHG emission data available for our study, while the other treatments were not measured. This study makes contributions to the maize LCA literature on tropical agriculture, particularly Brazil, by relying on a range of studies of field GHG emission measurements and measured soil C sequestration. The analysis points to crop and soil management options to mitigate GHG emissions.

2.3. Functional Units and System Boundary

We used two functional units to represent GHG emissions from summer-season NT maize production with different winter-season cover crops. One unit represents the GHG emission intensity per cultivated hectare of land per year, and the other represents the GHG emission intensity per kilogram of maize grain. We used both metrics to enable us to explain the results more completely and to distinguish the effects of different inputs or management practices per area and relative to the different yields.

The system boundary (Figure 1) of our analysis encompasses field-to-farm-gate activities to quantify the emission intensity of maize production based on three GHGs, namely, CO_2, CH_4, and N_2O. The energy expenditure and material flows associated with upstream fertilizer/chemical manufacturing and feedstock production stages are important components of field-to-farm-gate GHG emissions.

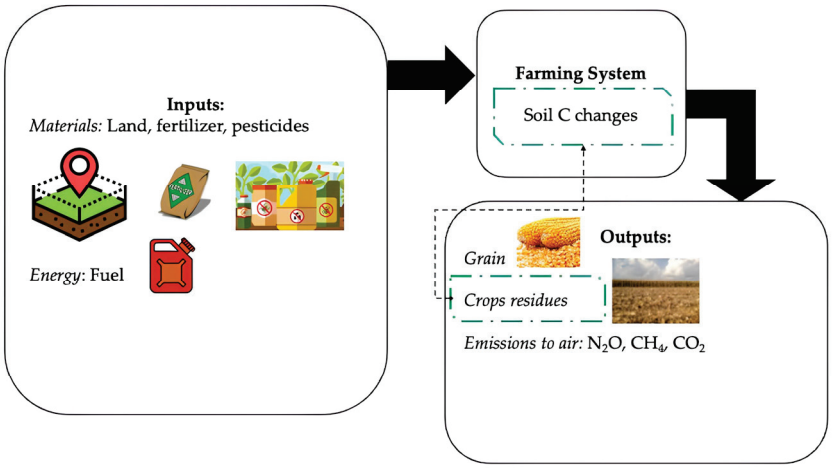


Figure 1. System boundaries of the farming systems in the life cycle of maize grain production "from field to farm gate".

2.4. Data Collection and Inventory Data

Emission data were measured in a long-term experiment for the main GHGs, N_2O and CH_4, during the 2003/2004, 2009/2010, 2010/2011, and 2011/2012 harvests, but not all the farming systems were measured during all the harvests. In 2003/2004, the farming systems where GHG measurements were collected were OV/MB, PM, and LM; in 2009/2010, measurements were taken for OV/M, OV/MB, and LM; in 2010/2011 and 2011/2012, measurements were taken for F/M, OV/M, and OV/MB. Gas collections began on the first or third days after soil preparation and management of cover crops; collections were more frequent up to 60 days after management and were subsequently carried out at intervals of every 15 days, and 30 collections were carried out per year.

To evaluate GHG emissions, the chamber method was used, with one chamber per plot, which was composed of two components: (i) an aluminum base (40 × 80 cm) inserted into the ground at a depth of 5 cm and (ii) an aluminum lid that was fitted onto the aluminum base during collection, constituting the sampling chamber. The lid has a carrying handle and holes to which a digital thermometer, an air collection extender, and the wiring for connecting the battery are connected. Internally, the chamber has two cooler-type fans.

Air samples were collected between 9:00 and 11:00 a.m., and emissions were considered as equivalent to average daily emissions. Samples were collected using BD® polypropylene syringes, with a volume of 20 mL, which were subsequently stored in a Styrofoam box at a low temperature [7]. The samples were analyzed using gas chromatography at the Environmental Biogeochemistry Laboratory of the Federal University of Rio Grande do Sul. Quantification was carried out using Shimadzu GC-2014 equipment in a model "greenhouse" under the following chromatographic conditions: a Porapak-Q column at 70 °C, N_2 carrier gas at 30 mL min^{-1}, a methanator at 380 °C, an FID detector at 250 °C, and an ECD at 325 °C.

We used the annual averages of N_2O and CH_4 emissions (Table 1) to calculate our study's GHG emission intensity. Annual cumulative emissions were estimated by integrating daily fluxes in the collection period.

Table 1. Field N_2O and CH_4 emissions for the agroecosystems and research thesis sources.

Thesis	Years	Unit	Farming System									
			F/M		OV/M		OV/MB		PM		LM	
			N_2O	CH_4	N_2O	CH_4	N_2O	CH_4	N_2O	CH_4	N_2O	CH_4
Gomes [24]	2003/2004	kg ha^{-1} yr^{-1}	-	-	-	-	2.5	0.2	2.1	2.0	−1.4	−0.02
Oliveros [25]	2009/2010	kg ha^{-1} yr^{-1}	-	-	23.4	−9.2	48.4	−10.6	-	-	15.4	−8.1
Denega [26]	2010/2011	kg ha^{-1} yr^{-1}	0.6	−0.4	2.2	−1.8	4.2	−1.4	-	-	-	-
	2011/2012	kg ha^{-1} yr^{-1}	0.2	−0.9	2.0	−0.3	5.2	−0.1	-	-	-	-
Average		kg ha^{-1} yr^{-1}	0.4	−0.6	9.2	−3.8	15.1	−3.0	2.1	2.0	7.0	−4.1

The equation used to calculate the gas flux was

$$f = \Delta Q/\Delta t \times PV/RT \times 1/A, \quad (1)$$

where Q is the mass of the gas (μg N_2O or CH_4 m^{-2}) inside the chamber in the time interval t ($hour^{-1}$); P is the pressure inside the chamber, assumed to be 1 atm; V is the volume of the chamber (L); R is the universal gas constant (0.08205 L atm K^{-1} mol^{-1}); T is the internal temperature (°K) inside the chamber; A is the area of the chamber (m^{-2}).

The SOC stocks and soil C sequestration rates (SOC storage rates) used in this study were calculated by Vieira [27] in his thesis (Table 2). Soil samples from 0 to 30 cm layers were collected in October 2002. The rates of change were determined by comparing the treatments

with the control and dividing by the length of the experiment: 19 years (1983–2002). Trenches were excavated with a backhoe to allow for the measurement of the soil bulk density in duplicate, using the volumetric ring method [28]. The soil samples were air-dried, ground, and sieved to 2 mm. After homogenization, a portion of each sample was ground in a mortar (0.5 mm) and subjected to C and total nitrogen analysis using dry combustion in Shimadzu TOC-V CSH equipment. SOC stocks were calculated using the equivalent mass method [29]. In this study, measured changes in SOC were used as a proxy for changes in CO_2 emissions because SOC increases are because of more biomass input to the soil, and that biomass C is accumulated from atmospheric CO_2.

Table 2. Soil organic C (SOC) stocks and SOC storage rates [27].

Farming System	SOC Stock	SOC Storage Rate
	0–30 cm	0–30 cm
	Mg C ha^{-1}	Mg C ha^{-1} yr^{-1}
F/M	50 ^{b}	0 ^{b}
OV/M	53.1 ^{b}	0.166 ^{b}
OV/MB	58.1 ^{ab}	0.427 ^{ab}
PM	60.5 ^{ab}	0.552 ^{ab}
LM	66.3 ^{a}	0.856 ^{a}

Superscript letters compare farming systems in columns; means with the same letter do not differ significantly according to the Tukey test ($p < 0.05$).

Average maize yields of the experimental farming systems were taken and calculated from 1983/84 to 2021/22, except for the 2019/20 season, where samples were not collected because of the COVID-19 pandemic.

The inventory data are contained in the results section.

2.5. Life-Cycle Impact Assessment

The long-term experimental data were incorporated into the Feedstock Carbon Intensity Calculator (FD-CIC) dynamic model version 2022 (greet.es.anl.gov/tool_fd_cic; accessed on 10 October 2023). Users can change the FD-CIC default settings that affect the GHG emission intensities from farming inputs and outputs. To run the model, the initial step involved incorporating production information for a maize grain into the "Maize Inputs" sheet. The relevant quantities were recorded in the "User Specific Value (NT with cover crops)" or "Default GREET (NT with fallow)" columns.

Modifications were made to the "Maize Results" sheet of the program to include GHG emission measurements from the long-term experiment; in default mode, CH_4 is not shown in the model, and N_2O emission rates are calculated based on nitrogen application rates, not external measurements. Specifically, the values for "N_2O emission due to nitrogen fertilizer and biomass residue" in row 18 were set to zero. Instead of relying on model calculations for these emissions, the measured soil C sequestration data (a proxy for CO_2) and CH_4 and N_2O emission measurements were included in rows 37, 38, and 39, respectively, using the necessary unit conversions.

2.6. Uncertainty Analysis and Comparison of Agroecosystems

Because of temporal factors that affect GHG emissions from fields in maize production, each GHG emission value in the maize life cycle has inherent variability. The relative impacts of GHG emissions were assessed in a sensitivity analysis, where average and standard deviation values were used in the LCA model. Monte Carlo simulations were applied to evaluate parameter variability and to generate a probability distribution of the expected GHG emission intensities. The program @Risk, by Palisade Corporation,

was used to perform 10,000 iterations of outputs by varying three parameters, consistent with their probability of occurrence (Table 3). The SOC sequestration rate, and CH_4 and N_2O emissions from the field were assigned normal distributions based on the standard deviation (SD) found in the databases from the theses of this experiment.

Table 3. Annual emissions from SOC changes, CH_4 from soil, and N_2O from soil used in Monte Carlo analysis to estimate the GHG emission intensities of maize production in different agroecosystems. SOC sequestration rates in Table 2 were converted to CO_2 equivalents.

Farming System	Unit	SOC	SD	CH_4	SD	N_2O	SD
F/M	kg CO_2 eq. ha^{-1}	0.0	0.0	−14.3	11.1	82.7	40.2
OV/M	kg CO_2 eq. ha^{-1}	−607.3	384.4	−101.9	18.0	2506.9	730.6
OV/MB	kg CO_2 eq. ha^{-1}	−1564.4	769.7	−80.7	10.6	4057.3	601.7
PM	kg CO_2 eq. ha^{-1}	−2023.7	407.4	55.1	33.7	556.0	341.7
LM	kg CO_2 eq. ha^{-1}	−3137.9	1292.7	−109.3	69.4	1915.2	1246.5

Analysis of variance (ANOVA) was performed using the software R 4.4.2 with the ExpDes package [30] to assess the differences between the agroecosystems; significant results ($p < 0.05$) were compared using the Tukey test ($p < 0.05$). ANOVA was performed on SOC stocks, SOC sequestration rates, and CH_4, N_2O, and GHG intensities.

3. Results

3.1. Life-Cycle Inventory (LCI) Analysis

In the LCI step, as a part of the LCA, an inventory table was constructed for maize grain production for each of the agroecosystems studied (Table 4); it should be noted that all the input values are the same except for the crop yields. The input data for the analyzed agroecosystems in the FD-CIC model were the quantities of the means of production used. The output data for the assessment of agroecosystems in the FD-CIC model were the quantities of the sources of GHG emissions (Table 5).

Table 4. Life-cycle inventory annual inputs for the five agroecosystems.

	F/M	OV/M	OV/MB	PM	LM	Unit
Farm size	1	1	1	1	1	hectare
Maize yield	3574	4740	5250	6296	6393	kg ha^{-1}
Annual inputs						
Diesel	3.8	3.8	3.8	3.8	3.8	L ha^{-1}
Monoammonium phosphate	50	50	50	50	50	kg ha^{-1}
K_2O	50	50	50	50	50	kg ha^{-1}
$CaCO_3$	167	167	167	167	167	kg ha^{-1}
Herbicide	6.3	6.3	6.3	6.3	6.3	kg ha^{-1}

Table 5. Annual GHG emissions from the agroecosystems per hectare. Superscript letters compare farming systems in lign; means with the same letter do not differ significantly according to the Tukey test ($p < 0.05$).

Annual Output	F/M	OV/M	OV/MB	PM	LM	Unit
Energy Diesel	12.0	12.2	12.2	12.0	12.2	kg CO_2e ha^{-1}
Phosphorus Fertilizer P_2O_5	23.5	23.5	23.5	23.5	23.5	kg CO_2e ha^{-1}
Potash Fertilizer K_2O	5.7	5.7	5.7	5.7	5.7	kg CO_2e ha^{-1}
Lime $CaCO_3$	0.3	0.3	0.3	0.3	0.3	kg CO_2e ha^{-1}
CO_2 emissions from $CaCO_3$ use	7.4	7.4	7.4	7.4	7.4	kg CO_2e ha^{-1}
Herbicide	118.9	118.9	118.9	118.9	118.9	kg CO_2e ha^{-1}
CO_2 SOC	0.0 ^{a}	−607.3 ^{ab}	−1564.4 ^{ab}	−2023.7 ^{ab}	−3137.9 ^{b}	kg CO_2e ha^{-1}
CH_4 Chamber	−14.3 ^{b}	−101.9 ^{c}	−80.7 ^{c}	55.1 ^{a}	−109.3 ^{c}	kg CO_2e ha^{-1}
N_2O Chamber	82.7 ^{d}	2506.9 ^{b}	4057.3 ^{a}	556.0 ^{cd}	1915.2 ^{bc}	kg CO_2e ha^{-1}

3.2. GHG Emissions from the Agroecosystems

In our results, shown in Figure 2, N_2O was the dominant source of GHG emissions from the agroecosystems. The N_2O emissions from the soil varied from 82.7 to 4057.3 kg CO_2e ha^{-1}, where agroecosystems using cover crops had higher emissions than the agroecosystem with fallow. The OV/MB agroecosystem had more cover crop rotations, being two legume cover crops per year, and had the highest N_2O emissions per kilogram of maize and per hectare. The agroecosystems (PM and LM) that used summer cover crops (pigeon pea and lablab) had lower N_2O emissions than the farming systems that used winter cover crops (oat and vetch), where summer cover crops had one-quarter of that emitted per kilogram and one-third of that emitted per hectare compared to the agroecosystems that used winter cover crops. The soil had a behavior as a sink of CH_4 in almost all the farming systems, except for the PM farming system, which emitted 55.4 kg CO_2e ha^{-1} of CH_4; the CH_4 influx was from −14.3 to −109.3 kg CO_2e ha^{-1} of CH_4 for F/M, OV/M, OV/MB, and LM. The highest influx of CH_4 was in the OV/M farming system. The CO_2 emissions from the soil were from −3137.9 to 7.4 kg CO_2e ha^{-1}, where measured soil C sequestration rates were a proxy for CO_2 emissions. The LM farming system had the lowest CO_2e emissions per kilogram of maize and per hectare. The use of chemicals was the third highest source of GHG emissions, and energy was the fourth highest source, responsible for 148 kg CO_2e ha^{-1} and 12.2 kg CO_2e ha^{-1}, respectively.

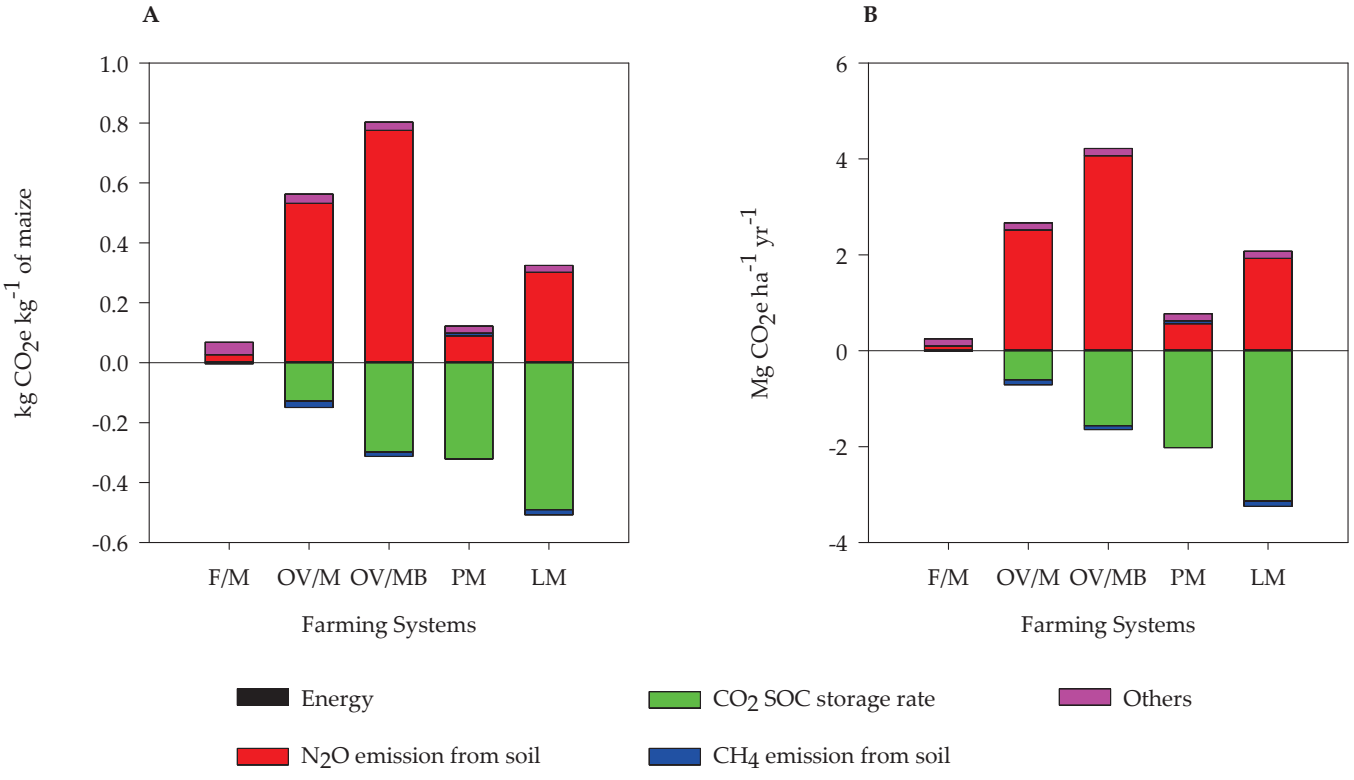


Figure 2. Greenhouse gas emissions per kilogram of maize (**A**) and hectare (**B**) from five agroecosystems. Net annual soil CO_2 emissions were calculated by taking the annual soil C storage rates in the agroecosystems compared to F/M system (control experiment).

In the five farming systems analyzed, N_2O emissions and SOC sequestration rates predominantly affected the GHG emission intensity in the life cycle of maize production (Figure 2). Monte Carlo analysis was used to analyze the effects of variations in SOC sequestration rates and CH_4 and N_2O emission rates on the life-cycle GHG emissions intensity of the agroecosystems. The N_2O emissions from the field were likely the most uncertain parameter when considering farming systems of maize production. This param-

eter was significant for GHG intensity because it depends on the amount of the biomass yield per year, the amount of N contained in the biomass, and the weather conditions for decomposing biomass by microorganisms' nitrification and denitrification processes to produce N_2O. SOC sequestration rates vary because of the randomized arrangement in the experimental field.

The estimated GHG emission intensities ranged from −7408.5 to 6215.1 kg CO_2e ha^{-1} for the agroecosystems (Table 6). Monte Carlo analysis provided data with a 90% confidence interval for each agroecosystem. The ranking of the farming systems according to Monte Carlo analysis together with ANOVA (Figure 3) was PM, LM, F/M, OV/MB, and OV/M, from the lowest to the highest average life-cycle emissions. However, Monte Carlo analysis showed that there were situations in which the farming systems changed their position in this ranking (Table 6). Using the minimum values, the alternative agroecosystems reduced emissions more than F/M; this is the best simulation scenario. However, using the maximum values is the worst scenario because F/M has the least emissions compared to those of the other agroecosystems.

Table 6. Summary of Monte Carlo analysis of GHG CO_2e ha^{-1} outputs from each farming system.

Farming System	GHG Intensity, kg CO_2e ha^{-1} yr^{-1}				
	Min.	Average	Max.	SD	CV% *
F/M	84.0	236.3	420.8	41.7	18%
OV/M	−1166.4	1965.8	5304.4	825.1	42%
OV/MB	−1017.8	2580.2	6115.9	972.8	38%
PM	−3276.9	−1244.8	693.8	533.1	−43%
LM	−7408.5	−1163.9	6215.1	1806.9	−155%

* Coefficient of variation.

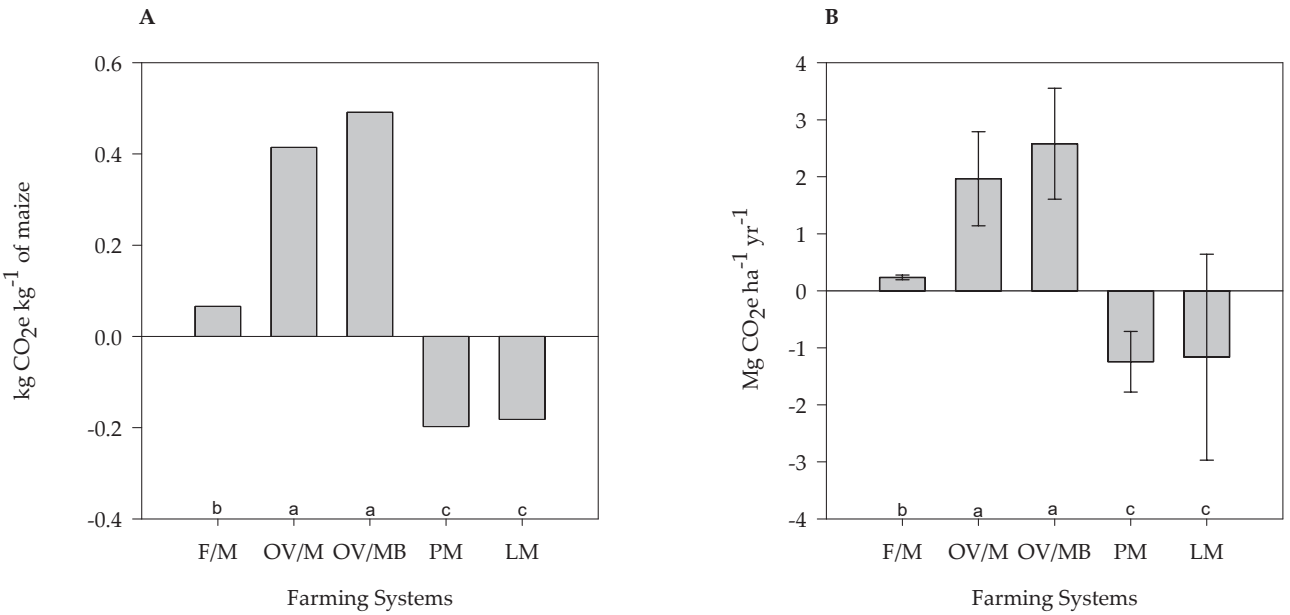


Figure 3. Life-cycle GHG emission intensities per kilogram of maize (**A**) and hectare of maize (**B**) for five agroecosystems; the sum of the data in Figure 2 is shown here. Monte Carlo averages and standard deviations are from Table 6; standard deviations are shown as error bars. Letters compare farming systems; means with the same letter do not differ significantly according to the Tukey test ($p < 0.05$).

The calculated life-cycle GHG emission values for one hectare of each agroecosystem of maize grain cultivation area were from −1.2 to 2.6 Mg CO_2e ha^{-1} (Figure 3B). The agroecosystems where cover crops were cultivated together with maize in the summer season had a life-cycle GHG emission value with an average of −1.2 Mg CO_2e ha^{-1}, while

the OV/MB agroecosystems with two winter cover crops had the highest life-cycle GHG emissions, with an average value of 2.6 Mg CO_2e ha^{-1}. Our study shows that the life-cycle GHG emissions per one kilogram of grain amounted to 0.07 kg CO_2e (Figure 3A) in the F/M farming system, which had a positive GHG emission value; the farming systems OV/M and OV/MB were not able to mitigate their GHG emissions and showed positive values of GHG emissions as well.

4. Discussion

Cover crops improved the resource use efficiency in these farming systems because of increases in crop yields compared to that of fallow. According to Blanco-Canqui et al. [31], the use of cover crops can increase crop yields if it is associated with long-term improvements in soil organic C, soil N, and soil properties. The adoption of legume cover crops in farming systems can provide atmospheric N fixation that can increase crop yields [32–34]. The use of crop rotations can improve the eco-efficiency of the agroecosystems, mainly via the use of legume cover crops, which enables a reduction in the use of synthetic N fertilizer, providing a higher efficiency per unit of input [33–36].

The treatments with the highest N_2O emissions had more crops per year. Although the F/M farming system had the least N_2O emissions, according to Bayer et al. [37], this was because of the relatively low biomass production of winter plants that grow during the fallow period and possibly because of less N availability compared to that in the other rotations. Legume cover crops have been found to reduce agricultural N_2O emissions indirectly by reducing inorganic N fertilizer and manure application requirements [31]. Yet, agroecosystems with crop succession showed higher N_2O emissions. Among the successions, the treatment with the introduction of cowpeas in spring/summer showed higher emissions than the treatment without this legume. The OV/MB farming system has the highest N_2O emission intensity, followed by OV/M. This short-term effect is related to the increase in the availabilities of C and N in the soil, through the mineralization of N-containing plant biomass and soil organic matter, increasing the substrate for N_2O production processes in the soil [38,39]. As we have found in this study, other studies [40–43] found, in a tropical area, higher N_2O emissions when adding residue compared to another fallow area. These results indicate that the soil in the different agroecosystems, mainly with summer cover crops, even with higher N_2O emissions, produced lower life-cycle GHG emissions than the agroecosystem with fallow because of soil C sequestration and higher crop yields. Although more N_2O measurements should be performed to confirm these life-cycle results, these long-term results demonstrate the beneficial environmental effect of including cover crops in agroecosystems to lower life-cycle GHG emissions.

All but one agroecosystem in this study was a sink of CH_4. Rainfed agroecosystems generally do not have large methane emissions because methanotrophs prevail in larger populations over methanogens in upland soils [44]. Thus, CH_4 oxidation in soil is mediated by methane monooxygenase, which requires the presence of O_2 [44]. According to Grassmann et al. [44], tropical clay soil is a weak sink for CH_4 because of methanotrophs. In our study, only PM had significant positive CH_4 emissions into the atmosphere, but this resulted from data from the first GHG measurements in this experiment; the observed positive emissions could also be because this agroecosystem had only a few years of data.

Soil C sequestration, in this study, was able to mitigate from ~40 to >100% of GHG emissions from agroecosystems. A study by Silva et al. [7] observed that soil C sequestration in agroecosystems under NT management can mitigate all the GHG emissions compared to CT. Six et al. [10] report that systems under NT management, in general, sequester C in the soil. However, the mitigation of GHG emissions is possible if the impact of this soil C sequestration reduces the GHG emissions to next to zero or negative GHG emissions, as

shown in this study, which used SOC measurements down to 0.3 m. Cover crop systems with summer legumes, from environmental and productivity points of view, were the most efficient in allowing the accumulation of soil C and increased the productivity of the maize crop. Numerous studies [18,37,45,46] have observed that NT management with summer cover crops in agroecosystems promotes soil C sequestration in low-fertility soils in the tropics and subtropics because of the high production of biomass by summer cover crops. The importance of creating management conditions that allow for the maximum rate of C sequestration in the soil makes the farming system a potential GHG emission mitigator.

Our life-cycle assessment demonstrates that the crop rotation strongly affects GHG emissions, primarily because of differences in the cover crops used. The PM and LM farming systems showed overall negative GHG emissions. The OV/M system had the greatest environmental impact related to GHG emissions. The agroecosystems with cover crops in winter and summer had higher GHG emissions than the agroecosystems with fallow because of increased N_2O emissions from crop residues. The same behavior was found by Prechsl et al. [19] in a similar experiment in Switzerland. Holka and Bieńkowski [47] measured GHG emissions of 1868.7 kg CO_2e ha^{-1} from maize grain production in Poland under NT management, which is similar to our results. For GHG emissions per kilogram of maize, our results were also similar to those found by Keshavarz Afshar and Dekamin [48], with results between 0.112 and 0.252 kg CO_2e kg^{-1} for maize under NT management. Although some studies [49–52] indicate that a greater diversity of crops can decrease GHG emissions, our data from this study showed that summer cover crops might have greater potential in mitigating GHG emissions than higher diversity crops (OV/M and OV/MB). This study shows how challenging it is to mitigate GHG emissions from agricultural systems that already adopt conservation practices, such as NT management. However, this study still shows that it is possible to reduce emissions with the appropriate crop rotations (PM and LM). Around 33 million hectares of agricultural area are under direct planting in Brazil, and these agroecosystems need to be improved to reduce their GHG emissions. This study provides evidence that the use of legumes with summer cover crops has high potential to increase soil C sequestration to mitigate other GHG emissions, particularly N_2O, in the life cycle of maize production.

5. Conclusions

This research assessed the life-cycle GHG emissions of five maize agroecosystems under NT management, based on data from a long-term field experiment. The comparison of the five farming systems, based on GHG emissions, showed greater performance for PM and LM compared to F/M, even though F/M has the lowest N_2O emissions. The obtained results reveal that cover crops can play an important role in increasing the grain yield of the maize in agroecosystems in southern Brazil; cover crops were found to increase the grain yield for the agroecosystems by ~30–80% compared to F/M.

Our work shows that the use of cover crops in agricultural systems can help to mitigate some of or all the life-cycle GHG emissions of maize production. This study shows that the use of summer cover crops is an efficient strategy for mitigating GHG emissions and increasing maize productivity in NT agroecosystems.

Author Contributions: Conceptualization, G.R.d.S., A.J.L. and C.B.; methodology, G.R.d.S., A.J.L. and C.B.; software, A.J.L.; validation, G.R.d.S., A.J.L. and C.B.; formal analysis, G.R.d.S.; investigation, G.R.d.S.; resources, A.J.L. and C.B.; data curation, C.B.; writing—original draft preparation, G.R.d.S.; writing—review and editing, G.R.d.S., A.J.L. and C.B.; visualization, A.J.L. and C.B.; supervision, A.J.L. and C.B.; project administration, C.B. and A.J.L.; funding acquisition, C.B. All authors have read and agreed to the published version of the manuscript.

Funding: This research was funded by the National Institute of Science and Technology in Low-Carbon-Emission Agriculture (INCT-ABC), sponsored by Brazil's National Council for Scientific and Technological Development (CNPq, grant no. 406635/2022-6); the Foundation for Research Support of the State of Rio Grande do Sul (FAPERGS, grant no. 22/2551-0000392-3); Bayer Crop Science S.A., through the ProCarbon Project (BAYER, grant no. BR135321048282P); and the Coordination for the Improvement of Higher-Education Personnel (CAPES) Foundation.

Data Availability Statement: The data presented in this study are available on request from the corresponding author.

Conflicts of Interest: The authors declare that this study received funding from CNPq (the National Council for Scientific and Technological Development), FAPERGS (the Foundation for the Support of Research in the State of Rio Grande do Sul), and Bayer Crop Science S.A. The funders were not involved in the study design; the collection, analysis, or interpretation of the data; the writing of this article; or the decision to submit it for publication.

References

1. IPCC. Emissions Trends and Drivers. In *Climate Change 2022-Mitigation of Climate Change*; Cambridge University Press: Cambridge, UK, 2023; pp. 215–294.
2. SEEG. *Análise das Emissões de Gases de Efeito Estufa e Suas Implicações para as Metas Climáticas do Brasil 1970-2021*; SEEG: Piracicaba, Brasil, 2022.
3. Blanco, H.; Lal, R. Tillage Systems. *Soil Conserv. Manag.* **2023**, *v.1*, 127–157. [CrossRef]
4. Kassam, A.; Friedrich, T.; Derpsch, R. Successful Experiences and Lessons from Conservation Agriculture Worldwide. *Agronomy* **2022**, *12*, 769. [CrossRef]
5. IBGE. *Censo Agropecuário 2017*; IBGE: Rio de Janeiro, Brasil, 2019.
6. Naseri, H.; Parashkoohi, M.G.; Ranjbar, I.; Zamani, D.M. Energy-Economic and Life Cycle Assessment of Sugarcane Production in Different Tillage Systems. *Energy* **2021**, *217*, 119252. [CrossRef]
7. Silva, G.R.; Liska, A.J.; Bayer, C. Life Cycle Greenhouse Gas Emissions in Maize No-Till Agroecosystems in Southern Brazil Based on a Long-Term Experiment. *Sustainability* **2024**, *16*, 4012. [CrossRef]
8. Houshyar, E.; Grundmann, P. Environmental Impacts of Energy Use in Wheat Tillage Systems: A Comparative Life Cycle Assessment (LCA) Study in Iran. *Energy* **2017**, *122*, 11–24. [CrossRef]
9. Zaher, U.; Stöckle, C.; Painter, K.; Higgins, S. Life Cycle Assessment of the Potential Carbon Credit from No- and Reduced-Tillage Winter Wheat-Based Cropping Systems in Eastern Washington State. *Agric. Syst.* **2013**, *122*, 73–78. [CrossRef]
10. Six, J.; Ogle, S.M.; Breidt, F.J.; Conant, R.T.; Mosiers, A.R.; Paustian, K. The Potential to Mitigate Global Warming with No-Tillage Management Is Only Realized When Practised in the Long Term. *Glob. Change Biol.* **2004**, *10*, 155–160. [CrossRef]
11. Kim, S.; Dale, B.E.; Jenkins, R. Life Cycle Assessment of Corn Grain and Corn Stover in the United States. *Int. J. Life Cycle Assess.* **2009**, *14*, 160–174. [CrossRef]
12. Triplett, G.B., Jr.; Dick, W.A. No-Tillage Crop Production: A Revolution in Agriculture! *Agron. J.* **2008**, *100*, S-153–S-165. [CrossRef]
13. Kim, S.; Dale, B.E. Life Cycle Assessment Study of Biopolymers (Polyhydroxyalkanoates) Derived from No-Tilled Corn. *Int. J. Life Cycle Assess.* **2005**, *10*, 200–210. [CrossRef]
14. Abdalla, M.; Hastings, A.; Helmy, M.; Prescher, A.; Osborne, B.; Lanigan, G.; Forristal, D.; Killi, D.; Maratha, P.; Williams, M.; et al. Assessing the Combined Use of Reduced Tillage and Cover Crops for Mitigating Greenhouse Gas Emissions from Arable Ecosystem. *Geoderma* **2014**, *223–225*, 9–20. [CrossRef]
15. Camargo, G.G.T.; Ryan, M.R.; Richard, T.L. Energy Use and Greenhouse Gas Emissions from Crop Production Using the Farm Energy Analysis Tool. *Bioscience* **2013**, *63*, 263–273. [CrossRef]
16. Malhi, S.S.; Lemke, R.; Wang, Z.H.; Chhabra, B.S. Tillage, Nitrogen and Crop Residue Effects on Crop Yield, Nutrient Uptake, Soil Quality, and Greenhouse Gas Emissions. *Soil Tillage Res.* **2006**, *90*, 171–183. [CrossRef]
17. Poeplau, C.; Don, A. Carbon Sequestration in Agricultural Soils via Cultivation of Cover Crops–A Meta-Analysis. *Agric. Ecosyst. Environ.* **2015**, *200*, 33–41. [CrossRef]
18. Bayer, C.; Gomes, J.; Zanatta, J.A.; Vieira, F.C.B.; Dieckow, J. Mitigating Greenhouse Gas Emissions from a Subtropical Ultisol by Using Long-Term No-Tillage in Combination with Legume Cover Crops. *Soil Tillage Res.* **2016**, *161*, 86–94. [CrossRef]
19. Prechsl, U.E.; Wittwer, R.; van der Heijden, M.G.A.; Lüscher, G.; Jeanneret, P.; Nemecek, T. Assessing the Environmental Impacts of Cropping Systems and Cover Crops: Life Cycle Assessment of FAST, a Long-Term Arable Farming Field Experiment. *Agric. Syst.* **2017**, *157*, 39–50. [CrossRef]

20. *ISO 14040:2006*; Environmental Management—Life Cycle Assessment—Principles and Framework. ISO: Geneva, Switzerland, 2006.
21. Schad, P. World Reference Base for Soil Resources—Its Fourth Edition and Its History. *J. Plant Nutr. Soil Sci.* **2023**, *186*, 151–163. [CrossRef]
22. USDA-NRCS. *Keys to Soil Taxonomy*, 13th ed.; NRCS: Washington, DC, USA, 2022.
23. Wang, M. *The Greenhouse Gases, Regulated Emissions, and Energy Use in Transportation (GREET) Model Version 1.5*; US Department of Energy: Washington, DC, USA, 1999.
24. Gomes, J. Emissão de Gases do Efeito Estufa e Mitigação do Potencial de Aquecimento Global por Sistemas Conservacionistas de Manejo do Solo. Ph.D. Thesis, Federal University of Rio Grande do Sul, Porto Alegre, Brazil, 2006.
25. Oliveros, L.F.C. Balanço da Emissão de Gases de Efeito Estufa Em Argissolo Vermelho Sob Sistemas de Cultura Em Plantio Direto. Ph.D. Thesis, Federal University of Rio Grande do Sul (UFRGS), Porto Alegre, Brazil, 2011.
26. Denega, G.L. Emissão de Gases de Efeito Estufa Em Argissolo Sob Sistemas de Preparo e Leguminosas de Cobertura No Sul do Brasil. Ph.D. Thesis, Federal University of Rio Grande do Sul (UFRGS), Porto Alegre, Brazil, 2014.
27. Vieira, F.C.B. Estoques e Labilidade da Matéria Orgânica e Acidificação de um Argissolo sob Plantio Direto Afetados por Sistemas de Cultura e Adubação Nitrogenada. Ph.D. Thesis, Federal University of Rio Grande do Sul (UFRGS), Porto Alegre, Brazil, 2007.
28. Blake, G.R.; Hartge, K.H. Bulk Density. In *Methods of Soil Analysis, Part 1—Physical and Mineralogical Methods*, 2nd ed.; American Society of Agronomy: Madison, WI, USA, 1986; pp. 363–375.
29. Ellert, B.H.; Bettany, J.R. Calculation of Organic Matter and Nutrients Stored in Soils under Contrasting Management Regimes. *Can. J. Soil. Sci.* **1995**, *75*, 529–538. [CrossRef]
30. Ferreira, E.B.; Cavalcanti, P.P.; Nogueira, D.A.; Ferreira, E.B.; Cavalcanti, P.P.; Nogueira, D.A. ExpDes: An R Package for ANOVA and Experimental Designs. *Appl. Math.* **2014**, *5*, 2952–2958. [CrossRef]
31. Blanco-Canqui, H.; Shaver, T.M.; Lindquist, J.L.; Shapiro, C.A.; Elmore, R.W.; Francis, C.A.; Hergert, G.W. Cover Crops and Ecosystem Services: Insights from Studies in Temperate Soils. *Agron. J.* **2015**, *107*, 2449–2474. [CrossRef]
32. Blanco, H.; Lal, R. Cover Crops. *Soil Conserv. Manag.* **2023**, *1*, 211–237. [CrossRef]
33. Nemecek, T.; von Richthofen, J.S.; Dubois, G.; Casta, P.; Charles, R.; Pahl, H. Environmental Impacts of Introducing Grain Legumes into European Crop Rotations. *Eur. J. Agron.* **2008**, *28*, 380–393. [CrossRef]
34. Nemecek, T.; Hayer, F.; Bonnin, E.; Carrouée, B.; Schneider, A.; Vivier, C. Designing Eco-Efficient Crop Rotations Using Life Cycle Assessment of Crop Combinations. *Eur. J. Agron.* **2015**, *65*, 40–51. [CrossRef]
35. Grassauer, F.; Herndl, M.; Nemecek, T.; Guggenberger, T.; Fritz, C.; Steinwidder, A.; Zollitsch, W. Eco-Efficiency of Farms Considering Multiple Functions of Agriculture: Concept and Results from Austrian Farms. *J. Clean. Prod.* **2021**, *297*, 126662. [CrossRef]
36. Zingale, S.; Ingrao, C.; Reguant-Closa, A.; Guarnaccia, P.; Nemecek, T. A Multifunctional Life Cycle Assessment of Durum Wheat Cropping Systems. *Agron. Sustain. Dev.* **2024**, *44*, 1–22. [CrossRef]
37. Bayer, C.; Dieckow, J.; Amado, T.J.C.; Eltz, F.L.F.; Vieira, F.C.B. Cover Crop Effects Increasing Carbon Storage in a Subtropical No-till Sandy Acrisol. *Commun. Soil Sci. Plant Anal.* **2009**, *40*, 1499–1511. [CrossRef]
38. Gomes, J.; Bayer, C.; de Souza Costa, F.; de Cássia Piccolo, M.; Zanatta, J.A.; Vieira, F.C.B.; Six, J. Soil Nitrous Oxide Emissions in Long-Term Cover Crops-Based Rotations under Subtropical Climate. *Soil Tillage Res.* **2009**, *106*, 36–44. [CrossRef]
39. Li, X.; Feng, J.; Zhang, Q.; Zhu, B. Warming Inhibits the Priming Effect of Soil Organic Carbon Mineralization: A Meta-Analysis. *Sci. Total Environ.* **2023**, *904*, 166170. [CrossRef]
40. Baggs, E.M.; Chebii, J.; Ndufa, J.K. A Short-Term Investigation of Trace Gas Emissions Following Tillage and No-Tillage of Agroforestry Residues in Western Kenya. *Soil Tillage Res.* **2006**, *90*, 69–76. [CrossRef]
41. Rigon, J.P.G.; Calonego, J.C.; Pivetta, L.A.; Castoldi, G.; Raphael, J.P.A.; Rosolem, C.A. Using Cover Crops to Offset Greenhouse Gas Emissions from a Tropical Soil under No-Till. *Exp. Agric.* **2021**, *57*, 217–231. [CrossRef]
42. Essich, L.; Nkebiwe, P.M.; Schneider, M.; Ruser, R. Is Crop Residue Removal to Reduce N2O Emissions Driven by Quality or Quantity? A Field Study and Meta-Analysis. *Agriculture* **2020**, *10*, 546. [CrossRef]
43. Shumba, A.; Chikowo, R.; Corbeels, M.; Six, J.; Thierfelder, C.; Cardinael, R. Long-Term Tillage, Residue Management and Crop Rotation Impacts on N2O and CH4 Emissions from Two Contrasting Soils in Sub-Humid Zimbabwe. *Agric. Ecosyst. Environ.* **2023**, *341*, 108207. [CrossRef]
44. Grassmann, C.S.; Mariano, E.; Rocha, K.F.; Gilli, B.R.; Rosolem, C.A. Effect of Tropical Grass and Nitrogen Fertilization on Nitrous Oxide, Methane, and Ammonia Emissions of Maize-Based Rotation Systems. *Atmos. Environ.* **2020**, *234*, 117571. [CrossRef]
45. Bayer, C.; Spagnollo, E.; Wildner, L.d.P.; Ernani, P.R.; Alburqueque, J.A. Incremento de Carbono e Nitrogênio Num Latossolo Pelo Uso de Plantas Estivais Para Cobertura Do Solo. *Ciênc. Rural* **2003**, *33*, 469–475. [CrossRef]
46. Spagnollo, E.; Bayer, C.; Wildner, L.P.; Ernani, P.R.; Albuquerque, J.A.; Proença, M.M. Leguminosas Estivais Intercalares Como Fonte de Nitrogênio Para o Milho, No Sul Do Brasil. *Rev. Bras. Ciênc. Solo* **2002**, *26*, 417–423. [CrossRef]

47. Holka, M.; Bieńkowski, J. Carbon Footprint and Life-Cycle Costs of Maize Production in Conventional and Non-Inversion Tillage Systems. *Agronomy* **2020**, *10*, 1877. [CrossRef]
48. Keshavarz Afshar, R.; Dekamin, M. Sustainability Assessment of Corn Production in Conventional and Conservation Tillage Systems. *J. Clean. Prod.* **2022**, *351*, 131508. [CrossRef]
49. Costa, M.P.; Chadwick, D.; Saget, S.; Rees, R.M.; Williams, M.; Styles, D. Representing Crop Rotations in Life Cycle Assessment: A Review of Legume LCA Studies. *Int. J. Life Cycle Assess.* **2020**, *25*, 1942–1956. [CrossRef]
50. Yang, X.; Gao, W.; Zhang, M.; Chen, Y.; Sui, P. Reducing Agricultural Carbon Footprint through Diversified Crop Rotation Systems in the North China Plain. *J. Clean. Prod.* **2014**, *76*, 131–139. [CrossRef]
51. Abdalla, M.; Hastings, A.; Cheng, K.; Yue, Q.; Chadwick, D.; Espenberg, M.; Truu, J.; Rees, R.M.; Smith, P. A Critical Review of the Impacts of Cover Crops on Nitrogen Leaching, Net Greenhouse Gas Balance and Crop Productivity. *Glob. Change Biol.* **2019**, *25*, 2530–2543. [CrossRef]
52. Gan, Y.; Liang, C.; Wang, X.; McConkey, B. Lowering Carbon Footprint of Durum Wheat by Diversifying Cropping Systems. *Field Crops Res.* **2011**, *122*, 199–206. [CrossRef]

Disclaimer/Publisher's Note: The statements, opinions and data contained in all publications are solely those of the individual author(s) and contributor(s) and not of MDPI and/or the editor(s). MDPI and/or the editor(s) disclaim responsibility for any injury to people or property resulting from any ideas, methods, instructions or products referred to in the content.

agronomy

MDPI

Article

Long-Term Annual Changes in Agricultural Carbon Footprints and Associated Driving Factors in China from 2000 to 2020

Xingyuan Xiao [1], Xuanming Hu [1], Yaqun Liu [1,2,*] and Changhe Lu [2,3]

[1] College of Geodesy and Geomatics, Shandong University of Science and Technology, Qingdao 266590, China; skd991338@sdust.edu.cn (X.X.); 202282020056@sdust.edu.cn (X.H.)
[2] Institute of Geographic Sciences and Natural Resources Research, Chinese Academy of Sciences, Beijing 100101, China; luch@igsnrr.ac.cn
[3] College of Resources and Environment, University of Chinese Academy of Sciences, Beijing 100049, China
* Correspondence: liuyaqun@igsnrr.ac.cn

Abstract: China is one of the world's largest agricultural producers, and its agricultural carbon footprint (CF) is a major contributor to global warming. However, the long-term annual changes in its agricultural CF and the underlying driving factors remain largely unknown, compromising the scientific basis for effective carbon reduction and sustainable agriculture management. To this end, we used the life cycle assessment (LCA) method and statistical data to calculate long-term annual agricultural CFs in China. We then adopted the linear regression slope and the Moran's I method to analyze the temporal trends and spatial clustering characteristics and revealed the correlations between the main drivers and agricultural CFs. The results showed that the total (TCF) and farmland-averaged carbon footprint (FCF) of crop production both increased first and then decreased in China from 2000 to 2020, with a turning point in 2015. Overall, the TCF increased by 6.82% (3022.16×10^4 t CO_2 eq), while the FCF slightly decreased by 0.004% (0.01 t CO_2 eq/ha). Both the TCF and the FCF showed spatial heterogeneity, with high values in the east and low values in the west, and the spatial clustering of the TCF and its components has weakened over time. Fertilizer (39.26%) and paddy (27.38%) were the main contributors to TCF. Driver analysis found that grain yield was positively correlated with TCF in most provinces, indicating that the continuous yield increase has brought greater pressure on agricultural carbon emission reduction in China. Agricultural stakeholders should optimize crop planting structures and patterns and improve resource-use efficiencies through technological and management innovation to adapt to these threats and achieve low-carbon agriculture. The findings of our research can aid the scientific research on spatiotemporal estimation and driver analysis of agricultural CFs and provide decision-making support for sustainable agricultural practices.

Keywords: agricultural carbon footprint; life cycle assessment; annual temporal trend; spatial autocorrelation; driving factors; crop production; climate change; sustainable agriculture development

1. Introduction

Agriculture provides essential food, fuel, feed and services for human society [1] and plays a key role in ensuring food security and improving the livelihoods and well-being of rural residents [2]. Global population and economic growth have increased food demand, leading to the expansion and intensification of farmland [3]. As a result, agricultural inputs such as fertilizers, pesticides, irrigation and machinery have increased,

intensifying greenhouse gas (GHG) emissions, environmental non-point source pollution and biodiversity loss [4]. Therefore, agricultural practices such as optimizing crop planting structure and improving resource-use efficiency are urgently needed to mitigate agricultural GHG emissions and promote low-carbon agriculture [5]. The key scientific basis for achieving these goals is to reveal the spatiotemporal changes in agricultural GHG emissions and the driving factors.

Carbon footprint (CF) is regarded as a pivotal metric for managing GHG emissions [6,7], which refers to refers to the total amount of greenhouse gases caused directly or indirectly by human activities [8]. It has been widely used to quantify GHG emissions across diverse sectors and scales [9], such as the food industry [10], transportation [11,12], biofuel production [13], chemistry [14,15] and the agricultural sector [16,17]. Studying CFs helps to comprehensively understand the GHG emission patterns across various activities and industries, as well as to assess the pressure of human activities on the ecology. For agricultural production, investigating its CF changes and driving factors can reveal the contribution of agricultural activities to GHG emissions, thereby aiding the agricultural sector to effectively manage and regulate itself. Thus, scholars have paid considerable attention to agricultural CFs, employing diverse methodologies for their quantification.

The commonly used methods for CF estimation include the economic input–output (EIO) method [18], life cycle assessment (LCA) [19] and hybrid LCA, which integrates EIO with LCA, known as EIO-LCA [20]. LCA is an effective method for evaluating the inputs, outputs and potential environmental impacts of a product system throughout its life cycle [21]. Since this method requires the collection of massive amounts of data throughout the product life cycle, the assessment scope and indicators should be primarily determined based on the research objectives and data availability. The EIO method calculates the CF of a specific production system based on a multi-sector input–output table and the interconnections and impacts between different sectors. However, in China, input–output tables are published once every five years, limiting the application of EIO in annual CF studies. Although the EIO-LCA method combines the advantages of EIO and LCA [22], it also faces similar time-interval limitations. Especially for crop production systems, existing data cannot support the construction of reliable annual input–output tables, which makes it difficult to reveal the fine spatiotemporal characteristics of agricultural CFs.

Benefiting from scholarly attention, previous studies have made great progress regarding the estimation, driving factors and reduction strategies of agricultural CFs. Some scholars have found that the CF of China's grain production was mainly due to fertilization, straw burning and paddy CH_4 emissions, among which paddy CH_4 emissions were significantly related to longitude, altitude and yield [23]. In Ethiopia, climate-smart agricultural technologies have achieved better performance than conventional agricultural practices in terms of crop yields, GHG emissions and economic benefits [24]. A study used the complete decomposition method to reveal agricultural CFs and their components in different European countries and found that improving labor productivity can effectively reduce GHG emission intensity [25]. Although there have been a large number of studies on agricultural CFs in China, there are still limitations, such as incomplete considerations (no subdivision of CFs by different fertilizers and the N_2O produced by nitrogen fertilizers being ignored) and short research time series.

As one of the world's largest agricultural producers, China's agricultural carbon footprint poses a huge challenge to its carbon-neutrality goals. Moreover, China has now replaced the United States as the world's largest carbon emitter [26]. However, the long-term annual agricultural CF and its changes and drivers remain largely unknown in China. This has hindered domestic and international scholars' understanding of China's agricultural CF and the decision-making support for effective agricultural management

strategies. Thus, we adopted the LCA method and statistical data to calculate annual agricultural CFs in China from 2000 to 2020 and used the linear slope and Moran's I index to reveal their temporal trends and spatial clustering characteristics. Furthermore, we analyzed the correlation between agricultural CFs and their main drivers and provide low-carbon practice strategies for sustainable agricultural management.

2. Materials and Methods

2.1. Study Area

China (Figure 1A) is located in East Asia and has a land area of 9.6×10^6 km^2. Its farmland covers an area of 1.276×10^6 km^2 [27], accounting for 13.29% of the total national land area, which is vital to agricultural production and food security. In recent decades, the rapid urbanization and industrialization in China has resulted in the loss of high-quality farmland and the expansion of low-yield farmland [28], accompanied by changes in crop planting structure. For example, from 1980 to 2011, the proportion of grain crops, such as rice, wheat and corn, decreased, while the proportion of economic and oil crops increased [29].

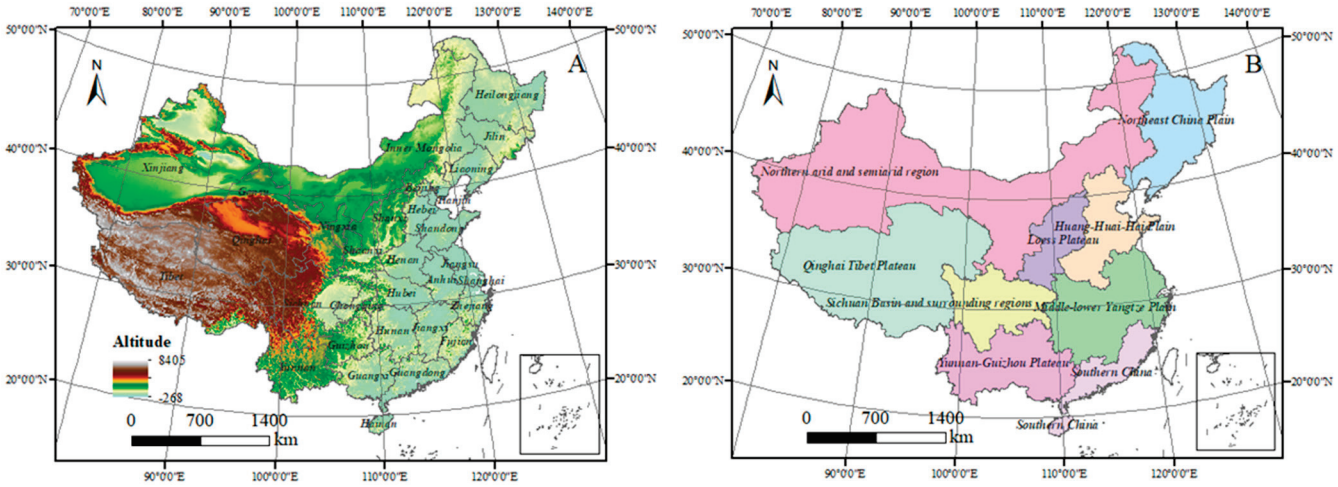


Figure 1. Provincial administrative districts (**A**) and nine agricultural regions (**B**) in China.

China's natural conditions, such as its climate, topography, soil and vegetation, are characterized by significant spatial heterogeneity, resulting in large spatial differences in planting structures. In the southern region, which is rich in water and heat resources, rice, wheat, vegetables and fruits are the main crops grown; in the arid northern region, wheat, corn, sorghum, cotton and oil crops are the main crops [30]. These differences in crop planting structure have led to the temporal evolution and spatial differentiation of agricultural CFs. In this research, we studied agricultural CFs at the provincial scale (including 31 provinces, excluding Hong Kong, Macao and Taiwan) and the agricultural region scale (Figure 1B). China is divided into 9 agricultural regions, including a northern arid and semiarid region, the Northeast China Plain, the Huang-Huai-Hai Plain, the Loess Plateau, the Qinghai–Tibet Plateau, the Sichuan Basin and surrounding regions, the Middle–Lower Yangtze Plain, the Yunnan–Guizhou Plateau, and southern China.

2.2. Data Sources

2.2.1. Statistical Data

The agricultural statistical data of 31 provinces in mainland China from 2000 to 2020 were obtained from the *China Statistical Yearbook (2001–2021)* and the *China Rural Statistical Yearbook (2001–2021)* on the China Economic and Social Big Data Research Platform

(https://data.cnki.net/, accessed on 15 February 2024). The agricultural statistics used in this study mainly include resource input, crop yield, population and cultivated area. Resource input data included fertilizer application (including nitrogen fertilizers, phosphate fertilizers, potash fertilizers and compound fertilizers; the application amounts were calculated according to the ratio of effective ingredients in each type of fertilizer), pesticide application, the total power of agricultural machinery (the sum of the rated capacity of machinery and equipment used for primary processing of agricultural products, farmland infrastructure construction, etc.), irrigated cultivated land area (the sum of paddy fields and irrigated fields), diesel consumption and agricultural film consumption. Crop yield refers to the total grain yield produced over the years. Population refers to the number of people employed in agriculture. Cultivated area data include rice, wheat, corn, soybean and other crop areas and crop sowing areas (that is, all land areas where crops are sown or transplanted and harvested in the calendar year). Data for the nine agricultural regions were obtained by provincial data division statistics.

2.2.2. Agricultural Region Data

A vector dataset of Chinese agricultural regions was sourced from the Resource and Environment Science and Data Center (https://www.resdc.cn/, accessed on 15 February 2024). China's nine agricultural regions are divided according to provincial administrative divisions.

2.2.3. Climate Dataset

The climate dataset used in the study was sourced from the National Qinghai–Tibet Plateau Scientific Data Center (https://data.tpdc.ac.cn, accessed on 20 February 2024). The dataset includes the monthly average temperature and monthly precipitation data in China from 2000 to 2020, with a spatial resolution of 1 km. The climate dataset required for this article was obtained through synthesis and projection transformation, and, finally, the annual average temperature and precipitation data of each province and region were obtained through zoning statistics.

2.3. Methods

In this study, we used the LCA methodology combined with agricultural statistical data to calculate agricultural CFs in China from 2000 to 2020 (Figure 2). We then adopted linear regression and spatial autocorrelation to analyze the temporal trend and spatial clustering characteristics of total (TCFs) and farmland-averaged CFs (FCFs). Finally, we used correlation coefficients to reveal the relationship between CFs and their driving factors.

2.3.1. System Boundary and Quantitative Index

Agricultural CFs are composed of several components, including GHG emissions from agricultural production processes, carbon sequestration from crop photosynthesis, etc. Within the scope of this study's system boundary, we only considered the CFs from resource inputs such as fertilizers, diesel and paddy cultivation.

In the agricultural production process, GHG emissions mainly include CO_2, CH_4 and N_2O. These emissions can be converted using global warming potential (GWP) values and represented uniformly as CO_2 eq [31]. This study employed two indexes to analyze agricultural CFs: TCF, which is the total GHG emissions expressed in t CO_2 eq, and FCF, which is the GHG emissions per unit of farmland area expressed in t CO_2 eq/ha.

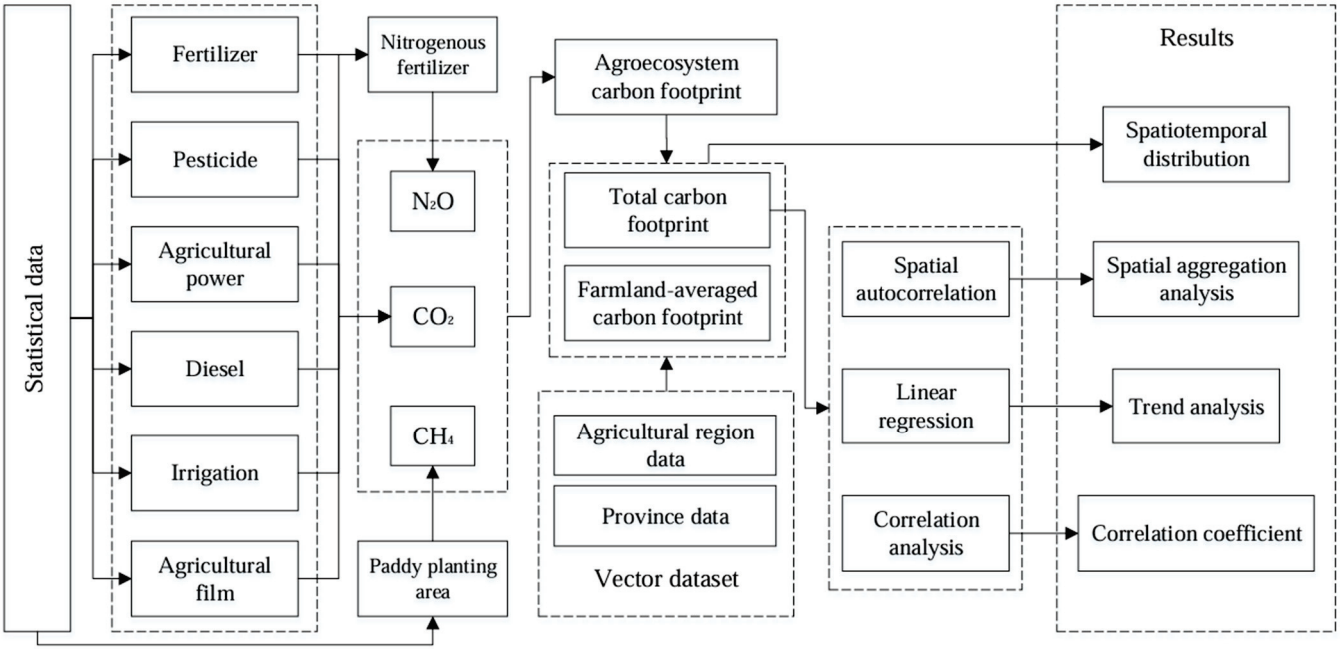


Figure 2. Analytical framework for agricultural carbon footprints.

2.3.2. LCA Method for Agricultural CF Calculation

In order to more accurately quantify the CFs of various types of agricultural inputs, the study employed the LCA method to calculate the CFs generated from agricultural inputs [32] (including irrigation, fertilizers, pesticides, diesel, agricultural film and the total power of agricultural machinery).

$$CF_{CO_2} = \sum_{i=1}^{9} (A_i \times EF_i) \quad (1)$$

where CF_{CO_2} represents the sum CF produced by agricultural inputs in t CO_2 eq; i represents various agricultural inputs; A_i represents the input quantity of the i-th substance in t, ha or 10^4 kW; 9 is the number of considered resources; and EF_i is the CO_2 emission factor of the corresponding A_i (Table 1). The C emission factor of irrigation and the total power of agricultural machinery are 266.48 kg C/ha and 0.18 kg C/kW [33], respectively. Due to CO_2 eq being used as the unit in this paper, the aforementioned two values were multiplied by 44/12 (C-to-CO_2 conversion factor) to obtain the emission factor values used in this study.

Table 1. Emission factors of different agricultural resources.

Emission Source	Emission Factor	Reference
N fertilizer	3.10 t CO_2 eq/t	[31]
P_2O_5 fertilizer	0.61 t CO_2 eq/t	[31]
K_2O fertilizer	0.44 t CO_2 eq/t	[31]
Compound fertilizer	1.38 t CO_2 eq/t	Average of fertilizer factors
Total power of agricultural machinery	6.6 t CO_2 eq/10^4 kW	The study's calculations
Diesel	3.70 t CO_2 eq/t	[34]
Pesticides	18.0 t CO_2 eq/t	[35]
Agricultural film	2.50 t CO_2 eq/t	[32]
Irrigation	0.98 t CO_2 eq/ha	The study's calculations

The formula used to calculate the CF generated by N_2O emissions from field application of nitrogen fertilizer is as follows [32].

$$CF_{N_2O} = B \times EF_{N_2O} \times \frac{44}{28} \times 265 \quad (2)$$

where CF_{N_2O} represents the CF from the application of nitrogen fertilizer in t CO_2 eq; B is the consumption of nitrogen fertilizer in t; EF_{N_2O} is the N_2O emission factor for nitrogen fertilizer, which is 0.01 t N_2O-N/t [36]; $\frac{44}{28}$ is the conversion factor from N_2 to N_2O; and 265 is the 100-year GWP of N_2O [37].

The CF calculation formula for CH_4 generated by paddy cultivation is as follows [32].

$$CF_{CH_4} = EF_{CH_4} \times T \times M \times 28 \quad (3)$$

where CF_{CH_4} represents the CF generated from paddy cultivation in t CO_2 eq; EF_{CH_4} is the CH_4 emission factor of paddy cultivation, which is 1.3×10^{-3} t CH_4/ha/d [36]; T is the duration of paddy growth in days; M is the farm area in ha; and 28 is the 100-year GWP of CH_4 [37]. The paddy growing season in China is generally around 100–150 days. Due to the lack of specific species differentiation in the cultivation area data used in this study, a duration of 125 days for the paddy growing season was chosen.

According to the above calculation process, the calculation formulas for TCF and FCF are as follows [32].

$$TCF = CF_{CO_2} + CF_{N_2O} + CF_{CH_4} \quad (4)$$

$$FCF = \frac{TCF}{S} \quad (5)$$

where the unit of FCF is t CO_2 eq/ha and S is the total of sown area of crops.

2.3.3. Moran's I Index for Spatial Clustering Analysis

In this paper, we used Geoda software (version 1.22) to conduct spatial autocorrelation analysis of Chinese agroecosystem TCFs and different CFs using the spatial weight method based on adjacency relationships. Due to the absence of geographic adjacency between Hainan and other provinces and its being in closest proximity to Guangdong, a spatial relationship was established by connecting Hainan with Guangdong to establish a mutual adjacency relationship during the spatial connectivity analysis. This study employed spatial autocorrelation analysis and utilized the global Moran's I index to measure the degree of spatial clustering of TCFs and CFs among different provinces. The calculation formula for Moran's I [38] is as follows.

$$I = \frac{N}{W} \times \frac{\sum_{i=1}^{N} \sum_{j=1}^{N} \omega_{ij}(x_i - \overline{x})(x_j - \overline{x})}{\sum_{i=1}^{N} (x_i - \overline{x})^2} \quad (6)$$

where I is the value of Moran's I; N is the number of provinces; x_i and x_j represent the TCF and CF generated by the i-th province and j-th province, respectively; $\overline{x}$ is the average value of x; ω_{ij} is the spatial weight matrix; and W is the sum of all ω_{ij}. $I > 0$ indicates a positive spatial autocorrelation, $I < 0$ means a negative spatial autocorrelation and $I = 0$ means spatial randomness.

2.3.4. Linear Regression Slopes for Trend Analysis

This study used the linear regression slope to analyze the trends of TCFs and CFs from 2000 to 2020. The slope [39] calculation formulas are as follows.

$$\text{slope} = \frac{n \times \sum_{t=1}^{n} t \times CF_t - \sum_{t=1}^{n} t \times \sum_{t=1}^{n} CF_t}{n \times \sum_{t=1}^{n} t^2 - \left(\sum_{t=1}^{n} t\right)^2} \quad (7)$$

$$\text{slope}\% = \text{slope} \times \frac{n}{\sum_{t=1}^{n} CF_t} \times 100 \quad (8)$$

where slope represents the interannual trend, n represents the number of study years, and CF_t represents the values of TCF and CFs in year t. Slope > 0 indicates an increasing trend, and slope < 0 indicates a decreasing trend, while slope% represents the ratio of the slope to the mean TCF and CFs, with the aim of calculating the magnitude of the change in the mean TCF and CFs.

2.3.5. Linear Correlation Coefficient for Driver Analysis

This study used the linear correlation coefficient to quantify the relationships between various natural–anthropogenic factors (i.e., annual precipitation, annual average temperature, paddy area, maize area, wheat area, soybean area, grain yield and employed population in primary industries) and agricultural TCFs. The calculation formula is as follows [40].

$$R = \frac{\sum (a - \bar{a})\left(b - \bar{b}\right)}{\sqrt{\sum (a - \bar{a})^2 \sum \left(b - \bar{b}\right)^2}} \quad (9)$$

where R is the correlation coefficient between two factors and a and b are different factors. $R > 0$ indicates a positive correlation; $R < 0$ indicates a negative correlation.

3. Results

3.1. Annual Distribution of Agricultural CFs

From 2000 to 2020, the agricultural TCF and FCF both increased first and then decreased in China, with a turning point in 2015 (Figure 3). The TCF increased from 44,334.88 $\times$ 10^4 t CO_2 eq to 47,357.04 $\times$ 10^4 t CO_2 eq, with an increase of 6.82% (3022.16 $\times$ 10^4 t CO_2 eq). The TCFs in the Northeast China Plain and the northern arid and semiarid region increased significantly from 3948.24 $\times$ 10^4 t CO_2 eq and 2315.62 $\times$ 10^4 t CO_2 eq to 6537.20 $\times$ 10^4 t CO_2 eq and 4218.17 $\times$ 10^4 t CO_2 eq, with increases of 61.01% (2588.96$\times$ 10^4 t CO_2 eq) and 82.16% (1902.55 $\times$ 10^4 t CO_2 eq), respectively. However, the TCFs in Southern China and the Huang-Huai-Hai Plain decreased significantly from 4168.28 $\times$ 10^4 t CO_2 eq and 8863.28 $\times$ 10^4 t CO_2 eq to 3667.32 $\times$ 10^4 t CO_2 eq and 7941.59 $\times$ 10^4 t CO_2 eq, with decreases of -12.02% (-500.96 $\times$ 10^4 t CO_2 eq) and -10.40% (-921.69 $\times$ 10^4 t CO_2 eq), respectively. China's FCF slightly declined from 2.84 t CO_2 eq/ha to 2.83 t CO_2 eq/ha (-0.004%). The FCFs in the Yunnan–Guizhou Plateau, the Sichuan Basin and surrounding regions, and the Huang-Huai-Hai Plain decreased by 4.02%, 6.78% and 10.10%, respectively. Other agricultural regions experienced varying degrees of increase. In particular, the FCFs in the northern arid and semiarid region and the Loess Plateau significantly increased from 1.65 t CO_2 eq/ha and 1.86 t CO_2 eq/ha to 2.08 t CO_2 eq/ha and 2.38 t CO_2 eq/ha, with increases of 26.38% and 27.94%, respectively.

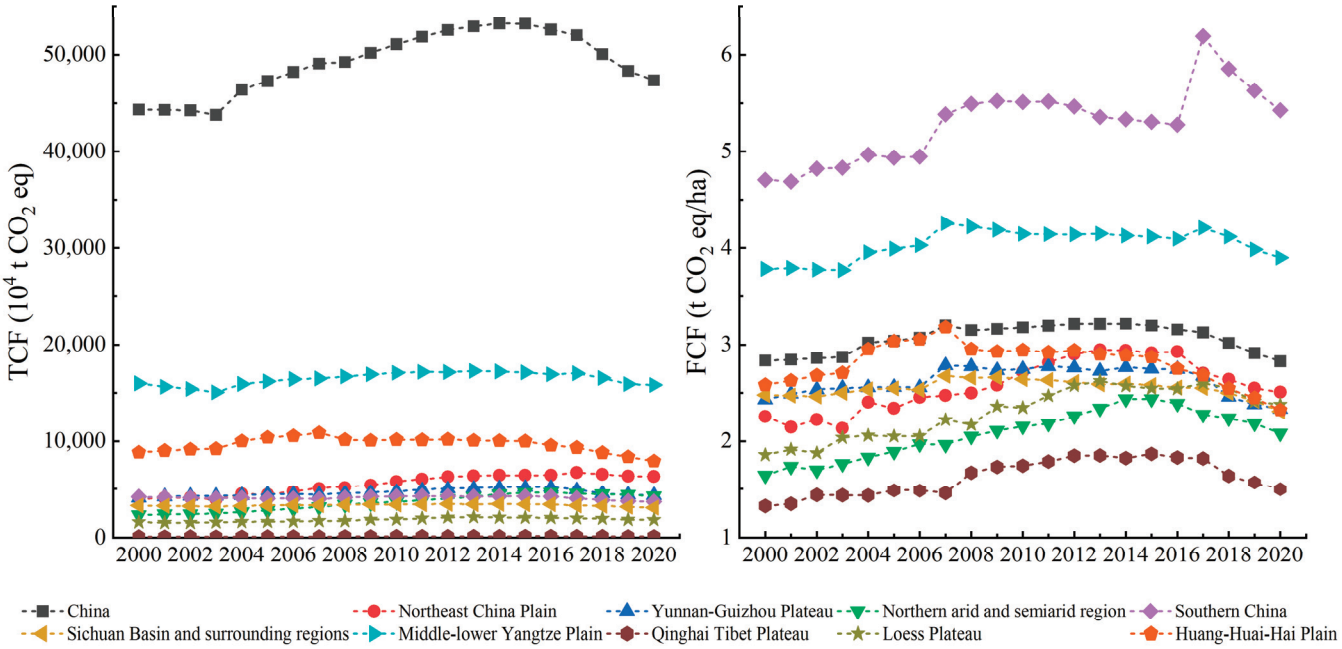


Figure 3. Annual changes in TCFs and FCFs of nine agricultural regions in China from 2000 to 2020.

Provinces with high TCFs were primarily located in East and Central China, while those in the western region generally had lower TCFs (Figure 4). Notably, the TCFs of Inner Mongolia, Heilongjiang, Tibet and Xinjiang significantly increased from 763.43 × 10^4 t CO_2 eq, 1736.83 × 10^4 t CO_2 eq, 29.65 × 10^4 t CO_2 eq and 878.01 × 10^4 t CO_2 eq to 1440.73 × 10^4 t CO_2 eq, 3679.25 × 10^4 t CO_2 eq, 57.29 × 10^4 t CO_2 eq and 1815.56 × 10^4 t CO_2 eq, with increases of 88.72%, 111.84%, 93.24% and 106.78%, respectively. Conversely, the TCFs in Beijing, Tianjin and Shanghai significantly decreased by 73.56%, 41.81% and 48.52%, from 165.07 × 10^4 t CO_2 eq, 196.05 × 10^4 t CO_2 eq and 293.78 × 10^4 t CO_2 eq to 43.65 × 10^4 t CO_2 eq, 114.08 × 10^4 t CO_2 eq and 151.24 × 10^4 t CO_2 eq, respectively. Both TCFs and FCFs showed spatial heterogeneity, with high values in the east and low values in the west, and the spatial clustering of the TCFs and their components has weakened over time. China's FCFs showed spatial heterogeneity, with higher values in the east and lower values in the west and the highest value located in the southeastern coastal area. Tibet's FCF significantly increased from 1.28 t CO_2 eq/ha to 2.11 t CO_2 eq/ha (64.09%). The FCFs of Heilongjiang, Fujian, Hainan, Shaanxi and Gansu increased by 32.55%, 34.55%, 35.67%, 37.03% and 39.96%, from 1.86 t CO_2 eq/ha, 4.97 t CO_2 eq/ha, 3.81 t CO_2 eq/ha, 2.23 t CO_2 eq/ha and 1.19 t CO_2 eq/ha to 2.47 t CO_2 eq/ha, 6.68 t CO_2 eq/ha, 5.16 t CO_2 eq/ha, 3.06 t CO_2 eq/ha and 1.66 t CO_2 eq/ha, respectively. The FCFs in Tianjin and Shandong significantly declined from 3.68 t CO_2 eq/ha and 2.80 t CO_2 eq/ha to 2.72 t CO_2 eq/ha and 2.25 t CO_2 eq/ha, with decreases of −25.99% and −19.49%, respectively.

3.2. Annual Distribution of Different CF Components

The CFs generated by various agricultural inputs made different contributions to TCFs (Figure 5). Fertilizer (39.26%) and paddies (27.38%) were the main contributors to TCFs. Among all CF components, only the CF of fertilizer decreased by 3.04%, dropping from 17,557.22 × 10^4 t CO_2 eq to 17,023.10 × 10^4 t CO_2 eq. The CFs from agripower and agrifilm markedly increased from 34.70 × 10^4 t CO_2 eq and 333.86 × 10^4 t CO_2 eq to 69.71 × 10^4 t CO_2 eq and 597.16 × 10^4 t CO_2 eq, with increases of 100.90% and 78.87%, respectively. The CFs from pesticides, diesel, irrigation and paddies increased by 2.64%, 31.56%, 28.50% and 0.39%, respectively.

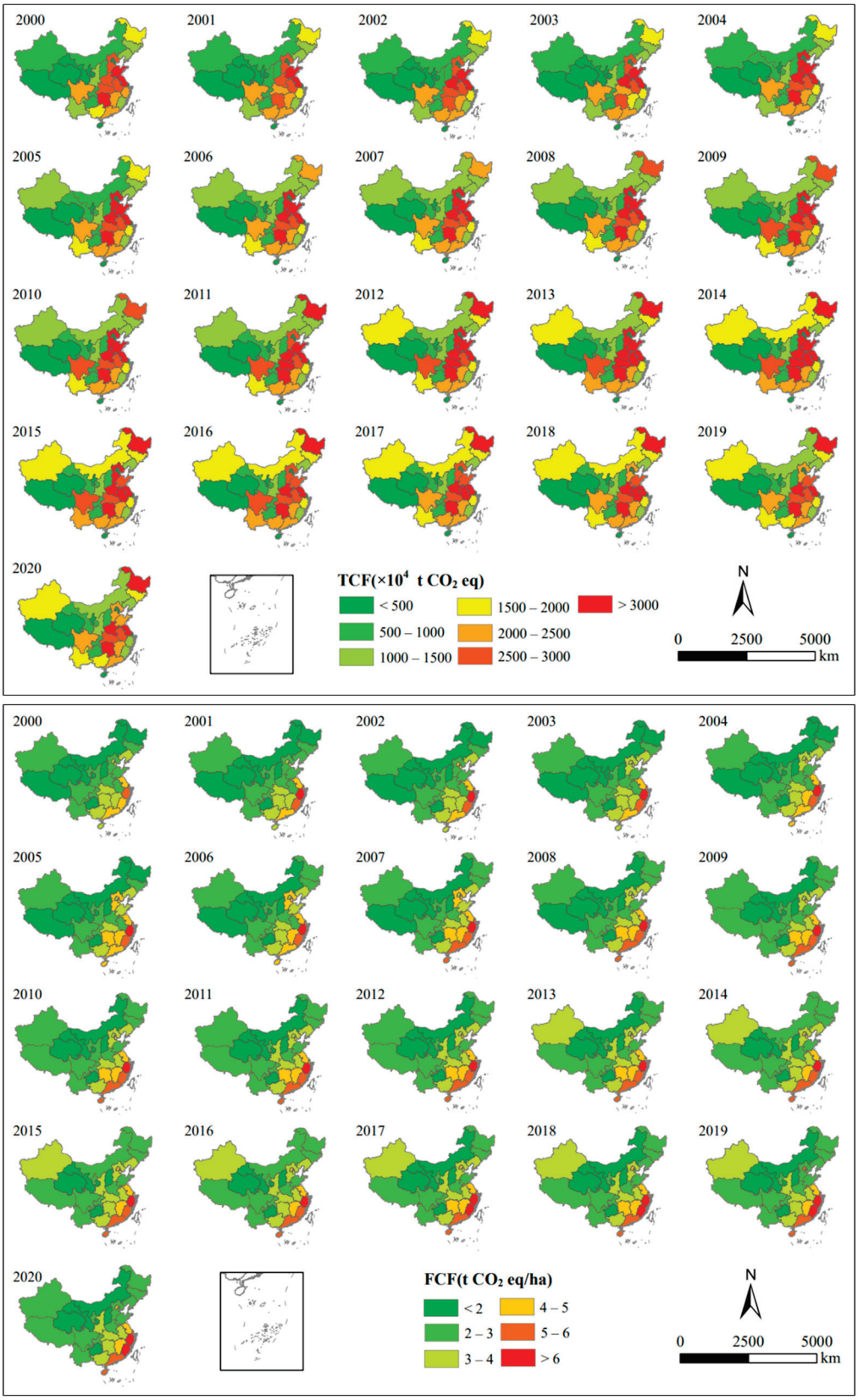


Figure 4. Annual distribution of TCFs and FCFs in different provinces in China from 2000 to 2020.

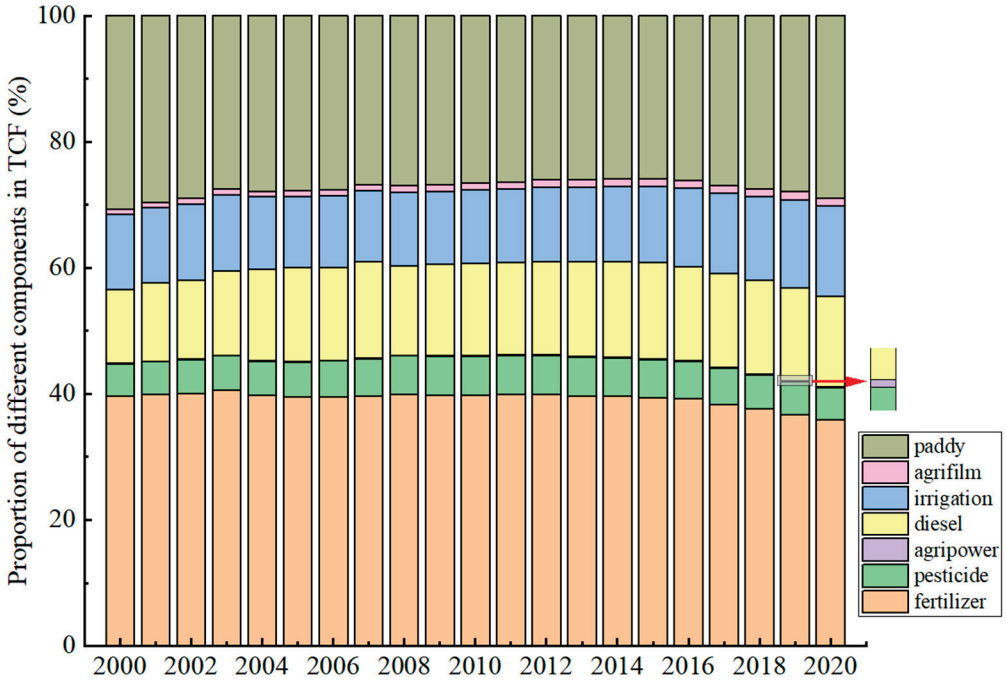


Figure 5. Annual proportions of TCF components in China from 2000 to 2020.

Various CF components in the Middle–Lower Yangtze Plain and the Huang-Huai-Hai Plain showed higher increases than other agricultural regions (Figure 6). In the northern arid and semiarid region, the CFs of fertilizer, pesticides and diesel saw significant increases of 91.68%, 147.16% and 128.34%, from 1045.08 × 10^4 t CO_2 eq, 63.90 × 10^4 t CO_2 eq and 357.79 × 10^4 t CO_2 eq to 2003.19 × 10^4 t CO_2 eq, 157.92× 10^4 t CO_2 eq and 816.96 × 10^4 t CO_2 eq, respectively. The CFs for fertilizer, pesticides and diesel in the Middle–Lower Yangtze Plain, the Sichuan Basin and surrounding regions, and the Huang-Huai-Hai Plain significantly declined by 20.84%, 26.32% and 17.51%. In the Northeast China Plain, the CFs of agripower and irrigation significantly increased by 231.15% and 102.80%, from 2.62 × 10^4 t CO_2 eq and 469.20 × 10^4 t CO_2 eq to 8.67 × 10^4 t CO_2 eq and 951.53 × 10^4 t CO_2 eq, respectively. The CFs for agripower, irrigation and agrifilm in all agricultural regions increased to varying degrees. Among them, agrifilm CF in the Qinghai–Tibet Plateau showed the largest growth of 1109.95%, from 0.19 × 10^4 t CO_2 eq to 2.31 × 10^4 t CO_2 eq.

There were significant differences in CF changes among provinces (Figure 7). In Beijing, the CFs for fertilizer, pesticides, agripower, diesel and irrigation decreased substantially by 75.56%, 60.50%, 69.89%, 78.48% and 66.67%, respectively. The CFs for agripower and diesel decreased by 38.47% and 87.95% in Tianjin. Shanghai showed decreases of 77.23%, 76.06%, 43.29% and 39.62% in the CFs for fertilizer, pesticides, irrigation and agrifilm. Conversely, Inner Mongolia experienced significant increases in CFs for fertilizer, pesticides, agripower and diesel of 104.26%, 163.07%, 200.42% and 161.20%. In Xinjiang, the CFs for fertilizer, agripower and agrifilm increased by 158.64%, 244.15% and 194.67%, respectively. The CFs for pesticides and agripower increased by 138.48% and 106.09% in Jilin and by 283.78% and 319.82% in Heilongjiang. Additionally, Jilin's diesel CF and Heilongjiang's irrigation CF increased by 134.16% and 203.72%. Gansu's CFs for pesticides and diesel increased by 253.15% and 131.41%. In Guizhou, the CFs for agripower and diesel increased by 317.46% and 200.00%. The CFs for agripower, diesel, irrigation and agrifilm increased by 403.76%, 442.86%, 80.73% and 1357.81% in Tibet. Agripower CFs in Hubei and Hainan and Hunan's diesel CF increased by 227.16%, 206.42% and 101.79%, respectively. Furthermore, the CFs

for agrifilm in Guangxi, Hainan, Qinghai and Ningxia increased by 174.64%, 5005.18%, 1060.06% and 241.35%, respectively.

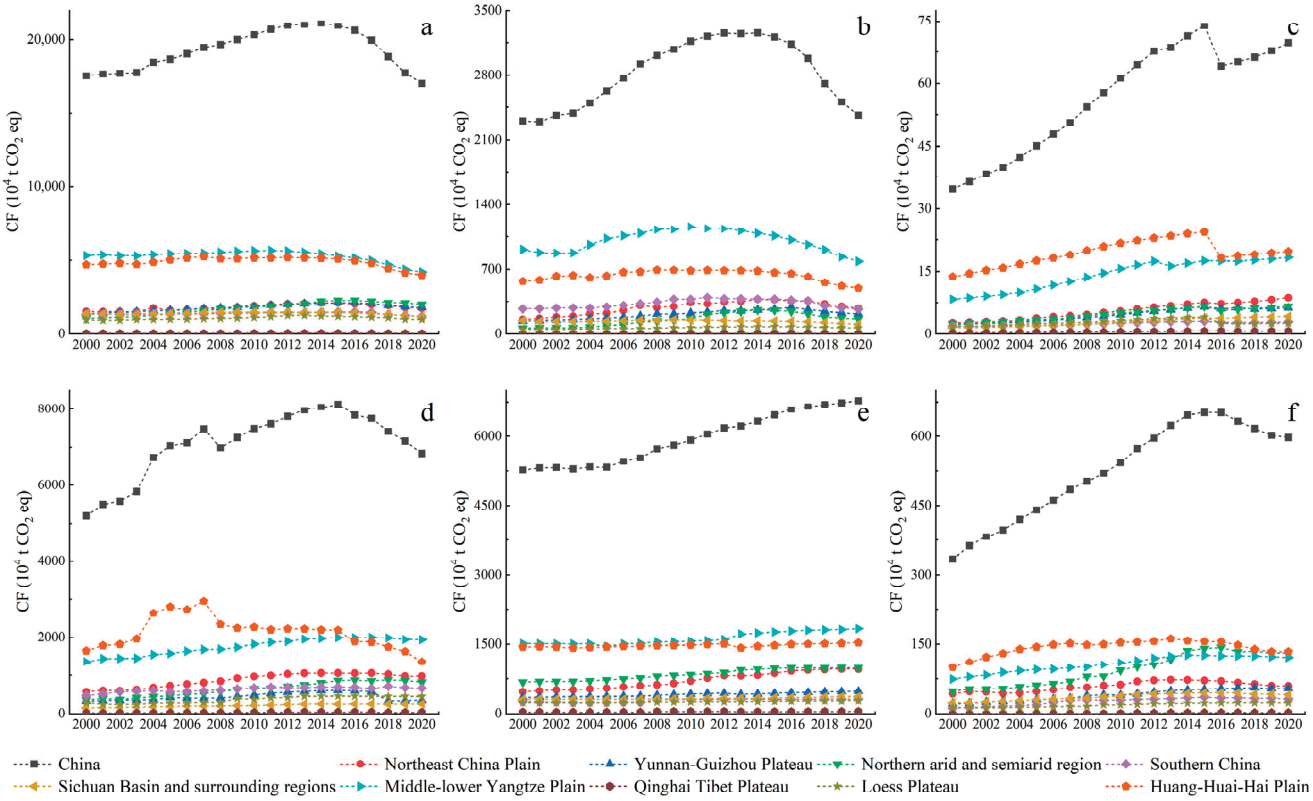


Figure 6. Annual changes in different CFs in nine agricultural regions in China from 2000 to 2020: (**a**) fertilizer CFs; (**b**) pesticide CFs; (**c**) agripower CFs; (**d**) diesel CFs; (**e**) irrigation CFs; (**f**) agrifilm CFs.

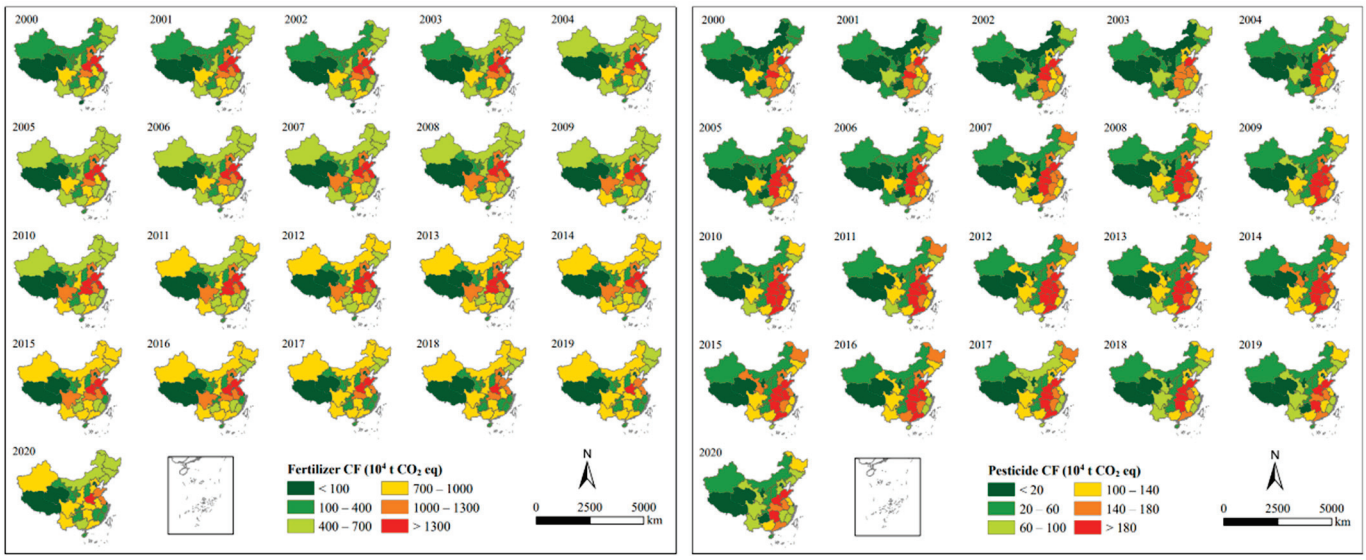


Figure 7. *Cont.*

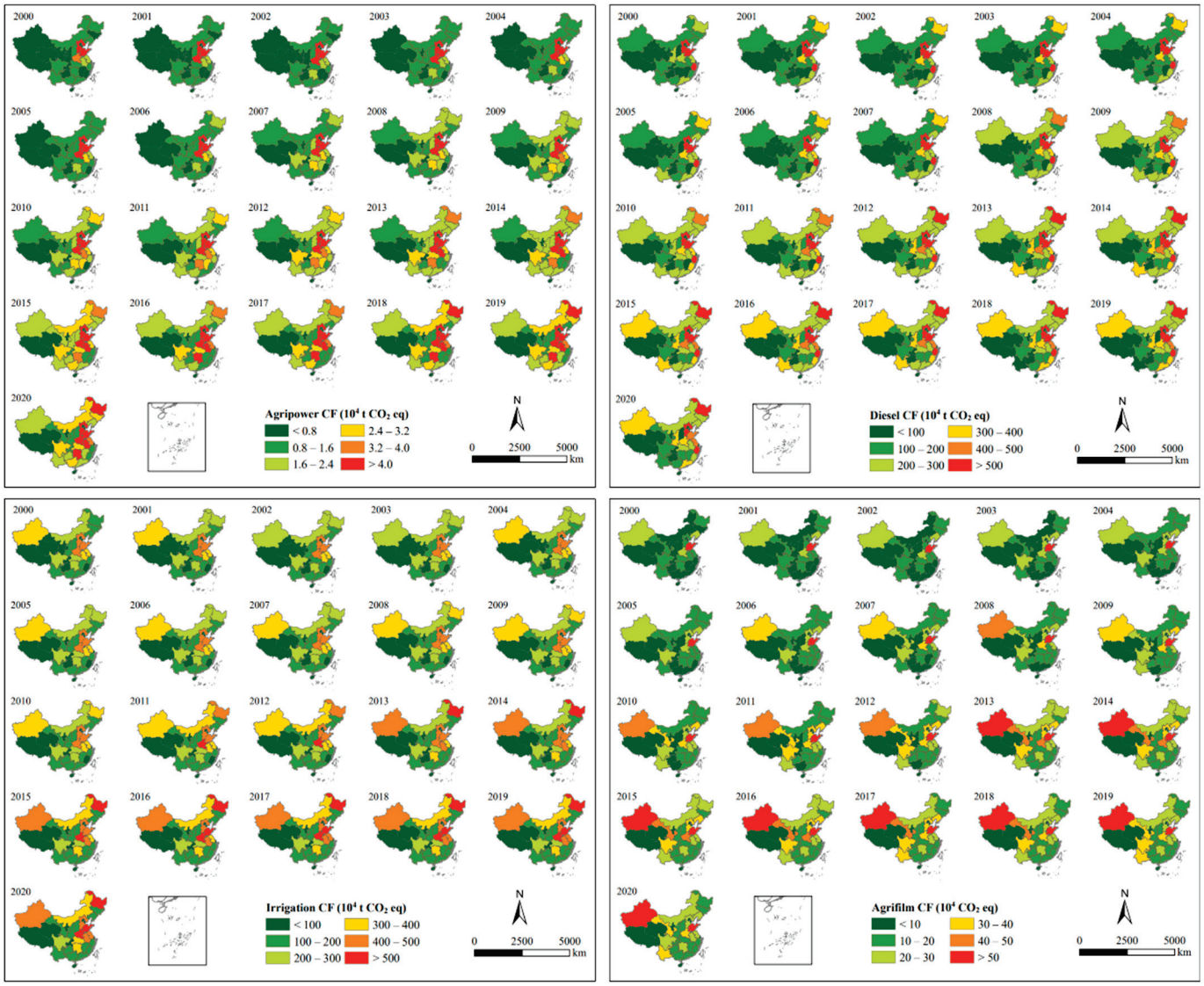


Figure 7. Annual distribution of different CFs in different provinces in China from 2000 to 2020.

3.3. Temporal Trends of Agricultural CFs

The temporal variations in TCFs and FCFs showed considerable differences (Figure 8). Inner Mongolia, Heilongjiang and Xinjiang experienced significant growth in TCFs, with slope values of 44.25 × 10^4 t CO_2 eq/yr, 125.44 × 10^4 t CO_2 eq/yr and 62.73 × 10^4 t CO_2 eq/yr and slope% values of 3.60%/yr, 4.47%/yr and 4.48%/yr, respectively. Hebei and Shandong showed significant declines in TCF, with slope values of −27.29 × 10^4 t CO_2 eq/yr and −30.36 × 10^4 t CO_2 eq/yr and slope% values of −0.93%/yr and −1.00%/yr, respectively. The FCFs of Zhejiang, Fujian and Hainan had slope values of 98.06 kg CO_2 eq/ha/yr, 91.17 kg CO_2 eq/ha/yr and 94.79 kg CO_2 eq/ha/yr and slope% values of 1.37%/yr, 1.55%/yr and 1.86%/yr, respectively. The slope of Tianjin's FCF was −30.52 kg CO_2 eq/ha/yr, and the slope% was −0.78%/yr, showing a noticeable declining trend.

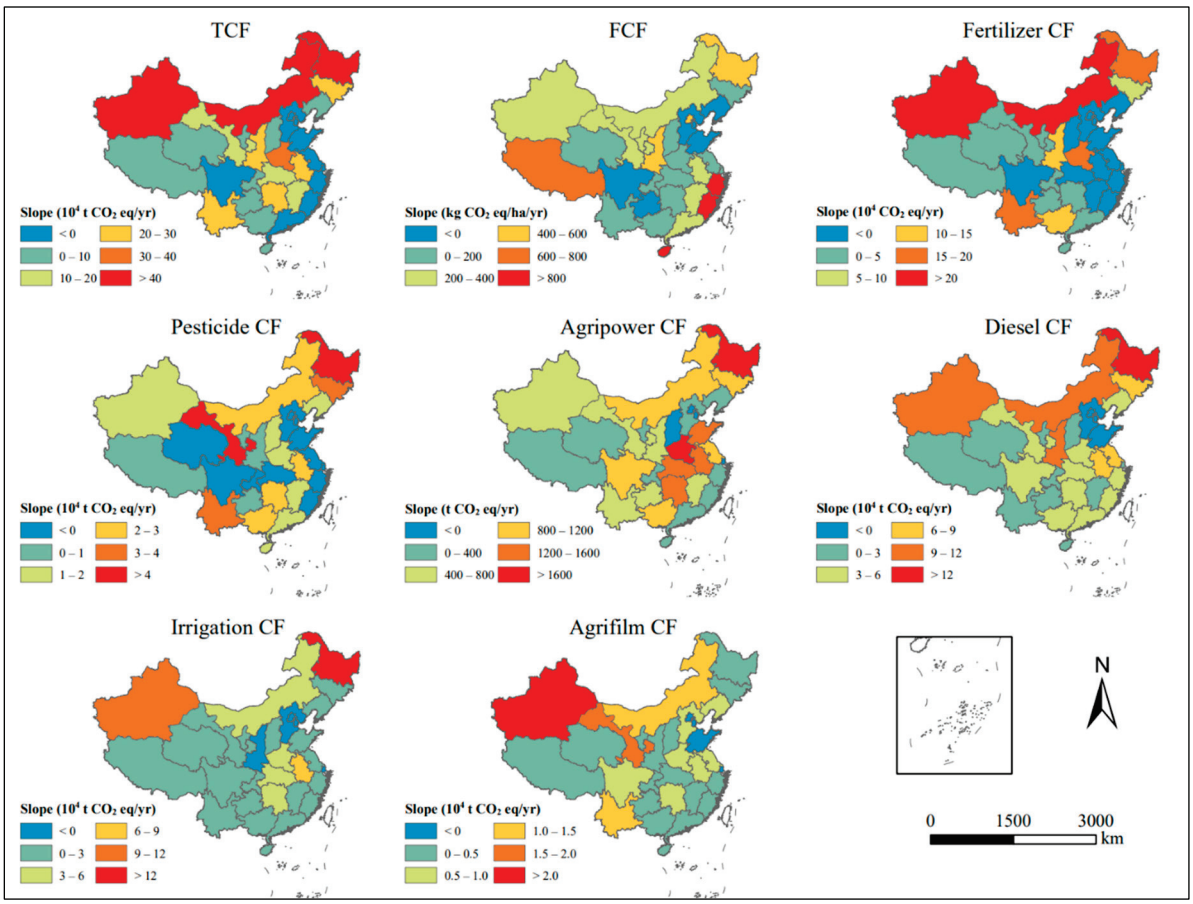


Figure 8. Slope values of TCFs, FCFs and different CFs in different provinces in China from 2000 to 2020.

In terms of changes in different CFs, the slope values of Inner Mongolia's CFs for fertilizer and diesel were 25.22 × 10^4 t CO_2 eq/yr and 10.52 × 10^4 t CO_2 eq/yr, and the slope% values were 4.02%/yr and 4.89%/yr, respectively. Conversely, the slope values for fertilizer CFs in Jiangsu and Shandong and the diesel CF in Hubei were −17.34 × 10^4 t CO_2 eq/yr, −23.91 × 10^4 t CO_2 eq/yr and −19.77 × 10^4 t CO_2 eq/yr, and the slope% values were −1.24%/yr, −1.58%/yr and −1.85%/yr, respectively. Additionally, the slope values for pesticide CFs in Jiangsu, Zhejiang and Shandong were −2.54 × 10^4 t CO_2 eq/yr, −2.29 × 10^4 t CO_2 eq/yr and −2.64 × 10^4 t CO_2 eq/yr, and the slope% values were −1.66%/yr, −2.17%/yr and −0.96%/yr, respectively. The slope values for Xinjiang's CFs for fertilizer, diesel, irrigation and agrifilm were 35.77 × 10^4 t CO_2 eq/yr, 11.16 × 10^4 t CO_2 eq/yr, 11.88 × 10^4 t CO_2 eq/yr and 2.64 × 10^4 t CO_2 eq/yr, and the slope% values were 5.47%/yr, 4.59%/yr, 3.05%/yr and 5.83%/yr, respectively. The slope values for Heilongjiang's CFs for pesticides, agripower, diesel and irrigation were 4.23 × 10^4 t CO_2 eq/yr, 1844.81 t CO_2 eq/yr, 14.04 × 10^4 t CO_2 eq/yr and 25.04 × 10^4 t CO_2 eq/yr, and the slope% values were 3.66%/yr, 7.22%/yr, 3.18%/yr and 6.33%/yr, respectively. The slope values for Gansu's CFs for pesticides and agrifilm were 4.98 × 10^4 t CO_2 eq/yr and 1.62 × 10^4 t CO_2 eq/yr, and the slope% values were 6.54%/yr and 5.27%/yr, respectively. The slope values for Henan's agripower CF and Shaanxi's diesel CF were 1650.98 t CO_2 eq/yr and 11.68 × 10^4 t CO_2 eq/yr, and the slope% values were 2.71%/yr and 4.48%/yr. The slope values for Beijing's CFs for agripower and irrigation were −100.30 t CO_2 eq/yr and −0.90 × 10^4 t CO_2 eq/yr, and the slope% values were −5.91%/yr and −4.87%/yr, respectively. The slope values for Tianjin's agripower CF and Shanghai's agrifilm CF were −78.42 t CO_2 eq/yr and −0.12 × 10^4 t CO_2 eq/yr, and the slope% values were −2.18%/yr and -2.43%/yr, respectively.

3.4. Spatial Clustering of Agricultural CFs

The Moran's I values for TCFs and different CFs decreased over time (Figure 9), indicating a weakening spatial clustering of CFs among provinces. The Moran's I values for TCFs, fertilizer CFs, irrigation CFs and agrifilm CFs declined from 0.231, 0.263, 0.159 and 0.142 to 0.122, 0.079, 0.106 and 0.024, respectively, suggesting that their spatial autocorrelation gradually shifted from a positive correlation towards randomness. The Moran's I values for pesticide CFs and agripower CFs decreased from 0.354 and 0.311 to 0.297 and 0.253, indicating a transition from strong to weak positive spatial autocorrelation. Unlike other categories, the Moran's I results for diesel CFs showed negative values, fluctuating between 0.078 and -0.031, indicating that the spatial autocorrelation for diesel CFs oscillated between positive and negative correlation.

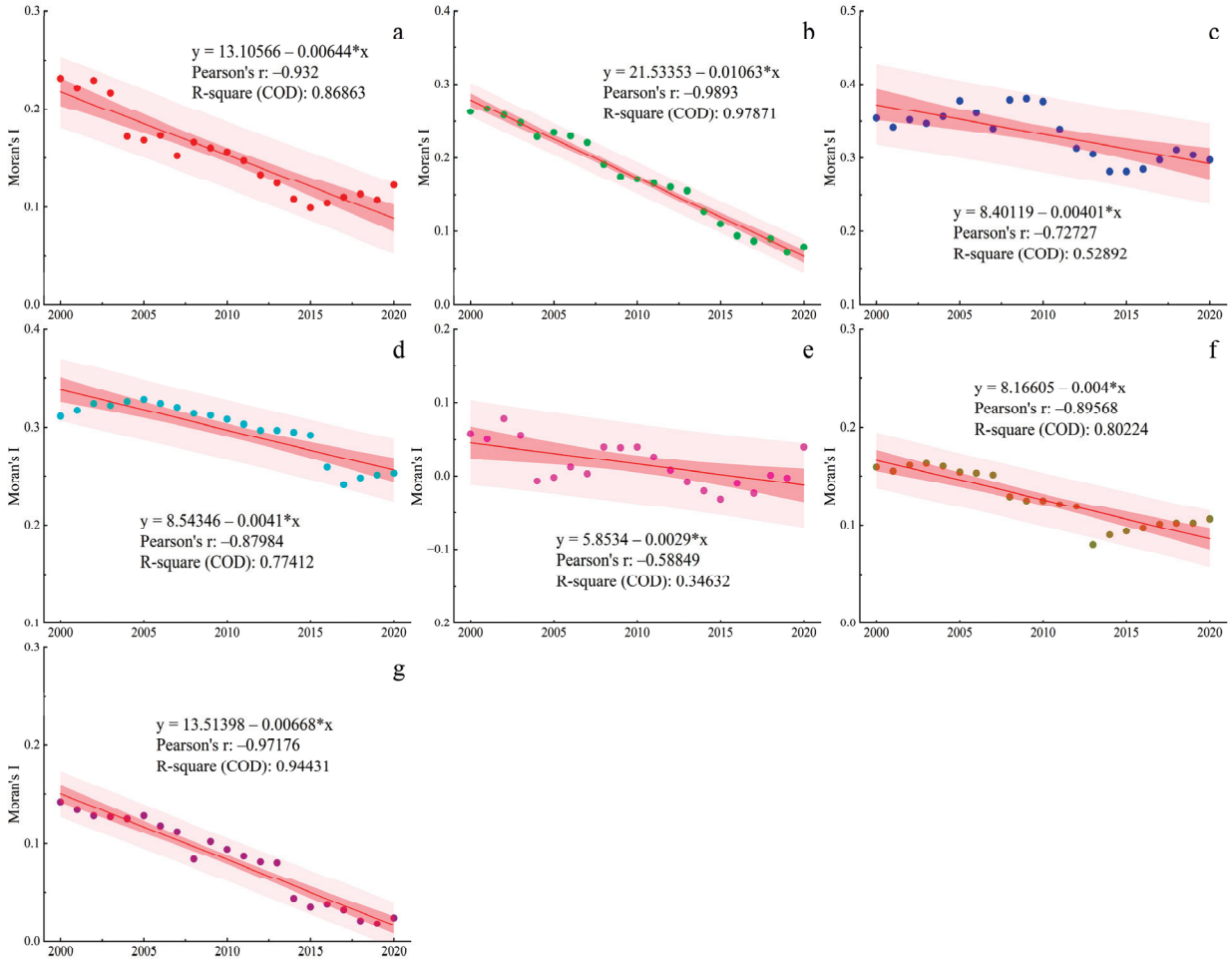


Figure 9. Temporal changes in Moran's I values for TCFs and different CFs in China from 2000 to 2020: (**a**) TCFs; (**b**) fertilizer CFs; (**c**) pesticide CFs; (**d**) agripower CFs; (**e**) diesel CFs; (**f**) irrigation CFs; (**g**) agripower CFs.

3.5. Main Factors Influencing TCFs

The influence of natural–anthropogenic factors on provincial TCFs showed significant differences (Figure 10). In Heilongjiang, Shanghai, Zhejiang, Fujian, Jiangxi, Henan and Hunan, TCFs showed a strong positive correlation with paddy cultivation. Maize showed a significant positive correlation with the TCFs of Inner Mongolia, Jilin, Heilongjiang, Guangdong, Tibet, Gansu, Ningxia and Xinjiang. Wheat had a strong positive correlation with TCF in Beijing, Anhui, Hubei and Xinjiang. There was a significant positive correlation between TCF and soybean production in Beijing and Fujian. Grain yield demonstrated a significant positive correlation with TCF in Inner Mongolia, Jilin, Heilongjiang, Shanghai,

Zhejiang, Anhui, Fujian, Jiangxi, Hunan, Shaanxi, Gansu, Ningxia and Xinjiang. The employed population in primary industries showed a significant positive correlation with TCF in Beijing, Shanghai, Zhejiang, Fujian and Shandong. Additionally, mean temperature and precipitation had a weak correlation with provincial TCFs, indicating no significant impact on TCFs. Annual precipitation was weakly positively correlated with TCFs in the water-scarce northern provinces but negatively correlated with TCFs in the precipitation-rich southern provinces.

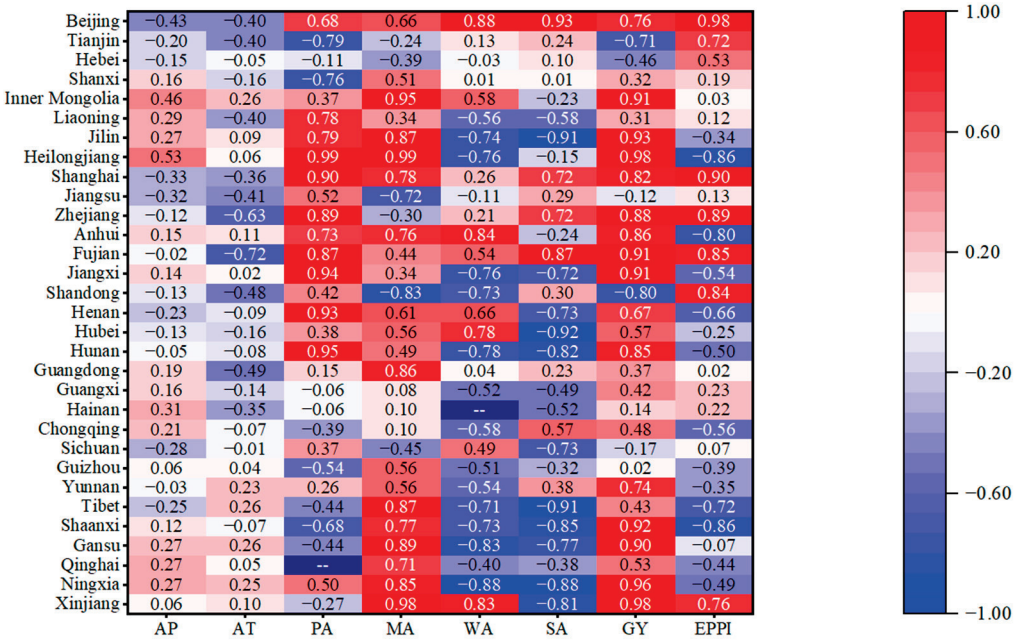


Figure 10. Correlations between natural–anthropogenic factors and TCFs. Abbreviations: annual precipitation (AP), annual average temperature (AT), paddy area (PA), maize area (MA), wheat area (WA), soybean area (SA), grain yield (GY), employed population in primary industries (EPPI).

4. Discussion

4.1. Reasons for the Spatiotemporal Heterogeneity of Agricultural CFs

China's vast territory is significantly heterogeneous in terms of climate, topography, vegetation and soil. Its crop planting types and resource inputs also vary across space, resulting in significant differences in agricultural CFs among provinces and agricultural regions [41]. The eastern and southern provinces of China have more suitable precipitation, temperature and terrain for crop production than the western and northern provinces. The crop planting intensity in the former is usually higher than that in the latter, resulting in high CFs in the southeast and low CFs in the northwest [42]. In addition, the economic development in the southeast is higher than that in the northwest, and its crop planting structure has a higher proportion of economic crops, such as vegetables and fruits with higher benefits, which usually also require higher resource inputs. Moreover, paddies with higher CFs were mainly planted in southeastern and northeastern China. These also caused the spatial differences in China's CFs.

During the study period, China's agricultural CFs generally showed an upward trend but declined significantly after 2015. This was mainly due to the promotion of modern agricultural technology and management innovation, which reduced agricultural CFs while promoting food production, especially significantly reducing fertilizer CFs. For example, compared with conventional tillage methods, the integration of no-till farming and straw return to the field not only enhanced crop yields but also effectively mitigated GHG emissions [43]. From a temporal perspective, there were obvious differences in

CFs between different regions and different components, which were mainly attributed to the changes in farmland patterns and policy orientations [44]. With the continuous advancement of China's ecological civilization construction [45], the concepts of low-carbon, circular and green agriculture also became known and were implemented by more and more farmers, and more advanced agricultural machineries and more scientific farmland management technologies were also widely used. All of these have led to China's continued increase in grain production, while agricultural CFs have gradually decreased since 2015. The formulation and implementation of policies have led to improvements in agricultural production and management, consequently reducing agricultural GHG emissions. However, in recent decades, China's farmland has shown an overall decrease in the south and an increase in the north, and the grain production pattern has also changed from "transporting grain from the south to the north" to "transporting grain from the north to the south". This has also led to a significantly higher increase in CFs in the northwest than in the southeast and even a decrease in CFs in the developed eastern coastal areas, despite the application of carbon-reducing agricultural technologies across the country.

4.2. Policy Implications for Low-Carbon Agriculture

As a major agricultural country, China has set ambitious goals to achieve its carbon peak by 2030 and carbon neutrality by 2060 [46]. It is urgent to reduce the CF of agriculture, a major contributor to GHG emissions. Therefore, the central and local governments have formulated targeted agricultural GHG emission-reduction policies and regulations based on regional characteristics [47]. Based on the findings of this study, we propose the following policy recommendations to differentially reduce agricultural CFs and mitigate China's agricultural GHG emissions.

Optimize paddy cultivation technology. Paddies make a large contribution to TCFs. Thus, in the pursuit of modernizing paddy cultivation, we should focus on enhancing cultivation practices and improving water and fertilizer management to mitigate CH_4 emissions [48]. At the same time, improving the use efficiencies of agricultural inputs is also important for reducing paddy CFs [49]. In addition, the use of intermittent irrigation technology can avoid long-term waterlogging and reduce CH_4 emissions. These measures need to be implemented effectively, especially in southeastern and northeastern China, where paddies are mainly grown.

Control the use of fertilizer and establish relevant reward and punishment mechanisms. Fertilizer is the main source of agroecosystem CFs, and promoting efficient fertilization technology is an important direction for improving agricultural practices. In addition, we found that the fertilizer CFs of Inner Mongolia and Xinjiang have grown rapidly. However, these regions are major pastoral areas in China with large numbers of livestock. Therefore, agricultural management departments should promote the planting–livestock cycle and benefit multiple stakeholders through policies and subsidies. This can not only reduce pollution of the ecological environment by livestock manure but also reduce agricultural fertilizer input and promote organic crop production.

Establish an intelligent agricultural system. Agricultural managers should improve resource utilization efficiency and reduce agricultural CFs by establishing an intelligent agricultural management and operation system. Intelligent and standardized modern agricultural technologies, such as soil testing and fertilizer formulation, remote sensing monitoring of crop growth conditions, drone fertilization and pesticide spraying, and agricultural machinery operations should be integrated into the agricultural system to help reduce CFs. Specific operation parameters need to be adjusted according to regional differences in crop types and CF intensity. In addition, the agricultural system should be

further upgraded to a climate-smart agricultural system to adapt to the climate conditions of different regions and future changes in the human–earth system.

Strengthen technological innovation and the use of green energy. In crop-productive Heilongjiang, Shandong and Henan, upgrading and renovating agricultural water supply networks has been shown to effectively reduce water evaporation and leakage, thereby reducing irrigation CFs [50]; thus, these measures should be implemented primarily in water-scarce northern China and the highly irrigated North China Plain. In addition, previous studies found that the use of biodiesel can effectively reduce agricultural CFs [51], which can be promoted through subsidy policies in Heilongjiang and the North China Plain, which have larger agripower CFs. In areas with abundant solar radiation and wind energy, such as Tibet, Qinghai and Xinjiang, the photovoltaic power generation industry and wind power generation can be vigorously developed to provide green energy for agricultural production and reduce CFs.

4.3. Comparison with Other Studies

In this study, the agricultural CFs of eastern provinces were higher than those of western provinces in China in the past two decades, which is consistent with previous studies [52]. We found that Chinese agricultural CFs showed a trend of increasing first and then decreasing from 2000 to 2020, with a turning point in 2015. Similar temporal change characteristics have been validated in existing research [53]. In addition, fertilizer and paddies were confirmed to be the main contributors to agricultural CFs, which was similar to previous studies, but the contribution rates were slightly different [4] due to the longer time period of this study. Previous local studies also found that fertilizer was the main contributor to and reduction pathway for CFs in coastal saline cropland ecosystems [54], and the CF of paddy production is generally higher than that of other crops [55]. Regarding driving factors, previous studies found that precipitation and temperature had limited effects on agricultural CFs [56], supporting the findings of this study. Although climate factors have no significant effect on CFs, they can intricately interact with CFs in combination with other natural–social factors.

4.4. Limitations and Prospects

This study revealed more detailed spatiotemporal characteristics of agricultural CFs in China, filling the knowledge gap in long-term annual trend analysis. However, it still has some limitations that need further improvement and in-depth research. First, the emission factors of various crop production inputs in this study were derived from previous studies without considering the differentiated impacts of factors such as changes in natural conditions and technological progress [57]. Future studies should investigate the spatiotemporal distribution of emission factors to estimate CFs more accurately. Second, this study adopted the widely used CF metric to characterize agricultural carbon emissions but did not analyze crop photosynthetic carbon fixation or soil carbon changes. Future research should integrate these important aspects of the agricultural carbon cycle to better serve sustainable agricultural development. Third, this study and previous studies found that paddy cultivation contributed significantly to agricultural CFs [58]. However, the estimation of paddy CFs involves many complex biological processes, and crop models are needed to conduct accurate evaluations in the future. Finally, although this study analyzed the annual trends of agricultural CFs, it was only conducted at the provincial level, such that the results may be different from the actual values. Future research can combine multi-source statistical and remote sensing data with machine learning algorithms to spatialize agricultural CFs and reveal more detailed spatiotemporal characteristics.

5. Conclusions

In this research, we used the LCA method and statistical data to calculate long-term annual agricultural CFs and revealed their spatiotemporal changes and driving factors in China from 2000 to 2020. The results showed that national agricultural CFs increased first and then decreased, with a turning point in 2015. The TCFs increased by 6.82%, while the FCFs slightly decreased by 0.004%. Spatially, both the TCFs and the FCFs showed the characteristics of high values in the east and low values in the west. The spatial clustering of TCFs and their components decreased over time. Further analysis revealed that the contributions of fertilizer and paddy to TCFs were 39.26% and 27.38%, these being the top two contributors. Grain yield was positively correlated with TCF in most provinces. This indicated that optimizing fertilizer use and paddy cultivation methods is key to the development of Chinese low-carbon agriculture. Improving crop planting structure, using green energy and adopting advanced technologies will promote the development of low-carbon agriculture in grain-producing areas. This research fills the gap in knowledge of Chinese long-term annual agricultural CFs and has guiding significance for the sustainable development of agriculture.

Author Contributions: Conceptualization, Y.L.; methodology, X.H. and Y.L.; software, X.H.; validation, X.X., X.H. and Y.L.; formal analysis, X.X. and X.H.; data curation, X.H.; writing—original draft preparation, X.X., X.H. and Y.L.; writing—review and editing, Y.L. and C.L.; visualization, X.H.; supervision, Y.L. and C.L.; project administration, Y.L. and X.X.; funding acquisition, Y.L. and X.X. All authors have read and agreed to the published version of the manuscript.

Funding: This research was funded by the National Natural Science Foundation of China (Grant Nos. 42201289, 42271273 and 41201266), the Natural Science Foundation of Shandong Province (Grant No. ZR2023MD018) and the Open Collaboration Fund of the State Key Laboratory of Black Soils Conservation and Utilization (Grant No. 2023HTDGZ-KF-09).

Data Availability Statement: The data presented in this research are available on reasonable request from the corresponding author. The data are not publicly available due to the data needing to be used for further research.

Acknowledgments: We greatly appreciate the editors and anonymous reviewers for their valuable time, constructive suggestions and insightful comments.

Conflicts of Interest: The authors declare no conflicts of interest.

References

1. Aguilera, E.; Reyes-Palomo, C.; Díaz-Gaona, C.; Sanz-Cobena, A.; Smith, P.; García-Laureano, R.; Rodríguez-Estévez, V. Greenhouse Gas Emissions from Mediterranean Agriculture: Evidence of Unbalanced Research Efforts and Knowledge Gaps. *Glob. Environ. Chang.* **2021**, *69*, 102319. [CrossRef]
2. Okeke, E.S.; Nweze, E.J.; Ezike, T.C.; Nwuche, C.O.; Ezorba, T.P.C.; Nwankwo, C.E.I. Silicon-Based Nanoparticles for Mitigating the Effect of Potentially Toxic Elements (Ptes) and Plant Stress in Agroecosystems: A Sustainable Pathway Towards Food Security. *Sci. Total Environ.* **2023**, *898*, 165446. [CrossRef]
3. Prosekov, A.Y.; Ivanova, S.A. Food Security: The Challenge of the Present. *Geoforum* **2018**, *91*, 73–77. [CrossRef]
4. Dong, G.; Mao, X.; Zhou, J.; Zeng, A. Carbon Footprint Accounting and Dynamics and the Driving Forces of Agricultural Production in Zhejiang Province, China. *Ecol. Econ.* **2013**, *91*, 38–47. [CrossRef]
5. Xiong, C.; Yang, D.; Huo, J.; Zhao, Y. The Relationship between Agricultural Carbon Emissions and Agricultural Economic Growth and Policy Recommendations of a Low-Carbon Agriculture Economy. *Pol. J. Environ. Stud.* **2016**, *25*, 2187–2195. [CrossRef] [PubMed]
6. Xu, X.; Lan, Y. A Comparative Study on Carbon Footprints between Plant-and Animal-Based Foods in China. *J. Clean. Prod.* **2016**, *112*, 2581–2592. [CrossRef]
7. Xu, X.; Zhang, B.; Liu, Y.; Xue, Y.; Di, B. Carbon Footprints of Rice Production in Five Typical Rice Districts in China. *Acta. Ecol. Sin.* **2013**, *33*, 227–232. [CrossRef]

8. Zorogastúa, P.; Feliciano, D.; Felipe de Mendiburu, D.; Quiroz, R. Combining Reference Trials, Farm Surveys and Mathematical Models to Assess Carbon Footprint and Mitigation Measures in Tropical Agriculture. *Ann. Agric. Sci.* **2019**, *64*, 188–195.
9. Baldo, G.L.; Marino, M.; Montani, M.; Ryding, S.-O. The Carbon Footprint Measurement Toolkit for the Eu Ecolabel. *Int. J. Life Cycle Assess.* **2009**, *14*, 591–596. [CrossRef]
10. Lin, B.; Guan, C. Assessing Consumption-Based Carbon Footprint of China's Food Industry in Global Supply Chain. *Sustain. Prod. Consum.* **2023**, *35*, 365–375. [CrossRef]
11. Chen, J.; Wang, W.; Sun, W.; Jiao, Y.; He, Y.; Li, D.; Gong, J. Tapping into the Potential CO_2 Emission Reduction of a Crude Oil Transportation System from Carbon Footprint Perspective. *J. Clean. Prod.* **2023**, *413*, 137409. [CrossRef]
12. Wu, J.; Liu, G.; Marson, A.; Fedele, A.; Scipioni, A.; Manzardo, A. Mitigating Environmental Burden of the Refrigerated Transportation Sector: Carbon Footprint Comparisons of Commonly Used Refrigeration Systems and Alternative Cold Storage Systems. *J. Clean. Prod.* **2022**, *372*, 133514. [CrossRef]
13. Therasme, O.; Volk, T.A.; Fortier, M.-O.; Kim, Y.; Wood, C.D.; Ha, H.; Ali, A.; Brown, T.; Malmsheimer, R. Carbon Footprint of Biofuels Production from Forest Biomass Using Hot Water Extraction and Biochemical Conversion in the Northeast United States. *Energy* **2022**, *241*, 122853. [CrossRef]
14. Sadiq, S.; Khan, I.; Humayun, M.; Wu, P.; Khan, A.; Khan, S.; Khan, A.; Khan, S.; Alanazi, A.F.; Bououdina, M. Synthesis of Metal–Organic Framework-Based Zif-8@ Zif-67 Nanocomposites for Antibiotic Decomposition and Antibacterial Activities. *ACS Omega* **2023**, *8*, 49244–49258. [CrossRef]
15. Chang, H.; Khan, I.; Yuan, A.; Khan, S.; Sadiq, S.; Khan, A.; Shah, S.A.; Chen, L.; Humayun, M.; Usman, M. Polyarylimide-Based Cof/Mof Nanoparticle Hybrids for CO_2 Conversion, Hydrogen Generation, and Organic Pollutant Degradation. *ACS Appl. Nano Mater.* **2024**, *7*, 10451–10465. [CrossRef]
16. Naorem, A.; Jayaraman, S.; Sinha, N.K.; Mohanty, M.; Chaudhary, R.; Hati, K.; Mandal, A.; Thakur, J.; Patra, A.; Srinivasarao, C. Eight-Year Impacts of Conservation Agriculture on Soil Quality, Carbon Storage, and Carbon Emission Footprint. *Soil. Tillage. Res.* **2023**, *232*, 105748. [CrossRef]
17. Wang, C.; Chen, Y.; Sun, M.; Wu, J. Potential of Technological Innovation to Reduce the Carbon Footprint of Urban Facility Agriculture: A Food–Energy–Water–Waste Nexus Perspective. *J. Environ. Manag.* **2023**, *339*, 117806. [CrossRef]
18. Weber, C.L.; Matthews, H.S. Quantifying the Global and Distributional Aspects of American Household Carbon Footprint. *Ecol. Econ.* **2008**, *66*, 379–391. [CrossRef]
19. Schulz, N.B. Delving into the Carbon Footprints of Singapore—Comparing Direct and Indirect Greenhouse Gas Emissions of a Small and Open Economic System. *Energy Policy* **2010**, *38*, 4848–4855. [CrossRef]
20. Suh, S.; Huppes, G. Methods for Life Cycle Inventory of a Product. *J. Clean. Prod.* **2005**, *13*, 687–697. [CrossRef]
21. Cucurachi, S.; Scherer, L.; Guinée, J.; Tukker, A. Life Cycle Assessment of Food Systems. *One Earth* **2019**, *1*, 292–297. [CrossRef]
22. Lenzen, M.; Crawford, R. The Path Exchange Method for Hybrid Lca. *Environ. Sci. Technol.* **2009**, *43*, 8251–8256. [CrossRef]
23. Tian, P.; Li, D.; Lu, H.; Feng, S.; Nie, Q. Trends, Distribution, and Impact Factors of Carbon Footprints of Main Grains Production in China. *J. Clean. Prod.* **2021**, *278*, 123347. [CrossRef]
24. Berhanu, Y.; Angassa, A.; Aune, J.B. A System Analysis to Assess the Effect of Low-Cost Agricultural Technologies on Productivity, Income and Ghg Emissions in Mixed Farming Systems in Southern Ethiopia. *Agric. Syst.* **2021**, *187*, 102988. [CrossRef]
25. Robaina-Alves, M.; Moutinho, V. Decomposition of Energy-Related Ghg Emissions in Agriculture over 1995–2008 for European Countries. *Appl. Energy* **2014**, *114*, 949–957. [CrossRef]
26. Liu, Y.; Gao, Y. Measurement and Impactor Analysis of Agricultural Carbon Emission Performance in Changjiang Economic Corridor. *Alex. Eng. J.* **2022**, *61*, 873–881. [CrossRef]
27. The Total Cropland Area in China Has Reached 1.276 × 106 km^2. Available online: www.moa.gov.cn/xw/shipin/202303/t20230306_6422302.htm (accessed on 4 March 2023).
28. Gao, X.; Cheng, W.; Wang, N.; Liu, Q.; Ma, T.; Chen, Y.; Zhou, C. Spatio-Temporal Distribution and Transformation of Cropland in Geomorphologic Regions of China During 1990–2015. *J. Geogr. Sci.* **2019**, *29*, 180–196. [CrossRef]
29. Liu, Z.; Yang, P.; Wu, W.; You, L. Spatiotemporal Changes of Cropping Structure in China During 1980–2011. *J. Geogr. Sci.* **2018**, *28*, 1659–1671. [CrossRef]
30. Chang, R.; Yao, Y.; Cao, W.; Wang, J.; Wang, X.; Chen, Q. Effects of Composting and Carbon Based Materials on Carbon and Nitrogen Loss in the Arable Land Utilization of Cow Manure and Corn Stalks. *J. Environ. Manag.* **2019**, *233*, 283–290. [CrossRef]
31. West, T.O.; Marland, G. A Synthesis of Carbon Sequestration, Carbon Emissions, and Net Carbon Flux in Agriculture: Comparing Tillage Practices in the United States. *Agric. Ecosyst. Environ.* **2002**, *91*, 217–232. [CrossRef]
32. Yan, M.; Cheng, K.; Luo, T.; Yan, Y.; Pan, G.; Rees, R.M. Carbon Footprint of Grain Crop Production in China–Based on Farm Survey Data. *J. Clean. Prod.* **2015**, *104*, 130–138. [CrossRef]
33. Duan, H.; Zhang, Y.; Zhao, J.; Bian, X. Carbon Footprint Analysis of Farmland Ecosystem in China. *J. Soil. Water. Conserv.* **2011**, *25*, 203–208. (In Chinese)

34. Chen, X.; Cui, Z.; Fan, M.; Vitousek, P.; Zhao, M.; Ma, W.; Wang, Z.; Zhang, W.; Yan, X.; Yang, J. Producing More Grain with Lower Environmental Costs. *Nature* **2014**, *514*, 486–489. [CrossRef] [PubMed]
35. Yang, X.; Gao, W.; Zhang, M.; Chen, Y.; Sui, P. Reducing Agricultural Carbon Footprint through Diversified Crop Rotation Systems in the North China Plain. *J. Clean. Prod.* **2014**, *76*, 131–139. [CrossRef]
36. Eggleston, H.S.; Buendia, L.; Miwa, K.; Ngara, T. Agriculture, Forestry and Other Land Use. In *IPCC 2006, 2006 IPCC Guidelines for National Greenhouse Gas Inventories*; Tanabe, K., Ed.; IPCC, IGES: Tokyo, Japan, 2006; Volume 4.
37. Pachauri, R.K. *IPCC, 2014: Climate Change 2014: Synthesis Report. Contribution of Working Groups I, II and III to the Fifth Assessment Report of the Intergovernmental Panel on Climate Change*; Meyer, L.A., Ed.; IPCC: Geneva, Switzerland, 2014.
38. Diniz-Filho, J.A.F.; Bini, L.M.; Hawkins, B.A. Spatial Autocorrelation and Red Herrings in Geographical Ecology. *Glob. Ecol. Biogeogr.* **2003**, *12*, 53–64. [CrossRef]
39. Xiao, X.; Zhang, J.; Liu, Y. Impacts of Crop Type and Climate Changes on Agricultural Water Dynamics in Northeast China from 2000 to 2020. *Remote Sens.* **2024**, *16*, 1007. [CrossRef]
40. Asuero, A.G.; Sayago, A.; González, A. The Correlation Coefficient: An Overview. *Crit. Rev. Anal. Chem.* **2006**, *36*, 41–59. [CrossRef]
41. Huang, X.; Xu, X.; Wang, Q.; Zhang, L.; Gao, X.; Chen, L. Assessment of Agricultural Carbon Emissions and Their Spatiotemporal Changes in China, 1997–2016. *Int. J. Environ. Res. Public Health* **2019**, *16*, 3105. [CrossRef] [PubMed]
42. Yin, C. Environmental Efficiency and Its Determinants in the Development of China's Western Regions in 2000–2014. *Chin. J. Popul. Resour. Environ.* **2017**, *15*, 157–166. [CrossRef]
43. Tan, Y.; Wu, D.; Bol, R.; Wu, W.; Meng, F. Conservation Farming Practices in Winter Wheat–Summer Maize Cropping Reduce GHG Emissions and Maintain High Yields. *Agric. Ecosyst. Environ.* **2019**, *272*, 266–275. [CrossRef]
44. Cui, Y.; Khan, S.U.; Deng, Y.; Zhao, M. Regional Difference Decomposition and Its Spatiotemporal Dynamic Evolution of Chinese Agricultural Carbon Emission: Considering Carbon Sink Effect. *Environ. Sci. Pollut. Res.* **2021**, *28*, 38909–38928. [CrossRef] [PubMed]
45. Liao, Y.; Wei, Y. Rural Social Justice Construction since the 18th National Congress of the Communist Party of China. *J. Agro-For. Econ. Manag.* **2019**, *18*, 702–708. (In Chinese)
46. China's Mid-Century Long-Term Low Greenhouse Gas Emission Development Strategy. Available online: https://unfccc.int/documents/307765 (accessed on 28 October 2021).
47. Han, J.; Qu, J.; Maraseni, T.N.; Xu, L.; Zeng, J.; Li, H. A Critical Assessment of Provincial-Level Variation in Agricultural GHG Emissions in China. *J. Environ. Manag.* **2021**, *296*, 113190. [CrossRef]
48. Xue, J.-F.; Pu, C.; Liu, S.-L.; Zhao, X.; Zhang, R.; Chen, F.; Xiao, X.-P.; Zhang, H.-L. Carbon and Nitrogen Footprint of Double Rice Production in Southern China. *Ecol. Indic.* **2016**, *64*, 249–257. [CrossRef]
49. Alam, M.K.; Bell, R.W.; Biswas, W.K. Decreasing the Carbon Footprint of an Intensive Rice-Based Cropping System Using Conservation Agriculture on the Eastern Gangetic Plains. *J. Clean. Prod.* **2019**, *218*, 259–272. [CrossRef]
50. Liu, M.; Yang, L. Spatial Pattern of China's Agricultural Carbon Emission Performance. *Ecol. Indic.* **2021**, *133*, 108345. [CrossRef]
51. Wu, Q.; He, Y.; Madramootoo, C.A.; Qi, Z.; Xue, L.; Bukovsky, M.; Jiang, Q. Optimizing Strategies to Reduce the Future Carbon Footprint of Maize under Changing Climate. *Resour. Conserv. Recy.* **2023**, *188*, 106714. [CrossRef]
52. Xu, X.; Lan, Y. Spatial and Temporal Patterns of Carbon Footprints of Grain Crops in China. *J. Clean. Prod.* **2017**, *146*, 218–227. [CrossRef]
53. Chen, X.; Ma, C.; Zhou, H.; Liu, Y.; Huang, X.; Wang, M.; Cai, Y.; Su, D.; Muneer, M.A.; Guo, M. Identifying the Main Crops and Key Factors Determining the Carbon Footprint of Crop Production in China, 2001–2018. *Resour Conserv Recy.* **2021**, *172*, 105661. [CrossRef]
54. Li, Y.; Zhang, D.; Wen, Y.; Liu, X.; Zhang, Y.; Wang, G. Spatiotemporal Patterns and Driving Factors of Carbon Footprint in Coastal Saline Cropland Ecosystems: A Case Study of the Yellow River Delta, China. *Land* **2024**, *13*, 2145. [CrossRef]
55. Sun, T.; Li, H.; Wang, C.; Li, R.; Zhao, Z.; Guo, B.; Yao, L.; Gao, X. The Carbon Footprint and Influencing Factors of the Main Grain Crops in the North China Plain. *Agronom* **2024**, *14*, 1720. [CrossRef]
56. Ju, H.; Zeng, G.; Zhang, S. Inter-Provincial Flow and Influencing Factors of Agricultural Carbon Footprint in China and Its Policy Implication. *Environ. Impact Assess. Rev.* **2024**, *105*, 107419. [CrossRef]
57. Chu, Y.; Xie, L.; Yuan, Z. Composition and Spatiotemporal Distribution of the Agro-Ecosystem Carbon Footprint: A Case Study in Hebei Province, North China. *J. Clean. Prod.* **2018**, *190*, 838–846. [CrossRef]
58. Hua, L.; Gao, Y.; Li, D.; Yang, Z.; Liu, Z. Effects of Different Straw Return Methods on Farmland Carbon Footprint and Water Footprint. *Agriculture* **2025**, *15*, 73. [CrossRef]

Disclaimer/Publisher's Note: The statements, opinions and data contained in all publications are solely those of the individual author(s) and contributor(s) and not of MDPI and/or the editor(s). MDPI and/or the editor(s) disclaim responsibility for any injury to people or property resulting from any ideas, methods, instructions or products referred to in the content.

agronomy

MDPI

Article

Rethinking Efficiency: How Increased Electricity Use Can Reduce Environmental Impacts in Controlled Hemp Cultivation—A Life Cycle Assessment (LCA) Study

Adéla Kalkušová [1,*], Jaroslav Neumann [1], Nina Veselovská [1], Eliška Kůrková [1], Petr Konvalina [1], Reinhard W. Neugschwandtner [2] and Jaroslav Bernas [1,*]

[1] Department of Agroecosystems, Faculty of Agriculture and Technology, University of South Bohemia in České Budějovice, Branišovská 1645/31A, 370 05 České Budějovice, Czech Republic
[2] Institute of Agronomy, Department of Agricultural Sciences, University of Natural Resources and Life Sciences, Vienna, Konrad-Lorenz-Straße 24, 3430 Tulln, Austria
* Correspondence: kalkua01@jcu.cz (A.K.); bernas@fzt.jcu.cz (J.B.)

Abstract

This study aims to assess the environmental profile and identify environmental hotspots of indoor hemp (*Cannabis sativa* L.) cultivation through environmental impact analysis under four scenarios combining two nutrient solutions and two lighting intensities (540 W and 900 W). Indoor cultivation of industrial hemp is becoming increasingly relevant as plant production shifts to controlled environments, raising the need to evaluate its environmental implications. The assessment was conducted using the Life Cycle Assessment (LCA) methodology in accordance with the ISO 14040 and ISO 14044 standards, applying a cradle-to-gate system boundary and a functional unit of 1 kg of dried hemp inflorescence. Primary data were obtained from a controlled cultivation experiment, while secondary data were drawn from validated databases. The carbon footprint ranged from 1050 to 1610 kg CO_2 eq per kilogram of dried inflorescence. Scenarios with 900 W lighting showed 30–35% lower impacts per kilogram compared to 540 W variants. Electricity production and consumption were identified as major environmental hotspots, dominating most impact categories. The study concludes that improving input–output efficiency is essential for sustainable indoor cultivation and that integrating renewable energy sources, such as photovoltaics or biomass, could further reduce environmental impacts.

Keywords: climate change; hemp inflorescence; hydroponics; indoor agriculture; LCA

1. Introduction

Hemp (*Cannabis sativa* L.) is a versatile plant whose applications are rapidly expanding across various industrial sectors, from construction [1] and textiles to food production, medicine, and biotechnology [2–4]. Thanks to its unique properties, the area designated for hemp fiber cultivation in the EU increased by 60% between 2015 and 2022 [5]. Several countries, including Germany, Canada, Malta, and Thailand, have moved to legalize non-medical cannabis use [6]. As more countries adopt similar policies, global cannabis production is likely to increase in the coming years. Hemp is gaining increasing attention not only as a traditional raw material but also as a key component of sustainable innovations, such as bioplastics [7], soil remediation [8], and renewable energy sources [9]. Industrial hemp is capable of absorbing heavy metals (e.g., Cd, Cr, Cu, Ni, Pb, and Zn) and radionuclides, while also reducing the content of polycyclic aromatic hydrocarbons

and cesium in contaminated soils [8]. These elements are absorbed by the plant's roots, which is beneficial for environmental remediation but can lead to their accumulation within the plant itself [10,11]. Therefore, hemp intended for medical purposes, such as the production of cannabidiol oils, tinctures, and food products, is typically grown using indoor systems [12].

Although industrial hemp is traditionally grown in Europe as a field crop primarily for fiber production [13], there are other production possibilities and alternative cultivation methods, particularly in controlled environments. Controlled environment cultivation provides stable and reproducible growth conditions. Indoor systems offer distinct advantages, including strict control of environmental variables, which minimizes the risk of contamination by undesirable substances and ensures consistent, high-quality production outputs [14]. Controlled environments in indoor plant-production systems, e.g., greenhouses, high tunnels, buildings, or container units with artificial lighting [15], allow precise manipulation of growth parameters, thereby facilitating optimization and improvements in productivity [16,17]. Vertical indoor farming systems have demonstrated potential to improve nutritional value and significantly reduce water consumption in agricultural production [18]. High light intensities with a high photosynthetic photon flux density in indoor settings can significantly increase cannabis yield. For instance, higher PPFD levels can result in 1.6 times increase in inflorescence dried weight, which is economically beneficial [19]. Indoor cultivation ensures a consistent quality of hemp products by maintaining stable growing conditions. This consistency is crucial for industries that rely on specific hemp qualities, such as the pharmaceutical and nutraceutical sectors [19,20]. However, these technological advantages come at the cost of substantially higher energy and material inputs, raising critical questions about the environmental sustainability of indoor cultivation systems.

While hemp is frequently presented as an environmentally friendly crop [21], the extent of its sustainability depends strongly on management practices. Irrigation and fertilization are essential for growth but can lead to environmental impacts when applied intensively or inefficiently [22,23]. Given the rapidly increasing scale of hemp production, it is essential to thoroughly analyze the environmental aspects of hemp cultivation to optimize indoor methods, ensure their long-term sustainability, and identify the most environmentally impactful stages of the cultivation cycle.

Indoor plant production facilities require considerable energy inputs. Some of the major inputs are high-intensity lighting for plant growth, dehuminification processes to prevent mold, and heating and cooling of the facility [24,25]. Light levels reach 500 times higher than those suitable for reading, ventilation rates are 6 times higher than in advanced laboratories, and power density can climb to 2000 W/m^2, comparable to contemporary data centers [26]. Additional energy is used for CO_2 generation [27], typically elevated to 4 times natural levels to boost growth efficiency, as well as for ventilation and waste heat removal. In the context of climate change mitigation and energy transition policies, such high energy intensity poses a significant challenge to the environmental viability of indoor agriculture. While these measures shorten growth cycles, they may also reduce overall energy intensity [26]. The primary challenges in achieving sustainability in indoor cultivation systems primarily involve high energy demands, significant capital costs, and the limited variety of crops suitable for cultivation [28].

Only two studies have investigated the carbon footprint of indoor cannabis production [26,27]. Some studies indicate that growing cannabis in controlled environments can have a higher carbon footprint than certain industrial sectors. Other studies have examined water consumption, particularly in regions where cannabis is cultivated outdoors or in

greenhouse systems, identifying high irrigation demands that may lead to local water scarcity issues [29].

However, this study is unique in that it evaluates four different cultivation systems based on variations in fertilizer concentration and light intensity in relation to yield across defined groups.

2. Materials and Methods

2.1. Goal and Scope Definition

This study evaluates the environmental impacts of different cultivation practices associated with the production of industrial hemp in indoor systems. The primary objective was to quantify environmental profiles using the Life Cycle Assessment (LCA) method and to assess them across selected impact categories, as well as through the analysis of material and energy flows throughout the entire life cycle of the defined indoor system.

Furthermore, the study aims to determine specific combinations of light intensity and nutrient input under which the environmental impacts per kilogram of dried hemp inflorescence are minimized and to quantify the extent of these reductions. The analysis examines whether increasing lighting power within the studied range raises yield enough to reduce the per kilogram environmental impact. The study also focuses on identifying the main environmental hotspots within the cultivation cycle and on assessing how input–output relationships influence the overall performance of the system.

It is hypothesized that higher (900 W) lighting intensity, when accompanied by a proportionally increased biomass yield, enhances input-use efficiency and consequently reduces environmental impacts per functional unit. Conversely, excessive nutrient application without adequate light supplementation may lead to an overall increase in environmental impacts. LCA is a standardized analytical tool used for evaluating the environmental aspects of a product, process, or service across its entire life cycle. It is structured in accordance with the international standards ISO 14040 and ISO 14044 [30,31], which provide the framework and requirements for conducting consistent and transparent analyses. The impact assessment was conducted using the ReCiPe 2016 Midpoint (H) method, V1.09, implemented in SimaPro Craft Analyst 10.2.0.0 (PRé Sustainability B.V., Amersfoort, The Netherlands) software. The Cut-off System Model was applied, in which the full environmental impact is attributed to the primary process entering the system, while secondary materials and by-products leave the system without carrying any additional environmental impacts [32]. The functional unit (FU) was defined as 1 kg of dried hemp inflorescence, representing the target output of the cultivation system.

Since primary data were available, the system boundaries were defined to include only the cultivation phase and post-harvest handling of the biomass, excluding any other post-harvest processes such as emissions from processing, recycling, packaging, and waste management. The environmental assessment considered impacts associated with water use, energy production and consumption, fertilizer production and application, material production and use, transportation of inputs to the cultivation facility, and hemp plant growth management.

All relevant inputs, ranging from the preparation of the cultivation setup to harvest and post-harvest handling of the biomass, were inventoried in detail. The system boundaries included unit processes, which are the smallest components of the production system for which specific data were collected. Economy allocation principles were applied in this study. The scope was limited to the defined experimental setup and did not consider the market value of co-products, because, in the case of the plant's green biomass (excluding inflorescence), composting was assumed without economic valorization. Therefore, accord-

ing to the economy allocation principles, the full environmental impact is connected with production of inflorescence only.

Propagation by cuttings was not included in the assessment, as all treatments were based on clones cultivated under identical conditions. This approach allowed for a consistent and reliable comparison of different cultivation scenarios, eliminating variability from the early growth phase.

The findings of this study contribute to the development of more environmentally responsible cultivation systems and offer practical insights for stakeholders engaged in indoor growing technologies. By promoting resource efficiency and reducing emissions, the study supports the transition toward more sustainable agricultural practices in indoor hemp production. The results also offer a clear perspective on the environmental profile of indoor cultivation, which is expected to become increasingly relevant due to factors such as population growth, climate change, and resource scarcity. New and existing indoor growers may use these results as guidance when evaluating sustainable cultivation investments. The system boundaries are illustrated in Figure 1.

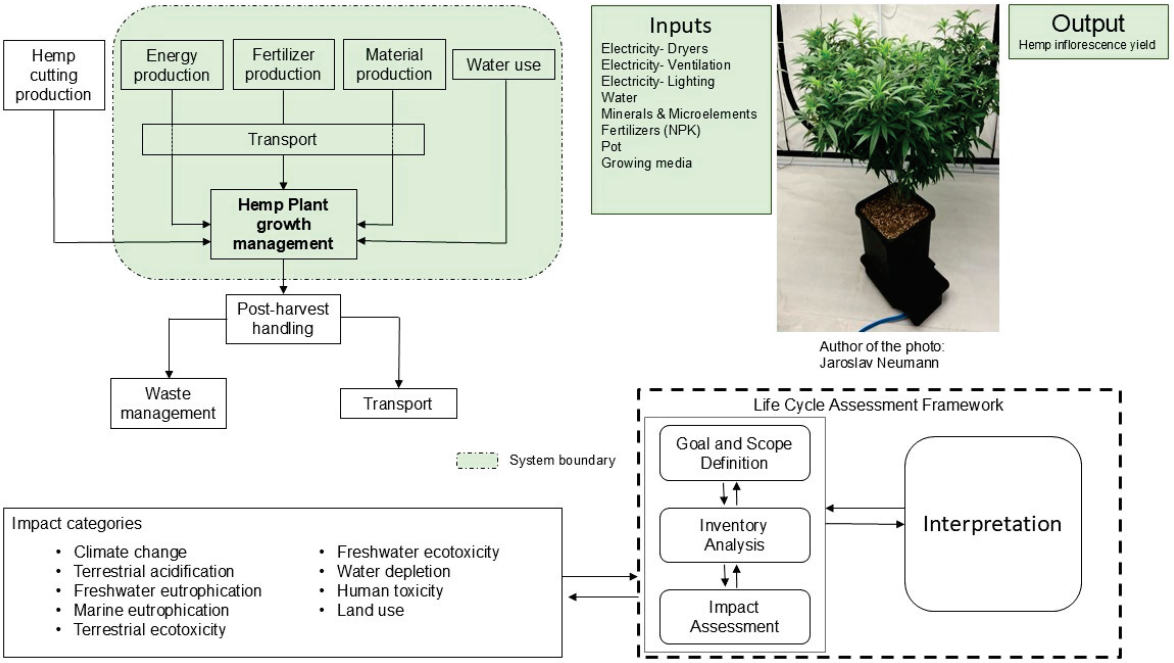


Figure 1. System boundaries.

2.2. Primary Data Collection (Hemp Cultivation)

This study assesses the environmental impacts associated with the indoor cultivation of industrial hemp using life cycle assessment (LCA), based on empirical data and the cultivation methodology described in [33]. Rather than cultivating hemp specifically for this research, data were obtained from controlled experimental setups designed to ensure methodological consistency and adherence to scientific standards. The cultivation process, including fertilization, lighting, and nutrient management, was thoroughly described in the previous study. This allowed the current LCA study to build on a validated and standardized cultivation framework.

The experiment was conducted in 2022 and lasted a total of 12 weeks. Plants were grown individually in 11-L plastic pots filled with a coconut fiber and perlite mix (60:40). The cultivation experiment was conducted in two independent runs on separate dates under identical controlled environmental conditions. Four treatment groups were established, combining two light intensities and two nutrient solutions, each consisting of eight plants per run. The experimental unit for yield was defined as the treatment group per run (batch

of eight plants). To address how between-run variability enters uncertainty, we quantified relative yield differences between the two runs and verified that these variations did not alter the relative ranking of scenarios. Therefore, averaged yield values were used for all subsequent LCA calculations. The recorded yield parameters serve as a fundamental basis for further analysis and discussion, particularly in the context of assessing the environmental footprint of indoor hemp cultivation under controlled conditions. An overview of all input data and average yields per treatment group is provided in Table 1.

Table 1. Inventory table: inputs and outputs of life cycle (for 1 kg of dried hemp inflorescence).

	Unit	**S1-L1**	**S1-L2**	**S2-L1**	**S2-L2**
Output					
Yield (⌀)	g	365	609	344	590
Input from Technosphere					
Tap water	l	156	156	156	156
Stone wool	g	20	20	20	20
Coconut fiber	kg	19	19	19	19
Perlite	kg	3.53	3.53	3.53	3.53
Flowerpot–1 year amortization	p	1	1	1	1
Inorganic nitrogen fertilizer as NO_3	g	16.1	16.1	16.1	16.1
Inorganic nitrogen fertilizer as NH_4	g	0.86	0.86	0.86	0.86
Inorganic phosphorus fertilizer as P_2O_5	g	4.36	4.36	34.7	34.7
Inorganic potassium fertilizer as K_2O	g	16.5	16.5	36	36
Calcium carbonate ($CaCO_3$)	g	39.4	39.4	37	37
Magnesium oxide (MgO)	g	6.5	6.5	12.6	12.6
Sulphite	g	5.01	5.01	27.2	27.2
Microelements (Fe, B, Cu, Zn, Mn, Mo)	g	0.58	0.58	0.51	0.51
Electricity production (Regional mix)–Lighting	kWh	272	419	272	419
Electricity production (Regional mix)–Fan, ventilation	kWh	158	158	158	158
Electricity production (Regional mix)–Dryers	kWh	515	515	515	515

S1-L1: solution 1, lighting 1, S1-L2: solution 1, lighting 2, S2-L1: solution 2, lighting 1, S2-L2: solution 2, lighting 2, between-run yield differences ranged from 3% to 54%.

The processes incorporated into the model system included tap water consumption for irrigation systems and dilution of plant protection products, as well as processes involving the production, use, and consumption of plastic containers/seed trays. Additionally, the model accounted for the production and use of the growing medium (coconut fiber and perlite), nutrient inputs including their production, distribution, and application, and electricity consumption for lighting, climate control, and drying.

After harvest, inflorescences were manually separated from stems and leaves. The separated flowers were then dried for ten days at a constant temperature of 20 °C and relative humidity of 50%. Waste biomass was considered composting material with negligible economic value. Therefore, no allocation was applied, as environmental impacts were attributed solely to the economically valuable product, the dried inflorescences. This assumption corresponds to the operational reality of the cultivation system, where inflorescence represents the only marketable output.

The nutrient solutions used in this study were divided into S1 (solution 1) and S2 (solution 2) formulations, with S2 further separated for the vegetative and flowering phases. The S1 solution contained moderate concentrations of nutrients, while S2 was designed with a higher phosphorus concentration and a specific potassium-to-calcium-to-magnesium ratio (1:2:4) to optimize plant growth. During the vegetative phase, S2 contained increased levels of nitrate nitrogen (NO_3), phosphorus (P_2O_5), and potassium (K_2O) to promote early plant development. In contrast, the flowering phase formulation of S2 had a significantly

higher phosphorus and sulphate (SO_4) concentration, supporting flower production and overall biomass yield. These adjustments ensured that nutrient availability was tailored to the specific needs of the plants at different growth stages.

The plants were exposed to two different lighting intensities (L1 = lighting 1, L2 = lighting 2) throughout their growth cycle, with separate settings for the vegetative phase, which lasted four weeks, and the flowering phase, which lasted eight weeks. For the vegetative phase, the photoperiod was set to 18 h for both lighting intensities; for the flowering phase, it was set to 12 h for both. The lighting configuration was specified to deliver an appropriate energy input for each developmental stage.

During the vegetative phase, the lighting system operated at:

- 360 W (≈300 μmol m^{-2} s^{-1} PPFD) under the first intensity setting (L1)
- 540 W (≈500 μmol m^{-2} s^{-1} PPFD) under the second, higher intensity setting (L2)

As the plants transitioned into the flowering phase, light intensity was significantly increased to support inflorescence development:

- 540 W (≈900 μmol m^{-2} s^{-1} PPFD) under the lower intensity setting (L1)
- 900 W (≈1300 μmol m^{-2} s^{-1} PPFD) under the higher intensity setting (L2)

The efficacy of the LED grow light used in this study is 2.8 μmol·J-1. The four cultivation groups were defined based on combinations of two lighting intensities and two nutrient solution regimes:

- S1-L1
- S1-L2
- S2-L1
- S2-L2

These data were used to determine the material, energy, and system requirements of each group. The collected information included input and output data related to individual cultivation treatments, as well as technosphere inputs (Table 1).

The quality of primary data used in the inventory phase was assessed in terms of temporal, geographical, and technological representativeness, as well as completeness and reliability, following ILCD guidelines [34]. The collected data were based on direct measurements from experimental cultivation (2022), corresponding to the Czech context and the specific crop system studied.

2.3. Secondary Data

Data were sourced from the following life-cycle inventory (LCI) databases: AGRIBALYSE® [35], the French national LCI database providing harmonized inventories and impacts for agricultural and food products; Agri-footprint 6.0 [36], a process-based LCI database covering global agri-food supply chains (crops, fertilizers, feed, processing); Ecoinvent 3.9 [37], a comprehensive multi-sector LCI database with geographically explicit datasets for energy, materials, transport, and waste; and WFLDB [38] (World Food LCA Database), a curated set of food- and agriculture-focused LCI datasets aligned with best-practice modeling for comparability. All inventoried data are part of the Life Cycle Inventory.

To ensure more precise and representative results, a specific energy mix for the Czech Republic in 2022 was modelled, incorporating all relevant energy sources available during the year in which the experiment was conducted. This energy mix was based on data from [39,40], ensuring alignment with the actual energy composition and providing a more accurate assessment of the environmental impacts associated with electricity consumption in the study.

2.4. Impact Categories and Impact Assessment Method

The selection of impact categories is based on the recommendations by Dijkman et al. [41], who identified suitable categories for the assessment of agricultural systems. Impact categories were chosen to reflect dominant pressure pathways in indoor hemp cultivation and to enable comparability with agricultural LCA practice. Following their approach, the following midpoint impact categories were included climate change, terrestrial acidification, freshwater eutrophication, marine eutrophication, terrestrial ecotoxicity, freshwater ecotoxicity, water depletion and human toxicity. In addition to the suggested categories, land use was also included due to its relevance for crop-based systems.

To enhance the interpretability of the results, the impact categories human carcinogenic toxicity and human non-carcinogenic toxicity, both quantified using the same reference unit (kg 1.4-DCB), were consolidated into a single category of human toxicity. This methodological decision is supported not only by the shared reference substance but also by the partially overlapping exposure routes and associated health effects.

3. Results

3.1. Environmental Impact per Cultivation Scenario

The environmental impact per 1 kg of dried hemp inflorescence was quantified. Table 2 (Table A1) presents the results of the total environmental impact per impact category, calculated based on the defined FU. The average yields of dried hemp inflorescence varied considerably across the cultivation scenarios: S1-L1 yielded 365 g, S1-L2 only 609 g, S2-L1 reached 344 g, and S2-L2 produced 590 g. Since the environmental impacts were calculated per kilogram of output, these yield differences are critical, as they directly influence the amount of input materials required to reach the defined FU. For example, under identical operating conditions and holding all other inputs constant, doubling the yield results in an approximately 50% reduction in per kilogram environmental impact across all scenarios.

Table 2. Environmental impact per functional unit (1 kg of dried hemp inflorescence).

Impact Category	Unit	S1-L1	S1-L2	S2-L1	S2-L2
CCH	kg CO_2 eq	1.52×10^3	1.05×10^3	1.61×10^3	1.08×10^3
TA	kg SO_2 eq	4.31×10^0	2.97×10^0	4.58×10^0	3.07×10^0
FE	kg P eq	2.40×10^0	1.66×10^0	2.54×10^0	1.71×10^0
ME	kg N eq	1.59×10^{-1}	1.10×10^{-1}	1.68×10^{-1}	1.13×10^{-1}
TE	kg 1.4-DCB	2.70×10^3	1.86×10^3	2.87×10^3	1.92×10^3
FX	kg 1.4-DCB	6.58×10^1	4.55×10^1	6.98×10^1	4.70×10^1
WD	m^3	6.78×10^0	4.64×10^0	7.21×10^0	4.79×10^0
HT	kg 1.4-DCB	2.72×10^3	1.88×10^3	2.89×10^3	1.94×10^3
LD	m^2a crop eq	3.97×10^1	2.74×10^1	4.22×10^1	2.83×10^1

S1-L1: solution 1, lighting 1, S1-L2: solution 1, lighting 2, S2-L1: solution 2, lighting 1, S2-L2: solution 2, lighting 2, CCH: Climate change, TA: Terrestrial acidification, FE: Freshwater eutrophication, ME: Marine eutrophication, TE: Terrestrial ecotoxicity, FX: Freshwater ecotoxicity, WD: Water depletion, HT: Human toxicity, LD: Land use. SimaPro Craft Analyst 10.2.0.0 software; ReCiPe 2016 Midpoint (H) V1.09/World (2010) H; Cut-off System Model approach; Characterization model.

Among all scenarios, S2-L1, which combines a higher nutrient input (S2) with standard lighting intensity (L1), consistently showed the highest environmental impact in most assessed impact categories. For instance, the climate change (CCH) impact reached 1610 kg CO_2 eq, which is 7% higher than in S1-L1 and more than 53% higher than in the lowest-emitting scenario, S1-L2. Similarly, human toxicity (HT) in S2-L1 was the highest at 2890 kg 1.4-DCB, which represents a 54% increase compared to S1-L2. The same trend was observed

in terrestrial ecotoxicity (TE–2870 kg 1.4-DCB) and land use (LD–42.18 m^2 crop eq), where S2-L1 also showed the highest values.

In contrast, S1-L2, which combines a lower nutrient input (S1) with higher lighting intensity (L2), showed the lowest values across nearly all categories. Compared to S2-L1, freshwater ecotoxicity (FX) was reduced by 35%, climate change impact by 35%, and water depletion (WD) by 36%. Its impact on marine eutrophication (ME) reached only 0.11 kg N eq, the lowest value among all tested setups.

The remaining two scenarios, S1-L1 and S2-L2, showed intermediate results, falling between the two extremes. S1-L1 exhibited lower environmental impacts than any scenario with higher nutrient input but had still higher impacts than S1-L2. For example, its water depletion was 6.78 m^3, which is 46% more than in the most efficient scenario, S1-L2. On the other hand, S2-L2, despite the higher lighting intensity, still showed significantly higher values. For instance, human toxicity reached 1940 kg 1.4-DCB, over 40% more than in S1-L2. This suggests that nutrient input has a more substantial influence on overall environmental impact than lighting intensity alone.

In general, the data highlighted the importance of input management in minimizing environmental impacts in hemp production systems. The values should be interpreted as indicative trends rather than absolute numerical constants [42]. Therefore, a stronger focus should be placed on the relative comparison between scenarios rather than on the absolute values. In this context, the results serve as a tool to identify cultivation strategies with higher or lower environmental impacts.

3.2. Contribution Analysis

3.2.1. Full System Aggregated Input Analysis

A contribution analysis was conducted for four indoor hemp cultivation treatments using the characterization model (Figure 2; Table A2). To improve comprehensibility and simplify interpretation of system inputs in the figure, detailed background flows were aggregated into broader, functionally relevant categories for graphical representation.

Electricity consumption, particularly from fossil-based sources, was identified as the dominant contributor across nearly all impact categories. Emissions from lignite mining and combustion played a critical role in the overall environmental impact, contributing significantly to greenhouse gases, sulphur oxides (SO_x), nitrogen oxides (NO_x), particulate matter, and heavy metals [35]. These emissions influenced multiple categories, including climate change, terrestrial acidification, both freshwater and marine eutrophication, and mainly human toxicity.

The highest climate change impacts were observed in scenario S2-L1, where electricity use constituted a major share of the carbon footprint. Specifically, lighting accounted for 460 kg CO_2 eq, ventilation for 270 kg CO_2 eq, and drying systems for as much as 870 kg CO_2 eq per kilogram of dried hemp inflorescence. Altogether, electricity-related emissions in S2-L1 were approximately 54% higher than in the lowest impact scenario, S1-L2, as high-lighting intensity scenarios (L2) showed lower environmental impacts per FU due to their substantially higher yields of hemp inflorescence.

In the categories of terrestrial acidification and eutrophication, emissions from lignite combustion and energy production residues (e.g., overburden, ash) played a key role. These by-products often contain nitrogen and phosphorus compounds that may leach into the environment, with pronounced effects in high-fertilization scenarios (S2).

Terrestrial and freshwater ecotoxicity were heavily influenced by the infrastructure of regional electricity mix, including the use of enriched uranium, natural gas, and photovoltaic components, as well as residues from coal extraction and combustion. The highest

impact within these categories was observed in treatment S2-L1, where electricity consumption by dryers emerged as the primary contributor.

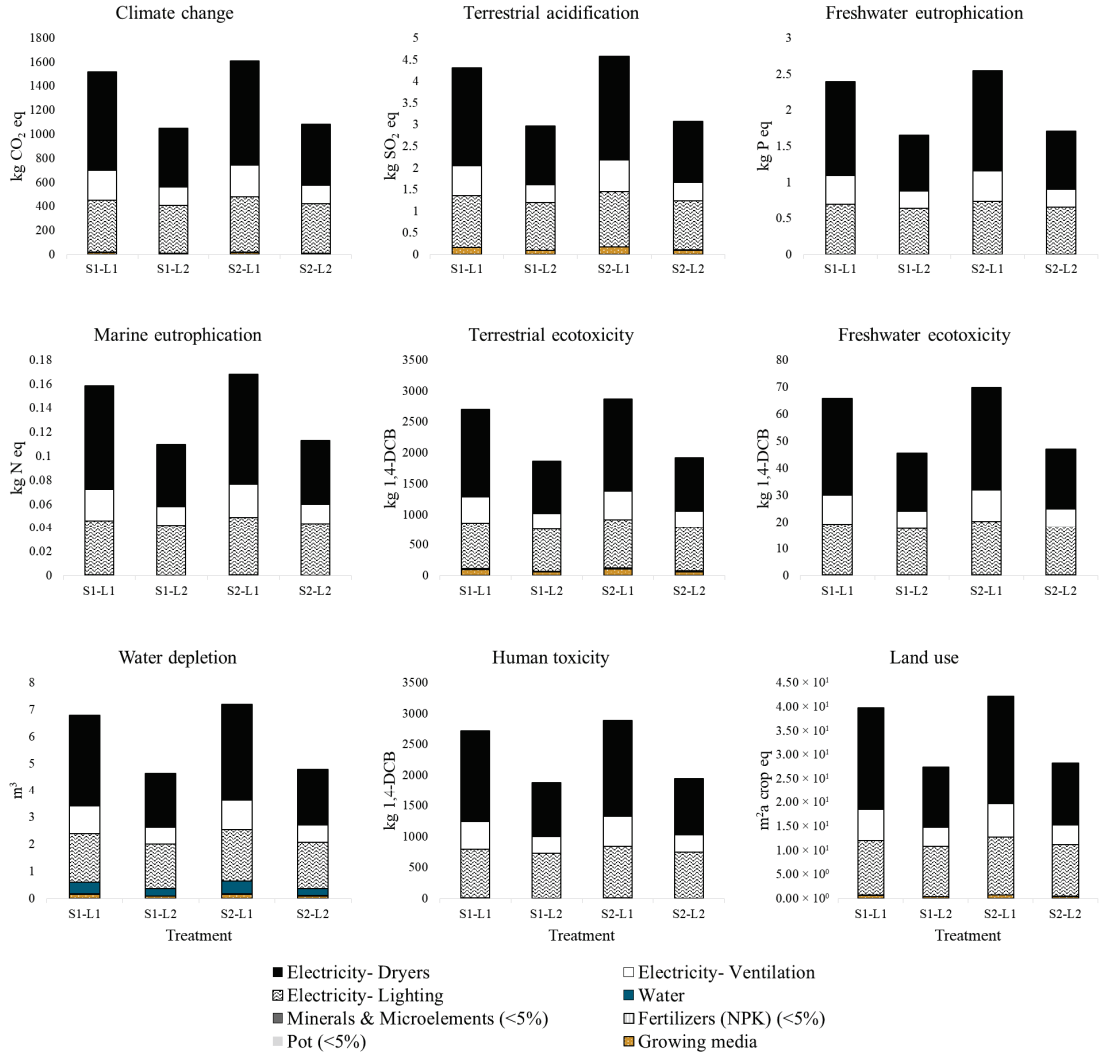


Figure 2. Contribution analyses: Environmental load per 1 kg of dried inflorescence, S1-L1: solution 1, lighting 1, S1-L2: solution 1, lighting 2, S2-L1: solution 2, lighting 1, S2-L2: solution 2, lighting 2, Climate change (kg CO_2 eq), Terrestrial acidification (kg SO_2 eq), Freshwater eutrophication (kg P eq), Marine eutrophication (kg N eq), Terrestrial ecotoxicity (kg 1.4-DCB), Freshwater ecotoxicity (kg 1.4-DCB), Water depletion (m^3), Human toxicity (kg 1.4-DCB), Land use (m^2a crop eq), Fertilizers (NPK): including NO_3^-, NH_4^+, P_2O_5, and K_2O fertilizers, Minerals & Microelements: including calcium carbonate, magnesium oxide, sulphite, and microelements (Fe, B, Cu, Zn, Mn, Mo), Growing media: including stone wool, coconut fiber, and perlite. Inputs contributing less than 5% in all categories are marked as '<5%'. SimaPro Craft Analyst 10.2.0.0 software; ReCiPe 2016 Midpoint (H) V1.09/World (2010) H; Cut-off System Model approach; Characterization model.

The highest levels of environmental impact in the category human toxicity were also recorded in scenario S2-L1, largely due to emissions associated with fossil-based electricity, steel production, and related industrial processes.

Likewise, scenario S2-L1 showed the highest water consumption, 7.24 m^3 per kilogram of dried biomass, with 50% of which was used for drying. Compared to S1-L2 (4.58 m^3), this represents an increase of more than 58%.

Land use was primarily driven by electricity generation from biomass, lignite, and wood residues. Across all impact categories, electricity consistently emerged as the main contributor, accounting for over 98% of the total impact in both S1-L1 and S2-L1 scenarios.

Fertilizer inputs had a secondary effect through indirect eutrophication and acidification. In scenarios with lower light intensity (L1), the influence of growing media also became more pronounced, particularly due to their relatively higher share in the total impact.

3.2.2. Fertilizer-Focused Contribution Analysis

To enhance the clarity and visibility of the results, environmental impacts were displayed as the contributions of individual mineral fertilizers (Figure 3; Table A3). Although the broader system analysis must account for the influence of electricity consumption, this section focuses exclusively on the environmental impact associated with fertilizer application. Given the varying biomass yields across scenarios, these differences were considered, enabling a realistic evaluation of the efficiency and environmental impact of different fertilization strategies.

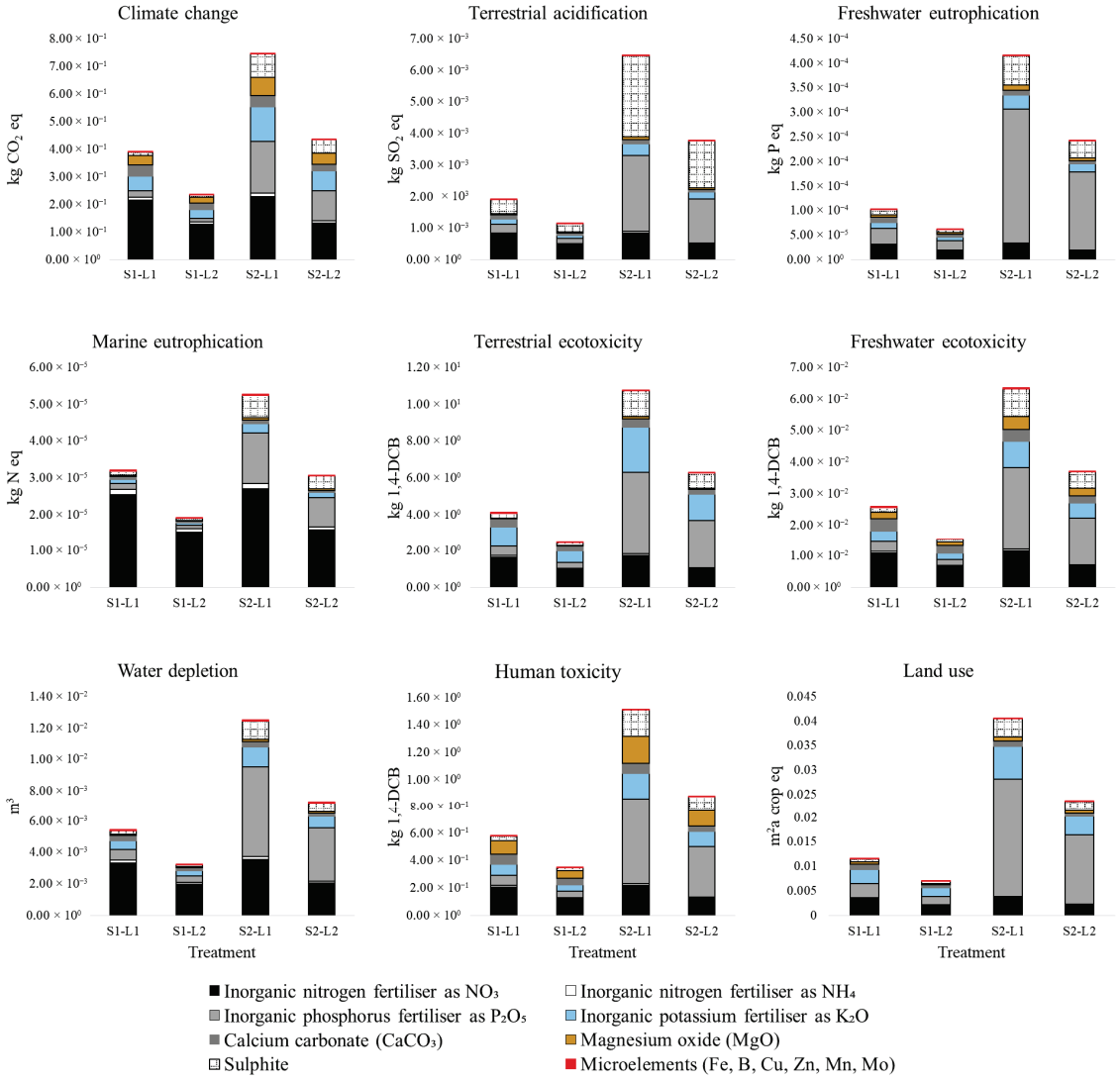


Figure 3. Contribution analyses: Environmental load of nutrients per 1 kg of dried inflorescence, S1-L1: solution 1, lighting 1, S1-L2: solution 1, lighting 2, S2-L1: solution 2, lighting 1, S2-L2: solution 2, lighting 2, Climate change (kg CO_2 eq), Terrestrial acidification (kg SO_2 eq), Freshwater eutrophication (kg P eq), Marine eutrophication (kg N eq), Terrestrial ecotoxicity (kg 1.4-DCB), Freshwater ecotoxicity (kg 1.4-DCB), Water depletion (m^3), Human toxicity (kg 1.4-DCB), Land use (m^2a crop eq), SimaPro Craft Analyst 10.2.0.0 software; ReCiPe 2016 Midpoint (H) V1.09/World (2010) H; Cut-off System Model approach; Characterization model.

The results showed that scenarios with higher fertilization intensity (S2) exhibited substantially higher environmental impacts on average by 88% in most categories compared to lower-dose variants (S1). Across scenarios, the fertilizer-only climate change impact per FU lies in the range 0.235–0.746 kg CO_2 eq. The S2-L1 variant with high fertilization under low lighting intensity, consistently showed the highest environmental impact among the tested scenarios. This suggests that simply increasing fertilizer input, without optimizing other parameters, amplifies environmental pressure per unit of product.

In the climate change category, ammonium nitrate (NH_4NO_3) was identified as the dominant emission source, due to the energy-intensive production processes of nitric acid (HNO_3) and anhydrous ammonia NH_3. This input significantly contributed to climate change category across all scenarios, particularly in S2-L1. Each additional 1 g of mineral N, applied as NO_3^- or NH_4^+, increases the climate change impact by 4.8 g CO_2 eq, whereas 1 g of P, applied as P_2O_5, adds 1.84 g CO_2 eq.

Terrestrial acidification was mainly influenced by nitric acid production, which is part of ammonium nitrate synthesis. In addition, sulphite production associated with sulphur dioxide emissions from industrial processes also contributed to acidification potential. The highest overall impact was observed in the S2-L1 treatment, where sulphite accounted for up to 39.6% of the total acidification impact, highlighting its considerable contribution under high-fertilization scenarios.

In both freshwater and marine eutrophication, the highest impacts were again observed in high-fertilization scenarios. For freshwater eutrophication, the combined effects of nitrogen and phosphorus inputs were evident, particularly from ammonium nitrate and single superphosphate. In marine systems, nitrogen-based fertilization, especially ammonium nitrate, was the key contributor. The S2-L1 treatment consistently showed the highest environmental impacts in both eutrophication categories. Each gram of mineral nitrogen applied to the system, as NO_3^- or NH_4^+, contributes 0.22 mg N eq to marine eutrophication and each gram of phosphorus applied, as P_2O_5, contributes 2.76 mg P eq to freshwater eutrophication.

Terrestrial ecotoxicity was primarily driven by nitrogen and potassium-based mineral fertilizers. Potassium chloride production, which involves potash mining, transport, steam use, and salt tailings, played a significant role in increasing environmental pressure. In freshwater ecotoxicity, the impact of calcium carbonate and phosphorus fertilizers was reflected in the results, due to emissions from their respective industrial production processes. The highest environmental impact in both categories was observed in the S2-L1 treatment, while the lowest values were recorded in the S1-L2 scenario, highlighting the importance of input optimization.

Human toxicity followed similar patterns to ecotoxicity. Nitrogen fertilizers, especially ammonium nitrate, were dominant contributors, with additional contributions from micronutrients and by-products from other fertilizer manufacturing processes. Notably, magnesium oxide also contributed to this category, accounting for up to 16.3% of the total impact in treatment S1-L1.

A particularly specific result was observed in the land use category, assessed under S1 and S2 scenarios. The highest land occupation was found in S2-L1, with the main contribution stemming from organic nitrogen fertilizer. Once again, this is due to the complex and resource-intensive production of ammonium nitrate including nitric acid, chemical facilities, and electricity use. Significant contributions also came from phosphate fertilizers through phosphate rock beneficiation and chemical conversion, potassium chloride due to energy and transport demands associated with potash mining, and magnesium oxide production due to reliance on industrial heat.

3.3. Normalization

The normalized environmental impact model calculated per FU (Figure 4; Table A4) revealed that the most affected categories were human toxicity (HT), freshwater eutrophication (FE), and freshwater ecotoxicity (FX). These categories showed the highest impact values across all scenarios, with the highest impacts found in S2-L1 and S2-L2, indicating a strong influence of fertilizer application and related field emissions. These results highlighted that nutrient inputs remain a critical factor shaping the environmental profile of indoor cultivation systems.

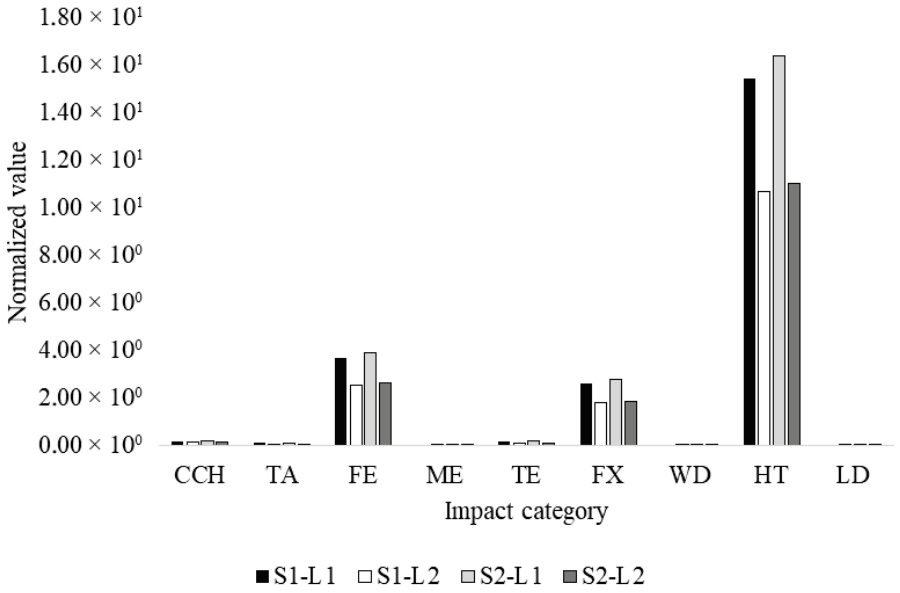


Figure 4. Normalization, S1-L1: solution 1, lighting 1, S1-L2: solution 1, lighting 2, S2-L1: solution 2, lighting 1, S2-L2: solution 2, lighting 2, CCH: Climate change, TA: Terrestrial acidification, FE: Freshwater eutrophication, ME: Marine eutrophication, TE: Terrestrial ecotoxicity, FX: Freshwater ecotoxicity, WD: Water depletion, HT: Human toxicity, LD: Land use, results are expressed as normalized values, SimaPro Craft Analyst 10.2.0.0 software; ReCiPe 2016 Midpoint (H) V1.09/World (2010) method; Normalization model.

In contrast, the least affected impact categories included water depletion, land use, and marine eutrophication. The impact values in these categories were consistently low compared to others, suggesting that indoor growing systems have relatively minor effects in these areas, likely due to closed-loop water use, spatial efficiency, and the limited interaction with marine ecosystems.

3.4. Sensitivity Analysis

The sensitivity analysis was conducted (Table A5) in accordance with the requirements of ISO 14044 [31], to verify the robustness of the results with respect to variations in the electricity mix. For all four cultivation scenarios, three alternative compositions of the Czech electricity mix were modeled. The first variant assumed a 25% increase in lignite share at the expense of nuclear energy, to evaluate the effect of a more fossil-intensive system. The second variant, reflecting a 25% increase in nuclear energy, corresponds to the current Czech energy mix [40], where the contribution of nuclear power has significantly increased. The third variant incorporated a 25% increase in renewable energy sources (hydropower, pumped storage, biomass, biogas, wind, solar, and geothermal), offset by a reduction in lignite, reflecting the decarbonization trend.

The results showed that increasing the share of lignite led to an average rise in total environmental impact by more than 100%, whereas scenarios with a higher share of nuclear

or renewable energy reduced impacts by approximately 20–30%. However, the results clearly demonstrate that the overall environmental performance of indoor cultivation systems is highly sensitive to the composition of the electricity mix. Shifting toward a more carbon-intensive mix substantially amplifies total impacts, whereas increasing the share of low-carbon or renewable sources markedly improves the sustainability profile of all scenarios.

4. Discussion

An LCA approach was adopted to evaluate the environmental impacts of indoor hemp cultivation under varying light and fertilization conditions. As a well-established and widely used environmental management tool, LCA enables a comprehensive evaluation of inputs and outputs across the entire production system [43].

4.1. Selection of the Functional Unit and Allocation Approach

In this study, the FU was defined as 1 kg of dried hemp inflorescence, in line with common practice in agricultural LCA [44]. This value was selected based on experimentally observed yields ranging from 344 g to 609 g per plant, with 1 kg representing a realistic and comparable amount of production. The choice of the FU has a significant impact on the interpretation of LCA results, especially when comparing agricultural systems. Using different FUs (e.g., mass-based, area-based, or nutritional) can lead to different rankings of environmental performance [45].

Economy allocation was applied in this study. The FU included only the market value of dried inflorescence, and no market value of co-products (e.g., seeds or stalks) were considered within the system boundaries. Some other studies focused on hemp cultivation applied, for example, mass allocation to divide the impacts between hemp seed oil (20%) and flour (80%) [46], but those co-products can be characterized by market value. In this study, an economy allocation was applied, as the dried inflorescence represented the only economically valuable output of the system, while the remaining biomass was treated as residual material without market value. The approach of allocation is based on the ISO 14044 [31]. Further, the weight ratio of the stems versus inflorescence was not carried out as this was not relevant for the experiment reproducibility, since the reproducibility of yield-related parameters in Cannabis sativa experiments is limited due to a wider range of cultivation practices in the industry. For example, the research of Reichel et al. [47] showed that stem diameter is strain (cultivar) dependent.

4.2. Comparison with Previous Studies on the Environmental Impacts of Indoor Hemp Cultivation

Direct comparisons are limited due to methodological inconsistencies across agricultural LCA studies, including differences in data quality, regional context, and interpretation. Presenting results as trends remains a valid and communicative approach [22]. A consistent finding, also observed in our study, is the dominant impact of electricity use.

A previous study found that greenhouse gas (GHG) emissions from indoor cannabis cultivation, accounting for modeled natural gas use, electricity use with geographically resolved grid emissions, and upstream/downstream processes, range from 2283 to 5184 kg CO_2 eq per kg of dried cannabis flower [27]. By contrast, this study restricts the system boundary to electricity-only (lighting, ventilation, drying) and applies the 2022 Czech grid emission factor. Under these conditions, GHG emissions range from 1040 to 1600 kg CO_2 eq per kg of dried cannabis flower, with electricity contributing 98.8–99.0% of the total climate change impact across all treatments.

Another study reports an approximate 4600 kg CO_2 per kg of dried indoor cannabis based on a model that converts operational energy for cultivation (light-

ing/HVAC/dehumidification, ventilation, pumps) and transportation into CO_2 emissions using building end-use modeling and market/manufacturer data [26]. Because prior work reports CO_2 and uses non-comparable system boundaries, we avoid a like-for-like quantitative comparison. Even so, it is reasonable to assume that electricity consumption and, where relevant, natural gas use are among the dominant contributors to total environmental impacts.

4.3. Strategies for Sustainable Indoor Cultivation of Hemp

Accurately quantifying energy use across all operational stages is crucial for reliable estimations of environmental impacts [48]. Methods such as Life Cycle Energy Assessment and Life Cycle Carbon Emissions Assessment enable a more precise identification of emission reduction opportunities. A key factor in this regard is the source of electricity consumed, which significantly influences the outcomes of carbon accounting and impact assessment in LCA [49].

The carbon intensity of electricity in the Czech Republic is substantially higher compared to countries with a higher share of renewable energy sources, because lignite constitutes a large part of the Czech electricity mix. Emissions from lignite-based electricity generation can reach up to 0.901 kg CO_2 eq/kWh [50], which is several times higher than that of wind (0.019 kg CO_2 eq/kWh) or solar energy (0.011 kg CO_2 eq/kWh). National energy mixes play a crucial role in LCA outcomes, with renewable-based systems achieving substantially lower greenhouse gas emissions [51].

Results of the sensitivity analysis indicated that an increased share of lignite in the electricity mix significantly amplified total environmental impacts across all cultivation scenarios, confirming the strong dependency of the overall results on the national energy structure. For these reasons, this study adopted a location-based approach based on data for the relevant period [39,40]. This method ensures a more realistic estimate of emissions [49].

However, while these constraints are central to indoor cultivation, shifting production outdoors is not a guaranteed remedy. Poorly managed field systems can introduce new trade-offs, nutrient and pesticide runoff, higher water use and land occupation, and weather-driven yield volatility, potentially raising inputs per kilogram of product [26,52,53]. One promising approach is the integration of renewable energy sources. For instance, the use of small-scale biomass gasifiers can enable partial energy self-sufficiency in indoor cultivation facilities. These systems can generate electricity, heat, and biochar, the last being a byproduct with potential soil-enhancing properties, thus reducing operational costs and increasing the overall sustainability of hemp production [20].

Another option with significant potential to reduce environmental impacts is the use of solar energy [54]. Carbon footprint calculations have shown a substantial difference between electricity supplied from the public grid and electricity generated through photovoltaic panels. In one analyzed system, the carbon footprint of electricity from the conventional grid reached 134.8 kg CO_2 eq per square meter, compared to only 4.1 kg CO_2 eq per square meter for photovoltaic energy [55]. This difference highlights the considerable environmental benefits of renewable energy sources in meeting the energy demands of indoor cultivation facilities. Our results also indicate a reduction in overall environmental impacts when 25% of electricity from lignite was substituted by renewable energy sources, although the effect was less pronounced than in studies assessing full photovoltaic replacement. This difference may be partly attributed to the model boundary assumptions, as in case of this study, the photovoltaic systems were not considered to be integrated directly at the cultivation site, where on-site generation could further reduce energy-related impacts.

Although increasing light intensity in indoor cultivation systems may initially appear to raise environmental impacts, recalculations per unit of production often reveal the

opposite. While higher light input increases energy use, it also significantly improves yields, thereby reducing the impact per kilogram of dried biomass. For indoor cultivation of hemp, the combination of 360 W during the vegetative stage and 900 W during the flowering stage, together with the S1 nutrient solution, reduced the environmental impacts per kilogram of dried inflorescence by approximately 30–32% compared to lower light treatments. This highlights that higher input does not necessarily result in higher impact, efficiency is the key.

This principle is supported by LCA case studies on microgreen production, where yield gains from intensified cultivation outweighed the associated environmental impact [56]. Similarly, our findings confirm that while fertilizers can contribute substantially to the overall impact, optimizing light conditions improves biomass production and resource efficiency. Light intensity is no longer just a biological parameter, but an economic and environmental one. Lower-concentration nutrient solutions can maintain yield and cannabinoid quality while reducing both costs and environmental impact. [33]. This confirms that thoughtful input management, whether related to lighting or fertilization, can offer both economic and ecological benefits, which aligns with the focus on resource-use efficiency in our assessment.

4.4. Environmental Implications of Fertilization Intensity and Nutrient Management

This study confirmed a significant environmental impact associated with the use of nitrogen-based fertilizers. Fertilizers containing nitrogen (N) and phosphorus (P) are responsible for approximately 78% of global freshwater and marine eutrophication [57]. Excessive nitrogen and phosphorus input is a major driver of eutrophication and biodiversity loss in global agricultural systems [58]. The environmental impact, however, is not limited to fertilizer application alone. The production phases of mineral fertilizers and agricultural operations each account for roughly 12% of the total cumulative energy demand [59]. This is primarily due to emissions generated during the extraction and industrial processing of raw materials such as ammonium nitrate, potassium chloride, and single superphosphate.

5. Conclusions

This study evaluated the environmental performance of indoor hemp cultivation under four controlled scenarios combining different lighting intensities and nutrient regimes. Optimizing input–output efficiency is essential. Higher lighting intensity can be justified when the yield scales proportionally. For indoor hemp cultivation, within the bounds of this study, four scenarios, a 12-week cycle, the 2022 Czech grid, and a cultivation-only scope with cradle-to-gate approach, priority should be given to the combination of S1 nutrient solution, and 900 W light intensity during the flowering stage, as this configuration achieved the most favorable balance between productivity and environmental performance. In this setting, the electricity intensity is 7000 kWh·kg^{-1}, with drying accounting for 47% of electricity use. If the share of renewable electricity in the national energy mix increases by approximately 25% at the expense of lignite-based generation, total environmental impacts decrease by about 17% and if, instead, nuclear increases by 25% at the expense of lignite, impacts decrease by 29%; conversely, a lignite-heavy shift leads to an increase of 113%

The conclusions are explicitly bounded to the tested four cultivation scenarios and the 2022 Czech electricity mix. Therefore, generalization to other regional contexts should be made with caution.

Further research should focus on identifying the optimal light design, specifically, determining the threshold where increased light intensity continues to enhance yield without proportionally raising. Future studies could also focus on the relationship between yield changes and corresponding variations in environmental impact.

Although the present study provides valuable insights, it has several limitations. The limited number of repetitions restricts statistical evaluation, and the system boundary did not include post-harvest waste management or potential material reuse. Future studies should incorporate additional replicates to strengthen data robustness and extend the system boundary to include waste valorization.

Author Contributions: Conceptualization, A.K., J.N. and J.B.; methodology, A.K., J.N. and J.B.; software, A.K. and J.B.; validation, J.N. and J.B.; formal analysis, A.K.; investigation, A.K.; resources, J.N.; data curation, A.K.; writing—original draft preparation, A.K., N.V., E.K., P.K., R.W.N. and J.B.; writing—review and editing, A.K., J.N. and J.B.; visualization, A.K.; supervision, J.B.; project administration, A.K. and J.B.; funding acquisition, P.K. All authors have read and agreed to the published version of the manuscript.

Funding: This research was funded by the Grant Agency of the University of South Bohemia in České Budějovice, grant number GA JU 122/2025/Z.

Data Availability Statement: The original contributions presented in this study are included in the article. Further inquiries can be directed to the corresponding authors.

Acknowledgments: This study is the output of the Laboratory of LCA under the Faculty of Agriculture and Technology, University of South Bohemia in České Budějovice.

Conflicts of Interest: The authors declare no conflicts of interest.

Abbreviations

The following abbreviations are used in this manuscript:

LCA	Life Cycle Assessment
FU	Functional unit
GHG	Greenhouse gas
NPK	Nitrogen (N), Phosphorus (P), and Potassium (K) fertilizers

Appendix A

Table A1. Uncertainty analysis of environmental impact categories (ReCiPe 2016 Midpoint).

	Treatment	Mean	Median	SD	CV	2.5%	97.5%	SEM
CCH	S1-L1	1.51×10^{3}	1.51×10^{3}	1.12×10^{2}	7.44×10^{0}	1.30×10^{3}	1.74×10^{3}	3.55×10^{0}
	S1-L2	1.05×10^{3}	1.05×10^{3}	8.20×10^{1}	7.80×10^{0}	9.06×10^{2}	1.23×10^{3}	2.59×10^{0}
	S2-L1	1.61×10^{3}	1.60×10^{3}	1.17×10^{2}	7.32×10^{0}	1.39×10^{3}	1.86×10^{3}	3.71×10^{0}
	S2-L2	1.09×10^{3}	1.09×10^{3}	8.18×10^{1}	7.53×10^{0}	9.27×10^{2}	1.25×10^{3}	2.59×10^{0}
TA	S1-L1	4.31×10^{0}	4.30×10^{0}	2.77×10^{-1}	6.42×10^{0}	3.80×10^{0}	4.92×10^{0}	8.75×10^{-3}
	S1-L2	2.97×10^{0}	2.96×10^{0}	1.93×10^{-1}	6.48×10^{0}	2.63×10^{0}	3.38×10^{0}	6.09×10^{-3}
	S2-L1	4.58×10^{0}	4.57×10^{0}	2.95×10^{-1}	6.44×10^{0}	4.02×10^{0}	5.19×10^{0}	9.33×10^{-3}
	S2-L2	3.07×10^{0}	3.06×10^{0}	1.98×10^{-1}	6.45×10^{0}	2.70×10^{0}	3.47×10^{0}	6.26×10^{-3}
FE	S1-L1	2.43×10^{0}	1.89×10^{0}	1.90×10^{0}	7.84×10^{1}	5.78×10^{-1}	7.33×10^{0}	6.01×10^{-2}
	S1-L2	1.70×10^{0}	1.32×10^{0}	1.48×10^{0}	8.70×10^{1}	4.14×10^{-1}	5.43×10^{0}	4.67×10^{-2}
	S2-L1	2.52×10^{0}	1.92×10^{0}	2.17×10^{0}	8.62×10^{1}	6.07×10^{-1}	8.49×10^{0}	6.86×10^{-2}
	S2-L2	1.72×10^{0}	1.33×10^{0}	1.51×10^{0}	8.76×10^{1}	4.08×10^{-1}	5.49×10^{0}	4.76×10^{-2}
ME	S1-L1	1.57×10^{-1}	1.53×10^{-1}	3.43×10^{-2}	2.18×10^{1}	1.01×10^{-1}	2.34×10^{-1}	1.08×10^{-3}
	S1-L2	1.10×10^{-1}	1.07×10^{-1}	2.46×10^{-2}	2.23×10^{1}	7.19×10^{-2}	1.66×10^{-1}	7.78×10^{-4}
	S2-L1	1.69×10^{-1}	1.64×10^{-1}	3.77×10^{-2}	2.23×10^{1}	1.10×10^{-1}	2.62×10^{-1}	1.19×10^{-3}
	S2-L2	1.13×10^{-1}	1.11×10^{-1}	2.40×10^{-2}	2.13×10^{1}	7.17×10^{-2}	1.62×10^{-1}	7.58×10^{-4}
TE	S1-L1	2.80×10^{3}	2.43×10^{3}	1.45×10^{3}	5.17×10^{1}	1.29×10^{3}	6.34×10^{3}	4.58×10^{1}
	S1-L2	1.85×10^{3}	1.62×10^{3}	8.78×10^{2}	4.74×10^{1}	8.77×10^{2}	4.09×10^{3}	2.78×10^{1}
	S2-L1	2.97×10^{3}	2.63×10^{3}	1.48×10^{3}	5.00×10^{1}	1.37×10^{3}	6.84×10^{3}	4.69×10^{1}
	S2-L2	1.90×10^{3}	1.69×10^{3}	8.52×10^{2}	4.49×10^{1}	9.18×10^{2}	4.44×10^{3}	2.69×10^{1}

Table A1. *Cont.*

	Treatment	Mean	Median	SD	CV	2.5%	97.5%	SEM
FX	S1-L1	6.74×10^{1}	4.83×10^{1}	7.28×10^{1}	1.08×10^{2}	2.30×10^{1}	2.30×10^{2}	2.30×10^{0}
	S1-L2	4.77×10^{1}	3.51×10^{1}	5.25×10^{1}	1.10×10^{2}	1.55×10^{1}	1.60×10^{2}	1.66×10^{0}
	S2-L1	7.24×10^{1}	5.27×10^{1}	7.71×10^{1}	1.07×10^{2}	2.49×10^{1}	2.57×10^{2}	2.44×10^{0}
	S2-L2	4.80×10^{1}	3.53×10^{1}	4.12×10^{1}	8.57×10^{1}	1.73×10^{1}	1.65×10^{2}	1.30×10^{0}
WD	S1-L1	4.12×10^{1}	1.50×10^{2}	1.31×10^{3}	3.18×10^{3}	-2.91×10^{3}	2.33×10^{3}	4.14×10^{1}
	S1-L2	-1.21×10^{1}	7.65×10^{1}	9.44×10^{2}	-7.81×10^{3}	-2.02×10^{3}	1.58×10^{3}	2.98×10^{1}
	S2-L1	7.67×10^{1}	1.72×10^{2}	1.30×10^{3}	1.70×10^{3}	-2.81×10^{3}	2.42×10^{3}	4.11×10^{1}
	S2-L2	-2.83×10^{0}	1.70×10^{2}	9.88×10^{2}	-3.49×10^{4}	-2.51×10^{3}	1.62×10^{3}	3.12×10^{1}
HT	S1-L1	1.39×10^{3}	9.94×10^{2}	2.60×10^{3}	1.86×10^{2}	1.28×10^{3}	1.51×10^{3}	5.81×10^{1}
	S1-L2	9.78×10^{2}	7.11×10^{2}	1.83×10^{3}	1.88×10^{2}	8.98×10^{2}	1.06×10^{3}	4.10×10^{1}
	S2-L1	1.52×10^{3}	1.09×10^{3}	2.91×10^{3}	1.91×10^{2}	1.39×10^{3}	1.65×10^{3}	6.50×10^{1}
	S2-L2	9.80×10^{2}	7.14×10^{2}	1.64×10^{3}	1.67×10^{2}	9.08×10^{2}	1.05×10^{3}	3.66×10^{1}
LD	S1-L1	3.86×10^{1}	3.88×10^{1}	2.04×10^{1}	5.29×10^{1}	-5.51×10^{0}	7.97×10^{1}	6.46×10^{-1}
	S1-L2	2.68×10^{1}	2.67×10^{1}	1.43×10^{1}	5.35×10^{1}	-3.08×10^{0}	5.55×10^{1}	4.53×10^{-1}
	S2-L1	4.20×10^{1}	4.25×10^{1}	2.07×10^{1}	4.94×10^{1}	-2.63×10^{0}	8.26×10^{1}	6.56×10^{-1}
	S2-L2	2.75×10^{1}	2.73×10^{1}	1.50×10^{1}	5.45×10^{1}	-2.49×10^{0}	5.57×10^{1}	4.75×10^{-1}

S1-L1: solution 1, lighting 1, S1-L2: solution 1, lighting 2, S2-L1: solution 2, lighting 1, S2-L2: solution 2, lighting 2, CCH: Climate change (kg CO_2 eq), TA: Terrestrial acidification (kg SO_2 eq), FE: Freshwater eutrophication (kg P eq), ME: Marine eutrophication (kg N eq), TE: Terrestrial ecotoxicity (kg 1.4-DCB), FX: Freshwater ecotoxicity (kg 1.4-DCB), WD: Water depletion (m^3), HT: Human toxicity (kg 1.4-DCB), LD: Land use (m^2a crop eq), SimaPro 9.3.0.2 software; ReCiPe 2016 Midpoint (H) V1.09/World (2010) H; Cut-off System Model approach; Characterization model, Confidence interval: 95%.

Table A2. Contribution analyses: Environmental load of full system per functional unit (1 kg of dried hemp inflorescence).

Impact Category	Treatment	Growing Media	Flowerpot-1 Year Amortization	Fertilizers (NPK)	Minerals & Microelements	Tap Water	Electricity-Lighting	Electricity-Ventilation	Electricity-Dryers
CCH	S1-L1	1.6×10^{1}	1.1×10^{0}	3.0×10^{-1}	8.9×10^{-2}	1.3×10^{-1}	4.3×10^{2}	2.5×10^{2}	8.2×10^{2}
	S1-L2	9.9×10^{0}	6.3×10^{-1}	1.8×10^{-1}	5.3×10^{-2}	7.9×10^{-2}	4.0×10^{2}	1.5×10^{2}	4.9×10^{2}
	S2-L1	1.8×10^{1}	1.1×10^{0}	5.5×10^{-1}	1.9×10^{-1}	1.4×10^{-1}	4.6×10^{2}	2.7×10^{2}	8.7×10^{2}
	S2-L2	1.0×10^{1}	6.5×10^{-1}	3.2×10^{-1}	1.1×10^{-1}	8.2×10^{-2}	4.1×10^{2}	1.5×10^{2}	5.1×10^{2}
TA	S1-L1	1.6×10^{-1}	3.2×10^{-3}	1.3×10^{-3}	6.3×10^{-4}	4.7×10^{-4}	1.2×10^{0}	6.9×10^{-1}	2.3×10^{0}
	S1-L2	9.6×10^{-2}	1.9×10^{-3}	7.7×10^{-4}	3.8×10^{-4}	2.8×10^{-4}	1.1×10^{0}	4.2×10^{-1}	1.4×10^{0}
	S2-L1	1.7×10^{-1}	3.3×10^{-3}	3.7×10^{-3}	2.8×10^{-3}	5.0×10^{-4}	1.3×10^{0}	7.4×10^{-1}	2.4×10^{0}
	S2-L2	9.9×10^{-2}	2.0×10^{-3}	2.1×10^{-3}	1.6×10^{-3}	2.9×10^{-4}	1.1×10^{0}	4.3×10^{-1}	1.4×10^{0}
FE	S1-L1	2.7×10^{-3}	2.7×10^{-4}	7.6×10^{-5}	2.6×10^{-5}	8.8×10^{-5}	6.9×10^{-1}	4.0×10^{-1}	1.3×10^{0}
	S1-L2	2.1×10^{-4}	1.6×10^{-4}	4.6×10^{-5}	1.6×10^{-5}	5.3×10^{-5}	6.4×10^{-1}	2.4×10^{-1}	7.8×10^{-1}
	S2-L1	2.8×10^{-3}	2.9×10^{-4}	3.3×10^{-4}	8.1×10^{-5}	9.3×10^{-5}	7.3×10^{-1}	4.2×10^{-1}	1.4×10^{0}
	S2-L2	1.7×10^{-3}	1.7×10^{-4}	2.0×10^{-4}	4.7×10^{-5}	5.4×10^{-5}	6.6×10^{-1}	2.5×10^{-1}	8.1×10^{-1}
ME	S1-L1	3.5×10^{-4}	2.3×10^{-5}	3.0×10^{-5}	2.5×10^{-6}	8.6×10^{-6}	4.6×10^{-2}	2.6×10^{-2}	8.6×10^{-2}
	S1-L2	2.1×10^{-4}	1.4×10^{-5}	1.8×10^{-5}	1.5×10^{-6}	5.2×10^{-6}	4.2×10^{-2}	1.6×10^{-2}	5.2×10^{-2}
	S2-L1	3.7×10^{-4}	2.4×10^{-5}	4.5×10^{-5}	7.9×10^{-6}	9.1×10^{-6}	4.8×10^{-2}	2.8×10^{-2}	9.1×10^{-2}
	S2-L2	2.2×10^{-4}	1.4×10^{-5}	2.6×10^{-5}	4.6×10^{-6}	5.3×10^{-6}	4.3×10^{-2}	1.6×10^{-2}	5.3×10^{-2}
TE	S1-L1	9.7×10^{1}	7.7×10^{-1}	3.3×10^{0}	8.0×10^{-1}	9.4×10^{0}	7.5×10^{2}	4.3×10^{2}	1.4×10^{3}
	S1-L2	5.8×10^{1}	4.6×10^{-1}	2.0×10^{0}	4.8×10^{-1}	5.6×10^{0}	6.9×10^{2}	2.6×10^{2}	8.5×10^{2}
	S2-L1	1.0×10^{2}	8.2×10^{-1}	8.8×10^{0}	2.0×10^{0}	9.9×10^{0}	7.9×10^{2}	4.6×10^{2}	1.5×10^{3}
	S2-L2	6.0×10^{1}	4.8×10^{-1}	5.1×10^{0}	1.2×10^{0}	5.8×10^{0}	7.1×10^{2}	2.7×10^{2}	8.7×10^{2}
FX	S1-L1	2.6×10^{-1}	1.2×10^{-2}	1.8×10^{-2}	7.7×10^{-3}	1.1×10^{-2}	1.9×10^{1}	1.1×10^{1}	3.6×10^{1}
	S1-L2	1.5×10^{-1}	6.7×10^{-3}	1.1×10^{-2}	4.6×10^{-3}	6.5×10^{-3}	1.7×10^{1}	6.6×10^{0}	2.1×10^{1}
	S2-L1	2.7×10^{-1}	1.3×10^{-2}	4.7×10^{-2}	1.7×10^{-2}	1.2×10^{-2}	2.0×10^{1}	1.2×10^{1}	3.8×10^{1}
	S2-L2	1.6×10^{-1}	7.4×10^{-3}	2.7×10^{-2}	9.9×10^{-3}	6.7×10^{-3}	1.8×10^{1}	6.8×10^{0}	2.2×10^{1}
WD	S1-L1	1.5×10^{-1}	1.1×10^{-2}	4.7×10^{-3}	7.1×10^{-4}	4.3×10^{-1}	1.8×10^{0}	1.0×10^{0}	3.4×10^{0}
	S1-L2	9.2×10^{-2}	6.5×10^{-3}	2.8×10^{-3}	4.2×10^{-4}	2.6×10^{-1}	1.6×10^{0}	6.2×10^{-1}	2.0×10^{0}
	S2-L1	1.6×10^{-1}	1.1×10^{-2}	1.1×10^{-2}	1.7×10^{-3}	4.6×10^{-1}	1.9×10^{0}	1.1×10^{0}	3.6×10^{0}
	S2-L2	9.5×10^{-2}	6.7×10^{-3}	6.3×10^{-3}	1.0×10^{-3}	2.7×10^{-1}	1.7×10^{0}	6.4×10^{-1}	2.1×10^{0}

Table A2. *Cont.*

Impact Category	Treatment	Growing Media	Flowerpot-1 Year Amortization	Fertilizers (NPK)	Minerals & Microelements	Tap Water	Electricity-Lighting	Electricity-Ventilation	Electricity-Dryers
HT	S1-L1	6.8×10^{0}	4.4×10^{-1}	3.7×10^{-1}	2.1×10^{-1}	5.8×10^{-1}	7.8×10^{2}	4.5×10^{2}	1.5×10^{3}
	S1-L2	4.1×10^{0}	2.6×10^{-1}	2.2×10^{-1}	1.3×10^{-1}	3.5×10^{-1}	7.2×10^{2}	2.7×10^{2}	8.9×10^{2}
	S2-L1	7.2×10^{0}	4.6×10^{-1}	1.0×10^{0}	4.7×10^{-1}	6.2×10^{-1}	8.3×10^{2}	4.8×10^{2}	1.6×10^{3}
	S2-L2	4.2×10^{0}	2.7×10^{-1}	6.1×10^{-1}	2.7×10^{-1}	3.6×10^{-1}	7.4×10^{2}	2.8×10^{2}	9.1×10^{2}
LD	S1-L1	6.8×10^{-1}	3.0×10^{-2}	9.4×10^{-3}	2.2×10^{-3}	4.7×10^{-3}	1.1×10^{1}	6.5×10^{0}	2.1×10^{1}
	S1-L2	4.1×10^{-1}	1.8×10^{-2}	5.6×10^{-3}	1.3×10^{-3}	2.8×10^{-3}	1.0×10^{1}	3.9×10^{0}	1.3×10^{1}
	S2-L1	7.3×10^{-1}	3.2×10^{-2}	3.5×10^{-2}	5.8×10^{-3}	5.0×10^{-3}	1.2×10^{1}	6.9×10^{0}	2.2×10^{1}
	S2-L2	4.2×10^{-1}	1.9×10^{-2}	2.0×10^{-2}	3.4×10^{-3}	2.9×10^{-3}	1.1×10^{1}	4.0×10^{0}	1.3×10^{1}

S1-L1: solution 1, lighting 1, S1-L2: solution 1, lighting 2, S2-L1: solution 2, lighting 1, S2-L2: solution 2, lighting 2, CCH: Climate change (kg CO_2 eq), TA: Terrestrial acidification (kg SO_2 eq), FE: Freshwater eutrophication (kg P eq), ME: Marine eutrophication (kg N eq), TE: Terrestrial ecotoxicity (kg 1.4-DCB), FX: Freshwater ecotoxicity (kg 1.4-DCB), WD: Water depletion (m^3), HT: Human toxicity (kg 1.4-DCB), LD: Land use (m^2a crop eq), "Fertilizers (NPK)" include NO_3^-, NH_4^+, P_2O_5, and K_2O fertilizers. "Minerals & Microelements" include calcium carbonate, magnesium oxide, sulphite, and microelements (Fe, B, Cu, Zn, Mn, Mo). "Growing media" include stone wool, coconut fiber, and perlite, SimaPro 9.3.0.2 software; ReCiPe 2016 Midpoint (H) V1.09/World (2010) H; Cut-off System Model approach; Characterization model.

Table A3. Contribution analyses: Environmental load of nutrients only system per functional unit (1 kg of dried hemp inflorescence).

Impact Category	Treatment	Total	Inorganic Nitrogen Fertilizer as NO_3	Inorganic Nitrogen Fertilizer as NH_4	Inorganic Phosphorus Fertilizer as P_2O_5	Inorganic Potassium Fertilizer as K_2O	Calcium Carbonate ($CaCO_3$)	Magnesium Oxide (MgO)	Sulphite	Microelements (Fe, B, Cu, Zn, Mn, Mo)
CCH	S1-L1	3.92×10^{-1}	2.15×10^{-1}	1.15×10^{-2}	2.22×10^{-2}	5.43×10^{-2}	4.00×10^{-2}	3.26×10^{-2}	1.46×10^{-2}	1.43×10^{-3}
	S1-L2	2.35×10^{-1}	1.29×10^{-1}	6.90×10^{-3}	1.33×10^{-2}	3.25×10^{-2}	2.39×10^{-2}	1.95×10^{-2}	8.75×10^{-3}	8.55×10^{-4}
	S2-L1	7.46×10^{-1}	2.29×10^{-1}	1.22×10^{-2}	1.87×10^{-1}	1.26×10^{-1}	3.98×10^{-2}	6.69×10^{-2}	8.41×10^{-2}	1.31×10^{-3}
	S2-L2	4.35×10^{-1}	1.33×10^{-1}	7.12×10^{-3}	1.09×10^{-1}	7.31×10^{-2}	2.32×10^{-2}	3.90×10^{-2}	4.90×10^{-2}	7.65×10^{-4}
TA	S1-L1	1.92×10^{-3}	7.96×10^{-4}	4.26×10^{-5}	2.84×10^{-4}	1.63×10^{-4}	1.32×10^{-4}	4.55×10^{-5}	4.46×10^{-4}	7.80×10^{-6}
	S1-L2	2.97×10^{0}	4.77×10^{-4}	2.55×10^{-5}	1.70×10^{-4}	9.78×10^{-5}	7.89×10^{-5}	2.73×10^{-5}	2.67×10^{-4}	4.67×10^{-6}
	S2-L1	6.46×10^{-3}	8.45×10^{-4}	4.52×10^{-5}	2.40×10^{-3}	3.77×10^{-4}	1.31×10^{-4}	9.35×10^{-5}	2.56×10^{-3}	7.18×10^{-6}
	S2-L2	3.77×10^{-3}	4.92×10^{-4}	2.63×10^{-5}	1.40×10^{-3}	2.20×10^{-4}	7.65×10^{-5}	5.45×10^{-5}	1.49×10^{-3}	4.18×10^{-6}
FE	S1-L1	1.02×10^{-4}	2.99×10^{-5}	1.60×10^{-6}	3.24×10^{-5}	1.21×10^{-5}	1.04×10^{-5}	4.97×10^{-6}	1.04×10^{-5}	5.31×10^{-7}
	S1-L2	1.66×10^{0}	1.79×10^{-5}	9.57×10^{-7}	1.94×10^{-5}	7.27×10^{-6}	6.25×10^{-6}	2.98×10^{-6}	6.20×10^{-6}	3.18×10^{-7}
	S2-L1	4.15×10^{-4}	3.17×10^{-5}	1.69×10^{-6}	2.73×10^{-4}	2.80×10^{-5}	1.04×10^{-5}	1.02×10^{-5}	5.96×10^{-5}	4.89×10^{-7}
	S2-L2	2.42×10^{-4}	1.85×10^{-5}	9.87×10^{-7}	1.59×10^{-4}	1.63×10^{-5}	6.06×10^{-6}	5.95×10^{-6}	3.47×10^{-5}	2.85×10^{-7}
ME	S1-L1	3.21×10^{-5}	2.55×10^{-5}	1.36×10^{-6}	1.63×10^{-6}	1.11×10^{-6}	8.36×10^{-7}	3.11×10^{-7}	1.06×10^{-6}	3.33×10^{-7}
	S1-L2	1.10×10^{-1}	1.53×10^{-5}	8.16×10^{-7}	9.75×10^{-7}	6.65×10^{-7}	5.01×10^{-7}	1.87×10^{-7}	6.32×10^{-7}	2.00×10^{-7}
	S2-L1	5.26×10^{-5}	2.70×10^{-5}	1.45×10^{-6}	1.37×10^{-5}	2.56×10^{-6}	8.33×10^{-7}	6.39×10^{-7}	6.07×10^{-6}	3.07×10^{-7}
	S2-L2	3.07×10^{-5}	1.58×10^{-5}	8.43×10^{-7}	8.00×10^{-6}	1.49×10^{-6}	4.85×10^{-7}	3.73×10^{-7}	3.54×10^{-6}	1.79×10^{-7}
TE	S1-L1	4.12×10^{0}	1.63×10^{0}	8.74×10^{-2}	5.30×10^{-1}	1.07×10^{0}	4.44×10^{-1}	5.31×10^{-2}	2.44×10^{-1}	5.82×10^{-2}
	S1-L2	1.86×10^{3}	9.78×10^{-1}	5.23×10^{-2}	3.17×10^{-1}	6.40×10^{-1}	2.66×10^{-1}	3.18×10^{-2}	1.46×10^{-1}	3.49×10^{-2}
	S2-L1	1.08×10^{1}	1.73×10^{0}	9.27×10^{-2}	4.47×10^{0}	2.47×10^{0}	4.42×10^{-1}	1.09×10^{-1}	1.40×10^{0}	5.36×10^{-2}
	S2-L2	6.28×10^{0}	1.01×10^{0}	5.40×10^{-2}	2.61×10^{0}	1.44×10^{0}	2.58×10^{-1}	6.35×10^{-2}	8.19×10^{-1}	3.12×10^{-2}
FX	S1-L1	259×10^{-2}	1.09×10^{-2}	5.83×10^{-4}	3.08×10^{-3}	3.62×10^{-3}	3.86×10^{-3}	1.96×10^{-3}	1.53×10^{-3}	3.27×10^{-4}
	S1-L2	4.55×10^{1}	6.53×10^{-3}	3.49×10^{-4}	1.84×10^{-3}	2.17×10^{-3}	2.31×10^{-3}	1.18×10^{-3}	9.14×10^{-4}	1.96×10^{-4}
	S2-L1	6.35×10^{-2}	1.16×10^{-2}	6.19×10^{-4}	2.60×10^{-2}	8.36×10^{-3}	3.85×10^{-3}	4.03×10^{-3}	8.78×10^{-3}	3.01×10^{-4}
	S2-L2	3.70×10^{-2}	6.74×10^{-3}	3.60×10^{-4}	1.51×10^{-2}	4.87×10^{-3}	2.24×10^{-3}	2.35×10^{-3}	5.12×10^{-3}	1.75×10^{-4}
WD	S1-L1	5.44×10^{-3}	3.32×10^{-3}	1.78×10^{-4}	6.89×10^{-4}	5.44×10^{-4}	3.38×10^{-4}	8.60×10^{-5}	1.96×10^{-4}	8.85×10^{-5}
	S1-L2	4.64×10^{0}	1.99×10^{-3}	1.06×10^{-4}	4.13×10^{-4}	3.26×10^{-4}	2.02×10^{-4}	5.15×10^{-5}	1.17×10^{-4}	5.30×10^{-5}
	S2-L1	1.25×10^{-2}	3.53×10^{-3}	1.89×10^{-4}	5.81×10^{-3}	1.26×10^{-3}	3.36×10^{-4}	1.77×10^{-4}	1.13×10^{-3}	8.15×10^{-5}
	S2-L2	7.29×10^{-3}	2.06×10^{-3}	1.10×10^{-4}	3.39×10^{-3}	7.32×10^{-4}	1.96×10^{-4}	1.03×10^{-4}	6.56×10^{-4}	4.75×10^{-5}

Table A3. *Cont.*

Impact Category	Treatment	Total	Inorganic Nitrogen Fertilizer as NO_3	Inorganic Nitrogen Fertilizer as NH_4	Inorganic Phosphorus Fertilizer as P_2O_5	Inorganic Potassium Fertilizer as K_2O	Calcium Carbonate ($CaCO_3$)	Magnesium Oxide (MgO)	Sulphite	Microelements (Fe, B, Cu, Zn, Mn, Mo)
HT	S1-L1	5.84×10^{-1}	2.07×10^{-1}	1.11×10^{-2}	7.43×10^{-2}	8.16×10^{-2}	7.30×10^{-2}	9.55×10^{-2}	3.36×10^{-2}	7.73×10^{-3}
	S1-L2	1.88×10^{3}	1.24×10^{-1}	6.64×10^{-3}	4.45×10^{-2}	4.89×10^{-2}	4.37×10^{-2}	5.72×10^{-2}	2.01×10^{-2}	4.63×10^{-3}
	S2-L1	1.52×10^{0}	2.20×10^{-1}	1.18×10^{-2}	6.27×10^{-1}	1.89×10^{-1}	7.27×10^{-2}	1.96×10^{-1}	1.93×10^{-1}	7.11×10^{-3}
	S2-L2	8.83×10^{-1}	1.28×10^{-1}	6.86×10^{-3}	3.65×10^{-1}	1.10×10^{-1}	4.24×10^{-2}	1.14×10^{-1}	1.13×10^{-1}	4.14×10^{-3}
LD	S1-L1	3.43×10^{-3}	1.83×10^{-4}	2.88×10^{-3}	2.90×10^{-3}	1.06×10^{-3}	4.35×10^{-4}	6.54×10^{-4}	3.13×10^{-5}	3.43×10^{-3}
	S1-L2	2.05×10^{-3}	1.10×10^{-4}	1.72×10^{-3}	1.74×10^{-3}	6.37×10^{-4}	2.61×10^{-4}	3.92×10^{-4}	1.88×10^{-5}	2.05×10^{-3}
	S2-L1	3.64×10^{-3}	1.94×10^{-4}	2.43×10^{-2}	6.70×10^{-3}	1.06×10^{-3}	8.94×10^{-4}	3.76×10^{-3}	2.88×10^{-5}	3.64×10^{-3}
	S2-L2	2.12×10^{-3}	1.13×10^{-4}	1.41×10^{-2}	3.90×10^{-3}	6.17×10^{-4}	5.21×10^{-4}	2.19×10^{-3}	1.68×10^{-5}	2.12×10^{-3}

S1-L1: solution 1, lighting 1, S1-L2: solution 1, lighting 2, S2-L1: solution 2, lighting 1, S2-L2: solution 2, lighting 2, CCH: Climate change (kg CO_2 eq), TA: Terrestrial acidification (kg SO_2 eq), FE: Freshwater eutrophication (kg P eq), ME: Marine eutrophication (kg N eq), TE: Terrestrial ecotoxicity (kg 1.4-DCB), FX: Freshwater ecotoxicity (kg 1.4-DCB), WD: Water depletion (m^3), HT: Human toxicity (kg 1.4-DCB), LD: Land use (m^2a crop eq), SimaPro 9.3.0.2 software; ReCiPe 2016 Midpoint (H) V1.09/World (2010) H; Cut-off System Model approach; Characterization model.

Table A4. Normalization model for unit of production (FU = 1 kg of dried hemp inflorescence.

Impact Category	S1-L1	S1-L2	S2-L1	S2-L2
CCH	1.90×10^{-1}	1.31×10^{-1}	2.01×10^{-1}	1.35×10^{-1}
TA	1.05×10^{-1}	7.25×10^{-2}	1.12×10^{-1}	7.49×10^{-2}
FE	3.69×10^{0}	2.55×10^{0}	3.92×10^{0}	2.64×10^{0}
ME	3.44×10^{-2}	2.38×10^{-2}	3.65×10^{-2}	2.46×10^{-2}
TE	1.78×10^{-1}	1.22×10^{-1}	1.89×10^{-1}	1.27×10^{-1}
FX	2.61×10^{0}	1.81×10^{0}	2.77×10^{0}	1.86×10^{0}
WD	2.54×10^{-2}	1.74×10^{-2}	2.70×10^{-2}	1.80×10^{-2}
HT	1.54×10^{1}	1.07×10^{1}	1.64×10^{1}	1.10×10^{1}
LD	6.44×10^{-3}	4.44×10^{-3}	6.83×10^{-3}	4.59×10^{-3}

S1-L1: solution 1, lighting 1, S1-L2: solution 1, lighting 2, S2-L1: solution 2, lighting 1, S2-L2: solution 2, lighting 2, CCH: Climate change, TA: Terrestrial acidification, FE: Freshwater eutrophication, ME: Marine eutrophication, TE: Terrestrial ecotoxicity, FX: Freshwater ecotoxicity, WD: Water depletion, HT: Human toxicity, LD: Land use, ReCiPe 2016 Midpoint (H) V1.09/World (2010) method, normalization model, results are expressed in pt (points).

Table A5. Sensitivity analysis of the electricity mix composition on the total environmental impact per functional unit (1 kg of dried hemp inflorescence).

Treatment	Baseline (CZ 2022)	Lignite	Nuclear	Renewables
S1-L1	4.17×10^{1}	8.87×10^{1}	2.96×10^{1}	3.46×10^{1}
S1-L2	2.88×10^{1}	6.13×10^{1}	2.04×10^{1}	2.39×10^{1}
S2-L1	4.43×10^{1}	9.42×10^{1}	3.14×10^{1}	3.68×10^{1}
S2-L2	2.97×10^{1}	6.33×10^{1}	2.10×10^{1}	2.47×10^{1}

S1-L1: solution 1, lighting 1, S1-L2: solution 1, lighting 2, S2-L1: solution 2, lighting 1, S2-L2: solution 2, lighting 2, the "Baseline (CZ 2022)" scenario represents the actual Czech electricity mix in 2022, the "Lignite" scenario assumes a 25% increase in the share of lignite-based electricity with a corresponding reduction in nuclear power, the "Nuclear" scenario assumes a 25% increase in nuclear share with reduced lignite contribution, the "Renewables" scenario models a 25% increase in renewable energy, with proportional contributions recalculated among hydropower, pumped storage, biomass, biogas, wind, solar, and geothermal sources, while reducing lignite proportion accordingly, ReCiPe 2016 Endpoint (H) V1.11/World (2010) H/A method, Single score model, results are expressed in pt (points).

References

1. Jami, T.; Rawtani, D.; Agrawal, Y.K. Hemp Concrete: Carbon-Negative Construction. *Emerg. Mater. Res.* **2016**, *5*, 240–247. [CrossRef]
2. Crini, G.; Lichtfouse, E.; Chanet, G.; Morin-Crini, N. Applications of Hemp in Textiles, Paper Industry, Insulation and Building Materials, Horticulture, Animal Nutrition, Food and Beverages, Nutraceuticals, Cosmetics and Hygiene, Medicine, Agrochemistry, Energy Production and Environment: A Review. *Environ. Chem. Lett.* **2020**, *18*, 1451–1476. [CrossRef]

3. Yano, H.; Fu, W. Hemp: A Sustainable Plant with High Industrial Value in Food Processing. *Foods* **2023**, *12*, 651. [CrossRef] [PubMed]
4. Zimniewska, M. Hemp Fibre Properties and Processing Target Textile: A Review. *Materials* **2022**, *15*, 1901. [CrossRef]
5. European Commission Hemp—Crop Production and Plant-Based Products 2025. Available online: https://agriculture.ec.europa.eu/farming/crop-productions-and-plant-based-products/hemp_en (accessed on 16 July 2025).
6. Fischer, B.; Hall, W. Germany's Evolving Framework for Cannabis Legalization and Regulation: Select Comments Based on Science and Policy Experiences for Public Health. *Lancet Reg. Health Eur.* **2022**, *23*, 100546. [CrossRef]
7. Mirpoor, S.F.; Ibáñez-Ibáñez, P.F.; Giosafatto, C.V.L.; Del Castillo-Santaella, T.; Rodríguez-Valverde, M.A.; Maldonado-Valderrama, J. Surface Activity of Protein Extracts from Seed Oil By-Products and Wettability of Developed Bioplastics. *Food Hydrocoll.* **2023**, *145*, 109091. [CrossRef]
8. Rheay, H.T.; Omondi, E.C.; Brewer, C.E. Potential of Hemp (*Cannabis sativa* L.) for Paired Phytoremediation and Bioenergy Production. *GCB Bioenergy* **2021**, *13*, 525–536. [CrossRef]
9. Milan, J.; Michalska, A.; Jurowski, K. The Comprehensive Review about Elements Accumulation in Industrial Hemp (*Cannabis sativa* L.). *Food Chem. Toxicol.* **2024**, *184*, 114344. [CrossRef]
10. Padmavathiamma, P.K.; Li, L.Y. Phytoremediation Technology: Hyper-Accumulation Metals in Plants. *Water Air Soil Pollut.* **2007**, *184*, 105–126. [CrossRef]
11. Burczyk, H.; Grabowska, L.; Kołodziej, J.; Strybe, M. Industrial Hemp as a Raw Material for Energy Production. *J. Ind. Hemp* **2008**, *13*, 37–48. [CrossRef]
12. Amaducci, S.; Scordia, D.; Liu, F.H.; Zhang, Q.; Guo, H.; Testa, G.; Cosentino, S.L. Key Cultivation Techniques for Hemp in Europe and China. *Ind. Crops Prod.* **2015**, *68*, 2–16. [CrossRef]
13. Jin, D.; Jin, S.; Chen, J. Cannabis Indoor Growing Conditions, Management Practices, and Post-Harvest Treatment: A Review. *Am. J. Plant Sci.* **2019**, *10*, 925–946. [CrossRef]
14. Ampim, P.A.Y.; Obeng, E.; Olvera-Gonzalez, E. Indoor Vegetable Production: An Alternative Approach to Increasing Cultivation. *Plants* **2022**, *11*, 2843. [CrossRef] [PubMed]
15. Choi, H.G.; Moon, B.Y.; Kang, N.J. Effects of LED Light on the Production of Strawberry during Cultivation in a Plastic Greenhouse and in a Growth Chamber. *Sci. Hortic.* **2015**, *189*, 22–31. [CrossRef]
16. Engler, N.; Krarti, M. Review of Energy Efficiency in Controlled Environment Agriculture. *Renew. Sustain. Energy Rev.* **2021**, *141*, 110786. [CrossRef]
17. Moosavi-Nezhad, M.; Salehi, R.; Aliniaeifard, S.; Winans, K.S.; Nabavi-Pelesaraei, A. An Analysis of Energy Use and Economic and Environmental Impacts in Conventional Tunnel and LED-Equipped Vertical Systems in Healing and Acclimatization of Grafted Watermelon Seedlings. *J. Clean. Prod.* **2022**, *361*, 132069. [CrossRef]
18. Pinstrup-Andersen, P. Is It Time to Take Vertical Indoor Farming Seriously? *Glob. Food Secur.* **2018**, *17*, 233–235. [CrossRef]
19. Llewellyn, D.; Golem, S.; Foley, E.; Dinka, S.; Jones, A.M.P.; Zheng, Y. Indoor Grown Cannabis Yield Increased Proportionally with Light Intensity, but Ultraviolet Radiation Did Not Affect Yield or Cannabinoid Content. *Front. Plant Sci.* **2022**, *13*, 974018. [CrossRef]
20. Pedrazzi, S.; Santunione, G.; Mustone, M.; Cannazza, G.; Citti, C.; Francia, E.; Allesina, G. Techno-Economic Study of a Small Scale Gasifier Applied to an Indoor Hemp Farm: From Energy Savings to Biochar Effects on Productivity. *Energy Convers. Manag.* **2021**, *228*, 113645. [CrossRef]
21. Ely, K.; Podder, S.; Reiss, M.; Fike, J. Industrial Hemp as a Crop for a Sustainable Agriculture. In *Cannabis/Hemp for Sustainable Agriculture and Materials*; Agrawal, D.C., Kumar, R., Dhanasekaran, M., Eds.; Springer: Singapore, 2022; pp. 1–28, ISBN 978-981-16-8777-8.
22. Bernas, J.; Bernasová, T.; Nedbal, V.; Neugschwandtner, R.W. Agricultural LCA for Food Oil of Winter Rapeseed, Sunflower, and Hemp, Based on Czech Standard Cultivation Practices. *Agronomy* **2021**, *11*, 2301. [CrossRef]
23. Ruviaro, C.F.; Gianezini, M.; Brandão, F.S.; Winck, C.A.; Dewes, H. Life Cycle Assessment in Brazilian Agriculture Facing Worldwide Trends. *J. Clean. Prod.* **2012**, *28*, 9–24. [CrossRef]
24. Desaulniers Brousseau, V.; Goldstein, B.P.; Lachapelle, M.; Tazi, I.; Lefsrud, M. Greener Green: The Environmental Impacts of the Canadian Cannabis Industry. *Resour. Conserv. Recycl.* **2024**, *208*, 107737. [CrossRef]
25. Mills, E. Energy-Intensive Indoor Cultivation Drives the Cannabis Industry's Expanding Carbon Footprint. *One Earth* **2025**, *8*, 101179. [CrossRef]
26. Mills, E. The Carbon Footprint of Indoor Cannabis Production. *Energy Policy* **2012**, *46*, 58–67. [CrossRef]
27. Summers, H.M.; Sproul, E.; Quinn, J.C. The Greenhouse Gas Emissions of Indoor Cannabis Production in the United States. *Nat. Sustain.* **2021**, *4*, 644–650. [CrossRef]
28. Ahamed, M.S.; Sultan, M.; Monfet, D.; Rahman, M.S.; Zhang, Y.; Zahid, A.; Bilal, M.; Ahsan, T.M.A.; Achour, Y. A Critical Review on Efficient Thermal Environment Controls in Indoor Vertical Farming. *J. Clean. Prod.* **2023**, *425*, 138923. [CrossRef]

29. Dillis, C.; Butsic, V.; Georgakakos, P.; Portugal, E.; Grantham, T.E. Water Demands of Permitted and Unpermitted Cannabis Cultivation in Northern California. Environ. *Res. Commun.* **2023**, *5*, 025005. [CrossRef]
30. *ISO 14040*; Environmental Management–Life Cycle Assessment–Principles and Framework. International Organization for Standardization: Geneva, Switzerland, 2006.
31. *ISO 14044*; Environmental Management–Life Cycle Assessment–Requirements and Guidelines. International Organization for Standardization: Geneva, Switzerland, 2006.
32. Steubing, B.; Wernet, G.; Reinhard, J.; Bauer, C.; Moreno-Ruiz, E. The Ecoinvent Database Version 3 (Part II): Analyzing LCA Results and Comparison to Version 2. *Int. J. Life Cycle Assess.* **2016**, *21*, 1269–1281. [CrossRef]
33. Konvalina, P.; Neumann, J.; Hoang, T.N.; Bernas, J.; Trojan, V.; Kuchař, M.; Lošák, T.; Varga, L. Effect of Light Intensity and Two Different Nutrient Solutions on the Yield of Flowers and Cannabinoids in *Cannabis sativa* L. Grown in Controlled Environment. *Agronomy* **2024**, *14*, 2960. [CrossRef]
34. European Commission; Joint Research Centre; Institute for Environment and Sustainability. *International Reference Life Cycle Data System (ILCD) Handbook: General Guide for Life Cycle Assessment: Detailed Guidance*; Publications Office: Luxembourg, 2010.
35. Koch, P.; Salou, T. *AGRIBALYSE®: Methodology*, version 1.3; ADEME: Angers, France, 2013.
36. Tyszler, H.B.M.; van der Voet, E.; van Paassen, M.; Braconi, N.; Kuling, L.; Durlinger, B.; Gual, P. *Agri-Footprint 6: Methodology Report*; Parts 1–2; Blonk Sustainability: Gouda, The Netherlands, 2022.
37. Wernet, G.; Bauer, C.; Steubing, B.; Reinhard, J.; Moreno-Ruiz, E.; Weidema, B. The Ecoinvent Database Version 3 (Part I): Overview and Methodology. *Int. J. Life Cycle Assess.* **2016**, *21*, 1218–1230. [CrossRef]
38. Nemecek, T.; Bengoa, X.; Lansche, J.; Roesch, A.; Faist-Emmenegger, M.; Rossi, V.; Humbert, S. *Methodological Guidelines for the Life Cycle Inventory of Agricultural Products*; Version 3.5; World Food LCA Database (WFLDB); Quantis and Agroscope: Lausanne/Zurich, Switzerland, 2019.
39. Ministry of Industry and Trade of the Czech Republic. Renewable Energy Sources 2022–2023. Available online: https://mpo.gov.cz/assets/cz/energetika/statistika/obnovitelne-zdroje-energie/2024/12/Obnovitelne-zdroje-energie-2022-2023_web.pdf (accessed on 10 July 2025).
40. Oenergetice.cz. EnergoStat. Available online: https://oenergetice.cz/energostat (accessed on 10 July 2025).
41. Dijkman, T.J.; Basset-Mens, C.; Antón, A.; Núñez, M. LCA of Food and Agriculture. In *Life Cycle Assessment*; Hauschild, M.Z., Rosenbaum, R.K., Olsen, S.I., Eds.; Springer International Publishing: Cham, Switzerland, 2018; pp. 723–754, ISBN 978-3-319-56474-6.
42. Bernas, J.; Bernasová, T.; Gerstberger, P.; Moudrý, J.; Konvalina, P.; Moudrý, J. Cup Plant, an Alternative to Conventional Silage from a LCA Perspective. *Int. J. Life Cycle Assess.* **2021**, *26*, 311–326. [CrossRef]
43. Hauschild, M.Z.; Rosenbaum, R.K.; Olsen, S.I. (Eds.) *Life Cycle Assessment: Theory and Practice*; Springer International Publishing: Cham, Switzerland, 2018; ISBN 978-3-319-56474-6.
44. Hayashi, K.; Gaillard, G.; Nemecek, T. Life Cycle Assessment of Agricultural Production Systems: Current Issues and Future Perspectives. In *Good Agricultural Practice (GAP) in Asia and Oceania*; Food and Fertilizer Technology Center: Taipei, Taiwan, 2005.
45. Pérez, R.; Argüelles, F.; Laca, A.; Laca, A. Evidencing the Importance of the Functional Unit in Comparative Life Cycle Assessment of Organic Berry Crops. *Environ. Sci. Pollut. Res.* **2024**, *31*, 22055–22072. [CrossRef]
46. Meffo Kemda, M.; Marchi, M.; Neri, E.; Marchettini, N.; Niccolucci, V. Environmental Impact Assessment of Hemp Cultivation and Its Seed-Based Food Products. *Front. Environ. Sci.* **2024**, *12*, 1342330. [CrossRef]
47. Reichel, P.; Munz, S.; Hartung, J.; Präger, A.; Kotiranta, S.; Burgel, L.; Graeff-Hönninger, S. Impact of Three Different Light Spectra on the Yield, Morphology and Growth Trajectory of Three Different *Cannabis sativa* L. Strains. *Plants* **2021**, *10*, 1866. [CrossRef] [PubMed]
48. Zheng, Z.; Fiddes, K.; Yang, L. A Narrative Review on Environmental Impacts of Cannabis Cultivation. *J. Cannabis Res.* **2021**, *3*, 35. [CrossRef] [PubMed]
49. Holzapfel, P.; Bach, V.; Finkbeiner, M. Electricity Accounting in Life Cycle Assessment: The Challenge of Double Counting. *Int. J. Life Cycle Assess.* **2023**, *28*, 771–787. [CrossRef]
50. Šerešová, M.; Štefanica, J.; Vitvarová, M.; Zakuciová, K.; Wolf, P.; Kočí, V. Life Cycle Performance of Various Energy Sources Used in the Czech Republic. *Energies* **2020**, *13*, 5833. [CrossRef]
51. Barros, M.V.; Salvador, R.; Piekarski, C.M.; De Francisco, A.C.; Freire, F.M.C.S. Correction to: Life Cycle Assessment of Electricity Generation: A Review of the Characteristics of Existing Literature. *Int. J. Life Cycle Assess.* **2020**, *25*, 55–56. [CrossRef]
52. Bauer, S.; Olson, J.; Cockrill, A.; Van Hattem, M.; Miller, L.; Tauzer, M.; Leppig, G. Impacts of Surface Water Diversions for Marijuana Cultivation on Aquatic Habitat in Four Northwestern California Watersheds. *PLoS ONE* **2015**, *10*, e0120016. [CrossRef]
53. Butsic, V.; Brenner, J.C. Cannabis (*Cannabis sativa* or *C. Indica*) Agriculture and the Environment: A Systematic, Spatially-Explicit Survey and Potential Impacts. *Environ. Res. Lett.* **2016**, *11*, 044023. [CrossRef]
54. Hassanien, R.H.E.; Li, M.; Dong Lin, W. Advanced Applications of Solar Energy in Agricultural Greenhouses. *Renew. Sustain. Energy Rev.* **2016**, *54*, 989–1001. [CrossRef]

55. Liantas, G.; Chatzigeorgiou, I.; Ravani, M.; Koukounaras, A.; Ntinas, G.K. Energy Use Efficiency and Carbon Footprint of Greenhouse Hydroponic Cultivation Using Public Grid and PVs as Energy Providers. *Sustainability* **2023**, *15*, 1024. [CrossRef]
56. Parkes, M.G.; Azevedo, D.L.; Cavallo, A.C.; Domingos, T.; Teixeira, R.F.M. Life Cycle Assessment of Microgreen Production: Effects of Indoor Vertical Farm Management on Yield and Environmental Performance. *Sci. Rep.* **2023**, *13*, 11324. [CrossRef] [PubMed]
57. Poore, J.; Nemecek, T. Reducing Food's Environmental Impacts through Producers and Consumers. *Science* **2018**, *360*, 987–992. [CrossRef]
58. Jwaideh, M.A.A.; Sutanudjaja, E.H.; Dalin, C. Global Impacts of Nitrogen and Phosphorus Fertiliser Use for Major Crops on Aquatic Biodiversity. *Int. J. Life Cycle Assess.* **2022**, *27*, 1058–1080. [CrossRef]
59. Bartzas, G.; Zaharaki, D.; Komnitsas, K. Life Cycle Assessment of Open Field and Greenhouse Cultivation of Lettuce and Barley. *Inf. Process. Agric.* **2015**, *2*, 191–207. [CrossRef]

Disclaimer/Publisher's Note: The statements, opinions and data contained in all publications are solely those of the individual author(s) and contributor(s) and not of MDPI and/or the editor(s). MDPI and/or the editor(s) disclaim responsibility for any injury to people or property resulting from any ideas, methods, instructions or products referred to in the content.

agronomy

MDPI

Article

Optimizing Vents Opening Configurations and Orientations for Effective Natural Ventilation in Sustainable Greenhouses: A Case Study

Ibrahim M. Al-Helal [1,*], Abdullah A. Alsadon [2], Abdullah A. Ibrahim [2] and Mohamed R. Shady [1]

[1] Department of Agricultural Engineering, College of Food and Agriculture Sciences, King Saud University, P.O. Box 2460, Riyadh 11451, Saudi Arabia; mshady@ksu.edu.sa
[2] Department of Plant Production, College of Food and Agriculture Sciences, King Saud University, P.O. Box 2460, Riyadh 11451, Saudi Arabia; alsadon@ksu.edu.sa (A.A.A.); adrahim@ksu.edu.sa (A.A.I.)
* Correspondence: imhelal@ksu.edu.sa; Tel.: +966-504420213

Abstract

For sustainable greenhouse design, natural ventilation is a vital component; it depends on the local climate. Therefore, optimizing the greenhouse orientation and vent opening configuration is a critical issue that needs to be addressed for a specific location (e.g., the central region of Saudia Arabia). Experiments were conducted in winter, in a curved-roof, single-span, N-S oriented greenhouse that includes roof and side-wall vents. Five different vent opening arrangements were examined. The outside and inside greenhouse environmental parameters were measured, and the ventilation rate ($kg \cdot s^{-1}$) and the number of air exchanges per hour (N_a) were estimated for each opening case using a modified energy balance equation. The results showed that the common wind directions are N-S and NW-SE. For effective ventilation, greenhouses should be oriented in the E-W or NE-SW directions. Opening the side-wall vents exhibited the highest wind-driven ventilation rate that is essential to control temperature and humidity at the crop level, while only opening the roof vents is not recommended. In the central region of Saudi Arabia, natural ventilation is sufficient for operating greenhouses ($\overline{N}_a > 30$). Opening the roof and side-wall vents (combined wind and buoyancy effects) is the most efficient as long as the greenhouse axis is aligned perpendicular to the wind direction. Such information is essential for sustainable greenhouse management in an arid environment.

Keywords: sustainable resources; greenhouse; natural ventilation; arid climate; orientation; vent opening

1. Introduction

In the arid environment (extremely hot and dry weather, with intensive solar irradiance) such as in Saudi Arabia, it is difficult to grow crops, especially vegetables, in the open fields; therefore, greenhouses are used to create an optimal environment for plant growth by controlling the microclimatic conditions [1]. Ventilation of greenhouses is an essential microclimatic parameter that needs to be adjusted for better crop growth. In general, ventilation is used for providing adequate microclimatic conditions by removing excess humidity and accumulated heat energy from the greenhouse [2]. Recently, most greenhouse ventilation studies have focused on the use of natural ventilation, instead of mechanical, to reduce electric energy consumption by greenhouses [1,2]. In the summer seasons of arid regions, natural ventilation is not appropriate. It replaces the inside greenhouse air

with the outside hot air too; therefore, an evaporative cooling system is commonly used to effectively reduce the inside greenhouse air temperature to the appropriate levels [3]. However, in the mild seasons (e.g., winter months), the natural ventilation may be an acceptable, low-cost technique; it may provide an adequate environment for crop growth in the greenhouses, and the operating cost would be reduced [3,4]. Natural ventilation depends on the wind force and its direction, and the temperature difference in air between the inside and outside of the greenhouse. Therefore, natural ventilation is driven by the combined effects of wind and buoyancy forces. This combination may offer, in most cases, an energy-efficient alternative to mechanical ventilation systems. However, the effectiveness of natural ventilation depends on several factors including structural design (that can be controlled such as greenhouse orientation, vents areas and arrangement) and climatic conditions such as the airflow dynamics, ambient air temperature and relative humidity, and radiation intensity (that cannot be controlled in most cases) [4,5].

Specifically, the wind-driven natural ventilation depends on the wind pressure differences between the windward and leeward sides of the greenhouse that create airflow into the greenhouse via its vents. This mainly depends on the number of vents, vent placement, and their opening area in the greenhouse and their opening configuration [5]. Accordingly, the wind direction and the location and the size of vents determine the volume of air exchange rates. In addition, greenhouse orientation is essential in determining the rate of ventilation; for example, aligning the greenhouse to prevailing wind directions enhances airflow efficiency [6]. Buoyancy-driven ventilation (the stack effect), caused by temperature-induced air density differences, drives warm air upward and out through the roof vents while cooler air enters through the lower openings. This mechanism is particularly effective in (i) the tall structures (increasing the height difference between inlet and outlet vents enhances buoyancy-driven airflow) and (ii) the hot climates (thermal gradients are naturally higher, boosting the stack effect) [4,7]. Under real conditions, wind and buoyancy forces often act together to induce natural ventilation. Therefore, understanding their interaction and interplay is essential for optimizing ventilation rate and enhancing its effectiveness. Because the efficiency of natural ventilation depends on the local climatic conditions (the geographic location of the greenhouse), therefore, optimizing the vent's openings and greenhouse orientation is essential to enhance wind-driven ventilation. For example, in Mediterranean climates, the combined side walls and roof ventilators significantly enhanced ventilation rate, reduced internal temperatures and improved humidity control [3–6].

A survey of the previous literature revealed that studies to optimize the vents' opening configurations for maximizing ventilation rate and to achieve optimum microclimatic conditions for crop growth in the desert of arid climate, such as in the central region of Saudi Arabia, are still missing, and more related information is essentially required for greenhouse growers and designers. Therefore, this study aimed to explore the wind directions commonly existing in this region, the optimum greenhouse orientation, and the most efficient vent opening configuration. An experimental, planted greenhouse was used; it includes side-walls and roof ventilators. Five configurations of vent openings were applied to explore the most efficient arrangement that can provide the highest ventilation rate. However, airflow characteristics and their effects on the crop growth behavior and CO_2 and humidity levels in the greenhouse are beyond the scope of this study. Results of this study would be useful for growers, greenhouse designers, and researchers by providing sufficient information for operating efficient, low-cost, environmentally friendly, and sustainable greenhouses in the central region of the Arabian Peninsula.

2. Materials and Methods

2.1. Experimental Set-Up and Vents Opening Configurations

The experiment was conducted in a curved-roof greenhouse, with a floor area of 160 m^2 (8 m × 20 m), covered with a double-layer, hollow-channeled, polycarbonate sheet of 8.15 mm thickness. The eaves and ridges heights are 4 m and 6.5 m, respectively, and the cover-to-floor surface area (ψ) was estimated to be 2.76 (Figure 1). The greenhouse was oriented in the north–south (N-S) direction in the Agricultural Research and Experiment Station, Agriculture Engineering Department, King Saud University (Riyadh, Saudi Arabia, 46°47′ E, longitude and 24°39′ N, latitude), and planted with a mature tomato crop. The radiative properties of the polycarbonate cover of the greenhouse were measured and reported in [8] to be as follows: the transmittance to global solar radiation (200–2500 nm) is 70%, to the photosynthetically active radiation (PAR: 400–700 nm) is 71%, and to the IR-thermal radiation (2500–12,500 nm) is 1%. The greenhouse was naturally ventilated using two identical roof ventilators (vents 3 and 4), and two identical side-wall ventilators (vents 1 and 2) as illustrated in Figure 1. The opening area of each roof vent is 20.9 m^2, and that of each side-wall vent is 22.8 m^2. The vents' opening configurations were arranged into five cases to cover all the possible airflow directions as illustrated in Figure 1. The case-I: opening the side-wall vents (vents 1 and 2), and closing the roof vents (vents 3 and 4); the case-II: opening the roof vents (vents 3 and 4) and closing the side-walls (vents 1 and 2); the case-III: opening the vents 1 and 4, and closing the vents 2 and 3; the case-IV: opening the vents 2 and 3 and closing 1 and 4; the case-V: opening the side-walls and roof ventilators (the vents 1, 2, 3, and 4) as illustrated in Figure 1.

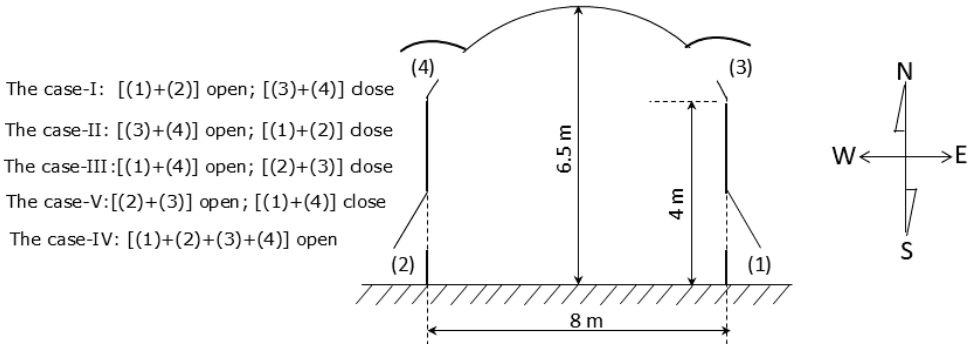


Figure 1. Schematic diagram showing the greenhouse with its ventilators used in the study.

2.2. Measuring the Required Parameters

In mild seasons, natural ventilation may be able to provide an optimal microclimate for crop growth. Therefore, the experiments were conducted on clear sunny winter days in the period from 15 to 30 December 2024; three consecutive days for each opening configuration of vents (Figure 1). The measured parameters were as follows: (i) The inside air temperature and relative humidity (T_i and RH_i) were recorded vertically at the center of the greenhouse in three locations (at 1, 2.5, and 4 m above the floor surface (Figure 2), and the average values were obtained to represent T_i and RH_i. The outside temperature and relative humidity (T_o and RH_o) were recorded outside the greenhouse, at 2 m height above the floor, and at a distance of 4 m from the greenhouse. The air temperature and relative humidity inside and outside the greenhouse were measured using combined temperature-humidity-data-logger sensors (OM-EL-USB2-LCD, Omega Inc., Norwalk, CT, USA). The sensors have a maximum error of ±0.5 °C and ±3% for the air temperature and relative humidity, respectively; a working temperature range of −35 to +80 °C and a relative humidity range of 0 to 100%. The sensors were protected against the solar and thermal radiation effects and have been calibrated before use by the supplier. (ii) The inside and

outside global solar radiation flux (S_i and S_o) were measured using CMP3 pyranometers (Kipp and Zonen, Sterling, VA, USA), having a time response of 18 µs, a maximum error of ±1%, a sensitivity of 5–20 µV $W^{-1} \cdot m^{-2}$, a working temperature range of −40 to +80 °C, and a wavelength range of 300 to 2800 nm. Two pyranometers for measuring S_i were placed at 4 m above the floor at two locations in the greenhouse (Figure 2), and the average value was obtained to represent S_i. A pyranometer to measure S_o was mounted outside the greenhouse at 2 m height above the ground level (Figure 2). The radiation sensors have been calibrated before use by the supplier. The wind speed values (V_w in $m \cdot s^{-1}$) and their directions were measured using wind sonic anemometer (Option-1, Gill Instruments Limited, Lymington, UK), installed over a building, near the greenhouse, 6 m above the ground floor. This just to show the magnitude and direction of the free wind stream, as a meteorological parameter, and its effect on the ventilation rate of a greenhouse having different vent opening configurations. However, measuring the wind speed at the vent opening was excluded because the airflow pattern and the characteristic behavior of air movement through the greenhouse vents are beyond the scope of this study. The wind speed sensor records eight directions of wind (i.e., N, E-W, N-E, E, S-E, S, S-W, and N-W), and the wind speed range of 0 to 60 $m \cdot s^{-1}$. All the measured parameters were recorded every 1 min, averaged every 10 min, and saved in a data logger (CR23X Micrologger, Campbell Scientific, Inc., Logan, UT, USA).

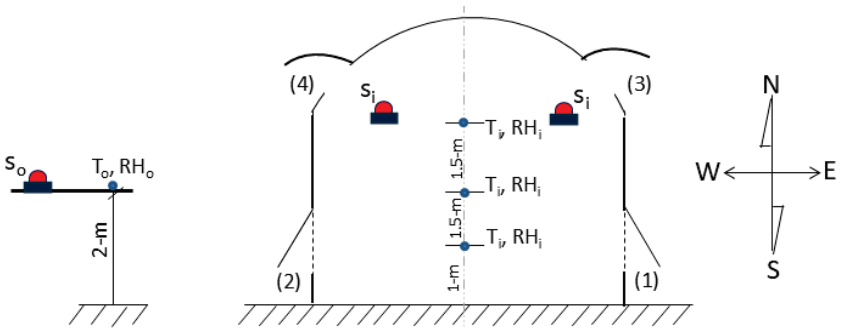


Figure 2. Schematic diagram of the greenhouse showing the locations of sensors used to measure the required parameters (locations of *T* and *RH* sensors, and radiation sensors).

2.3. Determination of the Ventilation Rate

The ventilation rate can be estimated by using either measuring methods [9–12], aerodynamic models [13–15], or energy balance models applied to the greenhouse air [2,16–19]. The aerodynamic models depend on two critical dimensionless coefficients (i.e., the discharge coefficient and the wind coefficient). These coefficients are usually determined by in situ measurements (as the measuring methods) and they differ from one greenhouse to another, and depend on the vents' design, greenhouse location, orientation, and the meteorological parameters outside the greenhouse. On the other hand, ventilation rate can be estimated by applying the sensible heat balance to the greenhouse air [17]. This method requires a determination of the fraction of solar energy used for evaporation in the greenhouse. This fraction depends on the plant and soil characteristics and is difficult to determine correctly, especially when the greenhouse includes an evaporative cooling system in summer [20]. The earliest popular formula used by Mihara (1983) to estimate the natural ventilation rate is based on a fundamental energy balance applied to the greenhouse air under the steady-state condition during the daytime [18]. This formula has been modified by Abdel-Ghany et al. [19] to include the most accurate expression for the overall heat loss coefficient (U) of the greenhouse cover. The U factor has been developed based on the transmitted solar radiation flux into the greenhouse (S_i), the thermal radiation outside and inside the greenhouse, and the convective and radiative heat transfer modes on the inside

and outside surfaces of the cover [21]. Then, the ventilation rate of moist air exchange through the greenhouse envelope is given by

$$\dot{m}_a = \{S_i - \psi U(T_i - T_o)\}/(h_i - h_o) \quad (1)$$

where $\dot{m}_a$ is the ventilation rate of moist air (kg·s^{-1}·m^{-2} [floor area]); S_i is the average solar radiation flux transmitted into the greenhouse (W·m^{-2}); ψ is the cover to floor surface area ratio (A_c/A_f); U is the cover overall heat loss coefficient (W·m^{-2}·°C^{-1}); T_i is the mean dry bulb temperature of air inside the greenhouse (°C); T_o is the dry bulb temperature of the outside air (°C); and ($h_i - h_o$) is the specific enthalpy difference in the moist air between inside and outside the greenhouse (J·kg^{-1}). The U value strongly depended on the environmental conditions inside and outside the greenhouse regardless of the covering material [21]. Therefore, the U factor can be used under the steady- or unsteady-state conditions (i.e., neglecting or considering the thermal mass of the covering material). Detailed analysis of the U factor under unsteady-state conditions for a naturally ventilated greenhouse under different environmental conditions is reported in [19,21], in which the value of U mainly depended on the wind speed outside the greenhouse (V_w) and the temperature difference between inside and outside ($T_i - T_o$). However, the relative humidity of air in the greenhouse has no significant effect [21]. Three-dimensional analysis was applied to the results reported in [21] using the Table Curve-3D package (Ver-4.0, SYSTAT). The U factor was correlated as a function of V_w in m·s^{-1} and ($T_i - T_o$) in °C with a coefficient of determination (R^2) of 0.92 and reported by [19] in the form:

$$U = Exp\left(1.108 - V_w^{0.5}[0.0895 \times \ln(V_w) - 0.359] + 753 \times 10^{-6}(T_i - T_o)^2\right) \quad (2)$$

The specific enthalpy of the moist air (kJ·kg^{-1}) inside and outside the greenhouse (h_i and h_o) can be approximated as a function of the dry bulb temperature (T), and the absolute humidity (ω), inside and outside the greenhouse as [22] by

$$h = (1.007T - 0.026) + \omega(2501 + 1.84T),\ T \text{ in}^\circ\text{C} \quad (3)$$

Using the measured relative humidity (RH_i and RH_o) and dry bulb temperatures inside and outside the greenhouse (T_i and T_o), the corresponding absolute humidity (ω) can be easily estimated by using the psychometric chart or simplified correlations reported in [22]. Once the value of $\dot{m}_a$ was determined, the number of greenhouse air changes per hour (N_a) can be determined as

$$N_a = \dot{m}_a \times 3600/(V_g \rho_a) \quad (4)$$

where ρ_a is the density of moist air in the greenhouse, and V_g is the greenhouse volume (m^3).

3. Results and Discussion

For each vent opening configuration (case-I to case-IV), the measurements were taken for 3 consecutive days (15 days in total). The results showed that the time courses of the measured meteorological conditions (T_o, RH_o, S_o, and V_w) were nearly similar during the 15 days of experiments. The transmitted solar radiation flux into the greenhouse (S_i) is the most important parameter that affects the inside air temperature and humidity (T_i and RH_i) and the natural ventilation rate as well. Figure 3 illustrates the transmitted solar radiation fluxes (S_i) taken for two consecutive days for each opening case. The diurnal variations in S_i through the different days of measurements were almost similar (Figure 3). Therefore,

for simplicity, the results of one day (24 h) was selected for each case (case-I to case-IV) to be presented in the upcoming results.

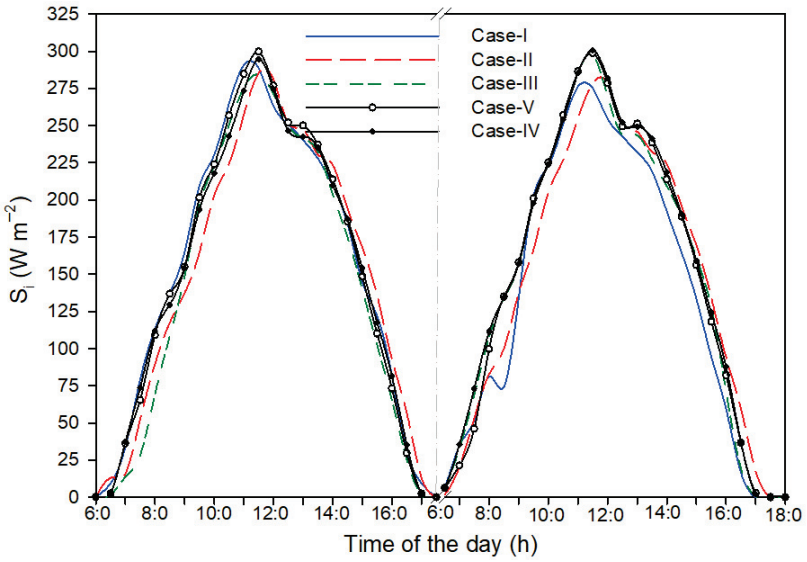


Figure 3. Diurnal variation in the transmitted solar radiation flux (S_i) into the greenhouse during two consecutive days were selected for each opening configuration (case-I to case-IV).

3.1. Wind Characterization

Diurnal variation in the wind speeds (V_w) for the selected five days (one day for each opening case) is illustrated in Figure 4. The highest wind speed was recorded when the side-wall vents were opened (the case-I), followed by the case-II (the roof vents were opened). For more clarification, a simple statistical analysis was applied to the data in Figure 4 and the results for each opening case are summarized in Table 1. This includes the daily mean of wind speed ($\overline{V}_w$), standard deviation (STD), and standard error (STE). The highest $\overline{V}_w$ value was recorded when the side-wall vents were opened (case-I), while the lowest was recorded when one roof and one side-wall vent were opened (case-III). The highest daily variation in V_w was observed when the roof vents were opened (case-II, STD = 1.37); while the lowest was when one roof and one side-wall vent were opened (case-III, STD = 0.58).

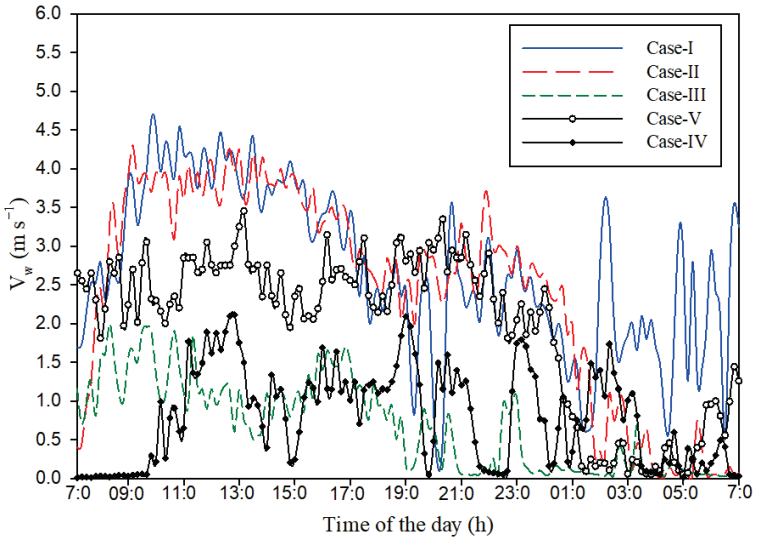


Figure 4. Time courses of the wind speed during a selected five days (one day for each opening configuration case).

Table 1. Descriptive statistics of wind speeds illustrated in Figure 4 for the five days of the experiment.

	Case-I	Case-II	Case-III	Case-V	Case-IV
$\overline{V}_w$ (m·s^{-1})	2.7	2.4	0.69	1.96	0.8
STD	1.04	1.37	0.58	1.01	0.623
STE	0.087	0.11	0.049	0.084	0.052

Wind speed and direction cannot be controlled (i.e., meteorological parameters), and the magnitude of wind speed alone is meaningless when studying the ventilation rate of a greenhouse; therefore, it should be allocated with the wind direction relative to the greenhouse orientation and vent opening configuration. Accordingly, this study explored the wind speed and direction during the 15 days of experiment as illustrated in Figure 5. The wind directions depicted in Figure 5 are common for most of the year and months in the central region of Saudi Arabia, not only during the experiment. To confirm this claim, data of wind speed and its direction for four consecutive months (November 2024–February 2025) could be collected from a meteorological station in the KSU campus, and are depicted in Figure 6. Based on Figure 6, the wind directions are mainly in the north and south directions (N-S or S-N), and sometimes in the NW and SE directions. This was also illustrated in the cases-I, II, III, and IV (Figure 5). It is uncommon (rarely) to be from the west to east direction (W-E) as in the case-V (Figure 5) and emphasized in Figure 6. Accordingly, orienting the greenhouse in the N-S direction is not appropriate, because the wind direction is, in common, parallel to the vent opening. To enhance the ventilation effectiveness, the wind direction should be perpendicular to the vent opening, and the greenhouse should be oriented in the E-W direction or in the NE-SW direction as illustrated in Figures 5 and 6. In general, the greenhouse should be oriented perpendicular to the prevailing wind direction to enhance the natural ventilation effectiveness.

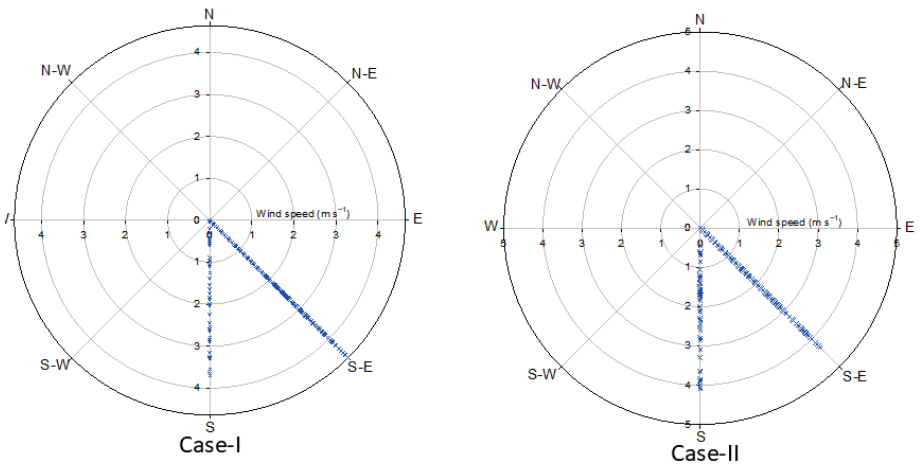


Figure 5. *Cont.*

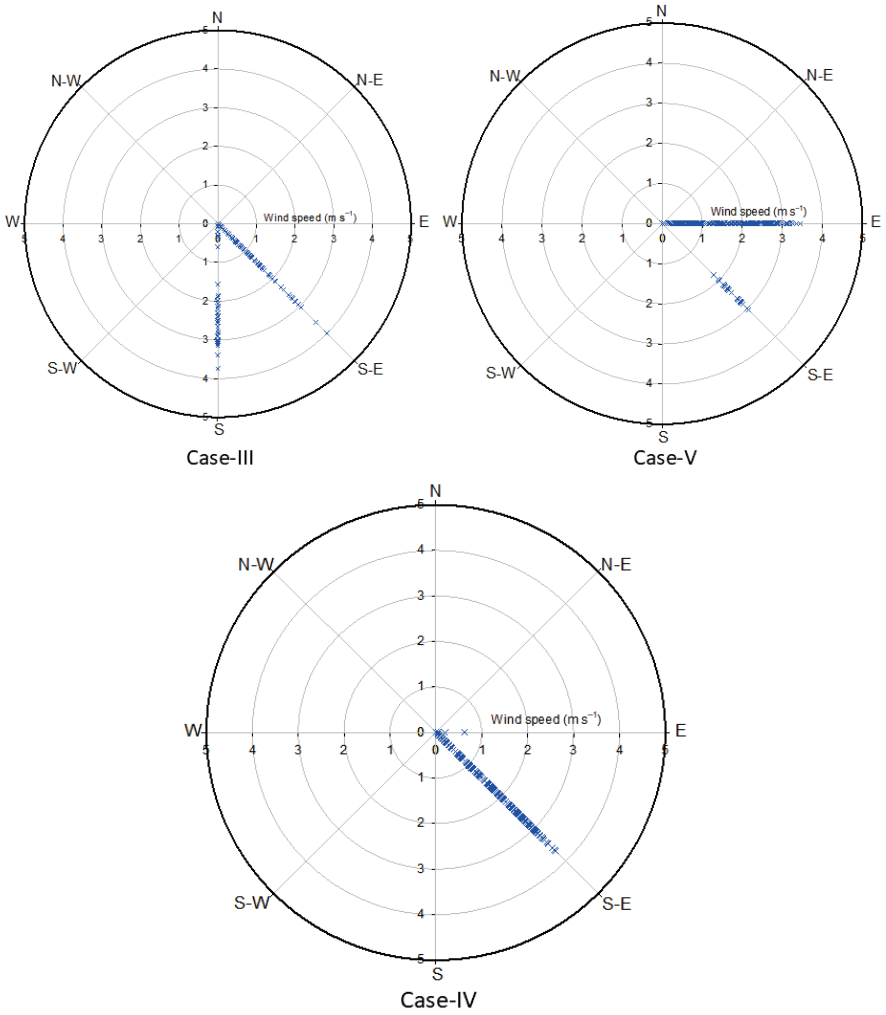


Figure 5. Polar plots representing the wind speeds and directions during the 15 days of experiment, (3 consecutive days for each opening configuration).

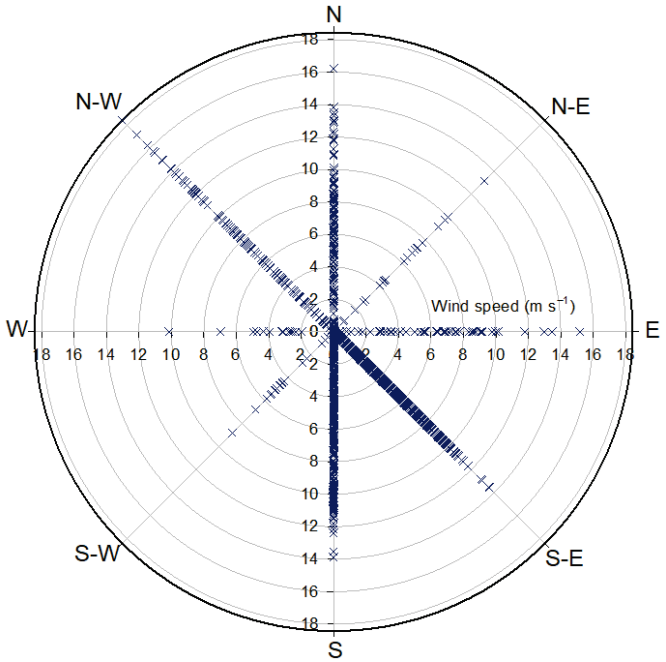


Figure 6. Polar plot representing the wind speeds and directions for 4 months (November 2024–February 2025), could be obtained from a meteorological station at KSU campus.

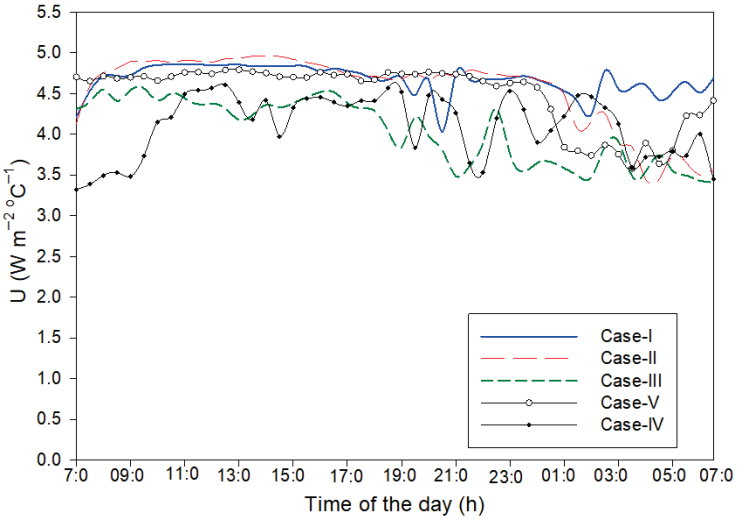


Figure 7. Diurnal variation in the overall heat losses coefficient (*U*) estimated for the five selected days (one day for each opening configuration) using Equation (2).

Using the enthalpy difference (h_i-h_o) in Equation (1) is more convenient than the form of sensible heat balance used in previous studies [17,23–26]. The enthalpy of air (Equation (3)) includes the thermal energy content of water vapor inside or outside the greenhouse in addition to the sensible heat content of the dry air. For the same 5 days selected in Figures 4 and 7, the diurnal variation in (h_i-h_o) is illustrated in Figure 8 for the five opening configurations (case-I to case-IV). Based on Equation (1), the low enthalpy difference is usually allocated with a higher ventilation rate (opening the side-wall vents, case-I in Figure 8). Opening the two roof vents together (case-II in Figure 8) showed the highest enthalpy difference and, consequently, would be allocated with the lowest ventilation rate.

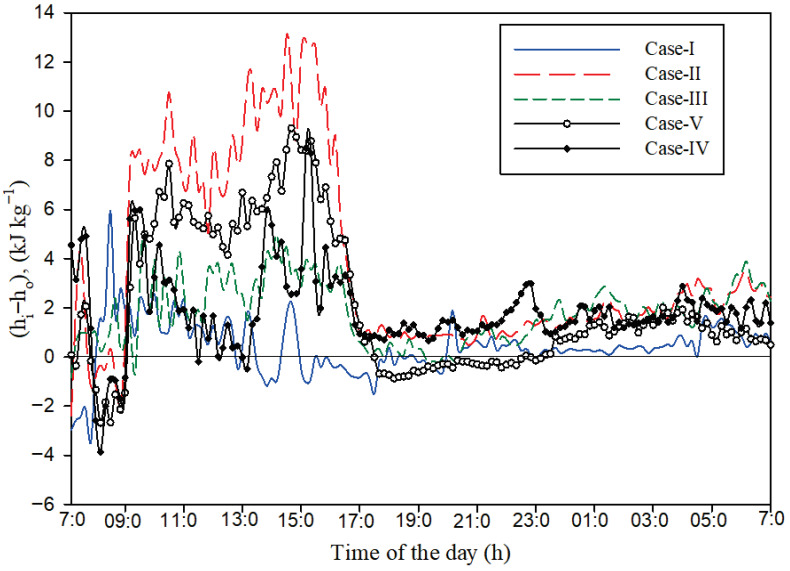


Figure 8. Diurnal variation in the enthalpy difference (h_i-h_o) between inside and outside the greenhouse, estimated for the five selected days (one day for each opening case).

In general, the buoyancy-driven ventilation (the stack effect) induced by the vertical density differences in the greenhouse air causes the warmer air to rise up and exit through the roof vents, while cooler air should enter the greenhouse through lower side-wall openings. Therefore, closing the side-wall vents and opening the roof vents would only deteriorate the stack effect and the buoyancy-driven ventilation as well (case-II, Figure 9). Moreover, opening the roof vents at the level of the hot air inside the greenhouse will

also deteriorate the wind-driven mechanism and allow only the air diffusion mechanism to exchange air through the greenhouse roof vents. Accordingly, opening the side-wall vents is more efficient in enhancing the ventilation rate than the roof vents. For an efficient ventilation rate, the side-wall and roof vents should be opened and aligning the greenhouse perpendicular to the wind direction; this is to enhance both wind-driven and buoyancy-driven ventilation. The negative values of (h_i-h_o) in Figure 8 around sunrise and sunset times are the result of the inside greenhouse air temperature being lower than outside during the early morning and late afternoon.

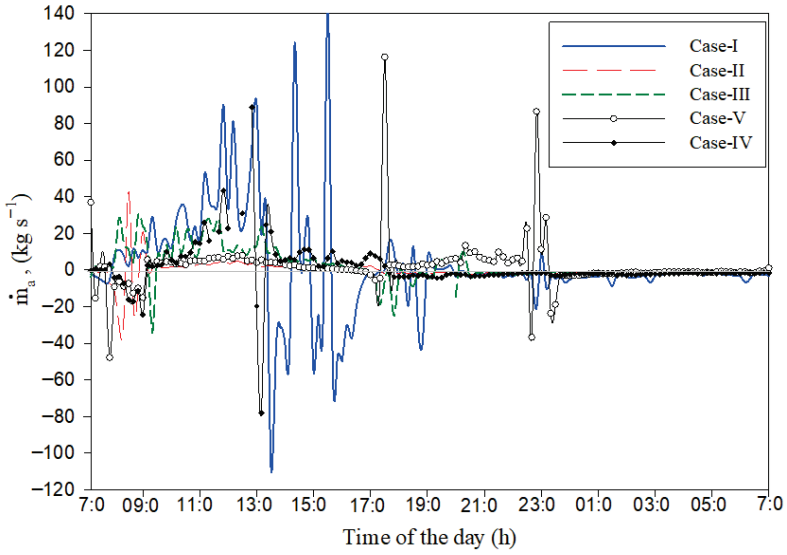


Figure 9. Diurnal variation in the ventilation rate ($\dot{m}_a$) in kg·s^{-1} estimated from Equation (1) for the five opening cases.

3.2. The Estimated Ventilation Rate

As we have mentioned previously, in the hot summer seasons of arid regions, natural ventilation is not enough for greenhouses to remove heat accumulation; it should be replaced with mechanical ventilation with evaporative cooling and shading [27]. Therefore, the experiment of this study was conducted in the winter season to examine the possibility of using natural ventilation alone, in winter months, for low-cost sustainable greenhouse operation. Figure 9 illustrates the natural ventilation rate ($\dot{m}_a$) estimated using Equation (1) in kg of air per second. The negative values of $\dot{m}_a$ in Figure 9 represent the opposite direction of airflow when the inside air temperature (T_i) is lower than that of the outside air (T_o). In the naturally ventilated greenhouses, in winter season, it is common for T_i to be lower than T_o in the morning and afternoon, and sometimes during the nighttime. In this case, the warm air enters the greenhouse from the roof (the upper) vents, and the cold air exits from the side-wall (the lower) vents. However, when T_i is higher than T_o (during most of the daytime), the inside warm air exits the greenhouse from the upper vents and the cold air enters from the side-wall (lower) vents.

These mechanisms make the two directions of airflow and the negative and positive values of the estimated $\dot{m}_a$ in Figure 9. The results of $\dot{m}_a$ in Figure 9 are in accordance with the results in Figure 8 and have emphasized four facts: (i) opening the side-wall vents significantly enhances the wind-driven ventilation rate at the crop level and is very useful for plant growth behavior (case-I), (ii) opening the roof vents alone is not recommended (case-II), (iii) opening the roof and side-wall vents in opposite directions (case-III and case-V) would be effective if the greenhouse was aligned longitudinally perpendicular to the wind direction, and (v) opening all the side-wall and roof vents (case-IV) would be more efficient if the greenhouse was aligned properly to prevailing wind directions. Moreover,

most of the existing greenhouses in the study region are CO_2 enriched and depend on the ambient CO_2 levels because they are used mainly for growing vegetable crops. Therefore, opening the side-walls and roof vents is strongly recommended.

The number of air exchange rates per hour (N_a) is commonly used to represent the required ventilation level for greenhouses; it depends on several parameters (e.g., the crop type, climate conditions, and ventilation method). Based on the literature, a minimum rate of 30 (h^{-1}) is able to maintain CO_2 levels for photosynthesis and prevent humidity buildup in the greenhouses. An optimum range of N_a from 60 to 90 (h^{-1}) is common for most crops, ensuring proper temperature control, humidity regulation, and CO_2 availability in the greenhouse for better crop growth [28]. However, in hot climates, a maximum rate of 180 (h^{-1}) is required to prevent overheating in the greenhouse [29]. The values of N_a estimated, using Equation (4), for the selected five days for the five cases of vent opening are depicted in Figure 10.

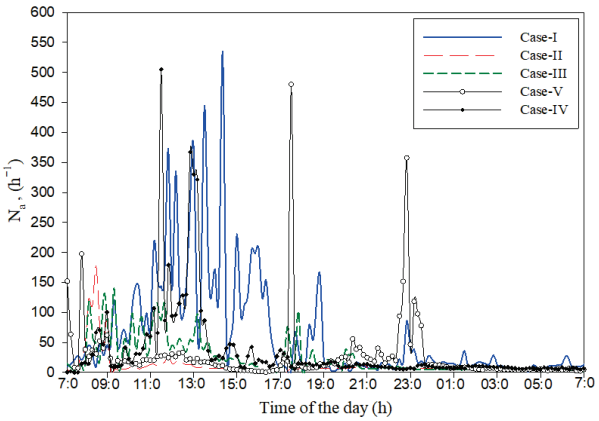


Figure 10. Diurnal variation in number of air exchange rate, N_a (h^{-1}) estimated from Equation (4) for the five opening cases.

A simple statistical analysis was applied to the data in Figure 10, and the results of each opening case (i.e., the mean value of the number of air exchange ($\overline{N_a}$), standard deviation (STD), and standard error (STE) are summarized in Table 2.

Table 2. Statistical analysis for the data in Figure 10 showing $\overline{N_a}$, STD, and STE of each opening configuration.

	Case-I	Case-II	Case-III	Case-V	Case-IV
$\overline{N_a}$ (h^{-1})	63.7	11.2	23.8	26.2	33.2
STD	90.15	21.7	30.2	55.5	67.2
STE	7.5	1.8	2.5	4.6	5.6

For the five opening cases, the level of N_a (in Figure 10) is higher during the daytime than nighttime for all opening cases because, during the daytime, ventilation is driven by the combination of the buoyancy and wind effects; however, during nighttime, ventilation is driven mainly by the wind effect. Based on Table 2, opening the side-wall vents (case-I) in the crop level exhibited the maximum ventilation rate ($\overline{N_a}$ = 63.7 h^{-1}) that is essential for better crop growth. Opening all vents (case-IV) also exhibited the optimum ventilation rate ($\overline{N_a} > 30$ h^{-1}). In addition, opening one roof and one side-wall vent (case-III and V) is a promising method if the greenhouse was oriented properly to enhance ventilation rates. The airflow in the greenhouse is steadier in the cases-III and V, (STD = 30.2 and 55.5, respectively) comparing to the cases-I and IV (STD = 90.15 and 67.2, respectively). Opening the roof vents alone (case-II) is not recommended at all, because the two roof vents are in

the hot air level; this deteriorates the buoyancy and wind effects. Even though in case-IV, all the side-wall and roof vents were opened, the value of $\overline{N_a}$ was 33.2 (h^{-1}) comparing with 63.7 (h^{-1}) when only the side-wall vents were opened (case-I); this is mainly attributed to the lower wind speed ($\overline{V}_w$ = 0.8 m·s^{-1}) compared with 2.7 m·s^{-1} of case-I (Tables 1 and 2).

3.3. Quantification of Ventilation Regime

Over the three days measured for each opening case, the ventilation rate ($\dot{m}_a$ in kg·s^{-1}) was quantified into three regimes according to the criteria reported in several greenhouse ventilation studies [30]. Based on the free wind stream velocities (V_w), the criteria are three categories: if [$V_w \leq 1$ m·s^{-1}], buoyancy is a substantial driver; if [$1 < V_w \leq 2$ m·s^{-1}], there is a combined regime of wind and buoyancy effect; and if [$V_w > 2$ m·s^{-1}], the wind effect is dominant. Table 3 summarized this quantification (the contribution percent).

Table 3. Quantification of the ventilation rate ($\dot{m}_a$) into three regimes for different opening cases.

Opening Cases	Buoyancy-Driven, % ($V_w \leq 1$ m·s^{-1})	Combined Regime, % ($1 < V_w \leq 2$ m·s^{-1})	Wind-Driven, % ($V_w > 2$ m·s^{-1})	$\overline{V}_w$ (m·s^{-1})
Case-I	18	14.5	67.5	2.7
Case-II	23.7	19.5	56.8	2.4
Case-III	24.7	7.6	67.6	0.69
Case-V	43.3	28.8	28.5	1.96
Case-IV	3.8	36	60	0.8

Even though the wind speed level was low ($\overline{V}_w$ = 0.8 m·s^{-1}, case-IV) opening the side-walls and roof ventilators deteriorated the buoyancy effect (contributed by 3.8%). In all cases of opening arrangements, the contribution of wind effect was dominant except in case-V. In this case, roof and side-wall vents were opened and both were not facing the wind direction (see Figures 1 and 6). In general, opening roof and side-wall ventilators would make the effect of wind force and buoyancy effect comparable if the greenhouse was properly oriented.

4. Conclusions and Recommendation

For sustainable low-cost greenhouse operation, natural ventilation can replace the energy-consuming mechanical ventilation in the central region of Saudi Arabia. For this purpose, experiments were conducted in a curved-roof, N-S oriented greenhouse that includes two roof vents and two side-wall vents. Five different opening configurations were examined to find the best opening arrangement that enhances the ventilation rate. Based on the results of this study, the following points could be drawn:

- Opening the side-wall vents is essential, exhibiting the highest ventilation rate; however, opening the roof vents alone is not recommended for greenhouse ventilation.
- Opening the roof and side-wall vents (in opposite directions) is effective if the greenhouse is properly oriented to make the vent opening perpendicular to the wind direction.
- According to the common wind direction in the central region of Saudi Arabia, the greenhouse should be oriented in the E-W or in the NE-SW directions.
- In winter seasons, natural ventilation for greenhouses is sufficient and can effectively replace the energy-consuming mechanical ventilation. However, in the summer, shading and evaporative cooling is required because ventilation replaces the inside greenhouse air with the outside hot air.

Future research is needed for optimizing greenhouse design, shape, and covering materials, and exploring hybrid ventilation systems by integrating renewable energy re-

sources and smart materials to enhance the efficiency of natural ventilation in arid climates. Expansions of this study should include different locations in the Arabian Peninsula, aiming to provide operational protocol for the greenhouse ventilation schedule in an arid environment.

Author Contributions: Conceptualization, I.M.A.-H. and A.A.A.; methodology, I.M.A.-H., A.A.A. and A.A.I.; software, M.R.S. and I.M.A.-H.; validation, I.M.A.-H., A.A.A., M.R.S. and A.A.I.; formal analysis, A.A.A., A.A.I. and I.M.A.-H.; investigation, I.M.A.-H., M.R.S. and A.A.A.; resources, I.M.A.-H., A.A.A., A.A.I. and M.R.S.; data curation, I.M.A.-H., A.A.A., M.R.S. and A.A.I.; writing—original draft, I.M.A.-H. and A.A.A.; writing—review and editing, I.M.A.-H., A.A.A., A.A.I. and M.R.S.; visualization, I.M.A.-H. and A.A.A.; supervision, I.M.A.-H. and A.A.A.; project administration, I.M.A.-H. All authors have read and agreed to the published version of the manuscript.

Funding: This research received no external funding.

Data Availability Statement: Data would be available upon request.

Acknowledgments: The authors would like to express their gratitude to the Ongoing Research Funding program, (ORF-2025-1394), King Saud University, Riyadh, Saudi Arabia for providing funding support for this research.

Conflicts of Interest: The authors declare no conflicts of interest.

Abbreviations

A_c	Surface area of the greenhouse cover, m^2
A_f	Surface area of the greenhouse floor, m^2
h_i	Enthalpy of the inside greenhouse air, $kJ \cdot kg^{-1}$
h_o	enthalpy of the outside greenhouse air, $kJ \cdot kg^{-1}$
$\dot{m}_a$	Ventilation mass flow rate, $kg \cdot s^{-1}$
N_a	Number of air exchange rate, h^{-1}
$\overline{N_a}$	Mean value of N_a
S_i	Solar radiation flux in the greenhouse, $W \cdot m^{-2}$
S_o	Solar radiation flux outside the greenhouse, $W \cdot m^{-2}$
T_i	Temperature of air in the greenhouse, °C
T_o	Temperature of air outside the greenhouse, °C
U	Overall heat transmission coefficient, $W \cdot m^{-2} \cdot °C^{-1}$
V_g	Volume of air in the greenhouse, m^3
V_w	Wind speed, $m \cdot s^{-1}$
$\overline{V}_w$	Daily average of wind speed, $m \cdot s^{-1}$
ρ_a	Density of air, $kg \cdot m^{-3}$
ψ	Cover to floor area ratio,
ω	Absolute humidity of air, kg of water vapor/kg dry air

References

1. Alsadon, A.A.; Al-Helal, I.M.; Ibrahim, A.; Abdel-Ghany, A.M.; Al-Zaharani, S.; Ashour, T. The effects of plastic greenhouse covering on cucumber (*Cucumis sativus* L.) growth. *Ecol. Eng.* **2016**, *87*, 305–312. [CrossRef]
2. Al-Helal, I.M.; Waheeb, S.A.; Shady, M.R.; Abdel-Ghany, A.M. Modified thermal model to predict the natural ventilation of greenhouses. *Energy Build.* **2015**, *99*, 1–8. [CrossRef]
3. Al-Ajlouni, M. Natural ventilation in greenhouses: Principles, design, and applications. *J. Agric. Eng.* **2020**, *13*, 58–72.
4. Raji, B.A.; Lal, S. Natural ventilation and its application in hot climates. *Renew. Energy Rev.* **2019**, *8*, 120–132.
5. Jafari, A.; Tavakol, A. Design and optimization of natural ventilation systems for greenhouses. *Energy Build.* **2018**, *166*, 71–82.
6. Pereira, L.S.; Rivas, R. Greenhouse climate control in hot regions. *Agric. Sys.* **2017**, *152*, 58–75.
7. Boulard, T.; Baille, A. Modelling and measurement of greenhouse ventilation. *Agric. For. Meteorol.* **1995**, *75*, 33–51.

8. Abdel-Ghany, A.M.; Picuno, P.; Al-Helal, I.M.; Alsadon, A.A.; Ibrahim, A.; Shady, M.R. Radiometric characterization, solar and thermal radiation in a greenhouse as affected by shading configuration in an arid climate. *Energies* **2015**, *8*, 13928–13937. [CrossRef]
9. Parra, J.P.; Baeza, E.; Montero, J.I.; Bailey, B.J. Natural ventilation of Parral greenhouses. *Boisyst. Eng.* **2004**, *87*, 355–366. [CrossRef]
10. Katsoulas, N.; Bartzanas, T.; Boulard, T.; Mermier, M.; Kittas, C. Effect of vent openings and insect screens on greenhouse ventilation. *Biosyst. Eng.* **2006**, *93*, 427–436. [CrossRef]
11. Samer, M.; Ammon, C.; Loebsin, C.; Fiedler, M.; Berg, W.; Sanftleben, P.; Brunsch, R. Moisture balance and tracer gas technique for ventilation rates measurements and greenhouse gases and ammonia emissions quantification in naturally ventilated buildings. *Build Environ.* **2012**, *50*, 10–20. [CrossRef]
12. Cui, S.; Cohen, M.; Stabat, P.; Marchio, D. CO_2 tracer gas concentration decay method for measuring air change rate. *Build. Environ.* **2015**, *84*, 162–169. [CrossRef]
13. Kittas, C.; Bartzanas, T. Greenhouse microclimate and dehumidification effectiveness under different ventilator configurations. *Build Environ.* **2007**, *42*, 3774–3784. [CrossRef]
14. Montero, J.I.; Anton, A.; Muñoz, P. Discharge coefficients of greenhouse windows with insect-proof screens. *Biosyst. Eng.* **2001**, *81*, 399–407. [CrossRef]
15. Fatnassi, H.; Boulard, T.; Poncet, C. Optimization of greenhouse insect-proof screens with computational fluid dynamics. *Biosyst. Eng.* **2006**, *93*, 301–312. [CrossRef]
16. Teitel, M. Greenhouse ventilation: Theory and practice. *Acta Hortic.* **2017**, *1170*, 243–248.
17. Seginer, I. Alternative design formulae for the ventilation rate of greenhouses. *J. Agric. Eng. Res.* **1997**, *68*, 355–365. [CrossRef]
18. Mihara, Y. *Fundamental and Practice of Greenhouse Design*, 1st ed.; Yokendo Inc.: Tokyo, Japan, 1983; pp. 160–169. (In Japanese)
19. Abdel-Ghany, A.M. Energy balance equation for natural ventilation of greenhouses under unsteady–state conditions. *Middle-East J. Sci. Res.* **2011**, *10*, 286–293.
20. Al-Helal, I.M.; Abdel-Ghany, A.M. Energy Partition and conversion of solar and thermal radiation into sensible and latent heat in a greenhouse under arid conditions. *Energy Build.* **2011**, *43*, 1740–1747. [CrossRef]
21. Abdel-Ghany, A.M.; Kozai, T. On the determination of the overall heat transmission coefficient and soil heat flux for a fog-cooled, naturally ventilated greenhouse: Analysis of radiation and convection heat transfer. *Energy Conver. Manag.* **2006**, *47*, 2612–2628. [CrossRef]
22. Abdel-Ghany, A.M.; Goto, E.; Kozai, T. Evaporation characteristics in a naturally ventilated, fog-cooled greenhouse. *Renew. Energy* **2006**, *31*, 2207–2226. [CrossRef]
23. Georgios, K.S. Temperature control and energy conservation in a plastic greenhouse. *J. Agric. Eng. Res.* **2001**, *80*, 251–259.
24. Swinkels, G.L.A.M.; Sonneveld, P.J.; Bot, G.P.A. Improvement of greenhouse insulation with restricted transmission loss through zigzag covering material. *J. Agric. Eng. Res.* **2001**, *79*, 91–97. [CrossRef]
25. Nijskens, J.; Deltour, J.; Coutisse, S.; Nisen, A. Heat transfer through covering materials of greenhouses. *Agric. For. Meteorol.* **1984**, *33*, 193–214. [CrossRef]
26. Zhang, Y.; Gauthier, L.; de Halleux, D.; Dansereau, B.; Gosselin, A. Effect of covering materials on energy consumption and greenhouse microclimate. *Agric. For. Meteorol.* **1996**, *82*, 227–244. [CrossRef]
27. Ahemd, H.A.; Al-Faraj, A.A.; Abdel-Ghany, A.M. Shading greenhouses to improve the microclimate, energy and water saving in hot regions: A review. *Sci. Hortic.* **2016**, *201*, 36–45. [CrossRef]
28. Baytorun, A.N.; Üstün, S.; Akyüz, A.; Önder, D. Determination of ventilation openings ratio in greenhouses under mediterranean climate conditions. *Turkish J. Agric. Food Sci. Tech.* **2017**, *5*, 409–415. [CrossRef]
29. Li, Y.; Zhao, S.; Dai, A.; Zhang, J.; Fan, Z.; Ding, T. Study on the natural ventilation model of a single-span plastic greenhouse in a high-altitude area. *Agronomy* **2024**, *14*, 2166. [CrossRef]
30. Kim, H.-K. Evaluating the ventilation performance of single-span plastic greenhouses with continuous screened side openings. *Agronomy* **2024**, *14*, 1447. [CrossRef]

Disclaimer/Publisher's Note: The statements, opinions and data contained in all publications are solely those of the individual author(s) and contributor(s) and not of MDPI and/or the editor(s). MDPI and/or the editor(s) disclaim responsibility for any injury to people or property resulting from any ideas, methods, instructions or products referred to in the content.

agronomy

MDPI

Article

Integrating Management and Digital Tools to Reduce Waste in Plant Protection Process

Marianna Cardi Peccinelli [1], Marcos Milan [2] and Thiago Libório Romanelli [2,*]

[1] Graduate Program on Agricultural Systems Engineering, Luiz de Queiroz College of Agriculture, University of Sao Paulo, Sao Paulo 13418-900, SP, Brazil; mcpeccinelli@gmail.com
[2] Department of Biosystems Engineering, Luiz de Queiroz College of Agriculture, University of Sao Paulo, Sao Paulo 13418-900, SP, Brazil; macmilan@usp.br
* Correspondence: romanelli@usp.br

Abstract

The search for higher efficiency in agribusiness supports the adoption of digital tools and Lean Production principles in agricultural spraying, a crucial operation for crops. Spraying is essential to ensure yield, quality, cost efficiency, and environmental protection. This study analyzed operational data from self-propelled sprayers in soybean and corn fields, classifying hours, calculating efficiencies, and applying statistical process control. Efficiencies were investigated by combining Lean Production principles with CAN-based digital monitoring, which enabled the identification of non-value-adding activities and supported the real-time management of spraying operations. The results showed that productive time accounted for 41.2% of total recorded hours, corresponding to effective operation and auxiliary tasks directly associated with the execution of spraying activities. A high proportion of unrecorded hours (21.2%) was also observed, reflecting discrepancies between administrative work schedules and machine-logged data. Additionally, coefficients of variation for operational speed and fuel consumption were 12.1% and 24.0%, respectively. Correcting special causes increased work capacity (4.9%) and reduced fuel consumption (0.9%). Economic simulations, based on efficiencies, operating parameters of the sprayer, and cost indicators, indicated that increasing scale reduces costs when installed capacity is carefully managed. Integrating telemetry with Lean Production principles enables real-time resource optimization and waste reduction.

Keywords: lean production; digital agriculture; precision agriculture; smart farm; agricultural mechanization

1. Introduction

Considered a Western model derived from the Toyota Production System (TPS), Lean Production is a management philosophy that seeks to maximize product or service value by eliminating waste. In Lean, waste is considered anything that does not add value to the final product or the customer: unnecessary transportation, excessive inventory, unnecessary movement, waiting, overproduction, overprocessing, and defects. Initially applied in industry, it has been adopted by several sectors, including the manufacture of prefabricated steel structures for buildings, resulting in a 34% reduction in time and a 16% reduction in costs [1–3].

Case studies and surveys have demonstrated that Lean tools, such as 5S, standard operating procedures, control charts, and value stream mapping, enhance operational efficiency, reduce waste, and foster safer and more organized farm environments. A survey of

132 fruit growers in South Africa found that larger farms implemented Lean concepts more easily, yielding consistent sustainability benefits. At a fruit distributor for short-shelf-life products, adopting Lean reduced losses, increased process efficiency, shortened cycle times, and optimized lead time. On dairy farms, the use of these concepts increased production and benefited animal health, and the application of 5S and standard operating procedures promoted a safer and more organized environment, improving process efficiency. Process stabilization is an essential requirement for reducing waste and increasing operational efficiency [4–6]. The integration of Lean and Green Production approaches allows agricultural systems to simultaneously pursue economic and environmental benefits, as demonstrated in studies that applied sustainable value stream mapping and process optimization on rural properties. In this case, Green Production is a concept related to practices that emphasize environmental sustainability in agribusiness through the rational use of inputs, improved resource utilization, and waste reduction [7].

In agriculture, one of the most important operations is spraying pesticides. It plays a vital role in crop protection, directly affecting productivity, quality, and economic outcomes, while also impacting the environment. The efficiency of this process depends not only on the sprayer design but also on operational parameters such as travel speed, nozzle type, working width, and control system precision. Variations in spray speed and control influence deposition, droplet size distribution, and drift potential, with significant effects on application quality and the environment. Technologies like application rate controllers and automatic sectioning systems have been introduced to reduce overlap, minimize application errors, and ensure more consistent deposition under varying field conditions. Localized spraying prevents unnecessary application of products, promoting less volume application, reduced costs, and less environmental impact [8–11].

In this context, variable rate spreading (VRT) emerges as a promising alternative to reduce waste and mitigate environmental impacts. By adjusting the application rate according to crop and field conditions, VRT minimizes excessive input use, improves application accuracy, and reduces the risks of drift and environmental hazards [12,13]. Although it involves higher investment costs and greater operational complexity, studies demonstrate its potential to increase pesticide use efficiency and make pollution practices more sustainable, reconciling economic and environmental benefits [14,15].

In spraying operations, only the time actually spent applying the pesticide, at the correct dose and location, adds value to the process. All other associated activities, such as machine maneuvers, refueling operations, and idle time, represent forms of waste. Most research focuses on isolated aspects, whether in the development of application technologies or in the ad hoc evaluation of operational indicators, without considering the combined application of management and sustainability tools. Given the importance of reducing inefficiencies and the need for real-time decision-making, and the fact that few studies have addressed the application of waste reduction concepts in real time and under field conditions, this study aims to analyze critical variables of the spraying process from the perspective of operational efficiency and waste reduction in soybean and corn crops.

2. Material and Methods

The study was conducted during the 2021/2022 harvest in commercial areas located in the state of Mato Grosso, Brazil (10°03′ S, 54°55′ W; altitude: 280 m), characterized by an average annual rainfall of 1721 mm and an average temperature of 24.1 °C. The total area covered approximately 6100 hectares, divided into 48 plots for soybean and corn cultivation.

Two self-propelled sprayers equipped with 183 kW (245 hp) engines and 36.0 m wide spray booms were used. Operational data—including equipment-related variables,

fuel consumption, engine speed, operating pressure, and ground speed—were obtained from the Controller Area Network (CAN) and integrated with GNSS (Global Navigation Satellite System) receivers. The data was captured at a frequency of 0.2 Hz and made available by an agricultural machinery company. The classification of operational events was obtained from the sprayers' on-board computer, which automatically recorded the allocation of time between different field activities, made available via commercial software. Manual records of 39 previously defined operational events were also integrated to ensure consistency. The 36.0 m boom enabled coverage of large areas per pass but required careful management of section overlap, particularly in irregularly shaped fields [16]. An average overlap of 4.0% was considered, resulting in an effective working width of 34.6 m, which was incorporated into the calculation of operational field capacity (ha h^{-1}). This study was structured in five main stages: (i) data collection and transmission; (ii) data processing; (iii) grouping; (iv) analysis; and (v) determination of operational costs.

In the first stage, data captured by two sprayers were transmitted via the internet to a cloud server and subsequently accessed through the company's management system. Data were collected during the 2021/2022 harvest for 168 days. Administrative work shifts (AWs) consisted of two daily shifts of 10 h each. Operational data include: timestamps (with millisecond resolution); machine status (operating or stopped); displacement speed (km h^{-1}); fuel consumption per time (L h^{-1}) and per area (L ha^{-1}). Specifically for spraying operations, the following data were recorded: dosage applied (L ha^{-1}), sprayer operating pressure (psi—pounds per square inch), overlap area (ha), and overlap percentage (%). The system also allows operators to enter up to 39 reasons for downtime, previously defined by company management. Additionally, it is mandatory to enter information such as the operator's identification, the field area (ha), product specifications, and the respective work order opening.

During the data processing stage, records were organized chronologically based on timestamps (tn). The time differences between consecutive records (tn + 1 − tn), expressed in seconds, were determined to define the intervals corresponding to each event identified by a specific code. The times associated with the events were classified based on the methodology proposed by [17] as: operation (TOp), active equipment performing its productive function; maneuver (TMn), active equipment, in motion, performing maneuvers necessary for the operation; supply (TSu), inactive equipment, stopped, supplying inputs; displacement for supply (TDs), active equipment, in motion, moving to the supply points; displacement (TDi): active equipment moving between plots or different areas; administrative (TAd), the equipment is available to operate but is not used due to administrative or managerial issues; maintenance (TMt): the equipment is unavailable due to corrective or preventive maintenance; climate (TCl): the equipment can operate but is not used due to unfavorable climate, soil or crop conditions; unreported (TUr): absence of record due to operator omission or system failure.

After classification, an analysis was performed to identify patterns of inconsistencies associated with processing errors, failures in event coding, incorrect nomenclature, or inaccuracies in sensor data capture. This analysis followed the methodology proposed by [18] for processing data with temporal constraints, considering three main criteria: (i) identification of interruptions in the temporal sequence of records; (ii) verification of the occurrence of unrecorded periods between two consecutive active times; and (iii) assessment of coherence between successive records by analyzing their temporal correlation.

Using the same logic applied to time classification, the amount of time (hours) was categorized according to the following events: operation (HOp); maneuver (HMn); supply (HSu); displacement for supply (HDs); displacement (HDi); administrative (HAd); maintenance (HMt); climate (HCl); unreported (HUr).

The determination of hours for each event was obtained by converting the sum of the times, recorded in seconds, using Equation (1):

$$Hj = 1/3600 \sum_{i=1}^{nj} Tij \quad (1)$$

where

Hj = Total time of event *j* (h);
3600 = Conversion factor (s/h);
Tij = Time of break *i* associated with event *j* (s);
nj = Total number of breaks associated with event *j*.

To reconcile the total number of recorded hours with the administrative work shifts (AWs), two categories of hours were defined: unrecorded hours (HNr), which represent the difference between the administrative workday and the sum of the hours recorded in all events; and unscheduled hours (HUs), which indicate the difference between the sum of the hours actually recorded and the administrative workday (Equations (2) and (3)).

$$HNr = Aws - (HOp + HMn + HSu + HDs + HDi + HAd + HMt + HCl + HUr) \quad (2)$$

where

HNr = Unrecorded time (h);
AWs = Administrative work shifts (h);
HOp = Operating time (h);
HMn = Maneuvering time (h);
HSu = Supply time (h);
HDs = Displacement for supply time (h);
HDi = Displacement time (h);
HAd = Administrative time (h);
HMt = Maintenance time (h);
HCl = Climate-related downtime (h);
HUr = Time for unreported activities (h).

$$HUs = (HOp + HMn + HAb + HDs + HDi + HAd + HMt + HCl + HUr) - \text{AWs} \quad (3)$$

where

HUs = Unscheduled time (h).

To align the terminology with daily operations, the term administrative work shifts (AWs) was used when the work shift was equal to or less than the 10 h scheduled by the company. When it exceeded this value, the term was actual working hours (AcWh), indicating that the number of actual operating hours exceeded the number scheduled by management (10 h). This occurs to address unforeseen situations such as finishing an area or taking advantage of favorable operating conditions. To evaluate equipment performance, the hours were grouped into operational classes.

The hours and efficiencies classifications related to spraying operations followed standard procedures in studies of agricultural machinery. In this study, however, these well-established indicators were collected from the CAN bus at a rate of 0.2 Hz, allowing a methodological approach to identify non-value-added activities and support real-time management decisions. The definitions of hours and efficiency classifications are presented in Appendix A.

The processed speed ($km \cdot h^{-1}$) and fuel consumption ($L \cdot h^{-1}$) data, obtained through the sprayers' on-board systems, were analyzed to understand the behavior of these vari-

ables during work shifts. For this analysis, control charts with standard deviation and variable sampling were used, as presented by [19].

The determination of the operational cost of spraying was performed using a model developed in a spreadsheet, whose input data included the area to be sprayed, the work shift, the hours associated with the events, and the sprayer and operation characteristics. The operational cost was determined by Equation (4):

$$OCs = (CHp/OFc) * 100 \quad (4)$$

where

OCs = Operational cost of the self-propelled sprayer (US\$ ha^{-1});
CHp = Hourly cost of the self-propelled sprayer (US\$ h^{-1});
OFc = Operational field capacity (ha h^{-1}).

To determine the hourly cost of the self-propelled sprayer, the methodology proposed by the American Society of Agricultural and Biological Engineers (ASABE) [20] was adopted, which includes the determination of fixed and variable costs. It should be noted that, in this study, only the cost related to the equipment was considered, without including labor costs. The hourly fixed cost was calculated according to Equation (5):

$$FCs = \{P * [(1 - S)/L) + ((1 + S)/2) * i + FAST]/TWi\} \quad (5)$$

where

FCs = Fixed cost per hour (US\$ h^{-1});
P = Purchase price of the sprayer (US\$);
S = Scrap price of the sprayer (decimal);
L = Useful life (years);
i = Interest rate (decimal);
$FAST$ = Safe housing factor and fees (US\$);
TWi = Time worked in a year (h year^{-1}).

The initial cost of the sprayer was obtained from the manufacturer, with reference to July 2024. The parameters for useful life, residual value, housing factor, insurance, and fees were adopted as per [20]. The hourly variable cost was calculated using Equation (6):

$$VCs = (FC * PF) + [(P * FRM)/L] \quad (6)$$

where

VCs = Variable cost of the sprayer (US\$ h^{-1});
FC = Fuel consumption (L h^{-1});
PF = Price per liter of fuel (US\$ L^{-1});
FRM = Repair and maintenance factor, decimal;
L = Useful life of the sprayer (h).

Thus, the hourly cost of the self-propelled sprayer is given by Equation (7):

$$CHp = FCs + VCs \quad (7)$$

The analysis of the sprayer's operational and economic performance was based on its working capacity (ha h^{-1}) and operational cost (US\$ ha^{-1}). For this purpose, a model in a spreadsheet was created based on the algorithm proposed by [21]. The model's input data allows for the calculation of the available hours for equipment operation throughout the harvest, based on the records. Based on the available hours and the total area to be sprayed, the work rate required to complete the spraying within the expected period is calculated. The amount of equipment is determined by the ratio between the work rate

and the operational field capacity. A rounding coefficient allows for an integer adjustment of the number of equipment, either upward or downward. The model allows, through simulations, for the analysis of operational and economic performance and the possibilities for reducing waste in the spraying operation.

3. Results

Data collected over 162 days of the 2021/2022 harvest totaled 1575.1 h of work. After processing the data, 5728 data points were reclassified. Because they represent only 5.5% of the total data collected, night shift records were not considered in the analysis. The distribution of hours during the analyzed period is shown in Figure 1.

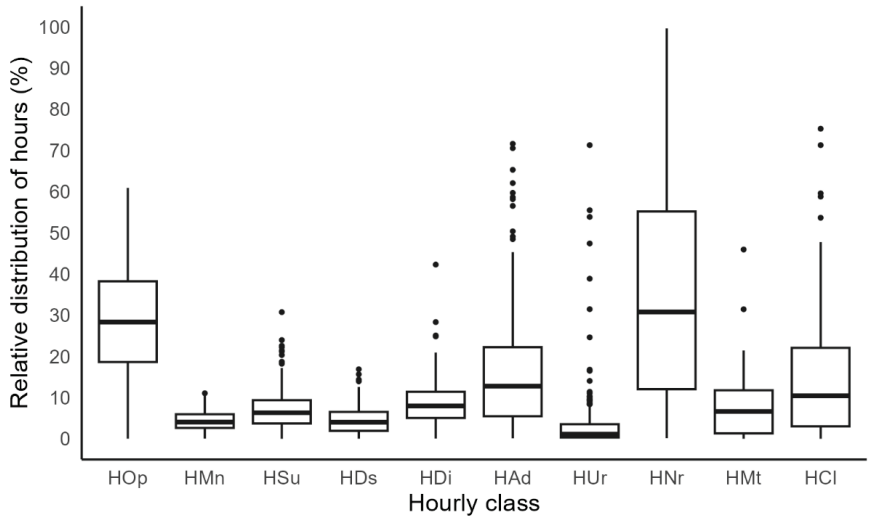


Figure 1. Distribution of hours throughout the workday (WD). HOp = operational; HMn = maneuver; HSu = supply; HDs = displacement for supply; HDi = displacement; HAd = administrative; HUr = unreported; HNr = unrecorded; HMt = maintenance; HCl = climate.

Regarding equipment efficiency, the results are presented in Figure 2.

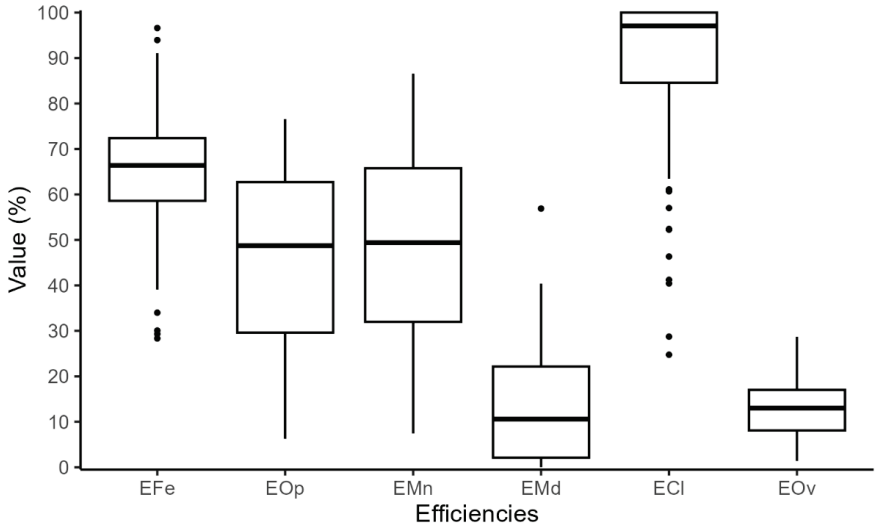


Figure 2. Equipment efficiencies. EFe = Field efficiency; EOp = Operational efficiency; EMn = Management efficiency; EMd = Mechanical downtime efficiency; ECl = Climate efficiency; EOv = Overall efficiency.

Speed is one of the factors that directly influences spray quality, spray deposition, work capacity, and, consequently, Operational costs. It is essential that it be maintained within specified limits throughout the entire operating period to ensure the expected results. Figure 3 shows the speed data recorded over the 162 days of spraying.

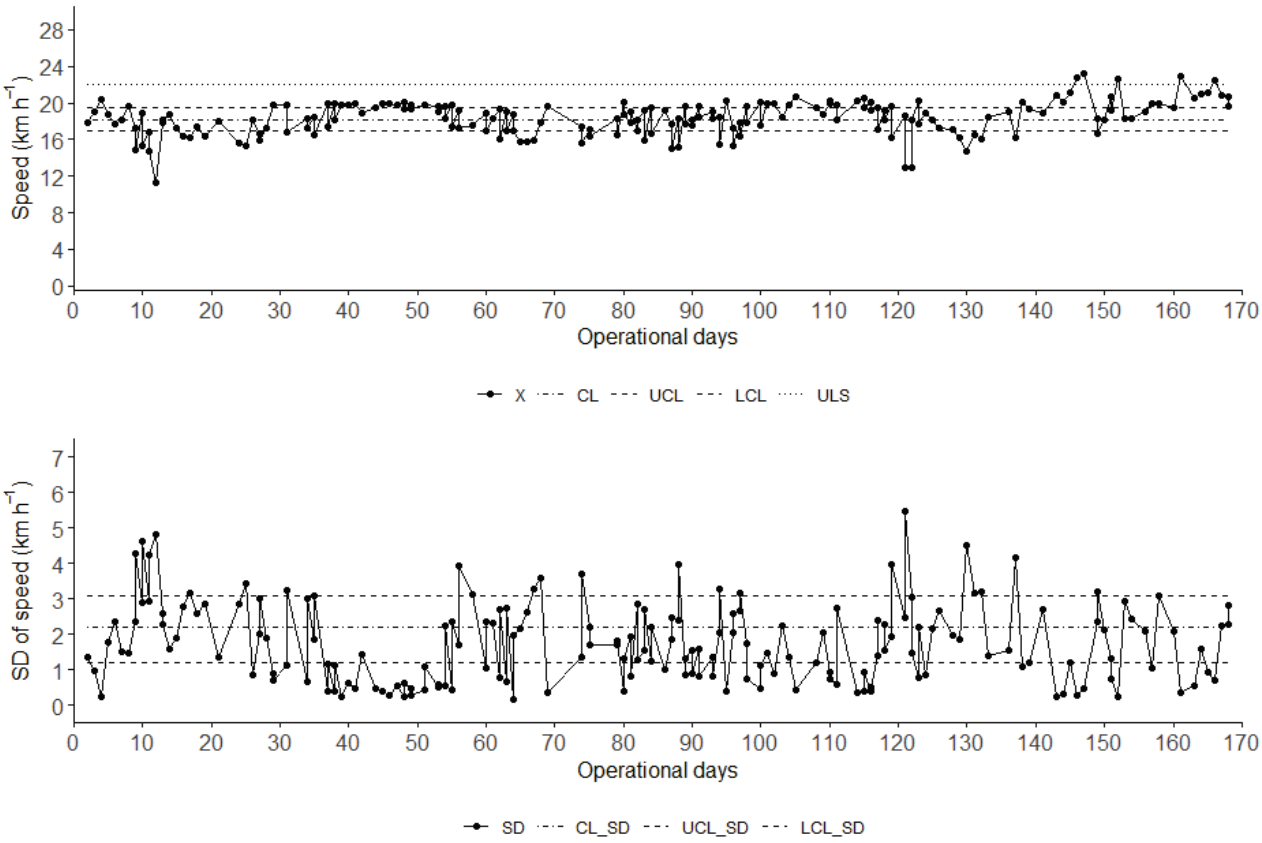


Figure 3. Speed (km h^{-1}) during operating hours (HOp) over the evaluated period (control chart by variable sample—mean and standard deviation). X = mean speed; CL = center line; UCL = upper control limit; LCL = lower control limit; ULS = upper specification limit (defined by the company, 22.0 km h^{-1}); SD = standard deviation of speed; CL_SD = center line for SD; UCL_SD = upper control limit for standard deviation; LCL_SD = lower control limit for standard deviation.

Regarding fuel consumption, the data remained mostly within the control limits (Figure 4), with an average of 22.1 L h^{-1}. However, the variable also showed instability, as evidenced by the presence of points outside the limits, points clustered near the limits, and an upward trend, especially after day 138. This behavior coincides with the period of increased speed, but it was not possible to establish a cause-and-effect relationship between the two variables in this study.

Figure 5 presents the relationship between the operational cost per hectare (OCs, US$ ha^{-1}) and the total area sprayed, expressed in thousand hectares. For areas smaller than 15,000 hectares, the OCs present high values, above 21.24 US$ ha^{-1}, decreasing sharply as the sprayed area increases.

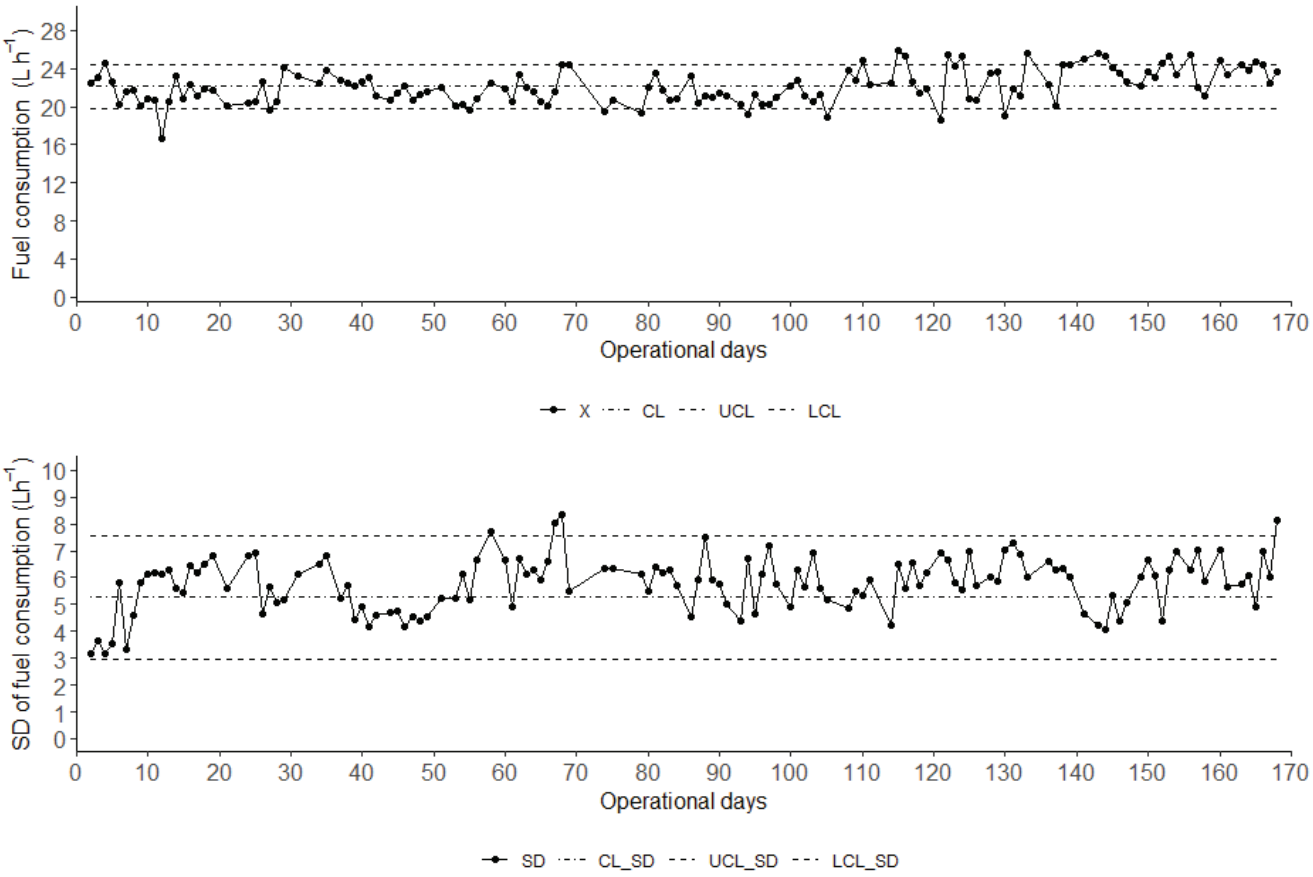


Figure 4. Fuel consumption (L h^{-1}) of the sprayers (set) in operating hours (HOp) over the evaluated period, eliminating special causes (control chart by variable sample—mean and standard deviation). X = mean speed; CL = center line; UCL = upper control limit; LCL = lower control limit; SD = standard deviation of speed; CL_SD = center line for SD; UCL_SD = upper control limit for standard deviation; LCL_SD = lower control limit for standard deviation.

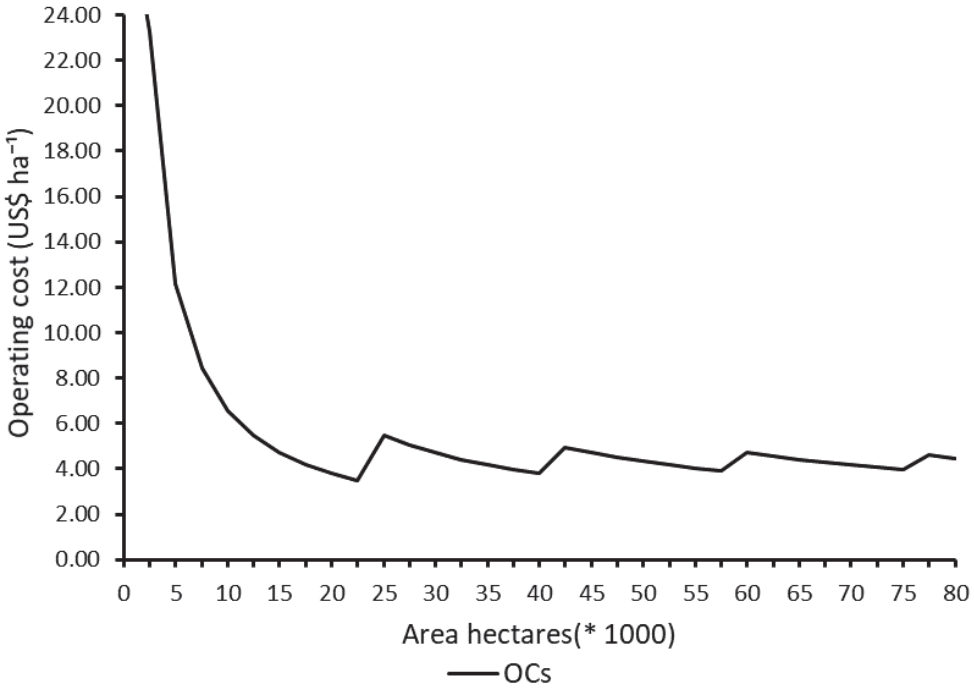


Figure 5. Operational cost (OC) as a function of area (ha) sprayed.

4. Discussion

4.1. Distribution of Hours

Operational hours (HOp), Figure 1, which directly correspond to spraying activities and add value to the process, had a median of 28.3%, representing less than a third of the available workday period dedicated to the main operation.

Auxiliary hours, which include maneuvering (HMn), supply (HSu), and displacement for supply (HDs), had relatively low medians and a concentrated distribution. However, the presence of outliers for HSu and HDs suggests the occurrence of abnormally high times, possibly associated with longer trips to supply points or long waiting times at these points.

Lost hours (HLt) refer to periods during which equipment was unavailable for operation, usually for managerial reasons. This category includes displacement (HDi), administrative activities (HAd), unreported records (HUr), and unrecorded records (HNr). Because they are not directly linked to the production process, these hours should be minimized whenever possible. Compared to auxiliary hours, reducing lost hours typically requires less effort and investment.

In the administrative category (HAd), the presence of outliers indicates idle time caused by managerial decisions, waiting periods, or organizational failures, such as the absence of work orders. These factors highlight the potential for operational improvements to increase the time dedicated to spraying.

The HNr (unrecorded) category had a median of 30.8% and high variability, highlighting serious problems in data collection and, consequently, in monitoring work hours. The high dispersion in the HNr and HUr categories may be related to data recording errors, interruptions in the temporal sequence of events, coding issues, or operational inconsistencies. Identifying the root causes of these errors is essential for improving data reliability and, consequently, operational management.

4.2. Equipment Efficiency

The median field efficiency (EFe) value of 65.6% indicates that approximately two-thirds of the time allocated to operation was spent on spraying, while the remainder corresponds to auxiliary operations such as maneuvering and supply (Figure 2). This value is in line with the parameters proposed by [20], which recommends a range between 50.0% and 80.0%, with an average of 65.0%. The presence of outliers may be related to variability in maneuvering and displacement times for supply, influenced, for example, by the shape of the fields [22] and the distance to supply points. Previous studies have reported that the field efficiency for full area spraying in cotton cultivation was approximately 61% [23], whereas site-specific spraying in soybean and corn fields reached up to 75% efficiency [11]. This improvement is associated with the targeted application of crop protection products only in necessary areas, which reduces the total volume used, the frequency of refills, and both the displacement for supply hours (HDs) and displacement hours (HDi). This practice directly contributes to the reduction in operational waste, unnecessary movement, and waiting time, while enhancing overall efficiency and sustainability in the spraying process.

Operational (EOp) and managerial (EMn) efficiencies assess the utilization of hours available for spraying. EOp considers exclusively the time dedicated to the operation, while EMn also incorporates the auxiliary hours essential for its completion. Both showed high variability. The averages of 44.8% for EOp and 46.4% for EMn indicate room for improvement, especially regarding the reduction in unproductive time associated with EMn. It is important to note that operations can present contrasts between different types of efficiency. For example, a sprayer may maintain high field efficiency (EFe) during the day, but if operational efficiency (EOp) is low due to long periods of inactivity or logistical delays, the area sprayed at the end of the day will be reduced.

Variations in efficiency values are common in agricultural environments, reflecting soil conditions, management practices, seasonal demands, and other factors. The efficiency of agricultural equipment use is directly related to logistical organization and operational planning. This behavior can be explained by improved input utilization and reduced losses associated with equipment idleness or underutilization. The adoption of precision agriculture technologies that monitor operational efficiency in real time can significantly contribute to reducing Operational costs [24–26]. The low mechanical downtime efficiency (EMd) value of 11.5% indicates that, over the 162 days analyzed, the sprayers operated almost without mechanical failures. On the other hand, the high suitability efficiency value reflects favorable climate conditions throughout the period. The overall efficiency, calculated based on 24 h equipment availability, showed a low value (12.9%) due to the assumed 10 h daily workday, even though the equipment is technically available for 24 h operation.

4.3. Spraying Speed

Regarding the speed variable (Figure 3), the process could not be considered stable, as several points fell outside the control limits, between the upper limit (UCL) and the lower limit (UCL). The company adopts 22.0 km h^{-1} as the upper specification limit (USL). It was observed that, for most of the analyzed period, the speed remained below this value, averaging 18.2 km h^{-1}. However, in the last days of operation, this limit was exceeded.

Based on a simulation of process improvements, the special causes identified in Figure 4, represented by points outside the control limits, were removed. After this intervention, the average speed increased from 18.2 km h^{-1} to 19.1 km h^{-1}, representing a gain of 0.9 km h^{-1} and a reduction in the variation range. The speed increase represents a 2.16 ha h^{-1} increase in the sprayer's working capacity, based on an effective width of 34.6 m and a field efficiency of 63.3%.

Keeping the speed variable within control limits is essential to ensure correct dosage and uniform foliar coverage, reducing product waste and environmental risks. Values above the upper control limit UCL can result in underdosing, uneven coverage, and increased drift, while values below the UCL can lead to overdosing, product runoff, and longer operating time [10,27]. These variations compromise both agronomic effectiveness and operational efficiency, generating waste that, according to Lean production principles, can be categorized as defects, rework, and overprocessing. Maintaining speed within statistically controlled limits supports process standardization, reduces variability, and promotes more efficient use of resources in pesticide application.

4.4. Fuel Consumption

Similar to the speed, fuel consumption (Figure 4) presented 34 points corresponding to special causes that were removed from the consumption control chart. As a result, the average consumption decreased to 21.9 L h^{-1}, a reduction of 0.2 L h^{-1}. With the removal of the points, the analysis indicated that the values in the control chart by the mean remained within the limits, but the standard deviation showed some points out of control, which prevents the process from being classified as stable. Although consumption reduction cannot be considered significant, 0.90%, the elimination of special causes and instabilities tends to reduce losses and waste, aligning with the principles of lean production [28], which advocates the systematic elimination of any factor that does not add value to the process.

Keeping fuel consumption within control limits is crucial, as this indicator (verification indicator) is directly related to operational costs and the sustainability of agricultural spraying. Values above the UCL (Upper Control Limit) indicate special causes that increase consumption and should be investigated, such as speed above the operating standard,

inadequate engine speed, incorrect gear usage, and more rugged terrain conditions, among others. Values below the LCL (Lower Control Limit) also require analysis. Although they may indicate lower consumption, it is necessary to assess whether they compromise application quality, as factors such as substandard speed or engine operating at inadequate speeds can impair performance. In these cases, if viability is confirmed, they can be treated as an opportunity for improvement to reduce costs without losing operational efficiency.

4.5. Operational Cost

Regarding the operational and economic performance of the spraying operation (Figure 5), the evaluation was performed through computer simulation in a spreadsheet, based on operational data obtained in the field, such as fuel consumption, average displacement speed, working width, pass overlap, and effective operating time. The scenario analyzed corresponded to an agricultural area of 6100 hectares, sprayed six times during the 2022 harvest, totaling 36,600 hectares treated. The administrative work shifts (AWs) adopted were 10 h per day, while the actual working hours (AcWh) observed were 10.3 h, of which 4.9 h were considered productive (HPr). The operating period covered 168 days, excluding Sundays and holidays.

The spraying-bar width was 36.0 m, but considering an average overlap of 4.0%, an effective width of 34.6 m was obtained. The average displacement speed during operations was 18.2 km h^{-1}. Based on these parameters, an operational efficiency (EOp) of 35.6% and a field efficiency of 63.3% were calculated, indicating the need for two sprayers to cover the total area within the stipulated timeframe. Each sprayer covered an average area of 18,300 hectares, accumulating a total of 919.8 productive hours. The estimated operational cost was 4.14 US$ ha^{-1}, considering exclusively the direct costs associated with the use of the equipment, excluding labor and inputs.

As the area increases, the cost per hectare tends to stabilize in the range of 3.65 to 4.57 US$ ha^{-1}. However, periodic fluctuations are observed at the transition points between area ranges, resulting from the addition of new mechanized equipment. This staggered behavior results from a temporary increase in fixed costs when new equipment is added, followed by a further reduction in the OCs (operational costs) as the total area is diluted [29].

The theoretical minimum area for full utilization of a sprayer, according to the simulated parameters, was estimated at 18,255.7 hectares. However, when the area size is approximately 22,500 ha, the operational cost increases due to the rounding criterion used to calculate the number of equipment required. Starting at a value of 0.30, the need to add another sprayer to meet demand was considered; if it is below, the calculated value is maintained. This threshold region is critical, as it marks the point where the addition of new sprayers becomes necessary and increases the fixed costs.

This pattern reinforces that expanding operational scale, combined with efficient use of installed capacity, is crucial for reducing costs per hectare and consequently eliminating waste, in line with Lean principles. Careful management of the number of machines, field efficiency, and fixed costs is essential to maximize operational efficiency and minimize unnecessary expenses [30,31].

5. Conclusions

Analyzing critical variables using real-time data allows us to identify opportunities for reducing waste, contributing to continuous process improvement, cost reduction, and sustainability.

The analysis of operational hours revealed that less than a third of the workday was dedicated to spraying, with a notable increase in unrecorded hours, highlighting flaws

in control and information management. The lost hours, assessed through managerial efficiency, represent potential for improvements typically associated with lower investment.

Statistical control of the speed and fuel consumption variables revealed the presence of special causes and instabilities in the process. Removing these causes resulted in an improvement in average speed and a small reduction in consumption, reinforcing the importance of maintaining operational parameters within control limits.

The simulation of operational and economic performance confirmed that expanding the operational scale contributes to reducing the cost per hectare, but that the staggered behavior resulting from the need to add new equipment requires careful management of installed capacity to avoid temporary increases in operational costs.

Author Contributions: Conceptualization, M.M. and T.L.R.; methodology, M.M. and M.C.P.; validation, M.M., M.C.P. and T.L.R.; formal analysis, M.M.; investigation, M.M. and M.C.P.; resources, M.C.P. and T.L.R.; writing—original draft preparation, M.C.P.; writing—review and editing, M.M. and T.L.R.; supervision, M.M. and T.L.R.; project administration, M.M. and T.L.R.; funding acquisition, T.L.R. All authors have read and agreed to the published version of the manuscript.

Funding: This research received no external funding.

Data Availability Statement: Restrictions apply to the availability of these data. Data were obtained from the company on which the study was carried out on and opted to remain anonymous.

Acknowledgments: First author thanks CAPES—Brazilian Federal Agency for Support and Evaluation of Graduate Education for the scholarship provided. The authors utilized Grammarly for language polishing and editing of the manuscript.

Conflicts of Interest: The authors declare no conflicts of interest.

Appendix A

Hours and efficiencies classifications related to spraying operations.

Table A1. Classification of hours related to spraying operations.

Grouped Classes							Activity Classification	Acronym	Unit	Calculation
Day (24 hours)	Actual working hours (AcWh)	Administrative work shifts (AWs)	Available time (HAt)	Mechanical Availability (HMa)	Productive (HPr)	Auxiliary (Hax)	Operation	HOp	h	Σ TOp
							Maneuver	HMn	h	Σ TMn
							Supply	HSu	h	Σ TSu
							Displacement for supply	HDs	h	Σ TDs
					Lost (HLt)		Displacement	HDi	h	Σ TDi
							Administrative	HAd	h	Σ TAd
							Unreported	HUr	h	Σ TUr
							Unrecorded	HNr	h	Σ AWs − Σ (HAt + HCl)
							Maintenance	HMt	h	Σ TMt
							Climate	HCl	h	Σ TCl
							Unscheduled	HUs	h	Σ AcWh − Σ AWs
							Unused	HUd	h	Day − Σ (AWs + HUs)

Auxiliary hours (HAx) represent the time dedicated to activities that support the operation but do not directly correspond to productive work, such as maneuvers, Equation (A1).

$$HAx = HMn + Hsu + HDs \quad \text{(A1)}$$

where

HAx = Auxiliary time (h).

Productive hours (HPr) correspond to the total time of effective operation, plus auxiliary activities directly related to task execution, Equation (A2).

$$HPr = Hop + HAx \quad \text{(A2)}$$

where

HPr = *Productive* time (h).

Lost hours (HLt) correspond to periods during which the equipment was unavailable for operation, primarily due to management reasons, Equation (A3).

$$HLt = HDi + HAd + HUr + HNr \quad \text{(A3)}$$

where

HLt = Lost *time* (h).

The available time (HAt) represents the time the equipment was available and ready for operation, including productive, lost and maintenance time (Equation (A4)).

$$HAt = (HPr + HLt + HMt) \quad \text{(A4)}$$

where

HAt = *Available* time (h).

Based on the classification of operational times, hours, and variables associated with spraying, analyses related to the performance of the operation and equipment were developed. The efficiencies analyzed, associated with time use and loss factors, were: field efficiency (EFe), operational efficiency (EOp), management efficiency (EMn), mechanical downtime efficiency (EMd), climate efficiency (ECl) and overall efficiency (EOv).

Field efficiency (EFe) indicates the extent to which auxiliary activities influence operational performance (Equation (A5)).

$$EFe = (HOp/HPr) * 100 \quad \text{(A5)}$$

where

EFe = Field *efficiency* (%).

Operational efficiency (EOp) measures how much of the available operating hours were used for the operation (Equation (A6)).

$$EOp = (HOp/HAt) * 100 \quad \text{(A6)}$$

where

EOp = *Operational* efficiency (%).

Management Efficiency (EMn) indicates the influence of lost hours on sprayer performance (Equation (A7))

$$EMn = (HPr/HAt) * 100 \quad \text{(A7)}$$

where

EMn = *Management* efficiency (%).

Downtime efficiency indicates how much of the available hours (equipment available for work) are used for maintenance (Equation (A8)).

$$EMd = (HMt/HAt) * 100 \quad \text{(A8)}$$

where

EMd = Mechanical downtime efficiency (%).

Climate efficiency (ECl) indicates how much the climate influences the workday, administrative or real (Equation (A9)).

$$ECl = (HAt/WD) * 100 \quad \text{(A9)}$$

where

ECl = Climate efficiency (%).

WD = Workday (h), shift (AWs) or actual (AcWh)

Overall efficiency (EOv) measures how much of the day was used to perform the operation for which the equipment was designed (Equation (A10)).

$$EOv = (HOp/Day) * 100 \quad \text{(A10)}$$

where

EOv = Overall Efficiency (%);

Day = 24 h

References

1. Ben Ruben, R.; Vinodh, S.; Asokan, P. State of Art Perspectives of Lean and Sustainable Manufacturing. *Int. J. Lean Six. Sigma* **2019**, *10*, 234–256. [CrossRef]
2. Emiliani, M.L. Origins of Lean Management in America. *J. Manag. Hist.* **2006**, *12*, 167–184. [CrossRef]
3. Heravi, G.; Firoozi, M. Production Process Improvement of Buildings' Prefabricated Steel Frames Using Value Stream Mapping. *Int. J. Adv. Manuf. Technol.* **2017**, *89*, 3307–3321. [CrossRef]
4. Pearce, D.; Dora, M.; Wesana, J.; Gellynck, X. Toward Sustainable Primary Production through the Application of Lean Management in South African Fruit Horticulture. *J. Clean. Prod.* **2021**, *313*, 127815. [CrossRef]
5. Proença, A.P.; Gaspar, P.D.; Lima, T.M. Lean Optimization Techniques for Improvement of Production Flows and Logistics Management: The Case Study of a Fruits Distribution Center. *Processes* **2022**, *10*, 1384. [CrossRef]
6. Melin, M.; Barth, H. Lean in Swedish Agriculture: Strategic and Operational Perspectives. *Prod. Plan. Control.* **2018**, *29*, 845–855. [CrossRef]
7. De Freitas, G.A.; Silva, M.H.d.P.e.; Silva, D.A.L. Overall Lean and Green Effectiveness Based on the Environmentally Sustainable Value Stream Mapping Adapted to Agribusiness. *Int. J. Lean Six Sigma* **2024**, *16*, 25–53. [CrossRef]
8. Al-Gaadi, K.A.; Ayers, P.D. Monitoring Controller-Based Field Sprayer Performance. *Appl. Eng. Agric.* **1994**, *10*, 205–208. [CrossRef]
9. Ayers, P.D.; Rogowski, S.M.; Kimble, B.L. An Investigation of Factors Affecting Sprayer Control System Performance. *Appl. Eng. Agric.* **1990**, *6*, 701–706. [CrossRef]
10. Sapkota, M.; Virk, S.; Rains, G. Spray Deposition and Quality Assessment at Varying Ground Speeds for an Agricultural Sprayer with and without a Rate Controller. *AgriEngineering* **2023**, *5*, 506–519. [CrossRef]
11. Zanin, A.R.A.; Neves, D.C.; Teodoro, L.P.R.; da Silva Júnior, C.A.; da Silva, S.P.; Teodoro, P.E.; Baio, F.H.R. Reduction of Pesticide Application via Real-Time Precision Spraying. *Sci. Rep.* **2022**, *12*, 5638. [CrossRef]
12. Farooque, A.A.; Hussain, N.; Schumann, A.W.; Abbas, F.; Afzaal, H.; McKenzie-Gopsill, A.; Esau, T.; Zaman, Q.; Wang, X. Field Evaluation of a Deep Learning-Based Smart Variable-Rate Sprayer for Targeted Application of Agrochemicals. *Smart Agric. Technol.* **2023**, *3*, 100073. [CrossRef]
13. Quan, C.; Zhang, J.; Feng, X.; Zhang, H.; Yang, M.; Zhu, Z.; He, X.; Wang, C. Spray Deposition and Weed Control Efficacy of a Real-Time Variable-Rate Boom Sprayer Applying Herbicide at Reduced Doses in Summer Maize Fields. *Agronomy* **2025**, *15*, 1953. [CrossRef]
14. Jiao, Y.; Zhang, S.; Jin, Y.; Cui, L.; Chang, C.; Ding, S.; Sun, Z.; Xue, X. Research Progress on Intelligent Variable-Rate Spray Technology for Precision Agriculture. *Agronomy* **2025**, *15*, 1431. [CrossRef]
15. Zhang, J.; Xu, X.; Lv, Y.; Zhao, X.; Song, J.; Yu, P.; Wang, X.; Zhao, E. Droplet Deposition and Efficacy of Real-Time Variable-Rate Application of Herbicides at Reduced Dose in Winter Wheat Fields. *Agronomy* **2024**, *14*, 211. [CrossRef]
16. Luck, J.D.; Pitla, S.K.; Zandonadi, R.S.; Sama, M.P.; Shearer, S.A. Estimating Off-Rate Pesticide Application Errors Resulting from Agricultural Sprayer Turning Movements. *Precis. Agric.* **2011**, *12*, 534–545. [CrossRef]

17. Gonçalves, N.H.; Lima, E.B.; Banchini, A.D.; Pinto, R.S.A.; Lopes, J.R. Eficiência de Uso de Máquinas Agrícolas. In Proceedings of the 5° Congresso Nacional da STAB, Águas de São Pedro, Brazil, Agosto 1993; Anais do 5° Congresso Nacional da STAB: Piracicaba, Brazil, 1993; pp. 165–168.
18. Song, S.; Huang, R.; Cao, Y.; Wang, J. Cleaning Timestamps with Temporal Constraints. *VLDB J.* **2021**, *30*, 425–446. [CrossRef]
19. Montgomery, D.C. *Design and Analysis of Experiments*; John Wiley & Sons: Hoboken, NJ, USA, 2017; ISBN 1119113474.
20. American Society of Agricultural and Biological Engineers (ASABE). *Agricultural Machinery Management Data ASABE D497.7*; American Society of Agricultural and Biological Engineers: St. Joseph, MI, USA, 2011.
21. Milan, M. Gestão Sistêmica e Planejamento de Máquinas Agrícolas (Systemic Management and Planning of Agricultural Machinery). Ph.D. Thesis, University of São Paulo, Piracicaba, Brazil, 2005.
22. Spekken, M.; de Bruin, S. Optimized Routing on Agricultural Fields by Minimizing Maneuvering and Servicing Time. *Precis. Agric.* **2013**, *14*, 224–244. [CrossRef]
23. Ghafoor, A.; Khan, F.A.; Khorsandi, F.; Khan, M.A.; Nauman, H.M.; Farid, M.U. Development and Evaluation of a Prototype Self-Propelled Crop Sprayer for Agricultural Sustainability in Small Farms. *Sustainability* **2022**, *14*, 9204. [CrossRef]
24. Zerbato, C.; Furlani, C.E.A.; da Silva, R.P.; Voltarelli, M.A.; dos Santos, A.F. Statistical Control of Processes Aplied for Peanut Mechanical Digging in Soil Textural Classes. *Eng. Agric.* **2017**, *37*, 315–322. [CrossRef]
25. Peloia, P.R.; Milan, M.; Romanelli, T.L. Capacity of the Mechanical Harvesting Process of Sugar Cane Billets. *Sci. Agric.* **2010**, *67*, 619–623. [CrossRef]
26. Colaço, A.F.; Rosa, H.J.d.A.; Molin, J.P. A Model to Analyze As-Applied Reports from Variable Rate Applications. *Precis. Agric.* **2014**, *15*, 304–320. [CrossRef]
27. Karadol, H.; Aybek, A.; Ucgul, M.; Kuzu, H.; Gunes, M. Field Sprayer with Application Rate Control Using Fast Response Proportional Valves under Variable Speed Conditions. *Agriculture* **2024**, *14*, 361. [CrossRef]
28. Womack, J.P.; Jones, D.T. Lean Thinking—banish Waste and Create Wealth in Your Corporation. *J. Oper. Res. Soc.* **1997**, *48*, 1148. [CrossRef]
29. Daum, T. Mechanization and Sustainable Agri-Food System Transformation in the Global South. A Review. *Agron. Sustain. Dev.* **2023**, *43*, 16. [CrossRef]
30. Sørensen, C.G.; Bochtis, D.D. Conceptual Model of Fleet Management in Agriculture. *Biosyst. Eng.* **2010**, *105*, 41–50. [CrossRef]
31. Bochtis, D.D.; Sørensen, C.G.C.; Busato, P. Advances in Agricultural Machinery Management: A Review. *Biosyst. Eng.* **2014**, *126*, 69–81. [CrossRef]

Disclaimer/Publisher's Note: The statements, opinions and data contained in all publications are solely those of the individual author(s) and contributor(s) and not of MDPI and/or the editor(s). MDPI and/or the editor(s) disclaim responsibility for any injury to people or property resulting from any ideas, methods, instructions or products referred to in the content.

agronomy

MDPI

Article

Weed Detection: Innovative Hyperspectral Image Analysis for Classification and Band Selection of Site-Specific and Selective Weeding Robot

Asi Lazar [1,2], Inbar Meir [1,3], Ran Nisim Lati [4] and Avital Bechar [1,2,*]

[1] Agricultural Research Organization, Institute of Agricultural and Biological Engineering, 68 Derech Hamacabim, P.O. Box 6, Rishon Lezion 5025001, Israel
[2] Department of Industrial Engineering and Management, Ben-Gurion University of the Negev, P.O. Box 653, Beer Sheva 84105, Israel
[3] School of Mechanical Engineering, Tel-Aviv University, Tel Aviv 6997801, Israel
[4] Department of Plant Pathology and Weed Research, Agricultural Research Organization, Newe Ya'ar Research Center, P.O. Box 6, Ramat Yishay 30095, Israel
* Correspondence: avital@volcani.agri.gov.il

Abstract

Weeding in melon and watermelon fields requires selective and pinpoint operation because the crop plants are sensitive to herbicides and tend to grow on the ground in all directions. Hyperspectral images have high spectral and spatial resolution, enabling an object's classification according to its spectral properties. Spectral band selection is a common practice with hyperspectral images, as it reduces the number of bands in use with only a minor effect on the results. This study's innovative contribution is the development and validation of a practical methodology to simplify complex hyperspectral data for real-world robotic weed management. This includes the introduction of the 'normalized crop sample index' (NCSI) to guide band selection and the use of machine learning methods, which revealed a set of four spectral bands—480 nm, 550 nm, 686 nm and 750 nm—that hold sufficient discriminating information between weeds and watermelon crop. This minimal set of bands enables the simulation and future development of a low-cost, high-speed multispectral camera system. An XGBoost model showed the lowest misclassification error level of 2–14%. The selected spectral bands were used to extract single-band images from the hyperspectral cube. In these images, vegetation pixels were separated using a normalized difference vegetation index filter, and each pixel was classified into a crop or weed class. The classified pixels were grouped into segmented objects, and weeding points were selected, suitable for robotic pinpoint operation.

Keywords: hyperspectral image; band selection; robotic weeding; watermelon; XGBoost

1. Introduction

Population growth and rising demand for quality agricultural products call for the production of the highest and best yields. Weeds are the number one cause of yield loss in some crops [1] and they can reduce the yield by around 45% [2,3]. Hence, their management is extremely important. Weeding in crops such as watermelon is conducted by non-chemical methods because these crops are sensitive to chemical treatment [4]. Non-chemical weed management focuses on preventative and direct physical weed-control methods [5]. Whereas preventative methods reduce weed germination and cultural meth-

ods improve crop durability, the direct physical weeding methods affect weed survival and robustness [6].

Recent developments in weeding mechanisms, such as low-energy electrophysical treatment [7], water jets [8], air-propelled abrasive grit [9,10], hot foam [11], mechanical systems [12] and more, enable highly accurate weed management while avoiding physical contact with the crop plants. This precision operation fundamentally relies on the first and most critical step: accurate and selective detection of the weed from the crop. Common methods to discriminate between crop and weed usually consist of the following phases: sensing, vegetation separation (segmenting) and classification [13]. Common RGB cameras use spatial data and morphological features for detection and classification; moreover, hyperspectral or multispectral cameras can increase the accuracy when spectral features are used. Hyperspectral imaging, with its hundreds of narrow bands, serves as a crucial research tool to identify the unique and subtle spectral differences between crop and weed, which may be missed by the broader bands of RGB cameras. These spectral differences provide features that are often more robust for classification than morphological features, especially when plants are young, overlapping, or morphologically similar. The key motivation for this study is to leverage the power of hyperspectral analysis to accurately locate the smallest subset of effective spectral bands. This selection will then enable the development of an efficient, low-cost multispectral camera system for real-time robotic applications, which is a major constraint for field deployment.

Modern classifiers of crops and weeds, using multispectral camera images, have been developed recently [14–16]. The images usually consist of four bands in the visible and near-infrared (VNIR) spectral range. A multispectral camera can produce sharp, high-resolution images at real-time speed, while reducing the computational power needed for the classification, resulting in lower costs. The normalized difference vegetation index (NDVI) is used to separate the vegetation from other objects in the image. For example, a vision-based classification system [15] used a random forest to classify sugar beet plants and weeds with a four-channel multispectral camera. Feature-based key point and object-based classification methods were employed, showing a 96% overall accuracy, segmenting plants and weeds based on object features. A convolutional neural network (CNN) method [17] was also used to classify sugar beet plants and weeds, in two stages: the first was removal of the background with a fast-segmenting network (sNet), based on NDVI; the second was classification of the vegetation pixels with a more complex classification network (cNet). The two-stage method had an accuracy of 95–98% with a processing time of 0.93 s, compared to 92–96% accuracy and 23 s for the classification network alone. These studies typically focus on pixel- or object-level classification accuracy.

Hyperspectral imaging is globally recognized as a powerful tool in precision agriculture, offering the unique capability to map subtle biochemical and biophysical properties of vegetation that are invisible to the human eye or standard cameras. This is crucial for tasks like early disease detection, nutrient monitoring, and, as in this study, high-accuracy species classification across various crops. Other approaches use hyperspectral camera images with hundreds of narrow bands to classify crops and weeds. Zhang et al. [18] presented a method for automated selection of spectral features from a hyperspectral image to differentiate rice from weeds. The data were collected with a hyperspectral camera with 512 narrow bands in the range 380–1080 nm. The 800-nm channel was used as a primary mask to select the crop leaf. After de-noising by wavelet transform, a successive projection algorithm (SPA) was used to select spectral features (bands). The SPA selected the six most important spectral features (705 nm, 1007 nm, 735 nm, 687 nm, 561 nm and 415 nm, ordered by importance). With the six SPA bands, a weighted support vector machine (SVM) model was used to achieve 100%, 100%, and 92% recognition rates for barnyard grass, weedy

rice, and rice, respectively. In Lauwers et al. [19], three classification models were used to distinguish between *Cyperus esculentus* weed and clones of morphologically similar weeds: random forest, regularized logistic regression and partial least-squares (PLS) discriminant analysis. Regularized logistic regression performed better than random forest or PLS discriminant analysis and was able to adequately classify the samples. The classification models were used on a hyperspectral reflectance dataset in the range of 500–800 nm. A low-cost multispectral camera based on four-band classification was used to simulate the results, and the simulated model classification accuracy was over 97%. In Diao et al. [20], a corn and weed classification was conducted by a spatial-spectral attention-enhanced Res-3D-OctConv model. The 350 spectral bands were reduced to four by principal component analysis, and the data were used by the model to classify the images. The model showed overall accuracy above 98% in the classification of the corn and weeds.

Many studies [21] have shown that band selection from hyperspectral data is very important to improving results. Band selection is based on the removal of highly correlated bands. Band selection also reduces the computational power needed for hyperspectral data processing. Various methods for selecting the most important spectral bands, such as linear discriminant analysis (LDA) [22], SVM [23], SPA [18] and random forest out of bag (OOB) [24] among others, are commonly used to reduce the number of bands. In the area of weed detection, spectral vegetation indices or image spatial indices have been used in many studies to classify vegetation [18,25].

Despite the promising high accuracy reported in the recent literature for crop and weed classification (e.g., 92–100%), two critical challenges remain for practical field implementation, particularly in crops like watermelon. First, a major challenge in watermelon cultivation is the need for extremely selective, pinpoint weed management, as the crop is sensitive to treatment and spreads in all directions on the ground, making standard weeding tools and methods unsuitable. The classification must be highly accurate and robust enough to avoid crop damage in close proximity. Second, many high-accuracy studies rely on full hyperspectral data with hundreds of bands, which demands significant computational power and specialized hardware, resulting in high costs that prevent wide-scale deployment on robotic platforms and are impractical for commercial use. Therefore, the critical issue is not simply achieving high accuracy but achieving high and robust accuracy with the minimal resources required for a cost-effective, real-time robotic system. This necessitates a precise methodology for spectral band selection.

The primary goal of this study was to find the most effective spectral bands for detecting weeds within a watermelon cultivation area [5]. To achieve this, an innovative and practical methodology was devised. The novelty of this approach lies in three critical aspects: first, the introduction of the 'normalized crop sample index' (NCSI), a new spectral analysis tool designed to simplify complex hyperspectral data for enhanced separation of two green vegetation types; second, the strategic use of conventional machine learning models for their ability to transparently and accurately select a minimal set of spectral bands from the original 840 bands in addition to optimize the classification performance; and third, the validation of this reduced spectral subset to enable the creation of a low-cost multispectral camera system for real-time robotic weed management. The objective was to identify a specific spectral range and the minimum number of bands that would be instrumental in the creation of a multispectral imaging system for weed detection.

As a result of careful consideration, the four most beneficial spectral bands were chosen, aligning with contemporary weed detection methodologies. It is important to note that this research forms a segment of an ongoing project dedicated to the advancement of a robotic weeding system.

2. Materials and Methods

The research comprised three main phases: firstly, conducting an experiment to collect hyperspectral data; secondly, performing band selection based on the spectral characteristics of the plants; and lastly, identifying potential weeding points (tool–weed contact points).

2.1. Experiment

An experiment was conducted in a commercial plot of watermelon (cv. *Malali*) where the common naturally grown weed population is of the genus *Convolvulus*. Hence, the focus of the study was on the *Convolvulus* as a weed. The plot was not weeded during the experiment for a period of 7 weeks from seeding. Hyperspectral images were collected from different regions of interest (ROIs) in the plot, which had both crop and weed plants. Each ROI was about 0.8 m long and between 0.4 and 1.2 m wide, depending on the growth stages of the crop and weed. Images were taken on three different dates in May and June 2019. On each measurement day, several crop rows were selected, and about eight ROIs were captured along 30 m in each row. The first measurement was conducted two weeks after seeding.

2.2. Experimental Apparatus

The data was collected using a hyperspectral camera, mounted on a custom data-collection cart (Figure 1a). The camera, a push-broom hyperspectral camera, VNIR HS (Specim, Oulu, Finland) with 840 spectral bands in the range of 395–1005 nm, a spectral resolution of 0.7 nm and spatial resolution of 1600 pixels, was attached to a rotary motor, Rotary (Specim, Oulu, Finland) (Figure 1b). The rotary motor was mounted on a cart, designed and built for the experiment at the Institute of Agricultural Engineering. The rotary motor was positioned at the front of the cart, at a height of 1.2 m above ground and at a 30-degree angle relative to the horizon. The motor rotated the camera at a constant speed, facilitating the line scanning process, where the camera direction traverses from one side of the Region of Interest (ROI) to the other. A sheet of square-patterned A4 paper (Figure 1c) was used as the "black and white" reference for the spectral reflectance and as a scale.

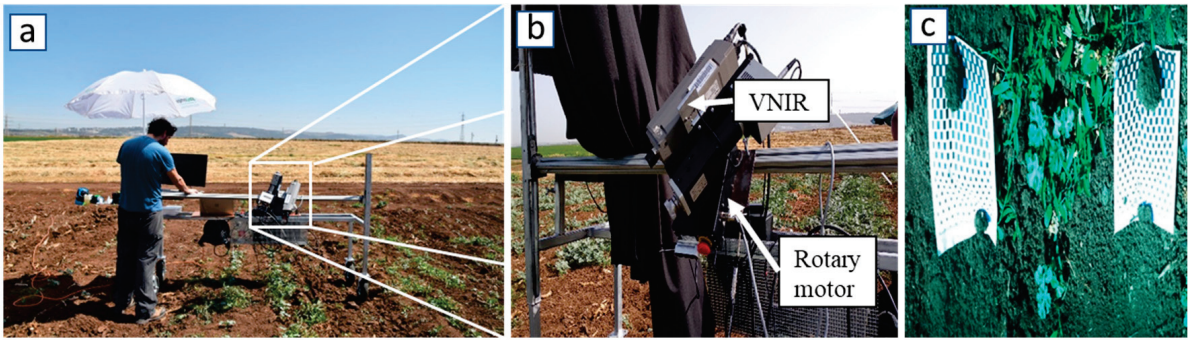


Figure 1. (**a**) The experimental apparatus. (**b**) The sensory system. (**c**) A VNIR pseudo RGB image of a single ROI [5].

2.3. Data Acquisition

At each visit, about 25 ROIs were captured. Each ROI (Figure 1c) consisted of crop plant, weed, soil, the "black and white" reference paper and other objects in the field, such as stones and dry crop material from the previous season. The hyperspectral camera captures images line by line (pushbroom), with each line composed of a 1600 × 840-pixel frame, 1600 spatial and 840 spectral pixels. To capture a full image, the rotary motor start

and end positions were set according to the stage and size of the plants of each ROI. The frame rate was set to 20 frames per second, and the number of lines varied between 1000 and 3000 according to the start and end positions. Hence, each ROI capture time was between 50 and 150 s. In addition, the hyperspectral data were presented as "pseudo RGB", where specific narrow band channels were used to create a common "RGB" image look-alike. The bands for the pseudo RGB image were 486 nm for blue, 550 nm for green and 686 nm for red from the VNIR camera (Figure 1c).

2.4. Data Pre-Processing

The hyperspectral image pre-processing procedure presented in Figure 2 was based on 26 selected images (ROIs) from the three visits, defined as day 1, day 2, and day 3. The images were labelled and studied using custom software that was developed in-house.

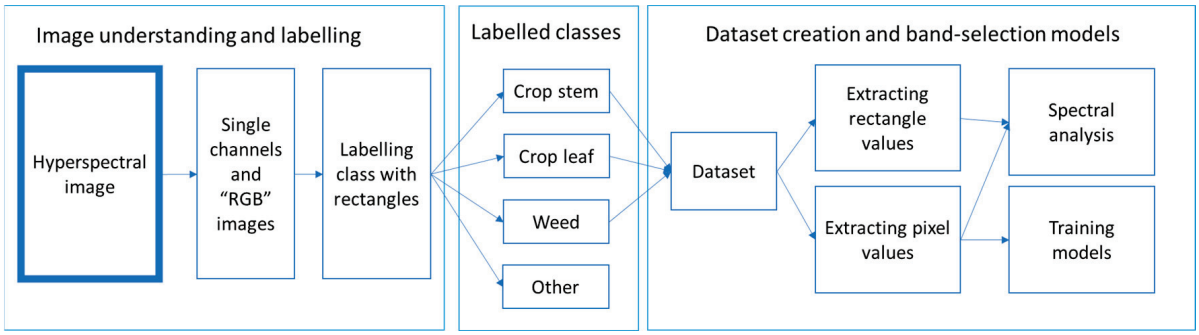


Figure 2. Data pre-processing of a hyperspectral image. The image is labelled, and the data are extracted for the spectral analysis and model training [5].

The selected hyperspectral images were used to extract each of the spectral bands from the image. Three single-band images were used to display a pseudo RGB image. Based on the pseudo RGB image and selected bands, several objects in the images were marked with rectangular frames and labelled as crop stem, crop leaf, weed, weed flower, "black and white" reference paper, and soil classes. The labels of crop stem and crop leaf were combined into a single class labelled 'crop'. An example of a labelled ROI image is given in Figure 3. The dataset for the classification models consists of the crop and weed labelled frames from the selected images, and for each pixel in the labelled frames, a vector of the spectral reflectance was extracted from the hyperspectral image. In all, 572 labelled frames of crop and weeds were extracted from the data. The frames contained 55,639 pixels labelled as crop and 40,389 pixels labelled as weeds.

2.5. Spectral Data Analysis

The crop and weed labelled frames were used to inspect the spectral response of each population (crop and weed) by taking the mean value of all of the pixels in each labelled rectangle as the intensity of each band.

2.6. Classification Models with Band Selection

To classify crops and weeds while reducing the number of spectral bands captured by the VNIR camera (Specim, Oulu, Finland), we used five distinct classification models: (i) Linear Discriminant Analysis (LDA), (ii) Logistic Regression, (iii) Partial Least Squares (PLS), (iv) Random Forest, and (v) XGBoost [26]. These models also served the dual purpose of band selection, with the goal of narrowing down the pool of 840 spectral bands into four. The target of four spectral bands was selected based on engineering constraints and performance requirements. It is common in relatively low-cost commercial multispectral cameras and represents a balance between spectral information for high accuracy and

minimal data for low computational cost and real-time operation in a robotic system. Two approaches were employed for band selection: "bottom up," primarily utilizing two-band analysis, and "top down," commencing from the complete set of 840 bands.

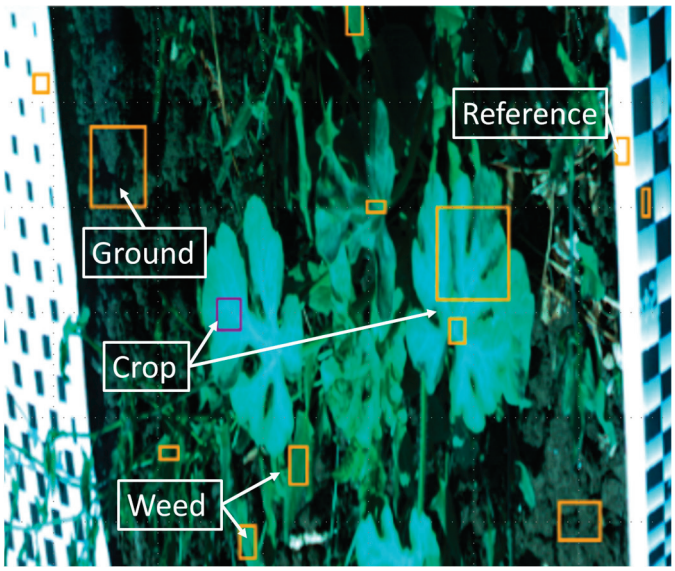


Figure 3. Pseudo RGB image labelled with custom software. Selected frames are labelled as Crop, Weed, Ground, or Reference classes, seen as orange rectangles. The purple rectangle was selected to be used with the proposed NCSI.

LDA (i) and Logistic Regression (ii) utilized the "bottom up" approach in a two-step process. The first step was to find a combination of two bands that minimized misclassification error. The second step used an iterative greedy approach: within each iteration, a single spectral band was added to reduce the misclassification error. In the first step, to reduce the computation time and avoid selecting adjacent bands, the spectrum of 840 bands was reduced to 84 bands with equal distribution along the spectrum (with approximately 7 nm spacing between spectral centres). On the reduced subset of 84 bands, a two-band analysis was conducted to generate a matrix of misclassification error levels, known as the "lambda–lambda graph". For each pair of bands, the misclassification was found by either LDA (i) or Logistic Regression (ii). The misclassification matrix was composed in the following manner: each cell outside the main diagonal holds the misclassification error of two bands together. The main diagonal holds the misclassification error of a single band, leading to a total of 7056 combinations that were calculated. From the misclassification error matrix, the two bands that showed the lowest error were selected as base bands for the second step, the greedy approach. The greedy approach, which utilizes a widely accepted heuristic technique for local optimization, was conducted iteratively. A single iteration of the greedy approach compared the misclassification error of the base bands with that of a single band from the 840 bands of the full spectrum. The band that reduced the misclassification error the most was added to the base bands for the next iteration. The algorithm stops once the misclassification error reduction is small or once the desired number of bands is reached. In this study, two more bands were added within the second step to reach a total of four bands.

PLS (iii), Random Forest (iv), and XGBoost (v) followed the "top to bottom" approach, utilizing all 840 bands in their operation. Each of these models calculated a unique contribution score for each spectral band, representing the band's significance as a feature in the model.

PLS (iii): PLS discriminant analysis is a versatile statistical method renowned for its ability in both classification and dimension reduction. In our context, it calculated Variable Importance in Projection (VIP) scores for each band. These VIP scores measured the cumulative importance of each band when considered in conjunction with all other bands. The VIP scores were instrumental in band selection, guiding the process.

Random Forest (iv): The Random Forest model, an ensemble of decision trees employing majority voting for classification, produced feature importance scores for each spectral band. These scores, generated using the Out-Of-Bag (OOB) method, reflected the band's importance within the learning process of the algorithm. The bands with higher feature importance scores were prioritized in the "top down" selection process.

XGBoost (v): Operating on the principle of tree boosting and gradient boosting, the XGBoost model constructed a collection of boosting trees. During its learning process, XGBoost computed a 'gain' score for each spectral band, which gauged the band's contribution to improved classification accuracy. The 'gain' score was the criterion for the "top down" band selection.

All classification models were implemented and trained using Python 3.10 with the scikit-learn and XGBoost libraries. For all models, a grid search hyperparameter tuning procedure was performed to optimize performance, focusing on minimizing the overall misclassification error. The computing environment used for all training and analysis consisted of a desktop PC with an Intel i7-9700K processor and 32 GB of RAM, running Windows 10. For each model, the key hyperparameters tuned during the grid search were as follows: LDA model: solver type ('svd', 'lsqr', 'eigen') and shrinkage parameter; Logistic Regression model: regularization strength (C) and penalty type ('l1', 'l2'); PLS model: number of latent variables; Random Forest model: number of estimators (trees), maximum tree depth, and minimum samples per leaf; and XGBoost model: number of estimators (100–1000), maximum tree depth (2–8), learning rate (0.01–0.3), subsample ratio, and column sampling rate per tree. Furthermore, to validate the classification, a k-fold cross-validation was conducted with five folds. The k-fold cross-validation was used for all the models in each fitting process.

To ensure that the selected bands contributed meaningfully to classification, a spectral distance of at least 20 nm was maintained between the chosen bands. This precaution was taken because neighbouring bands tend to be highly correlated, potentially causing redundancy and describing the same spectral phenomena. Following the band selection process, a subset comprising the chosen bands was employed to train the classifiers. The models were rigorously tested on data from each visit day individually, as well as on the aggregated dataset spanning all days. Each model underwent training and fitting using 80% of the data and was then evaluated on the remaining 20%. Importantly, in each training session of each algorithm, multiple train–test splits were employed to ensure robustness in the model's performance assessment.

2.7. Weeding-Point Selection

The weeding point is considered as the physical contact point between the weeding tool electrode and the weed. The selection of weeding points involves a structured image-processing workflow, encompassing four key steps:

(i) NDVI Vegetation Mask Application: Initially, an NDVI vegetation mask was applied. This mask identified living plants by utilizing two specific bands (686 nm and 750 nm) to separate the plant pixels from the background. Subsequent image processing steps focused exclusively on this masked vegetation data.

(ii) Pixel Classification: Classification was conducted using grayscale images of specific spectral bands from the hyperspectral VNIR camera. In this study, four spectral bands

were selected by the classification models. Each of these bands contributed a set of four images used for classification. Every pixel within the vegetation mask was represented as a four-value vector. Each classification model was applied to this labelled data, generating a classification image for each of the four spectral bands. A pixel-wise majority vote from all the classification models produced a comprehensive classification mask distinguishing between crop and weed.

(iii) Segmentation of Contoured Objects: To ensure the separation of crops from weeds, a distance had to be maintained between the crop and the weeding tool. Achieving this involves enlarging the crop objects through morphological dilation and removing all weed pixels within the expanded crop area. This segmentation process unfolded in two steps: first for the crop population and then for the weed population. For the crop population, the steps included noise filtration, contour detection, and contour shape dilation to create a crop mask. For the weed population, the process commenced with the subtraction of the crop mask and then proceeded with noise filtration, contour detection, and contour shape erosion. This resulted in a segmented image, effectively distinguishing crop and weed objects.

(iv) Selection of Weeding Point: The final step involved selecting weeding points while maintaining a safe distance from the crop plants. A minimal distance of approximately six cm was preserved, considering data analysis that indicated this to be less than the average distance between two weed plants, effectively treating them as the same plant. To ensure this distance, the image was divided into small sections, approximately 6 × 6 cm in size, by averaging the values of the surrounding area. Sections containing crop values were excluded, retaining only the segments with weed presence. The image with the isolated weed section was then divided into overlapping tiles. The number of weed pixels within each tile was calculated. These tiles were then ranked based on the quantity of weed pixels they contained, without any overlap. Weeding points were selected by choosing tiles with the highest weed pixel count, thereby facilitating precise weed removal.

3. Results

3.1. Spectral Data Analysis—Development of the 'Normalized Crop Sample Index' (NCSI)

The spectral response of the labelled frames of crop and weed classes from the ROIs images was analyzed, as seen in Figure 4. Each labelled frame out of the 572 samples, represented as a vector $\vec{\lambda}_i$ of the mean intensity values of the pixels of the frame in each band. The NCSI, denoted as $\Lambda_{(i)}$ (Equation (1)), was used for the normalization of the samples. The NCSI uses a normalization vector $\vec{\lambda}_{mean}$, which can be one crop pixel's spectral values, one crop-labelled frame's mean spectral values, or another selection of n_j samples from the crop population. Therefore, each element $\vec{\lambda}_{mean_j}$ (Equation (2)) is the mean spectral reflectance of the n_j samples, used for the normalization of band j in $\vec{\lambda}_{mean}$ normalization vector. The n_j samples represented as $\lambda_{i,j}$ where i considered to be one of the $\vec{\lambda}_i$ vectors and j the specific spectral band. The NCSI, when applied to one labelled frame, divides the spectral response of a sample $\vec{\lambda}_i$ with the normalization vector $\vec{\lambda}_{mean}$ element wise. In the study, $\vec{\lambda}_{mean}$ was developed with samples of the crop population.

$$\Lambda_{(i)} = \frac{\vec{\lambda}_i}{\vec{\lambda}_{mean}} \quad (1)$$

$$\vec{\lambda}_{mean_j} = \frac{\sum_{i=1}^{n_j} \lambda_{i,j}}{\mathrm{n}_j} \quad (2)$$

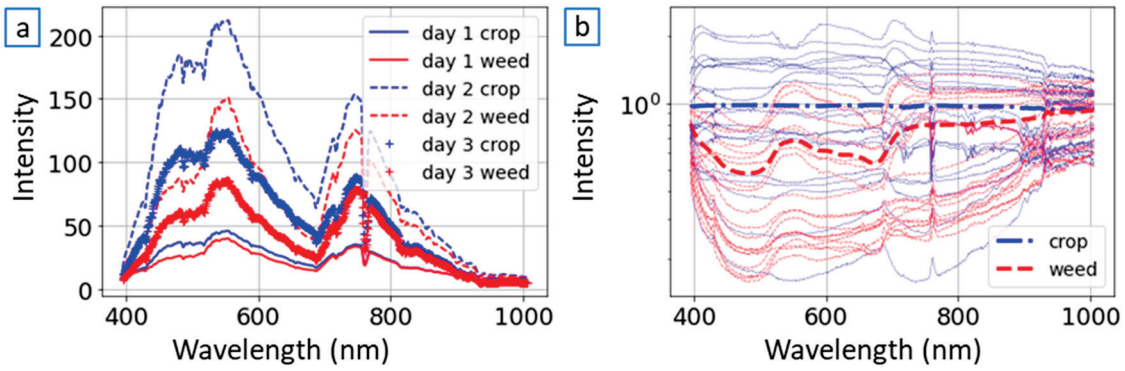


Figure 4. (**a**) Average spectral response of each population crop in blue and weed in red, for each visit day. (**b**) NCSI of the response on a logarithmic scale. Thin lines represent selected specific samples, from 20 crop-labelled frames and 20 weed-labelled frames. Bold lines represent the average of all samples [5].

The underlying principle of the NCSI can be simplified in the case that $\vec{\lambda}_{mean}$ was selected as specific $\vec{\lambda}_i$ vector from the dataset. In this case, the expectation is that when the NCSI is applied to a different sample of the same type of plants, the watermelon crop in the study, the index values will exhibit a relatively straight and levelled pattern parallel to the straight line that represents the chosen sample. Conversely, the NCSI spectra of weed samples are anticipated to demonstrate fluctuations, as seen in Figure 4b. The average spectral reflectance for each population for each trial day is seen in Figure 4a, while the bold representation in Figure 4b depicts the average NCSI spectral reflectance (as defined in Equation (1)) across all samples. Upon analyzing the NCSI spectral response, specific characteristics were observed for the crop-labelled frames within the designated ROIs. Specifically, within the spectral range of 450 nm to 690 nm and 750 nm to 900 nm, the spectral response remained generally stable, forming a consistent line. However, a marked transition in the spectral response was identified in the range between 690 nm and 750 nm. In contrast, the normalized response of the weed samples displayed fluctuations within the range of 450 nm to 690 nm, with a distinct change occurring between 690 nm and 750 nm. Other portions of the spectral response were found to be unstable due to the sensor's limited signal-to-noise ratio in these specific spectral bands. In certain instances, particularly those involving low intensity (such as on trial day 1) or suboptimal selection of the crop sample frame, fluctuations were observed in the crop response. While variations were noticeable in the weed samples based on the selection of different crops, the regions corresponding to local minimum and maximum responses remained consistently positioned within the same spectral regions.

The four bands that were manually selected in the spectral analysis were in the areas of the local minimum and maximum points of the NCSI spectral response of the weed, and at the edges of the sharp spectral change seen between 690 nm and 750 nm. The four selected bands were: 480 nm, 550 nm, 686 nm and 750 nm. This set of four bands was defined as the 'NCSI band selection', to be compared in all classification models as the reference selection of bands for the model.

3.2. Classification and Band-Selection Models

The spectral response of each pixel in the crop and weed-labelled rectangles was used to train five classification models: greedy LDA (i), greedy logistic regression (ii), PLS (iii), random forest (iv) and XGBoost (v). For each pixel, an 840-value vector of the intensity of each spectral band was extracted, for a total of about 100,000 pixels.

The models were trained for each trial day separately and on all days together. For each day, the spectral response of each pixel was normalized using the NCSI, where $\vec{\lambda}_{mean}$ is the vector of the mean response of all crop pixels on the same day. The baseline of the misclassification error level was assessed on the dataset of labelled pixels with 840 bands. All models showed similar results, with misclassification error levels of about 5%, 1.5% and 2% for days 1, 2, and 3, respectively. For each model, the method specified in Section 2 was used to find the set of four bands with the lowest misclassification error level. As mentioned in Section 2, a k-fold cross-validation was used for all training of the models. The spectral reflectance of the measurements on each day differed in intensity due to camera calibration and the changes in environmental conditions (e.g., varying sunlight intensity and angle), where day 2 had the highest intensity and the camera calibration was sharp and detailed, and day 1 had the lowest intensity and was the least detailed. The diverse levels of intensity during and between the days posed a challenge for the band selection of each model, because the bands that contributed most on each day differed with respect to the intensity difference. The successful normalization of the spectral response using the NCSI, which utilizes the mean crop response of the same day for normalization, alleviated the effect of these environmental changes, demonstrating a path toward robust daily operation. Furthermore, during the band selection procedure, a deliberate exclusion was made with respect to the spectral region exceeding 850 nm. This exclusion was motivated by the presence of a notably low signal-to-noise ratio within this specific spectral range in the specific outdoor conditions in which we took the images. This limitation is generally tied to the sensitivity of the VNIR sensor at the higher end of its range and the specific lighting/field conditions. This limitation could potentially be mitigated through the use of cameras with improved sensitivity at higher wavelengths or by implementing more sophisticated spectral pre-processing techniques, such as advanced filtering or specific sensor calibration for the NIR range.

For the LDA (i) and logistic regression (ii) models, the bands that reduced the misclassification error level the most over all 3 days were selected according to the greedy selection algorithm. In the first stage of the algorithm, two-band analysis, as shown in Figure 5, produced a matrix of misclassification error rate for each of the two bands in the matrix. The two-band misclassification matrix is characterized by regions where the misclassification was low (black); these areas of the matrix indicate that multiple selections of specific two bands can produce low misclassification error. Notably, the main diagonal of the matrix shows high misclassification errors, occurring when the same band was selected twice, since analyzing a single band effectively employs only a single feature. Figure 6 shows the process of the greedy selection and highlights the bands chosen for the LDA model. This selection process commenced by establishing a set of base bands (represented by vertical red lines), which were the bands selected in the two-band analysis. For every consecutive band, a classifier was trained to assess the contribution of that band toward reducing misclassification errors. The most advantageous band, optimizing misclassification rate reduction across the three days, was determined by identifying regions where misclassification was minimal while maintaining a spectral distance of 20 nm between the base bands. Furthermore, in the band selection procedure, the introduction of the third and fourth bands was guided by the lowest misclassification error rates observed on days 1 and 3, respectively, due to their significant contributions. Consequently, for day 2, the addition of these bands resulted in a comparatively minor reduction in misclassification when contrasted with the base bands.

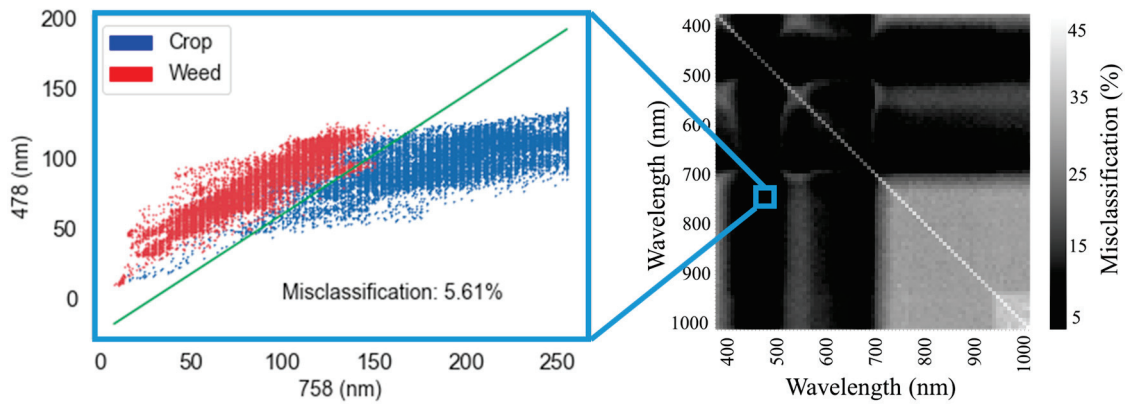


Figure 5. Two-band analysis of day 2 data using LDA backbone. The LDA misclassification of the two-band (478 nm and 758 nm) graph (**left**) is calculated and considered as a single value in the two-band analysis matrix (**right**). The matrix holds the misclassification error level of each of the 7056 combinations of two bands [5]. The green line represents the boundary between crop and weed classes.

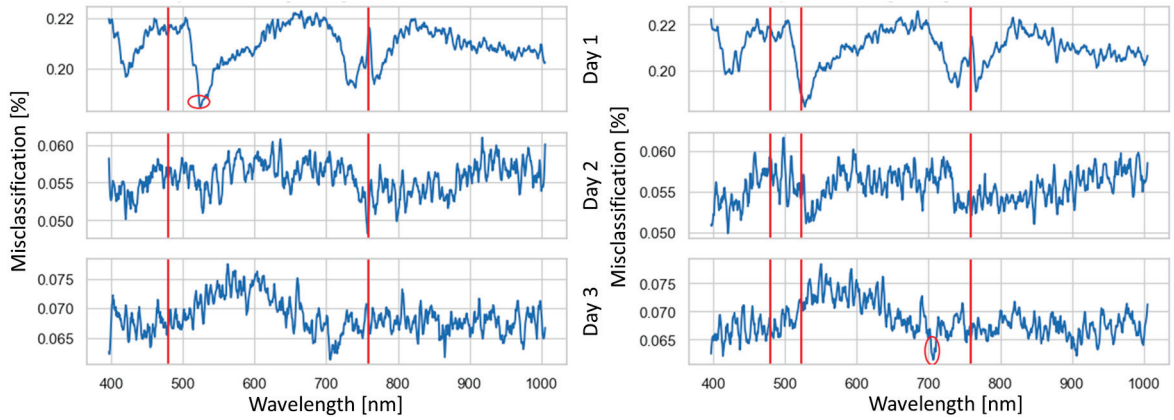


Figure 6. Band Selection using Greedy Selection Algorithm for LDA Model ((**left**): Third Band, (**right**): Fourth Band). Each subplot represents the Savitzky and Golay [27] approximation of the misclassification error values for each combination on a specific day. The vertical red lines denote the bands constituting the base bands for the greedy algorithm. The initial two (base) bands were 478 and 758 nm, while the third band selected at 529 nm is indicated based on day 1 (highlighted by a red ellipse in the top left subplot), and the fourth band chosen at 705 nm is highlighted based on day 3 (red ellipse in the bottom right subplot).

In the case of the PLS (iii), random forest (iv), and XGBoost (v) models, the bands that were chosen for inclusion in the models were those that demonstrated substantial feature importance, as outlined in Section 2 specific to each model. As shown in Figure 7, the XGBoost model's band selection process is illustrated.

The misclassification error level of the data from all days for the four bands selected by each model was 12% on average, whereas the misclassification error level when using the NCSI reference bands was between 11% and 14% (Table 1). The random forest and XGBoost showed the lowest misclassification error levels with the reference bands selected by the NCSI; however, for the LDA, logistic regression and PLS, the model method of band selection gave better results than the NCSI reference bands. The set of four bands selected by the model-specific method tended to classify better on days 1 and 3 because the selection method was influenced by the reduction in misclassification error level, which was larger for those days.

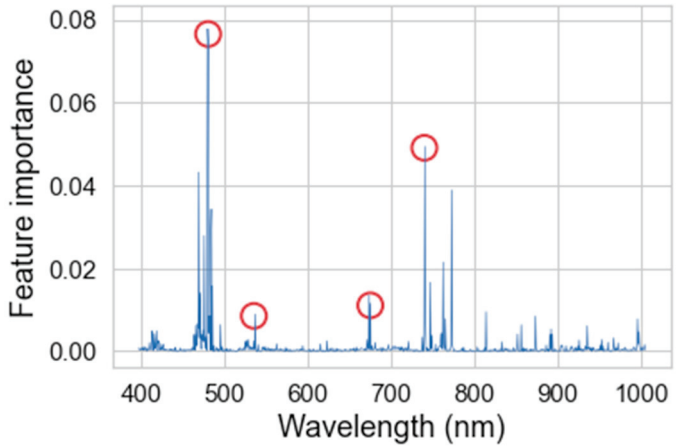


Figure 7. The band selection for the XGBoost algorithm bands, by gain feature importance, is at 485 nm, 554 nm, 668 nm, and 735 nm. The feature importance was calculated with the data from all days. The red circles represent the selected bands.

Table 1. Four-band misclassification error level of each model based on the selection of four bands from the NCSI spectral analysis (480 nm, 550 nm, 686 nm, and 750 nm) and on the selection of four bands according to each model-specific method. The bold figures represent the best results for each day and all days data. The bands selected by each model are presented in Table 2.

Model	Day 1	Day 2	Day 3	All Days
NCSI bands				
LDA	0.201 ± (0.003)	0.051 ± (0.001)	0.080 ± (0.004)	0.141 ± (0.003)
Logistic regression	0.183 ± (0.003)	0.037 ± (0.002)	0.064 ± (0.003)	0.134 ± (0.004)
PLS	0.203 ± (0.003)	0.056 ± (0.001)	0.074 ± (0.002)	0.135 ± (0.003)
Random forest	0.145 ± (0.002)	0.028 ± (0.002)	0.050 ± (0.001)	0.110 ± (0.004)
XGBoost	**0.142** ± (0.004)	0.022 ± (0.001)	0.050 ± (0.001)	**0.108** ± (0.003)
Model-method bands				
Greedy LDA	0.182 ± (0.003)	0.049 ± (0.002)	0.047 ± (0.003)	0.119 ± (0.003)
Greedy logistic regression	0.175 ± (0.004)	0.035 ± (0.002)	**0.042** ± (0.003)	0.120 ± (0.004)
PLS—VIP	0.169 ± (0.003)	0.051 ± (0.001)	0.046 ± (0.003)	0.120 ± (0.003)
Random forest—OOB	0.160 ± (0.004)	0.035 ± (0.002)	0.046 ± (0.002)	0.119 ± (0.004)
XGBoost—gain importance	0.144 ± (0.004)	**0.022** ± (0.002)	0.052 ± (0.005)	0.109 ± (0.001)

Table 2. Selection of bands by each model (Lazar and Bechar, 2021) [5].

Model	Band 1 (nm)	Band 2 (nm)	Band 3 (nm)	Band 4 (nm)
NCSI—manually selected	480	550	686	750
Greedy LDA	478	529	705	758
Greedy logistic regression	478	522	677	758
PLS	470	527	705	759
Random forest	484	552	758	813
XGBoost	485	554	668	735

Overall, the misclassification error using the four bands for pixel classification was below 5% for most days, but higher than the baseline levels found with all 840 spectral bands. Moreover, while it is not crucial to calibrate the cameras properly to achieve less than 12% misclassification error over all days, for day 2, where the images were the most detailed due to good camera calibration, the misclassification was lower than 2% (Table 1).

Investigation of the four-band combinations selected by the models (Table 2) showed that most of the bands were found near the NCSI manually selected bands. This indicates that the NCSI explains the spectral differences through a simple interpretation of the data. In addition, the selection made by the spectral analysis consisted of bands that had been used in previous studies for plant classification [25].

3.3. Weeding-Point Selection

The weeding-point selection consisted of five main stages: the first was to extract the image from the hypercube, followed by the four stages mentioned in Section 2. Figure 8 shows the workflow of the process.

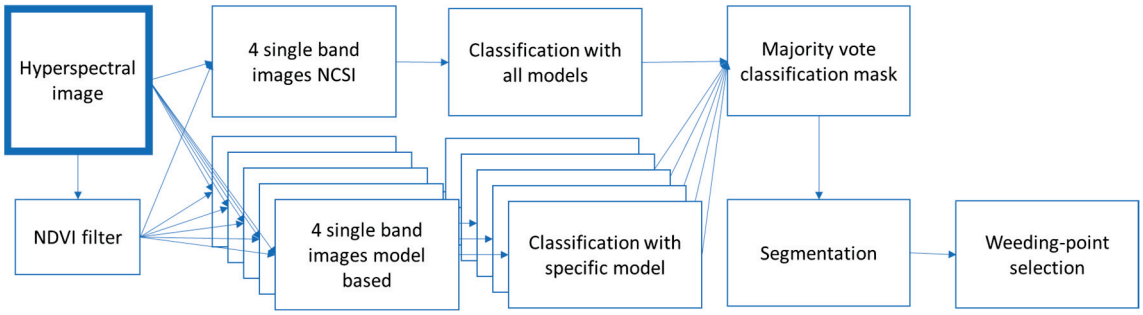


Figure 8. Weeding-point selection workflow. The hyperspectral image is used to extract four-band images for the classification models and the NDVI filter. The classified images are combined using a majority vote for each pixel, and the pixels are segmented to crop and weed objects. Weeding points are selected using the segmented image.

3.4. Image Classification with Four Bands

The hyperspectral images of the ROIs were used to classify the vegetation pixels in each ROI image into crop and weed. The classification was based on a four-band classification according to the selection of each method (Table 2). For each set of bands, four single-band images were extracted from the hyperspectral cube according to the selection of the classification model. Five sets of four single-channel images were extracted for the machine learning algorithm band selection. An additional set of four single-channel images was extracted for the NCSI manual band selection, resulting in six sets of images.

To separate the vegetation from the background, an NDVI filter was used with two of the four bands from the NCSI set—the 750 nm and 686 nm bands—to create a vegetation mask (Figure 9) of the ROI. Consistently, the same vegetation mask was used for all classification models to extract the pixels that represent vegetation for classification.

For qualitative assessment of the models, the six different sets were used, where each set of four single-band images was used for classification. Each vegetation pixel was classified 10 times, five times for the NCSI reference bands used by each classification model, and five times for the bands that were selected and used by the classification models (Table 2). The pixels were represented by $\vec{\lambda}_i$, which was a four-value vector, one for each band. The vectors of the pixels were classified by the models to produce 10 classification masks (Figure 10) of the classified pixels. The masks were produced by the classification models that were trained with data from the day on which the ROI image was taken. Inspection of the classification masks shows that all the classification models correctly classified most vegetation pixels. However, each mask differs in the classified pixels, with some pixels correctly classified and others misclassified.

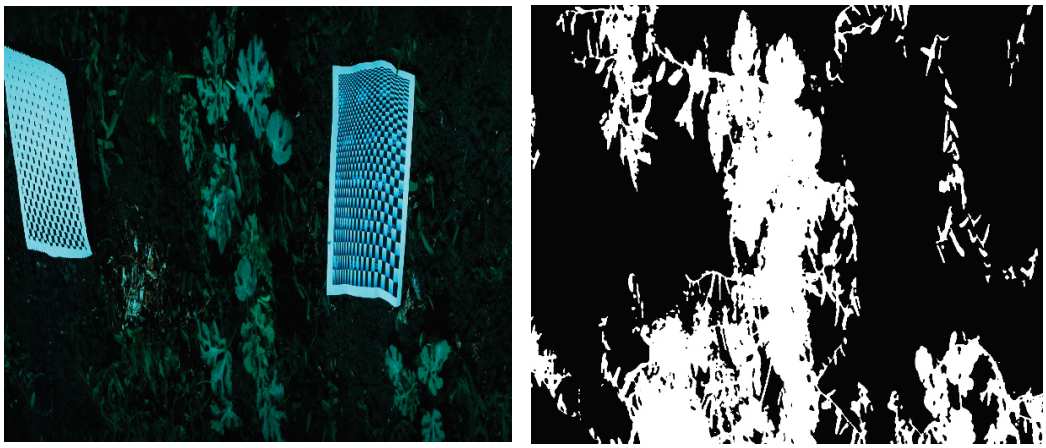


Figure 9. Pseudo RGB on the left and NDVI mask of the vegetation on the right form a single ROI image (sample 24 from day 3, Lazar and Bechar, 2021) [5].

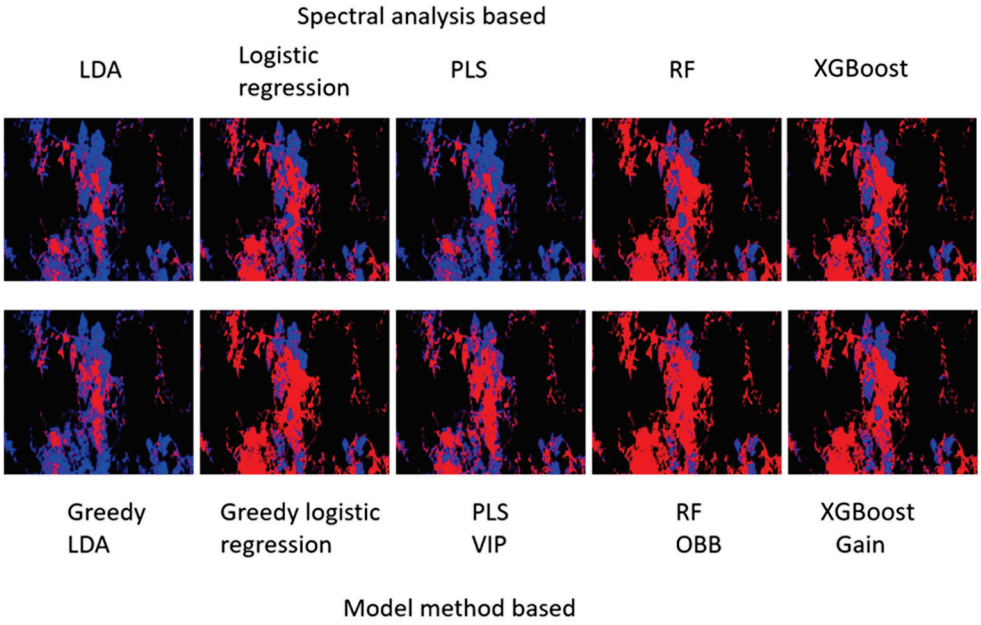


Figure 10. Classification masks of an ROI image. The classification fitting data were from the same visit day as the ROI image. Blue pixels represent crop; red pixels represent weed.

Most misclassifications occur at the edges of vegetation objects, where there can be shading from other plants, resulting in a low spectral difference. Random forest and XGBoost tend to classify these pixels as weeds, whereas the other methods classify them as crop. To resolve the conflict between the classification mask, for each pixel, a majority vote of all 10 models was used to create a classification mask that reduces misclassification. Each pixel (x, y) in the majority classification image was considered a weed pixel if six or more (out of the 10) models classified it as a weed; otherwise, the pixel was considered to be a crop. Furthermore, the classification masks showed better results when the model training data were normalized using the NCSI, where $\vec{\lambda}_{mean}$ (Equation (2)) was calculated as the mean response of the crop-labelled pixels from the same day that the image was taken, and each vegetation pixel $\vec{\lambda}_i$ was normalized using NCSI $\Lambda_{(i)}$ (Equation (1)).

To investigate the classification quality when using data from different days to train the classification models, each ROI image was classified 30 more times for a total of 40 classification masks. For each day, 10 classification masks were trained only on that day's data. An additional 10 classification masks were generated by models trained on data

from all days. All 40 classification masks, 10 for each day and 10 for all days, are presented in Figure 11 to provide a more comprehensive understanding of the classification outcomes generated by each classifier. Inspection of Figure 11 shows that XGBoost and Random Forest produce robust classification for all the masks, while with the other models, the classification changes when using different day data. The assessment of the classification mask indicates that the best classification was achieved when using the same-day data for classification. However, using data from day 2, which showed the lowest misclassification error (Table 1), produced masks that correctly classified most pixels, indicating the possibility of achieving similar results with high-quality stored data.

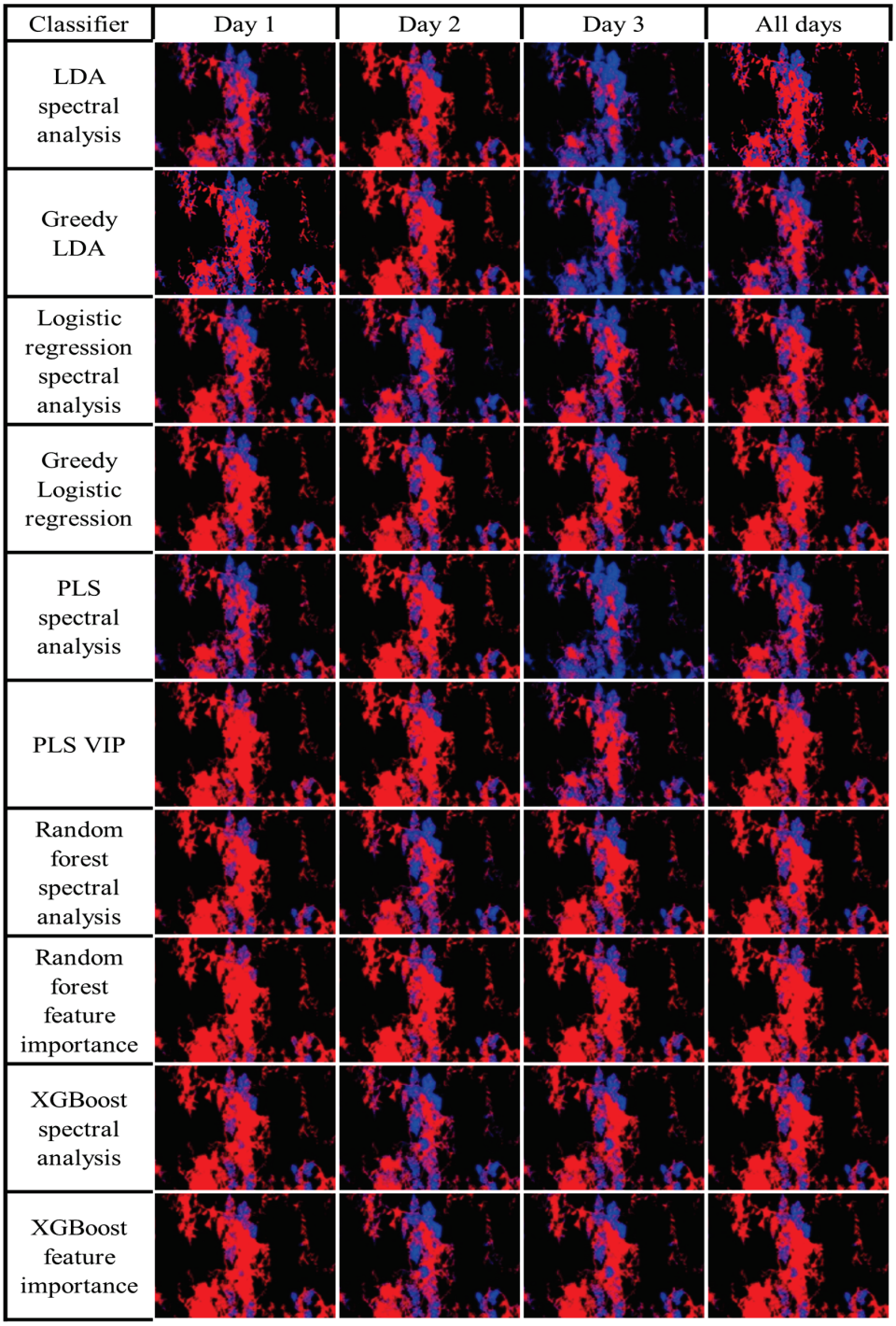


Figure 11. Classification masks based on each model for sample 24 from day 3, a total of 40 classifiers. Blue pixels represent crop; red pixels represent weed.

The final image classification workflow, which relies on a majority vote across 10 classification masks derived from both the NCSI-selected and model-optimized four-band subsets, serves as an effective mechanism for error mitigation and maximizing robustness. The qualitative assessment of the classification masks clearly highlights the ability of the reduced four-band set to accurately differentiate vegetation, with most misclassifications occurring in challenging areas like plant edges or shaded regions. Crucially, the finding that normalization via NCSI significantly improves classification quality across the board underscores the index's operational value, and the demonstration that high-quality, normalized data can yield correct classification even for unseen images suggests a viable path toward a generalized, high-accuracy model that requires only periodic, not continuous, field calibration.

3.5. Image Segmentation and Point Selection

The segmentation procedure is based on a majority vote classification mask. Using the algorithms presented in Section 2, the crop and weed objects were classified. Figure 12 shows the segmented objects, and the crop (blue) objects include some weed pixels, which are either between or near the crop pixels. The segmentation objective is to avoid weeding of the crop. In addition, weed objects are to be evaluated as smaller than the area of classified weed pixels, and are to be considered crop-free.

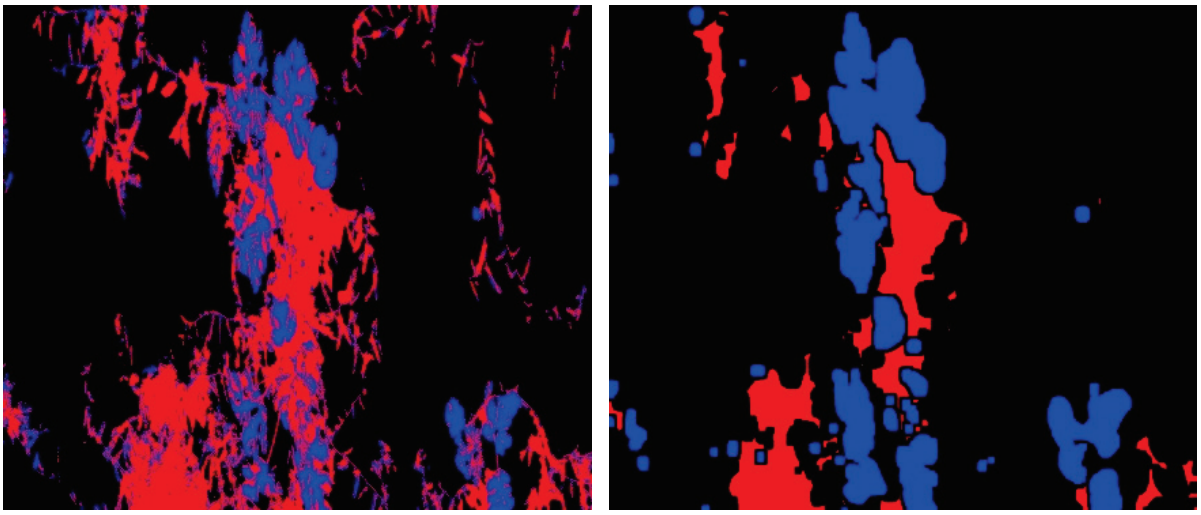


Figure 12. The majority classification mask (**left**) and the segmented mask (**right**). Blue: pixels represent crop; red pixels represent weed.

The segmented mask was resized by averaging to a small image of about 15 pixels in height, where each pixel represents about 6 × 6 cm, to find weed areas that are remote from the crop. In the small 15-pixel high image, pixels that had some crop (blue) values were disregarded. The result was a crop-free weed area image (Figure 13). The weeding points selected from the crop-free tiled image followed the distance rules and did not touch any of the crop pixels. All of the ROI VNIR hyperspectral images were used in this procedure, and weeding points were selected for each ROI image that contained weeds. An expert evaluation of the quality of the number and location of the weeding points found that all weeding point positions were weed pixels in the images and that it is sufficient for the process of handling intra-row weeds with pinpoint selection. However, the objective evaluation of final weeding-point selection accuracy, as well as metrics like detection time and rate of successful weed removal, requires further field-based research to be conducted using the algorithm in a commercial plot.

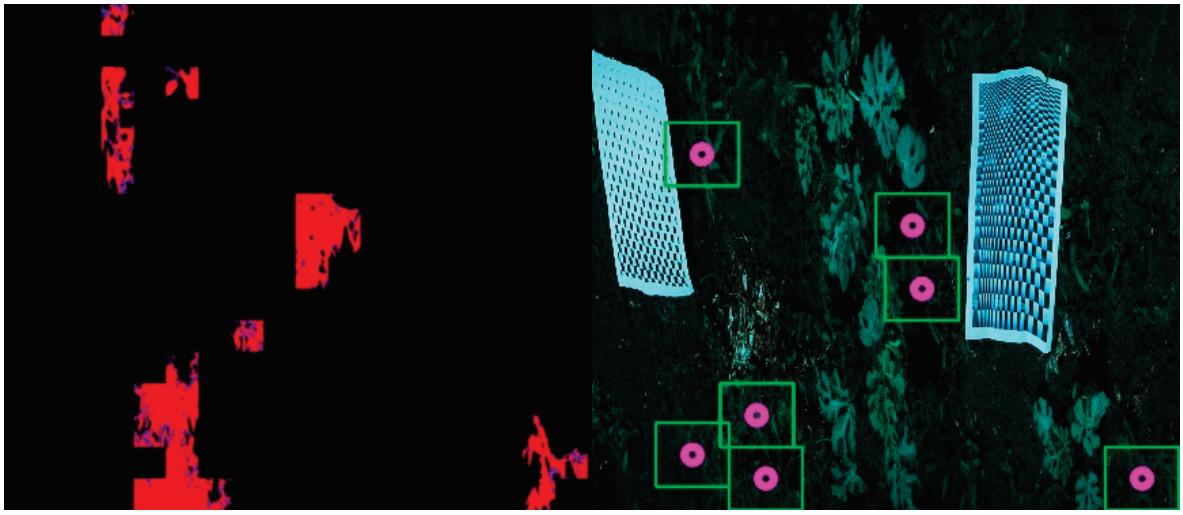


Figure 13. The crop-free weed tile mask (**left**) and the weeding points corresponding with high weed density in the non-overlapping tiles (**right**). Red pixels represent weed; purple rings represent weeding points and the green rectangles represent weeding point zones.

4. Discussion and Conclusions

A case study was conducted for the classification of cv. Malali watermelon crop and weeds of the genus *Convolvulus*. Four-band subsets selected from 840 bands of the VNIR camera (400–1000 nm) demonstrated that four-band subsets achieved sufficient accuracy for targeted weeding. This success was critically supported by the introduction of the Normalized Crop Sample Index (NCSI), a practical innovation that simplifies complex hyperspectral data for real-world agricultural use by normalizing the sample's spectral response against the mean crop signature. This normalization effectively amplifies the subtle, vital spectral differences between the crop and the weed, minimizing the impact of day-to-day environmental variability. The NCSI proved a powerful, straightforward tool for feature engineering, as the four manually selected bands (480 nm, 550 nm, 686 nm, and 750 nm) precisely aligned with the index's critical spectral inflection points and produced similar results, in terms of selected bands and low misclassification error, to those selected by five different machine learning models. The misclassification error levels were similar as well.

The NCSI is a novel contribution as it functions as a comprehensive spectral normalization tool, unlike a simple two-band spectral index such as the NDVI. The NDVI is primarily used for binary segmentation, separating all vegetation from non-vegetation. The NCSI, by contrast, normalizes the full spectral vector of an unknown plant against the average full spectral vector of a known crop sample. This process effectively minimizes external noise and variations due to illumination or camera calibration, which can cause intensity shifts across the spectrum. The NCSI's main advantage is that the resulting normalized spectrum (Figure 4b) emphasizes the subtle spectral differences between the weed and the crop, transforming the problem from distinguishing between two similar absolute reflectance curves into classifying based on a distinct pattern of deviation from the crop's baseline. This ability to simplify the interspecies difference across the full spectrum proved instrumental in manually identifying the optimal distinguishing bands.

It was found that the greedy LDA, greedy logistic regression and PLS are sensitive to the differences in daily conditions and to the band-selection method, as seen in Figure 11. The classification masks produced by those models show a high difference when the classifiers were trained on the same day or on different days. These models therefore operate with relatively lower performance when the training and testing images are from

different days; on the other hand, random forest and XGBoost show robust performance even when the tested data are taken from days that differ from those of the training data. This robust performance of Random Forest and XGBoost, which are tree-based models, is likely due to their non-linear nature and their internal mechanisms for handling feature variance and outliers more effectively than linear models like LDA or Logistic Regression. They create multiple decision trees, which effectively average out the noise and variability present in the data collected across the different days, leading to a classification decision that is more stable and more robust than a single linear model. Overall, the use of random forest or XGBoost as classification models is preferred because the classification showed the overall lowest misclassification error level and was more robust across dynamic field conditions. This insight suggests that future robotic systems should prioritize the use of these robust, non-linear classification methods for reliable performance in dynamic, real-world agricultural environments and low-dimensional spectral features.

Due to the distinct spectral characteristics exhibited by crops as compared to weeds, the labelling process was efficient, requiring only a relatively small number of frames. Specifically, 572 frames were selected from 26 chosen ROI (Region of Interest) images to create the classifiers. These labelled rectangles were carefully chosen from the VNIR ROI images for each class. A modest amount of labelled data, approximately 100,000 pixels, proved to be more than adequate for training classification models that hinged on the four spectral bands. These models demonstrated a remarkable ability to classify unknown data with a high degree of accuracy. The spectral characteristics identified by the NCSI and selected bands are derived from the spectral contrast between the watermelon (cv. Malali) and the weed (*Convolvulus*). However, the developed methodology using NCSI is a universally applicable method to distinguish between melon (crop plant) and different types of weeds since it is normalized by the crop spectral signature. The machine learning for band selection is portable and can be adapted to different crop/weed species. The methodology developed in this context and the approach of working with a compact dataset could easily be adapted for use with different weed varieties. Periodic calibration, such as at the outset of each day or whenever environmental conditions undergo significant changes, could be facilitated by labelling a limited number of crop and weed plants and subsequently updating the classification models with real-time data. Furthermore, the quality of the camera calibration played a crucial role. In cases where calibration was suboptimal, as seen on day 1, certain classifiers exhibited superior performance in classifying unseen images. However, under conditions of good calibration, all the classifiers consistently demonstrated proficient image classification.

The final steps of image segmentation and weeding-point selection demonstrate the method's transition from spectral science to robotic engineering. The segmentation algorithm, by aggressively prioritizing crop protection through dilation and weed-object erosion, generates distinct, crop-free weed objects suitable for physical intervention. The use of spatial averaging to create large (6 cm $\times$ 6 cm) tiles and then ranking them by weed pixel density effectively converts the pixel data into a discrete, manageable set of high-confidence treatment locations. This tiling process is the practical bridge between accurate classification and the constraints of a mechanical weeding tool, ensuring that the selected points are not only weeds but are also spatially isolated and dense enough to warrant a precision treatment, thereby completing the robust workflow necessary for a functional, selective weeding robot.

The study indicates that future application of a robotic platform equipped with a four-band multispectral camera may be able to detect and apply treatment for weeds in watermelon plots with pinpoint operation. Such a camera, which uses four narrow bands, can produce fast and accurate crop and weed detection with low cost and low

computational resources in comparison to an 840-band hyperspectral camera. This is due to the significant reduction in data dimensionality from 840 to only four spectral bands, making real-time processing substantially easier and enabling the use of less expensive hardware. Further studies are required to determine the actual operational metrics, such as model response speed and power consumption, with reference to the weeding tool and the critical weeding period, and to increase the diversity of the crop and weed data.

The NCSI, with a minimal set of four bands, is highly effective for crop-weed discrimination. The key advantage of the NCSI approach lies in its simplicity and inherent spectral interpretability. By normalizing the spectral response of a sample against the mean crop signature, NCSI effectively isolates the subtle, differential reflectance characteristics critical for separating crop and weed. This approach demonstrated strong efficacy, as the NCSI-selected bands were consistently near the optimal bands identified by more complex, purely algorithmic methods like Greedy LDA, PLS, and XGBoost. In contrast, automated dimension reduction techniques, such as the Principal Component Analysis (PCA) used by Diao et al. [20] or the Successive Projection Algorithm (SPA) used by Zhang et al. [18], are effective for data compression but often yield spectral features that are linear combinations of the original bands, thereby losing direct physical interpretability. The SPA method, for example, selected six specific features [18], achieving high accuracy but necessitating a larger feature set than our target. The NCSI approach, by focusing on spectral inflection points derived from biophysical differences (chlorophyll absorption and cellular structure), provides a transparent, low-cost alternative to these automated methods. This transparency is crucial for the engineering development of a low-cost, multispectral camera system, confirming that the minimal four-band subset is sufficient for high-accuracy discrimination.

A limitation of this study is that although NCSI was designed to cope with several weeds, it was examined on a single crop-weed pair, which, while proving the methodology, limits the immediate universal applicability. Furthermore, while the model was robust, the data collection covered only three non-consecutive days. However, the models, particularly XGBoost, demonstrated a remarkable ability to classify unknown data with a high degree of accuracy with a modest amount of labelled data, alleviating the concern of a small training set size or potential overfitting. Future research should focus on three main directions: expanding the dataset to include greater diversity of weed species and crop growth stages; performing a direct, objective field validation of the entire robotic system to measure real-time operational metrics like detection speed and successful weeding rates; and, adapting the NCSI-based band selection methodology to other high value crops to accelerate the adoption of cost-effective multispectral weeding systems.

Author Contributions: Conceptualization, A.B.; methodology, A.L. and I.M.; software, A.L.; validation, A.B.; formal analysis, A.L.; investigation, R.N.L.; writing—original draft preparation, A.L.; writing—review and editing, A.B. and R.N.L.; supervision, A.B.; project administration, A.B. All authors have read and agreed to the published version of the manuscript.

Funding: This study was funded by the Chief Scientist of the Ministry of Agriculture, Israel. We are grateful to Aviad Ozeri and Shai Ladani for their help in carrying out the experiments.

Data Availability Statement: The original contributions presented in this study are included in the article. Further inquiries can be directed to the corresponding author(s).

Conflicts of Interest: The authors declare no conflict of interest.

References

1. Froud-Williams, R.J. Weed Science Research: Past, Present and Future Perspectives. *Weed Res. Expand. Horiz.* **2017**, 1–32. [CrossRef]
2. Flessner, M.L.; Burke, I.C.; Dille, J.A.; Everman, W.J.; VanGessel, M.J.; Tidemann, B.; Manuchehri, M.R.; Soltani, N.; Sikkema, P.H. Potential wheat yield loss due to weeds in the United States and Canada. *Weed Technol.* **2021**, *35*, 916–923. [CrossRef]
3. Korav, S.; Dhaka, A.; Singh, R.; Chandramohan Reddy, G. A study on crop weed competition in field crops. *J. Pharmacogn. Phytochem.* **2018**, *7*, 3235–3240.
4. Cohen, R.; Eizenberg, H.; Edelstien, M.; Horev, C.; Lande, T.; Porat, A.; Achdari, G.; Hershenhorn, J. Evaluation of herbicides for selective weed control in grafted watermelons. *Phytoparasitica* **2008**, *36*, 66–73. [CrossRef]
5. Lazar, A.; Bechar, A. Four-band weed detection using machine learning algorithms based on hyperspectral images. In Proceedings of the 13th European Conference on Precision Agriculture, Mons, Belgium, 18–20 July 2022; Wageningen Academic: Wageningen, The Netherlands, 2021.
6. Melander, B.; Liebman, M.; Davis, A.S.; Gallandt, E.R. Non-Chemical Weed Management: Expanding Horizons. In *Weed Research*; Wiley: Oxford, UK, 2017; pp. 245–270.
7. Lati, R.N.; Rosenfeld, L.; David, I.B.; Bechar, A. Power on! Low-energy electrophysical treatment is an effective new weed control approach. *Pest Manag. Sci.* **2021**, *77*, 4138–4147. [CrossRef]
8. Khort, D.; Shutenko, A.; Filippov, R.; Semichev, S. Automated stand for the study of injectors made of polymer materials for hydraulic weed destruction. In *E3S Web of Conferences*; EDP Sciences: Les Ulis, France, 2020; Volume 193. [CrossRef]
9. Forcella, F. Potential use of abrasive air-propelled agricultural residues for weed control. *Weed Res.* **2009**, *49*, 341–345. [CrossRef]
10. Forcella, F. Air-Propelled Abrasive Grit for Postemergence In-Row Weed Control in Field Corn. *Weed Technol.* **2012**, *26*, 161–164. [CrossRef]
11. Antonopoulos, N.; Kanatas, P.; Gazoulis, I.; Tataridas, A.; Ntovakos, D.; Ntaoulis, V.; Zavra, S.-M.; Travlos, I. Hot foam: Evaluation of a new, non-chemical weed control option in perennial crops. *Smart Agric. Technol.* **2023**, *3*, 100063. [CrossRef]
12. Chandel, N.S.; Chandel, A.K.; Roul, A.K.; Solanki, K.R.; Mehta, C.R. An integrated inter- and intra-row weeding system for row crops. *Crop Prot.* **2021**, *145*, 105642. [CrossRef]
13. Coleman, G.R.Y.; Bender, A.; Hu, K.; Sharpe, S.M.; Schumann, A.W.; Wang, Z.; Bagavathiannan, M.V.; Boyd, N.S.; Walsh, M.J. Weed detection to weed recognition: Reviewing 50 years of research to identify constraints and opportunities for large-scale cropping systems. *Weed Technol.* **2022**, *36*, 741–757. [CrossRef]
14. Amziane, A.; Losson, O.; Mathon, B.; Macaire, L.; Duménil, A. Weed detection by analysis of multispectral images acquired under uncontrolled illumination conditions. *SPIE-Int. Soc. Opt. Eng.* **2021**, *11794*, 12. [CrossRef]
15. Lottes, P.; Hörferlin, M.; Sander, S.; Stachniss, C. Effective Vision-based Classification for Separating Sugar Beets and Weeds for Precision Farming. *J. Field Robot.* **2017**, *34*, 1160–1178. [CrossRef]
16. Sa, I.; Chen, Z.; Popović, M.; Khanna, R.; Liebisch, F.; Nieto, J.; Siegwart, R. weednet: Dense semantic weed classification using multispectral images and mav for smart farming. *IEEE Robot. Autom. Lett.* **2017**, *3*, 588–595. [CrossRef]
17. Potena, C.; Nardi, D.; Pretto, A. Fast and accurate crop and weed identification with summarized train sets for precision agriculture. In *Advances in Intelligent Systems and Computing*; Springer: Berlin/Heidelberg, Germany, 2017; Volume 531, pp. 105–121. [CrossRef]
18. Zhang, Y.; Gao, J.; Cen, H.; Lu, Y.; Yu, X.; He, Y.; Pieters, J.G. Automated spectral feature extraction from hyperspectral images to differentiate weedy rice and barnyard grass from a rice crop. *Comput. Electron. Agric.* **2019**, *159*, 42–49. [CrossRef]
19. Lauwers, M.; De Cauwer, B.; Nuyttens, D.; Cool, S.R.; Pieters, J.G. Hyperspectral classification of cyperus esculentus clones and morphologically similar weeds. *Sensors* **2020**, *20*, 2504. [CrossRef]
20. Diao, Z.; Guo, P.; Zhang, B.; Yan, J.; He, Z.; Zhao, S.; Zhao, C.; Zhang, J. Spatial-spectral attention-enhanced Res-3D-OctConv for corn and weed identification utilizing hyperspectral imaging and deep learning. *Comput. Electron. Agric.* **2023**, *212*, 108092. [CrossRef]
21. Sun, W.; Du, Q. Hyperspectral band selection: A review. *IEEE Geosci. Remote Sens. Mag.* **2019**, *7*, 118–139. [CrossRef]
22. Jayaprakash, C.; Damodaran, B.B.; Viswanathan, S.; Soman, K. Randomized independent component analysis and linear discriminant analysis dimensionality reduction methods for hyperspectral image classification. *J. Appl. Remote Sens.* **2020**, *14*, 036507. [CrossRef]
23. Nagasubramanian, K.; Jones, S.; Sarkar, S.; Singh, A.K.; Singh, A.; Ganapathysubramanian, B. Hyperspectral band selection using genetic algorithm and support vector machines for early identification of charcoal rot disease in soybean stems. *Plant Methods* **2018**, *14*, 86. [CrossRef]
24. Chan, J.C.W.; Paelinckx, D. Evaluation of Random Forest and Adaboost tree-based ensemble classification and spectral band selection for ecotope mapping using airborne hyperspectral imagery. *Remote Sens. Environ.* **2008**, *112*, 2999–3011. [CrossRef]
25. Thenkabail, P.S.; Enclona, E.A.; Ashton, M.S.; Van Der Meer, B. Accuracy assessments of hyperspectral waveband performance for vegetation analysis applications. *Remote Sens. Environ.* **2004**, *91*, 354–376. [CrossRef]

26. Liakos, K.G.; Busato, P.; Moshou, D.; Pearson, S.; Bochtis, D. Machine learning in agriculture: A review. *Sensors* **2018**, *18*, 2674. [CrossRef] [PubMed]
27. Savitzky, A.; Golay, M.J.E. Smoothing and Differentiation of Data by Simplified Least Squares Procedures. *Anal. Chem.* **1964**, *36*, 1627–1639. [CrossRef]

Disclaimer/Publisher's Note: The statements, opinions and data contained in all publications are solely those of the individual author(s) and contributor(s) and not of MDPI and/or the editor(s). MDPI and/or the editor(s) disclaim responsibility for any injury to people or property resulting from any ideas, methods, instructions or products referred to in the content.

MDPI AG
Grosspeteranlage 5
4052 Basel
Switzerland
Tel.: +41 61 683 77 34

Agronomy Editorial Office
E-mail: agronomy@mdpi.com
www.mdpi.com/journal/agronomy



Disclaimer/Publisher's Note: The title and front matter of this reprint are at the discretion of the Guest Editor. The publisher is not responsible for their content or any associated concerns. The statements, opinions and data contained in all individual articles are solely those of the individual Editor and contributors and not of MDPI. MDPI disclaims responsibility for any injury to people or property resulting from any ideas, methods, instructions or products referred to in the content.





Academic Open
Access Publishing

mdpi.com

ISBN 978-3-7258-9296-9